SAND81-0763
Unlimited Release
UC-62

Handbook for the Conceptual Design of Parabolic Trough Solar Energy Systems

Process Heat Applications

Raymond W. Harrigan

Prepared by Sandia National Laboratories, Albuquerque, New Mexico 87185
and Livermore, California 94550 for the United States Department
of Energy under Contract DE-AC04-76DP00789

Printed July 1981

Sandia National Laboratories

SF 2900-Q(3-80)

Issued by Sandia National Laboratories, operated for the United States Department of Energy by Sandia Corporation.

NOTICE: This report was prepared as an account of work sponsored by an agency of the United States Government. Neither the United States Government nor any agency thereof, nor any of their employees, nor any of their contractors, subcontractors, or their employees, makes any warranty, express or implied, or assumes any legal liability or responsibility for the accuracy, completeness, or usefulness of any information, apparatus, product, or process disclosed, or represents that its use would not infringe privately owned rights. Reference herein to any specific commercial product, process, or service by trade name, trademark, manufacturer, or otherwise, does not necessarily constitute or imply its endorsement, recommendation, or favoring by the United States Government, any agency thereof or any of their contractors or subcontractors. The views and opinions expressed herein do not necessarily state or reflect those of the United States Government, any agency thereof or any of their contractors or subcontractors.

Printed in the United States of America

Available from
National Technical Information Service
U. S. Department of Commerce
5285 Port Royal Road
Springfield, VA 22161

NTIS price codes
Printed copy: $17.00
Microfiche copy: A01

SAND81-0763
Unlimited Release
Printed July 1981

UC-62

HANDBOOK FOR THE CONCEPTUAL DESIGN OF PARABOLIC TROUGH SOLAR ENERGY SYSTEMS

PROCESS HEAT APPLICATIONS

R. W. Harrigan
Component and Subsystem Development Division 4716
Sandia National Laboratories
Albuquerque, NM 87185

ABSTRACT

This report presents the techniques needed to execute conceptual designs of process heat systems employing parabolic trough solar collectors. The design tools are presented in graphical format, and each of 26 SOLMET sites is explicitly represented. The conceptual design resultant from the application of the design charts contained within this handbook approximates the collector area needed to displace a constant thermal demand, the land area needed for collector deployment, the appropriate quantity of sensible heat storage, the fraction of fossil fuel displaced by solar, and the capital cost of the collector-storage subsystem.

CONTENTS

CONTENTS (Continued)

ILLUSTRATIONS

ILLUSTRATIONS (Continued)

TABLE

HANDBOOK FOR THE CONCEPTUAL DESIGN OF PARABOLIC TROUGH SOLAR ENERGY SYSTEMS

PROCESS HEAT APPLICATIONS

1. INTRODUCTION

The goal of this handbook is to provide easily used techniques which will allow the rapid achievement of conceptual designs. Much has been learned about expected collector performance, variation of solar radiation within the United States, and how parabolic trough solar collectors can be integrated with thermal energy storage. This handbook integrates this and other state-of-the-art information into the conceptual design process.

A conceptual design evaluates the ability of alternative design options to meet the energy demands of a potential process heat application. The objective is to quickly sort through the various potential solar energy system designs and to choose one or two, if any, that have good potential for servicing a thermal energy demand cost-effectively. The conceptual design should estimate

1. The area of solar collectors required,
2. The land area needed by the solar collectors,
3. Storage requirements, and
4. The fraction of the fossil fuel which could reasonably be displaced by a solar thermal energy system.

In addition, a well-executed conceptual design allows approximation of the capital cost of the solar energy system needed to service the demand.

As a result, the conceptual design serves as a screening tool. If the conceptual design reveals severe constraints on the solar energy system (e.g., too little land available for collector deployment), the application of solar energy to the process should be questioned before continuing with the design process. If the conceptual design indicates good compatibility between the solar energy system concept and the application, the conceptual design serves as a foundation from which the preliminary and detailed design processes can begin.

Handbook design procedures are needed to help instill reliability and safety of design and to lower costs resultant from custom designing. Furthermore, there will not be a single system design which services all process heat applications efficiently. This handbook is a statement of design procedures which do not vary from application to application. This allows design of the solar energy system which best interfaces with a specific application. Development of standard design procedures is an evolutionary process based upon experience in the design, construction, and operation of actual systems. This handbook attempts to initiate that evolution by presenting an assembly of conceptual design techniques developed through the design of solar thermal systems employing parabolic troughs. The handbook is meant to be revised as experience with solar thermal systems grows.

Preliminary design, which evaluates considerations such as system control, thermal losses from piping manifolds, fluid pump power requirements, preferred piping and wiring layouts, and system safety follows conceptual design. These considerations are necessary inputs into any decision to build and result in a reasonably accurate definition of system configuration and costs.

1.1 APPROACH

The handbook stresses the use of graphs and figures in the design process to allow the designer to visualize the importance of the different factors impacting the design. A primary concern is not only to achieve a conceptual design of a solar thermal process heat system, but to develop an understanding of the factors strongly influencing

the design. Extensive text has been provided in Sections 2 and 3 in order to describe the development of the design techniques and indicate their validity and limitations as well as their use. It is important that, as tradeoffs are made in arriving at a final design, the impact of any design change is fully understood by the designer. All pertinent design charts are reproduced in the appendices for easy reference.

Emphasis has been placed on developing techniques to allow designers to quickly evaluate solar thermal energy systems. No attempt is made to decide a priori whether or not solar energy is appropriate to a given application's needs. This handbook provides the tools to execute conceptual designs, building on parabolic trough collector performance test data. The interaction of storage and collectors is examined. The approach is to use Storage Sizing Graphs* which relate collector area to Storage Capacity for a given displacement of a defined thermal energy demand. The concept of a Maximum Displacement Point is developed and used to determine the practical limit to fossil fuel Displacement by a parabolic trough solar thermal energy system.

Because costs are ill defined in any developing technology, a design strategy stressing maximum Utilization of solar equipment is employed. Since a solar energy system is capital intensive, efficient use (i.e., high Utilization) of the solar equipment is required to maximize the return on investment. Thus, as will be shown, deployment of collectors and storage to provide energy for infrequent occasions, such as cloudy days, is usually not cost effective since the Utilization of the extra collectors and storage is low. Typically, systems should be designed to allow near 100% Utilization of the energy collected.

The handbook is structured to allow the designer to factor costs which are current at the time of design execution into the design

---

* Capitalized terms are explicitly defined in Appendix A, "Glossary of Handbook Terminology."

process where needed. Thus, the design procedures are not limited by any costs assumed at the date of publication.

The handbook is divided into four principal sections together with appendices. Sections 2 and 3 provide the background information needed to understand the development of the conceptual design techniques. Section 4 presents the conceptual design procedures and illustrates their use. Section 4 is written to stand alone as much as possible, and the design techniques can be used without reading Sections 2 and 3. It is recommended, however, that Sections 2 and 3 be read to achieve an understanding of the development and the limitations of the design techniques to prevent their inadvertent misuse. A brief summary of each section follows.

Performance of Parabolic Trough Collectors -- This first major section of the handbook addresses the conversion of measured collector test data into average annual and monthly thermal collector performance for a particular site. Average annual and monthly collector performance information is developed as a function of Collector Operating Temperature and orientation. Nomographs are presented which allow the generation of integrated performance information for any single-axis tracking parabolic trough collector for which standard test data are available.

Thermal Energy Storage -- Thermal energy storage must be incorporated into a solar thermal energy system if significant amounts of fossil fuel Displacement are to be achieved. Graphs relating fossil fuel Displacement and Storage Capacity are developed in this section together with estimates of storage costs. Evidence supporting the design philosophy of achieving maximum utilization of the solar equipment is presented.

Conceptual Design -- Techniques for quickly determining the basic compatibility of a solar thermal process heat system with an application are developed in this section. The role of storage in solar process heat systems is examined, leading to a determination of the

area of collector and quantity of storage needed to service a given thermal energy Demand. The fossil fuel Displacement is estimated along with the land area needed for deployment of the system. Design rules-of-thumb are presented. A first order estimate of system costs can be developed based on the conceptual design.

In addition to the main sections within the body of the handbook, appendices are presented which provide detailed discussions of selected topics as well as a glossary of commonly used terms and site-specific design charts for each of 26 SOLMET sites.

Glossary of Handbook Terminology -- In order to discuss the execution of system designs using parabolic trough collectors, it is important to clearly define terms and then use these terms consistently. To facilitate this, a "Glossary of Handbook Terminology" has been included as Appendix A. Every attempt is made to insure consistent use of the terms in Appendix A throughout the handbook. In a few cases, accurate definition of a term may require a rather extensive discussion; an example of this is the definition of efficiency. These expanded definitions are contained in Appendix B. Terms which are explicitly defined in the appendices are capitalized within the text to tell the reader that this term is being used with a specific definition.

Site-Specific Design Information -- Each of 26 SOLMET[1] sites is explicitly addressed in the appendices. These sites are maintained by the National Climatic Center, and an hourly solar data base is available for each location. All the graphs needed to perform solar thermal system design at each site are reproduced together with any nomographs needed to support site-specific design.

In summary, the handbook allows the stepwise design of parabolic trough solar thermal process heat systems. The resultant design should represent a reasonable beginning to allow system performance and economic evaluation with confidence. In fact, given the uncertainty in the inputs to the design, such as the solar resource data

base, the conceptual design resulting from use of this handbook may well be within the limits of error of a fully optimized conceptual design developed through computer simulation.

1.2 LIMITATIONS

Before beginning the development of the conceptual design techniques, it is worthwhile to explicitly state the limitations of the handbook. This is done to avoid confusion over applicability of the handbook and to prevent misuse of the design charts and techniques to be presented. Each of the major limitations is listed together with a brief discussion.

1. Single-Axis Tracking Parabolic Troughs -- The handbook is limited to system designs employing single-axis tracking parabolic troughs. This limitation arises primarily from the nomographs for predicting average collector performances. Use of the nomographs requires knowledge of the Direct Insolation entering the collector aperture. This in turn requires knowledge of the tracking of the collector. Charts of the Direct Insolation incident on single-axis tracking collectors are presented in Appendix H for each of 26 SOLMET sites.

2. Geographic Location -- Explicit design data are present only for each of 26 SOLMET sites within the continental United States. Use of these data for other sites should be considered high risk. A Direct Insolation map is presented in Section 2 to help in selecting the SOLMET site best representative for design of a system located at a non-SOLMET site. However, maps such as this are approximate, and local climatological conditions can vary greatly from those indicated on Direct Insolation maps.

3. Conceptual Design Only -- The techniques presented in this handbook lead to a conceptual design only. Design considerations such as thermal losses in the collector field manifold piping, pump power requirements, optimum insulation thicknesses, optimum collector row spacing, control strategies, dirt on reflector surfaces, etc., are not covered.

2. PERFORMANCE OF PARABOLIC TROUGH COLLECTORS

The basic principle used in the design of parabolic trough collectors is to concentrate the solar energy incident upon a large area onto a smaller receiver area. By reducing the area of the hot receiver, the thermal losses from the receiver are reduced, allowing operation at high temperatures with high efficiency. Typically, parabolic trough collectors have concentration ratios (i.e., aperture area/receiver area) between 20 and 50. Figure 1 is a sketch of a parabolic trough collector, showing the principal component parts.

The linear reflector is made of a material which exhibits high Specular Reflectance and is formed with high accuracy to a parabolic contour. The receiver is generally a steel tube coated with a black selective coating having a high Absorptance for visible light and a low Emittance for infrared radiation. Heat transfer fluid is used within the receiver tube to remove the thermal energy. A concentric glass envelope suppresses convective thermal losses from the receiver. The collector is rotated, using a drive motor and gear box assembly, in order to maintain the Direct Insolation focused on the receiver tube. A tracking device is employed to determine the proper position of the parabolic trough throughout the day. Typically, a flexible metal hose is used to connect the rotating collector to the rigid pipe fluid distribution network.

Parabolic trough collectors are usually laid out horizontal to the ground to take advantage of their linear geometry and to reduce interconnecting plumbing and complex collector support structure. Multiple rows of parabolic troughs are employed to achieve a given thermal energy output from the collector field as indicated in Figure 2.

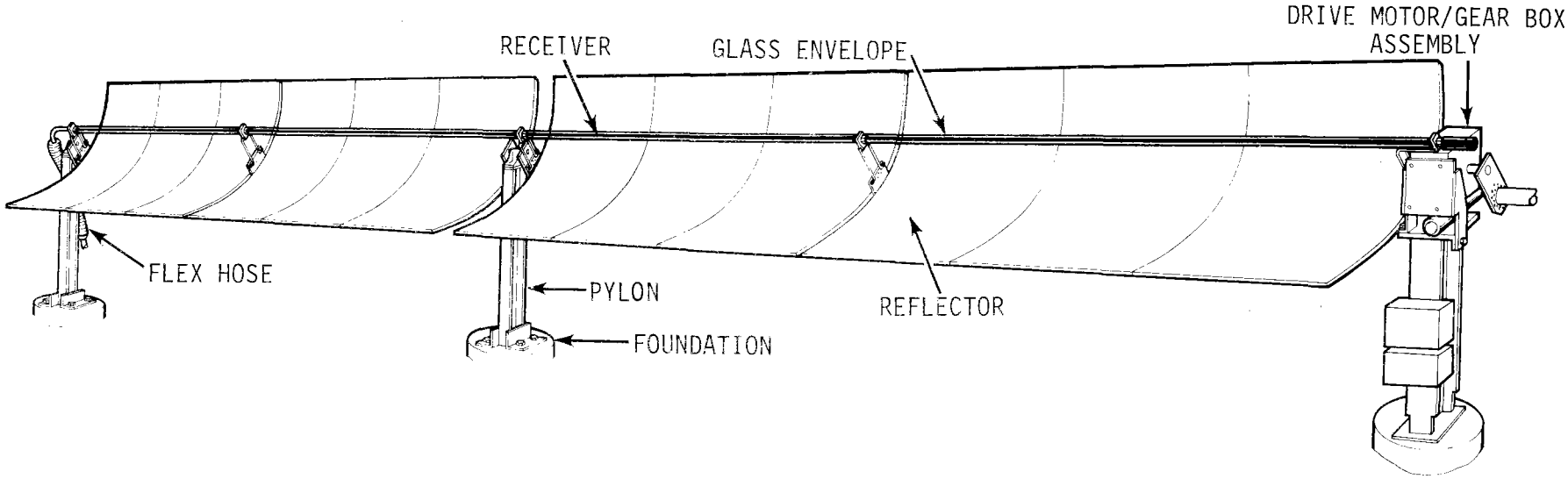

Figure 1. Typical Line-Focusing Collector Design

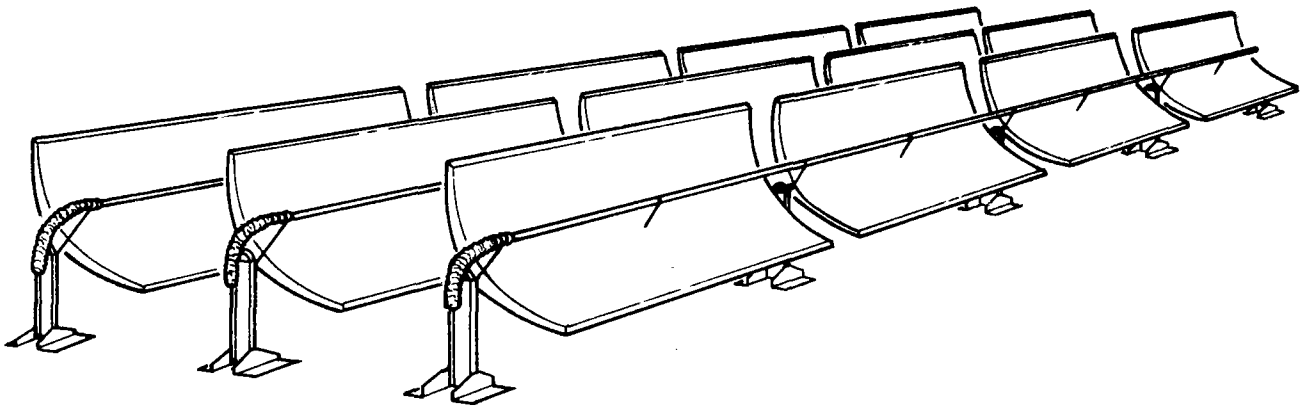

Figure 2. Deployment of Parabolic Trough Collectors in Rows

The following discussion examines the performance of parabolic trough collectors and the effect of single-axis tracking on collector performance throughout the day. In addition, nomographs are developed for projecting thermal energy output from a parabolic trough collector during a year. This projection requires an estimate of the Direct Insolation and knowledge of the collector efficiency as a function of operating temperature as typically measured by test facilities evaluating collector performance.

To facilitate discussion, it is convenient to use the generic term "collector efficiency" as long as what is meant by that term is understood. Various definitions of collector efficiency have been presented in detail in Appendix B. In the body of this handbook, collector efficiency will be defined as the Instantaneous Direct Insolation Aperture Efficiency. In addition, the average collector efficiency over a given period of time (e.g., average annual efficiency) will refer to the Average Direct Insolation Efficiency over the time period indicated. The reader is directed to Appendices A and B for further definition of terms used in this handbook.

2.1 COLLECTOR PERFORMANCE TEST DATA

The performance of a parabolic trough collector is usually reported as a plot of collector efficiency versus the function $(T_{col} - T_{amb})/I$ (see Reference 2) where

I = the instantaneous Direct Insolation passing through a unit area of collector aperture and

$(T_{col} - T_{amb})$ = the difference between the Collector Operating Temperature (average of fluid inlet and outlet temperatures) and the ambient temperature.

Figure 3 shows a plot of performance data for a clean parabolic trough collector evaluated at Sandia National Laboratories, Albuquerque (SNLA).

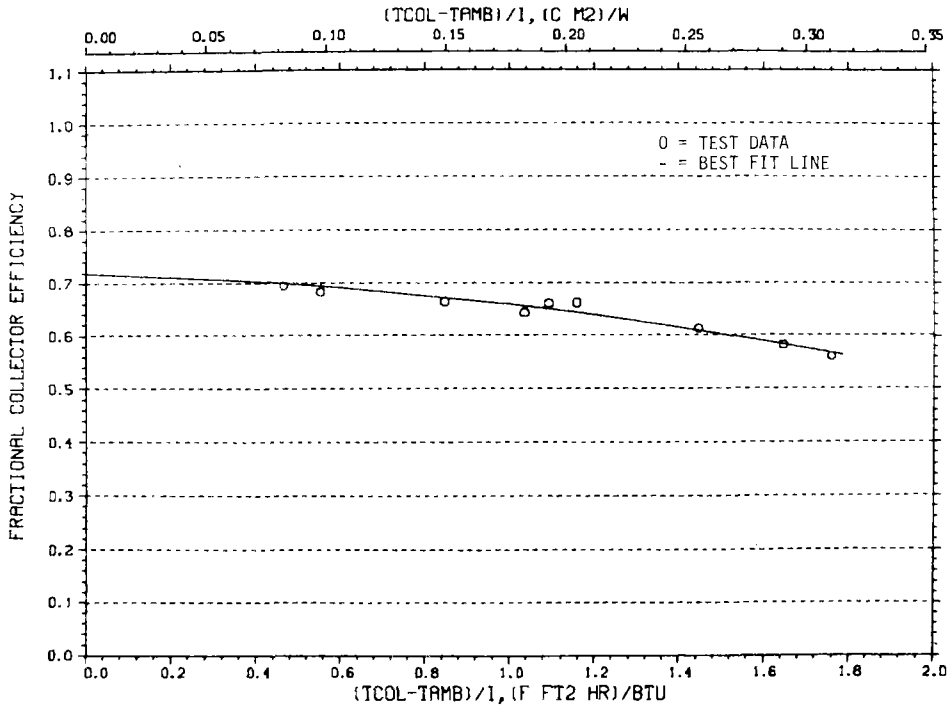

Figure 3. Performance Plot for a Clean Parabolic Trough Collector

Since the Direct Insolation used in the function $(T_{col} - T_{amb})/I$ is the Direct Insolation passing through the collector aperture, data for graphs such as Figure 3 are obtained with the plane of the collector aperture oriented normal to the position vector pointing toward the sun.*

*Recently, collector performance data have been obtained when the collector aperture is not normal to the position vector pointing toward the sun. This is done by mounting the collector on a turntable and allows evaluation of effects due to the Direct Insolation striking the collector off normal.[3]

While these data are of value in evaluating the peak efficiency of one collector versus another, they do not directly indicate the amount of energy a collector will deliver over an extended period of time (e.g., a year). In order to do this, data of the type presented in Figure 3 must be combined with knowledge of the collector tracking and resulting Solar Incidence Angles as well as knowledge of the time-varying Direct Insolation available for collection.

2.2 TRACKING OF PARABOLIC TROUGH COLLECTORS

A single-axis tracking parabolic trough rotates about only one axis in its attempt to follow the sun's apparent path. The minimum Solar Incidence Angle occurs when the collector rotates about its axis so that the plane defined by the sun and the collector's receiver tube is normal to the plane of the collector aperture. As a result, a parabolic trough tracks the so-called "profile angle" of the sun in the plane normal to the axis of rotation. A profile angle is defined as the projection of the position vector pointing from a point on the receiver tube to the sun onto some vertical plane.

Figure 4 graphically depicts the E/W and N/S profile angles by showing the shadows resultant from the sun's rays striking a geometrical object. The object is a rectangular box with its front (south side) and left (west side) removed. The back of the box lies in the E/W vertical plane while the right side of the box lies in the N/S vertical plane. The shadows cast (i.e., projected) onto the back and the side of the box represent the E/W and N/S profile angles, (GHI and DEF, respectively).

By convention, the Tracking Angle of a collector is usually defined as 0° when the collector aperture is horizontal up-facing. Thus, in keeping with this convention, the collector Tracking Angles are the complementary angles to the respective profile angles, as indicated in Figure 4. In addition, a negative tracking angle for a N/S trough indicates that the collector is facing west while a negative tracking angle for an E/W trough indicates a south-facing trough.

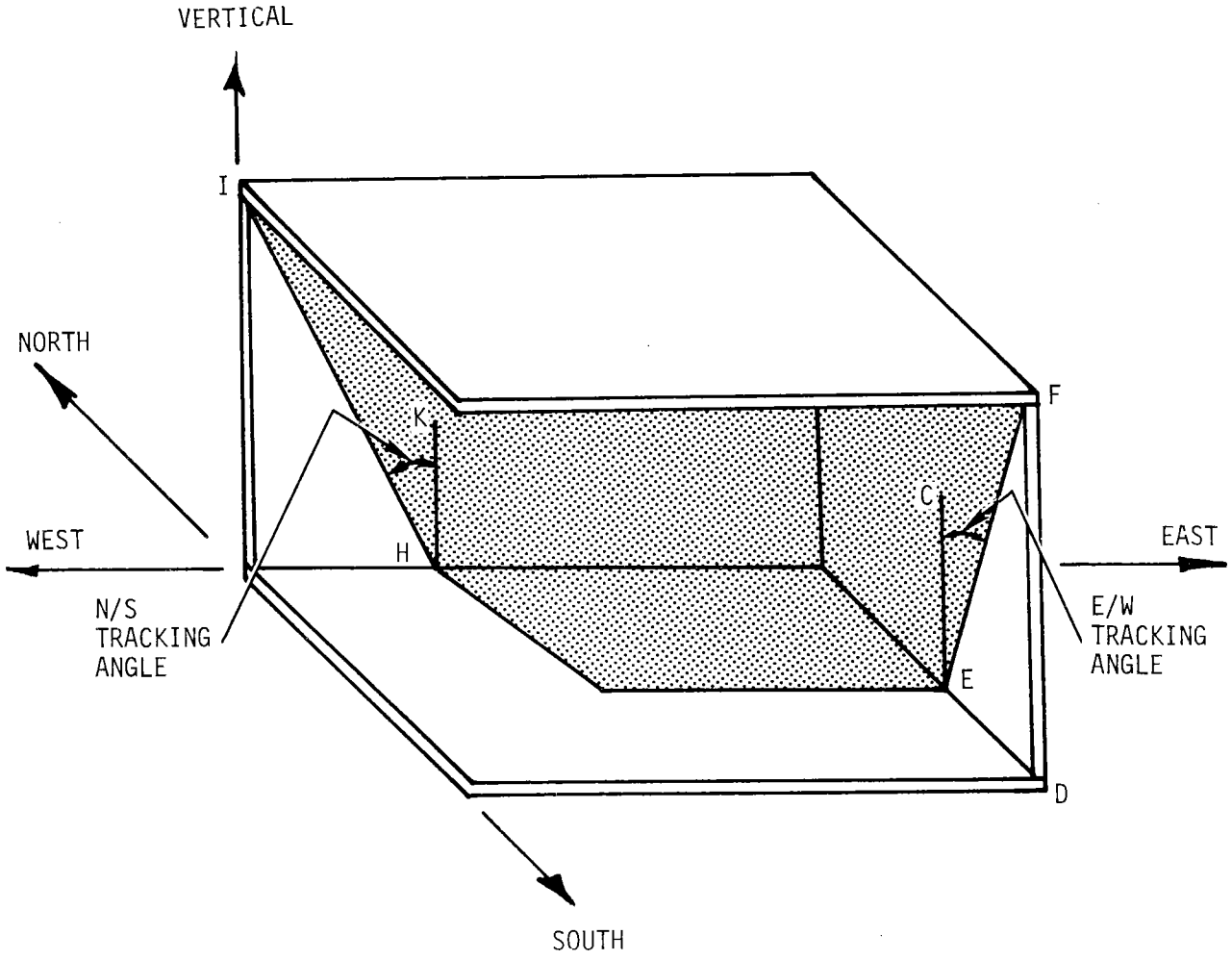

Figure 4. Definition of Sun Profile Angles

Tracking angles can similarly be defined for parabolic troughs having orientations other than E/W and N/S. A general analytical tracking equation will be developed below, followed by an evaluation of the effect of single-axis tracking on collector performance.

2.2.1 The Tracking Equation

To illustrate the development of the tracking equation for a parabolic trough collector, it is easiest to derive the equation for the specific case of a N/S collector and then generalize the equation to any orientation.

As shown in Figure 5, the position vector of the sun, defined in terms of solar azimuth (AZ) and elevation angles (EL)*, can also be described in terms of position vectors s_j, e_j, and v_j. The N/S tracking angle is then, as shown in Figure 5, defined by the position vectors e_j and v_j leading to the expression

$$\text{N/S Tracking Angle} = \tan^{-1}\left[\frac{\cos(EL)\cdot\sin(AZ)}{\sin(EL)}\right]$$

where the tracking angle is 90° when the elevation angle (EL) is equal to 0°.

This equation can be generalized to any collector orientation by defining a Collector Azimuth (CAZ) angle. The Collector Azimuth has the same sign convention as the solar azimuth angle where a clockwise rotation away from the N/S line is a negative angle while a counter clockwise rotation is a positive angle. This sign convention is illustrated in Figure 6. The generalized tracking equation then follows from subtracting CAZ from the solar azimuth, as shown in Figure 5.

The cosine of the incidence angle that the sun's rays make with the normal to the collector aperture is obtained by taking the dot product of the collector aperture normal and the sun's position vector. The result of this is

$$CINC = \cos(EL)\cdot\sin(TA)\cdot\sin(AZ - CAZ) + \sin(EL)\cdot\cos(TA)$$

where CINC = cosine of the Solar Incidence Angle and all other variables are defined as above. The Solar Incidence Angle (SI) is then

$$SI = \cos^{-1}(CINC)$$

---

*The definitions of solar azimuth and elevation angles are found in Appendix C.

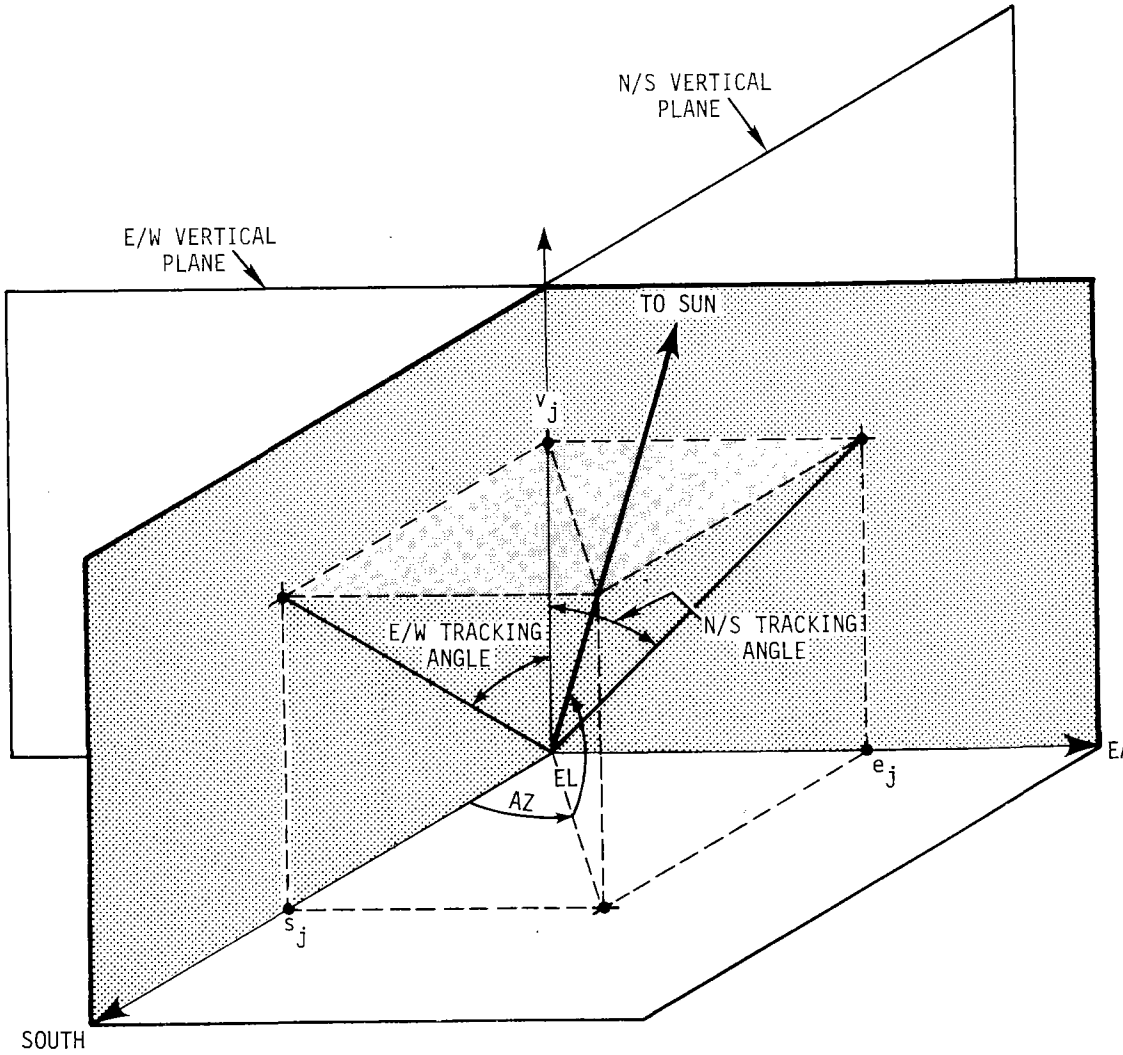

PROJECTION OF SUN VECTOR ON AXES

$s_j = \cos(EL)*\cos(AZ)$

$e_j = \cos(EL)*\sin(AZ)$

$v_j = \sin(EL)$

N/S TRACKING ANGLE (N/S TA)

$$N/S\ TA = \tan^{-1}\left(\frac{e_j}{v_j}\right) = \tan^{-1}\left[\frac{\cos(EL)*\sin(AZ)}{\sin(EL)}\right]$$

WHERE N/S TA = 90° FOR EL = 0°, |AZ| < 90°
TA = 90° FOR EL = 0°, |AZ| > 90°

GENERAL TRACKING ANGLE (TA)

$$TA = \tan^{-1}\left[\frac{\cos(EL)*\sin(AZ-CAZ)}{\sin(EL)}\right]$$

WHERE TA = 90° FOR EL = 0°, |AZ| < 90°
TA = -90° FOR EL = 0°, |AZ| > 90°

CAZ = COLLECTOR AZIMUTH ANGLE (SEE FIGURE 6)

Figure 5. Analytical Expressions for Parabolic Trough Tracking and Incidence Angles

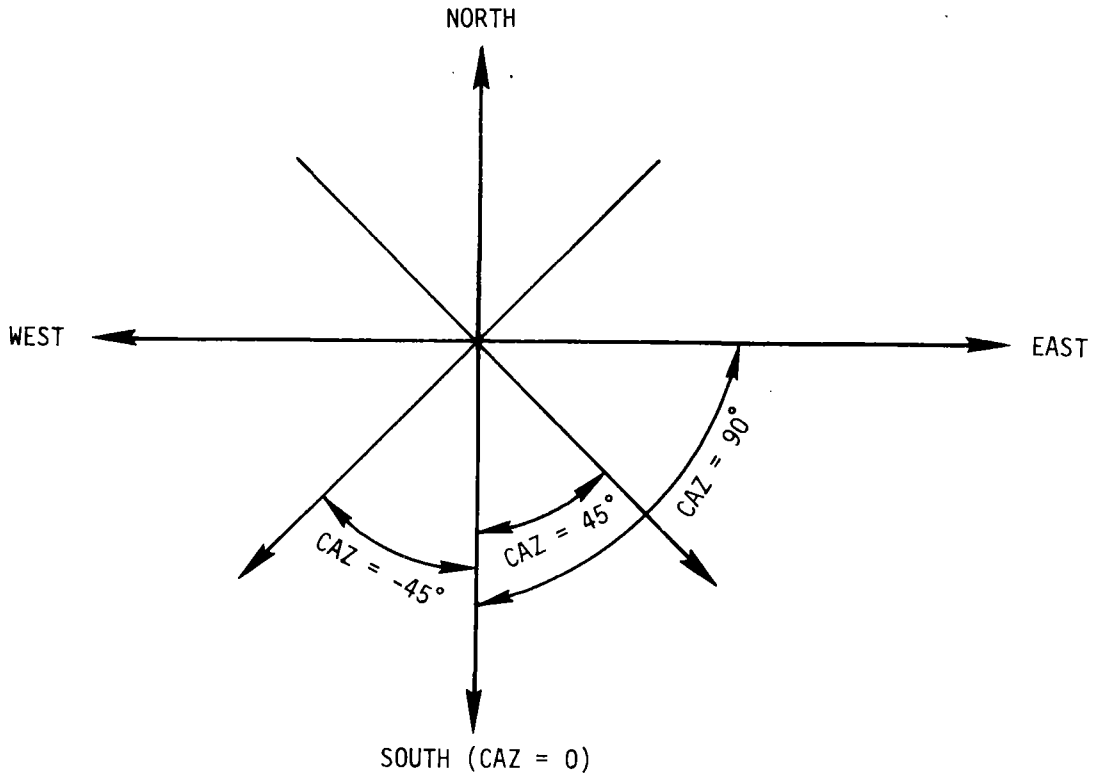

Figure 6. Definition of Sign Convention for Collector Azimuth Angle (CAZ)

2.2.2 Solar Energy Incident on Tracking Collectors

The relative value of tracking collectors in increasing the amount of Direct Insolation available to the collector aperture is shown in Figure 7 for Albuquerque, which experiences reasonably clear weather year-round. Figure 7 was prepared using the Typical Meteorological Year data tape for Albuquerque. These data tapes are discussed in Section 2.3. Curve 1, which represents the Direct Normal Insolation available to a two-axis tracking collector, is the maximum available to any concentrator. Curves 2 and 3 show the penalties associated with restricting tracking to a single axis oriented along either a N/S or an E/W horizontal line, respectively. Had no tracking been employed and the collectors oriented horizontal face up, a severe penalty in solar availability would have resulted (see Curve 4).

As illustrated in Figure 7, the N/S collector has significantly more Direct Insolation striking its aperture in summer than does the

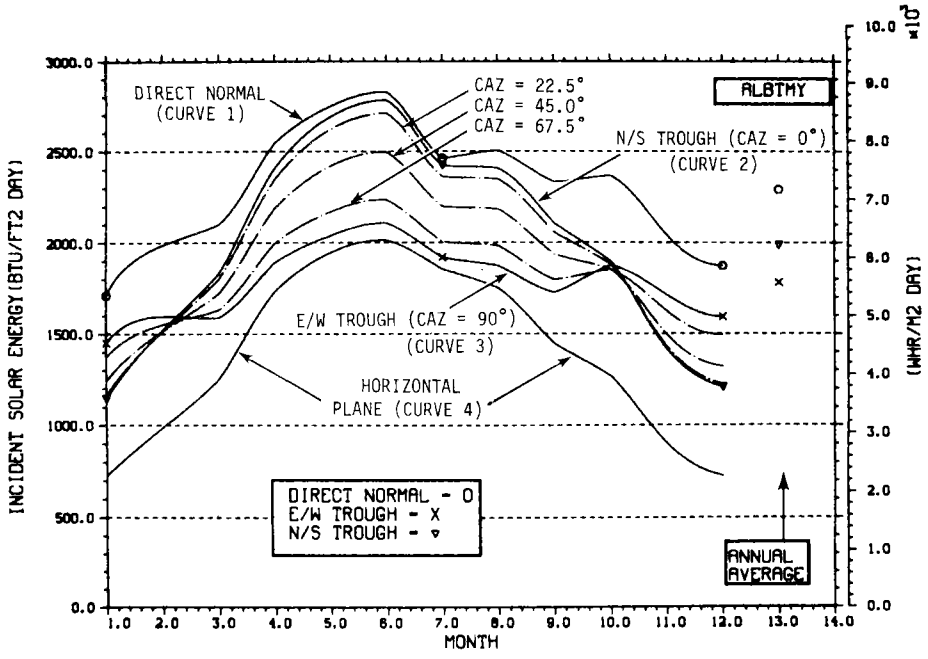

Figure 7. Effect of Tracking on Interception of Direct Insolation. (Month 13 gives annual average for direct normal, E/W Trough, and N/S Trough.)

E/W collector. This can be qualitatively understood by observing the apparent motion of the sun as depicted in Figure 8. In Albuquerque, the sun, on the summer solstice, rises slightly north of the E/W line, moves 11.5° south of the Zenith by noon, and then sets slightly north of the E/W line. Thus, a N/S collector tracking about a N/S line can rotate and look almost directly at the sun for all hours of the day (i.e., the N/S Solar Incidence Angle is relatively small at all times during the day). On the other hand, the E/W collector, which is following the N/S profile angle of the sun, remains virtually unmoving during the day, suffering large Solar Incidence Angle losses in the morning and afternoon.

The effect of tracking on the hourly interception of Direct Insolation by N/S and E/W parabolic trough collectors on clear days near the solstices is shown in Figure 9. In summer, the energy incident upon the aperture of a N/S collector closely follows the available Direct Normal Insolation, reflecting the fact that the Albuquerque

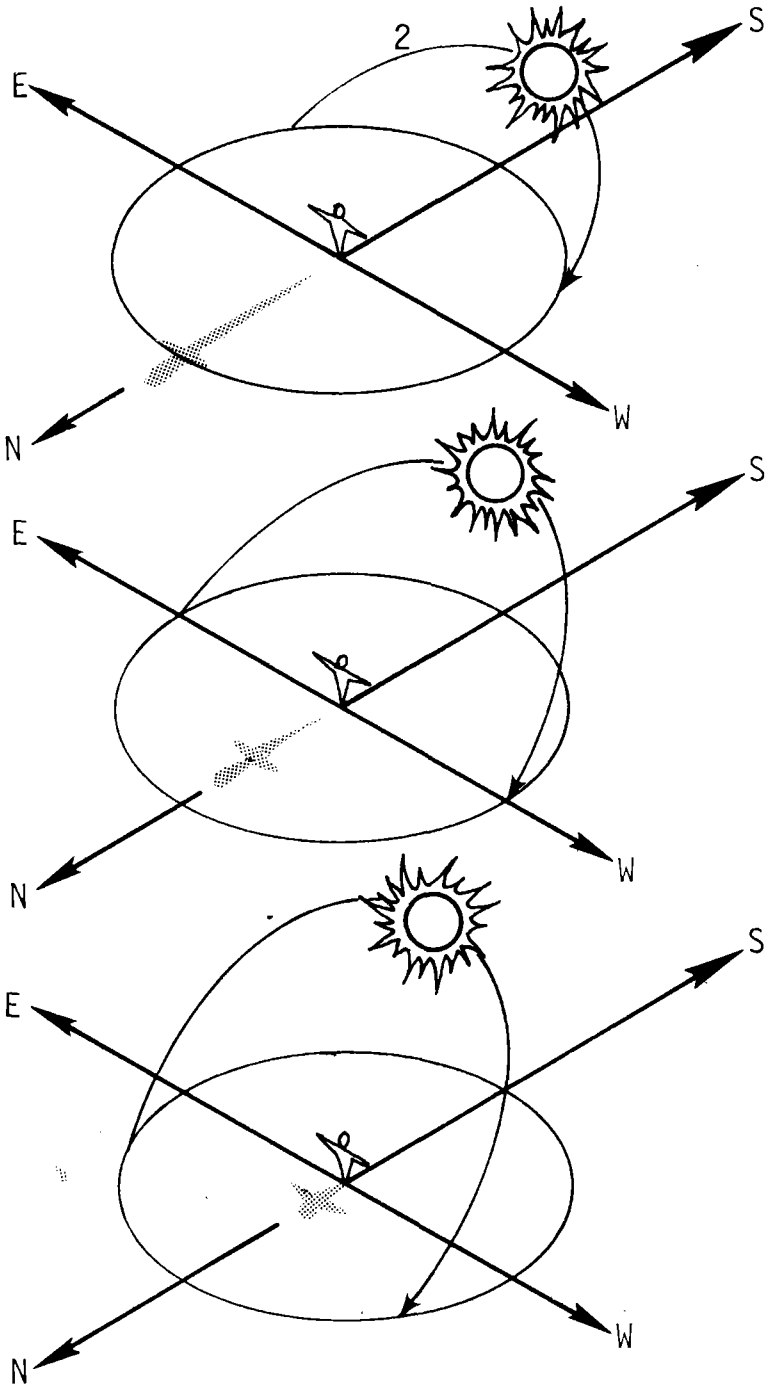

WINTER SOLSTICE

SPRING & FALL EQUINOXES

SUMMER SOLSTICE

Figure 8. The Movement of the Sun from Season to Season*

*Reproduced from Edward Mazria and David Winitzky, Solar Guide and Calculator, (Eugene, OR: The Center for Environmental Research, University of Oregon, 1976) by permission.

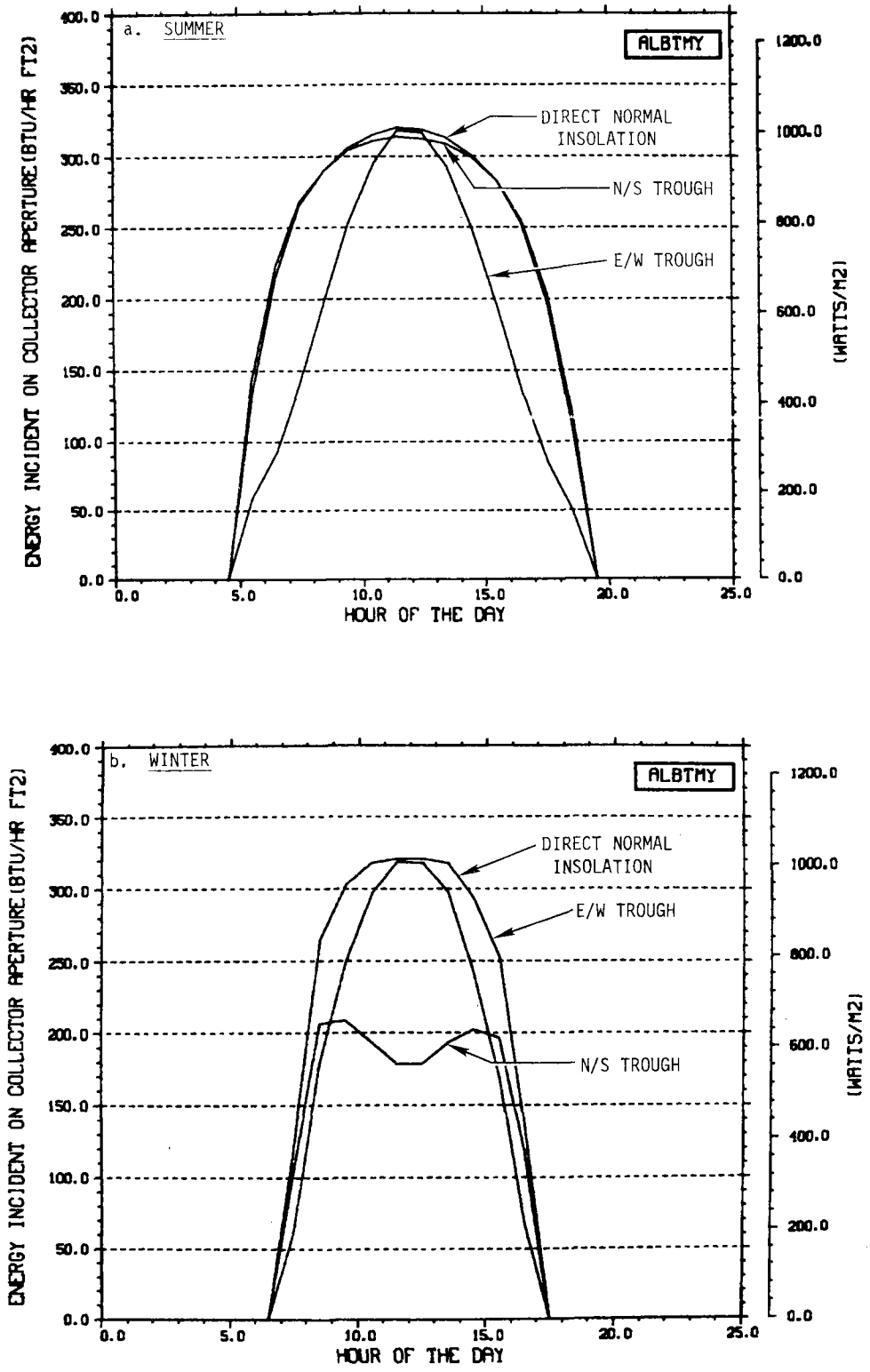

Figure 9. Hourly Incident Energy on E/W and N/S Troughs

summer sun basically follows an east-to-west path directly overhead. This summer solar path strongly penalizes the E/W collector in the morning and afternoon, as illustrated in Figure 9a. It is interesting to note that at noon the E/W collector aperture actually intercepts slightly more energy than the N/S collector aperture since the E/W collector can rotate along the E/W line to directly face the sun at noon.

During the winter (see Figure 9b), the situation essentially reverses itself, with the E/W aperture intercepting more energy than the N/S aperture. Since the sun remains rather low in the southern sky in winter, the N/S collector, with no degrees of freedom about the E/W line, suffers large cosine losses compared with the E/W collector, which can rotate down to look at the low sun angles. It is interesting to note that the most favorable incidence angle of the sun with a N/S collector located in Albuquerque in winter occurs 2 to 3 hours either side of noon, producing the characteristic double-humped N/S collector curve of Figure 9b.

These seasonal tracking differences are responsible for the characteristically flat curve of an E/W parabolic trough collector throughout the year and the sharply summer peaking curve of a N/S parabolic trough collector, as depicted in Figure 7. Basically, an E/W collector performs best during winter, when solar availability is low, but poorly during summer, when solar availability is high. A N/S collector's seasonal response is just the reverse.

As might be anticipated, the Direct Insolation incident upon the aperture of a parabolic trough oriented somewhere between the N/S and E/W limits is intermediate between that incident on the E/W and N/S troughs. This is illustrated in Figure 7 for troughs rotated 22.5°, 45°, and 67.5° counterclockwise from a true N/S orientation (i.e., CAZ = 22.5°, 45°, and 67.5°). The curves for a trough with CAZ equal to -22.5°, -45° and -67.5° are the same as those shown in Figure 7 indicating that, on the average, the Direct Normal Insolation in Albuquerque is symmetric about solar noon.

The variation with CAZ of the annual average Direct Insolation incident upon the aperture of a single-axis tracking parabolic trough is shown in Figure 10. Also included in Figure 10 is the variation in thermal output, at 600°F (316°C), of the Nominal Collector defined below in Section 2.4. These curves are symmetric about CAZ = 0, indicating that on the average over a year in Albuquerque, the Direct Insolation available before solar noon is equal to the Direct Insolation after solar noon (i.e., over the year, clouds do not significantly affect Direct Insolation more in the morning versus the afternoon or vice versa). This is not true for all SOLMET sites. Figure 10 is reproduced in Appendix H for all SOLMET sites and some (e.g., Omaha) show asymmetry. The asymmetry is usually small, and, typically, the performance of a parabolic trough collector at any Collector Azimuth can be approximated by a linear combination of the E/W and N/S performance, using a cosine function of the form

$$\text{Collector Performance} = \frac{1}{NS}\left[\frac{EW + NS}{2} + \left(\frac{NS - EW}{2}\right)\cos(2 \cdot CAZ)\right]$$

where

NS = annual performance of N/S parabolic trough
EW = annual performance of E/W parabolic trough
CAZ = Collector Azimuth.

For conceptual design, the performance of a parabolic trough collector at some Collector Operating Temperature below 600°F (316°C) can be obtained by interpolating between the 600°F (316°C) curve and the Direct Insolation curve. The temperature dependence of collector performance is discussed further in Section 2.5.2. The purpose of Figure 10 is to give the designer an understanding of what happens to collector performance if he does not choose to orient the collectors along strict E/W or N/S lines.

As a general rule, the performance change in going from a N/S orientation to an E/W orientation will be somewhat greater for a

collector operating at 600°F (316°C) than for the incident Direct Insolation since collector efficiency is, as discussed in Section 2.1, a function of Direct Insolation. In locations where the amount of Direct Normal Insolation is low (e.g., Boston), however, this trend may be reversed since some of the available Direct Insolation may not be sufficient to operate the collector at 600°F (316°C). Thus, any change in the availability of the Direct Insolation upon reorienting the collector would not result in a change in the trough's performance at 600°F (316°C). For this reason, Figure 10, which is the result of hourly computer simulations, was computed and reproduced in Appendix H for each SOLMET site.

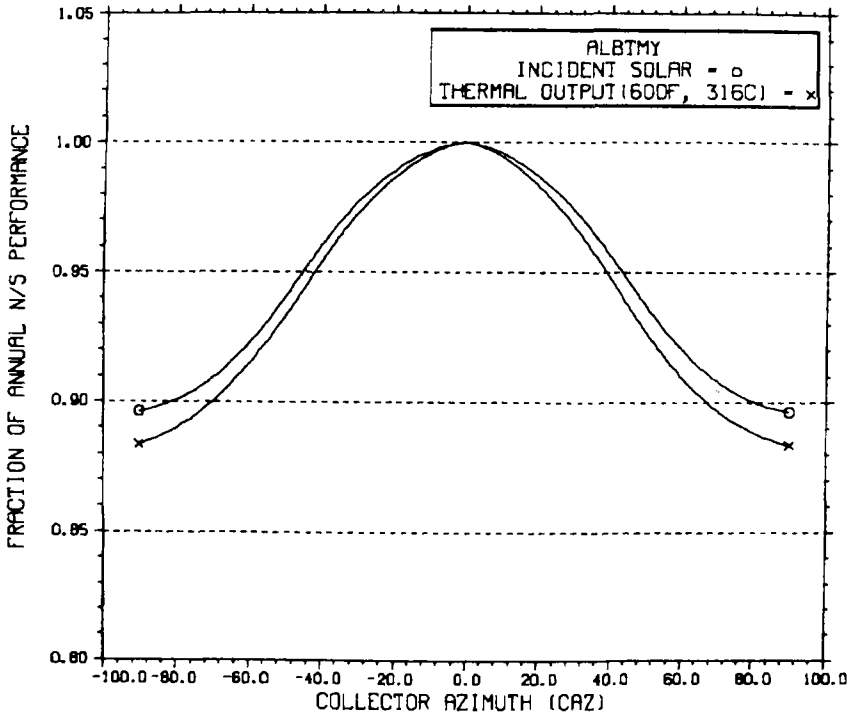

Figure 10. Variation in Parabolic Trough Performance with Collector Azimuth

2.3 INSOLATION DATA

In order to accurately predict expected typical performance of a solar collector over a given period of time, accurate information on Insolation must be available. A widely accepted source of accurate Insolation and climatological data is the Typical Meterological Year

(TMY)[1] data tapes. The tapes are available for each of 26 SOLMET sites. Each tape contains measured hourly Insolation and weather data synthesized into a composite year statistically typical of 20 years' worth of climatological data at each site. These TMY data tapes were used in computing the curves shown in Figures 7, 9, and 10 and the Nominal Collector performance to be discussed below.

A map of the continental United States is shown in Figure 11, indicating the location of the 26 SOLMET sites. Superimposed on this map are contours showing the annual average Direct Normal Insolation. This map was drawn using the techniques described by E. C. Boes et al.[4] Contour maps, such as Figure 11, are useful in determining which TMY data to use if the site of interest is not located at a specific SOLMET site. Typically, a SOLMET site which is geographically near and has an annual average Direct Normal Insolation similar to the site of interest, as determined from Figure 11, is chosen as the data source. This procedure should be used with great care since local weather variations not reflected in the gross contours of Figure 11 can greatly influence solar availability. If, however, site-specific solar data are lacking, this procedure can be used for conceptual design, but it must be emphasized that designing a solar energy system without site-specific data must be considered high risk.

2.4 DEFINITION OF A NOMINAL COLLECTOR

Performance data for parabolic trough collectors are typically reported in the form shown in Figure 3. Since projected annual collector performance profiles are needed to execute designs of solar thermal systems, nomographs for use in this handbook have been developed to project annual collector performance data. To allow the use of nomographs, the performance of a clean nominal parabolic trough collector (i.e., Nominal Collector) has been defined and will be used as the basis for the projection of the annual performance of actual collectors for which $(T_{col} - T_{amb})/I$ versus efficiency test data exist.

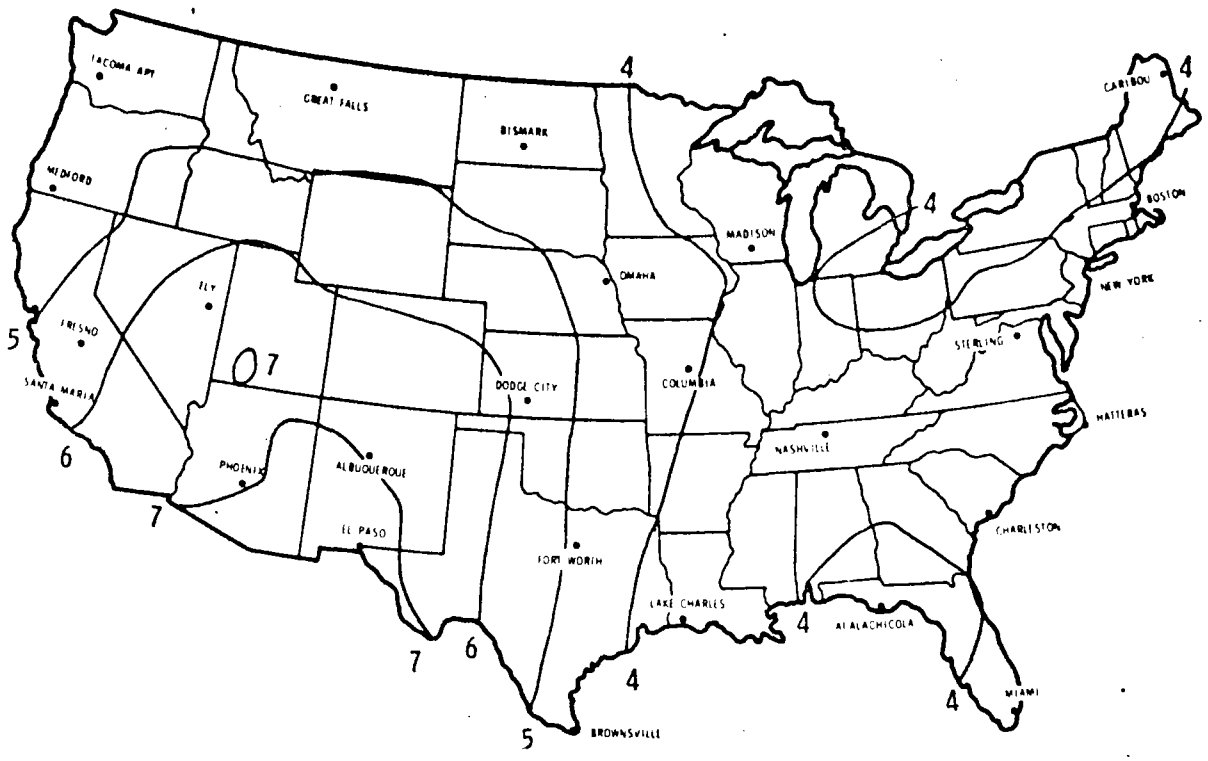

Figure 11. TMY Sites and Map of Mean Daily Direct Normal Insolation--Annual Average ($kW \cdot h/m^2 \cdot day$)

The basic technique involves computing the annual performance profile for the Nominal Collector, starting with $(T_{col} - T_{amb})/I$ versus efficiency data. The nomographs developed in the next section allow adjustment to the annual performance profile computed for the Nominal Collector. This is done by compensating for the differences between the $(T_{col} - T_{amb})/I$ versus efficiency data for the actual collector and the Nominal Collector. This section describes how the annual performance profiles for the Nominal Collector were determined and why there is confidence that the computational techniques are accurate.

The $(T_{col} - T_{amb})/I$ versus efficiency curve defined for the Nominal Collector used in this handbook is shown in Figure 12. It is a straight line which intercepts the efficiency axis at 0.8 and has a slope of -0.088 $Btu/h \cdot ft^2 \cdot °F$ (-0.5 $W/m^2 \cdot °C$). Using the efficiency function in Figure 12, the annual performance for the Nominal Collector in both E/W and N/S orientations can be computed. Figure 13 shows

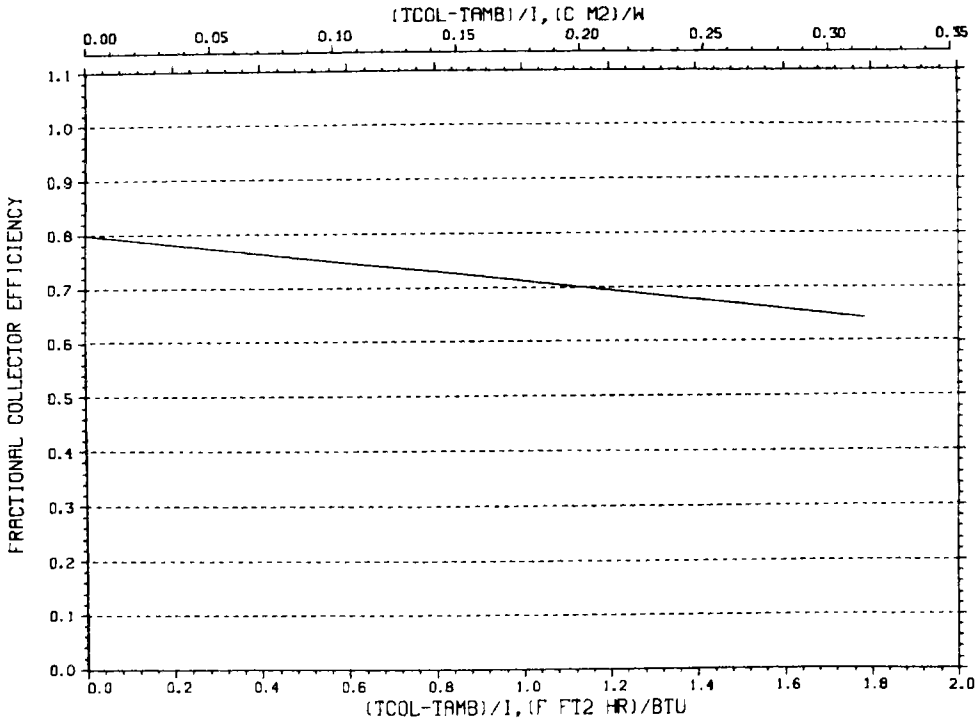

Figure 12. Performance of Nominal Collector

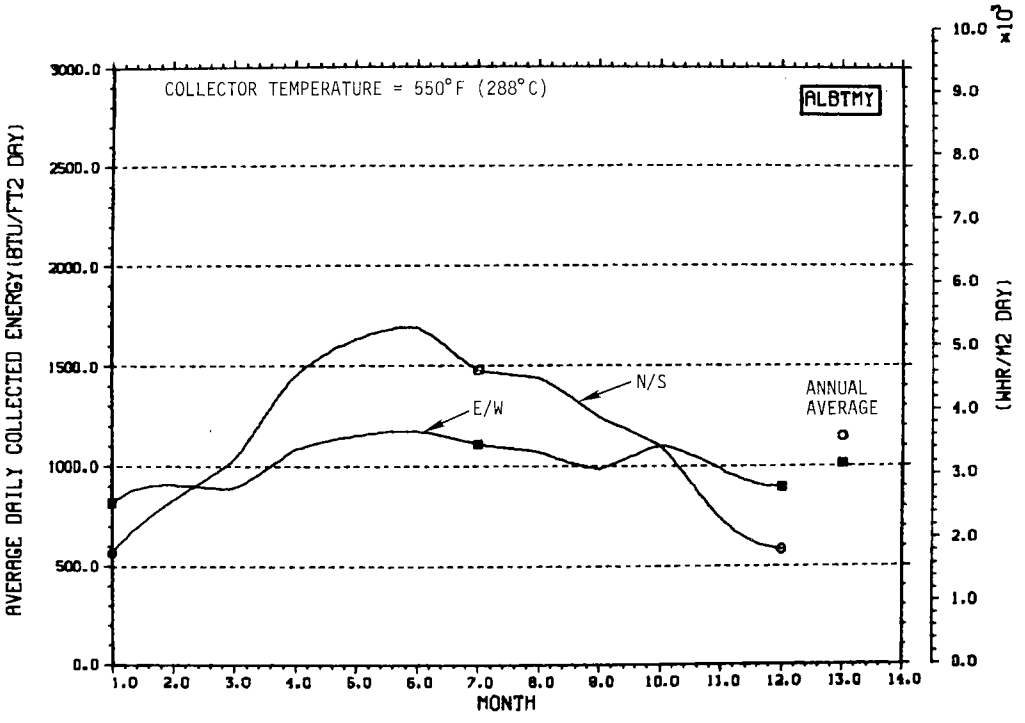

Figure 13. Monthly Performance of Nominal Collector. (Month 13 is annual average.)

the projected monthly performance profiles and annual average performance for the above-defined Nominal Collector if it were located in Albuquerque, New Mexico. Generation of collector performance curves such as those in Figure 13 is done on an hourly basis using TMY data tapes. The cosine of the Solar Incidence Angle (as defined in Section 2.2) is computed and multiplied by the Direct Insolation read hourly from the TMY solar data tape. The resultant is the Direct Insolation passing through the aperture of the trough. Knowledge of the ambient temperature (obtained from the TMY tape) and collector operating temperature allows evaluation of the function $(T_{col} - T_{amb})/I$ and, as a result, the corresponding collector efficiency. This collector efficiency, when multiplied by the Direct Insolation entering the collector aperture, defines the quantity of thermal energy leaving the collector in the fluid at the given receiver temperature. Averaged over the month, the collected solar energy computed in this manner yields the points from which collector performance plots such as Figure 13 are made. A Collector Operating Temperature of 550°F (288°C) was arbitrarily chosen for Figure 13. The effect of Collector Operating Temperature is addressed in Section 2.5.2.

It should be noted that at this point, no consideration has been given to angle-of-incidence factors, such as the variation in Reflectance and Absorptance with incidence angle and end-losses where, due to the angle of incidence, the reflected beam misses the receiver tube. These factors, along with others which tend to degrade collector performance, are typically small and would be considered in preliminary design.

The computer code used to compute the annual average performance profiles for parabolic trough collectors is described in greater detail in Appendix D. The predictions of the code were compared with actual all-day performance data measured at Sandia National Laboratories and found to provide good agreement with measured test results. The nomographs described below were developed to obviate the need for designers to develop and run similar computer codes to predict the average annual performance profiles of a collector of interest.

2.5 ANNUAL PERFORMANCE OF PARABOLIC TROUGH COLLECTORS

In conceptual design, initial collector field sizing employs only the performance of an isolated collector with no parasitic losses considered.* The purpose of this field sizing is to allow estimation of the collector and land areas required to displace a given load and provide a starting point from which more detailed field design (incorporating such considerations as pump power and field piping heat losses) can proceed. This section deals with determining the annual collector thermal energy output, the knowledge of which is needed to execute a conceptual design.

If a collector being considered for a given application has the same performance characteristics as the Nominal Collector defined above, conceptual design can proceed. However, when the collector under consideration for use in a given solar energy system has performance characteristics different from the Nominal Collector or when the Collector Operating Temperature is different from that assumed in generating the performance profiles of Figure 13, a projection of annual performance must be made for the new collector. The objective here is to provide simple nomographs which allow adjustments to the Nominal Collector performance profiles reported in Figure 13 to permit collector field sizing without resorting to computer simulation.

2.5.1 Variations in Collector Performance

It is unlikely that the performance of a parabolic trough collector under consideration will be identical to that assumed for the Nominal Collector in this handbook. Figure 14 shows the conversion of the Nominal Collector thermal performance over a given period of time,

---

*It should be pointed out that system parasitics are not negligible. In fact, in fields of parabolic trough collectors, shading (see Section 2.6), field piping heat losses, dirt on the collectors, and other system parasitics typically amount to 20 to 25% of the solar energy that would be collected by an isolated clean collector. These losses will be accounted for in Section 4.2, "Conceptual Design Rules of Thumb." At this stage, however, only an isolated, clean (as tested) collector will be considered.

in a given location, to the thermal performance of a different parabolic trough collector over the same period of time in the same location.

As an example, consider the problem of determining the average annual thermal energy output from an E/W parabolic trough collector (denoted here and throughout the rest of the handbook as Collector 2) having the efficiency versus $(T_{col} - T_{amb})/I$ curve shown in Figure 14. Figure 13 indicates that the annual average thermal energy output of the E/W Nominal Collector located in Albuquerque and operating at an average receiver temperature of 550°F (288°C) is about 1010 Btu/ft^2·day (3.2 kWh/m^2·day). The annual average Direct Insolation incident on a tracking E/W aperture in Albuquerque is given in Figure 7 as 1740 Btu/ft^2·day (5.5 kWh/m^2·day) resulting in annual Average Direct Insolation Aperture Efficiency of 0.59 for the Nominal Collector.

Figure 14 indicates that the annual average value of $(T_{col} - T_{amb})/I$, which corresponds to the Nominal Collector annual Average Direct Insolation Aperture Efficiency of 0.59, is 2.35°F·ft^2·h/Btu (0.41°C·m^2/W). This is, however, the same $(T_{col} - T_{amb})/I$ observed by any E/W parabolic trough collector operating with an average receiver temperature of 550°F (288°C) in Albuquerque. Thus, the annual Average Direct Insolation Aperture Efficiency for Collector 2 is about 0.35. This efficiency value multiplied by the solar energy incident on the collector aperture yields the annual average collector thermal output for Collector 2. In this case: (1740)(0.35) = 609 Btu/ft^2·day (1.93 kWh/m^2·day). This value is very close to the annual average thermal output for Collector 2 computed by hourly simulation. Hourly simulation results in a predicted annual average thermal output from Collector 2 of about 620 Btu/ft^2·day (1.97 kWh/m^2·day). Similarly, the output from Collector 2 oriented N/S is calculated as 660 Btu/ft^2·day (2.09 kWh/m^2·day) from Figure 14 while hourly simulation predicts about 700 Btu/ft^2·day (222 kWh/m^2·day).

Collector 2 was purposely chosen to illustrate that even if the performance curve is not linear, the procedure presented in Figure 14

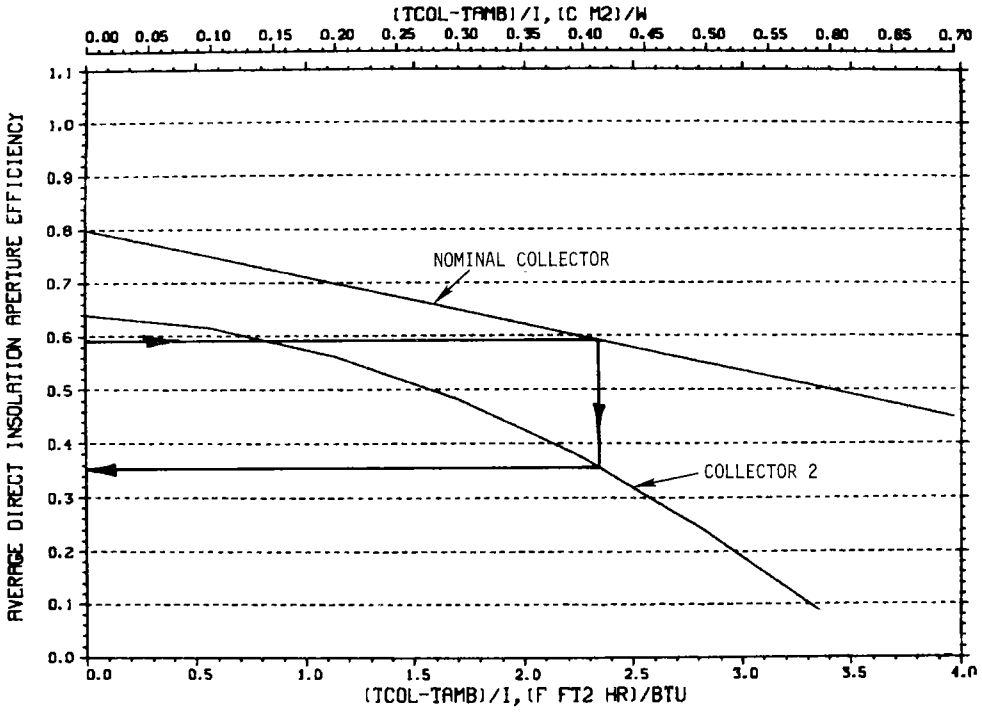

Figure 14. Prediction of Long-Term Collector Performance

yields a reasonable estimate of annual collector performance. Many collectors have performance curves which have much less curvature than that for Collector 2.[2] The predicted annual performance of collectors, as obtained from the use of Figure 14, typically agrees to within 5 to 6% of the annual performance computed using hourly simulations. Predictions of monthly collector performance using this technique were also found to typically agree to within 5 to 6% of the monthly performance computed using hourly simulations. Agreement between the graphical technique discussed here and computer simulation has not been seen to change significantly if performance curves different from those of Collector 2 were used. However, performance curves with more curvature than Collector 2's were not evaluated.

2.5.2 Variations in Collector Operating Temperature

The above techniques can be used to obtain the thermal energy output from any single-axis tracking parabolic trough collector if the effect of temperature on the thermal energy output of the Nominal Collector is known. Figure 15 reports the average monthly thermal energy

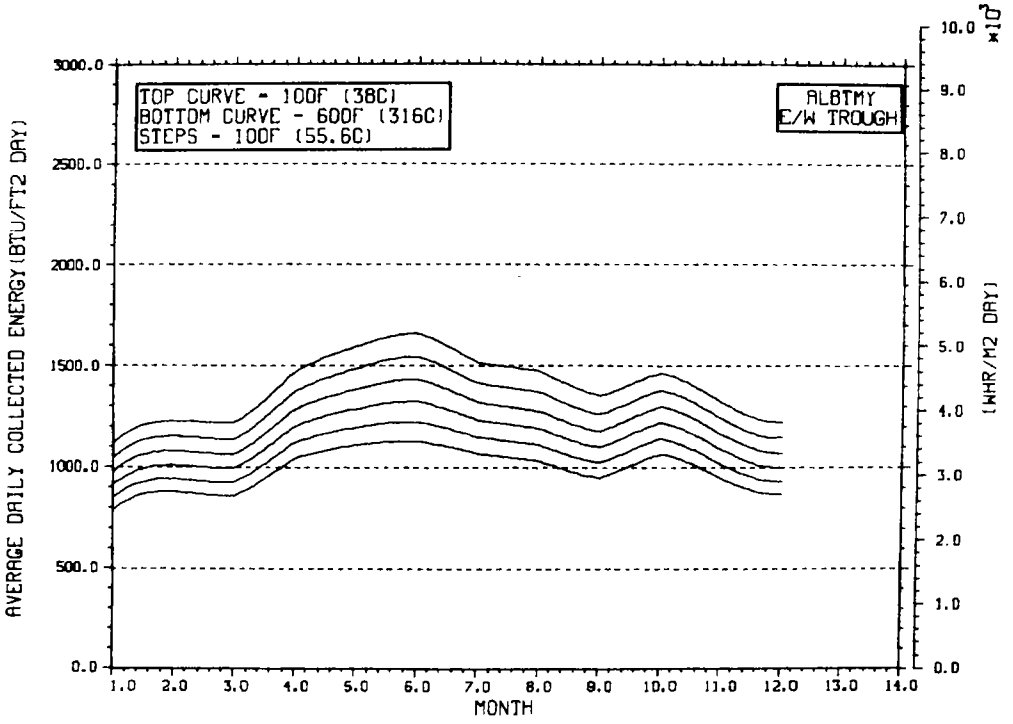

Figure 15. Temperature Dependence of E/W Nominal Collector Performance

output from an E/W Nominal Collector. The effect is a smooth increase in collector performance as the Collector Operating Temperature decreases. Figure 16 reports the temperature dependence of the annual average output from both E/W and N/S Nominal Collectors. These graphs are used to determine the Average Direct Insolation Aperture Efficiency for the Nominal Collector at the operating temperature of interest. This efficiency is then used to predict the performance of the new collector, as discussed above, at the temperature of interest.

2.6 COLLECTOR SHADING

The collector performance presented in Sections 2.4 and 2.5 was for an isolated collector operating as if uninfluenced by its surroundings. In actual systems, however, parabolic trough collectors will be deployed in fields consisting of multiple rows of collectors. Shading within the field due to the proximity of one collector row to the next will reduce collector performance from the idealized situation. Almost any parabolic trough collector field will suffer some

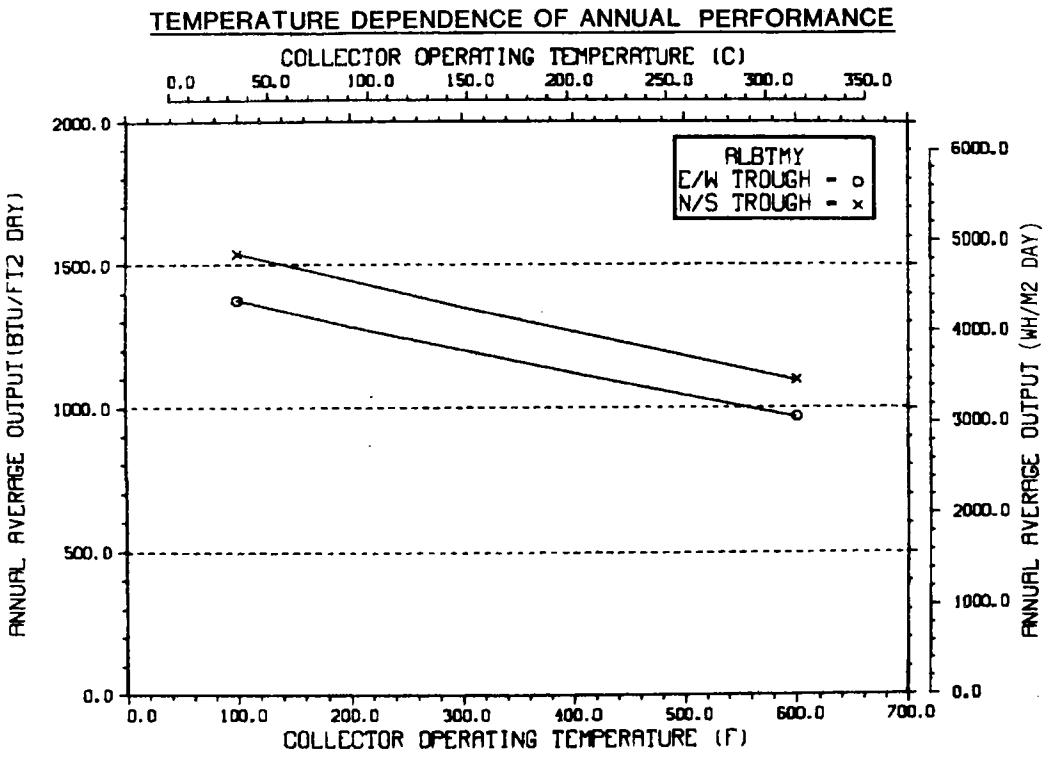

Figure 16. Variation of Nominal Collector Annual Performance with Temperature

shading loss due to the desire to minimize collector spacing in order to decrease land area requirements and the length of the thermal distribution network required by the collector field.

The fractional reduction in Direct Insolation incident upon the nonfirst row collector due to shading is shown in Figure 17 for parabolic troughs in both E/W and N/S orientations. The use of the terminology "nonfirst row" refers to the fact that in any parabolic trough collector field, one row of collectors will be unshaded since there are no collectors between it and the line to the sun. Thus, for example, in an E/W collector field, the north row is unshaded when the sun is north of the east-west line while the south row is unshaded when the sun is south of the east-west line. Likewise, the east row in a N/S collector field is unshaded before solar noon while the west row is unshaded after solar noon.

In order to use Figure 17, it is necessary to account for the unshaded row. Consider, for example, a N/S collector field containing

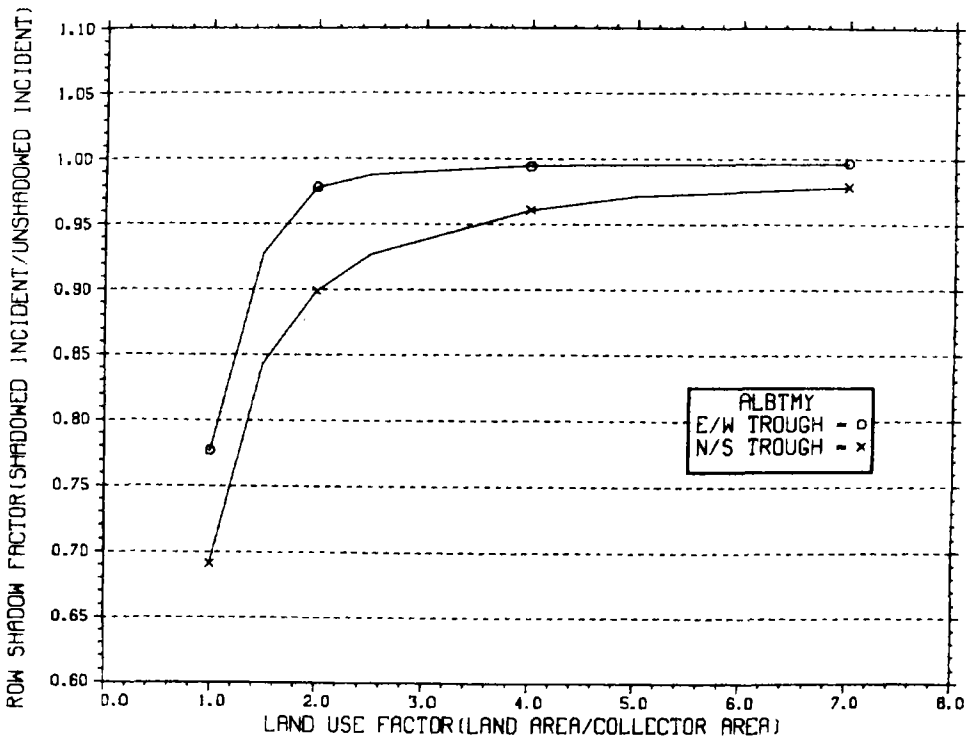

Figure 17. Nonfirst Row Shading of Annual Incident Direct Insolation

two rows with a Land Use Factor of 2.0. The Direct Insolation incident upon the nonfirst row collector is reduced to 0.895 (i.e., Row Shadow Factor = 0.895) of the unshaded solar input (see Figure 17). However, the Direct Insolation incident upon the total field is reduced to only 0.948 (i.e., Field Shadow Factor = [1.0 + 0.895]/2) that of the unshaded field. The general equation for computing the Field Shadow Factor is

$$\text{Field Shadow Factor} = \frac{1.0 + (N-1)(\text{Row Shadow Factor})}{N}$$

where N is the number of rows in the collector field. This equation is plotted in Figure 18 which converts Row Shadow Factor to Field Shadow Factor, accounting for the unshaded first row.

As an example of the use of Figure 18, consider a N/S field of 10 rows of parabolic trough collectors located in Albuquerque and

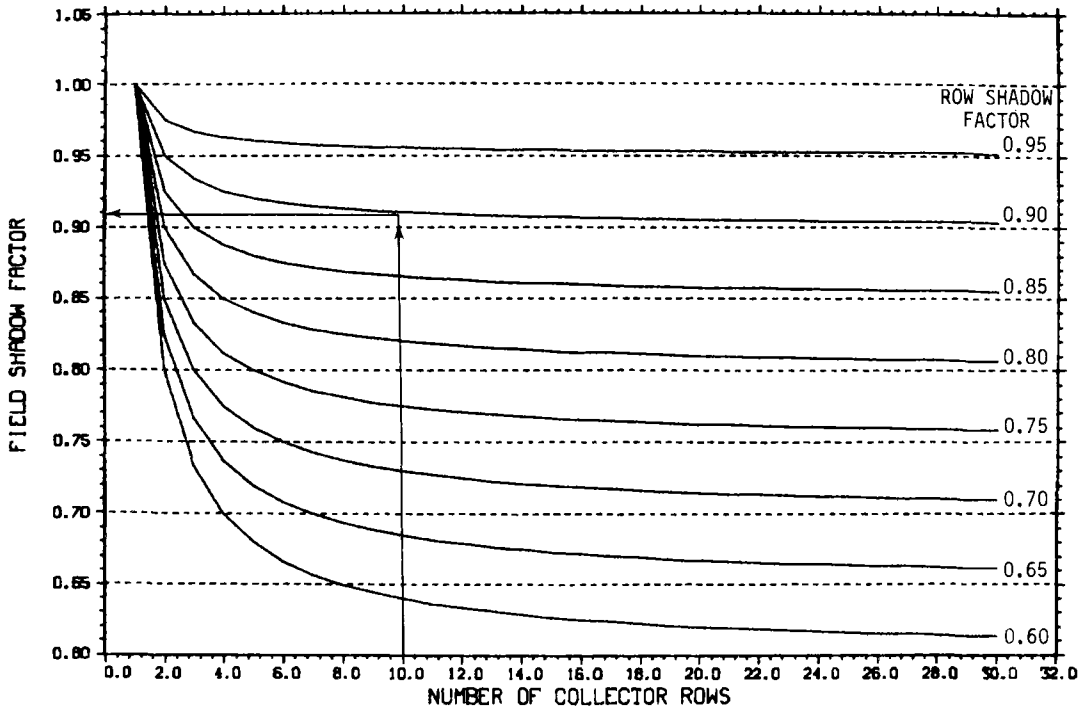

Figure 18. Effect of Number of Collector Rows on Field Shading Prediction of Average Collector Output

deployed with a Land Use Factor of 2.0. From Figure 17 the Row Shadow Factor is 0.895, resulting in a Field Shadow Correction of 0.91, as indicated in Figure 18.

It is interesting to note that for any given Land Use Factor, shading is greater for a N/S field than an equivalent E/W field. This increased shading tends to bring the annual performance of an N/S parabolic trough collector field closer to an E/W field. Appendix G examines shading on a monthly basis and discusses the reasons for increased shading in N/S parabolic trough collector fields. In order to reduce the impact of shading, E/W parabolic trough collector fields are typically deployed with a Land Use Factor of 2.0 to 3.0. N/S fields are typically deployed with a Land Use Factor of 3.0 to 4.0.

2.7 SUMMARY OF TECHNIQUE FOR PROJECTING COLLECTOR PERFORMANCE

In summary, the basic technique used in predicting the long-term performance of a given collector involves the use of Figure 14 as

outlined in Figure 19. The $(T_{col} - T_{amb})/I$ performance curve for the parabolic trough collector is plotted on Figure 14 together with the performance curve for the Nominal Collector. Knowledge of the thermal energy output from the Nominal Collector, at a given temperature, coupled with the Direct Insolation incident on the Nominal Collector aperture yields the Average Direct Insolation Aperture Efficiency of the Nominal Collector. This, in turn, defines the average $(T_{col} - T_{amb})/I$ for the Nominal Collector which is the average $(T_{col} - T_{amb})/I$ for all parabolic troughs with similar tracking. Since the average $(T_{col} - T_{amb})/I$ for the new collector is now known, the Average Direct

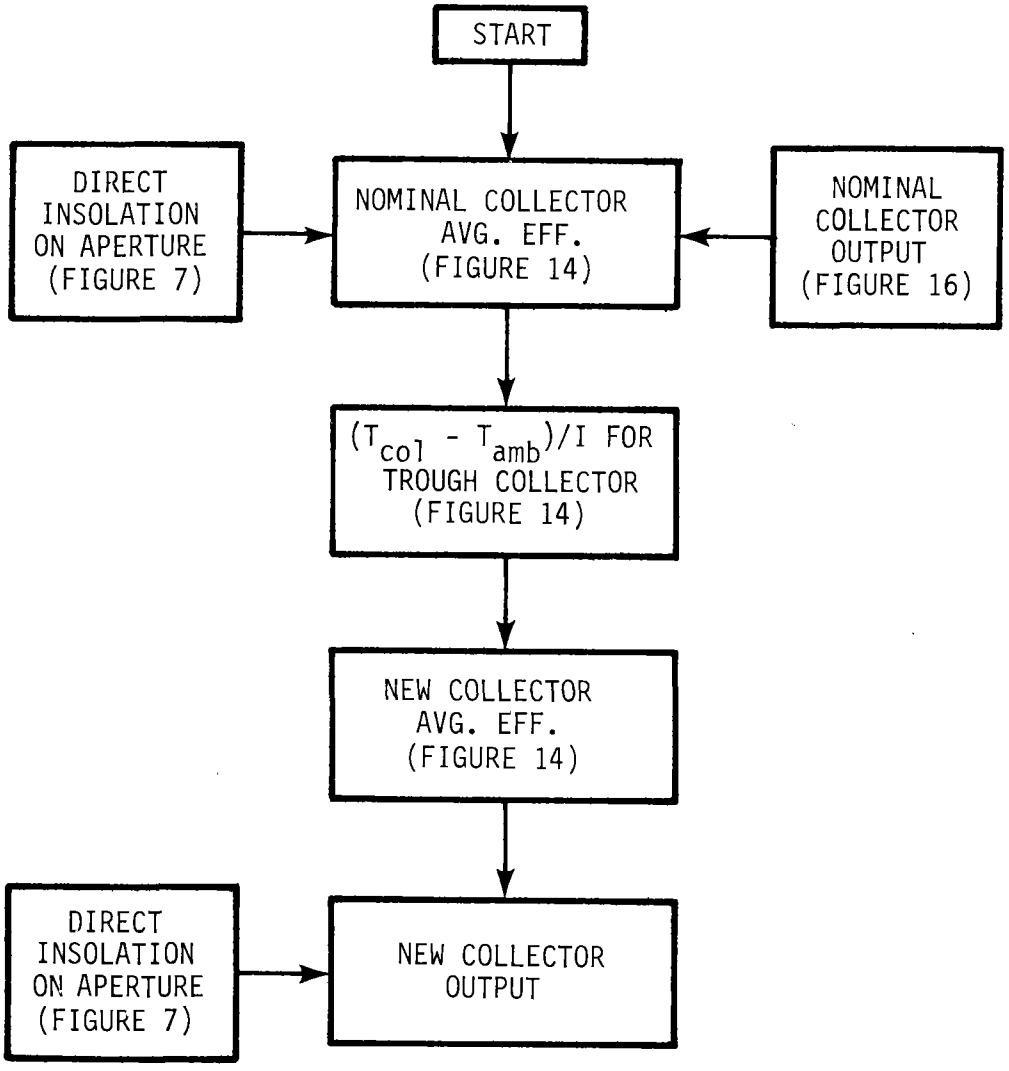

Figure 19. Prediction of Average Collector Output

Insolation Aperture Efficiency is defined by Figure 14. This efficiency, when multiplied by the Direct Insolation incident upon the collector aperture, yields the thermal energy output for the new collector. The collectors, when deployed in a field of multiple rows, would have a Land Use Factor of 2.0 to 3.0 for an E/W field and 3.0 to 4.0 for a N/S field to minimize shading losses. The tradeoff of land costs versus decreased collector field output could be performed, of course, if the value of the land and thermal energy from the collector field were known. The Land Use Factors listed above are good starting points for such tradeoff analyses and are appropriate for conceptual design.

Figure 7, showing the Direct Insolation incident upon E/W and N/S parabolic trough collectors, is given for each SOLMET site in Appendix H. In Addition, Figure 10, Figure 15 (both E/W and N/S collectors), Figure 16, and Figure 17 are given in Appendix H for each SOLMET site.

3. THE ROLE OF STORAGE

This section provides the tools, generically termed Storage Sizing Graphs, needed to determine the proper combination of collector area and thermal energy storage capacity required to meet constant thermal energy requirements (i.e., Demands). Constant Demands were selected since industrial process heat requirements are usually constant during specific periods of plant operation.

The determination of the proper collector field size to service a defined Demand is intimately tied to the amount of storage provided. As long as all of the thermal energy produced by a solar collector field can be effectively utilized to satisfy a Demand, a solar energy system which employs no thermal energy storage will be the lowest cost system. Solar energy systems which have no thermal energy storage are usually capable of meeting only a rather small fraction of the total Demand. If no storage is provided and the collector area is increased, the ability of the application to effectively use all the thermal energy produced by the collector field rapidly diminishes. This decrease in Utilization of the collected solar energy results from mismatches between the Demand profile of the application and the energy supply profile of the solar collector field. Increasing the Utilization of the collected solar energy requires storage of some of the energy until periods when the Demand by the application exceeds the collector field's ability to produce energy. Thus, a primary role of thermal energy storage is to allow increased displacement of fossil fuel energy while maintaining high Utilization of collected solar energy.

This is illustrated in Figure 20 where the role of storage in solar energy systems servicing both daylight-only and 24-hour-per-day

a) DAYLIGHT HOURS-ONLY DEMAND

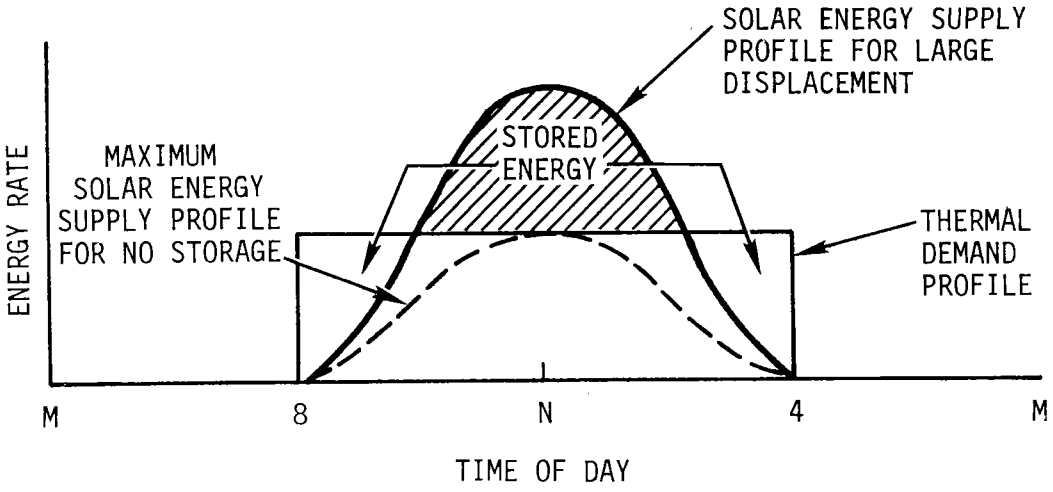

b) OVERNIGHT STORAGE

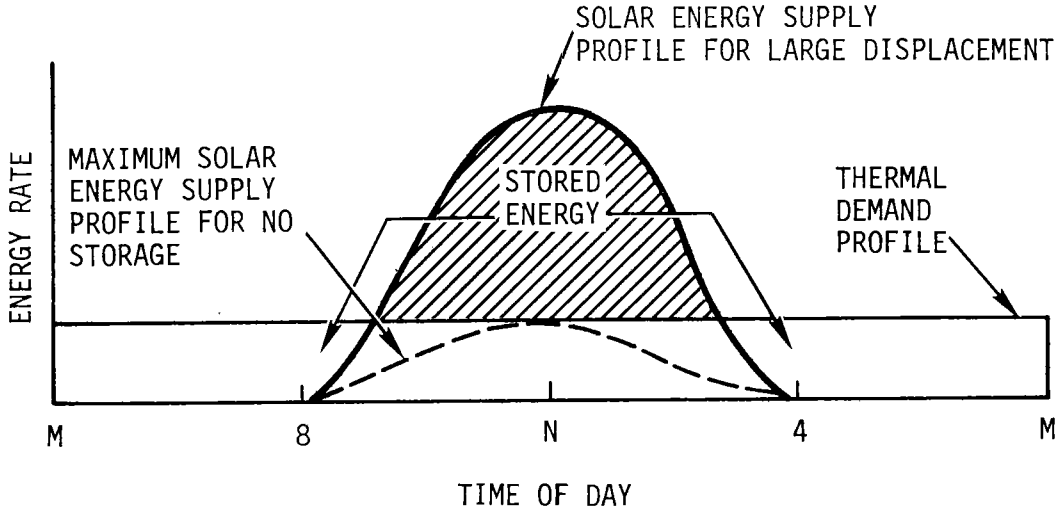

Figure 20. The Role of Storage in a Solar Energy System

Demands is shown. Storage is needed, even for a daytime-only demand, if large Displacement is desired. Storage of the solar energy collected near noon in excess of the Demand provides energy for the early morning and late afternoon when the thermal output from the collector field is insufficient to provide enough thermal energy to meet the Demand. Without storage, the excess energy collected near noon would have to be discarded without significantly contributing to increased displacement of fossil fuel. A similar situation occurs with a 24-hour-per-day Demand. The quantity of storage required to provide large Displacement of a 24-hour-per-day Demand is, as illustrated, much larger than for the daylight-only Demand. In the case of applications which shut down on weekends, thermal energy storage is required to enable Utilization, during the week, of solar energy collected on the weekend. The amount of increased Utilization of collected solar energy resultant from the inclusion of storage in the system determines the allowable cost of storage.

Several different constant Demand profiles will be evaluated in this section. The first Demand profile will be a constant, 24-hour-per-day, 365-day-per-year Demand. This profile will be evaluated in some detail since it is one of the more common industrial Demand profiles, and many of its characteristics which influence conceptual design (e.g., the significance of the Maximum Displacement Point) appear in other types of demands. Discussion of the 24-hour-per-day, 365-day-per-year Demand profile will be followed by examination of constant thermal energy demands, which occur only during the daytime (8 am to 5 pm). This will allow determination of a chart which shows the proper quantity of storage for Demands of any duration longer than daytime-only. Design of solar thermal energy systems which service Demands which shut down on weekends will also be evaluated. A final section will address the design of solar energy systems for servicing applications whose thermal Demands are not constant throughout an entire day but can be considered as combinations of constant Demands.

All Storage Sizing Graphs provide the required Storage Capacity without regard to efficiency of the storage unit. The actual quantity

of storage needed would have to incorporate some appropriate efficiency factor for the storage unit. Storage Sizing Graphs are provided for E/W and N/S collector orientations only. These charts are adequate for conceptual design if it is recognized that collector fields having different orientations can be approximated as linear combinations of E/W and N/S fields, as described in Section 2.2.1. As will be described below, the Storage Sizing Graphs are useful for determining which combinations of collector area and Storage Capacity are needed to achieve a given Actual Displacement. In addition, they illustrate which of the various collector field and Storage Capacity combinations are reasonable candidates for conceptual design.

3.1 24-HOUR-PER-DAY CONSTANT THERMAL DEMAND STORAGE SIZING GRAPHS

Perhaps one of the most common Demand profiles in the industrial process heat sector is a constant requirement for thermal energy, 24 hours per day, 365 days per year. This section evaluates the collector area needed to service this type of Demand profile and the concomitant thermal energy storage requirements for both E/W and N/S collectors. The computations used in generating the Storage Sizing Graphs are described in Appendix E.

3.1.1 E/W Collector Field

Figure 21 plots the Utilization of the energy collected over a year by a field of E/W parabolic trough collectors as a function of Nominal Displacement. Nominal Displacement is defined as the fraction of the Demand which could be displaced if all the collected solar energy could be used in displacing the thermal energy demand. Thus, Nominal Displacement is the ratio of the average daily collector output for a year to the average daily Demand for the year. The Actual Displacement of the Demand is determined by how efficiently the collected solar energy is used (i.e., the Utilization of the collected solar energy).

The Nominal Displacement is a convenient parameter since it, in effect, sizes the collector field required to service a given constant

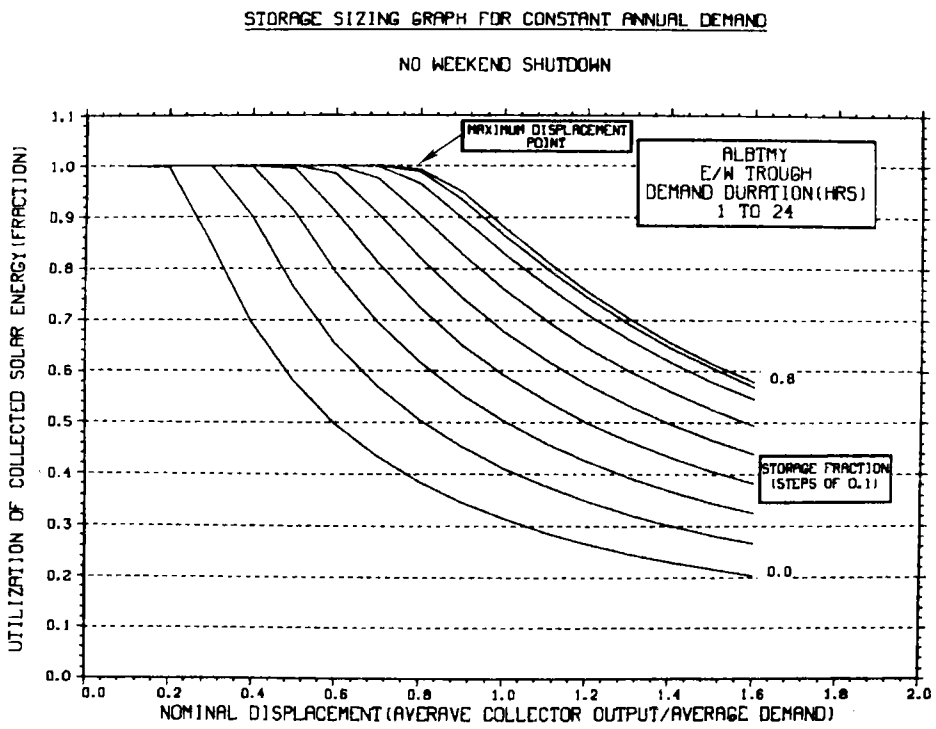

Figure 21. Storage Sizing Graph for E/W Trough--24 h/day

Demand. If an application's average daily Demand and the desired Nominal Displacement are known, the required average daily collector output can be calculated. The solar collector area is simply the partial average daily Demand associated with the desired Nominal Displacement divided by the average daily collector output per unit area for the year, computed as described in Section 2.5.

$$\text{COLLECTOR AREA} = \frac{(\text{DEMAND}) \cdot (\text{NOMINAL DISPLACEMENT})}{(\text{AVERAGE DAILY COLLECTOR OUTPUT})}$$

The purpose of Figure 21 is to illustrate what Nominal Displacements are reasonable to try to achieve with different amounts of storage. A goal in all designs is high Utilization of all collected solar energy (i.e., minimum waste of energy). Section 3.6 discusses the use of the Storage Sizing Graphs for computing collector and storage subsystem costs and provides rationale for designing for high Utilization.

Storage Capacity is represented in Figure 21 by the parameter Storage Fraction. Storage Fraction is defined as the ratio of the Storage Capacity to the average daily Demand. The Storage Capacity required to achieve a given Nominal Displacement with a defined Utilization of collected solar energy is thus equal to the average daily Demand multiplied by the Storage Fraction, as determined from Figure 21.

STORAGE CAPACITY = (DAILY DEMAND)·(STORAGE FRACTION)

Suppose, for example, it were desired to provide a Nominal Displacement of 60% of a constant 24-hour-per-day Demand of 10^8 Btu/day (29.4 kWh/day) and have near-100% Utilization of the collected solar energy. From Figure 21, approximately $0.5\times10^8 = 5\times10^7$ Btu (14.8 kWh) of storage would have to be provided. Figure 21 provides all the tools needed to determine preliminary Storage Capacities and E/W collector areas for servicing a constant 24-hour-per-day Demand.

The Actual Displacement of a thermal energy Demand by a given solar energy system is determined by multiplying the system's Nominal Displacement by the Utilization of the collected solar energy, as defined by Figure 21.

$$\text{ACTUAL DISPLACEMENT} = (\text{NOMINAL DISPLACEMENT})\cdot(\text{UTILIZATION})$$

$$= \frac{(\text{ENERGY COLLECTED})}{(\text{DEMAND})} \cdot \frac{(\text{UTILIZED ENERGY})}{(\text{ENERGY COLLECTED})}$$

$$= \frac{(\text{UTILIZED ENERGY})}{(\text{DEMAND})}$$

For convenience, the results of such calculations are presented in Figure 22, which shows the Actual Displacement achieved by solar energy systems having different Nominal Displacements and Storage Fractions.

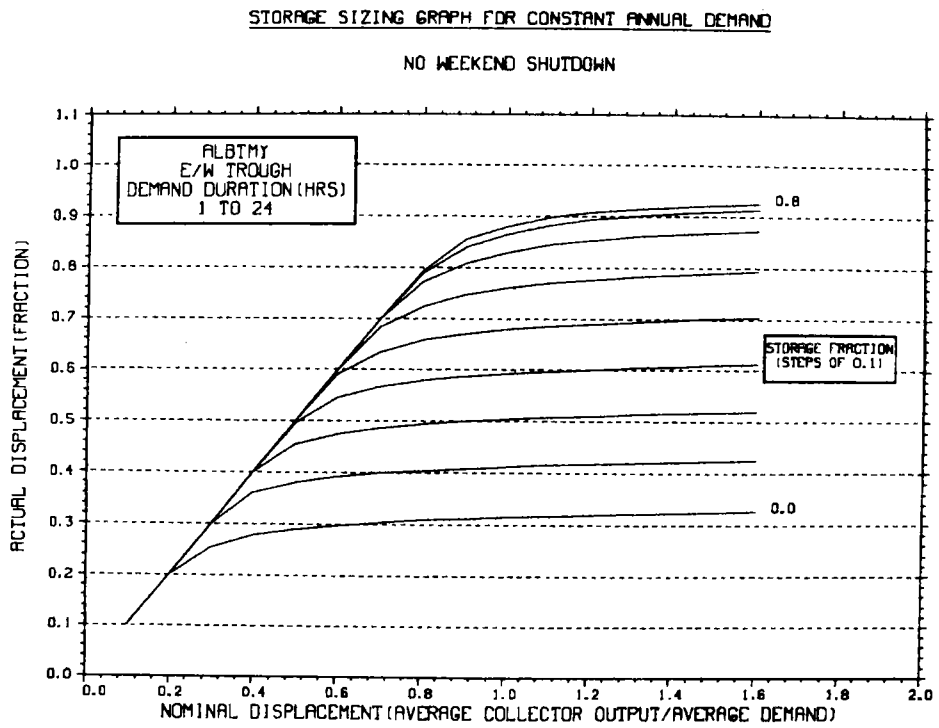

Figure 22. Displacement of 24-Hour-per-Day Demand--E/W Trough

Figure 22 shows that above a Nominal Displacement of 0.8, increasing the collector field size (i.e., Nominal Displacement) has a diminishing effect on Actual Displacement and that incremental increases in Storage Fraction above about 0.6 have less and less impact on increasing the Actual Displacement. As indicated in Figure 22, an Actual Displacement of 0.6 could be achieved with a collector field size equivalent to a Nominal Displacement of 1.2 and a Storage Fraction of 0.3 or a field size equivalent to a Nominal Displacement of 0.6 and a Storage Fraction of 0.4. Due to the expense of solar collectors, the smaller collector field and larger Storage Fraction will usually be most cost effective. High Utilization is chosen as a design criterion in this handbook to identify reasonable starting points for system design.

Figures 21 and 22 are specific to Albuquerque because they incorporate weather characteristics. Storage Sizing Graphs for other SOLMET sites are presented in Appendix H.

3.1.2 General Characteristics of E/W Collector Fields

One of the most striking characteristics of an E/W parabolic trough collector field revealed in Figures 21 and 22 is that without the ability to store thermal energy (i.e., Storage Fraction is 0.0), only a small fraction (about 20%) of the constant 24-hour Demand can be displaced while maintaining near-100% Utilization of the collected solar energy. If an E/W parabolic trough field were sized for a Nominal Displacement of 0.4 with no provision for storage, the resultant Utilization of the collected solar energy would be only 0.7. Wasting 30% of the collected solar energy would, in effect, increase by 30% the cost of the energy produced by the collector field. Even at very large field sizes (i.e., large Nominal Displacement), Actual Displacement would not exceed much over 30 to 35% with no storage.

The decrease in Utilization associated with increasing the Nominal Displacement above 0.2 for an E/W field reveals the allowable cost for thermal energy storage if it is desired to achieve an Actual Displacement of 0.4 (i.e., a Nominal Displacement of 0.4 with 100% Utilization). Figure 21 reveals that a Storage Fraction of 0.2 will permit 100% Utilization. Thus, on the average, 50% of the collected solar energy must be stored daily (i.e., Storage Fraction/Nominal Displacement = Storage Capacity/Average Daily Collector Output). If the cost to store this quantity of energy were greater than 30% of the collector field cost, it would be more expensive to include storage than to accept the decrease in Utilization in collected solar energy. Storage costs will be discussed further in Section 3.5, and it will be seen that, typically, the minimum storage/collector subsystem costs occur at Storage Fractions which allow near-100% Utilization of the collected solar energy.

3.1.3 Maximum Displacement Point

Another general conclusion which can be obtained from Figure 21 is that E/W parabolic trough solar collector fields cannot displace more than about 80% of a constant 24-hour Demand in Albuquerque and still maintain near-100% Utilization of the collected solar energy

even with large Storage Capacities. This is denoted as the Maximum Displacement Point on Figure 21. Above a Storage Fraction of 0.6 to 0.7, additional increments of storage have little impact on the Utilization of collected solar energy. One reason for this can be observed in Figure 13, which shows that the thermal energy output from an E/W solar collector field in Albuquerque varies about ±10% around the annual average from season to season. Increasing Displacement above 80% for an E/W parabolic trough field in Albuquerque would require seasonal storage. Up to the Maximum Displacement Point, the combination of collectors and storage serve mainly to displace the recurring daily overnight thermal Demand.

It should be remembered that Albuquerque is a reasonably clear climate with little cloud cover. In cloudy climates, the Maximum Displacement Point will occur at relatively small values of Nominal Displacement due to the many cloudy days throughout the year. As the Storage Sizing Graphs for these sites indicate (see Appendix H), only rather small Actual Displacements are practical in such climates.

The Maximum Displacement Point in Figure 21 and all other Storage Sizing charts has design significance in that it represents a design goal for solar energy systems incorporating storage. In general, if the economic decision is made to incorporate storage in a solar energy system, there is no additional economic penalty for deploying the collectors and storage concomitant with the Maximum Displacement Point. The decision is really one of whether or not to include any storage at all. If storage is to be included, the Maximum Displacement Point indicates the appropriate quantity to assess potential for fossil fuel Displacement.

The logic which drives the design of a solar energy system to the Maximum Displacement Point is reduced to graphical form in Figure 23. This graph plots a term called the Incremental Storage Ratio versus Nominal Displacement. The Incremental Storage Ratio is defined as the incremental change in Storage Fraction divided by the resultant incremental change in Actual Displacement as defined in Figure 22. The

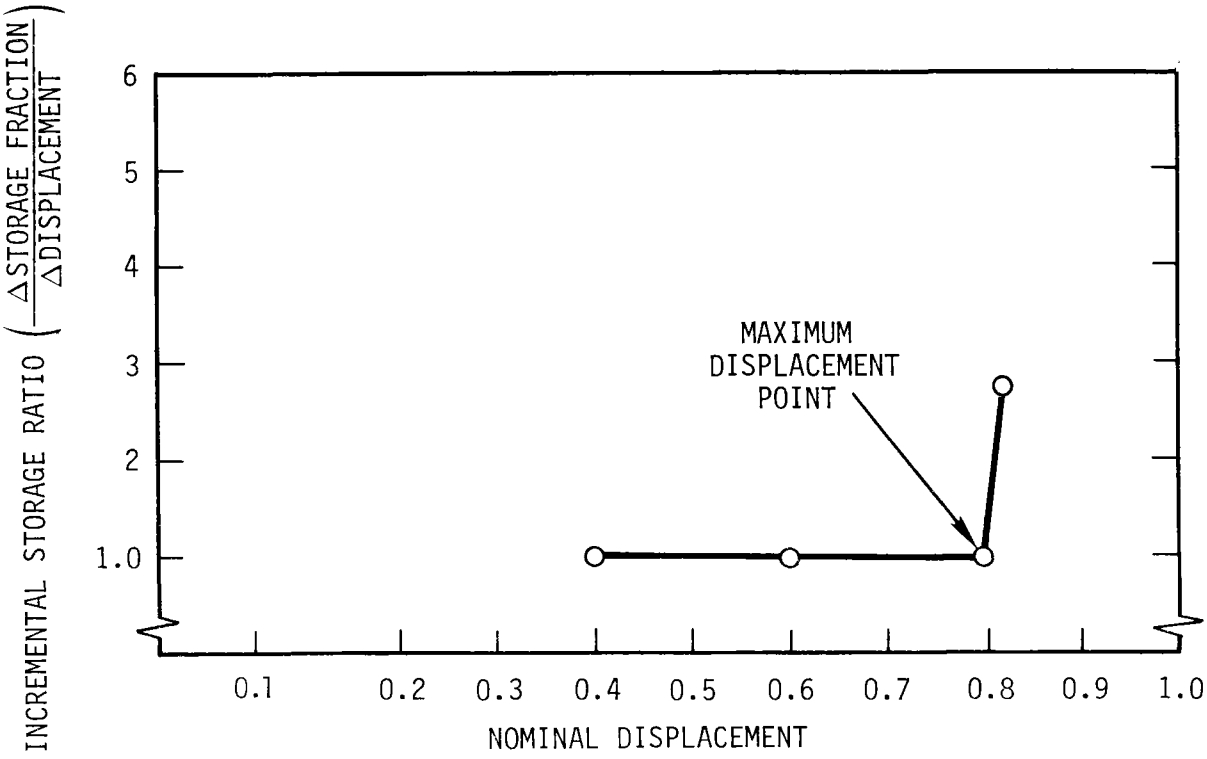

Figure 23. Effect of Storage on Displacement

Incremental Storage Ratio is a measure of how effective added storage is in increasing Actual Displacement.

Thus, for example, the Incremental Storage Ratio associated with the Storage Fraction (0.2) needed to go from an Actual Displacement of 0.2 to 0.4 is 0.2/0.2. Likewise, the Incremental Storage Ratio associated with an additional Storage Fraction of 0.2 is also 0.2/0.2 since this additional Storage Fraction results in the Actual Displacement increasing from 0.4 to 0.6 (see Figure 22). The points plotted in Figure 23 were calculated this way and show that the Incremental Storage Ratio does not change significantly until the Maximum Displacement Point is approached. At this point, a further increase in the Storage Fraction of 0.2 leads to an increase in Displacement of only 0.07 (see Figure 22) which results in a sharp increase in the Incremental Storage Ratio. The conclusion to be drawn from Figure 23 is that subsequent increments of storage and collector area are equally effective up to the Maximum Displacement Point.

In conceptual design, the Maximum Displacement Point will identify the design point for assessing the maximum practical potential a solar energy system has for displacing fossil fuel. While the selection of the proper storage/collector combination will be determined by economics, the Maximum Displacement Point represents a good initial selection of collector area and Storage Capacity. Section 3.6 will address the calculation of subsystem costs and provide further evidence for the rationale of selecting the Maximum Displacement Point as the design point in a conceptual design which includes storage.

3.1.4 N/S Collector Field

Figures 24 and 25 are plots of Utilization and Actual Displacement versus Nominal Displacement, respectively, for N/S parabolic trough solar energy systems servicing constant, 24-hour-per-day, 365-day-per-year, thermal energy Demands in Albuquerque. All parameters are as defined above for the E/W collector field.

A N/S parabolic trough field (Figure 24) shows characteristics similar to those of an E/W field except that the Maximum Displacement Point occurs at a Nominal Displacement of 0.6 in Albuquerque. This is due to the even larger variations in the seasonal output of N/S collectors than in E/W collectors in Albuquerque.

3.2 DAYTIME-ONLY CONSTANT THERMAL DEMAND STORAGE SIZING GRAPHS (8 am to 5 pm)

Figures 26 and 27 show the Utilization and Actual Displacement, respectively, for an E/W parabolic trough collector field servicing a constant thermal Demand lasting from 8 am to 5 pm sun time. Figures 28 and 29 display similar information for N/S collectors. As might be expected, Figures 26 and 27 show that with Demands for thermal energy present only during the daytime, greater Actual Displacement (i.e., Nominal Displacement at 100% Utilization) can be achieved with less storage than in the case of 24-hour Demands. In fact, with no storage, up to 40% Actual Displacement can be achieved by E/W parabolic trough collector fields while maintaining high Utilization. Addition of small amounts of storage can increase Actual Displacement up to 60% with high Utilization.

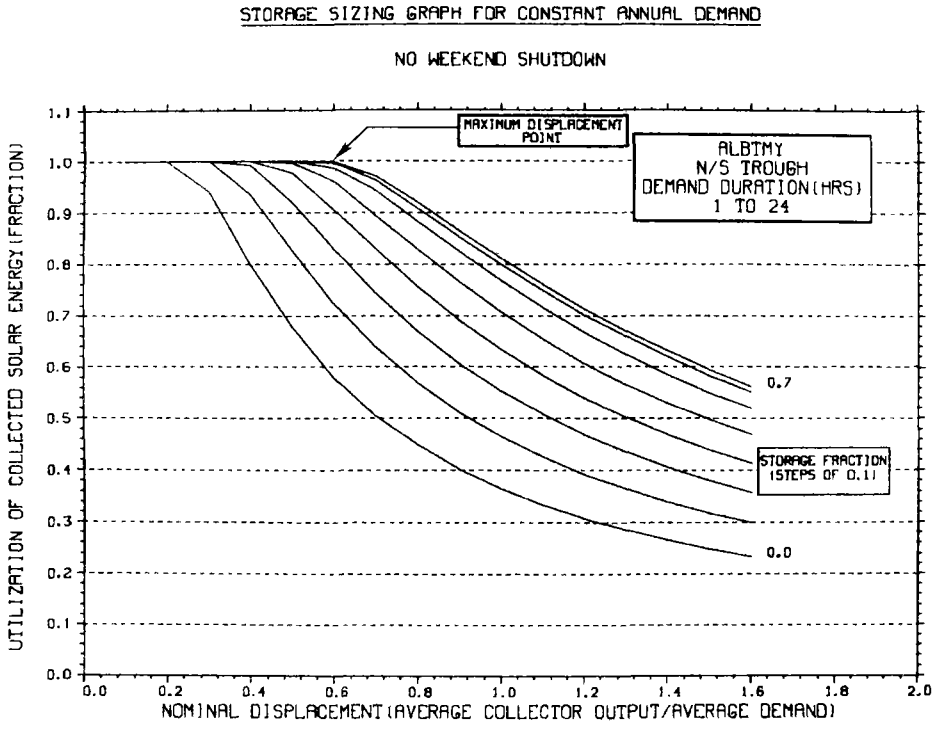

Figure 24. Storage Sizing Graph for N/S Trough--24 h/day

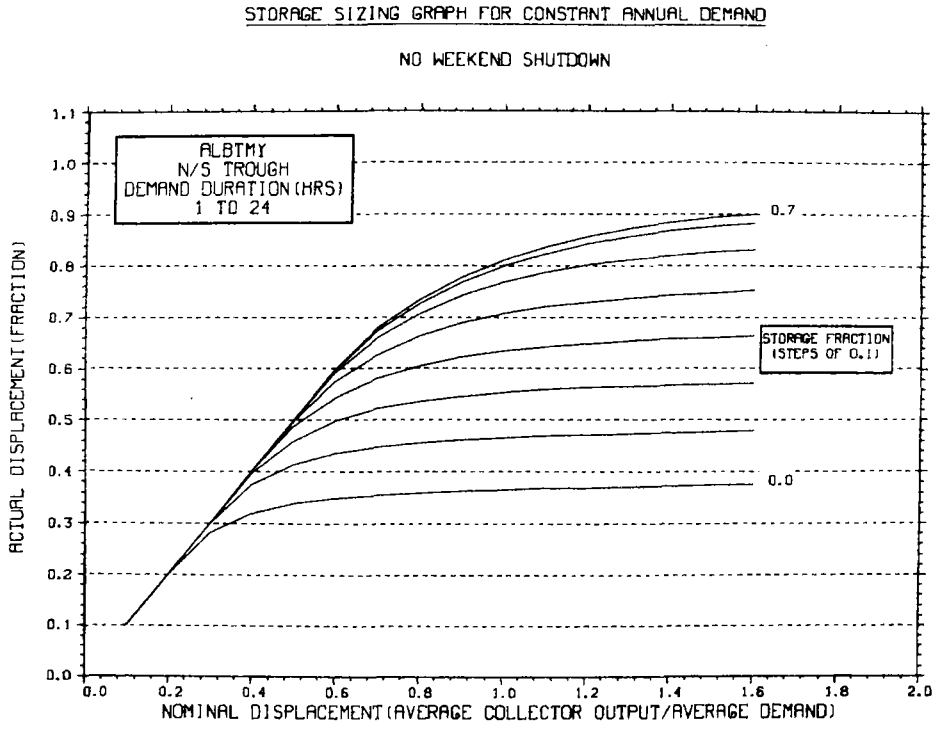

Figure 25. Displacement of 24-Hour-per-Day Demand--N/S Trough

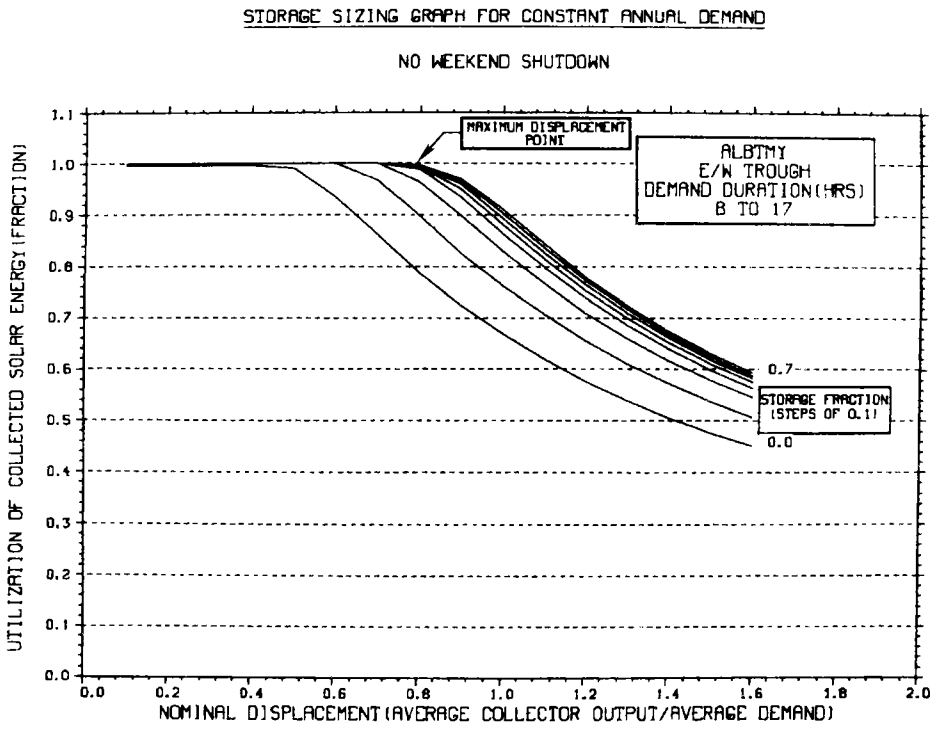

Figure 26. Storage Sizing Graph for E/W Trough--Daytime Demand

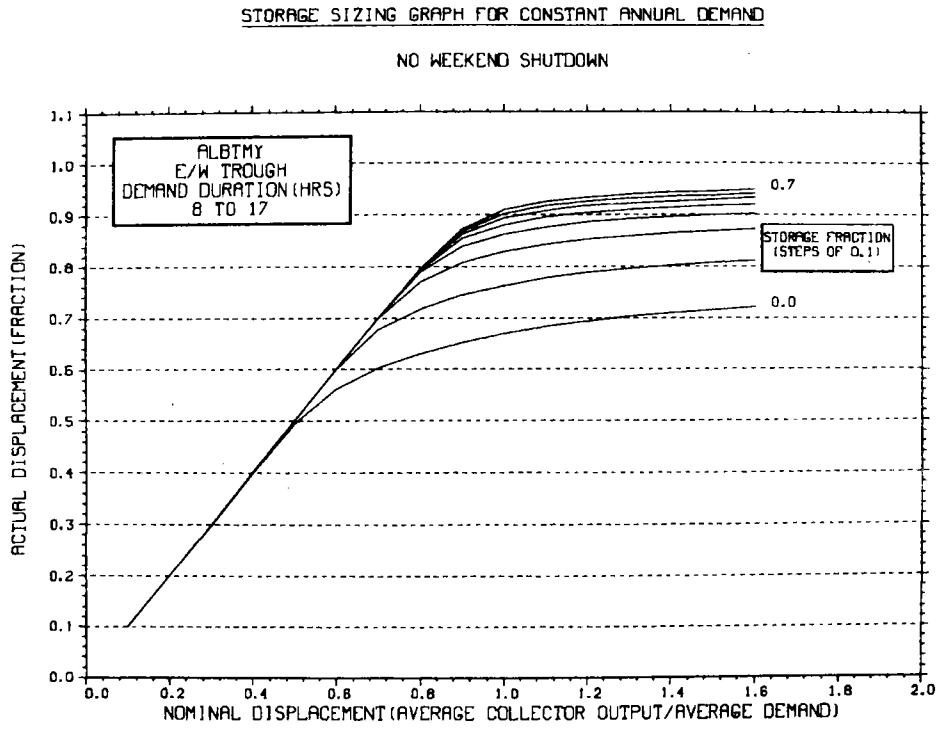

Figure 27. Displacement of Daytime Demand--E/W Trough

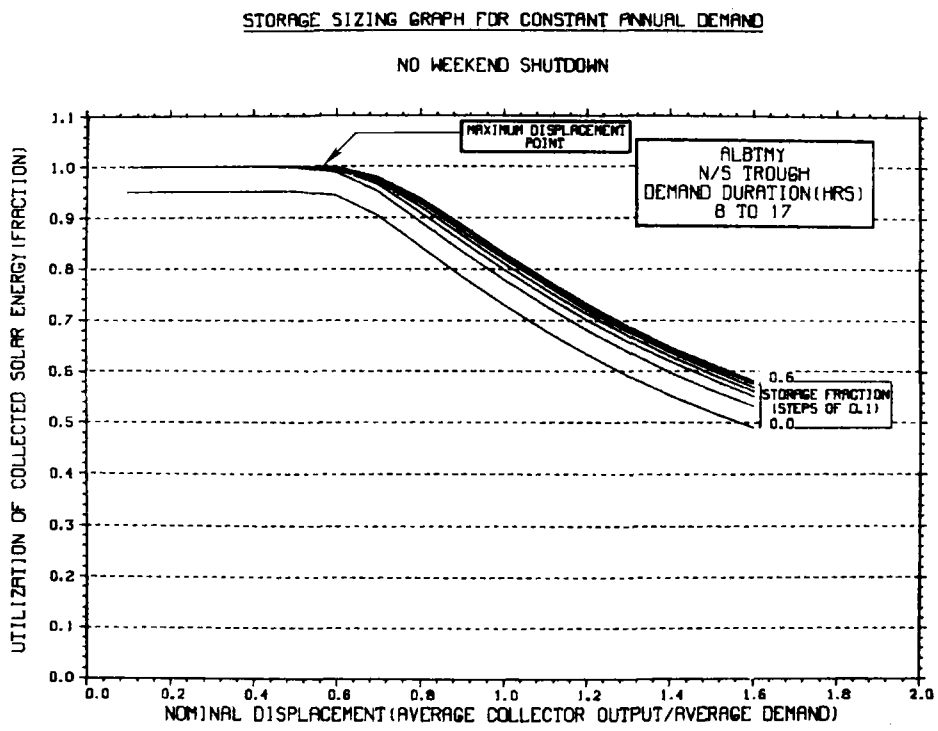

Figure 28. Storage Sizing Graph for N/S Trough--Daytime Demand

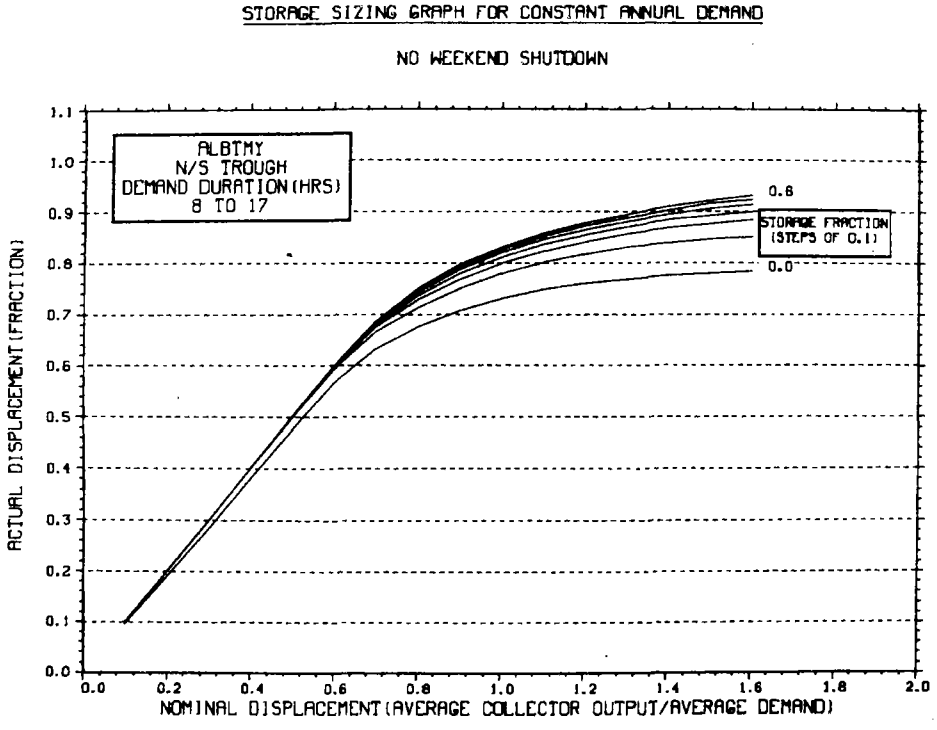

Figure 29. Displacement of Daytime Demand--N/S Trough

Notice in Figures 28 and 29, that with no storage, the highest Utilization attained by a N/S trough is 0.95. This results from the summer performance profile at which time the N/S trough produces energy before 8 am and after 5 pm. With no storage, this energy is wasted. This situation does not occur for an E/W trough. Due to the high Solar Incidence Angles in the early morning and late afternoon during the summer, an E/W trough does not produce significant energy outside the 8 am to 5 pm time period.

Figures 26 and 28 reflect that, in Albuquerque, the Actual Displacement (i.e., Maximum Displacement Point) available to E/W and N/S collector fields with reasonable Storage Capacities and near-100% Utilization is about 0.8 and 0.6, respectively. This, as discussed above, is due to the seasonal variation of the thermal energy output from the two fields.

3.3 STORAGE CAPACITY FOR CONSTANT DEMANDS OF INTERMEDIATE DURATION

The appropriate Storage Capacity for any constant Demand which lasts longer than the 8 am to 5 pm time period discussed above can be determined from the daytime-only Storage Sizing Graphs. The daytime-only Storage Sizing Graphs give the Storage Fraction required for daytime operation. Any operation outside the 8 am to 5 pm period must be done exclusively from storage. As an example of how the daytime-only Storage Sizing Graph can be used to predict Storage Capacities for Demands with longer duration, consider a constant Demand which lasts 24 hours (i.e., the situation represented by Figure 21).

If a constant daily Demand of 10^8 Btu/day (29.4 MWh/day) is assumed and a Nominal Displacement of 0.8 is desired, the quantity of Demand which occurs outside daylight hours is $(15/24)(0.8\times10^8) = 0.5\times10^8$ Btu/day (14.7 MWh/day). From Figure 26, it is seen that a Storage Fraction of about 0.3 is needed to provide near-100% Utilization for the daytime-only portion of the load. The 8 am to 5 pm portion of the 24-hour load is $(9/24)(0.8\times10^8) = 0.3\times10^8$ Btu/day (8.8 MWh/day). Thus, the Storage Capacity required for the 8 am to 5 pm

portion of the constant 24-hour Demand is $(0.3)(0.3\times10^8) = 0.09\times10^8$ Btu (2.6 MWh). The resultant total Storage Capacity for a Nominal Displacement of 0.8 with near-100% Utilization of the constant 24-hour Demand is 0.59×10^8 Btu (17.3 MWh). This corresponds to a Storage Fraction of $0.59\times10^8/10^8$ or about 0.6 Btu/day. This is in agreement with Figure 21, which reveals a Storage Fraction of 0.6 to 0.7 for a Nominal Displacement of 0.8.

This computation of Storage Fraction for Demands with durations greater than 8 am to 5 pm has been reduced to graphical format in Figure 30. Figure 30 plots the ratio of Storage Fraction to Nominal Displacement versus the number of hours that the demand lasts outside the 8 am to 5 pm time period. Thus, for the 24-hour example above, the ratio of Storage Fraction to Nominal Displacement is 0.74, as shown in Figure 30. At a Nominal Displacement of 0.8, this results in a Storage Fraction of (0.8)(0.75) = 0.6, in agreement with the above calculation. Likewise, a Storage Fraction of about 0.5 would be required for a Nominal Displacement of 0.8 for a constant Demand lasting from 8 am to 12 MN.

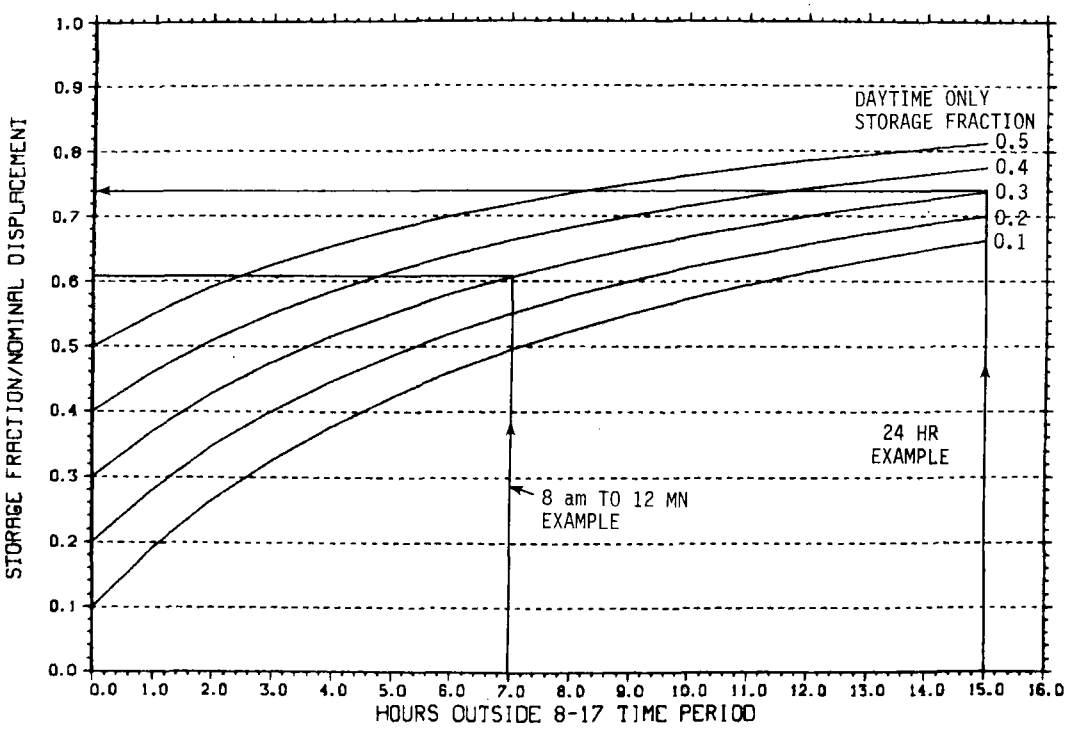

Figure 30. Computation of Storage Fraction

Although Figure 30 could be used to compute Storage Fractions for any Demand lasting longer than 8 am to 5 pm, both the daytime-only and the 24-hour-per-day Storage Sizing Graphs are presented in Appendix H. This was done for convenience since the 24-hour-per-day Demand is very common. Other time periods can be analyzed using Figure 30, which is also reproduced in Appendix H.

3.4 ADDITIONAL DEMAND PROFILES

3.4.1 Weekend Shutdown Storage Sizing Graphs

Weekend shutdown is a unique type of Demand in that the no-storage system may, in fact, not be the least costly solar thermal energy system. The reason for this is that the collectors can produce energy during the weekend, but there is no coincident Demand. This leads to poor Utilization in the case of no storage, effectively increasing the cost of energy produced by the collector field.

From the point of view of evaluating the proper collector area-storage capacity combination, the question of whether or not to provide sufficient storage to store the thermal energy produced during the weekend should be addressed first. This is simply an economic question of whether it is less expensive to waste the weekend energy or pay for the storage capacity to use it.

If the weekend energy were discarded due to lack of storage, the Effective Collector Cost would increase by 7/5. Thus, in the case of $\$20/ft^2$ ($\$215/m^2$) collectors, used with near-100% Utilization during the week, the Effective Collector Cost would be (20)(7/5) = $\$28/ft^2$ ($\$301/m^2$) in the case of weekend shutdown and no storage. This increased cost of the collectors would have to be compared with the cost of storing the weekend energy. Consider, for example, a collector field located in Albuquerque and producing, on the average, 1000 Btu/ft^2·day (3.15 kWh/m^2·day). Weekend storage would have to be sized for 2 days of energy production, or in the case of this example, 2000 Btu/ft^2 (6.30 kWh/m^2). Thus, if the cost of thermal energy storage were

less than (28 - 20)/2000 = $4/kBtu ($13.64/kWh), weekend storage would be cost effective.*

Once a decision has been made concerning the incorporation of weekend storage, conceptual design can proceed using the appropriate Storage Sizing Graphs for the no-weekend-shutdown case. If it is decided not to incorporate weekend storage, conceptual design progresses as in the no-weekend-shutdown case except with the realization that the Utilization will be 5/7 of the Utilization shown in the Storage Sizing Graph.

In the case where a decision is made to provide weekend storage, the total amount of storage is equal to the weekend storage plus the storage needed for the hourly mismatches between Demand and solar energy production on a day-to-day basis. The no-weekend-shutdown Storage Sizing Graphs show the Nominal Displacement associated with the Maximum Displacement Point. However, with weekend shutdown, energy produced during the weekend when there is no Demand is applied to the Demand during the week. The net result is that, for weekend shutdown, the Storage Sizing Graphs should be used with a corrected Nominal Displacement equal to 5/7 times the Nominal Displacement of the no-weekend-shutdown case. Figure 31 correlates Nominal Displacement, no-weekend shutdown, with Nominal Displacement, weekend shutdown. (Weekend shutdowns of both 1 and 2 days are shown since the above discussion could, of course, be applied to a 1-day-per-week shutdown.)

As an example of the above reasoning, consider an E/W parabolic trough collector field located in Albuquerque and producing, on the average, 1000 Btu/ft^2·day (31.5 kWh/m^2·day). The Demand is assumed to be constant 24 hours per day. The appropriate Storage Sizing Graph is presented in Figure 21. As seen, the Maximum Displacement Point occurs at a Nominal Displacement of 0.8. Since this example deals with

*This example is meant only to illustrate the basic computational technique and does not include a storage efficiency. Storage efficiency would have be considered in an actual design.

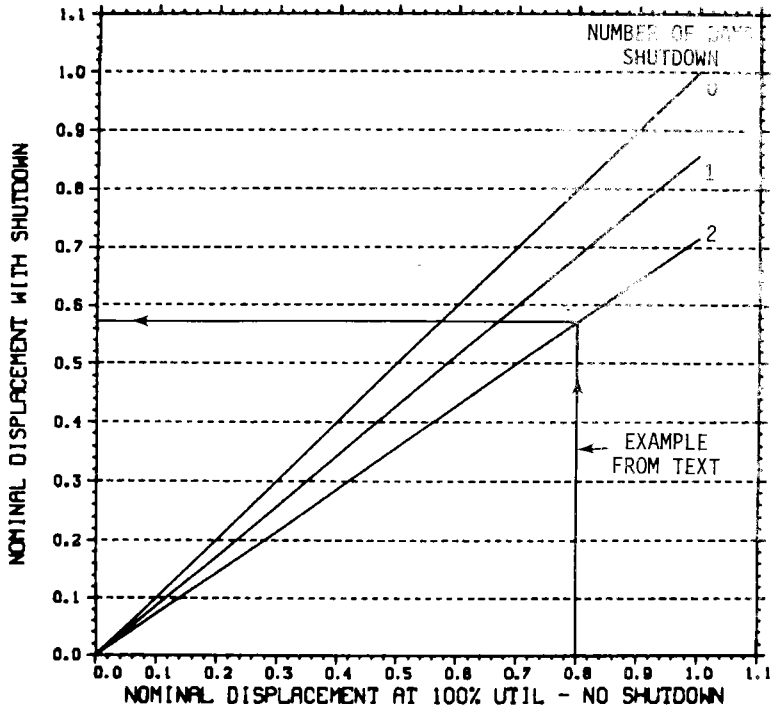

Figure 31. Nominal Displacement for Weekend Shutdown

a 2-day shutdown on the weekends, the appropriate Nominal Displacement is approximately 0.57 (see Figure 31). Thus, from Figure 21, the appropriate Storage Fraction associated with near-100% Utilization for daily storage is 0.4 to 0.5. The Storage Fraction for weekend storage will be twice the Nominal Displacement since enough storage must be provided for 2 days of unused collector output. In other words,

$$\text{WEEKEND STORAGE FRACTION} = \frac{\text{STORAGE CAPACITY}}{\text{DAILY DEMAND}}$$

$$= \frac{2(\text{DAILY COLLECTOR OUTPUT})}{\text{DAILY DEMAND}} = 2(\text{NOMINAL DISPLACEMENT})$$

The total approximate storage capacity is then represented by the sum of the Storage Fraction for daily operation (0.4 to 0.5) and the Storage Fraction for weekend storage (2)(0.57) or 1.5 to 1.7. In addition, a Nominal Displacement of 0.57 would be chosen as the design point corresponding to the Maximum Displacement Point for weekend shutdown.

The Storage Sizing Graph for weekend shutdown for an E/W trough located in Albuquerque is shown in Figure 32 for comparison with the above computation. As seen in Figure 32, the Storage Sizing Graph shows the Maximum Displacement Point occurring at a Nominal Displacement of about 0.6 and a Storage Fraction of 1.4 to 1.6. This agrees with the above calculation.

Figure 33 correlates Actual Displacement with Nominal Displacement and Storage Capacity for the case of no weekend Demand. To understand the Displacement curves, recall that there is a Demand only 5/7 of the time during which there is the potential for collecting solar energy. Thus, even though the Utilization at a Nominal Displacement of 0.2 is only 0.71 for an E/W collector with no storage, Actual Displacement also is 0.2 since the decreased Utilization is due to wasting thermal energy on weekends only and not during the week when a Demand exists. Thus, in the case where the demand is shutdown 2 days per week, Actual Displacement can be calculated by

$$\text{Actual Displacement} = (\text{Nominal Displacement}) \frac{\text{Utilization}}{5/7}$$

Individual Storage Sizing Graphs for weekend shutdown are not explicitly presented in Appendix H since the conceptual design can be accomplished using the no-weekend shutdown Storage Sizing Graphs as discussed above. Figure 31 is reproduced in Appendix H for convenience in executing conceptual designs for Demands which shutdown on weekends.

3.4.2 Demands Which Are Not Constant

The Storage Sizing Graphs for constant Demands can also be used to allow conceptual design to proceed in cases where the Demand can be considered a composite of the constant Demands discussed above. If, for example, an application's Demand had the profile illustrated in Figure 34, the solar energy system to service the Demand may be considered to be two separate systems. The increased daytime Demand is considered a separate Demand serviced by a particular collector area

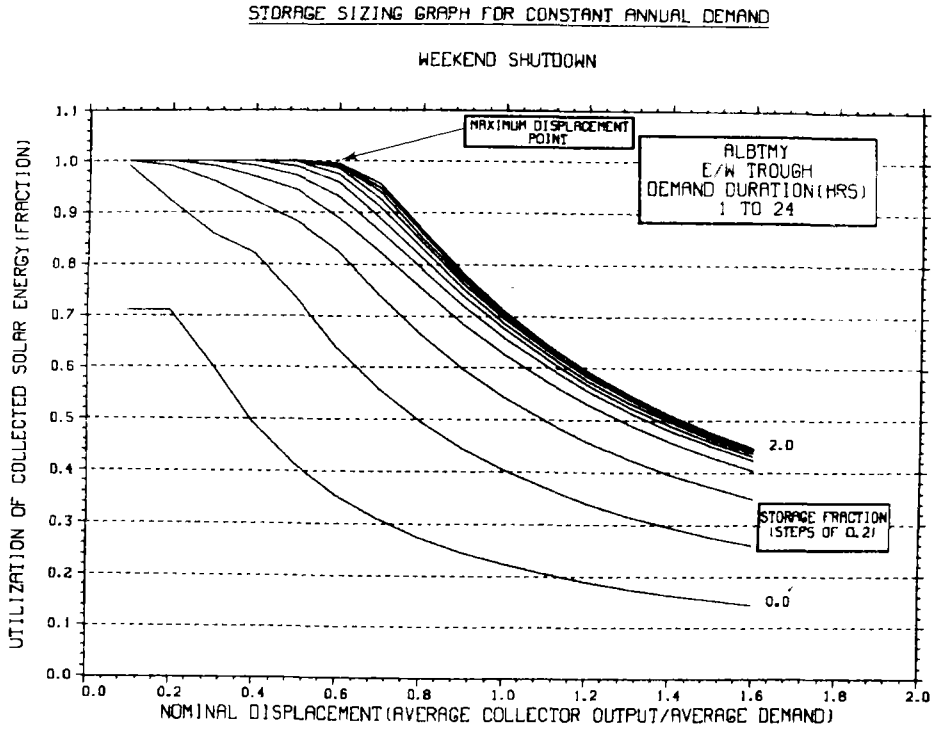

Figure 32. Storage Sizing Graph for E/W Trough--Weekend Shutdown

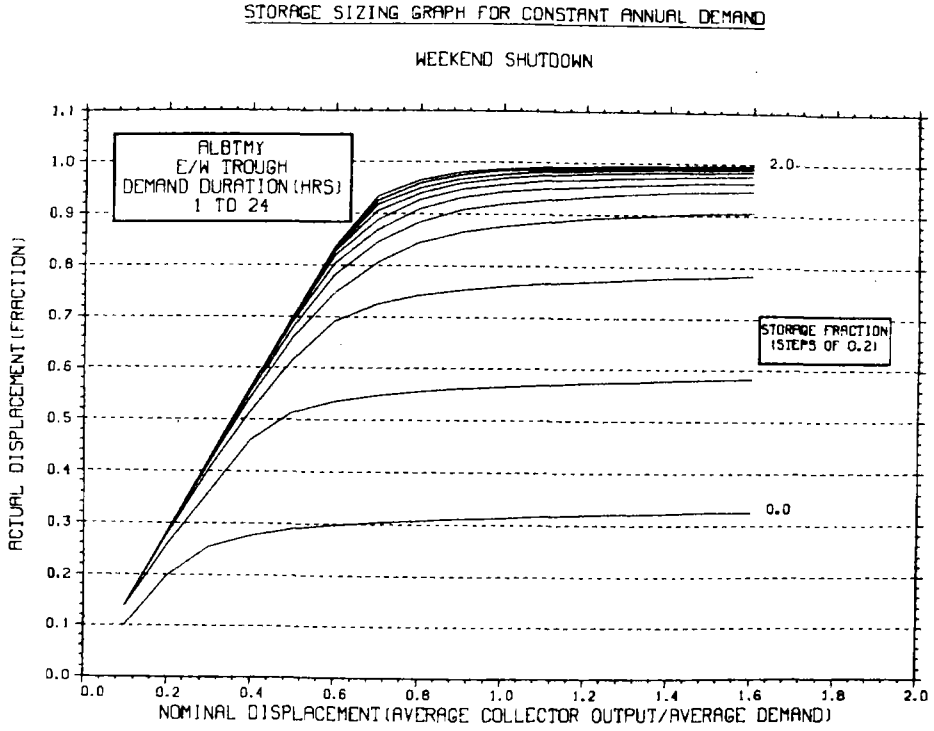

Figure 33. Displacement of Demand Which Shuts Down on Weekends

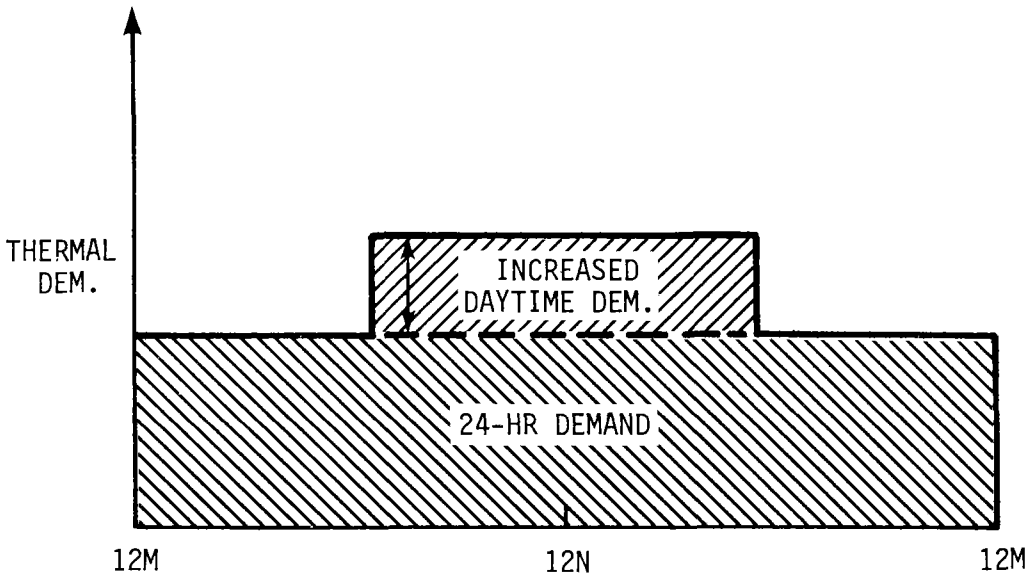

Figure 34. A Stepped Demand Profile

and storage combination while the constant 24-hour Demand is considered separately and serviced by a different collector area and storage combination. The solar energy system servicing the entire Demand is the total collector area and total Storage Capacity of the two separately analyzed Demands. An example illustrating design of a solar energy system servicing such a stepped Demand profile is presented later in Section 4.4.

3.5 COST FOR SENSIBLE HEAT STORAGE

Before beginning a discussion of the proper sizing of parabolic trough collector fields, the costs associated with sensible heat storage will be investigated. Sensible heat is the type of storage currently in most common use. Details on the derivation of the nomographs described here are presented in Appendix F. The purpose of including a brief discussion of sensible heat storage costs at this point is to allow the designer to make some preliminary decisions on the potential role of storage in solar energy systems. If firm costs for storage are available, the designer should by all means use those costs in place of the generic costs outlined here.

For storage systems operating in the temperature range of 300°F (149°C) to 600°F (315°C), organic heat transfer fluids are typically used as the heat storage medium. The best understood storage systems are neat oil systems, which employ either multiple hot and cold storage tanks, or thermocline storage tanks, in which the hot oil floats on top of the cold oil. In a mixed-media storage system, rock or some other inert material is added to either the multiple tanks or thermocline tank to displace part of the expensive heat transfer oil. In any case, the cost of storage for large systems is essentially the cost of the oil* for oil costs in the range of $3 to $5/gal ($800 to $1320/$m^3$). Figure 33 graphically computes the cost of storage in $/kBtu (kBtu = 10^3 Btu) and $/kWh, starting with the storage medium cost in $/gal or $/$m^3$. The cost in $/kBtu or $/kWh is convenient since, typically, a parabolic trough will deliver approximately 10^3 Btu/ft^2·day (3.17 kWh/m^2·day) in a clear climate.

As an example of the use of Figure 35, consider a sensible heat storage system employing neat oil, which costs $5/gal ($1320/m^3). During storage of thermal energy, the heat transfer fluid is heated from 350°F (177°C) to 500°F (260°C). At the average temperature of 425°F (219°C), the fluid density and heat capacity will be assumed to be 7.0 lb/gal (839 kg/m^3) and 0.55 Btu/lb·°F (0.55 cal/g·°C), respectively.

The graphical computation is performed by first finding the intercept of the $5/gal ($1320/m^3) cost line and the 7.0 lb/gal (840 kg/m^3) density line in Chart A of Figure 35. A vertical line is then drawn, and the intercept with the 0.55 Btu/lb·°F (0.55 cal/g·°C) heat capacity in Chart B is located. Finally a horizontal line is drawn to Chart C. The intercept with the 150°F (83°C) ΔT line in Chart C is

*Appendix F presents a derivation of storage costs. Limitations to the assumption that storage costs equals oil costs are presented in Appendix F.

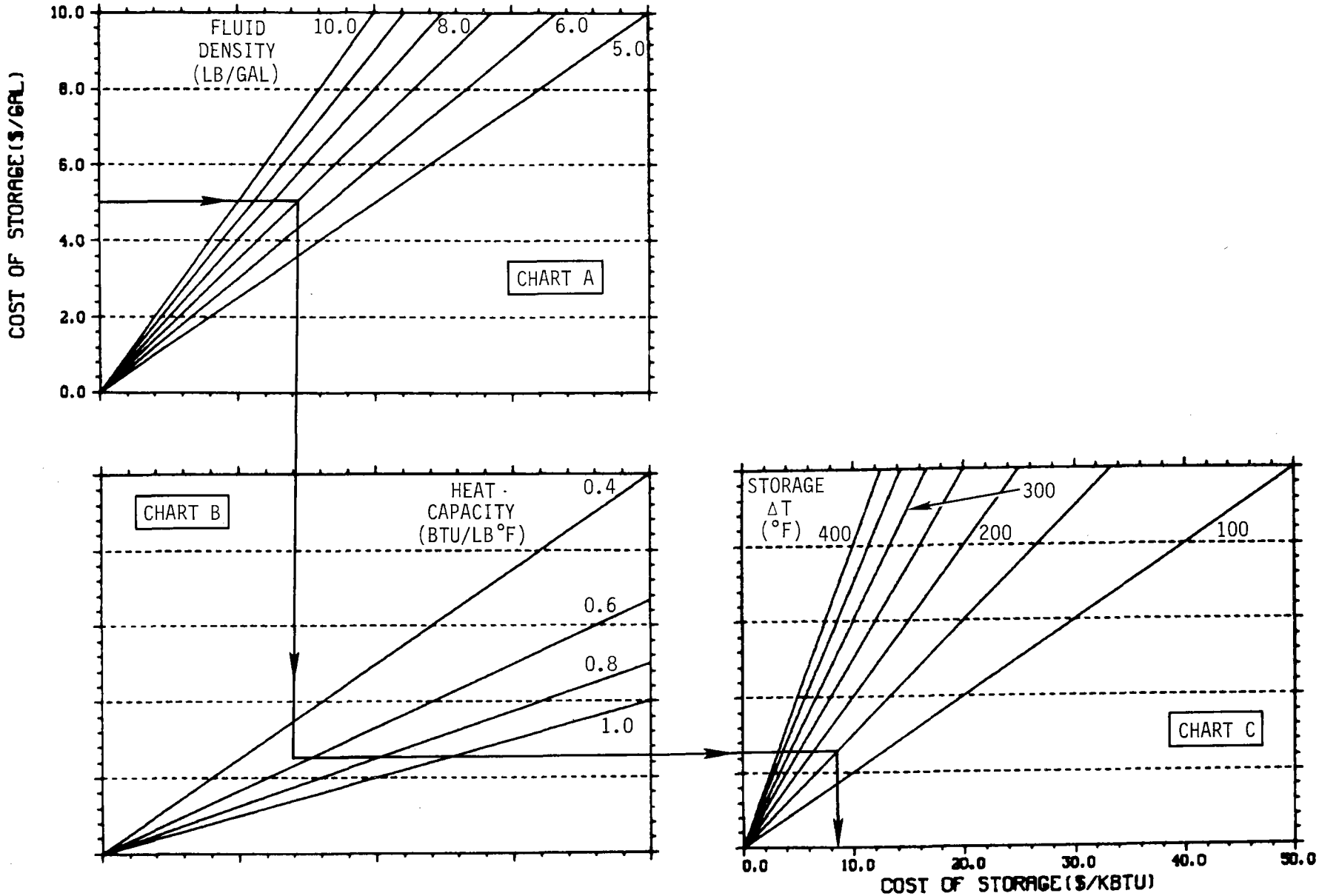

Figure 35a. Estimation of Sensible Heat Storage Costs--English Units

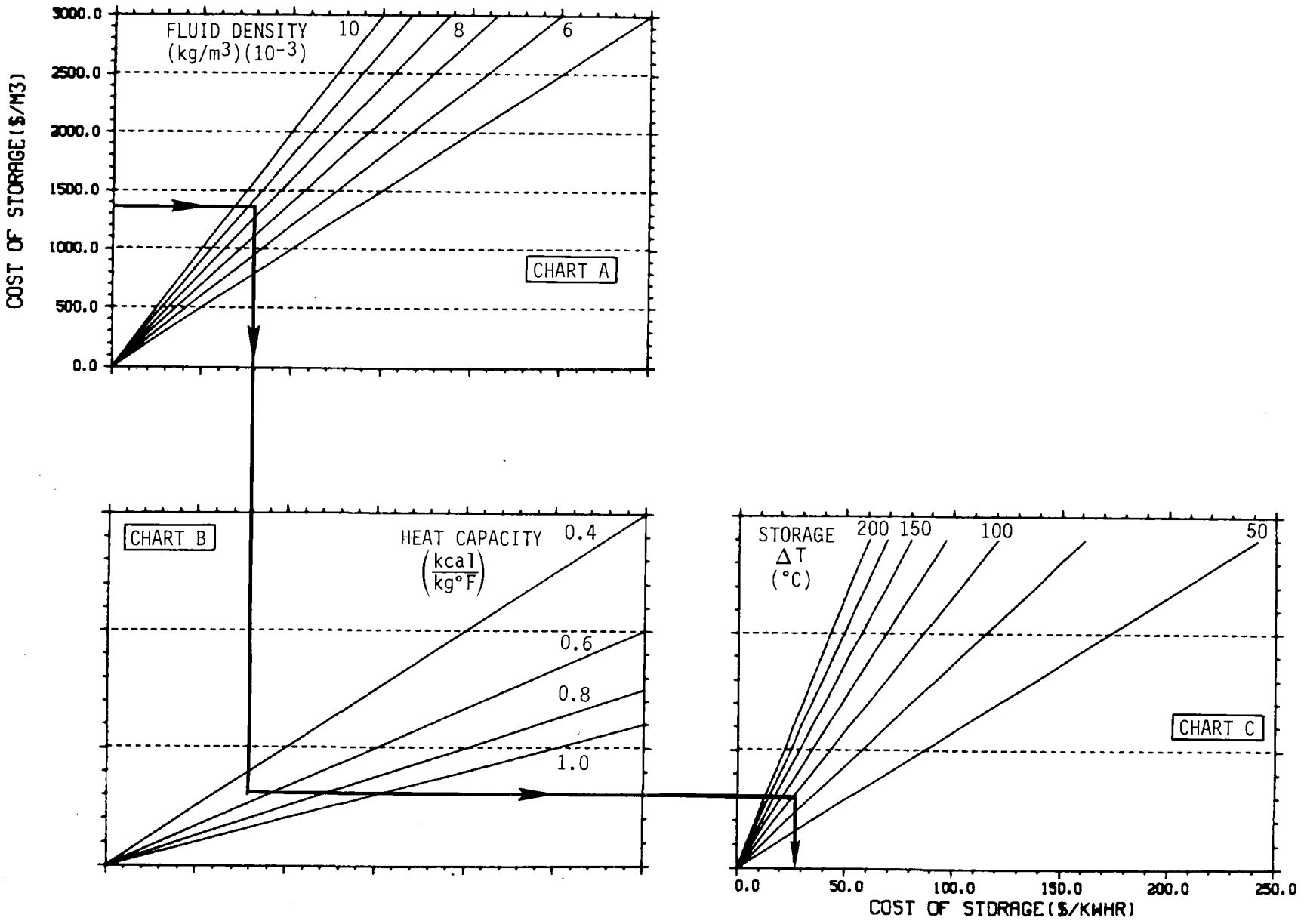

Figure 35b. Estimation of Sensible Heat Storage Costs--Metric Units

then projected onto the horizontal axis of Chart C. This reveals the cost of the storage system to be about $8.60/kBtu ($29.20/kWh).*

In order to use Figure 35 with mixed-media storage, the storage cost can be approximated by multiplying the price of the oil by the void fraction in the mixed-media tank. If, for example, the above storage system were replaced by a mixed-media system in which 60% of the tank was filled with rock, the storage cost would then be reduced by 60% to $3.44/kBtu ($11.68/kWh). This assumes the cost of the solid media (e.g., rock) to be negligible. Usually, the cost of rock is small compared to that of oil, and this approximation is acceptable for conceptual design purposes. However, there is little experience with mixed-media storage systems. It is possible that the cost for properly installing the rock and the cost of a reinforced tank to hold the rock may be large.

As will be discussed in Section 4.1, the designer has some control over the choice of the temperature difference across storage and, as a result, will be able to vary storage costs somewhat. The purpose of Figure 35 is to facilitate computation of sensible heat storage costs, starting with basic, generally available information. A Design Rule-of-Thumb will be developed in Section 4.2 using Figure 35.

3.6 IMPACT OF STORAGE COSTS ON STORAGE AND COLLECTOR SUBSYSTEM COSTS

Knowledge of thermal energy storage costs, when combined with information on the effects of storage on solar energy Utilization such as that presented in Figure 21, allows estimation of subsystem costs.

---

*Note that at a cost of $8.60/kBtu, storage represents a considerable extra cost to the solar collector system even if storage is 100% efficient. If installed collector costs are about $20/ft^2, for example, and 1 ft^2 of collector provides about 1000 Btu/day, storage could effectively lead to an increase in collected energy costs of about 22% if half the collected thermal energy were stored. For this reason, inexpensive oils and mixed-media storage are receiving much attention from the designers of collector and storage systems. Typically, the same heat transfer oil is used both in the collector field and storage to avoid the need for a heat exchanger.

The logic flow in determining storage and collector subsystem costs is shown in Figure 36. As indicated, the costs of the collectors and storage are evaluated separately and then combined to provide a total storage and collector subsystem cost on a per-unit-collector-area basis.

The cost of the parabolic troughs is usually obtained from collector manufacturers. This cost information, when divided by the Utilization of the parabolic trough, yields the Effective Collector Cost.* This says, in effect, that a collector which is poorly utilized is more costly than the purchase price indicates because it produces less useful energy than it is capable of supplying to the Demand.

The quantity of storage and area of collectors needed to service a given Demand is determined from the Storage Sizing Graphs described previously in Sections 2.1 and 2.2.** When combined with the area of collectors under consideration (e.g., the Nominal Collector represented in Figure 13), the quantity of storage per unit of collector area is determined. Vendor quotes or, in the absence of firm price data, the storage costs from Figure 35 may be used to estimate the cost of storage per unit collector area. This information can be combined with the Effective Collector Costs to determine the minimum cost collector and storage subsystem.

The computations of collector and storage subsystem costs can be best illustrated by an example. To simplify the discussion, a Demand equal to the output from 1 ft^2 (0.0929 m^2) of an E/W Nominal Collector

---

* At this stage, it is still assumed that the collector performance is equal to the clean, as tested, collector performance and system parasitics are not considered. These factors are incorporated into the conceptual design in Section 4.2, Conceptual Design Rules-of-Thumb.

** The Storage Sizing Graphs do not include an efficiency for thermal energy storage. Thus, the quantity of storage would have to be increased by an appropriate storage efficiency factor, if known, in a manner similar to determining the Effective Collector Cost.

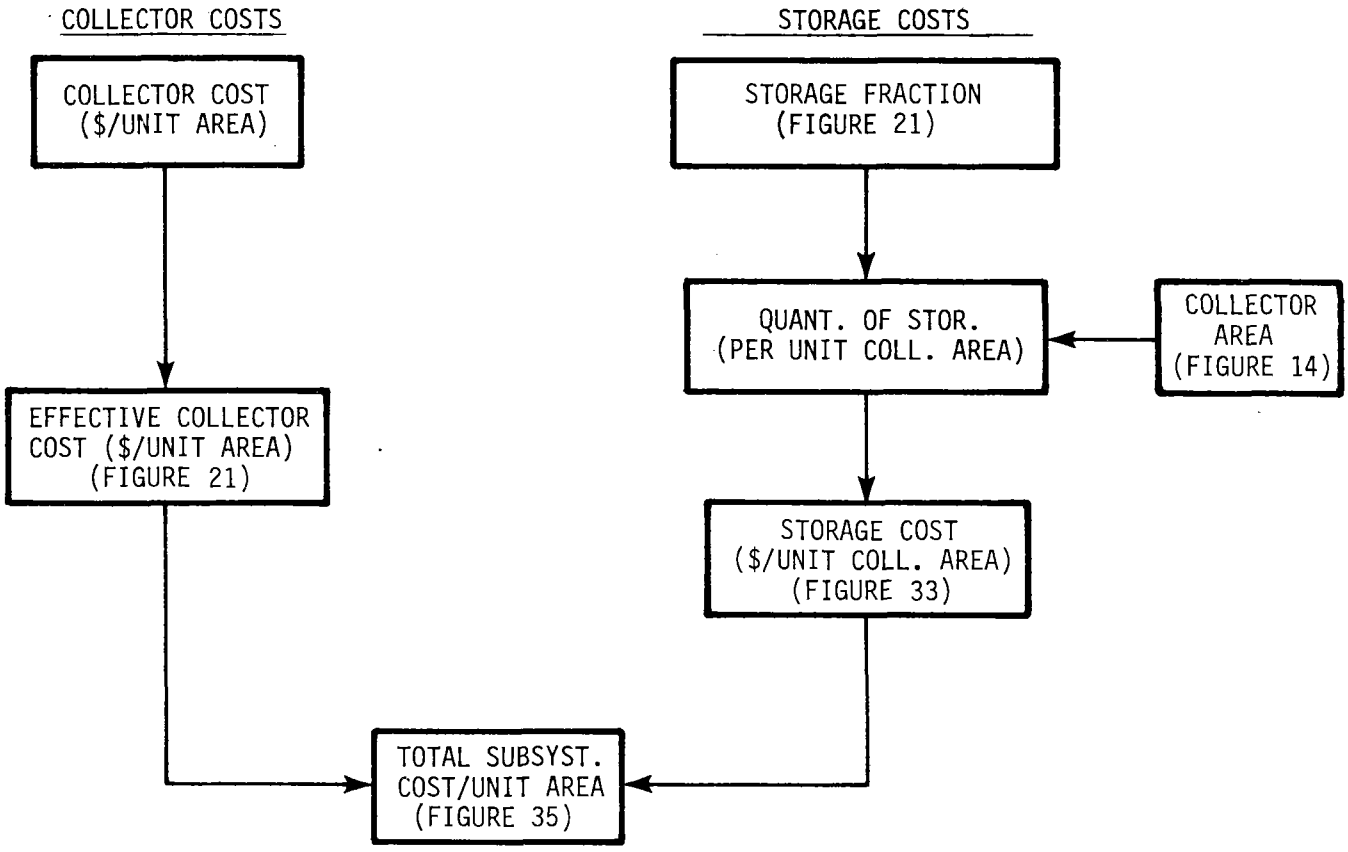

Figure 36. Logic Flow for Determining Collector/Storage Subsystem Costs

operating at 550°F (288°C) in Albuquerque will be assumed. This reduces all the computations to a per-unit-area basis directly, which will facilitate plotting the results. The Demand is assumed to be constant, 24 hours per day, 365 days per year (i.e., Figure 21 is applicable).

For the sake of illustration, the installed cost of the parabolic trough collectors will be assumed to be $\$20/ft^2$ ($\$215/m^2$). In the absence of cost data for thermal energy storage, the cost of \$8.60/kBtu (\$29.20/kWh) determined in the example in Section 3.5 will be used, and it will be assumed that storage is 100% efficient. At this point, these costs are used only to illustrate the computational techniques employed and are not meant to be indicative of any real component costs.

Since the Demand was assumed equal to the output from 1 ft^2 (0.0929 m^2) of Nominal Collector, the Storage Fraction reported in Figure 21, when multiplied by the average daily output from the Nominal Collector (see Figure 13), yields the storage capacity per ft^2 of collector directly for any given Nominal Displacement and Utilization. The Storage Capacity per ft^2 of collector, when multiplied by the cost of storage, defines the cost of storage per ft^2 of collector, i.e., $(Btu/ft^2)(\$/Btu) = \$/ft^2$.

The storage and collector costs, each multiplied by a scaling factor of 0.5, are graphically added in Figure 37* to show the trends in subsystem costs. Five different curves are shown. Each curve represents the calculation of Effective Storage and Collector Subsystem Cost for each combination of Storage Fraction and Utilization shown in Figure 21 for the indicated Nominal Displacement. The curves in Figure 37 support the design criterion that the lowest-cost storage and collector subsystem is one which does not include storage yet permits high Utilization. If storage is incorporated, sufficient storage should be provided to allow near-100% Utilization of the collected solar energy for a given Nominal Displacement. For example, in the case of a Nominal Displacement of 0.8, Effective Storage and Collector Subsystem Cost decreases until a Storage Fraction of about 0.5 to 0.6 is achieved. Beyond this Storage Fraction, additional storage becomes less effective (as was seen in Figure 21), and subsystem costs increase. Computation of Effective Storage and Collector Subsystem Costs can be used to determine the lowest cost combination of collector area and storage capacity if component costs are known. Figure 37 will be used again in Section 4.4 during execution of the example conceptual design.

---

*Figure 37 was drawn to be used with any system of units employed by the designer. Thus, both the x- and y-axes are per unit area, with no defined units. To use Figure 37 with Effective Collector and Storage Costs larger in magnitude than the numbers shown in Figure 37, simply multiply all costs by the scaling factor needed to make these costs fit on the graph. The actual Effective System Costs will then simply be the Effective System Costs from Figure 37 divided by the scaling factor. In the current example, a scaling factor of 0.5 is used.

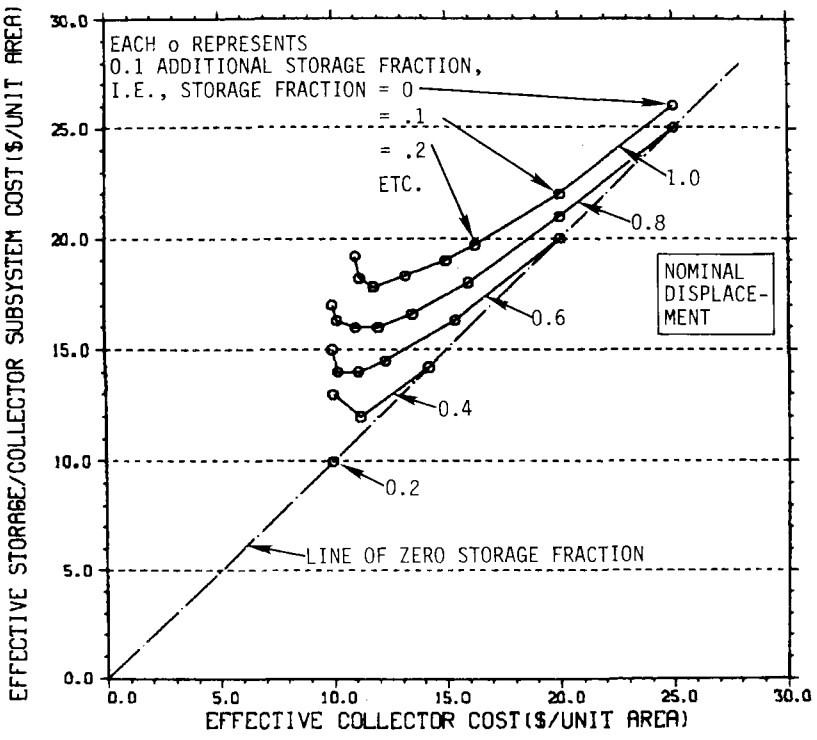

Figure 37. Determination of Subsystem Costs

Notice that as the Nominal Displacement increases, the Effective Storage/Collector Subsystem Cost increases, reflecting the increasing role of storage. If, however, the incremental costs of storage were evaluated, as was the Incremental Storage Ratio in Section 2.1.1 (see discussion of Maximum Displacement Point), it would be found that the incremental storage costs per unit of increased Actual Displacement remain constant up to the Maximum Displacement Point of the Storage Sizing Graphs. At this point, incremental storage costs would increase rapidly, as did the Incremental Storage Ratio in Figure 23.

4. CONCEPTUAL DESIGN PROCEDURE

The basic characteristics of both the collectors and storage have been defined to the extent necessary to complete the conceptual design. At this stage in the design process, the objective is to look at the solar energy system's ability to interface with a process heat demand. Of primary importance is an approximation of the collector and land area needed and the portion of the fossil fuel demand which can reasonably be displaced by the solar energy system. If at this point the concept appears feasible, the preliminary design stage can be started.

This section assembles the methods discussed in Sections 2 and 3 for predicting collector performance and Storage Capacity into a procedure for achieving a conceptual design of a solar thermal energy system using parabolic troughs. The influence of the application on the Collector Operating Temperature is examined. In addition, the inclusion of thermal storage in the solar energy system can influence the desired Collector Operating Temperature. Thus, the application and whether or not the system includes storage combine to define the appropriate Collector Operating Temperature. These effects are evaluated in Section 4.1, "System Integration."

Once the influence of the application and storage on system design is understood, Design Rules-of-Thumb are formulated in Section 4.2. These Design Rules-of-Thumb can then be used as the starting point for conceptual design. The logic flow in achieving a conceptual design is then presented in Section 4.3, followed by several examples in Section 4.4 to illustrate the design procedure.

While specific recommendations are made for selecting appropriate collector area and Storage Capacities in the form of Conceptual Design Rules-of-Thumb, other designs can, of course, be formulated. There is sufficient information in the Storage Sizing Graphs to determine the collector area and Storage Capacity needed to achieve a reasonable Actual Displacement desired. In areas having low availability of Direct Insolation, a designer may, for example, elect to deploy a larger collector field and storage combination than suggested by the Maximum Displacement Point in order to achieve a larger Actual Displacement. The Conceptual Design Rules-of-Thumb that are derived from the concept of the Maximum Displacement Point simply help to define the most cost-effective deployment of collector and storage capital equipment. Other designs could be developed which would have higher Effective Storage and Collector Subsystem Costs but might better suit the particular needs of a given application.

4.1 SYSTEM INTEGRATION

System integration begins with an examination of how the type of Demand affects selection of the appropriate Collector Operating Temperature. Two significantly different types of thermal energy Demands are examined. Each strongly influences the solar energy system design. One type of Demand is a sensible heating system in which the process heat transfer fluid experiences large temperature swings, and the second type of Demand is a phase change system, such as steam, which tends to operate within rather narrow temperature limits.

4.1.1 Sensible Heat Demand

A sensible heat Demand, in which the temperature of the process fluid varies over a wide temperature range, is perhaps the type of Demand most easily serviced by a parabolic trough collector. This type of Demand, which may, for example, involve heating a heat transfer oil in an existing process heat system, closely matches the thermal characteristics of the solar collector field. The collector field collects thermal energy through a sensible heat mechanism and, as a result, undergoes large temperature swings. Thus, it is conceivable

that the temperature in the collector field could be made to conform closely to the temperatures of the process heat transfer fluid. Conceptual design of the solar energy system can proceed in a rather straightforward manner because the average operating temperature of the collector field is approximately equal to the average process temperature. This is not the case with a latent heat demand such as a process steam system.

4.1.2 Latent Heat Demand (Process Steam)

Process heat is most commonly delivered to an application in the form of steam. The design difficulty encountered in a process steam system is the interfacing of a sensible heat solar collection system with a latent heat (i.e., steam) process heat system. The problem is illustrated schematically in Figure 38 for a hypothetical case in which 150 psi (1.1×10^6 Pa) saturated steam at 360°F (182°C) is desired.

In transit to the point of use, the steam will suffer a small pressure drop and heat loss in the pipe. Any line condensate that results is usually removed by traps. These pressure and heat losses, however, are typically very small and are not explicitly shown in Figure 38.

After condensation of the steam by the process, the hot water is returned to the boiler for revaporization. While the hot condensate may be used for preheating, this is not shown on Figure 38 in order to simplify the discussion at this point. The hot condensate is assumed to be saturated. The primary design problem here is how to interface the relatively constant temperature process steam system with a solar energy collection system which operates best with large swings in temperature.

Sensible heat addition to the process steam generator is indicated on Figure 38 in the form of straight lines. As shown, several options are available with the constraint imposed by the second law of thermodynamics--the temperature of the collector fluid must, at any

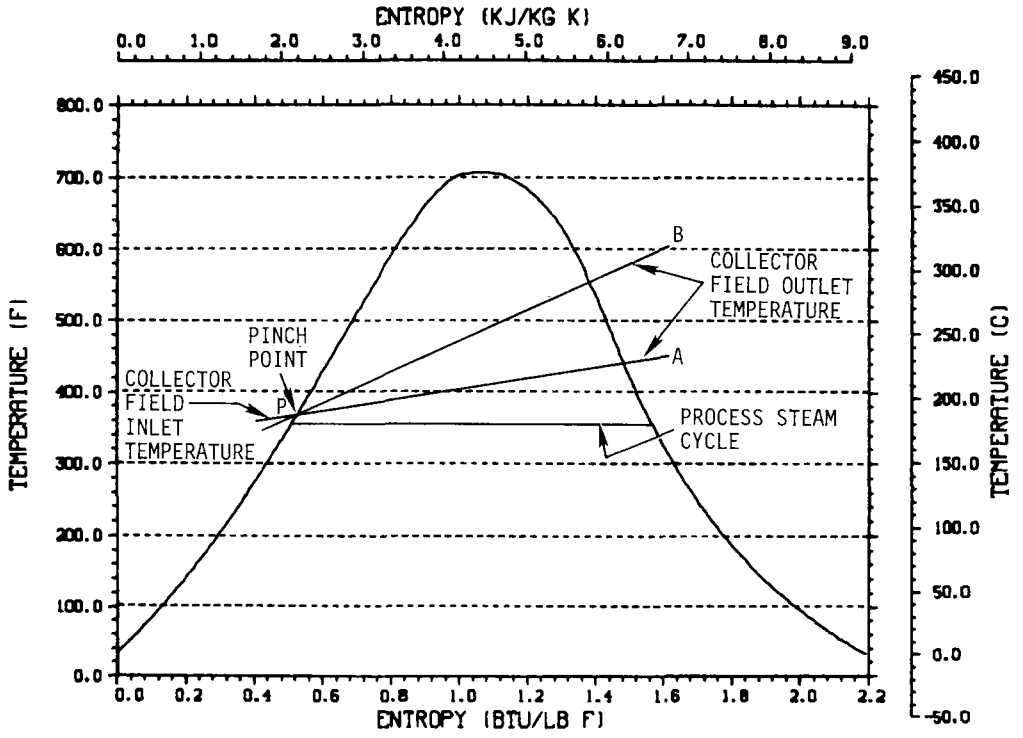

Figure 38. Process Steam Cycle (Adopted from Keenan and Keyes, Thermodynamic Properties of Steam)

given point, be greater than the corresponding temperature of the process fluid in order for heat transfer from the collector fluid to the process fluid to occur. The two different heat addition lines for the collector fluid (lines PA and PB) represent different ΔT's across the collector field.

At first consideration, heat addition line PA might appear best. This heat addition process would result in the lowest average collector temperature of the two situations and, as discussed in Section 2.5, collector performance increases with decreasing operating temperature. There are, however, system considerations which can force a system design away from one in which the ΔT across the collector field is small and toward designs in which the ΔT is large, such as represented by line PB.

A system level consideration which favors a large collector field ΔT is storage. Most storage concepts developed to the point where

they would be used in near-term solar energy systems employ sensible heat. The ΔT across the storage system is essentially the ΔT across the collector field. As the sensible heat storage ΔT increases (and thus the collector field ΔT increases), the volume of storage required to store a given quantity of energy decreases, resulting in decreased storage costs.

These trade off considerations are represented schematically in Figure 39. As the collector field ΔT increases, the collector field efficiency decreases, effectively increasing the cost of the collectors. On the other hand, as the collector field ΔT increases, storage costs decrease. The challenge for the designer is to find the conditions representing the most cost-effective system.

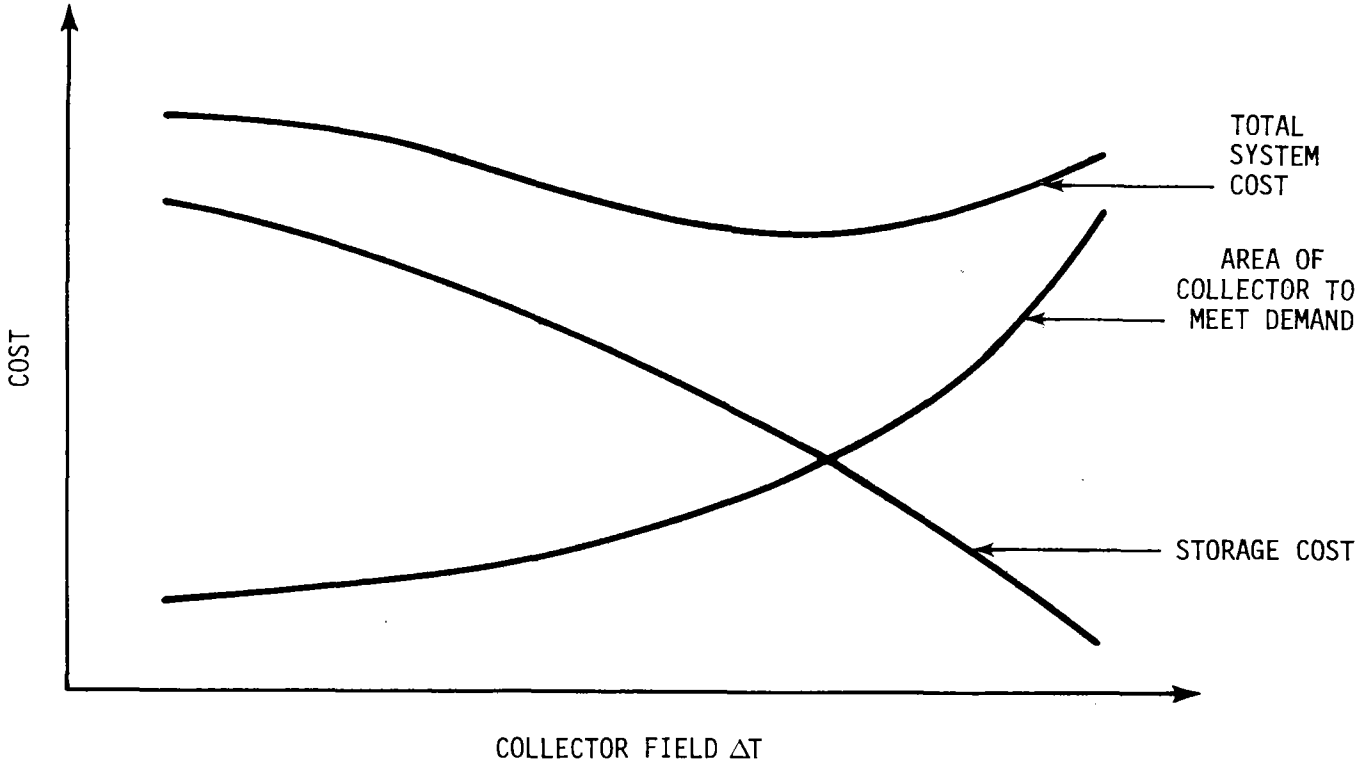

Figure 39. Effect of Collector Field ΔT on Solar Energy Subsystem and System Costs

4.2 CONCEPTUAL DESIGN RULES-OF-THUMB

At this stage, approximate rules-of-thumb can be formulated which are applicable to the design of process heat systems. The purpose of

these rules-of-thumb is to provide a starting point for the conceptual design. The rules will be listed simply as a group to provide easy reference. The list is followed by the rationale for each rule.

4.2.1 Process Steam Demands

Rule 1. Collector Field ΔT (No Storage). In the absence of storage, the collector field ΔT will be approximately 100°F (56°C) to 150°F (83°C) or the difference between 600°F and the steam delivery temperature, whichever is smaller.

Rule 2. Collector Field ΔT (Sensible Heat Storage). If significant storage capacity is to be provided in the solar energy system, the collector field ΔT will be approximately the difference between 600°F (315°C) and the steam delivery temperature or 250°F (121°C), whichever is smaller.

Rule 3. Collector Operating Temperature. The Collector Operating Temperature will be one-half the collector field ΔT above the steam delivery temperature.

4.2.2 Sensible Heat Demands

Rule 4. Collector Field ΔT (No Storage). When a solar energy system services a process heat Demand which uses a sensible heating mechanism (i.e., not a process steam system), the collector field ΔT will be approximately 100°F (56°C) to 150°F (83°C) or the process ΔT, whichever is greater.

Rule 5. Collector Field ΔT (Sensible Heat Storage). If significant Storage Capacity is to be provided in the solar energy system, the collector field ΔT will be approximately the difference between the process low temperature and 600°F (315°C) or 250°F (121°C), whichever is smaller.

Rule 6. Collector Operating Temperature. The Collector Operating Temperature will be one-half the collector field ΔT above the process low temperature.

4.2.3 General

Rule 7. Land Area Requirements. The land area required for the deployment of both E/W and N/S parabolic trough solar collectors is approximately 2.0 to 3.5 times the total aperture area of the collectors.

Rule 8. Collector Orientation. Unless the performance of E/W and N/S collectors differs more than 20% at a given site, the conceptual design should be executed using the performance of an E/W parabolic trough collector.

Rule 9. Storage Capacity. If storage is to be incorporated into the system conceptual design and there is no a priori reason to limit collector field size, the proper collector area and Storage Capacity are those associated with the Maximum Displacement Point in the appropriate Storage Sizing Graph.

Rule 10. Cost of Sensible Heat Storage. The cost of sensible heat storage in neat oil can be estimated for conceptual design purposes by the following relationship:

$$\text{Storage cost (\$/kBtu)} = 260\ P_1 V/(\Delta T_1 E)$$

$$\text{Storage cost (\$/kWh)} = 1.86\ P_2 V/(\Delta T_2 E)$$

where

ΔT = Temperature rise across the collector field
P_1 = Cost of oil (\$/gal)
P_2 = Cost of oil (\$/m^3)
V = Void fraction (1.0 for neat oil systems)
E = Efficiency of Thermal Energy Storage (Fraction)
ΔT_1 = °F
ΔT_2 = °C

Rule 11. Decrease of Collector Output for System Parasitics. The thermal energy output from an installed parabolic trough collector

field will be 75% to 80% of the output from a clean, as tested, isolated collector.

4.2.4 Rationale for Design Rules-of-Thumb

The rationale for the Design Rules-of-Thumb is based primarily upon the above discussions concerning the interaction of the collector field and storage and the costs of oil sensible heat storage. The rules are repeated for easy reference.

Rule 1. Collector Field ΔT (No Storage). In the absence of storage, the collector field ΔT will be approximately 100°F (56°C) to 150°F (83°C) or the difference between 600°F and the steam delivery temperature, whichever is smaller.

In the absence of storage, the lowest field ΔT (and, hence, average operating temperature of the collector field) compatible with reasonable pumping power requirements and thermal losses from field piping is desirable. This will usually lead to a field ΔT of about 100°F to 150°F (56°C to 83°C) (based upon the parabolic trough development program). As can be seen in Figure 38, the lowest temperature the collector field heat transfer fluid can normally achieve approximates the steam temperature because of the pinch point at P.

Rule 2. Collector Field ΔT (Sensible Heat Storage). If significant storage capacity is to be provided in the solar energy system, the collector field ΔT will be approximately the difference between 600°F (315°C) and the steam delivery temperature or 250°F (121°C), whichever is smaller.

The second Rule-of-Thumb is a result of the desire to reduce storage costs by increasing the ΔT across storage. While the proper ΔT would typically be determined through an economic optimization, changes in the average Collector Operating Temperature due to adjustment of the collector field ΔT usually affects storage costs more than

collector costs. This Rule-of-Thumb yields a good starting point for design. Thus, in the absence of Collector Operating Temperature limitations, the least-cost storage will result when the collector field is operated at its maximum ΔT. Due to the pinch point, the minimum temperature experienced by the collector field heat transfer fluid will be, as discussed above, close to the steam temperature. The 600°F (315°C) temperature limit of Rule 2 is imposed by fluid stability. Most organic oil heat transfer fluids currently in use in parabolic trough collector fields and sensible heat storage are not recommended for use much above 600°F. The 250°F (121°C) limit on ΔT comes from current collector designs typically not allowing a greater ΔT due to the excessive pumping parasitics required for long ΔT strings. Typical collector designs provide for a fluid temperature rise of about 0.5°F (0.3°C) per linear foot of trough when the fluid flow is just above the transition to turbulent flow region.

Rule 3. Collector Operating Temperature. The Collector Operating Temperature will be one-half the collector field ΔT above the steam delivery temperature.

The average collector temperature is simply the average between the collector inlet and outlet temperatures. Rule 3 follows from the collector inlet temperature being defined by the steam temperature (see Rule 1).

Rule 4. Collector Field ΔT (No Storage). When a solar energy system services a process heat Demand which uses a sensible heating mechanism (i.e., not a process steam system), the collector field ΔT will be approximately 100°F (56°C) to 150°F (83°C) or the process ΔT, whichever is greater.

In a process heat system with no storage that uses sensible heat rather than a latent heat system, the temperature of the collector field tends to closely follow the process temperatures, as discussed in Section 4.4.1, unless the ΔT across the process is small. If the

process ΔT is small, the minimum collector field ΔT will be about 100°F (56°C) to 150°F (83°C) in order to keep pumping parasitics within reason.

Rule 5. Collector Field ΔT (Sensible Heat Storage). If significant Storage Capacity is to be provided in the solar energy system, the collector field ΔT will be approximately the difference between the process low temperature and 600°F (315°C) or 250°F (121°C), whichever is smaller.

As in Rule 2, the cost of storage tends to drive the collector field ΔT as large as possible without allowing the collector fluid to exceed 600°F (315°C). The 250°F (121°C) limit on the ΔT stems from current collector designs typically not allowing ΔTs of much more than 250°F (121°C) due to the excessive pump power required to maintain turbulent flow conditions in long ΔT strings within the collector field (see Rule 2).

Rule 6. Collector Operating Temperature. The Collector Operating Temperature will be one-half the collector field ΔT above the process low temperature.

The average collector temperature is simply the average between the collector inlet and outlet temperatures. Rule 6 follows from the desire to maintain the collector field inlet temperature close to the sensible heat demand low temperature.

Rule 7. Land Area Requirements. The land area required for the deployment of both E/W and N/S parabolic trough solar collectors is approximately 2.0 to 3.5 times the total aperture area of the collectors.

Land area requirements are based upon trade off analyses of collector shading and thermal heat losses in the collector field piping. The shading within trough collector fields was discussed in Section 2.6.

Rule 8. Collector Orientation. Unless the performance of E/W and N/S collectors differs more than 20% at a given site, the conceptual design should be executed using the performance of an E/W parabolic trough collector.

In the absence of shading, N/S collectors typically produce more thermal energy than equivalent E/W collectors. However, N/S collectors suffer more shading losses in real situations than do E/W collectors (see Section 2.6). This tends to reduce N/S collector performance with respect to E/W collector performance. In addition, the annual collector output profile for an E/W collector tends to be flatter than that for a N/S collector. This, as discussed in Section 3.1, allows an E/W collector field greater potential fossil fuel displacement during a year.

The net result of these somewhat counteracting influences is that doing a conceptual design using an E/W trough provides a reasonable estimate of collector area and the maximum potential for fossil fuel Displacement if storage is provided. Differences between E/W and N/S collector arrays would be further evaluated in preliminary design. The proper selection of either a N/S or an E/W field can only be made by computing the cost of both and determining whether or not the extra Displacement allowed by an E/W collector field warrants any increase in costs.

Rule 9. Storage Capacity. If storage is to be incorporated into the system conceptual design and there is no a priori reason to limit collector field size, the proper collector area and Storage Capacity are those associated with the Maximum Displacement Point in the appropriate Storage Sizing Graph.

The justification for this Design Rule-of-Thumb is presented in Section 3.1.

Rule 10. Cost of Sensible Heat Storage. The cost of sensible heat storage in neat oil can be estimated for conceptual design purposes by the following relationship:

$$\text{Storage cost (\$/kBtu)} = 260\ P_1 V/(\Delta T_1 E)$$

$$\text{Storage cost (\$/kWh)} = 1.86\ P_2 V/(\Delta T_2 E)$$

where

ΔT = Temperature rise across the collector field
P_1 = Cost of oil (\$/gal)
P_2 = Cost of oil (\$/m^3)
V = Void fraction (1.0 for neat oil systems)
E = Efficiency of Thermal Energy Storage (Fraction)
ΔT_1 = °F
ΔT_2 = °C

At elevated temperatures, an oil storage medium is typically used to avoid pressurized systems. This Rule-of-Thumb is based upon the use of Figure 35, employing generalized physical properties of oil heat transfer fluids. Many of the high-temperature oil heat transfer fluids in use in solar energy systems have heat capacities in the range of 0.5 to 0.6 Btu/lb·°F (0.5 to 0.6 cal/g·°C) and densities in the range of 7.5 to 6.5 lb/gal (900 kg/m^3 to 780 kg/m^3) in the temperature range of 300°F (149°C) to 700°F (371°C). The equation given in Rule 4 was obtained from Figure 35, choosing nominal values of 0.55 Btu/lb·°F (0.55 cal/g·°C) and 7.0 lb/gal (840 kg/m^3) for the oil heat capacity and density, respectively. If known, actual properties can be used to obtain storage costs from Figure 35, but in the absence of such information, Rule 10 provides a reasonable starting point for the conceptual design process (see Appendix F for limitations).

Rule 11. Decrease of Collector Output for System Parasitics. The thermal energy output from an installed parabolic trough collector field will be 75% to 80% of the output from a clean, as tested, isolated collector.

As mentioned in Section 2.5, thermal losses from field piping, dirt on the collectors, and to a lesser extent intercollector shadowing will reduce the collector field thermal energy output calculated using test data. Experience has indicated that this reduction will be about 75% to 80% for a typical field. While these losses are not explicitly evaluated in conceptual design, applying a correction factor of 0.75 to 0.80 to the calculated collector output will provide a realistic approximation of actual installed collector field performance.

4.3 SUMMARY OF CONCEPTUAL DESIGN METHOD

The procedure for arriving at a conceptual design is fast and easily applied when the Design Rules-of-Thumb listed in Section 4.2 are employed. The application of these rules, when employed in conjunction with the Storage Sizing Graphs (Section 3.1, Appendix E), quickly yields a credible conceptual design. The logic path from definition of the Demand through achievement of the conceptual design is outlined in Figure 40. Where appropriate, the Design Rule-of-Thumb, together with the section in the Handbook that discusses development of the design charts used, is indicated.

The design process starts with the definition of the Demand characteristics. The temporal profile of the Demand defines which Storage Sizing Graph to use. The temperature characteristics of the Demand, when taken together with the desire to have a system which either includes storage or has no storage, define the collector field ΔT. Typically both storage and no-storage designs are performed.

Rules 1 and 2 apply to process steam systems and Rules 4 and 5 to sensible heat demands. The collector field ΔT in turn defines the Collector Operating Temperature which, together with collector performance characteristics, provides the average annual collector performance. Nomographs developed in Section 2.4 and reproduced in Appendix H allow projection of annual collector performance for collectors which have only efficiency versus $(T_{col} - T_{amb})/I$ test data available. Published average annual performance data can be used if available.

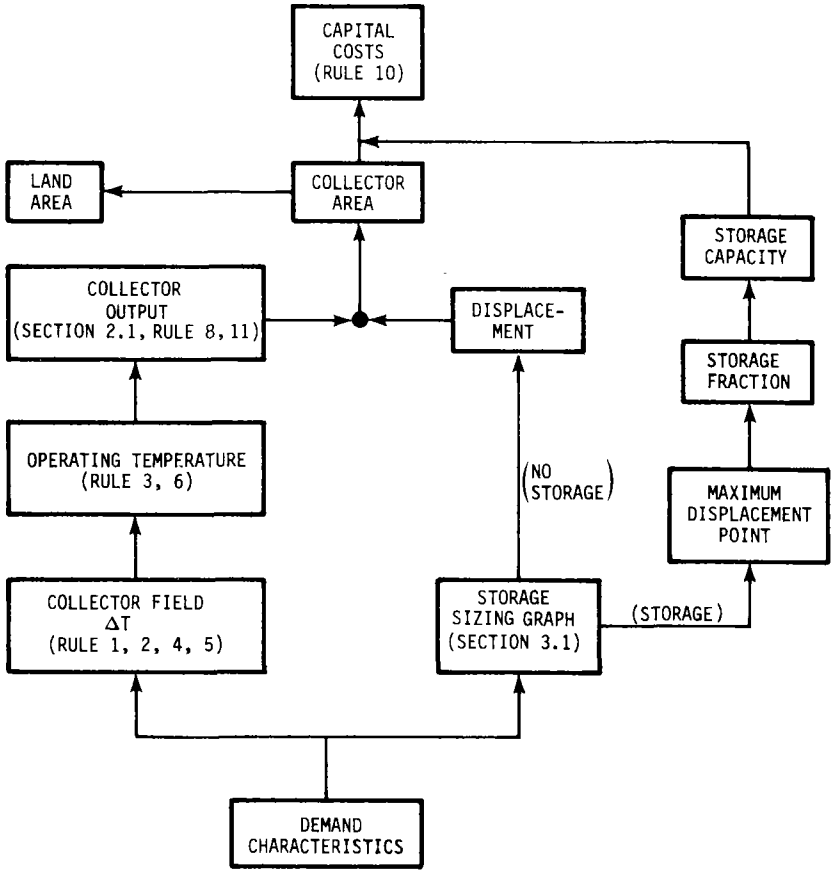

Figure 40. Logic Flow of Conceptual Design Process

The Storage Sizing Graphs are used to determine the relationship between needed collector output, Storage Capacity, and Demand. Only solar energy systems which provide near-100% Utilization of the collected solar energy are selected. In the case of systems incorporating storage, the design point is the Maximum Displacement Point. Multiplying the Nominal Displacement by the Demand yields the quantity of energy displaced by the solar energy system. Dividing the quantity of energy displaced by the per-unit-area collector output and adjusting for field losses (Rule 11) yields the required collector area. Finally, multiplying the Storage Fraction by the average daily Demand yields the necessary Storage Capacity.

If estimates of storage costs (Rule 10) and collector costs are available, total storage/collector subsystem capital costs can be approximated. The net results of the conceptual design are the Displacement of fossil energy, the collector area and Storage Capacity

needed to achieve this displacement, the approximate land area needed for collector deployment, and an estimate of the total capital costs.

4.4 CONCEPTUAL DESIGN -- EXAMPLE PROBLEMS

To illustrate the preceding design procedures, a hypothetical 150-psi (1.1×10^6-Pa) process steam system has been defined, and a retrofit solar energy system will be designed to service the Demand for thermal energy. Figure 41 outlines the thermal energy flow paths of the fossil fuel energy system, located in Albuquerque, together with the important temperatures and pressures needed to define the system. The solar retrofit, consisting of an E/W collector field and sensible heat storage, is also shown with the fossil fuel system retained for backup. The first Demand profile considered will be constant, 24 hours per day, 365 days per year. The temperature-entropy (T-S) diagram in Figure 42 traces the thermal characteristics of the process heat supply.

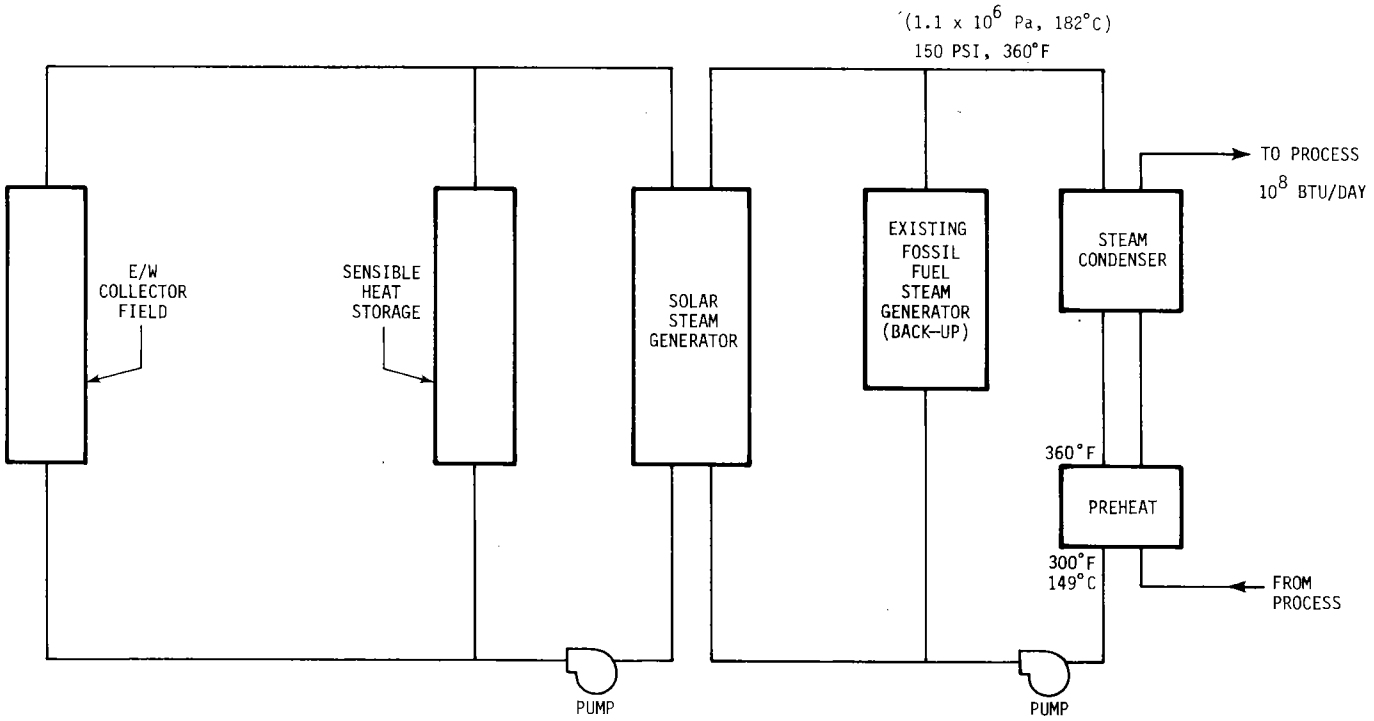

Figure 41. Thermal Energy Flows in Example Problem

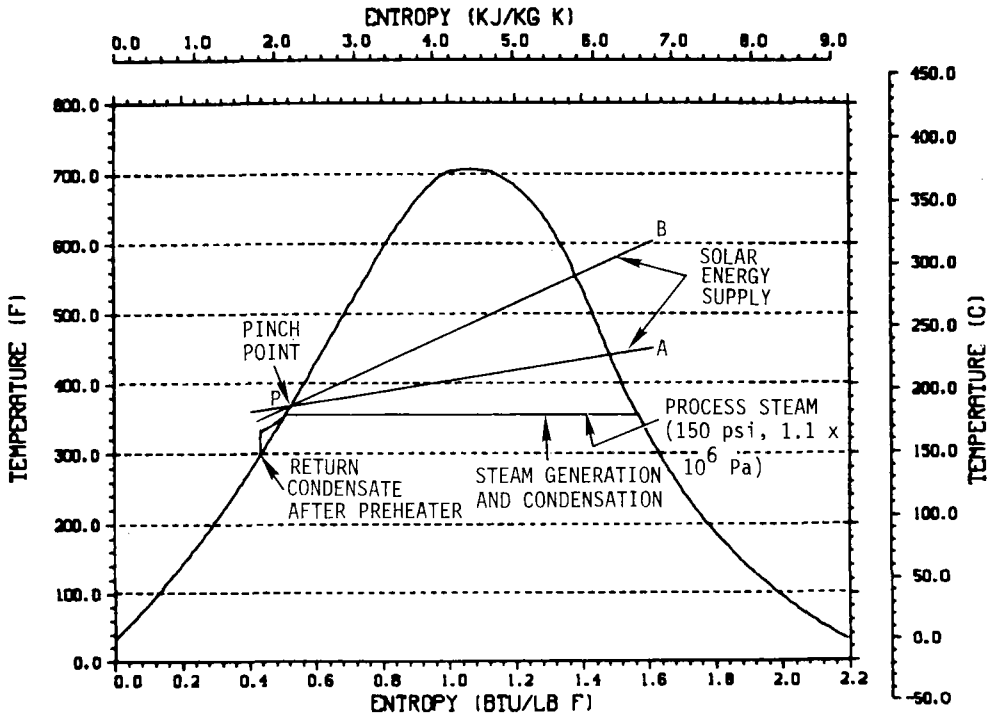

Figure 42. Temperature-Entropy Diagram for Example Problem (Section 2.4) (Adapted from Keenan and Keyes, Thermodynamic Properties of Steam)

Two basic choices are available for the solar energy system--a system including storage and a system without storage. Typically, both options are considered at the conceptual design stage. This example illustrates the design of both storage and no-storage systems. An E/W collector orientation is chosen for the conceptual design in concert with Design Rule-of-Thumb No. 8.

A hypothetical parabolic trough collector performance will be assumed. The performance of this collector is plotted in Figure 43 and is denoted as "Example Collector." This plot of Collector Efficiency versus $(T_{col} - T_{amb})/I$ is typical of the form in which performance data is published for commercial collectors. The Nominal Collector is also shown in Figure 43. Figure 43 is the nomograph which will be used to project the annual average thermal energy output from the Example Collector (see Section 2).

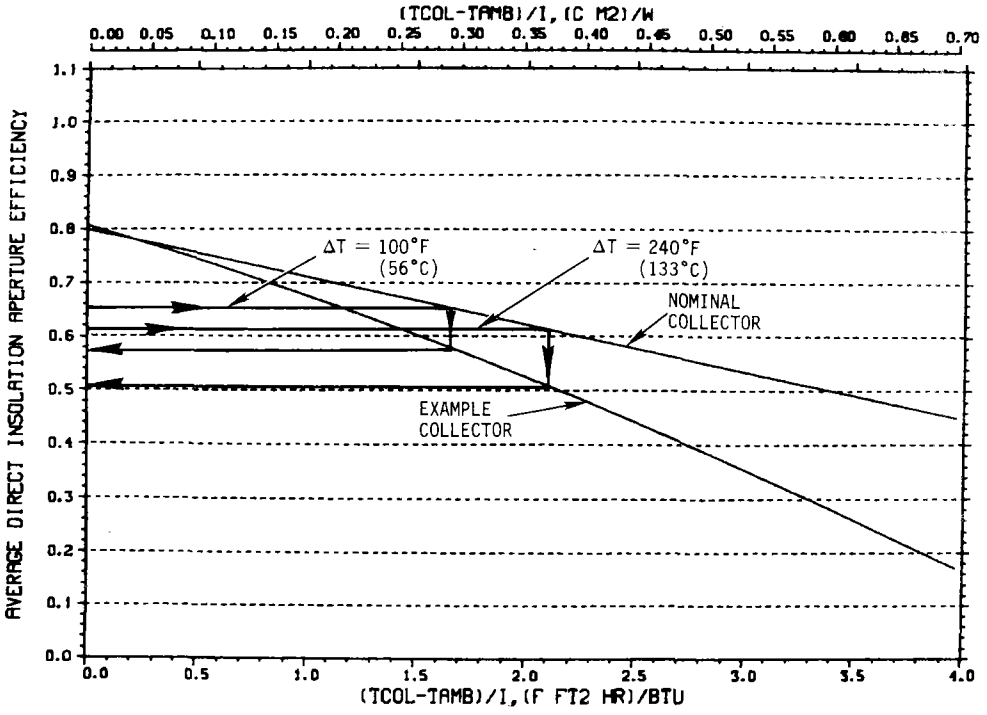

Figure 43. Performance Characteristics of Collector Used in Example Conceptual Design

4.4.1 No Storage

As observed in the Storage Sizing Graphs for this type of Demand profile (see Figure 22 or Appendix H), the main effect of having no storage in a solar thermal energy system is to restrict the amount of the Demand which can be displaced to a small fraction of the total Demand. In the case of Albuquerque, only about 20% of the Demand can be displaced with near 100% Utilization by an E/W collector field having no thermal energy storage.

Using Design Rule-of-Thumb No. 1 for a no-storage system, the average operating temperature of the collector field will be about 410°F (210°C), reflecting a ΔT across the collector field of 100°F (56°C) (line PA, Figure 42). In order to determine the annual output from the Example Collector, Figure 43 is used. From Appendix H (or Figure 16), the annual average output of the Nominal Collector at 410°F (210°C) is seen to be about 1140 Btu/day.ft^2 (3.6 kWh/day.m^2).

The direct insolation incident on the collector aperture (see Figure 7 or Appendix H) is 1750 Btu/day·ft^2 (5.5 kWh/day·m^2). From Figure 43, the annual Average Direct Insolation Aperture Efficiency for the Example Collector is seen to be about 0.57, resulting in an energy output of 998 Btu/day·ft^2 (3.1 kWh/day·m^2) at an average operating temperature of 410°F (210°C).

Figure 43 also shows that increasing the collector field ΔT to 240°F (133°C), as represented by line PB of Figure 42, reduces the efficiency of the Example Collector. Increasing the collector field ΔT effectively increases the Collector Operating Temperature to 480°F (249°C). The annual Average Direct Insolation Aperture Efficiency decreases to 0.605 for output from the Nominal Collector at 480°F. This converts into an Average Direct Insolation Aperture Efficiency of about 0.50 for the Example Collector or an annual average output of 875 Btu/day·ft^2 (2.8 kWh/day·m^2). This represents a 12% decrease in collector field output and supports design Rule-of-Thumb No. 1.

Given a 24-hour-per-day constant Demand of 10^8 Btu/day (29.4 MWh/day) and an average Collector Operating Temperature of 410°F (210°C), the area of E/W collector which best services the Demand can be determined. From the Storage Sizing Graph (reproduced here as Figure 44, from Appendix H), it is seen that, at best, 20% of the daily Demand can be displaced while maintaining near-100% Utilization of the collected solar energy. Thus, the collector field should be sized to provide 2.0×10^7 Btu/day (5.9 MWh/day), on the average, throughout the year. The average annual output at 410°F (210°C) of the Example Collector is, as calculated above, 998 Btu/ day·ft^2 (3.6 kWh/day·m^2). This results in a required Example Collector area of 26,720 ft^2 (2483 m^2) when adjusted by 0.75 to account for field losses (Rule 11).

If greater than 20% displacement of the fossil fuel energy is desired, additional collectors could, of course, be deployed. If no storage is added along with the additional collectors, Utilization of the collected energy falls rapidly. Thus, for example, doubling the

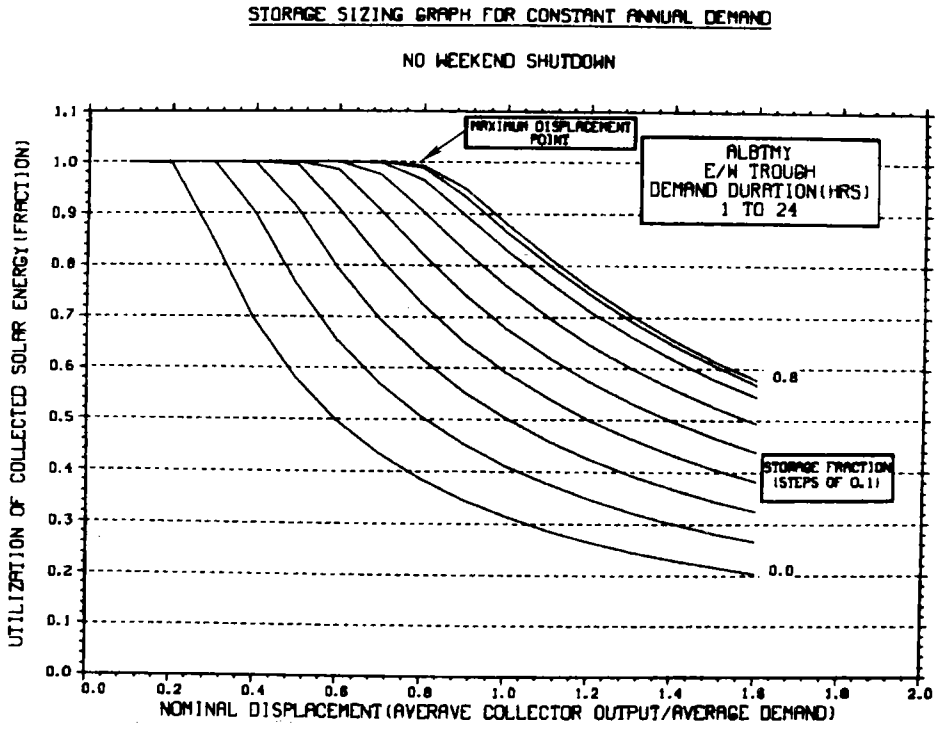

Figure 44. Storage Sizing Graph for E/W Trough--24 h/day

collector area to 53,440 ft^2 (4965 m^2) at a Nominal Displacement of 0.4 and without adding storage (i.e., Storage Fraction = 0.0), the output from the collector field increases to only (53,440)(998)(0.75)(0.7) = 2.8×10^7 Btu/day (8.2 MWh/day). This is an increase in energy delivered to the Demand of only 40%. The addition of storage would have to be quite expensive to make deploying additional collectors with a Utilization of only 40% a cost-effective way of increasing fossil fuel displacement. The land area required for collector deployment, in accordance with Design Rule-of-Thumb No. 6, is about 2.5 times the collector area or approximately 66,800 ft^2 (6207 m^2 or about 1.6 acres).

4.4.2 Sensible Heat Storage

The addition of storage to the above solar thermal energy system allows consideration of deploying larger fields of solar collectors to displace more than 20% of the Demand. The decision to add storage is an economic one. If the value of the additional fossil fuel energy

displaced is greater than the cost of the extra collectors and storage required, the increase in Displacement is worthwhile. The selection of the proper quantity of storage is not too sensitive to the cost of storage as long as the decision is made to incorporate more than just the small amount typically used for control purposes. Once the decision is made to include storage, the form of the dependence of solar energy Utilization on Storage Capacity tends to drive the design to the Maximum Displacement Point of the appropriate Storage Sizing Graph regardless of cost (see Section 3.1.3).

Thus, a conceptual design can proceed in the absence of cost figures since, for a given Displacement of a Demand, a preferred Storage Capacity can be identified. As capital costs are factored into the evaluation, the costs associated with providing more than nominal fossil fuel Displacement would become evident.

Employing Rule-of-Thumb No. 2, a collector ΔT of 240°F (133°C) is chosen and is represented in Figure 42 by line PB. This results in an average collector temperature (in accordance with Rule-of-Thumb No. 3) of 480°F (249°C). Since a collector with the performance characteristics of the Example Collector is assumed, the average daily collector output is, as computed above from Figure 43, about 875 Btu/ft^2.day (2.8 kWh/m^2.day). Following Rule-of-Thumb No. 9, the solar energy system will be designed to the Maximum Displacement Point in the Storage Sizing Graph shown in Figure 44. Sizing of the collector field and storage follows directly.

The Nominal Displacement associated with the Maximum Displacement Point in Figure 44 is 0.8. Thus, the quantity of thermal energy which must be provided by the collector field is 8×10^7 Btu/day (23.5 MWh/day). Dividing this daily demand by the average daily collector output of 875 Btu/ft^2.day (2.8 kWh/m^2.day) and 0.75 to account for field losses (Rule 11) yields the collector area needed to achieve a Nominal Displacement of 0.8. The required collector area is 121,905 ft^2 (11,324 m^2) of Example Collector. The associated Storage Capacity (i.e., Storage Fraction x daily Demand) is approximately 60% of the

average daily Demand or 6×10^7 Btu (17.6 MWh),* and the area required for collector deployment is about 304,763 ft^2 (28,310 m^2 or about 7 acres). This land area was calculated using 2.5 units of land area per unit of collector area in accordance with Rule-of-Thumb No. 6. The results of these two conceptual designs are summarized in Table 1.

Table 1

Results of Example Conceptual Design Demand = 10^8 Btu/day (29.4 MWh/day)

	Collector Area	Storage Capacity	Displacement	Land Area
No Storage	26,720 ft^2 (2483 m^2)	0	2×10^7 Btu/day (5.9 MWh/day)	1.6 acres (6207 m^2)
Storage	121,905 ft^2 (11,324 m^2)	6×10^7 Btu (17.6 MWh)	8×10^7 Btu/day (23.5 MWh/day)	7.0 acres (28,310 m^2)

An approximation of the capital costs for this solar energy system can be obtained with the help of Rule-of-Thumb No. 10. If it is assumed that the collectors could be purchased and installed for \$20/ft^2 (\$215/m^2), the capital cost for the collector field is $\$2.44\times10^6$. Using Design Rule-of-Thumb No. 10, storage costs are estimated to be \$312,000 (assuming a storage efficiency of 100%) for oil that costs about \$3.60/gal (\$950/m^3). This results in a total storage plus collector subsystem capital cost of about $\$2.75\times10^6$.

Figure 37 in Section 3.6 can be used to verify that the storage-collector subsystem sizing performed using the Design Rules-of-Thumb does indeed result in the lowest cost design for a system including storage. This is shown in Figure 45, which reproduces Figure 37 for

*Assuming 100% storage efficiency is not realistic since storage tanks lose heat and suffer degradation by other mechanisms. However, there is a general lack of information on the efficiency of thermal storage. Since the purpose here is to illustrate the design techniques and not suggest the status of storage technology development, 100% efficiency has been chosen for this example.

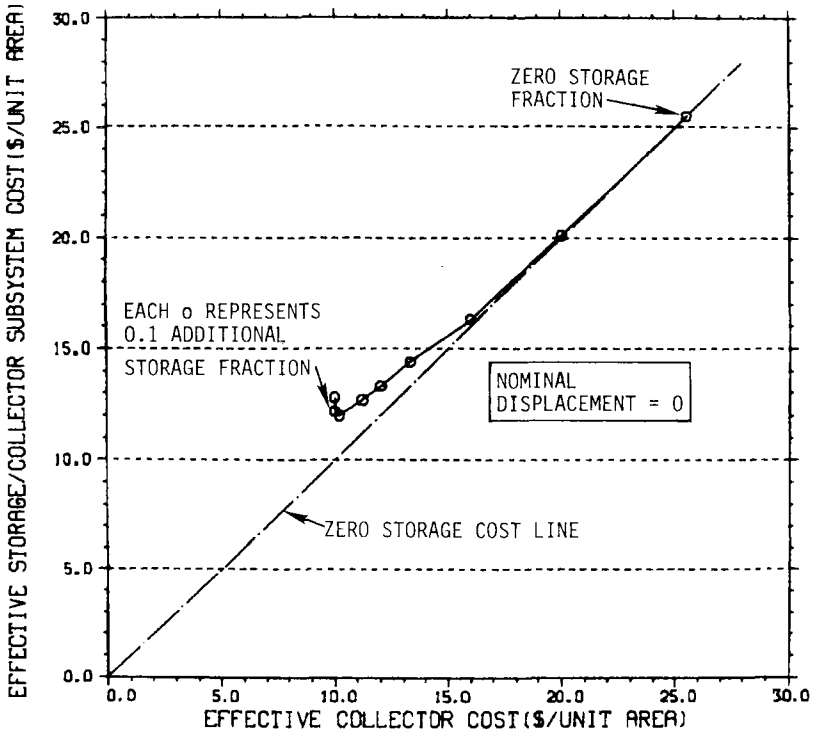

Figure 45. Determination of Minimum Cost Collector/Storage Combination for Example Problem

use with this example. The Effective Storage-Collector Subsystem Costs for a Nominal Displacement of 0.8 (see Figure 44) are shown. All costs have been scaled by 0.5 to fit on the graph. Storage cost can be computed since the cost representing a Storage Fraction of 0.6 is \$312,000. Thus, each 0.1 Storage Fraction costs \$52,000. Since there are 121,905 ft^2 of collector, the storage cost representing each 0.1 Storage Fraction is \$0.43/ft^2 of collector. The curve showing combined storage/collector costs for the various Storage Fractions at a Nominal Displacement of 0.8 is drawn in Figure 45. The minimum cost subsystem, as illustrated in Figure 45, is approximately \$24/ft^2 for a total subsystem capital cost of about $\$2.9\times10^6$. This is in agreement with the results obtained using the Design Rules-of-Thumb.

4.4.3 Example Design for a Stepped Demand Profile

As an example of how a stepped Demand profile is handled, consider the Demand profile shown in Figure 46. The application is assumed identical to that defined in Section 4.4.2 except for the Demand

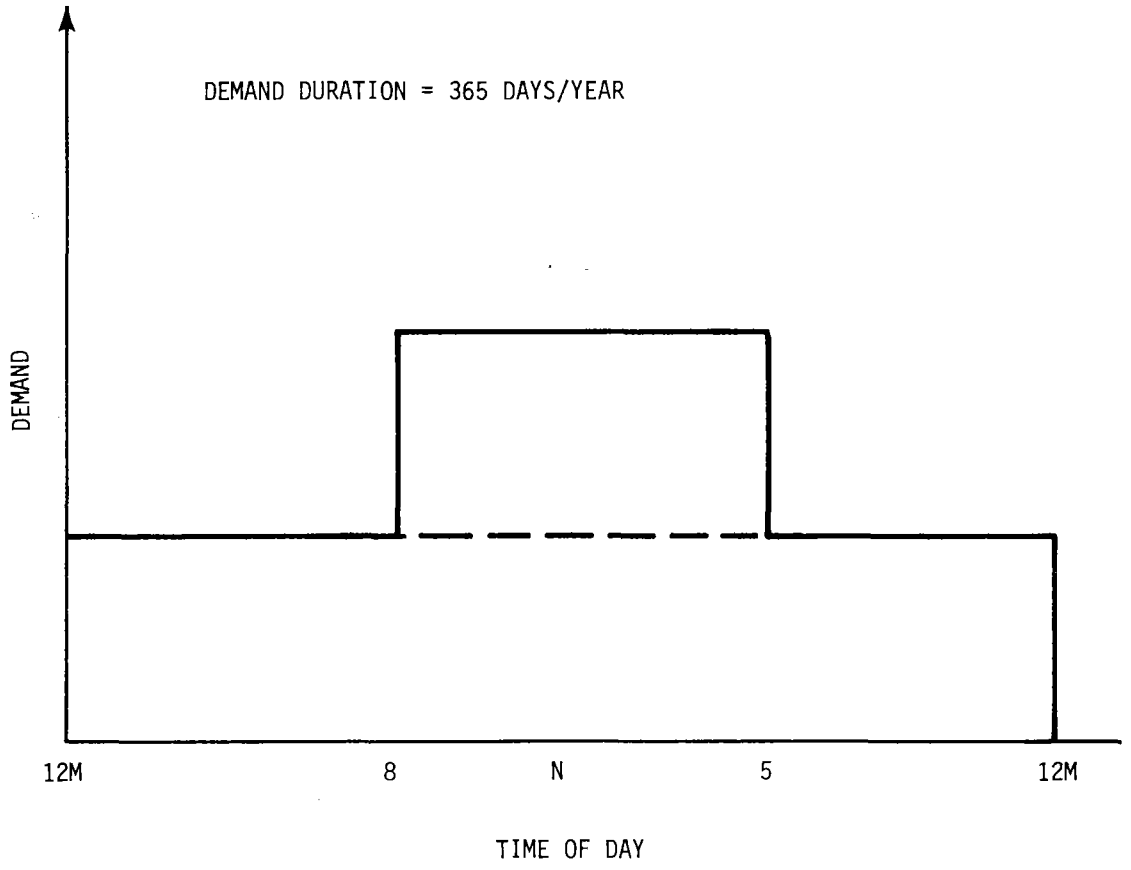

Figure 46. Example Stepped Demand Profile

profile. The Demand for this example will be assumed constant at 4.167×10^6 Btu/h (1.2 MW) between midnight and 8 am and between 5 pm and midnight. During the hours between 8 am and 5 pm, the Demand is assumed to double to 8.33×10^6 Btu/h (2.4 MW). This stepped Demand can be thought of as the superposition of two Demands. One Demand is constant, 24 hours per day, 365 days per year, while the other is also constant but present only during daylight hours. The 24-hour Demand is equal to $(24)(4.167 \times 10^6) = 10^8$ Btu/day (29.3 MWh/day). This is the Demand of the example conceptual design performed in Sections 4.4.1 and 4.4.2. The separate daytime-only Demand is equal to $(9)(4.167 \times 10^6) = 3.75 \times 10^7$ Btu/day (10.8 MWh/day).

The 24-hour Demand serviced by an E/W Baseline Collector has already been examined, and the design procedures need not be repeated. Thus, a conceptual design need only be performed for the daytime Demand and the resulting collector area and Storage Capacity added to

that of the 24-hour Demand conceptual design. For brevity, only a solar energy system employing E/W Example Collectors and containing storage will be designed.

Figure 47 reproduces the appropriate Storage Sizing Graph from Appendix H. The Maximum Displacement Point in Figure 47 occurs at a Nominal Displacement of 0.8 and a Storage Fraction of 0.3. Thus, the appropriate area of Example Collector, which has an average thermal output of 875 Btu/ft^2·day (3.35 kWh/m^2·day), is $(3.75\times10^7)(0.8)/[(875)(0.75)]$ = 45,714 ft^2 (4247 m^2). The capacity of thermal storage is obtained by multiplying the Storage Fraction (0.3) at the Maximum Displacement Point by the separate daytime Demand of 3.5×10^7 Btu/day (10.8 MWh/day). This results in a required Storage Capacity of 11.25×10^6 Btu (3.31 MWh).

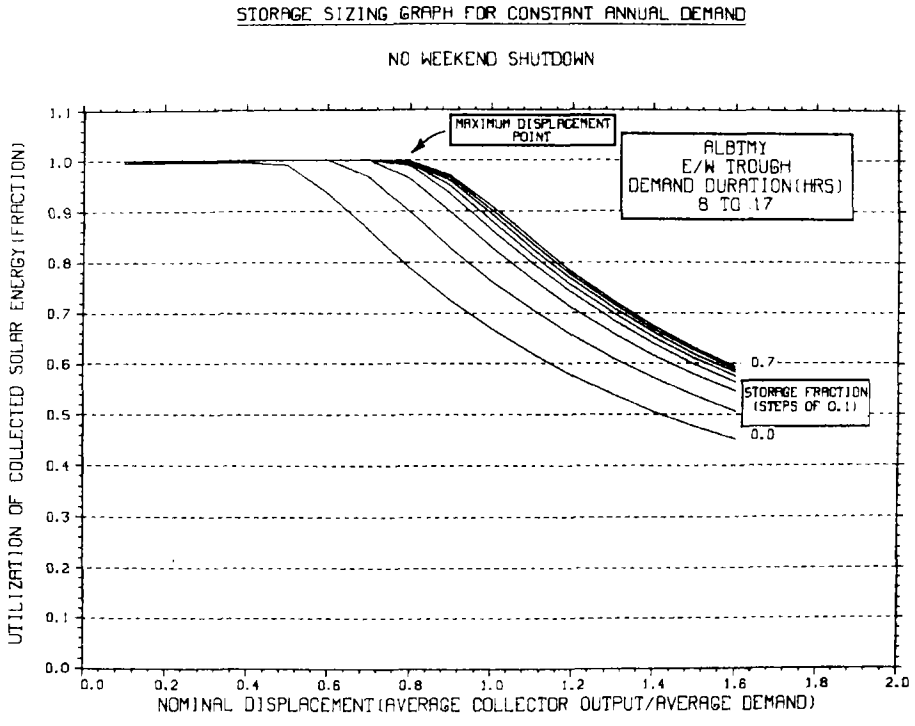

Figure 47. Storage Sizing Graph for Stepped Demand Conceptual Design Example

When the collector field sizes and Storage Capacities for the two subsystems are added, the resultant conceptual design consists of

7.125×10^7 Btu (21.0 MWh) of Storage Capacity coupled with 167,619 ft^2 (15,490 m^2) of Example Collector. If the same unit collector and storage capital costs are assumed as in Section 4.4.2, the total storage/collector capital costs for the E/W solar energy system servicing the stepped Demand of Figure 44 is $\$3.72 \times 10^6$.

Had a N/S collector orientation been chosen, the same procedures would have been followed, resulting in a system displacing only 60% of the Demand.

REFERENCES

[1] I. Hall et al, Generation of Typical Meteorological Years for 26 SOLMET Stations, SAND78-1601 (Albuquerque: Sandia Laboratories, 1978).

[2] V. E. Dudley and R. M. Workhaven, Summary Report: Concentrating Solar Collector Test Results. Collector Module Test Facility (CMTF). January-December 1978, SAND78-0977 (Albuquerque: Sandia Laboratories, 1979).

[3] John V. Otts, Midtemperature Solar System Test Facility Program Status Report, SAND80-1681 (Albuquerque: Sandia National Laboratories, 1980).

[4] E. C. Boes et al, Distribution of Direct and Total Solar Radiation Availabilities for the USA, SAND76-0411 (Albuquerque: Sandia Laboratories, 1976).

APPENDIX A

Glossary of Handbook Terminology

Absorptance -- The ratio of the actual radiant flux absorbed by a body to the radiant flux incident upon it.

Collector Azimuth -- The angle that the axis about which a parabolic trough tracks makes with the N/S line. The collector azimuth has the same sign convention as the sun azimuth angle where a clockwise rotation away from the N/S line is a negative angle while a counterclockwise rotation is a positive angle (see Figure 6, Section 2.2.1).

Collector Efficiency -- Collector efficiency can be used in many different ways, each meaning something different. The various definitions of collector efficiency are examined in detail in Appendix B. In the body of this handbook, collector efficiency will be defined as the Instantaneous Direct Insolation Aperture Efficiency (see Appendix B). Additionally, the average collector efficiency over a given period of time (e.g., average annual efficiency) will refer to the Average Direct Insolation Efficiency when applied to a parabolic trough over the time period indicated unless otherwise specified.

Collector 2 -- A hypothetical collector defined in Section 1.5.1. It was defined in order to illustrate the techniques employed in predicting long-term performance from instantaneous collector performance test data.

Collector Operating Temperature -- The average operating temperature of a parabolic trough collector. It is the arithmetic mean of the collector inlet and outlet temperatures. This definition is used both for individual collector modules and collector strings comprised of several modules to achieve large ΔTs.

ΔT -- The temperature increase associated with collection of solar energy in a parabolic trough collector field.

Demand -- The thermal energy requirements of an application.

Displacement

Actual Displacement -- That fraction of an application's average daily Demand over a year which is satisfied by thermal energy produced by a solar energy system.

Nominal Displacement -- That fraction of an application's average daily Demand over a year which could be satisifed if all the thermal energy produced by a solar energy system could be used without waste.

Effective Collector Cost -- The purchase price of a parabolic trough divided by the fractional Utilization of the thermal energy produced by the parabolic trough.

Effective Storage and Collector Subsystem Cost -- The capital costs associated with storage plus the Effective Collector Cost.

Emittance -- The ratio of the actual radiation emitted by a body to the radiation emitted by a black body at the same temperature.

Field Shadow Factor -- The ratio of the Direct Insolation incident upon all collectors in a field when shading is considered to the unshaded Direct Insolation incident upon all the collectors in a field (see Section 2.6).

Incremental Storage Ratio -- The incremental change in Storage Fraction divided by the resultant change in Actual Displacement resultant from increasing storage at a given Nominal Displacement (see Section 2.1.1 for detailed discussion).

Insolation -- The solar energy incident on a unit surface in unit time.

Direct Insolation -- The Insolation which comes from within the solid angle subtended by the solar disk.

Diffuse Insolation -- Any contribution to the Insolation that is not direct, excluding specular reflections from other objects.

Total Insolation -- The sum of Direct and Diffuse Insolation.

Direct Normal Insolation -- The Insolation on a surface perpendicular to a ray of sunlight from the center of the solar disk.

Total Normal Insolation -- The Total Insolation on a surface perpendicular to a ray of sunlight from the center of the solar disk.

Direct Aperture Insolation -- The Direct Insolation passing through the aperture of a collector. Direct Aperture Insolation is related to the Direct Normal Insolation by the Solar Incidence Angle.

Total Aperture Insolation -- The Total Insolation passing through the aperture of a collector. Total Aperture Insolation is related to the Total Normal Insolation by the Solar Incidence Angle.

Land Use Factor -- The ratio of the land area upon which a collector field is deployed to the collector aperture area.

Maximum Displacement Point -- That point on the Storage Sizing Graphs which indicates the largest practical Nominal Displacement which can be achieved with a parabolic trough field/storage combination.

Nominal Collector -- The parabolic trough, defined here only for the development of the design nomographs used in this handbook, is termed the Nominal Collector. Its purpose is to illustrate the use of design techniques only, and it is not meant to reflect the characteristics of an existing parabolic trough collector. The performance of the Nominal Collector is defined in Section 2.4.

Reflectance -- The ratio of the reflected radiant flux to the incident radiant flux.

Row Shadow Factor -- The ratio of the Direct Insolation incident upon the nonfirst row collectors in a field when shading is considered to the unshaded Direct Insolation incident upon the nonfirst row collectors (see Section 2.6).

Solar Incidence Angle -- The angle of the sun's rays with the normal to the collector aperture. By definition, the Solar Incidence Angle is zero when the sun's rays are normal to the plane of the collector aperture (see Section 1.2 for detailed discussion).

Specular Reflectance -- Refers to the radiation reflected from a surface such that the angle of reflection is equal to the angle of incidence.

Storage Capacity -- That quantity of thermal energy storage which is provided for the storage of excess solar thermal energy produced by a solar collector field.

Storage Fraction -- The ratio of the Storage Capacity provided in a solar energy system to the average daily Demand.

Storage Sizing Graphs -- A series of graphs defined in Section 3 which relate Nominal and Actual Displacement as a function of Storage Fraction. These graphs are used to size the collector field and storage in the conceptual design process.

Tracking Angle -- The angle a vector normal to the collector aperture makes with the zenith as it attempts to follow the sun. By definition, the tracking angle is 0° when the collector is up-facing. In addition, a negative tracking angle for a N/S trough indicates that the collector is facing west while a negative tracking angle for an E/W collector indicates a south-facing trough (see Section 1.2 for detailed discussion).

Transmittance -- The ratio of the radiant flux transmitted by a body to the incident radiant flux.

Utilization -- The fraction of the thermal energy produced by a solar collector field which is used in displacing an application's Demand.

Zenith -- The point in space directly overhead.

APPENDIX B

Definitions of Collector Efficiency

Several different definitions of collector efficiency are currently in use. For example, the efficiency of a parabolic trough collector is typically based only upon available Direct Insolation while the efficiency of flat plate collectors is typically based upon the available Total (Direct plus Diffuse) Insolation. In other words, a 50% efficient parabolic trough typically means that 50% of the Direct Insolation available to the collector is converted into useful thermal energy leaving the collector. A 50%-efficient flat plate collector, on the other hand, usually implies that half the Direct plus Diffuse Insolation available to the flat plate collector is converted into useful thermal energy leaving the flat plate collector. To further confuse the issue, collector efficiencies can be based either upon the Insolation passing through the collector aperture regardless of the collector's position relative to the sun (i.e., Direct or Total Aperture Insolation) or the Direct or Total Normal Insolation.

While it might be argued that only one definition of Collector Efficiency should be used, each definition has its value, and thus multiple definitions will continue in use. For example, plots of efficiency versus $(T_{col} - T_{amb})/I$, as presented in Figure 3 of Section 2.1, are based upon the Direct Aperture Insolation. However, it is also useful to consider average Collector Efficiencies based upon Total and Direct Normal Insolation since this definition of efficiency points out the difference in daily performance between tracking and nontracking collectors.

The point here is to caution the reader that several conventions for expressing Collector Efficiency are in current use. It is important to know with certainty which convention is being employed before

attempting to use published efficiency data. For the purposes of this report, the definitions below will be adhered to unless explicitly stated to the contrary.

Instantaneous Direct Insolation Aperture Efficiency -- The efficiency typically used to define the performance of concentrating collectors, as in the case of Figure 3 of Section 2.1, where the Collector Efficiency of a parabolic trough collector is plotted as a function of $(T_{col} - T_{amb})/I$. Instantaneous Direct Insolation Aperture Efficiency is defined as the ratio of the instantaneous thermal energy output from a collector to the Instantaneous Direct Aperture Insolation.

Average Direct Insolation Efficiency -- The efficiency typically used to describe the performance of a concentrating collector over some defined period of time (i.e., day, month, or year). Average Direct Insolation Efficiency is defined as the ratio of the integrated thermal energy output from a collector over some known period of time to the integrated Direct Normal Insolation over the same period of time.

Average Direct Insolation Aperture Efficiency -- The efficiency used to predict the performance of a concentrating collector over some defined period of time (i.e., day, month, or year), as described in Section 1.5.1. Average Direct Insolation Aperture Efficiency is defined as the ratio of the integrated thermal energy output from a collector over some known period of time to the integrated Direct Aperture Insolation over the same period of time.

APPENDIX C

Sun Angles

In order to provide for accurate tracking of parabolic trough solar collectors, the position of the sun must be known at all times during the year. The position of the sun is usually defined, relative to any position on earth, by two time-dependent angles: the solar azimuth angle (AZ) and the solar elevation angle (EL). This appendix provides the analytical expressions needed to calculate these two angles.

The general approach employed in this appendix follows that of E. C. Boes,[1] and the reader is referred to that reference for further detailed information on computing the sun's position. While the resultant equations are accurate enough for computing collector performance, they may not be accurate enough for collector tracking requirements. John Zimmerman[2] has recently reviewed the accuracy of various equations and computer programs for calculating the sun's position. Basically, the solar declination and hour angles are defined and these two angles, together with local latitude, are then used to define the solar azimuth and elevation angles. The hour angle incorporates the equation of time which corrects local standard time to solar time.

Solar Declination Angle (D)

The planar orbit of the earth about the sun is an ellipse having semimajor and semiminor axes of $(9.3007)(10^7)$ miles, or $(1.4968)(10^8)$ km, and $(9.2994)(10^7)$ miles, or $(1.4966)(10^8)$ km, respectively. The axis about which the earth rotates is inclined to the plane of the earth's orbit by 23.45°. The orbit of the earth about the sun, with the tilt of the earth's axis of rotation, is shown in Figure C1.

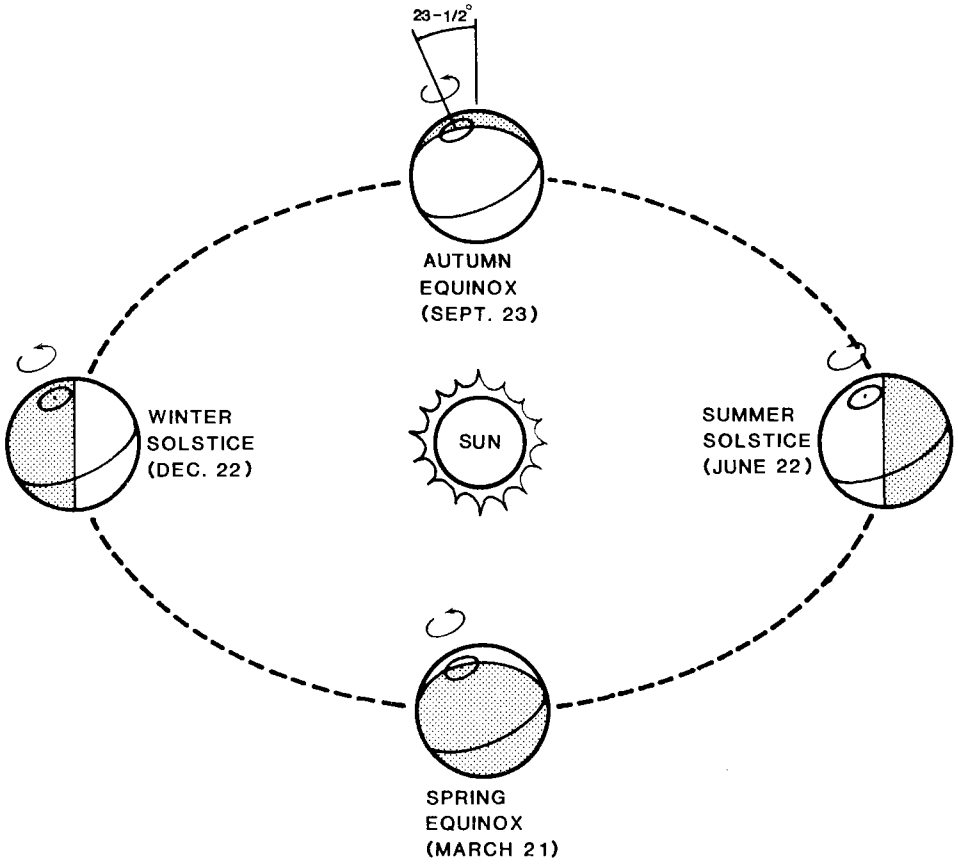

Figure C1. Motion of Earth Relative to Sun

On the summer solstice in the northern hemisphere, the inclination of the earth's rotation axis at the north pole is 23.45° toward the sun. On the winter solstice, the earth's rotation axis points 23.45° away from the sun. At the solar equinox, the earth's rotation axis is normal to the sun/earth vector, resulting in the sun rising due east and passing directly overhead to an observer located on the equator. The angle of tilt of the earth's rotation axis toward the sun is called the solar declination angle. By definition, it is +23.45° on the summer solstice in the northern hemisphere. As a result, it is then -23.45° on the northern hemisphere winter solstice and 0° on the spring and fall equinoxes. Analytically, the solar declination angle is approximately

$$\sin(D) = 0.39795 \cos [0.98563 (N-173)] \qquad (1)$$

where N is the day number of the year, starting with 1 January. The formula is accurate to about ±1°.

Determination of Solar Time

The sun does not necessarily cross the local meridian (i.e., solar noon) when the local standard time (LST) indicates 12 noon. One difference between the LST and solar time is called the equation of time (EOT) and is approximated by

$$EOT = -(0.1236 \sin x - 0.0043 \cos x + 0.1538 \sin 2x + 0.0608 \cos 2x) \quad (2)$$

where the angle x, in degrees, is a function of the day of the year N, starting at 1 January.

$$x = 360(N-1)/365.242 \quad (3)$$

To complete the conversion from LST to solar time, a correction (L) in hours for longitude must also be included where

$$L = [(\text{local longitude in degrees}) - (\text{longitude of local standard time meridian in degrees})]/15 \quad (4)$$

Thus solar time at any specified location, in hours, can be expressed as

$$\text{Solar Time} = LST + EOT - L \quad (5)$$

The local time meridians are 75° for Eastern Standard Time, 90° for Central Standard Time, 105° for Mountain Standard Time, and 120° for Pacific Standard Time.

Hour Angle (H)

For computing the solar azimuth and elevation angles which follow, it is convenient to express solar time in degrees rather than in hours. The conversion is based upon the fact that the earth rotates 360° on its axis in 24 hours and thus the hour angle (H) changes 15° per hour. H is measured from solar noon and is positive before 12 noon (up to midnight) and negative after 12 noon (up to midnight). For example, 8 am solar time is +60° while 9 pm solar time is -105°.

Recall that since solar time varies with longitude, so does the hour angle H.

Solar Azimuth (AZ) and Solar Elevation (EL) Angles

As mentioned above, the sun's position is usually defined by AZ and EL, respectively. These angles are shown in Figure C2. AZ measures the sun's angular distance from the south while EL measures the sun's angular position up from the horizon. The definition employed in this handbook is that a positive solar azimuth implies that the sun is east of the north/south line, and a negative solar azimuth implies that the sun is west of the north/south line. A frequently employed term is the solar Zenith angle (Z), which is simply the complement of the solar elevation angle

$$Z = 90° - EL$$

The solar elevation and azimuth angles are defined by the equations

$$\sin(EL) = \cos(LAT)\cdot\cos(D)\cdot\cos(H) + \sin(LAT)\cdot\sin(D) \ , \qquad (6)$$

$$\sin(AZ) = [\cos(D)\cdot\sin(H)]/\cos(EL) \ , \qquad (7)$$

where LAT = latitude of location.

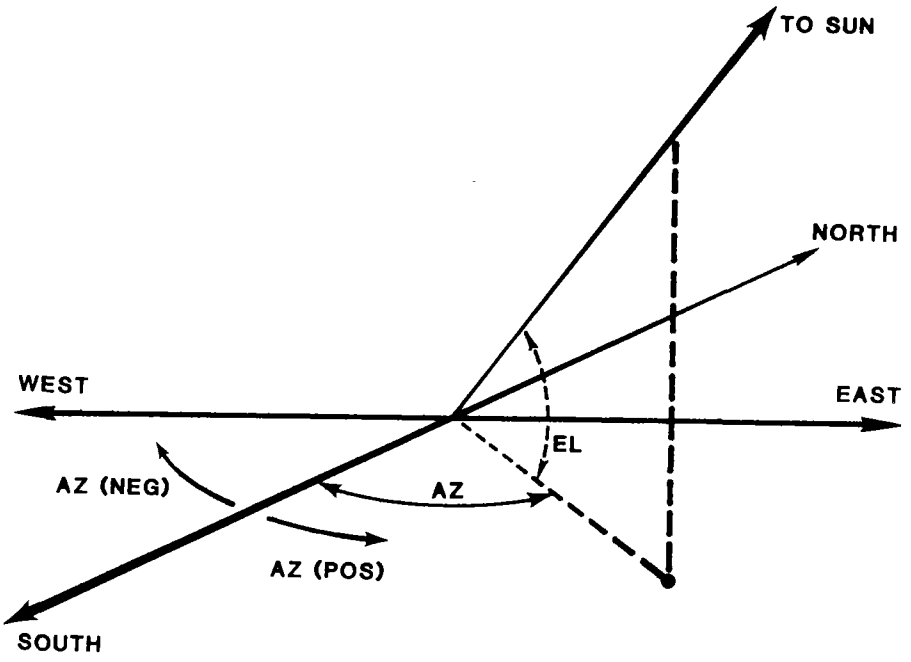

Figure C2. Definition of Solar Azimuth (AZ) and Solar Elevation (EL) Angles

Since the elevation angle varies only between 0° and 90°, the inverse sine function of Eq. (6) yields the elevation angle directly. However, it is necessary to distinguish when the sun is in the northern half of the sky and when it is in the southern half in order to use Eq. (7). This is done by

$$AZ = \begin{cases} \sin^{-1}(Q) \text{ if } \cos(H) > \dfrac{\tan(D)}{\tan(LAT)} \\ 180° - \sin^{-1}(Q) \text{ if } \cos(H) < \dfrac{\tan(D)}{\tan(LAT)}, \text{ and } H > 0 \\ -180° - \sin^{-1}(Q) \text{ if } \cos(H) < \dfrac{\tan(D)}{\tan(LAT)}, \text{ and } H < 0 \end{cases}$$

where

$$Q = [\cos(D) \cdot \sin(H)]/\cos(EL)$$

In the case where

$$\cos(H) = \tan(D)/\tan(LAT) ,$$

the solar azimuth angle is ±90°, depending upon the sign of the solar hour angle H.

References

[1]E. C. Boes, Fundamentals of Solar Radiation, SAND79-0490 (Albuquerque, Sandia Laboratories, 1979).

[2]John C. Zimmerman, Sun-Pointing Programs and Their Accuracy, SAND81-0761 (Albuquerque: Sandia National Laboratories, to be published).

APPENDIX D

Computation of Collector Performance

A computer code which employs experimentally determined $\Delta T/I$ versus efficiency data and the TMY weather tapes was used to predict the long-term collector output reported in Sections 2.4 through 2.6 and Appendix H. The logic flow of the computer program is shown in Figure D1. The computation begins with an interrogation of the TMY weather tape for the ambient temperature and Direct Insolation at a given time of day and day of the year. From knowledge of the operating temperature of the collector (predetermined by the user), the ΔT that the collector is operating above ambient is determined. The angle of incidence (see Section 2.2) is computed from knowledge of collector orientation, collector location, and the sun's position in the sky. The cosine of the angle of incidence multiplied by the Direct Normal Insolation read from the TMY tape results in the Direct Insolation entering the collector aperture. This allows computation of $\Delta T/I$ for that particular time of day and that day of the year.

Since, as described in Section 2.1, the Instantaneous Direct Insolation Aperture Efficiency for a given collector is a unique function of $\Delta T/I$, the Collector Efficiency can be determined from published test data of $\Delta T/I$ versus efficiency for the collector of interest. In Section 2.4 this was the Nominal Collector. Once the Instantaneous Direct Insolation Aperture Efficiency is determined, it can be multiplied by the direct insolation entering the collector aperture to obtain the thermal energy output from the collector. This computation is typically repeated hourly for a year's worth of TMY data to obtain collector output plots such as those for the Nominal Collector which were reported in Sections 2.4 through 2.6 and Appendix H.

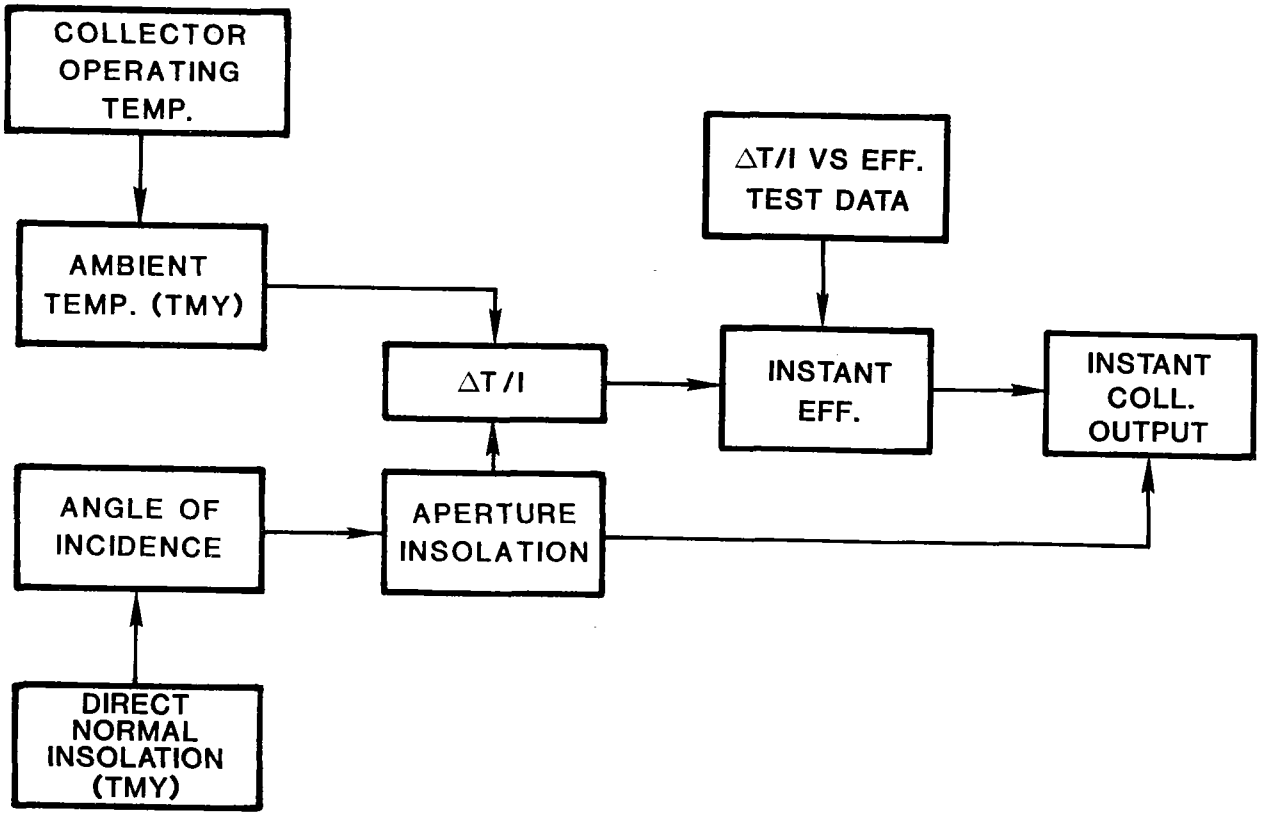

Figure D1. Logic Flow for Computing Collector Thermal Output

The validity of this approach to calculating the thermal energy output from a collector was evaluated using measured all-day performance of two different parabolic trough collectors with the $\Delta T/I$ versus efficiency characteristics shown in Figure D2. Figures D3 through D6 show the computed versus measured thermal energy output for the two different parabolic trough collectors tested at SNLA. The computed collector performance used the measured Direct Normal Insolation and ambient temperatures obtained during the day of each test. Two different collectors and orientations were selected, together with different times of the year, in order to provide widely diverse conditions to allow a reasonably rigorous test of the computer code. Since the tested collectors were short-test modules, end losses due to the reflected beam missing the end of the receiver tube were evaluated. End losses become important at high incidence angles for short modules. End losses proved significant in only one test (see Figure D5)

5520

SAND80-1666
Unlimited Release

4722 - R. Champion
extra copy

Proceedings of the Line-Focus Solar Thermal Energy Technology Development A Seminar for Industry

Albuquerque, New Mexico
September 9, 10, 11, 1980

FEB 27 1981

To	Org	Code
	5800	
✓	~~5821~~	
	~~5822~~	
	5823	Cej
✓	~~5824~~	
✓	5520	Champion

1. Action 4. File
2. Info 5. Destroy
3. See Me

Roscoe L. Champion, Editor

Prepared by Sandia National Laboratories, Albuquerque, New Mexico 87185 and Livermore, California 94550 for the United States Department of Energy under Contract DE-AC04-76DP00789

Printed February 1981

Sandia National Laboratories

SF 2900-Q(3-80)

Distribution (cont)

1520 T. J. Hoban
1530 W. E Caldes
1550 F. W. Neilson
2320 K. L. Gillespie
2323 C. M. Gabriel
2324 R. S. Pinkham
2326 G. M. Heck
3161 J. E. Mitchell
3600 R. W. Hunnicutt
Attn: H. H. Pastorius, 3640
3700 J. C. Strassel
4000 A. Narath
4231 J. H. Renken
4700 J. H. Scott
4710 G. E. Brandvold
4713 B. W. Marshall
4714 R. P. Stromberg (20)
4715 R. H. Braasch
4718 E. Burgess
4719 D. G. Schueler
4720 V. L. Dugan (100)

4721 J. V. Otts
4722 J. F. Banas
4723 W. P. Schimmel
4725 J. A. Leonard
4750 V. L. Dugan
5510 D. B. Hayes
5513 D. W. Larson
5520 T. B. Lane
5523 R. C. Reuter
5810 R. G. Kepler
5820 R. E. Whan
5830 M. J. Davis
5833 J. L. Jellison
5840 N. Magnani
8266 E. A. Aas (2)
8450 R. C. Wayne
8451 C. F. Melius
8452 A. C. Skinrood
8452 T. Bramlette
8453 W. G. Wilson
3141 T. L. Werner (5)
3151 W. L. Garner (3)
(Unlimited Release)
For DOE/TIC
(Unlimited Release)
6011 Patents

☆U.S. GOVERNMENT PRINTING OFFICE: 1981-0-777-023/516

DESIGN OF COLLECTOR SUBSYSTEM PIPING LAYOUTS

Robert E. Morton
Jacobs Engineering Group
Pasadena, California 91101

Introduction

Review of current designs show that the process piping systems in solar collector arrays are being built around design criteria long established as acceptable by process industries. Although these criteria are known to be conservative when applied to solar collector fields, designers are still forced to use them because guidelines do not exist yet for solar applications. The use of conservative process piping design criteria undoubtedly increases capital and operating costs when used without consideration for the special nature of solar energy fields.

In early 1979, Sandia Laboratories commissioned Jacobs Engineering Group to study the piping criteria in depth as they apply to the design of solar field piping layouts. Field layout; optimum insulation type and thickness; method and frequency of pipe support; ΔT string length; pump type; driver type and many other related factors were to be studied. The long range goal of these studies is to develop special guidelines tailored to facilitate design of modular solar piping systems.

The initial design studies have been performed on a 50 thousand square foot solar collector field layout. As a result of these studies, recommendations for configuration; ΔT string length; header piping profile; and insulation material and thickness have been developed. The insulation recommendations can be applied to the design of any size solar array because it was possible to decouple the insulation study from the piping study. The other recommendations, however, apply strictly to the design of the 50 thousand square foot E-W collector array. Future studies should be made to determine the need to modify the piping recommendations for modular collector arrays which are larger or smaller than the one studied.

Design Criteria

The studies are based on certain design criteria established by Sandia. These are presented below in Table I.

Table I

Initial Design Criteria

Parameter	Value
Wind Velocity	5 ft/sec. normal to pipe
Size of collector field	50,000 ft^2
Drive string length	80 ft
Collector orientation	E-W
Collector spacing	15 feet
Heat transfer fluid	Therminol MCS-2046
Fluid ΔT	150°F
Fluid outlet temperature	600°F
Energy value out of collectors	$10 per million BTU
Annual capital charge	15% of initial investment
Foundation design	Optimum Sandia design
Minimum flow rate	50 gpm
Peak flow rate	300 gpm

Piping Study

Several alternative field layouts were proposed and, of these, two were selected for preliminary study. These are shown schematically in Figures 1 and 2. Heat transfer fluid enters and leaves the system via the center of the collector array in Figure 1, and via the edges of Figure 2.

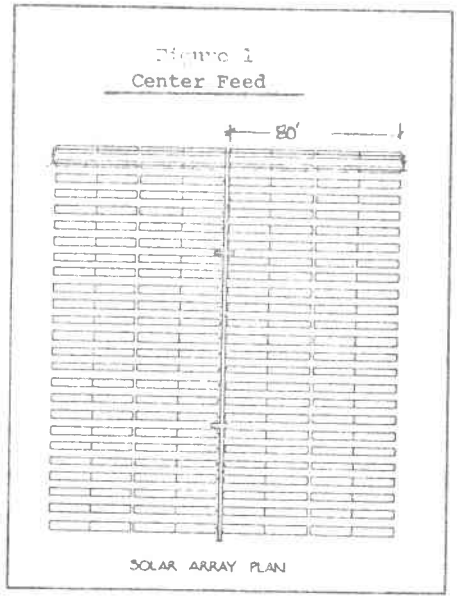

The preliminary screening process consisted of a capital cost estimate, estimates of heat loss and a subjective critique of the arrays utility as a module in larger collector fields. It was found during this process that the capital costs of both configurations were about the same, however the center feed configuration of Figure 1 would not economically lend itself to larger modules. Each of the collector rows in Figure 1 requires two additional fifteen foot long 1" pipe return bends not required by the array in Figure 2. The extra pipe results in substantially higher heat losses for larger arrays. The edge feed configuration of Figure 2 was selected for detailed study for this reason.

Once the general configuration was established, cost comparisons were made of optimized edge feed 50 thousand square foot collector arrays to arrive at a recommendation for ΔT string length and receiver tube diameter. Four ΔT string lengths were considered. They ranged in size from 240' to 480' in length. Receiver tubes under consideration were 1" and 1.25" o.d. schedule 40 steel pipe. Each of the final candidate arrays evolved from optimization studies which considered the minimization of capital, heat loss and pumping cost in the piping size selection.

The results of the study indicate that the ΔT string length should be 320'. Receiver tube diameter can be 1" or 1.25" o.d.

Table 2 presents the total annual estimated operating costs for the range of ΔT strings studied. These costs are plotted in Figure 3. This figure shows the relative insensitivity of the estimated operating costs to ΔT string length and receiver tube diameter.

Table 2

Total Annual Operating Costs

Length of ΔT string,	Receiver dia., in.	Pumping Cost,$/yr	Heat Loss Cost,$/yr	Capital Charge,$/yr	Total Cost,$/y
240	1.0	6800	9100	12900	28800
320	1.0	7300	8000	11250	26550
400	1.0	8550	7700	10400	26650
480	1.0	11300	7600	9900	28800
240	1.25	6400	9100	12900	28400
320	1.25	6540	8000	11250	25800
400	1.25	6950	7700	10400	25050
480	1.25	8300	7600	9900	25800

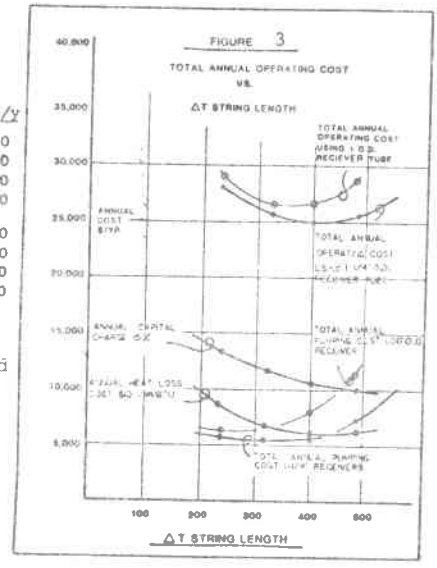

Figure 4 is a plan view of the conceptual 50 thousand square foot collector array developed in this project. The design is the result of otpimization studies made to find a design in which the pumping cost, heat loss cost and capital charge were minimized. This collector layout consists of twenty-four 320' long ΔT strings spaced at 15 foot intervals. Each ΔT string is composed of four 80' drive strings, a 1-1/4" o.d. receiver tube; two gate valves and

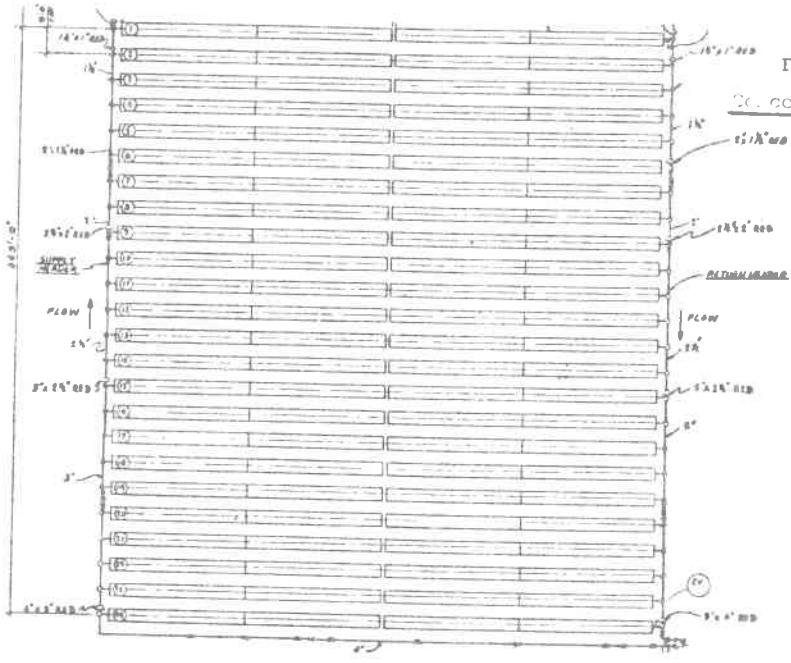

Figure 4

Conceptual Layout

a control valve. The telescoped header profile shown on Figure 4 results in the minimum overall operating cost, based on heat and power costs provided by Sandia. Heat is valued at $10/million Btu. Electric power costs 10¢/Kwh and the annual capital charge is 15 percent of initial capital investment. It has been shown by sensitivity study (see Figures 5, and 6) that these costs can vary substantially without affecting the design recommendation.

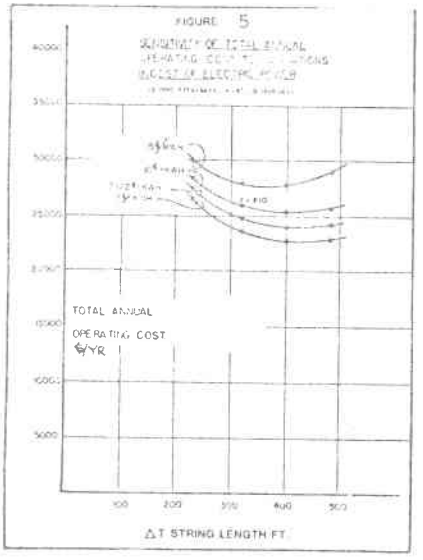

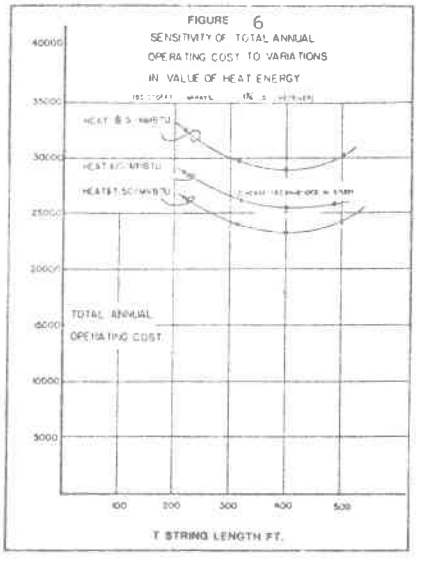

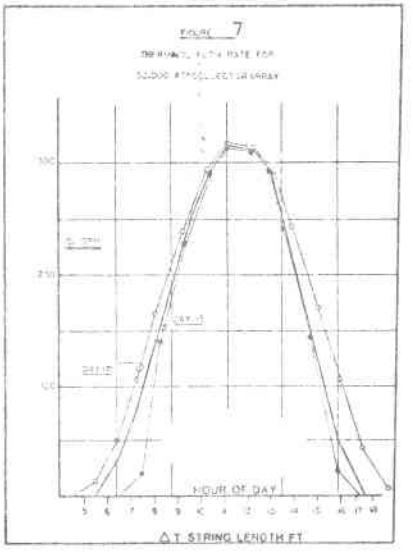

Pump Driver Study

Solar energy input to the collector is not constant over the operating day. Since it is desirable to maintain a constant fluid temperature rise across the ΔT string, the fluid flow must vary in proportion to the changing energy input. The flow rate in the ΔT string, and header piping, will rise from a minimum in the morning, peak at solar noon and fade off to a minimum value in the evening. The array will be shut down and allowed to cool overnight.

Various alternatives are available for pumping fluid through the collector piping. We have studied the use of centrifugal pumps in solar arrays. The pump is assumed to operate in one of three modes: continuous speed; two speed; and SCR drive variable speed. Annual

operating costs were developed for each of the three modes in order to select the most economical. The pumping and capital costs were based on vendor pump price quotations, the pipe configuration shown in Figure 4, energy value of 10¢/Kwh and an annual capital charge of 15 percent of capital costs. Receiver tube o.d. was 1.25 inches.

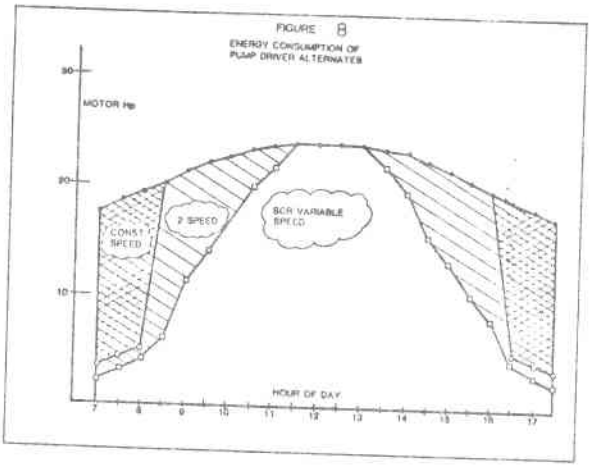

Energy consumption was estimated using the daily estimated flow curve shown in Figure 7. Using quantity-discharge curves provided by the pump manufacturer and calculated pipe system curves, estimates were made of pump BHP requirements. The BHP requirement was calculated over one operating day for half hour intervals. The calculated BHP values were then corrected for motor efficiency. The resultant gross Hp was converted to Kwh. The annual energy cost was based on the integrated daily energy consumption.

Figure 8 shows the calculated gross motor Hp for each of the three cases. The area under the curve is the total daily energy consumption for each case. Clearly, the continuous speed case uses the most energy, followed by the two speed case. It is evident from this figure that speeding up the pump impeller in proportion to energy input through the use of an SCR drive results in the lowest energy consumption.

Table 3 presents a breakdown of the total costs associated with pumping. The annual capital charge is 15 percent of the initial cost of the pump and controls. Even though the SCR drive is substantially more costly than the other two types of driver the energy savings justifies its selection.

Table 3

Total Annual Pumping Cost

Mode	Capital Charge,$	Energy Cost,$	Total,$
Continuous speed	1570	6540	8110
Two speed	1570	5510	7080
Variable speed	2730	3810	6540

Insulation Studies

Calcium silicate, mineral wool, fiber glass, and cellular glass were selected for study. These four were picked because they seemed to fulfill such basic considerations as cost, and resistance to high temperature and abuse. The optimum insulation material was found by weighing cost advantages of all four at their optimum thickness against ease in installation and service life. Part of the study consisted of evaluating insulation materials under changing conditions of heat loss and annual capital charge. To expedite the analysis one of the four materials (Base Case) was subjected to post-optimality analysis which showed the sensitivity of the calculated optimum thickness to changes in certain parameters. The behavior of the other three insulation materials to changes in the same variable was assumed to be consistent with the response shown by the Base Case. Calcium silicate was selected to be the Base Case because of its wide acceptance as an insulating material. As it turned out, fiberglass or mineral wool are preferred to calcium silicate.

Determining optimum insulation thickness for a given material involves the trade-off of insulation materials costs with the value of the energy saved. Estimating the energy savings requires calculating daily heat losses. The total heat loss calculated in this study was the sum of three individual component losses, the operating heat loss, the overnight cooldown heat loss and the startup heat loss. The capital cost of the insulation material and installation labor were obtained from insulation contractors. The cost data included the insulation material, vapor barrier, 0.016" aluminum covering, and all labor charges, installed in New Mexico.

The calculated optimum thickness of 4" for the Base Case (calcium silicate, over a 4" schedule 40 steel pipe) is shown by curve 3 on Figure 9 . The curve is relatively flat in the optimum region allowing a range of selection between 3" to 5" before significant change is made in overall annual costs. Curves 1 and 2 show the component capital costs and heat loss costs, respectively. Figure 10 shows the relative sensitivity of this optimum to energy costs of $3, $7.50, and $10 per million btu; and three annual payback rates of 10, 15, and 20 percent. As expected, higher energy values tend to drive one to thicker insulation thicknesses.

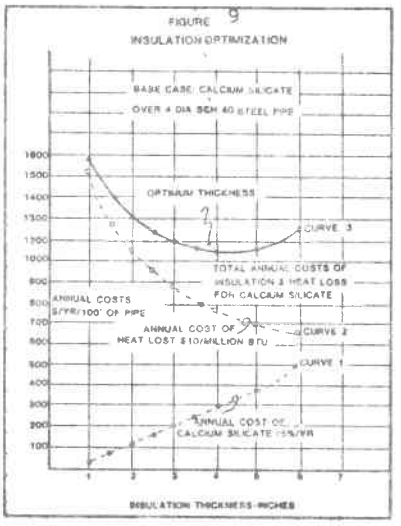

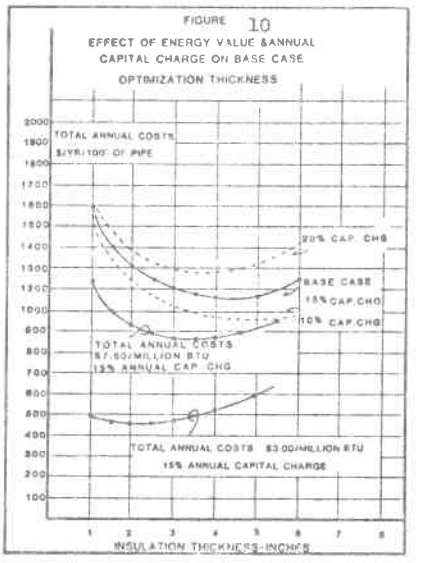

Figure 11 presents the relative performance of each of the four materials under Base Case conditions for a 4" pipe. Clearly, fiberglass or mineral wool have cost advantage over cellular glass or calcium silicate. The optimum thickness for all four is about the same. Figure 12 presents similar results for 2" and 8" pipes.

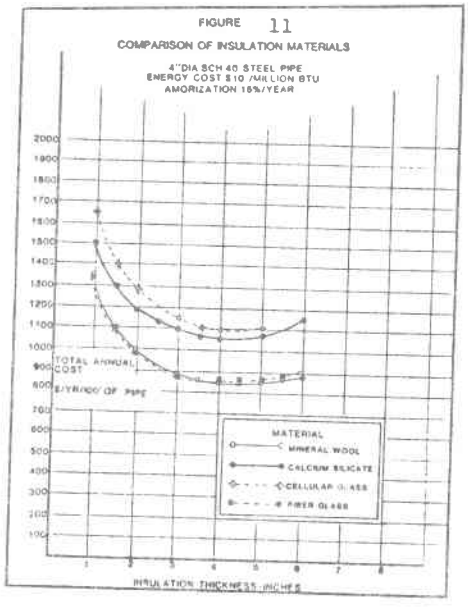

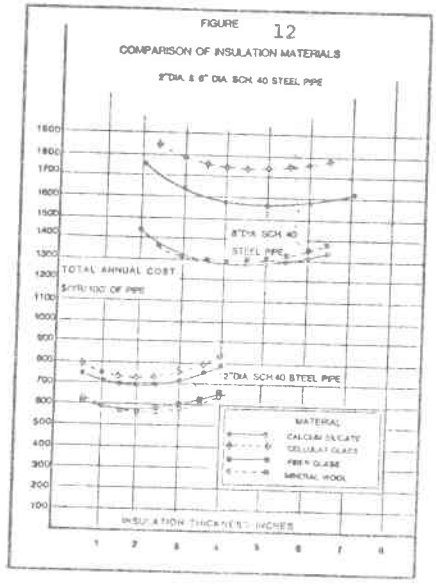

A schedule of recommended insulation thicknesses for various diameter pipes is presented below in Table 5. Preformed fiber glass or mineral wool insulation is preferred for those applications where physical abuse is not a problem. Calcium silicate can be used in combination with fiberglass in those areas of the array where the fiberglass could be damaged by rough treatment.

Table 5

Recommended Insulation Thickness
(Basis: $10/million Btu and 15% amortization)

Nominal Pipe Diameter, in.	Recommended Thickness, in.
1	1-2
1.5	1.5-2
2	2-3
2.5	3-4
3	3-4
4	4-5
6	4-5
8	6

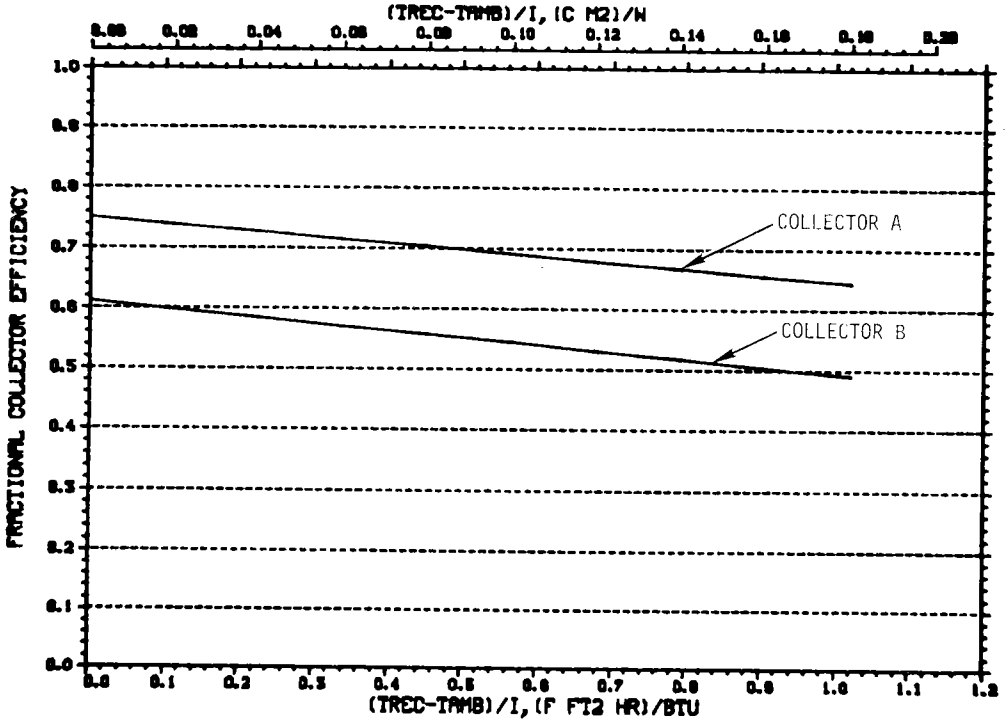

Figure D2. Performance of Collectors Used to Validate Simple Collector Model

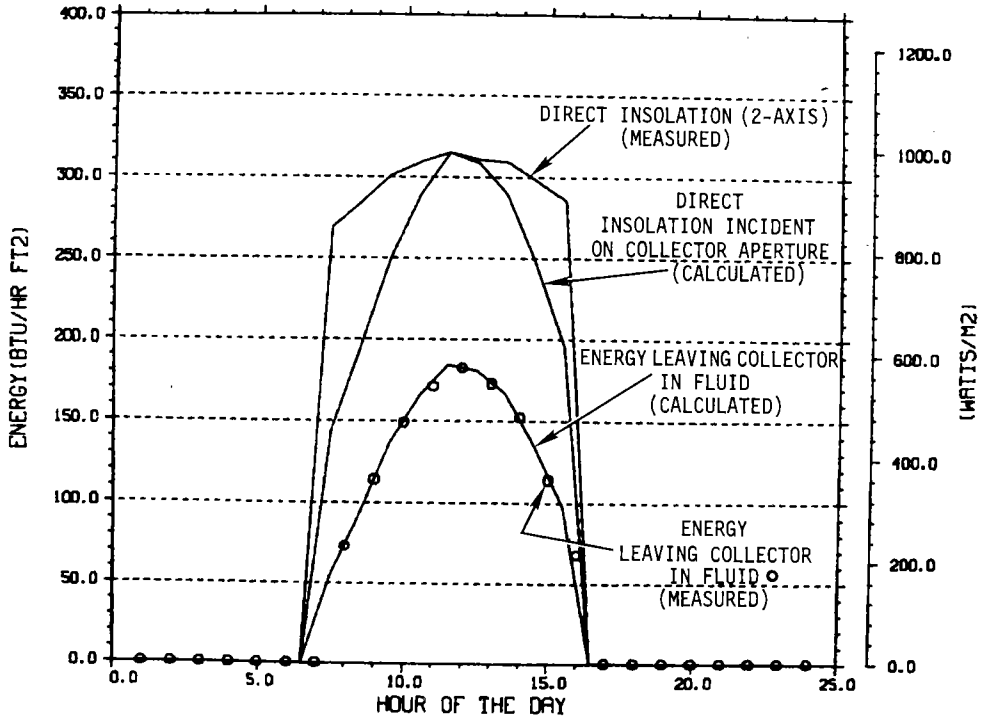

Figure D3. Hourly Thermal Output from E/W Collector A, Day 179

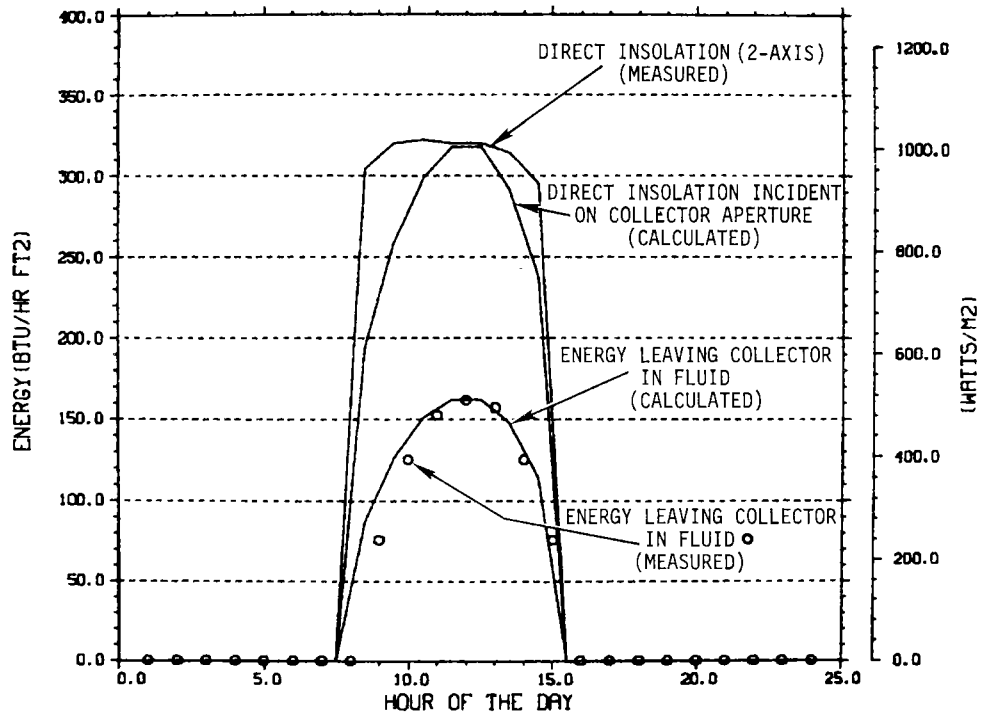

Figure D4. Hourly Thermal Output from E/W Collector B, Day 44

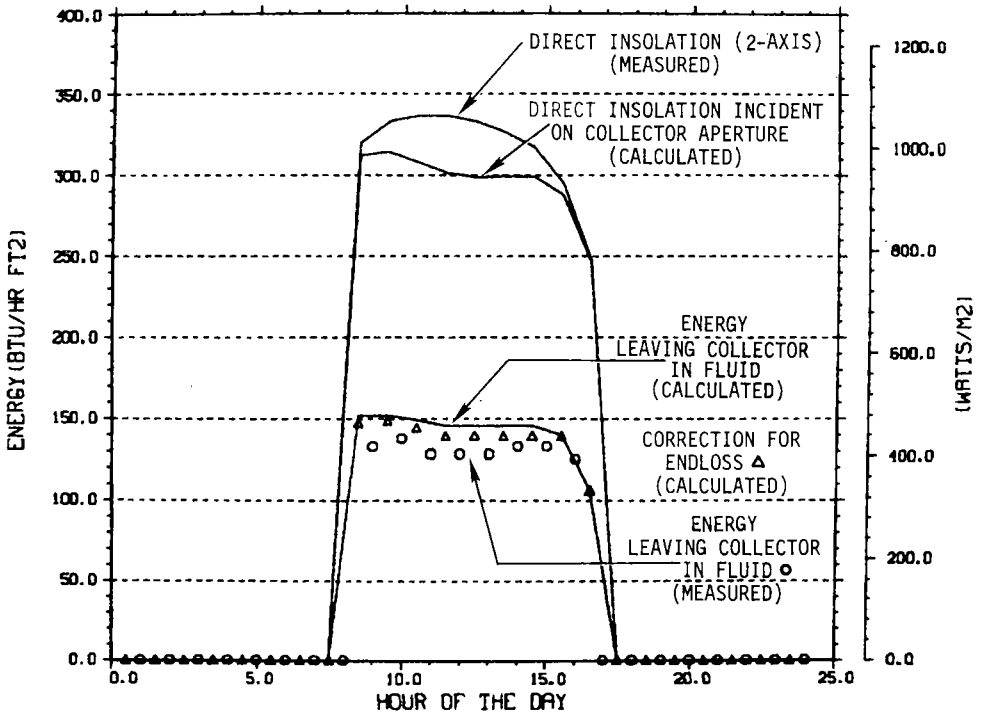

Figure D5. Hourly Thermal Output from N/S Collector B, Day 103

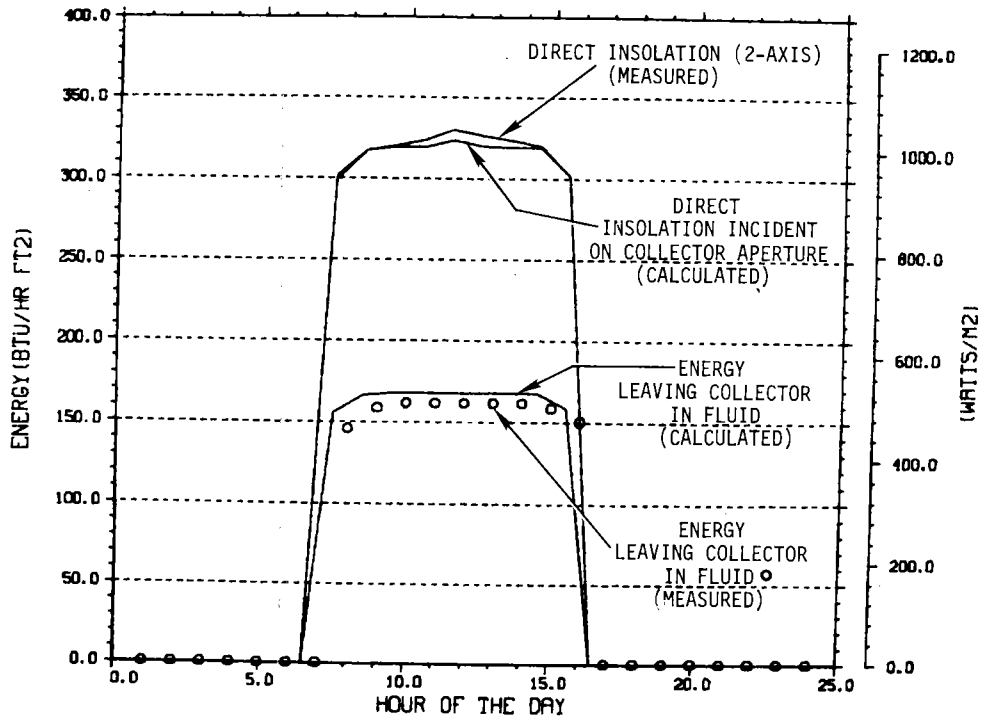

Figure D6. Hourly Thermal Output from N/S Collector, Day 170

and thus are not shown in the other plots to improve clarity. Typically, end losses are not anticipated as being large in actual installations where long rows of collectors are used. Thus, end losses are not directly included in the simple computed code outlined in Figure D1.

As illustrated in Figures D3 and D4, agreement between computed and measured E/W hourly performance is good. The end losses were relatively small and thus are not shown. It should be noted that morning test results must be used with caution since, during this time period, the collector was warming up and stabilizing. Thus, for example, deviations from the test results in the morning (reported in Figure D4) from the computed performance may not be indicative of predictive ability of the computer program but may be due simply to the test collector not being stabilized. Agreement between the computed and measured collector performance during the afternoon is much better.

Figures D5 and D6 show similar results for a N/S-oriented Collector B parabolic trough. During the summer (day 170), the comparison between computed and measured performance is, as illustrated, good. Due to the path of the sun near the summer solstice, the angle of incidence between the sun and the collector aperture is always small. The resultant small end losses are, for this reason, not shown in Figure D6. As above, morning test results are not considered as valid as the afternoon test data.

The basic conclusion which can be drawn from Figures D3 through D6 is that the simplified collector mode, using $\Delta T/I$ versus efficiency performance data, is capable of predicting hourly collector thermal output with accuracy. The results obtained in predicting the hourly performance for different collector orientations during different times of the year also imply that the simplified model can be used with confidence to predict annual collector performance from $\Delta T/I$ versus efficiency data.

APPENDIX E

Storage Sizing Graph Determination

In order to examine the effect of collector area and Storage Capacity on the Utilization of collected solar energy, it is necessary to look at the hour-by-hour production of thermal energy by the collector field. This energy supply profile must then be contrasted with the application's hour-by-hour Demand and the Storage Capacity available for storing excess solar-derived thermal energy. The logic flow for a computer program to do this is outlined in Figure E1.

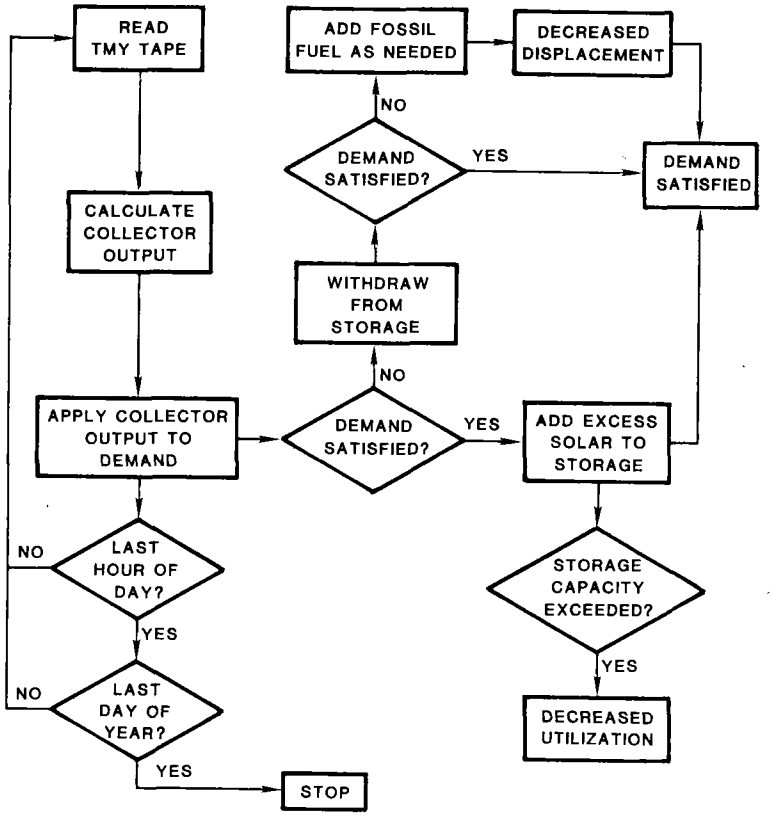

Figure E1. Logic Used To Prepare Storage Sizing Graphs

The computer program calculates the hourly collector thermal energy output, using TMY data as described in Appendix D. The collector thermal energy output at any given hour is compared to the application's Demand at that hour. If the Demand is less than the thermal energy output of the collector field, the thermal energy in excess of the Demand is placed in storage if such is available. If the thermal energy Storage Capacity is exceeded, the excess energy is considered wasted and acts as a debit against the Utilization of the collected solar energy. If the Demand for thermal energy by the process is greater than the collector output, energy is withdrawn from storage to help satisfy the Demand. If the combined thermal energy output from the collector field and the thermal energy in storage is insufficient to meet the application's Demand, fossil fuel is consumed in order to satisfy the Demand, resulting in decreased Displacement of the Demand by the solar installation. Analyses of this type were performed, employing several different Demand scenarios, and the results are reported in Section 3.1.

APPENDIX F

Sensible Heat Oil Storage Costs

As discussed in Section 3.5, sensible heat oil thermal energy storage is currently the most highly developed storage technology for application in solar thermal energy systems. This appendix provides the rationale behind the development of the storage cost nomograph contained in Figure 35.

To obtain the cost of sensible heat oil storage, a good first approximation is to assume that the cost of the storage system is the cost of the oil. This is based upon work done at Atomics International (AI) as part of a study executed to evaluate the application of solar total energy to the commercial sector.[1] AI concluded that the cost ($1976) of the storage could be approximated by

$$\text{Storage Cost} = 352\ (\text{vol, ft}^3)^{0.515} + \text{oil cost (vol, ft}^3)$$

for storage systems in the size range of 150 to 150,000 ft^3 (4.2 to 42,000 m^3). Thus, for oil that cost about $3/gal ($790/m^3$, $22.5/ft^3$), the cost for oil begins to exceed the nonoil cost at a storage size of about 250 ft^3 (14 m^3). Above this size, oil costs quickly overshadow nonoil costs. Thus, for conceptual design purposes, the assumption is made that storage costs are reflected in the oil costs. This assumption can be reevaluated if the design gets to the Preliminary Design stage.

Figure 35 simply performs the calculation which converts the cost of oil into an equivalent cost for storage. Figure 35a, in English units, is reproduced here as Figure F1 for convenience of discussion. Chart A performs the calculation which divides the cost of the oil

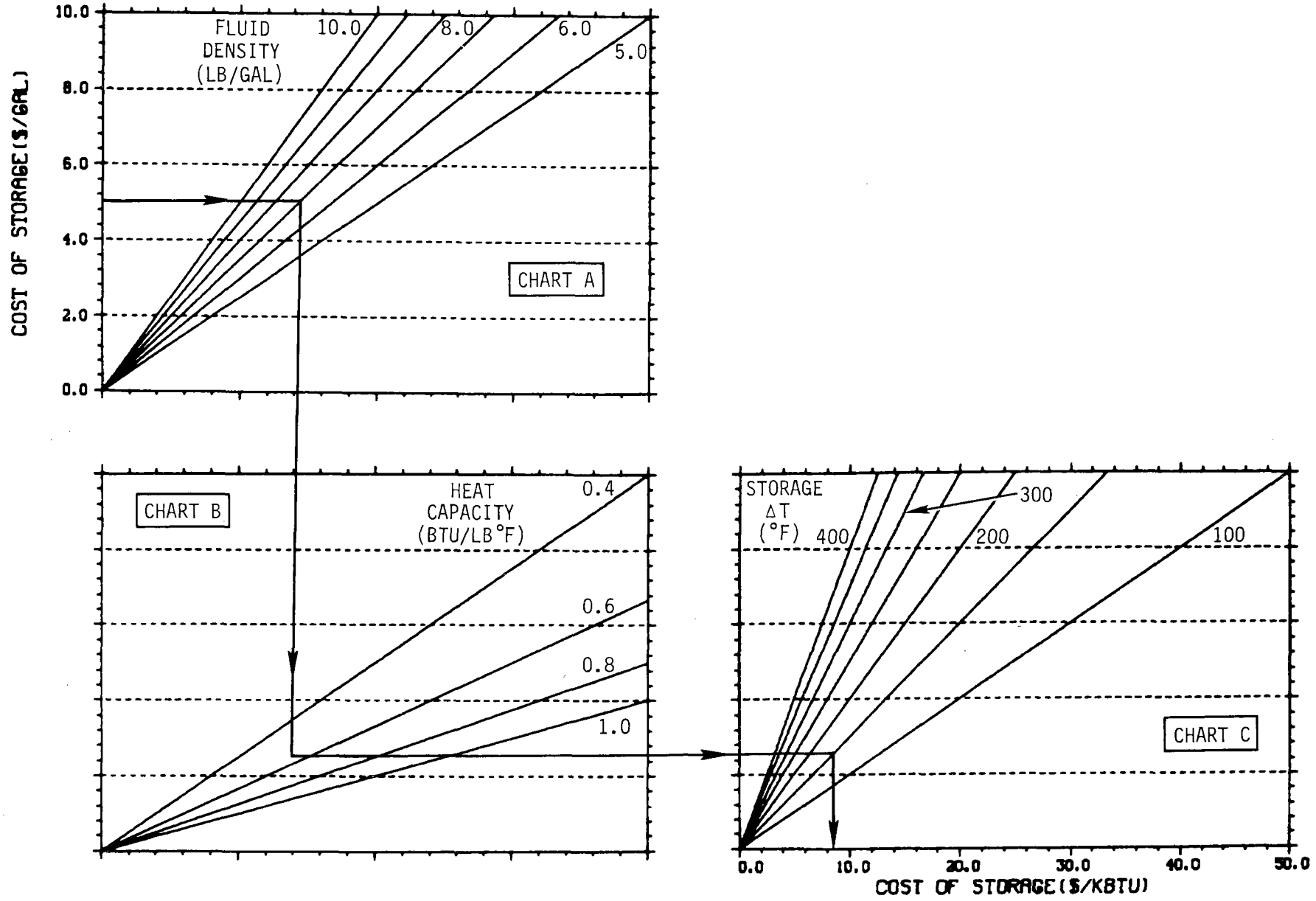

Figure F1. Estimation of Sensible Heat Storage Costs--
English Units

storage medium ($/gal) by the density of the oil (lb/gal) to obtain the cost per unit weight of oil.

$$\text{Oil cost } (\$/\text{lb}) = (\$/\text{gal}) \div (\text{lb/gal})$$

The cost per unit weight of oil, when divided by the heat capacity of the oil (Btu/lb·°F) yields the cost of the oil storage for a 1°F ΔT.

$$\text{Storage cost } \frac{\$ \cdot °F}{\text{Btu}} = (\$/\text{lb}) \div (\text{Btu/lb} \cdot °F)$$

Although the axes are not explicitly labeled to show it, this calculation is performed in Chart B. The final computation of sensible heat storage costs is performed by dividing the costs from Chart B by the ΔT across the sensible heat storage unit. Multiplying by 1,000 provides a cost in a per kBtu Basis.

$$\text{Storage cost } (\$/\text{kBtu}) = \left[\frac{\$ \cdot °F}{\text{Btu}} \div (°F)\right] \cdot 1000 \frac{\text{Btu}}{\text{kBtu}}$$

This final computation is performed in Chart C of Figure F1.

Thus, for an example where $5/gal oil with a density of 7.0 lb/gal and heat capacity of 0.55 Btu/lb·°F undergoes a ΔT of 150°F, Figure F1 graphically performs the computation.

$$(\$5/\text{gal}) \frac{\text{gal}}{7.0 \text{ lb}} \frac{\text{lb} \cdot °F}{0.55 \text{ Btu}} \frac{1}{150°F} = \$8.65/\text{kBtu}$$

Reference

[1]Commercial Applications of Solar Total Energy Systems, Second Quarterly Progress Report, August 1, 1976, October 31, 1976 Report No. AI-ERDA-13200 (Canoga Park, CA: Rockwell International, Atomics International Division, April 1977).

APPENDIX G

Difference in Shading in E/W and N/S Parabolic Trough Collector Fields

As discussed in Section 2.6, "Collector Shading," there is a significant difference in the shading suffered by a N/S field of parabolic trough collectors and an E/W field of parabolic trough collectors. The plot showing the annual shading suffered by parabolic trough collectors located in Albuquerque is reproduced here in Figure G1. In order to understand why E/W and N/S collector fields experience different amounts of shading, it is helpful to look at shading on a monthly basis. Figure G2 plots the Direct Insolation incident upon both E/W and N/S nonfirst row collectors as a function of Land Use (i.e., land area/collector aperture area). As can be seen in Figure G2, the Direct Insolation incident on a N/S field of parabolic trough collectors approaches that incident on an E/W field of parabolic trough collectors at high Land Use.

The differences in shading between E/W and N/S collectors is due to the fact that shading for both orientations is greatest at low sun angles. During the summer, for example, the performance of a N/S collector is greater than that of an E/W collector because the N/S collector can rotate over and look directly at the morning and afternoon sun at low sun angles while an E/W collector suffers high incidence angle effects. This advantage is really applicable only to the east row (or west row in the afternoon), however, since subsequent rows of N/S collectors will not have an unencumbered view of the sun but will instead be partially, if not completely, blocked. The E/W-oriented collector will, in the summer, be virtually free of significant shading effects, as suggested by Figure G2. This is a result of

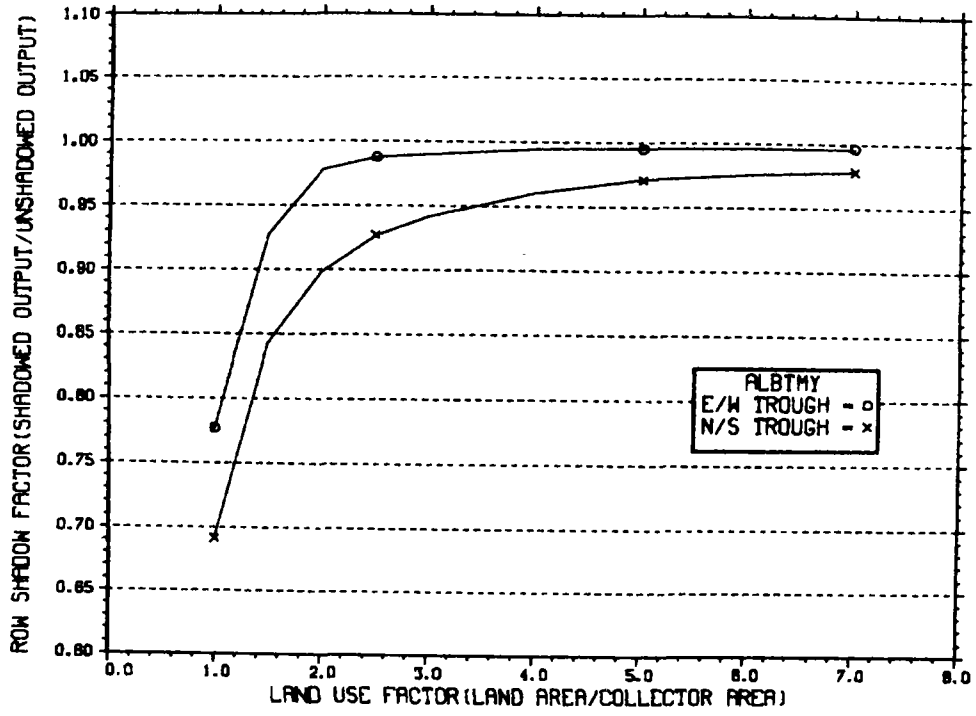

Figure G1. Annual Nonfirst Row Shading

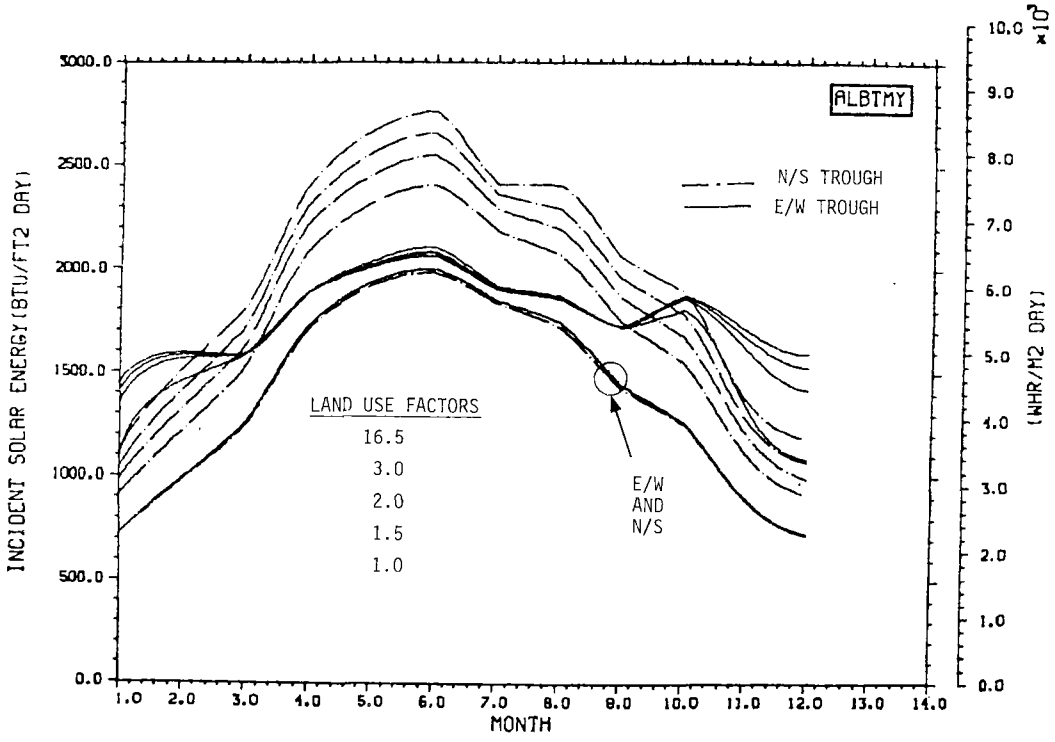

Figure G2. Monthly Shadowing of E/W and N/S Parabolic Troughs

the fact that any shading that does occur will occur during the early morning and late afternoon when E/W trough performance is lowest anyway due to large incidence angle effects.

This is further illustrated in Figures G3 and G4 which present the hourly Direct Insolation incident upon nonfirst row E/W and N/S collectors at different Land Use factors. As illustrated in Figure G3, some early morning shading occurs in an E/W system but, even with a Land Use Factor of 1.0, reduction in incident Direct Insolation is small. For a parabolic trough with a N/S orientation, on the other hand, Figure G4 illustrates significant shading up to the point where the hourly Direct Insolation incident upon a N/S collector output approaches that incident upon an E/W collector. It is interesting to note that at a Land Use Factor of 1.0, the Direct Insolation incident upon E/W and N/S collectors will be equal since, from the sun's viewpoint, the Direct Insolation incident on both fields will be equal to that incident on a flat plate. The combined shading and angle of incidence effects for both the E/W and N/S fields will be equivalent to the angle of incidence effects of a large flat plate filling the same area.

The shading losses suffered by both E/W and N/S in winter are also shown in Figure G2. As indicated, both orientations suffer shading losses but, as opposed to the summer situation, the losses suffered by the E/W-oriented parabolic trough collectors are somewhat larger than the losses suffered by the N/S-oriented collector.

The net result of the different seasonal dependence of shading for E/W and N/S parabolic trough fields is that, over a year, shading penalizes a N/S orientation more than an E/W orientation up to the point where, at the extreme case of a Land Use Factor of 1.0, the N/S and E/W field performances are the same.

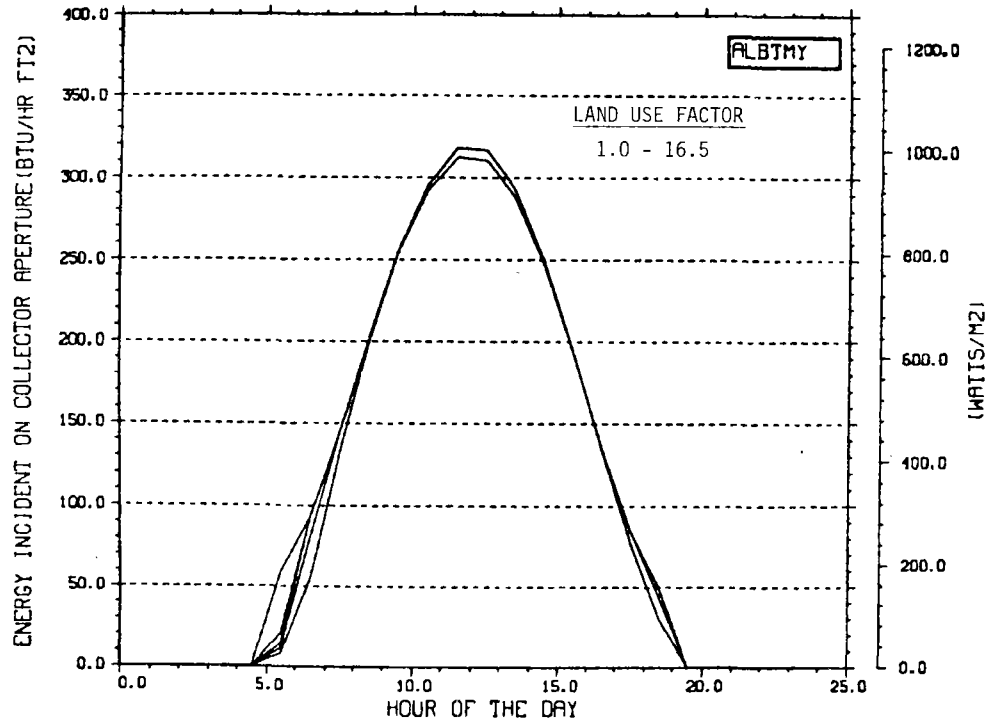

Figure G3. Shadowing of an E/W Parabolic Trough (Summer Solstice)

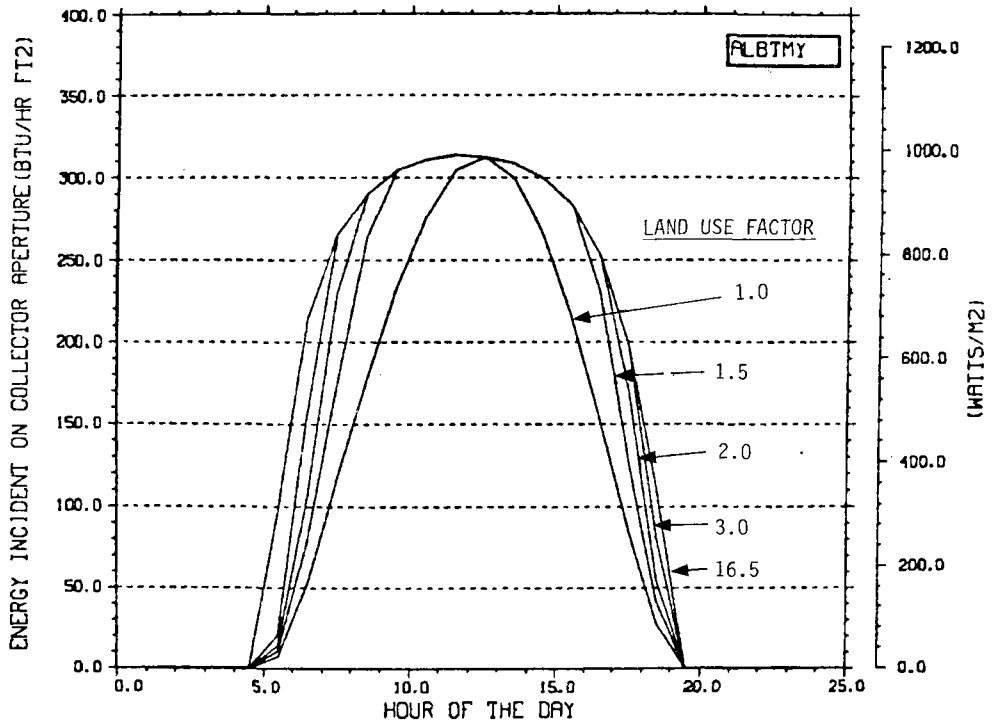

Figure G4. Shadowing of a N/S Parabolic Trough (Summer Solstice)

APPENDIX H

Site-Specific Design Information

This appendix is divided into two parts. The first part reproduces six design nomographs from the main body of the handbook. These six charts are needed during the design process and are reproduced here so that the reader need not search through the handbook for these charts.

The second part of this appendix gives the design information, in chart form, needed to execute conceptual designs. Design information for each of the 26 SOLMET sites is presented. The design charts are for the Nominal Collector defined in Section 2.4 and should be adjusted to reflect the collector under evaluation, as described in the body of the handbook (see, for example, Section 4, Conceptual Design Procedures).

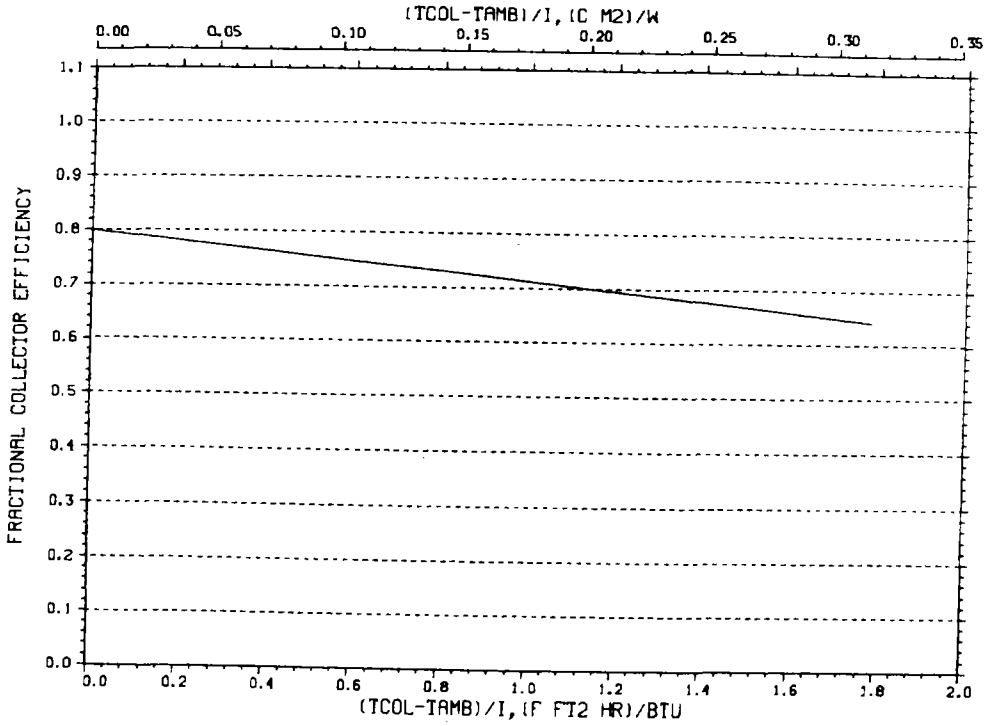

Figure H1. Performance of Nominal Collector

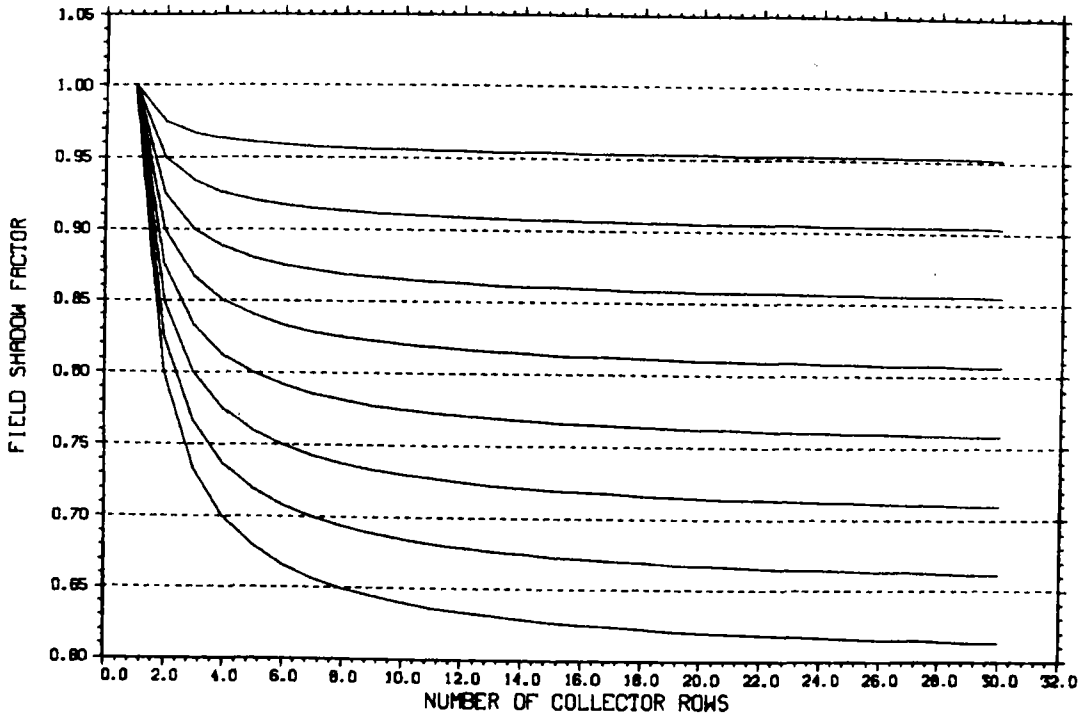

Figure H2. Effect of Number of Collector Rows on Field Shading Prediction of Average Collector Output

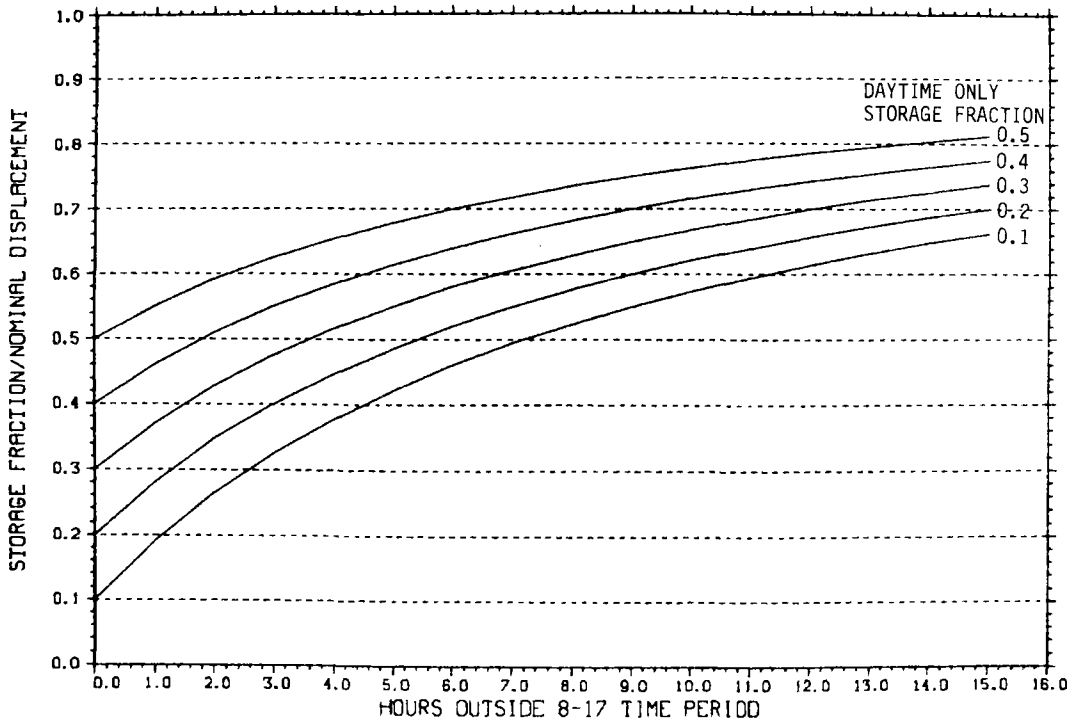

Figure H3. Computation of Storage Fraction

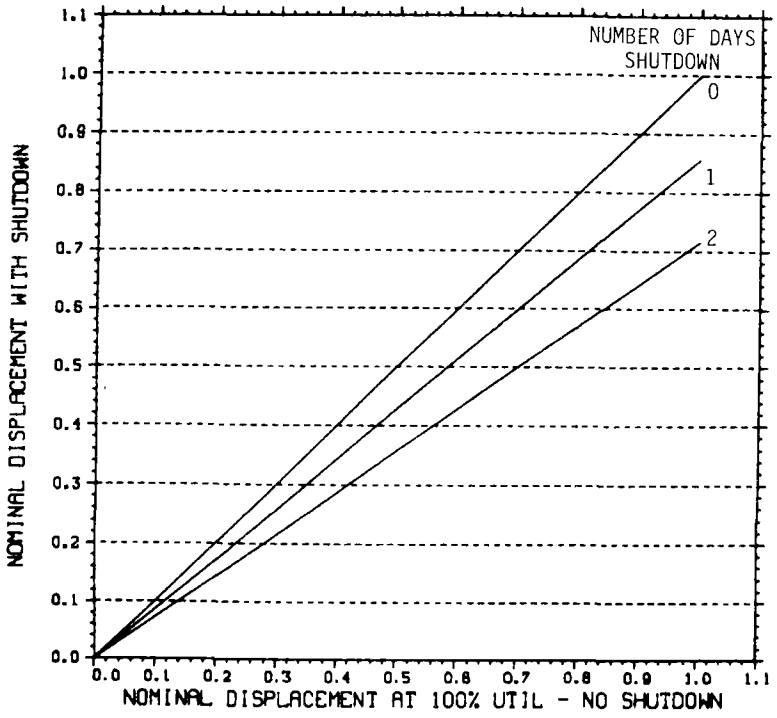

Figure H4. Nominal Displacement for Weekend Shutdown

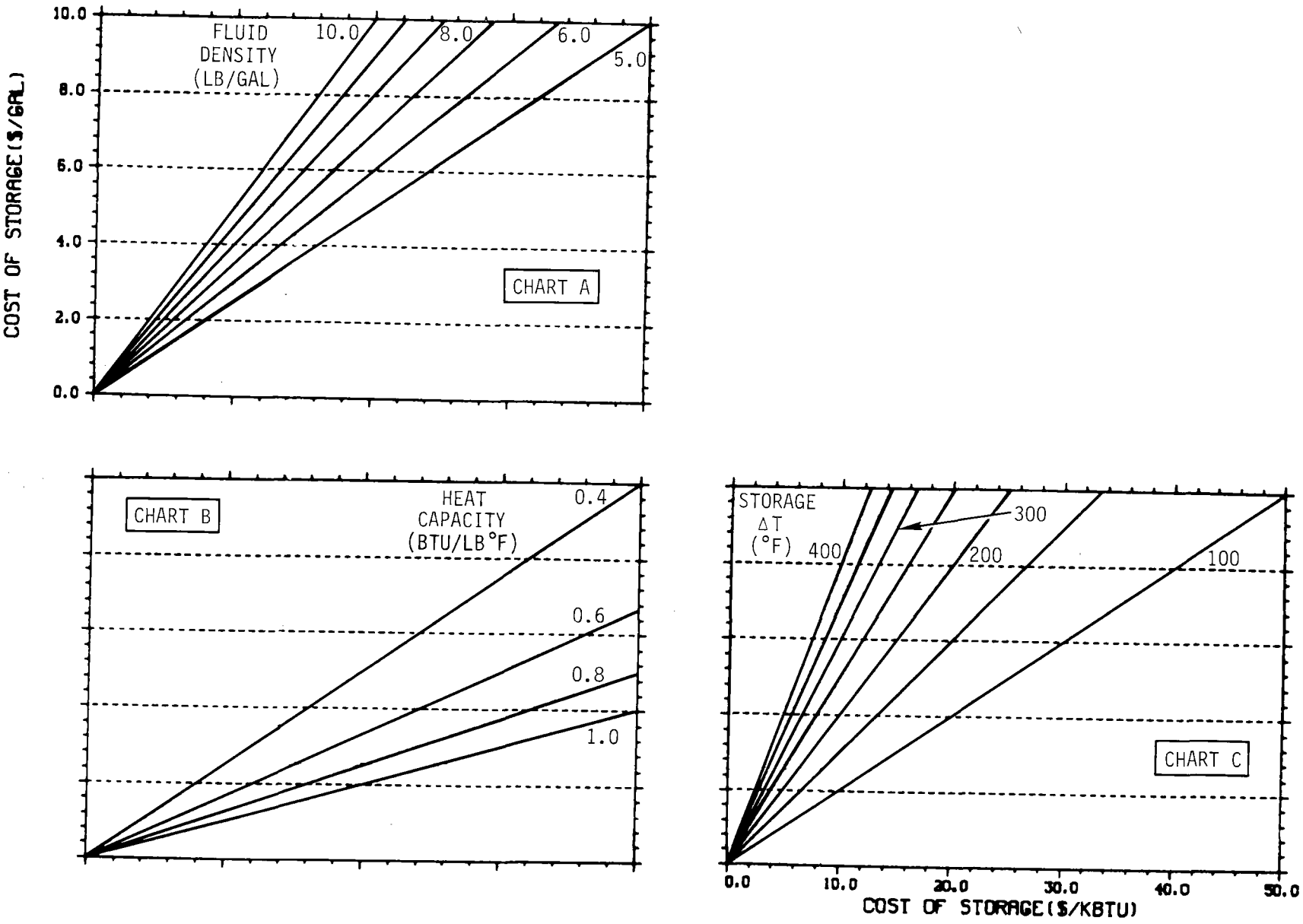

Figure H5. Estimation of Sensible Heat Storage Costs--
English Units

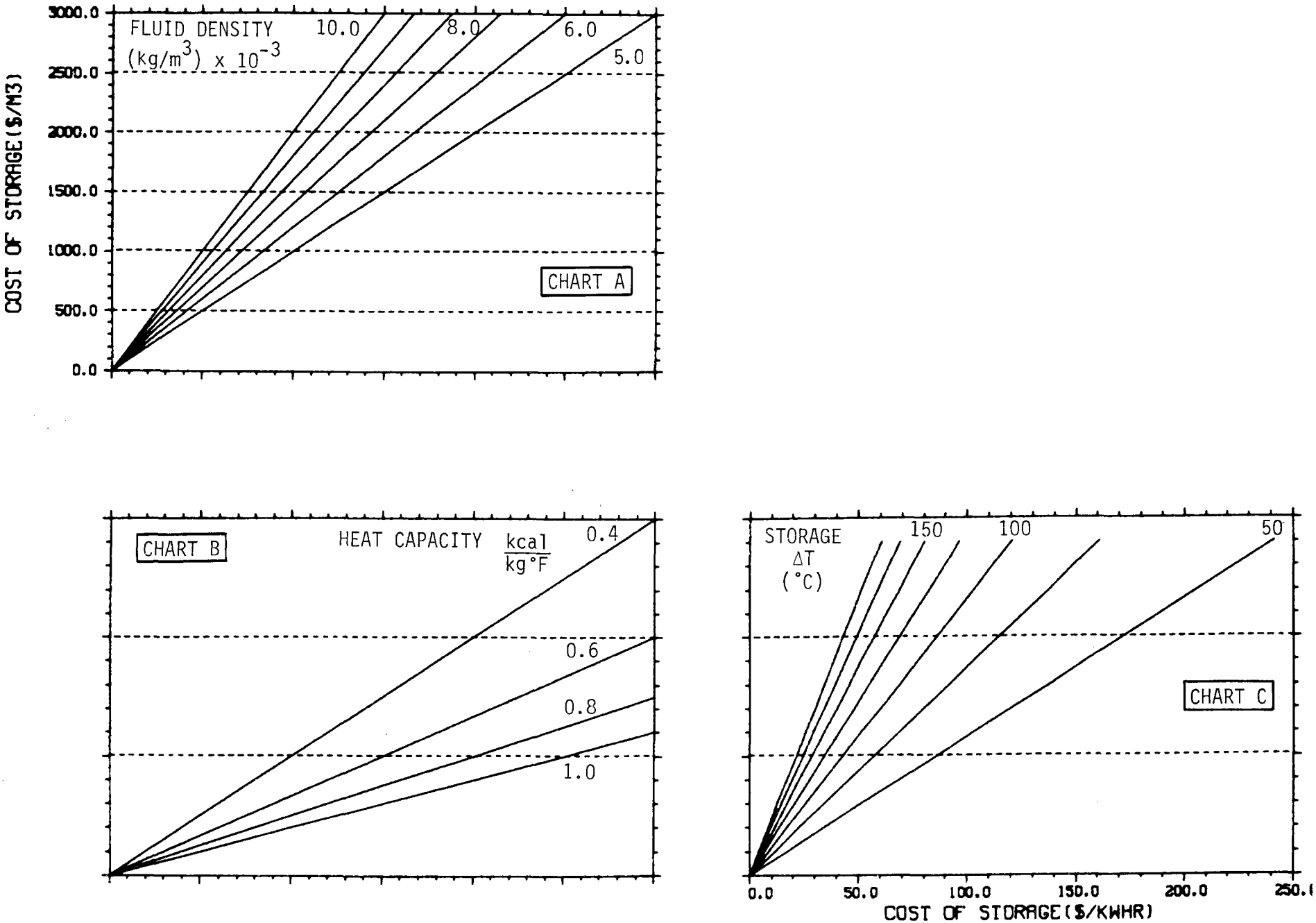

Figure H6. Estimation of Sensible Heat Storage Costs--
Metric Units

Part 2

Site-Specific Design Charts

ENERGY INCIDENT ON COLLECTOR APERTURE

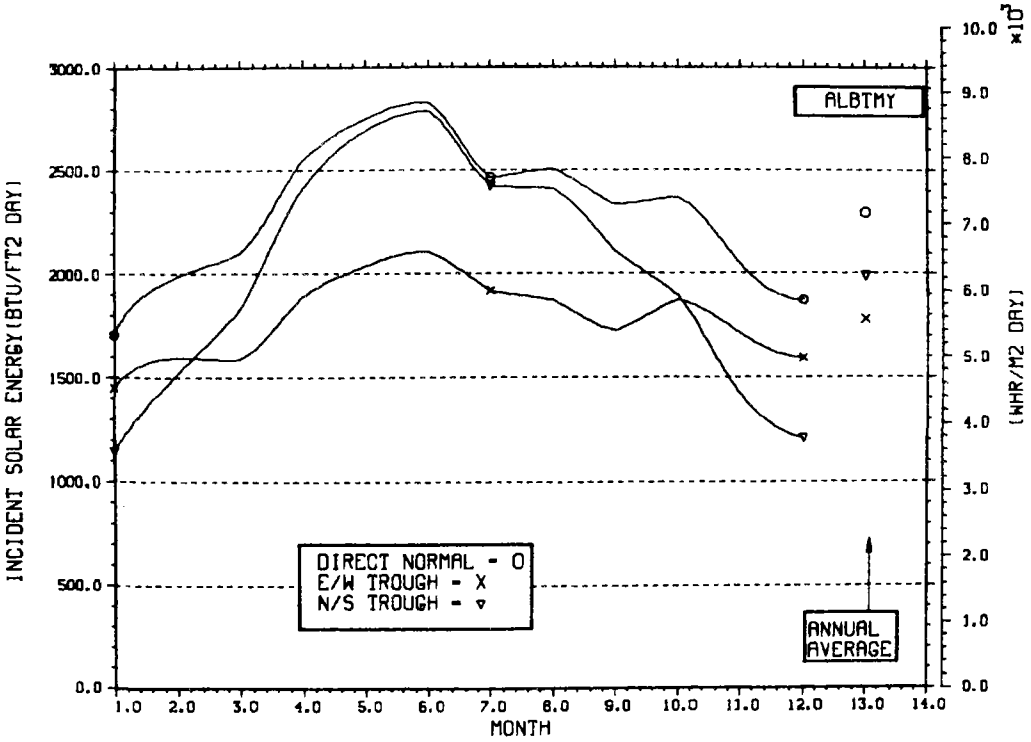

ANNUAL NONFIRST ROW SHADING

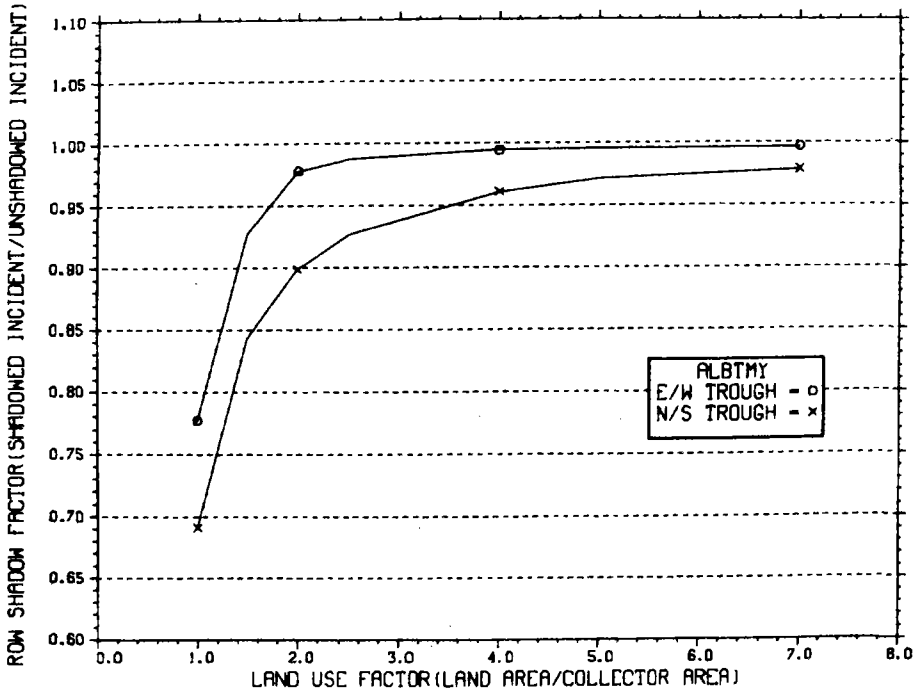

PERFORMANCE VARIATION WITH COLLECTOR AZIMUTH

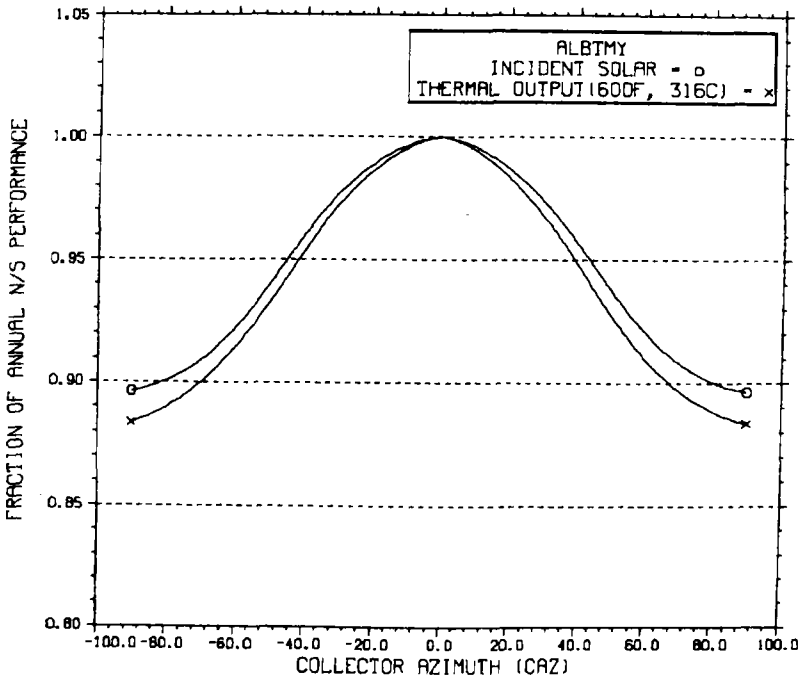

TEMPERATURE DEPENDENCE OF ANNUAL PERFORMANCE

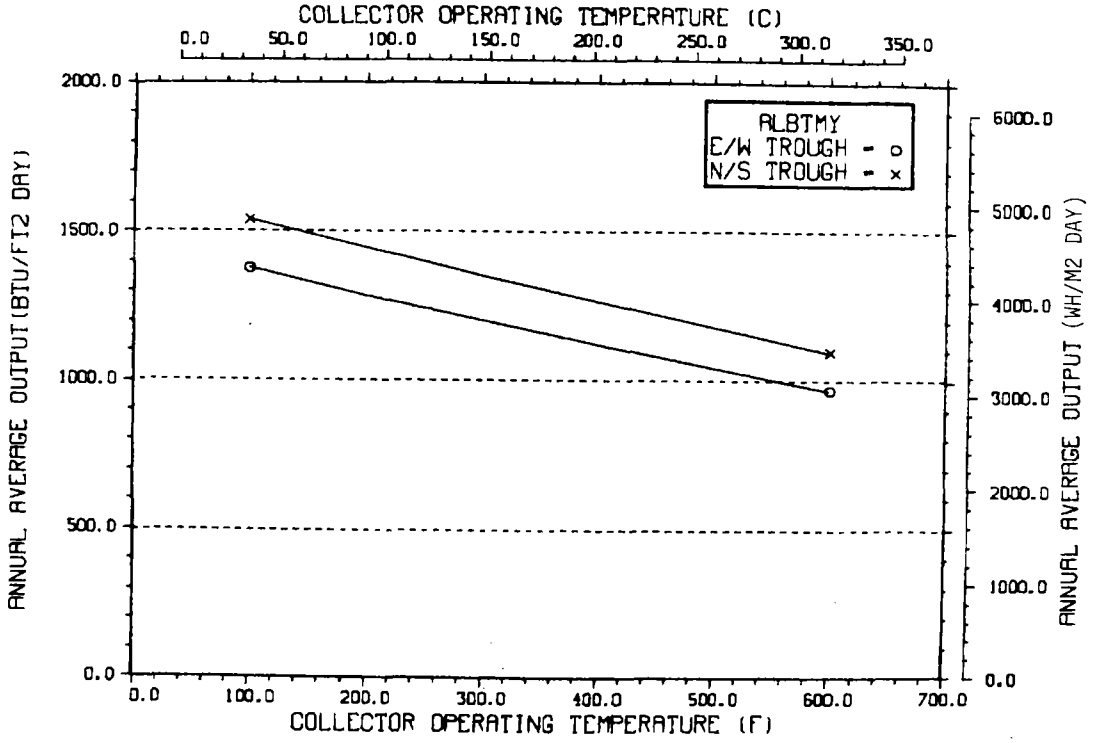

TEMPERATURE DEPENDENCE OF MONTHLY PERFORMANCE

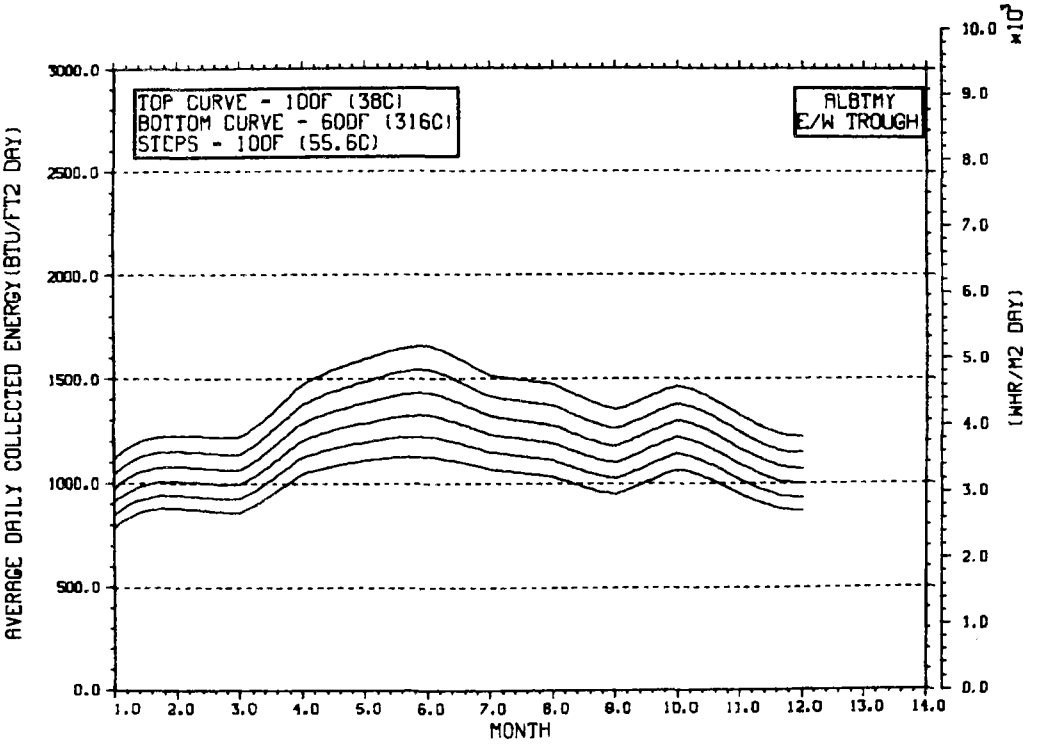

TEMPERATURE DEPENDENCE OF MONTHLY PERFORMANCE

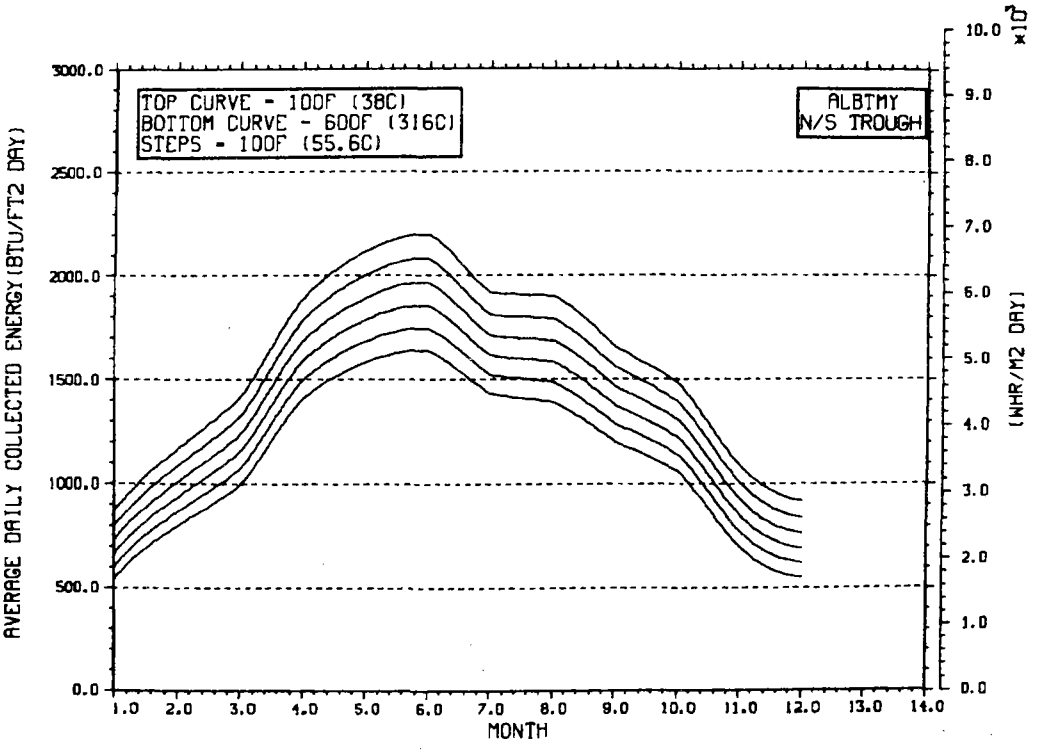

STORAGE SIZING GRAPH FOR CONSTANT ANNUAL DEMAND

NO WEEKEND SHUTDOWN

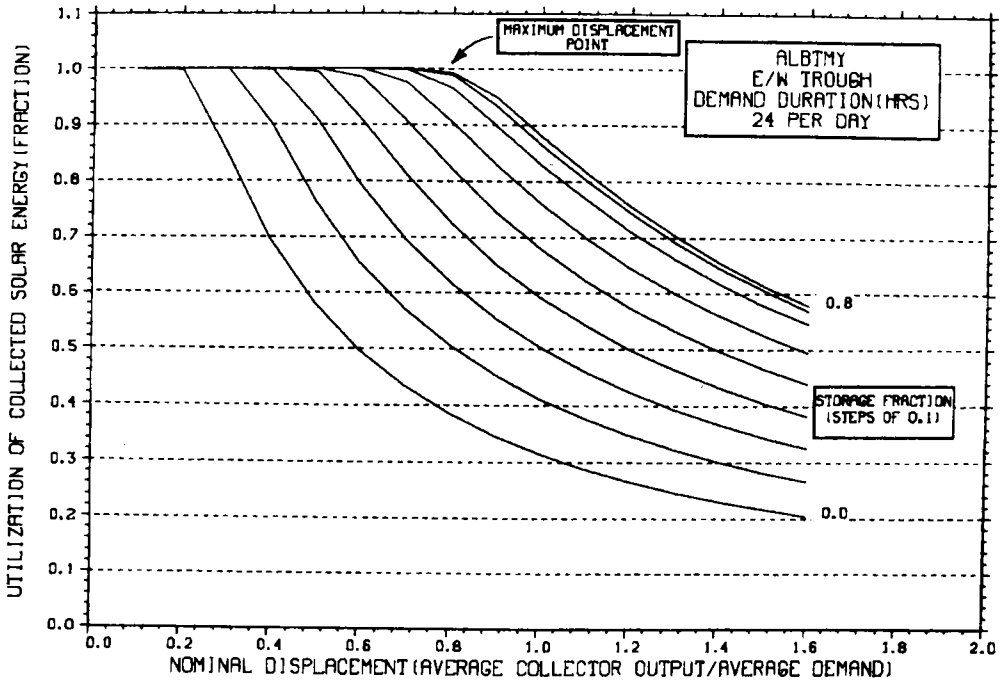

STORAGE SIZING GRAPH FOR CONSTANT ANNUAL DEMAND

NO WEEKEND SHUTDOWN

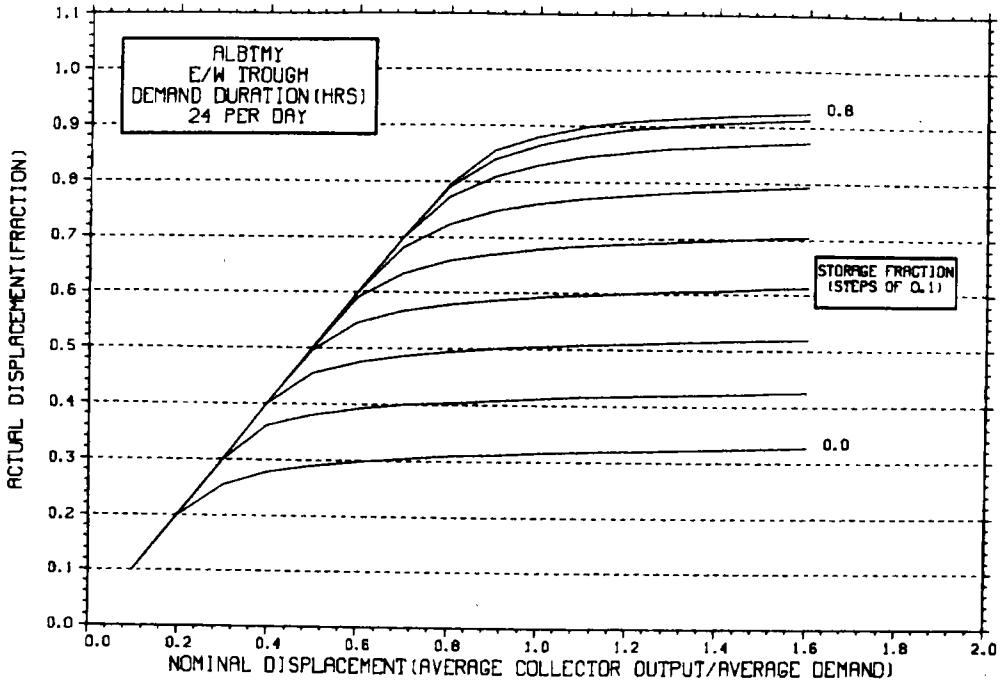

STORAGE SIZING GRAPH FOR CONSTANT ANNUAL DEMAND

NO WEEKEND SHUTDOWN

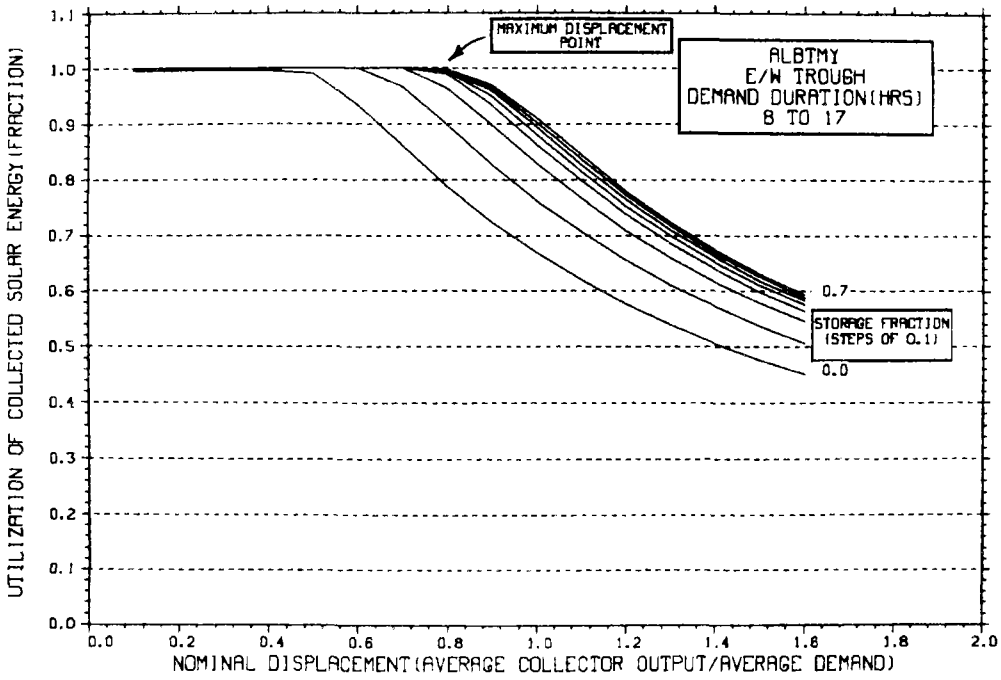

STORAGE SIZING GRAPH FOR CONSTANT ANNUAL DEMAND

NO WEEKEND SHUTDOWN

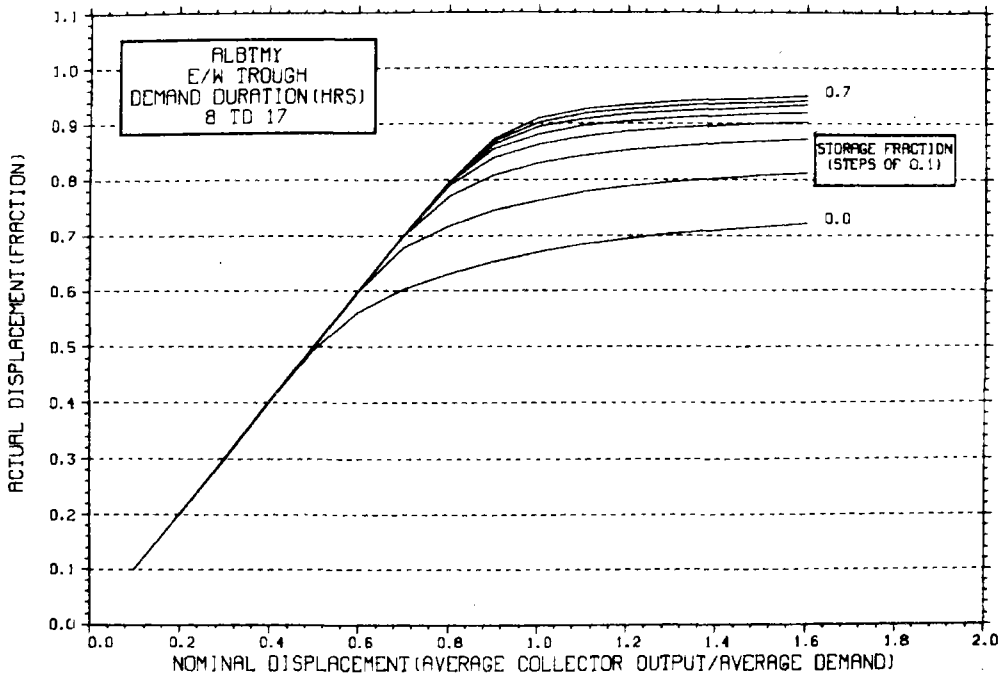

STORAGE SIZING GRAPH FOR CONSTANT ANNUAL DEMAND

NO WEEKEND SHUTDOWN

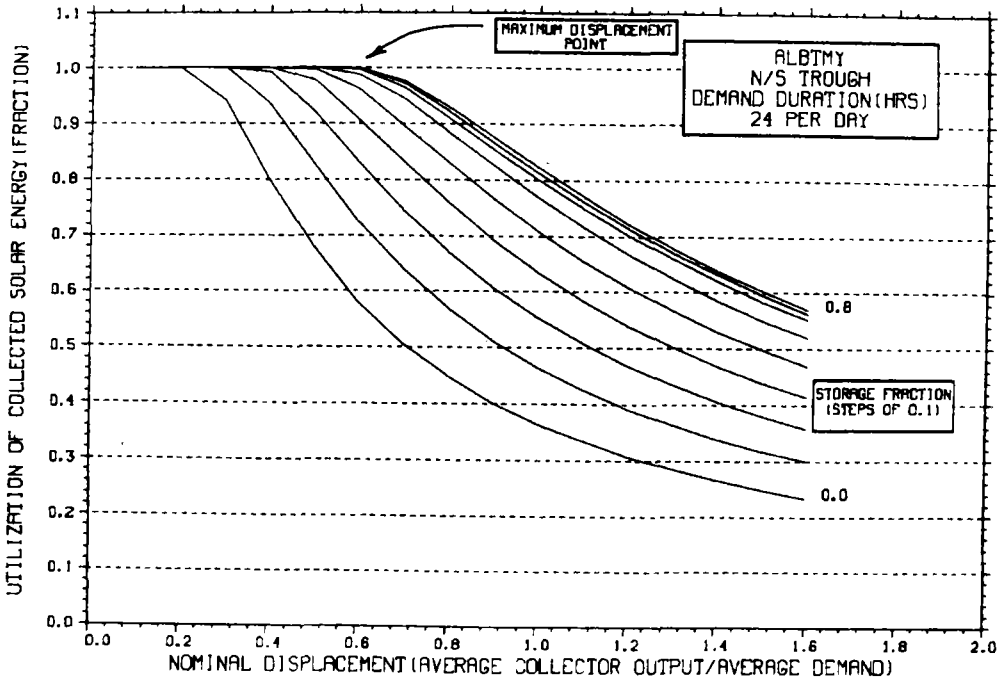

STORAGE SIZING GRAPH FOR CONSTANT ANNUAL DEMAND

NO WEEKEND SHUTDOWN

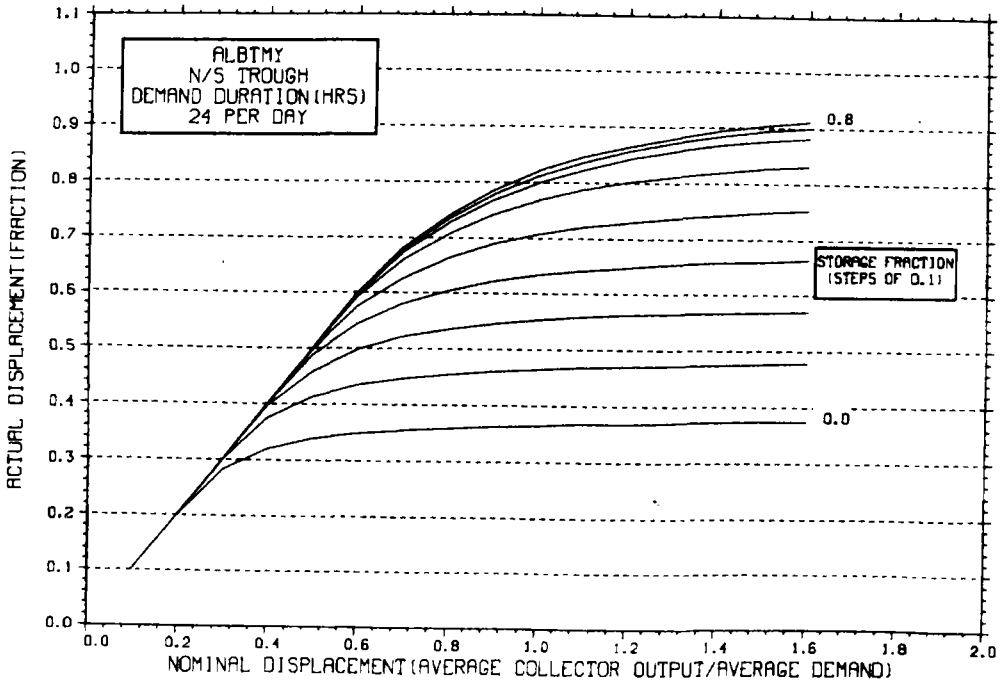

STORAGE SIZING GRAPH FOR CONSTANT ANNUAL DEMAND

NO WEEKEND SHUTDOWN

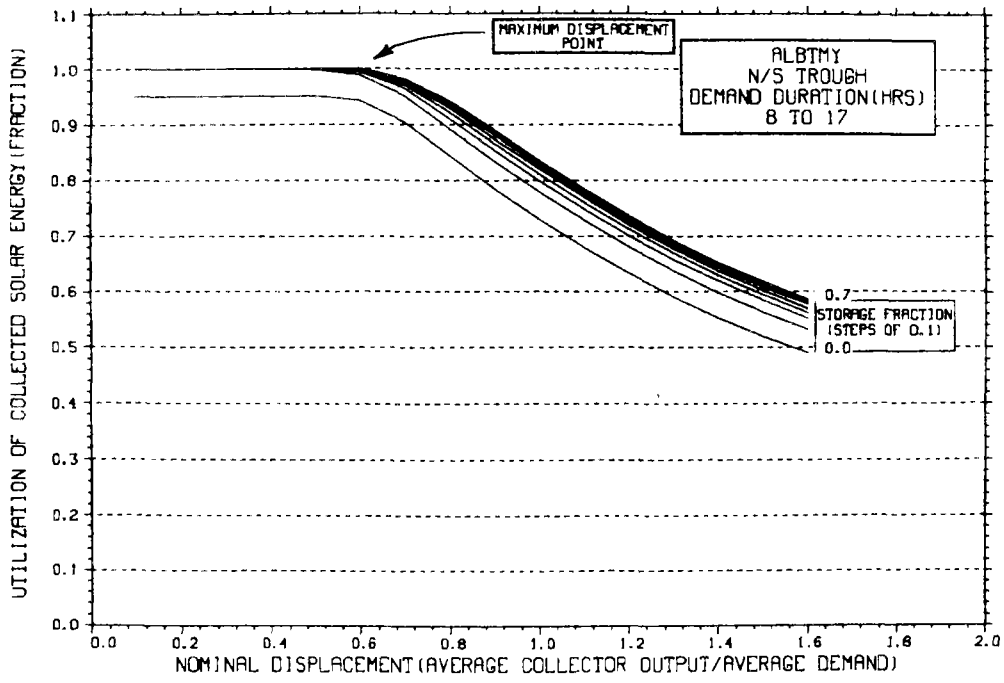

STORAGE SIZING GRAPH FOR CONSTANT ANNUAL DEMAND

NO WEEKEND SHUTDOWN

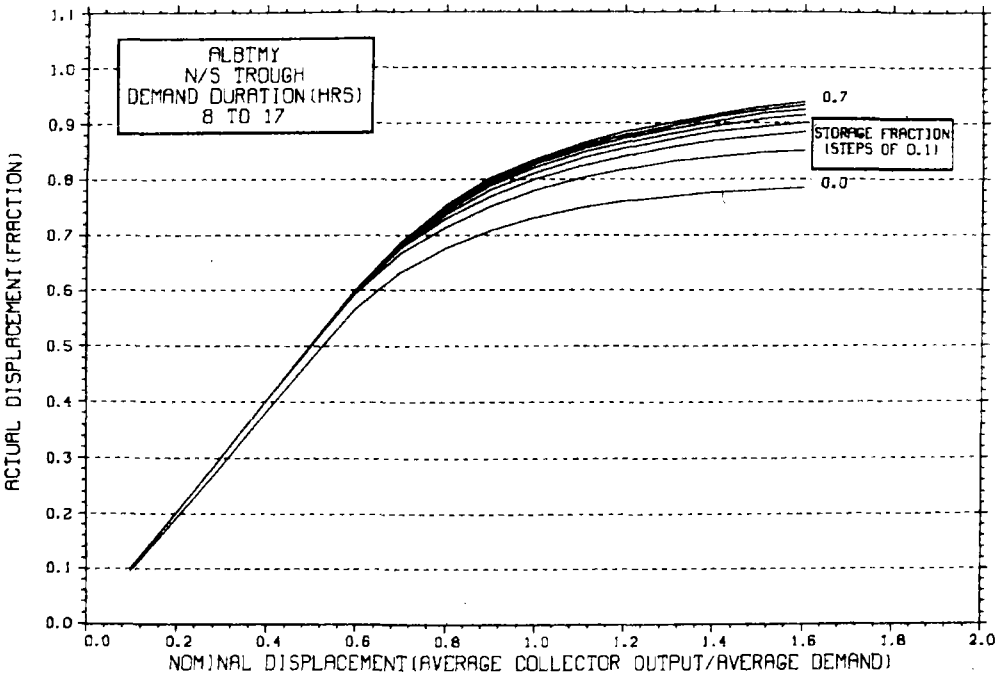

ENERGY INCIDENT ON COLLECTOR APERTURE

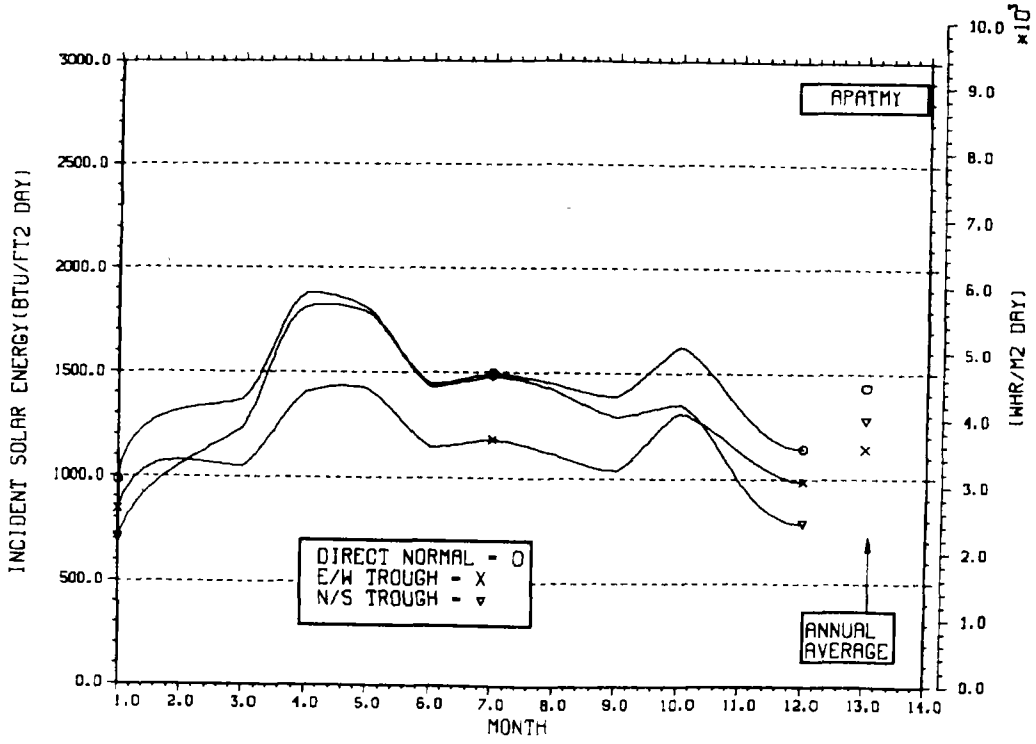

ANNUAL NONFIRST ROW SHADING

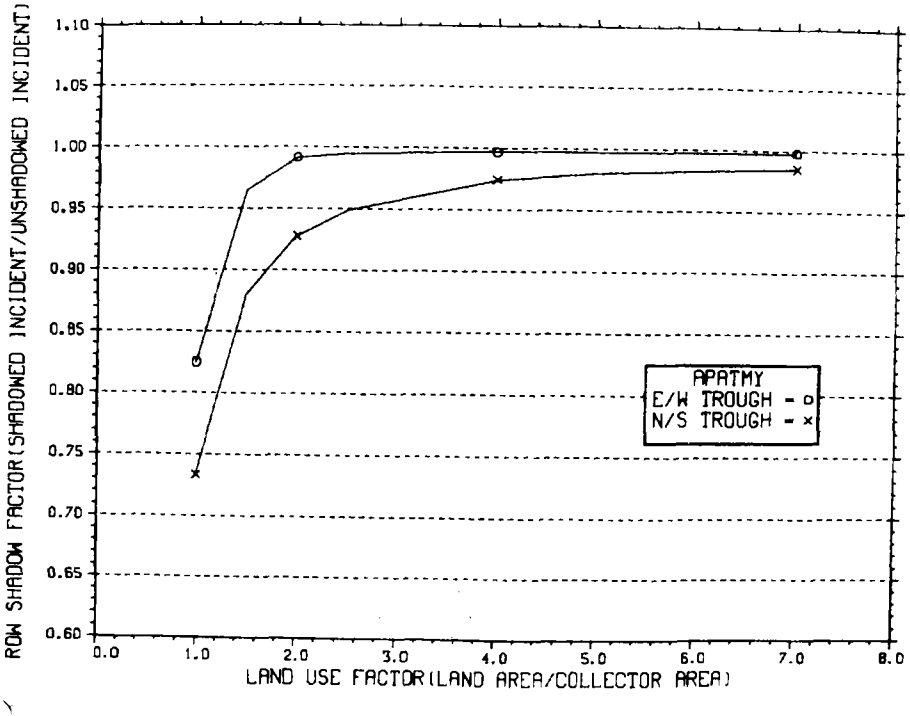

PERFORMANCE VARIATION WITH COLLECTOR AZIMUTH

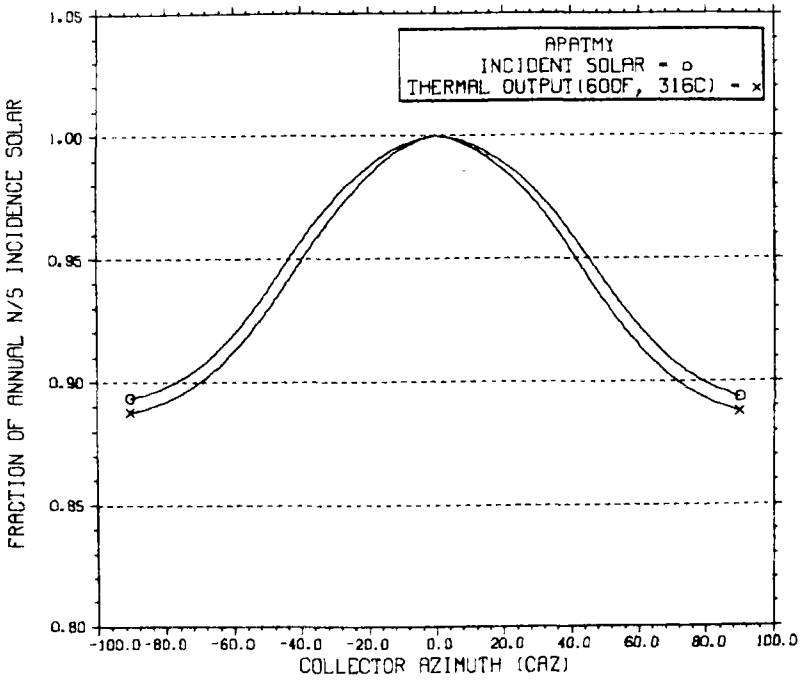

TEMPERATURE DEPENDENCE OF ANNUAL PERFORMANCE

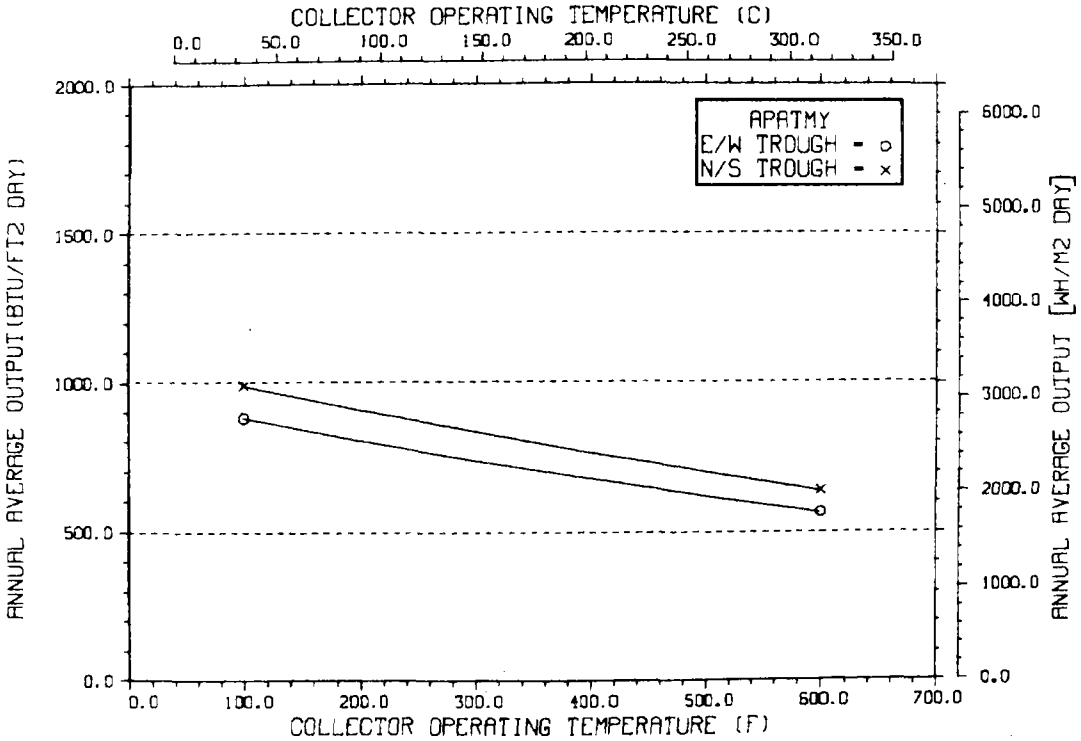

TEMPERATURE DEPENDENCE OF MONTHLY PERFORMANCE

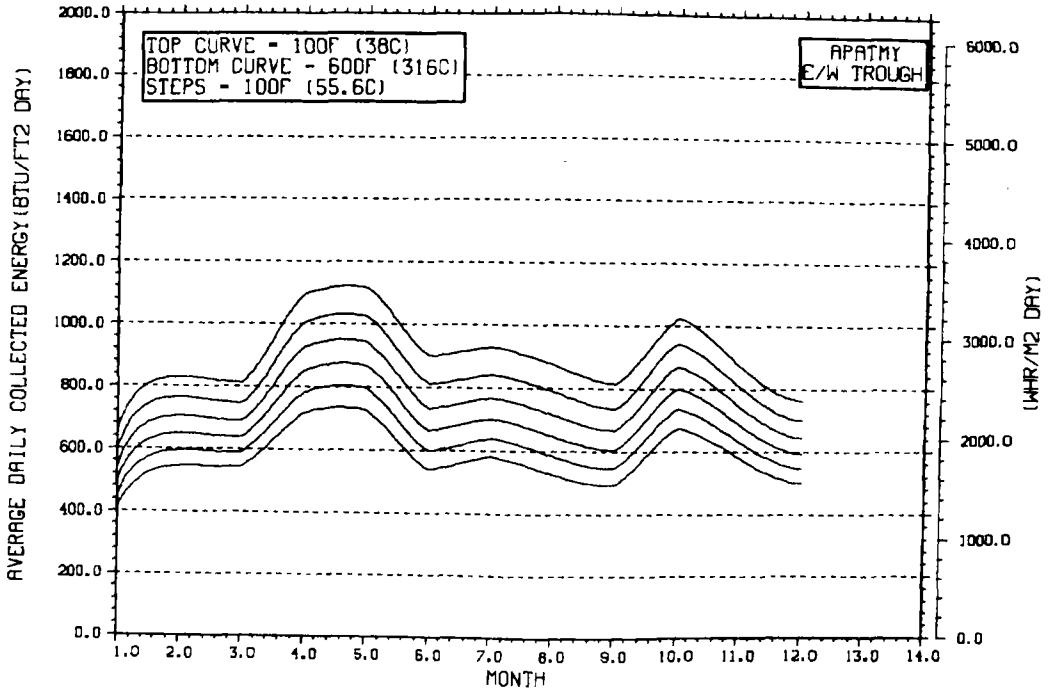

TEMPERATURE DEPENDENCE OF MONTHLY PERFORMANCE

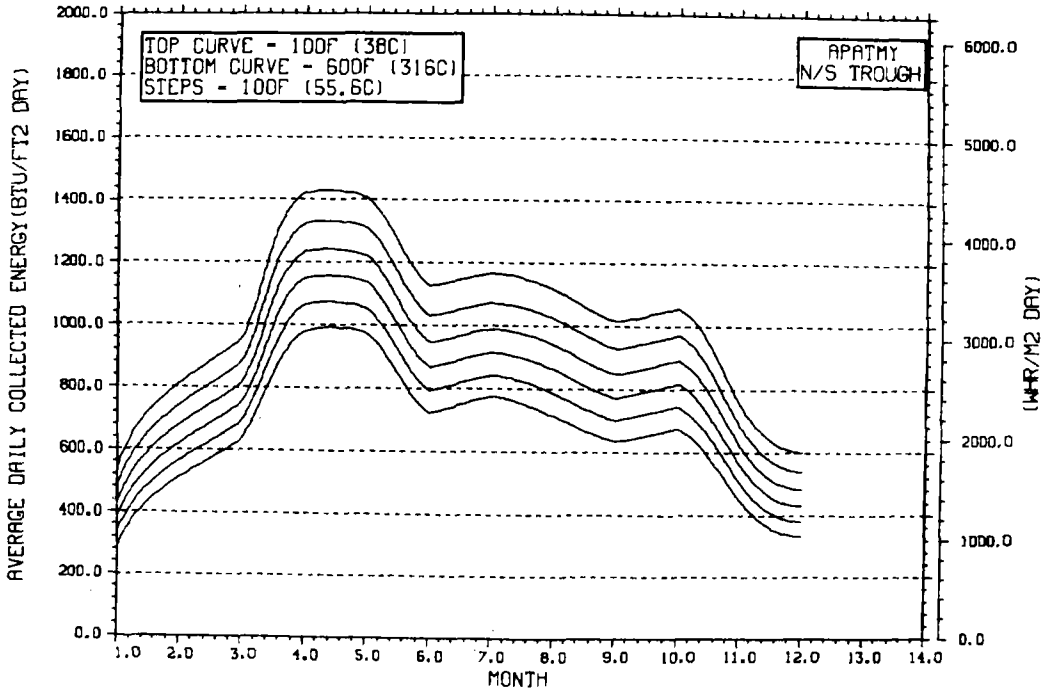

STORAGE SIZING GRAPH FOR CONSTANT ANNUAL DEMAND

NO WEEKEND SHUTDOWN

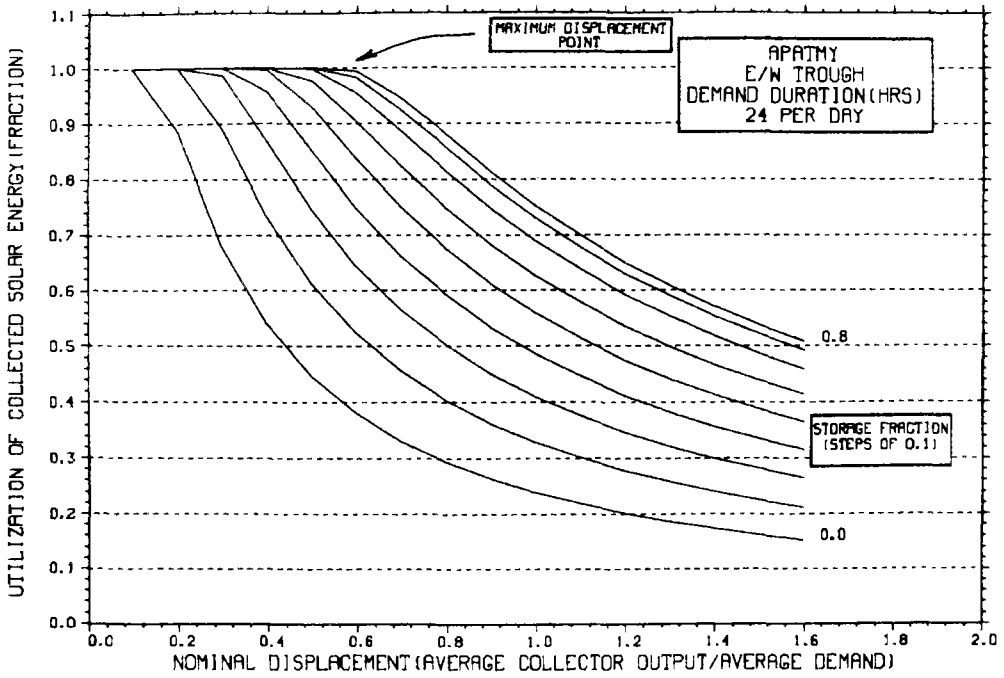

STORAGE SIZING GRAPH FOR CONSTANT ANNUAL DEMAND

NO WEEKEND SHUTDOWN

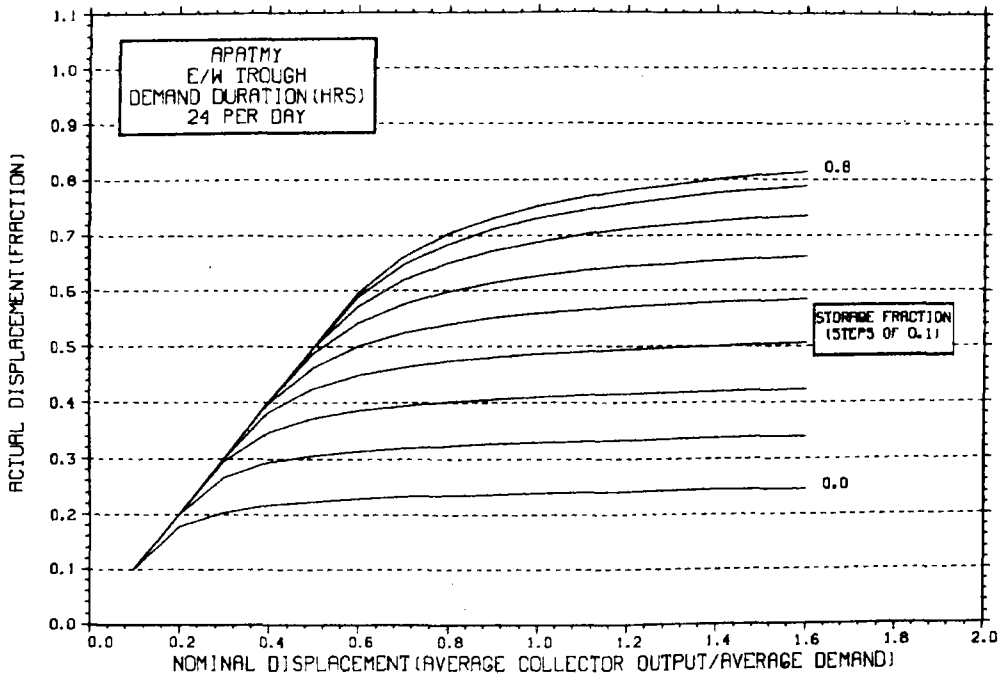

STORAGE SIZING GRAPH FOR CONSTANT ANNUAL DEMAND

NO WEEKEND SHUTDOWN

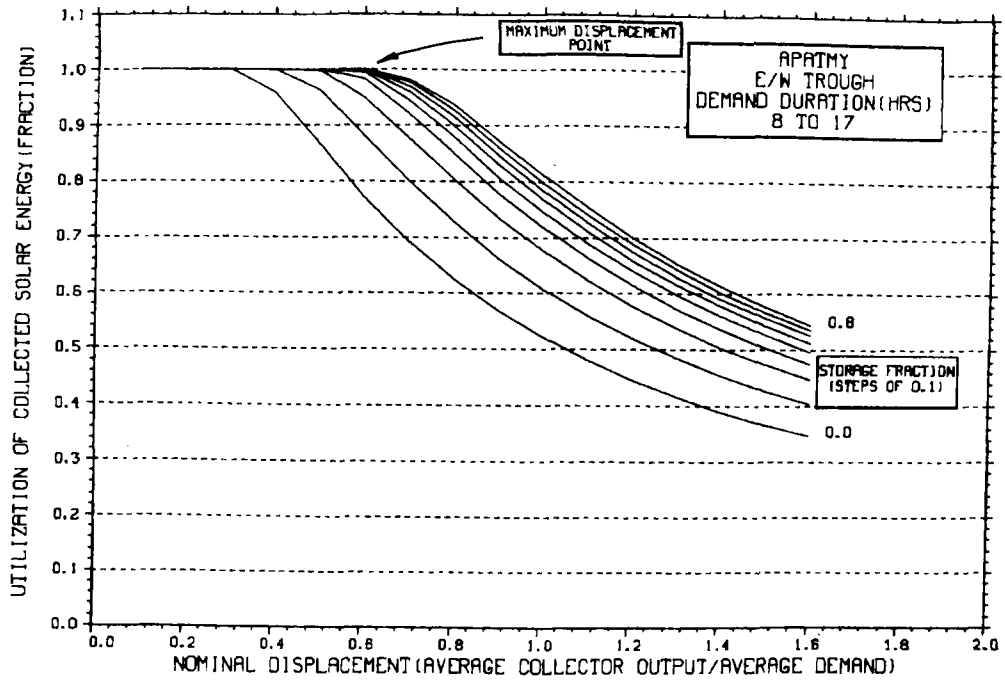

STORAGE SIZING GRAPH FOR CONSTANT ANNUAL DEMAND

NO WEEKEND SHUTDOWN

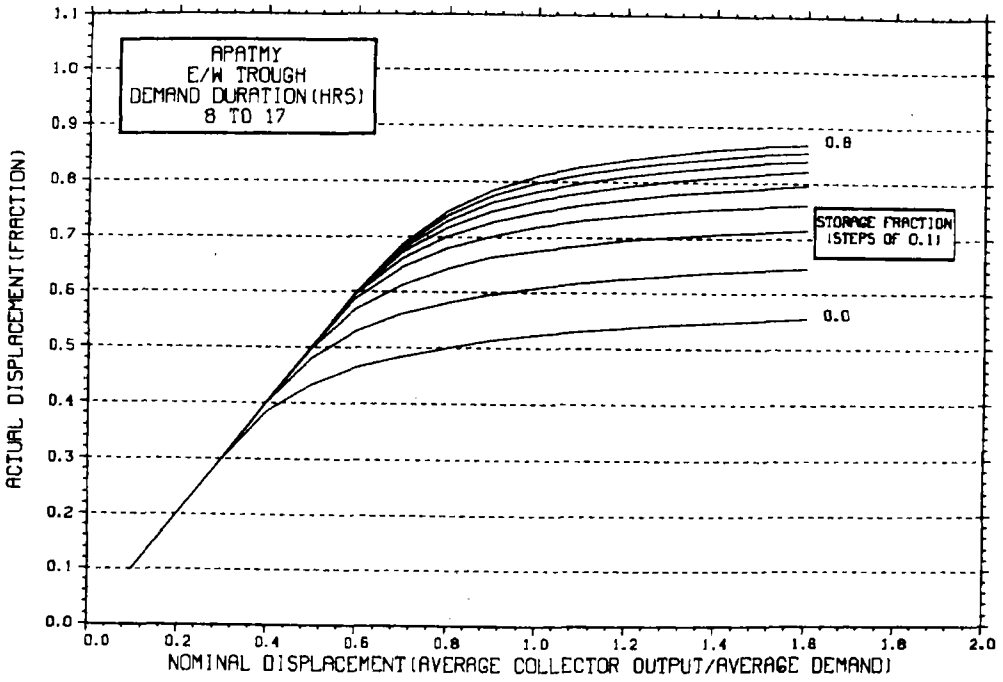

STORAGE SIZING GRAPH FOR CONSTANT ANNUAL DEMAND

NO WEEKEND SHUTDOWN

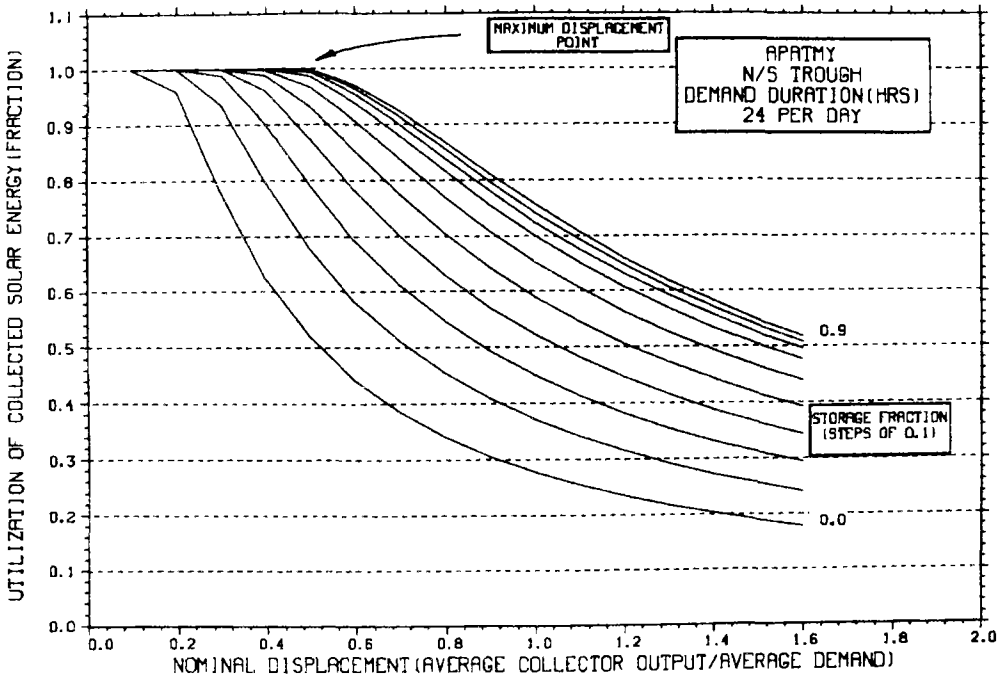

STORAGE SIZING GRAPH FOR CONSTANT ANNUAL DEMAND

NO WEEKEND SHUTDOWN

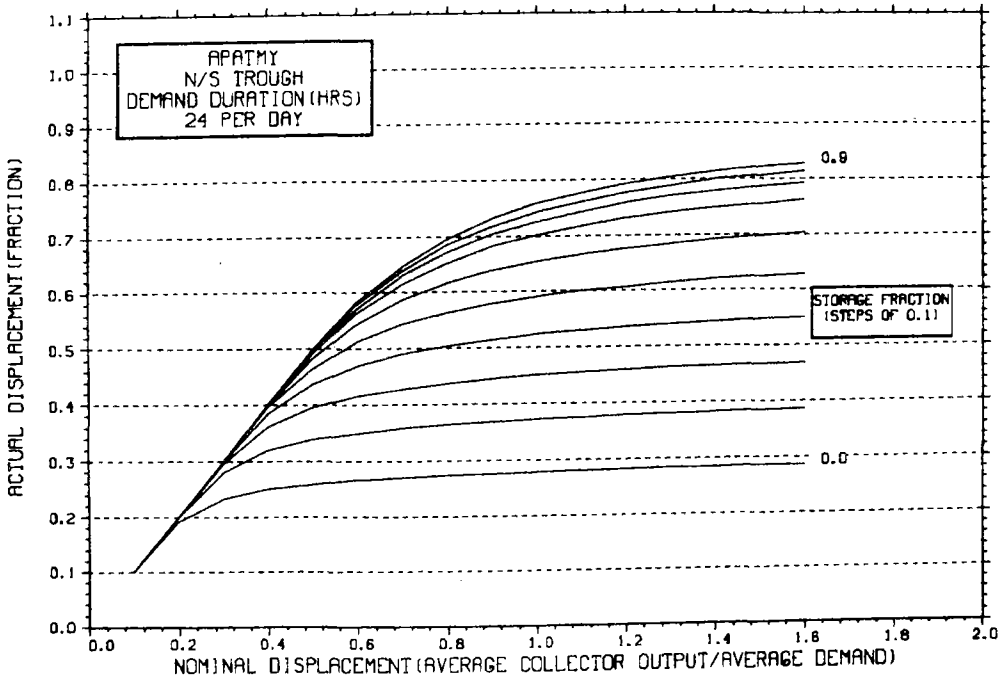

STORAGE SIZING GRAPH FOR CONSTANT ANNUAL DEMAND

NO WEEKEND SHUTDOWN

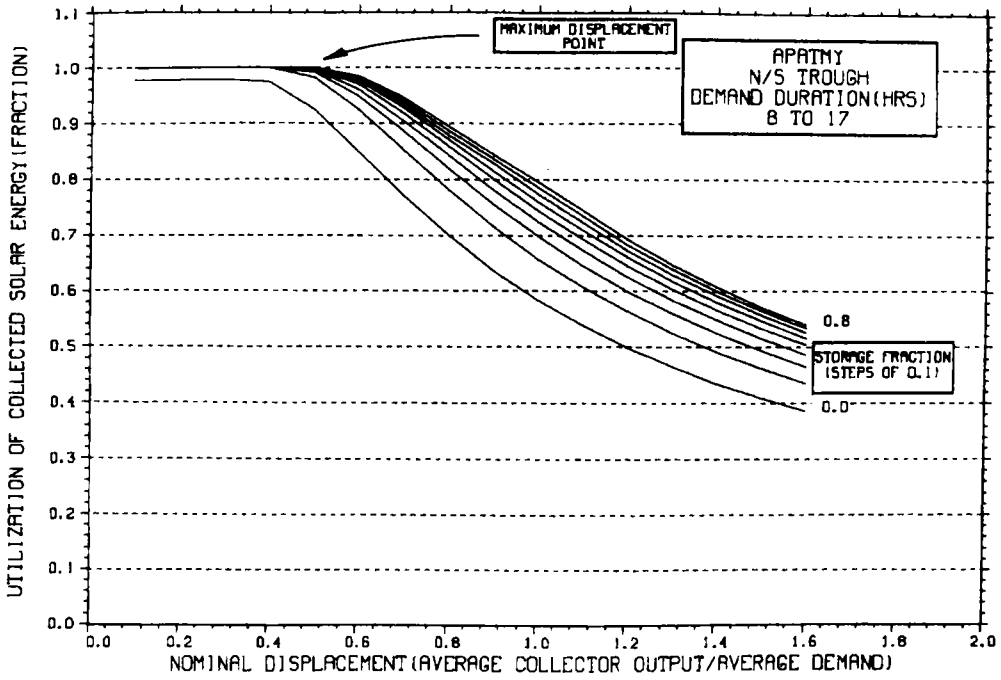

STORAGE SIZING GRAPH FOR CONSTANT ANNUAL DEMAND

NO WEEKEND SHUTDOWN

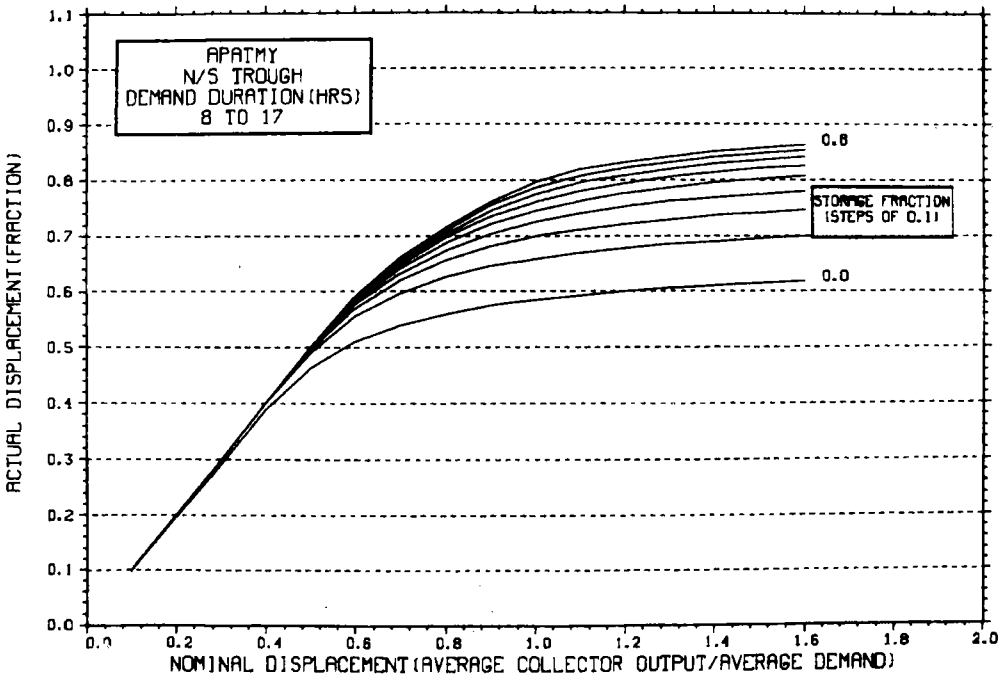

ENERGY INCIDENT ON COLLECTOR APERTURE

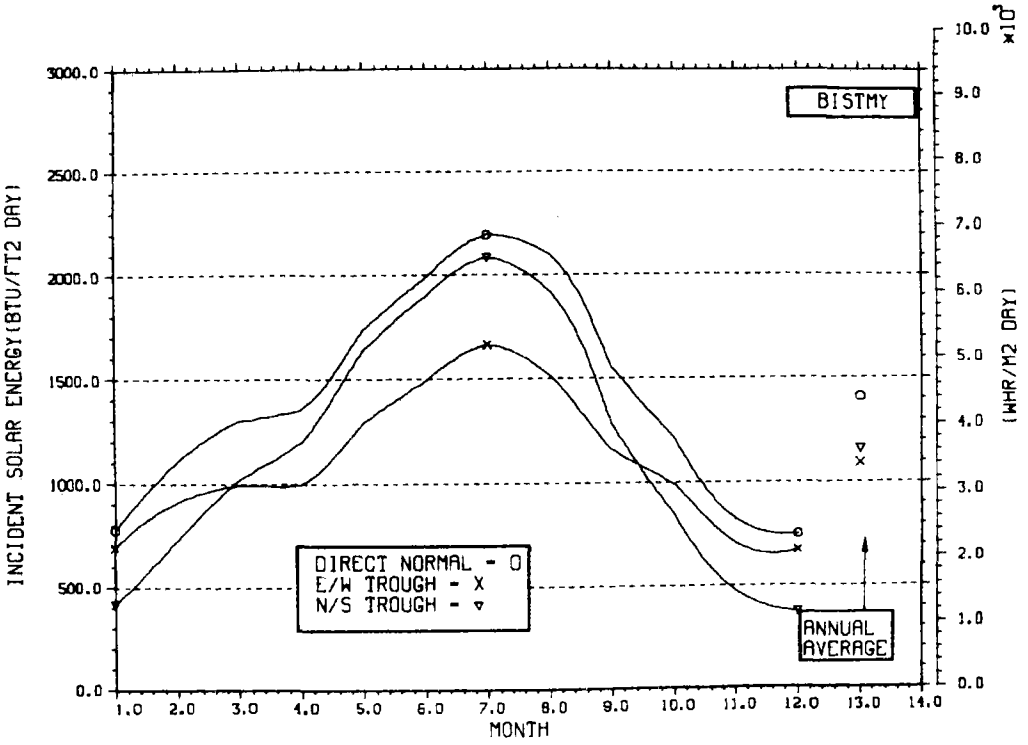

ANNUAL NONFIRST ROW SHADING

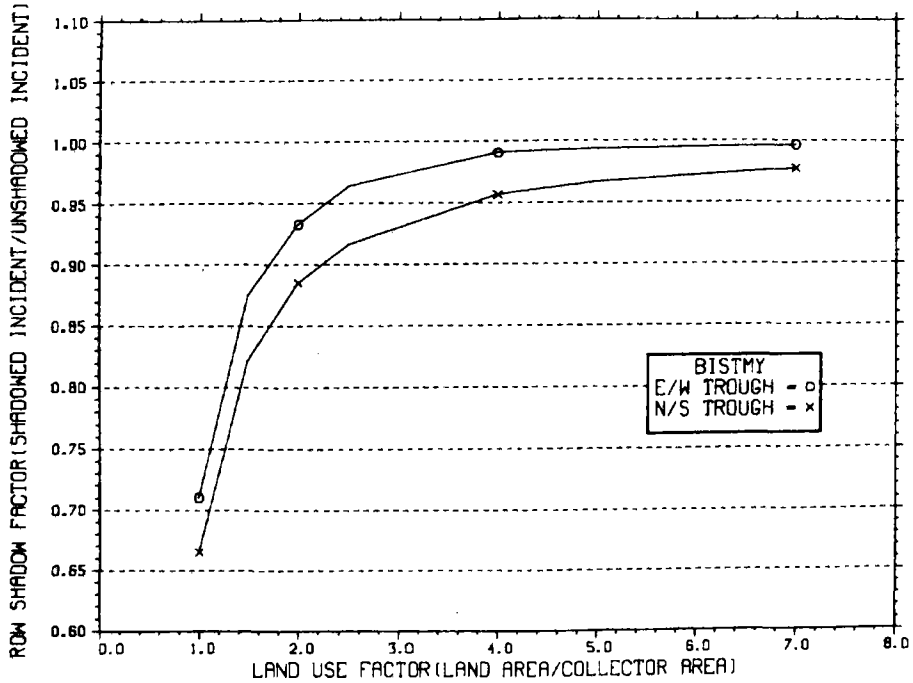

PERFORMANCE VARIATION WITH COLLECTOR AZIMUTH

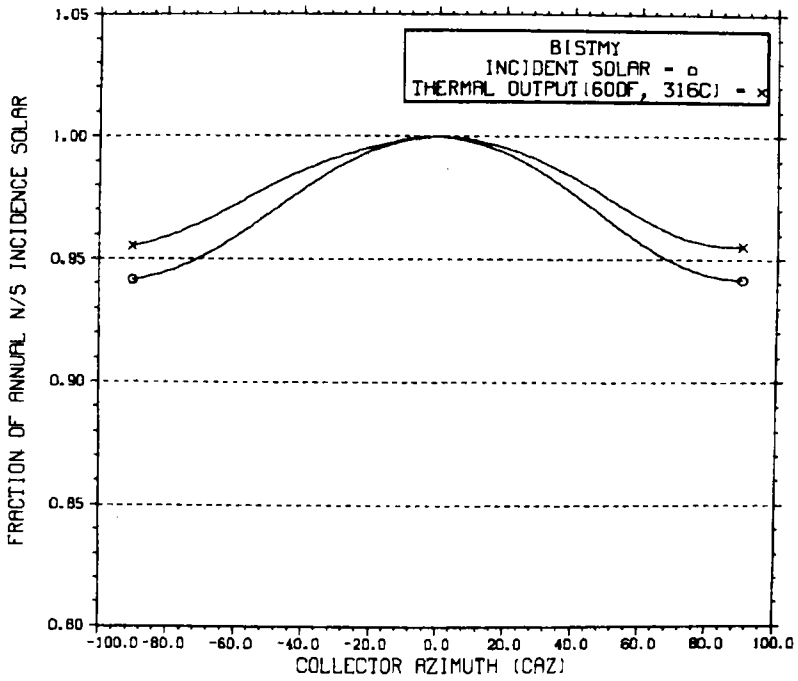

TEMPERATURE DEPENDENCE OF ANNUAL PERFORMANCE

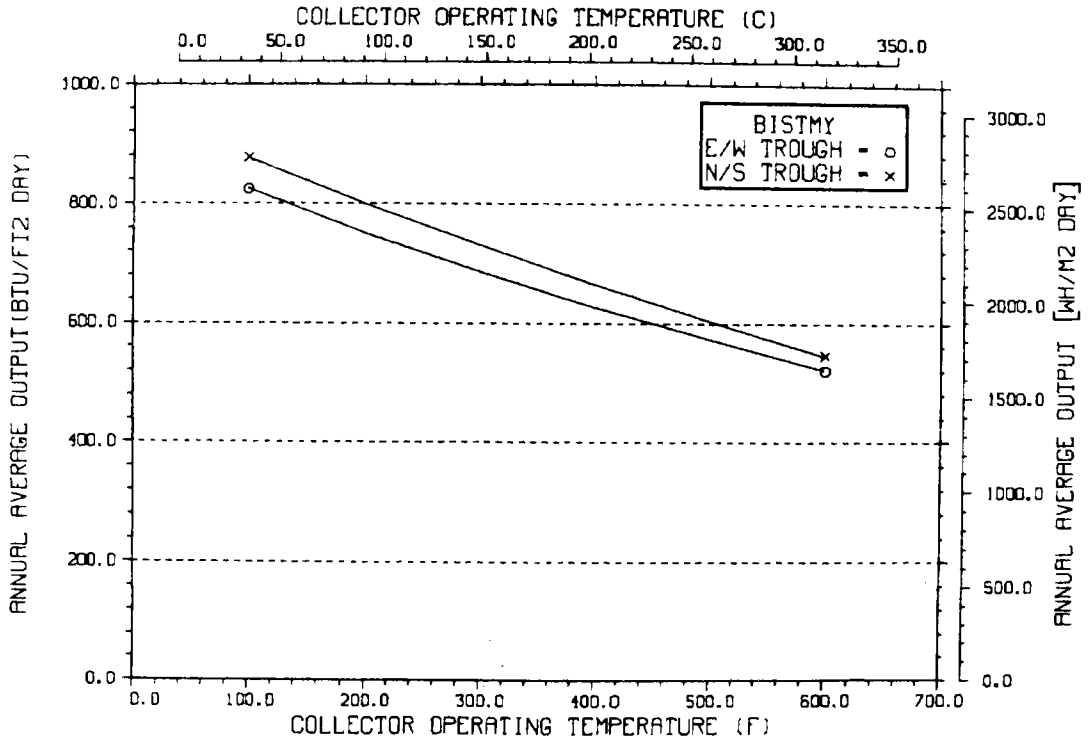

TEMPERATURE DEPENDENCE OF MONTHLY PERFORMANCE

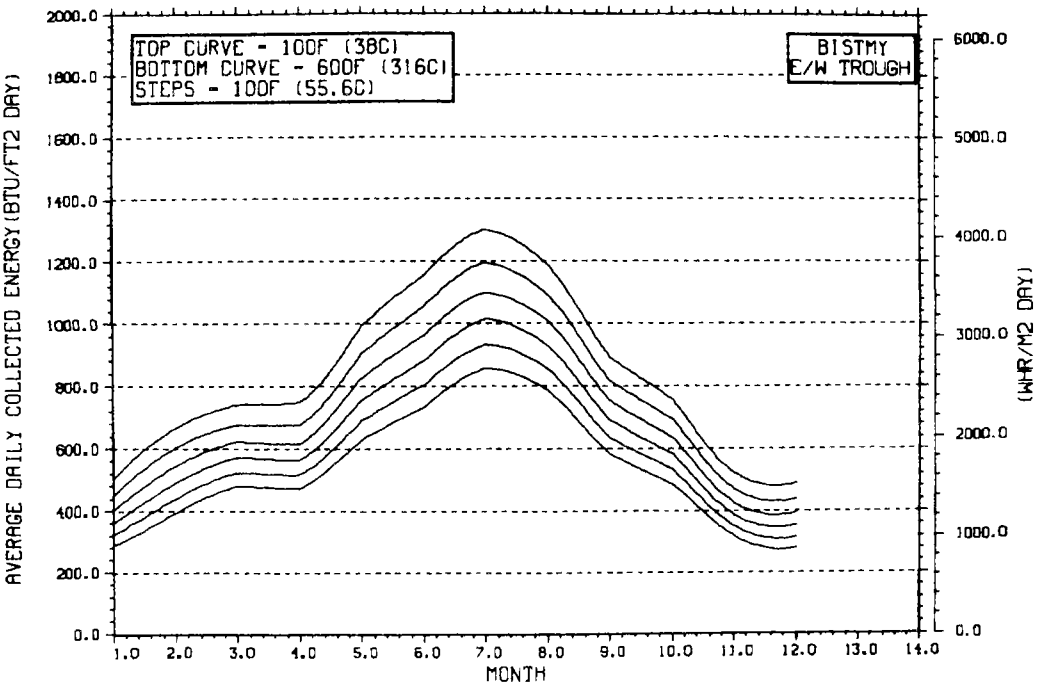

TEMPERATURE DEPENDENCE OF MONTHLY PERFORMANCE

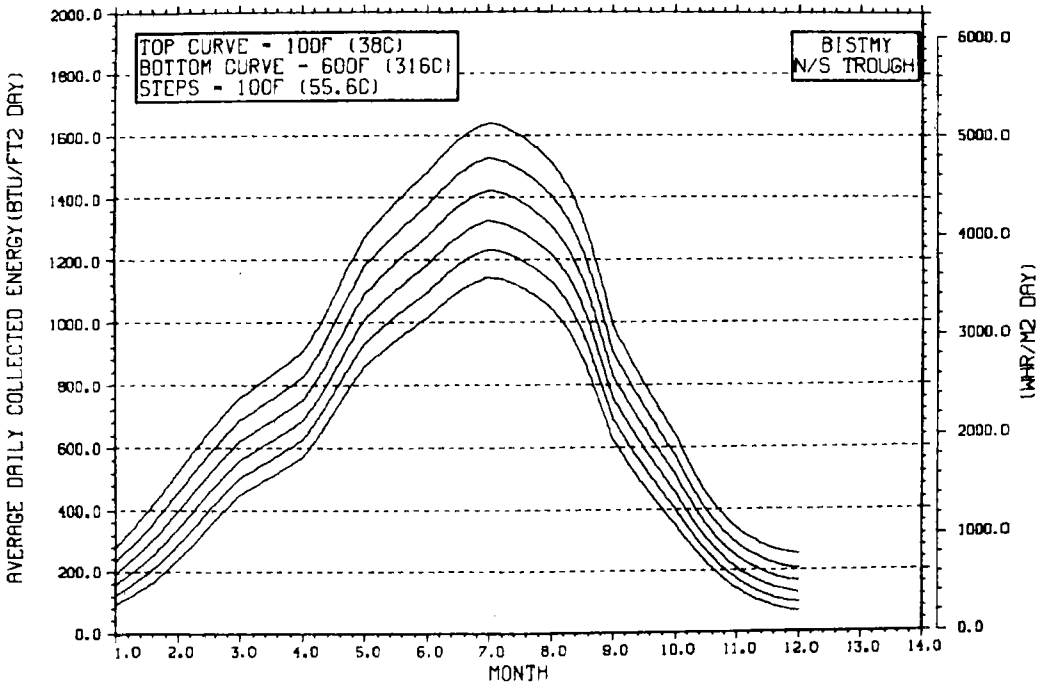

STORAGE SIZING GRAPH FOR CONSTANT ANNUAL DEMAND

NO WEEKEND SHUTDOWN

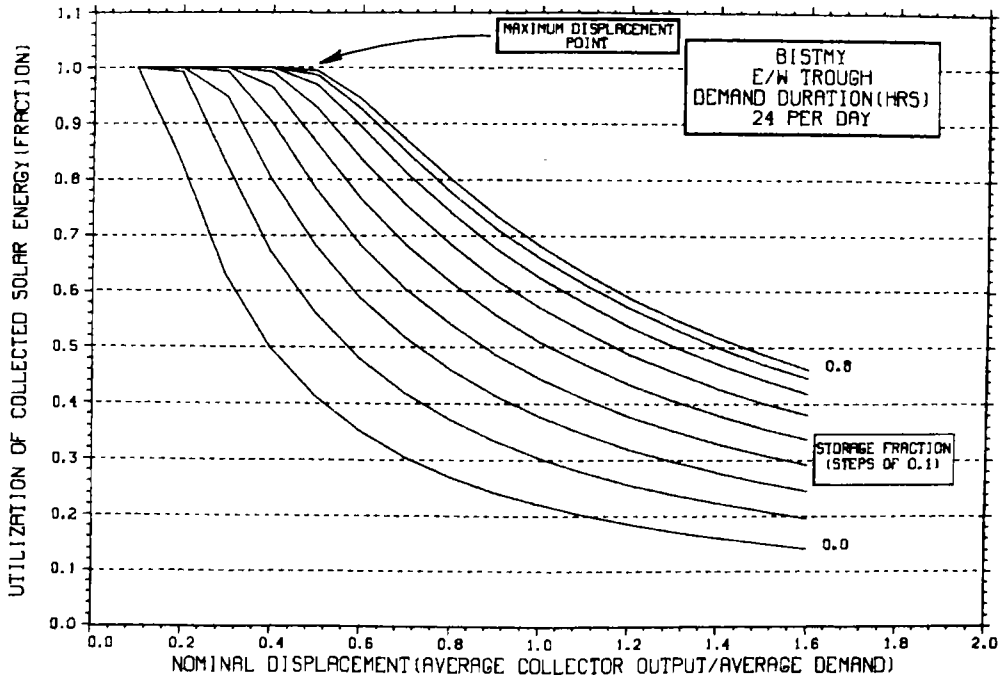

STORAGE SIZING GRAPH FOR CONSTANT ANNUAL DEMAND

NO WEEKEND SHUTDOWN

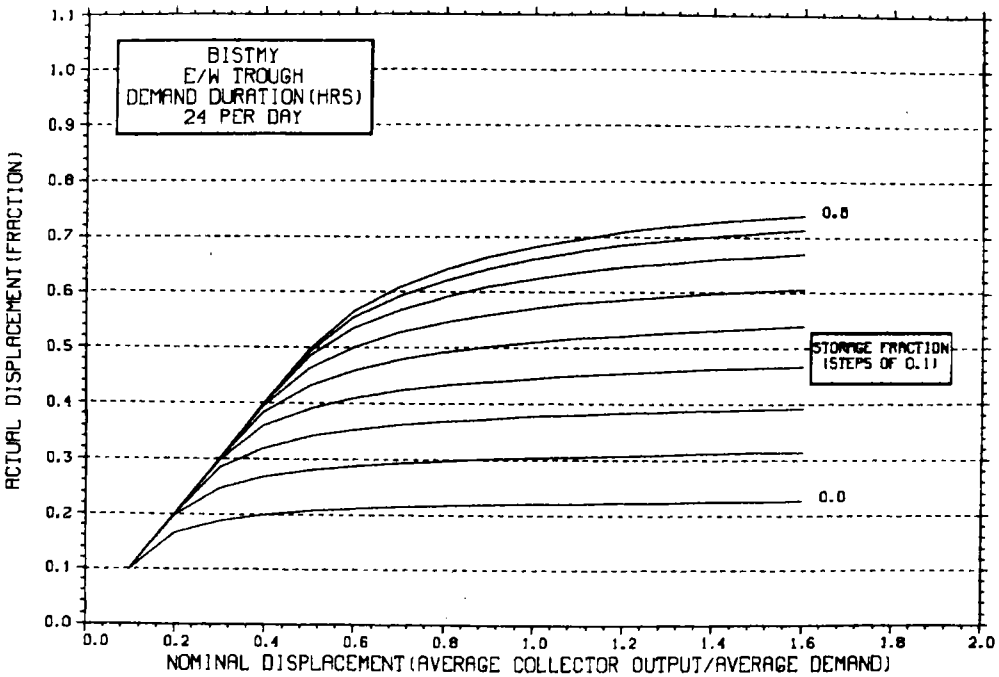

STORAGE SIZING GRAPH FOR CONSTANT ANNUAL DEMAND

NO WEEKEND SHUTDOWN

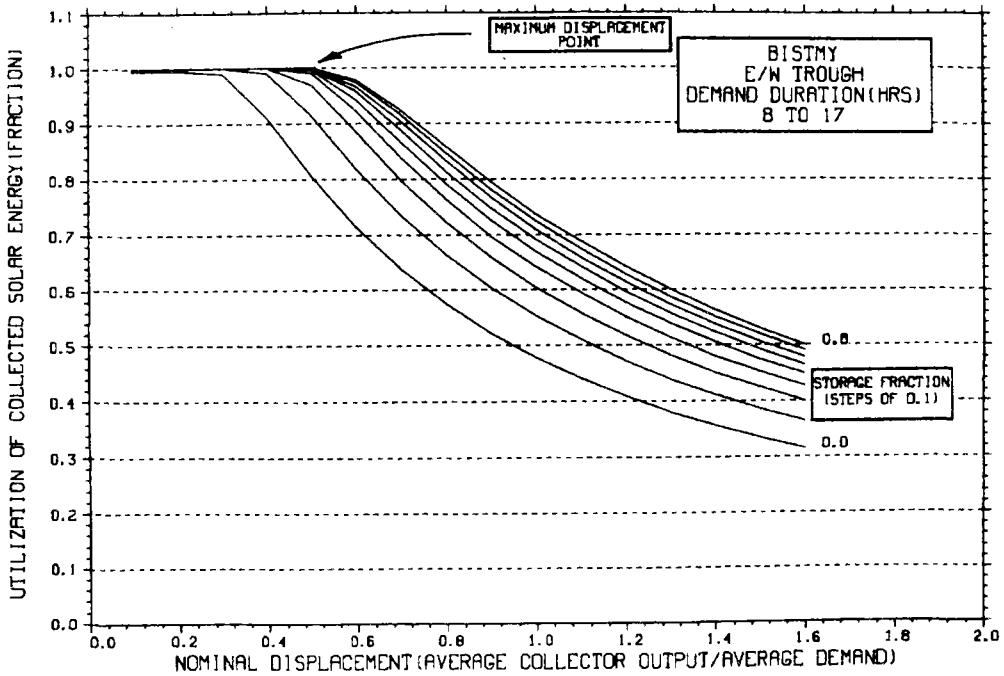

STORAGE SIZING GRAPH FOR CONSTANT ANNUAL DEMAND

NO WEEKEND SHUTDOWN

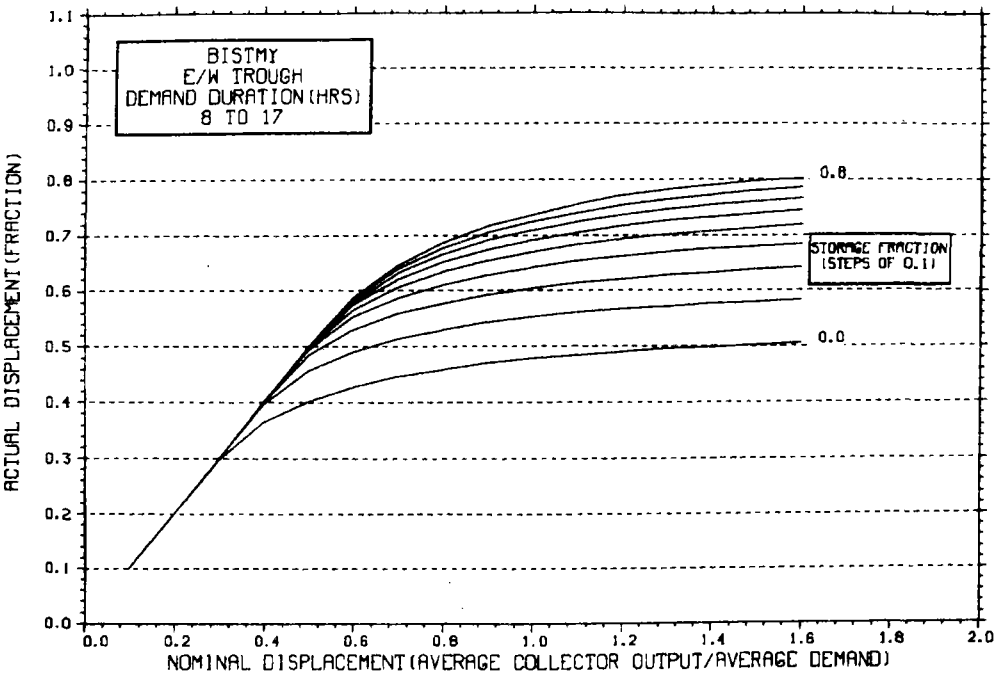

STORAGE SIZING GRAPH FOR CONSTANT ANNUAL DEMAND

NO WEEKEND SHUTDOWN

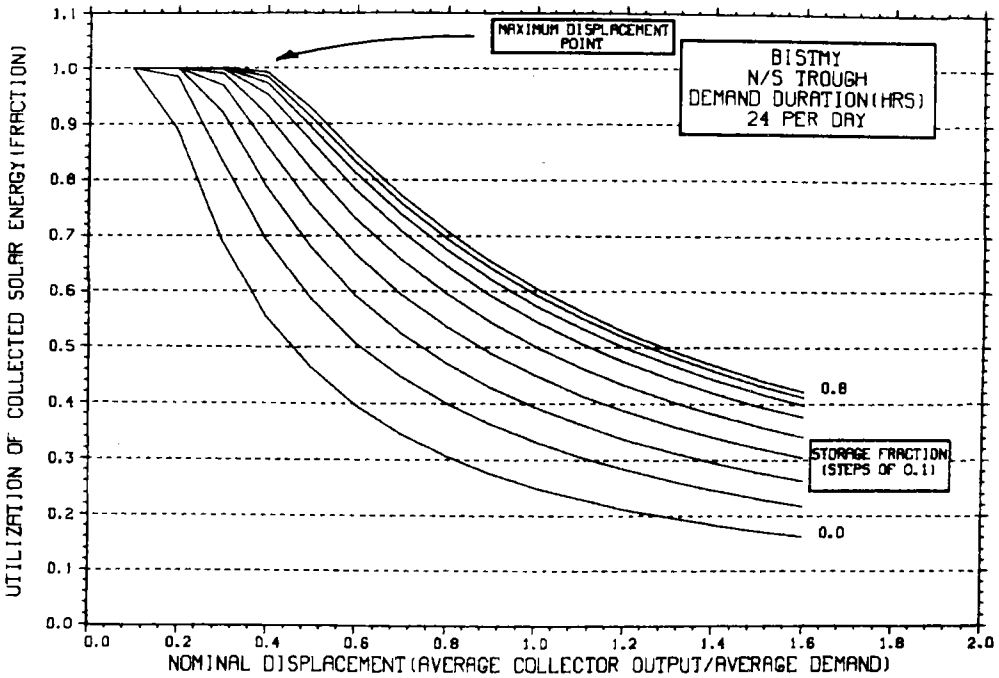

STORAGE SIZING GRAPH FOR CONSTANT ANNUAL DEMAND

NO WEEKEND SHUTDOWN

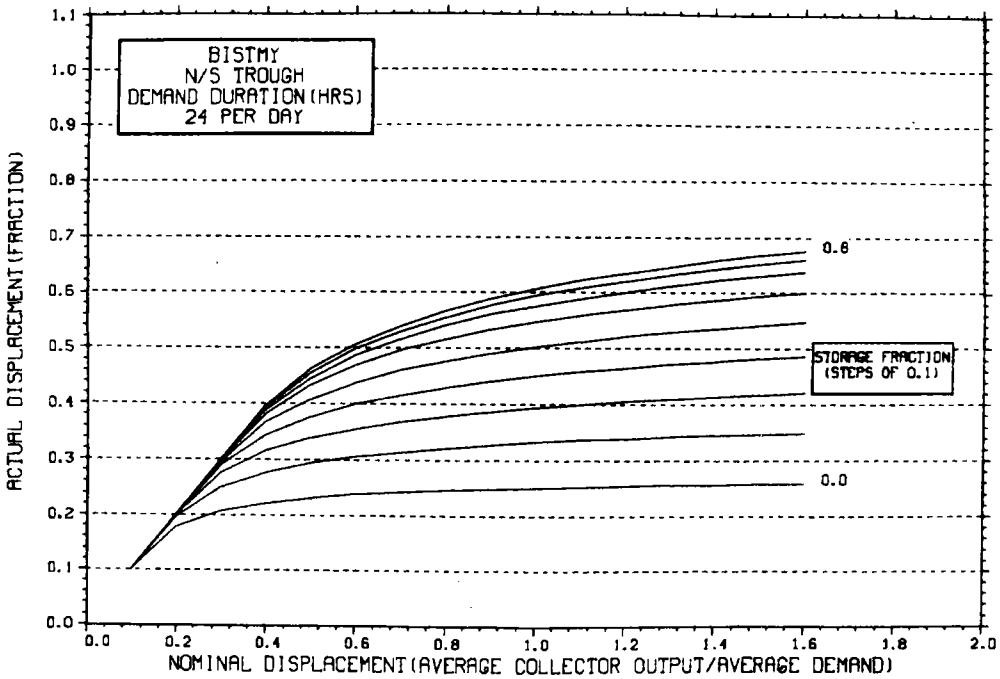

STORAGE SIZING GRAPH FOR CONSTANT ANNUAL DEMAND

NO WEEKEND SHUTDOWN

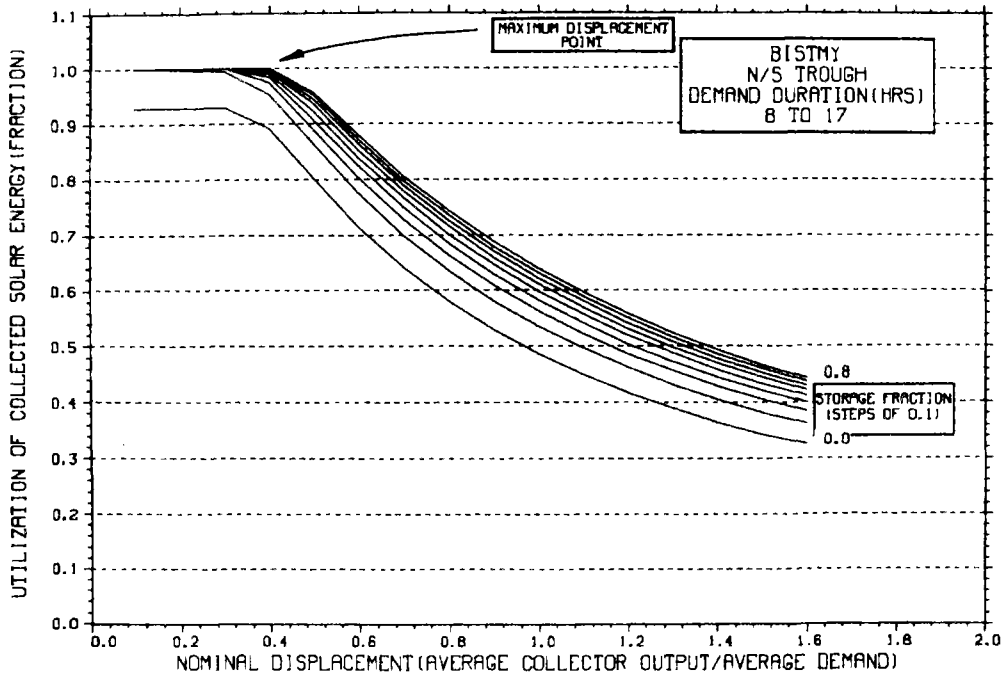

STORAGE SIZING GRAPH FOR CONSTANT ANNUAL DEMAND

NO WEEKEND SHUTDOWN

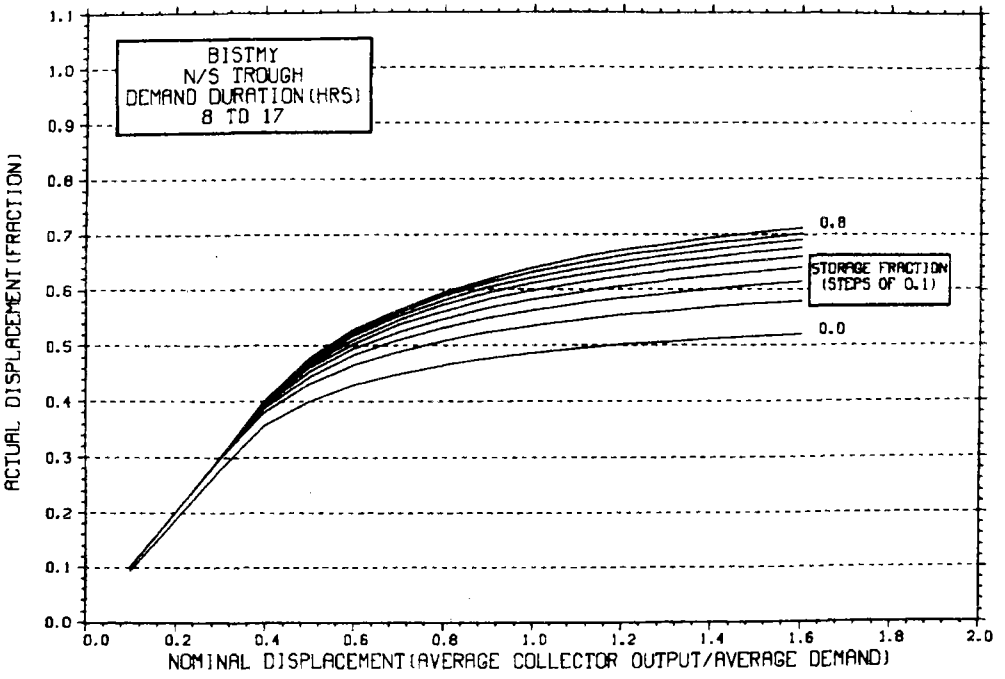

ENERGY INCIDENT ON COLLECTOR APERTURE

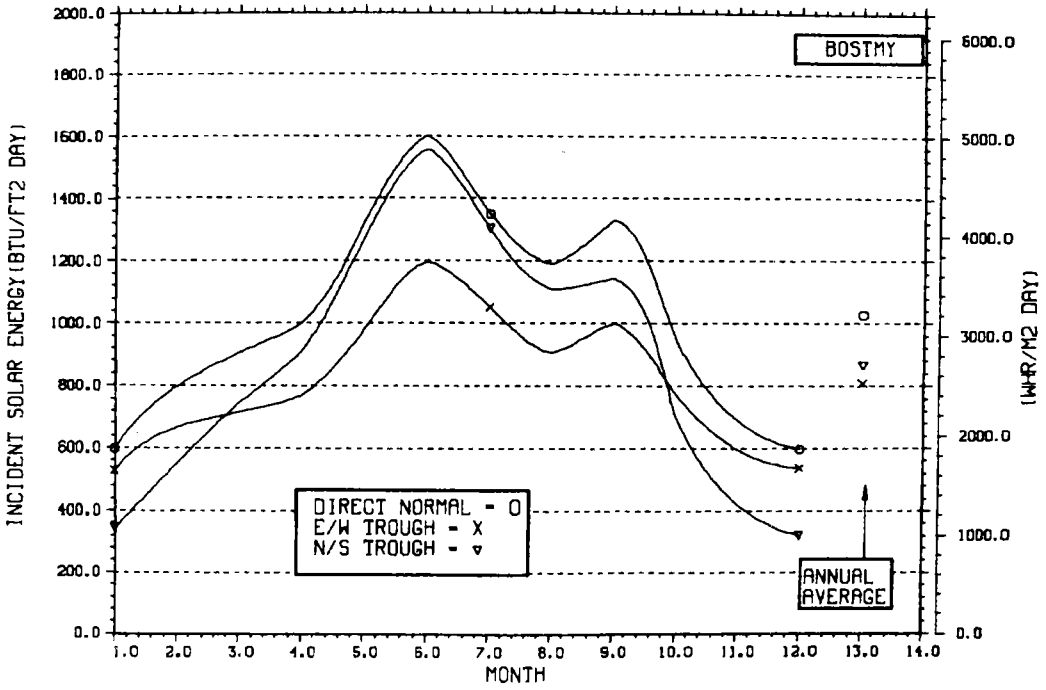

ANNUAL NONFIRST ROW SHADING

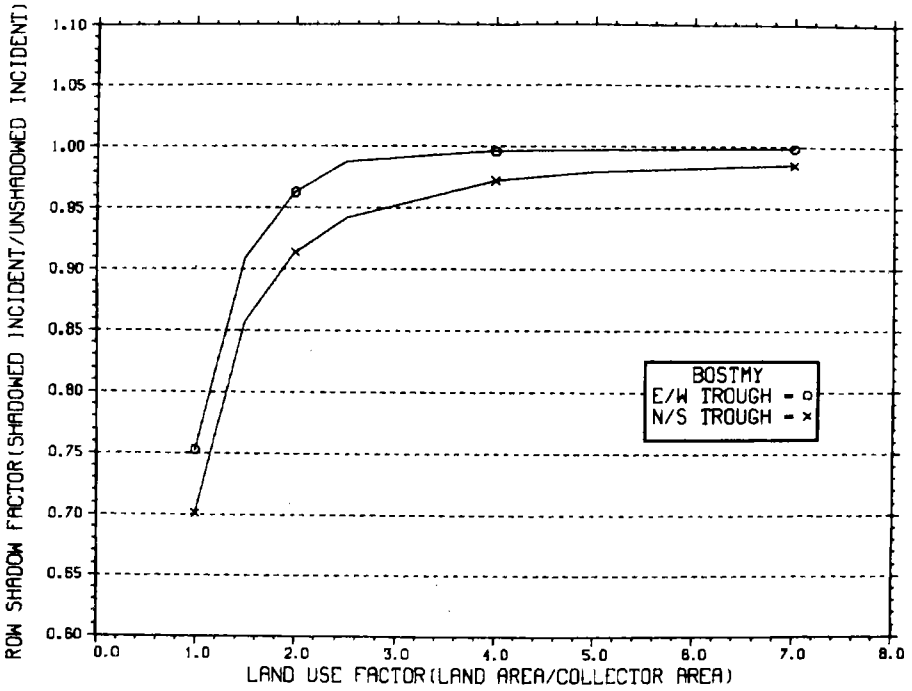

PERFORMANCE VARIATION WITH COLLECTOR AZIMUTH

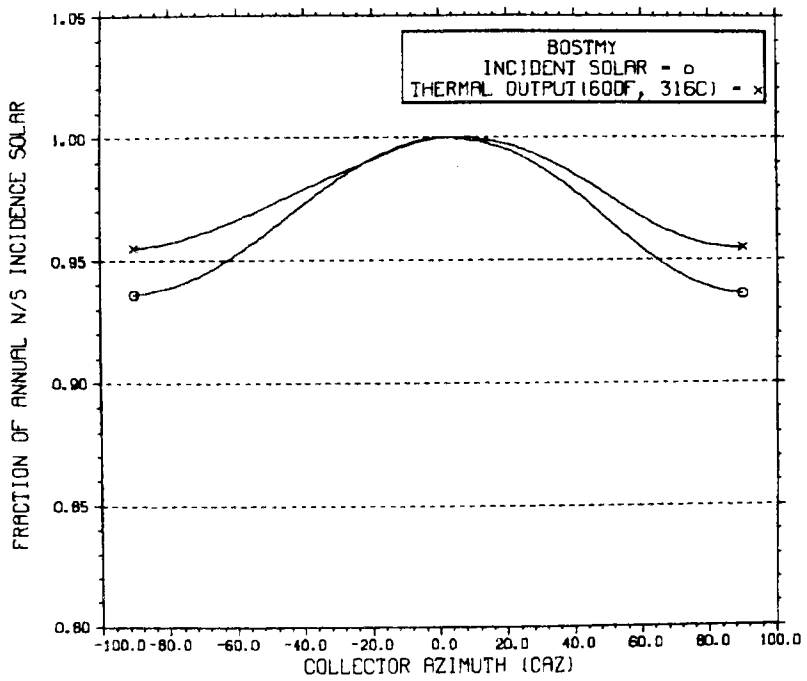

TEMPERATURE DEPENDENCE OF ANNUAL PERFORMANCE

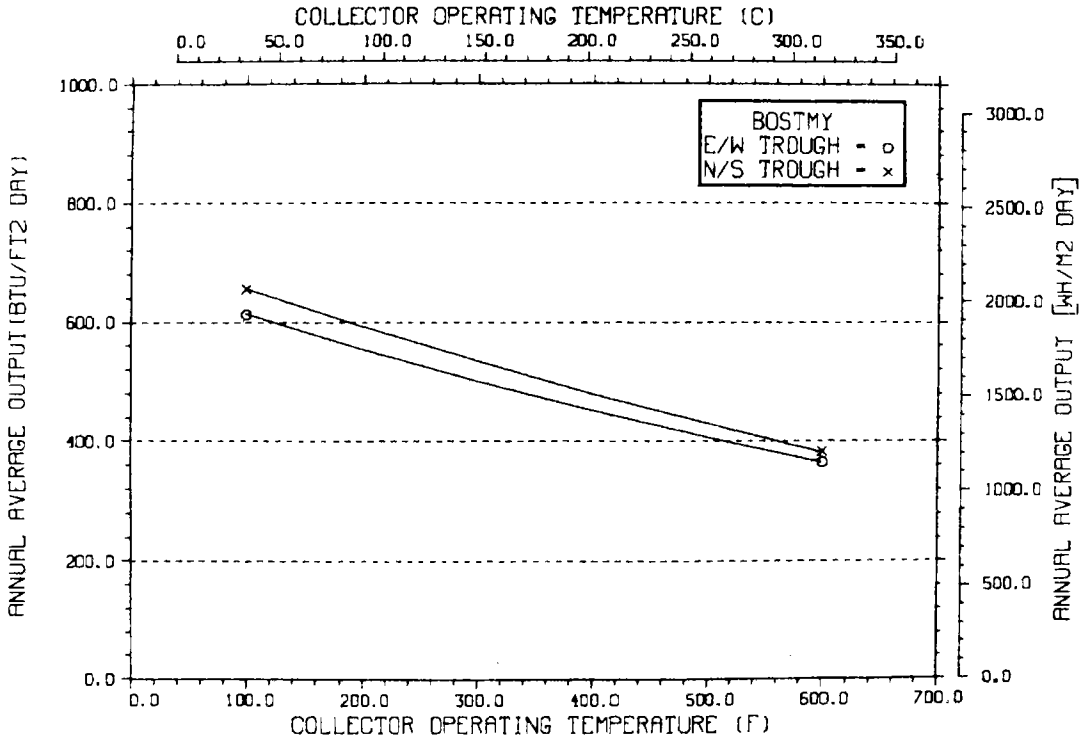

TEMPERATURE DEPENDENCE OF MONTHLY PERFORMANCE

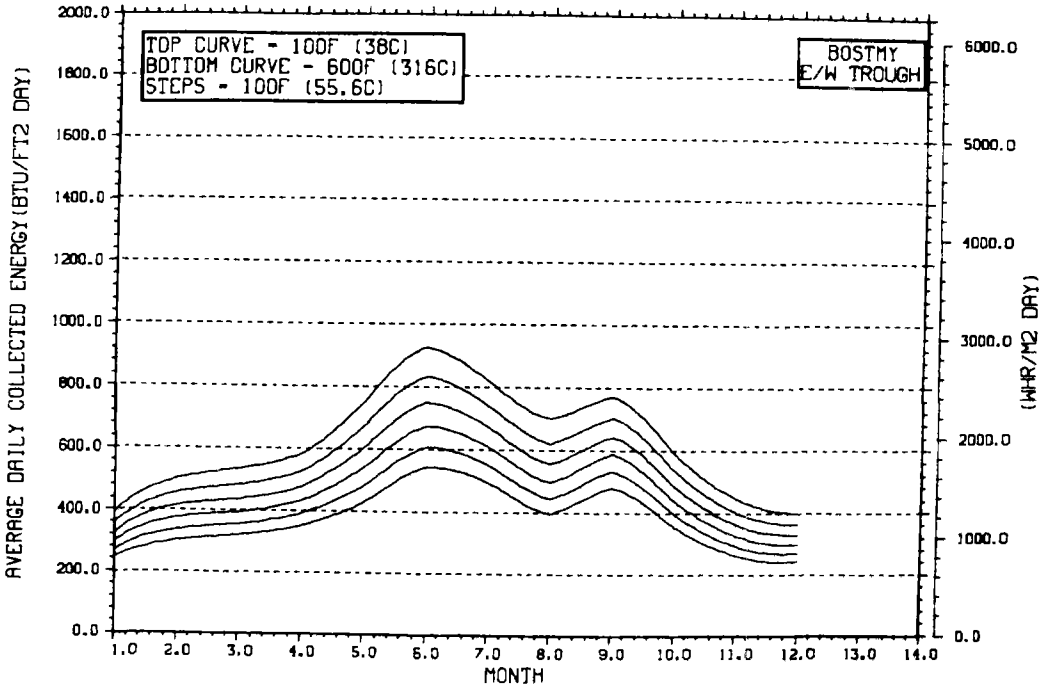

TEMPERATURE DEPENDENCE OF MONTHLY PERFORMANCE

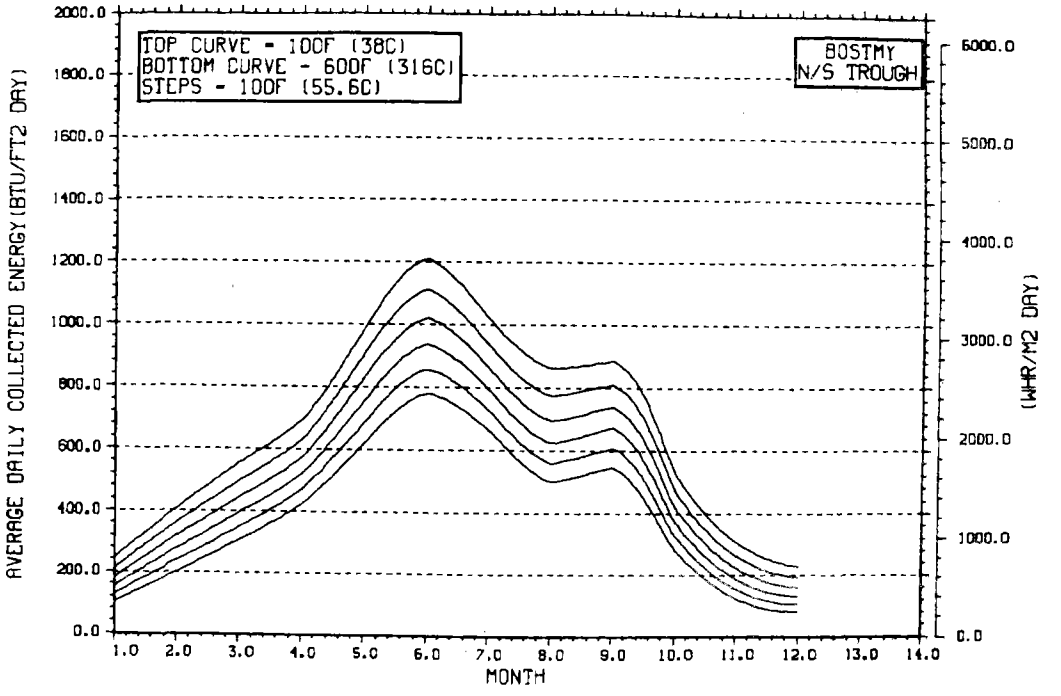

STORAGE SIZING GRAPH FOR CONSTANT ANNUAL DEMAND

NO WEEKEND SHUTDOWN

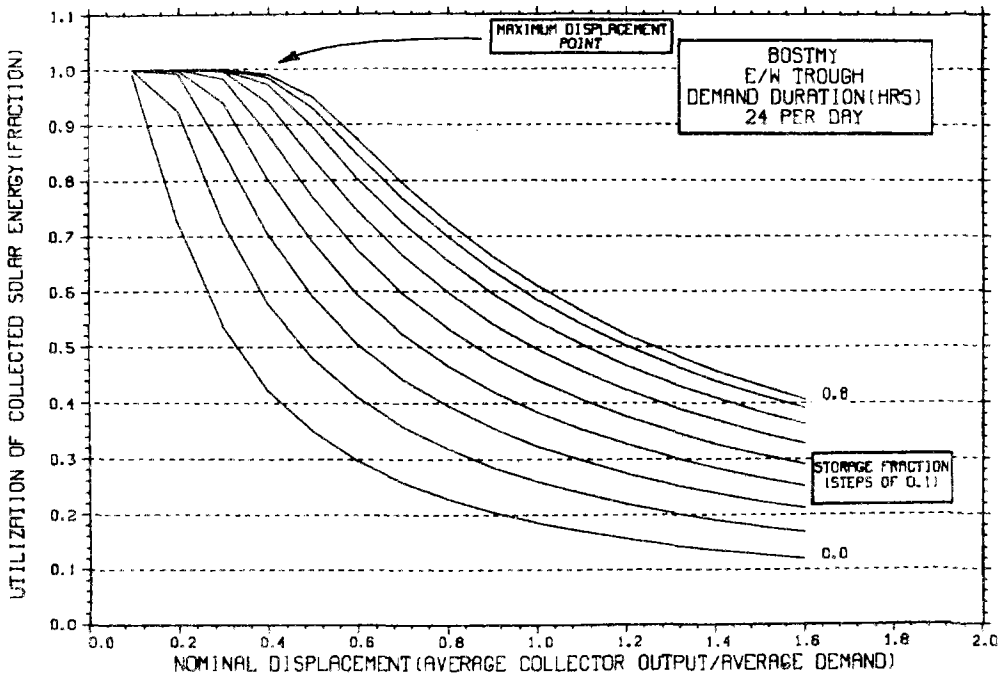

STORAGE SIZING GRAPH FOR CONSTANT ANNUAL DEMAND

NO WEEKEND SHUTDOWN

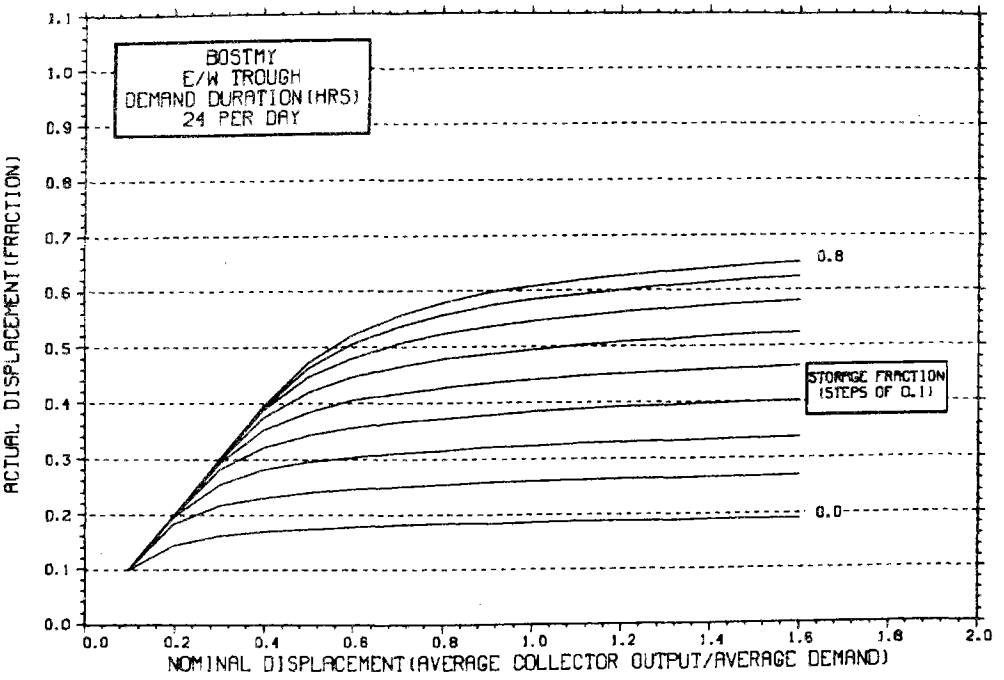

STORAGE SIZING GRAPH FOR CONSTANT ANNUAL DEMAND

NO WEEKEND SHUTDOWN

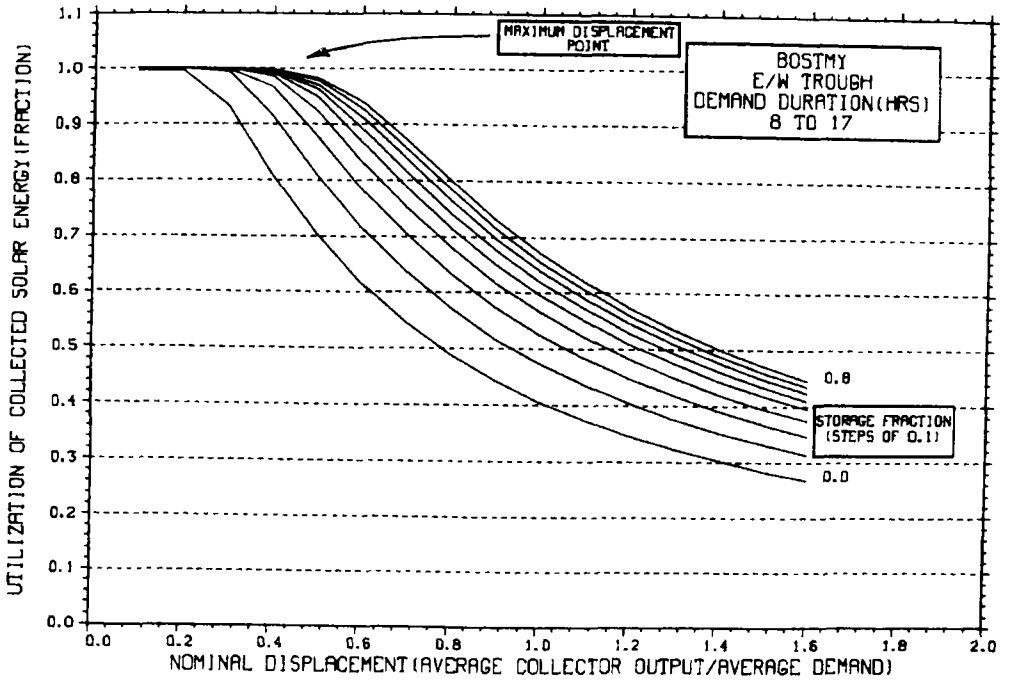

STORAGE SIZING GRAPH FOR CONSTANT ANNUAL DEMAND

NO WEEKEND SHUTDOWN

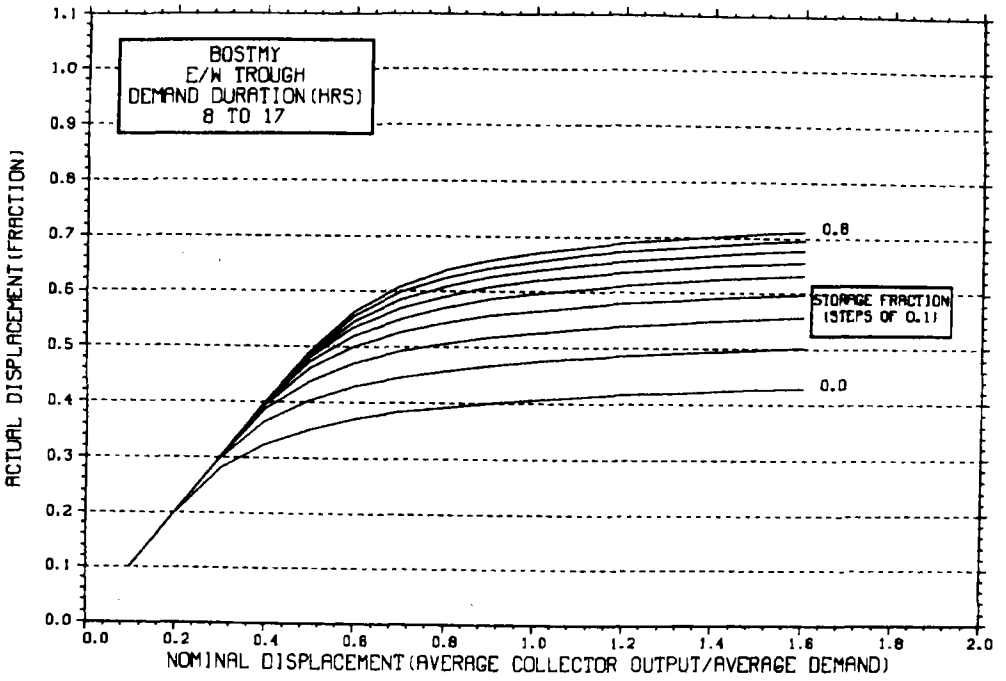

STORAGE SIZING GRAPH FOR CONSTANT ANNUAL DEMAND

NO WEEKEND SHUTDOWN

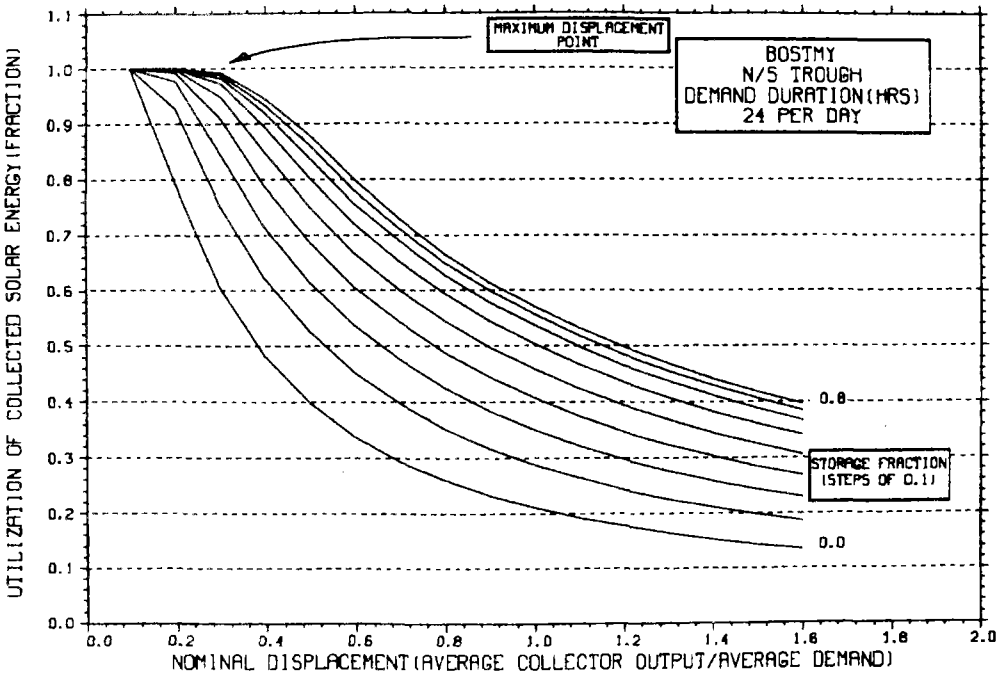

STORAGE SIZING GRAPH FOR CONSTANT ANNUAL DEMAND

NO WEEKEND SHUTDOWN

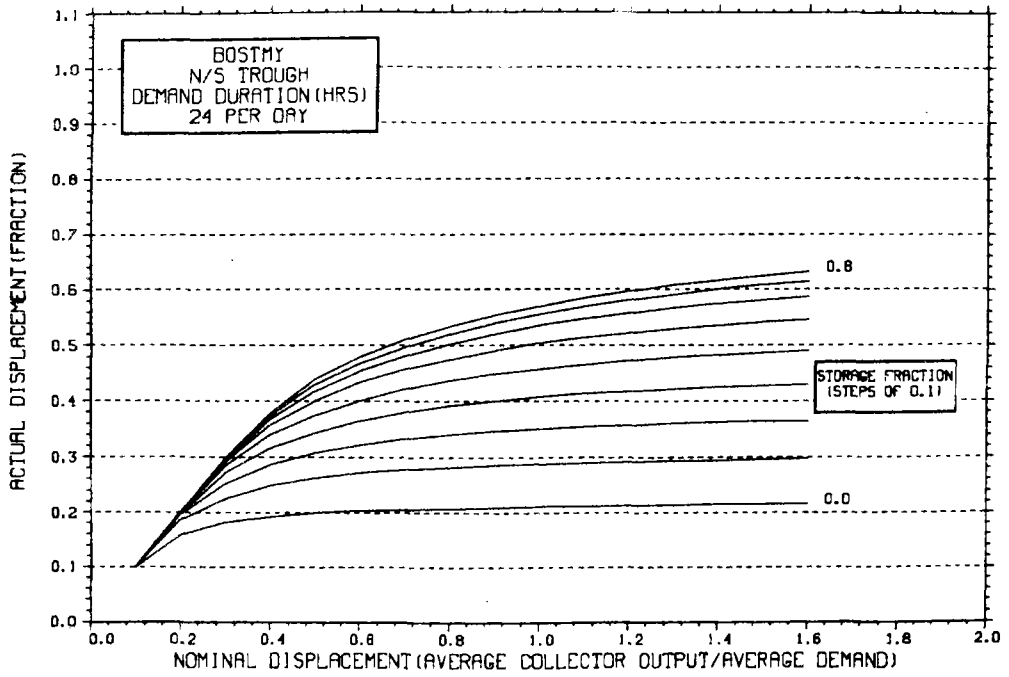

STORAGE SIZING GRAPH FOR CONSTANT ANNUAL DEMAND

NO WEEKEND SHUTDOWN

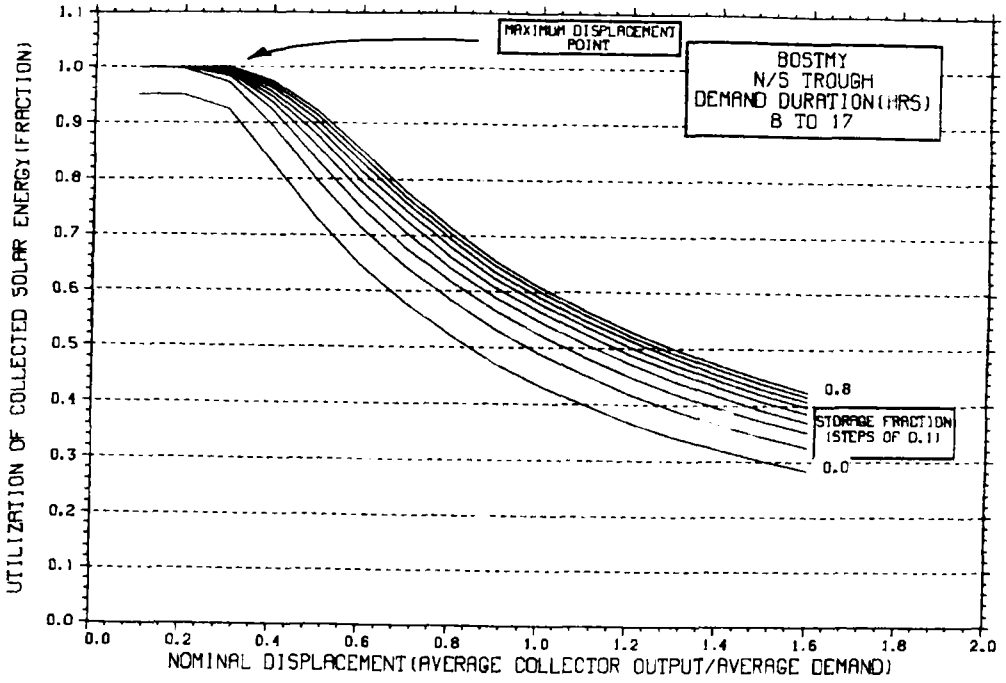

STORAGE SIZING GRAPH FOR CONSTANT ANNUAL DEMAND

NO WEEKEND SHUTDOWN

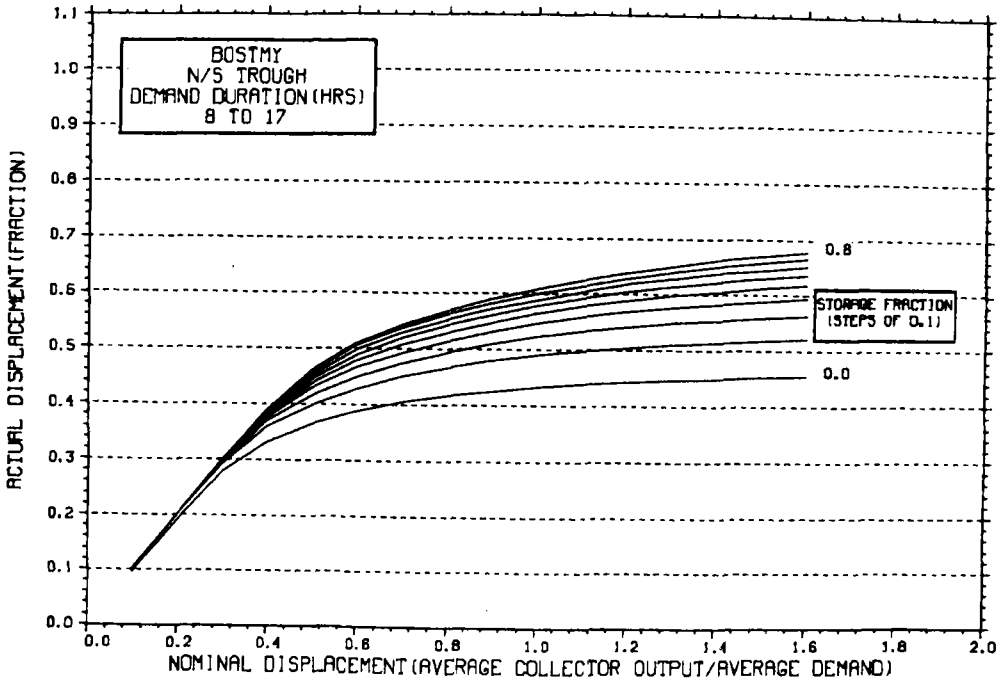

ENERGY INCIDENT ON COLLECTOR APERTURE

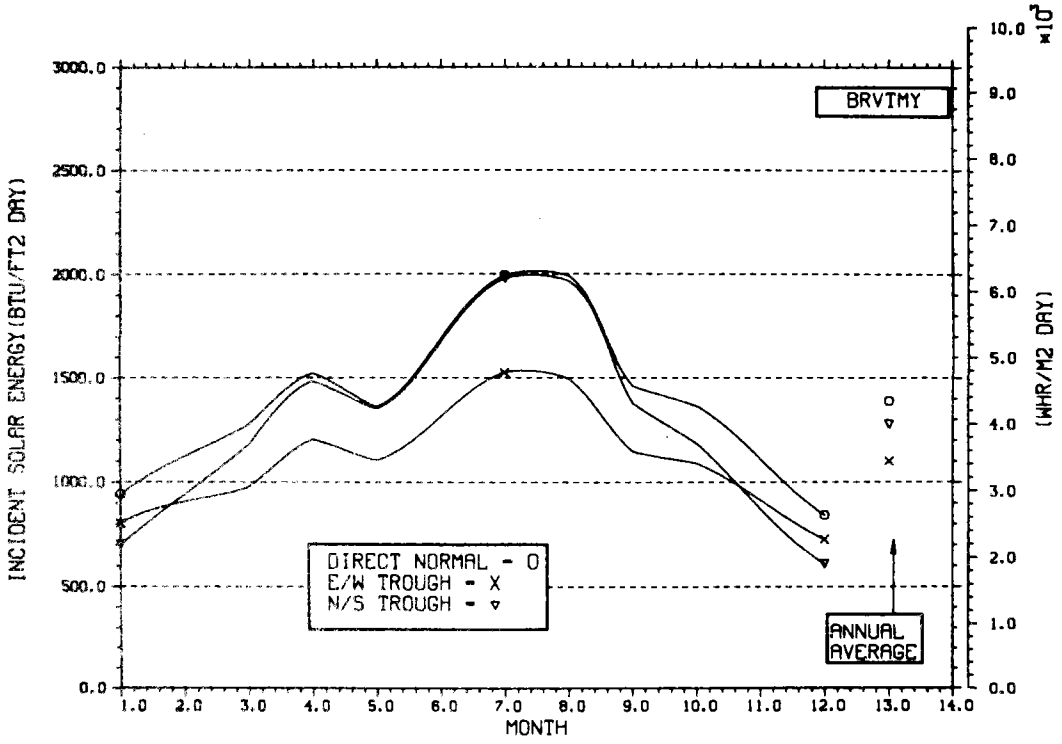

ANNUAL NONFIRST ROW SHADING

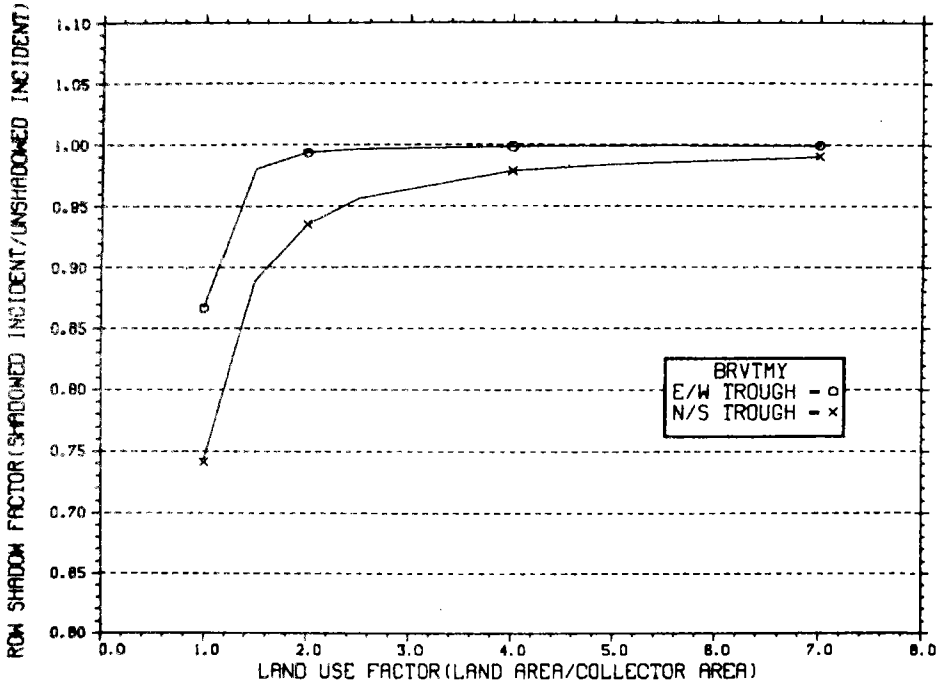

PERFORMANCE VARIATION WITH COLLECTOR AZIMUTH

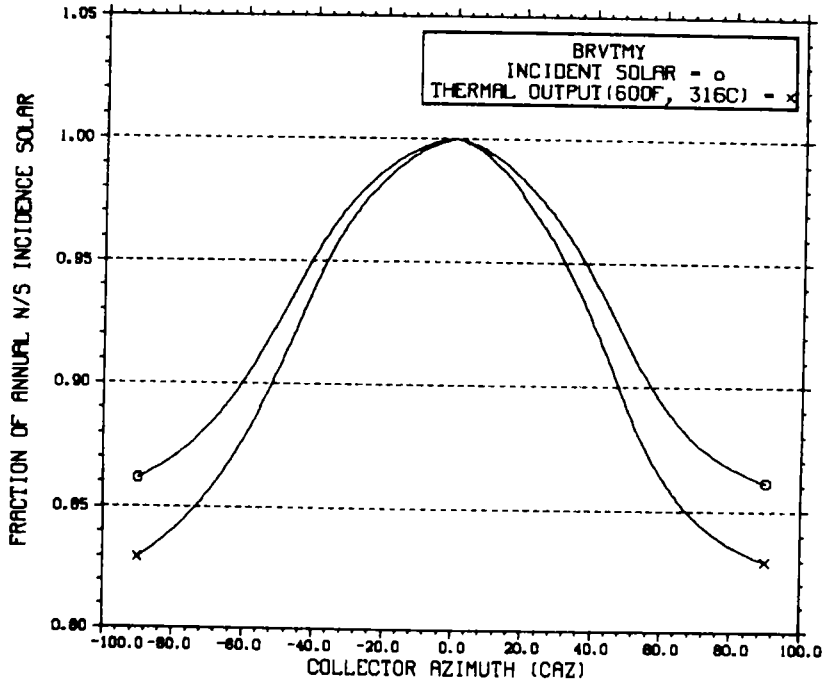

TEMPERATURE DEPENDENCE OF ANNUAL PERFORMANCE

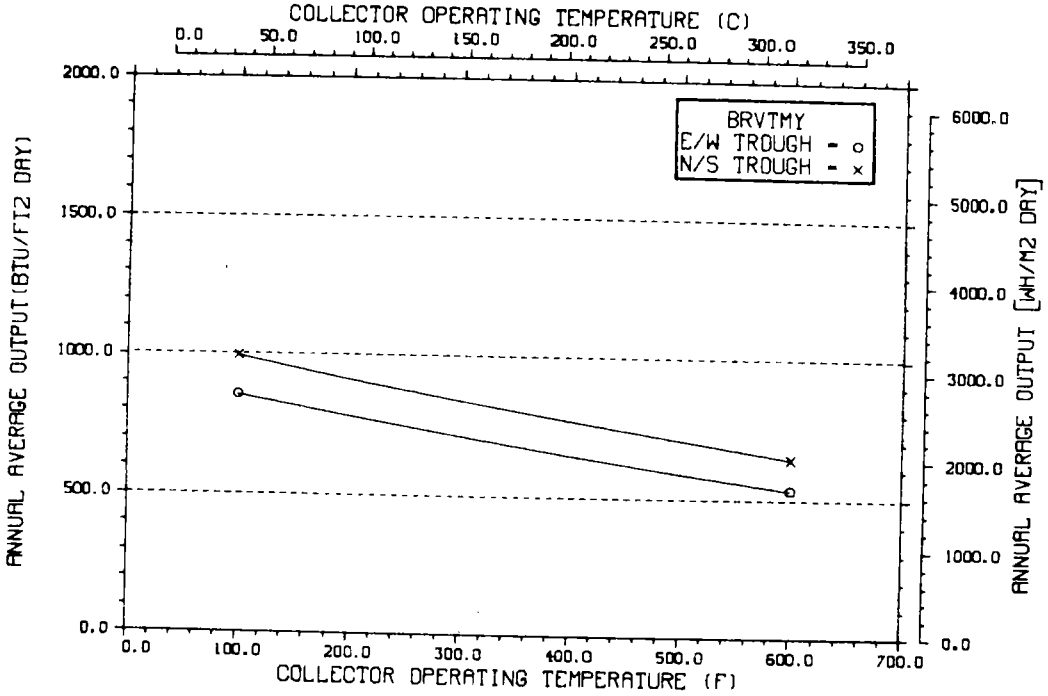

TEMPERATURE DEPENDENCE OF MONTHLY PERFORMANCE

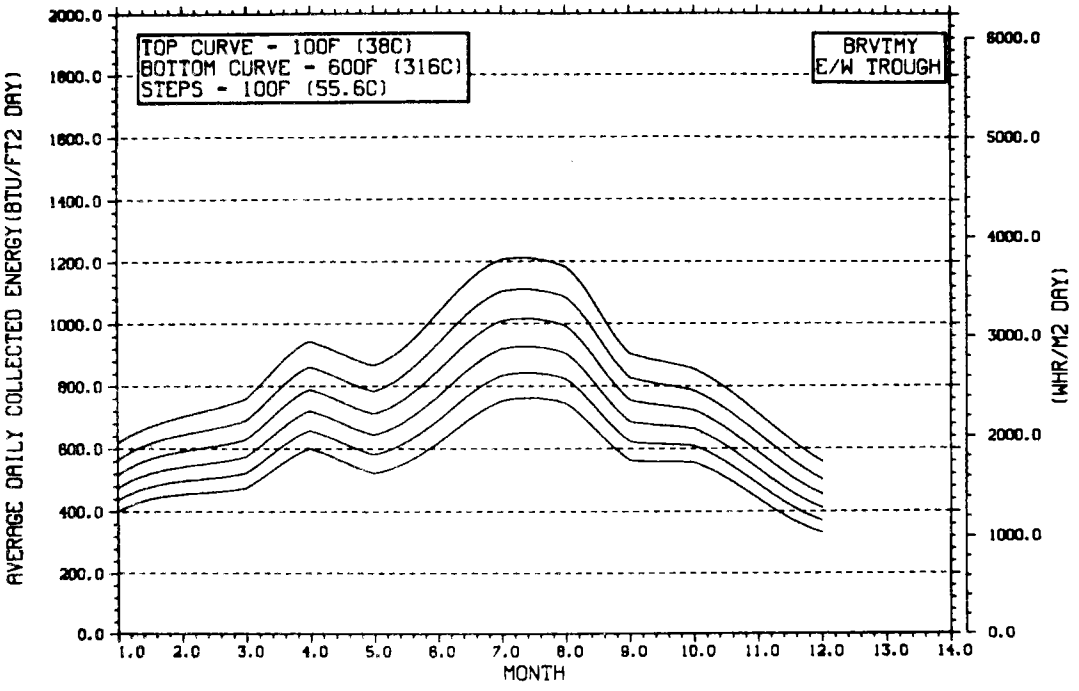

TEMPERATURE DEPENDENCE OF MONTHLY PERFORMANCE

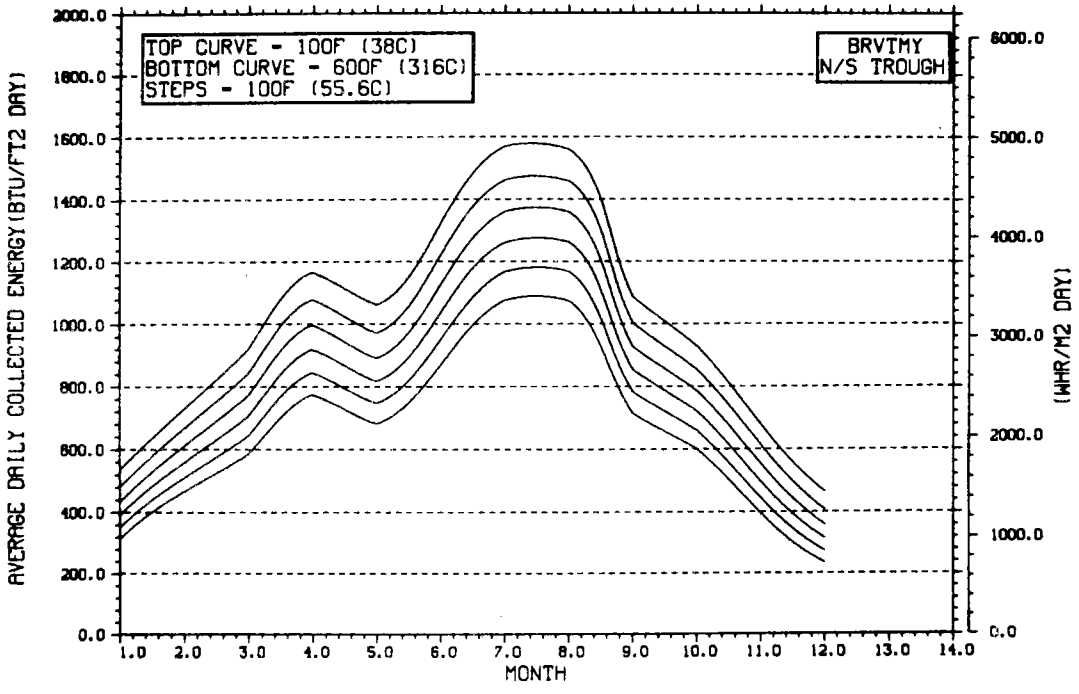

STORAGE SIZING GRAPH FOR CONSTANT ANNUAL DEMAND

NO WEEKEND SHUTDOWN

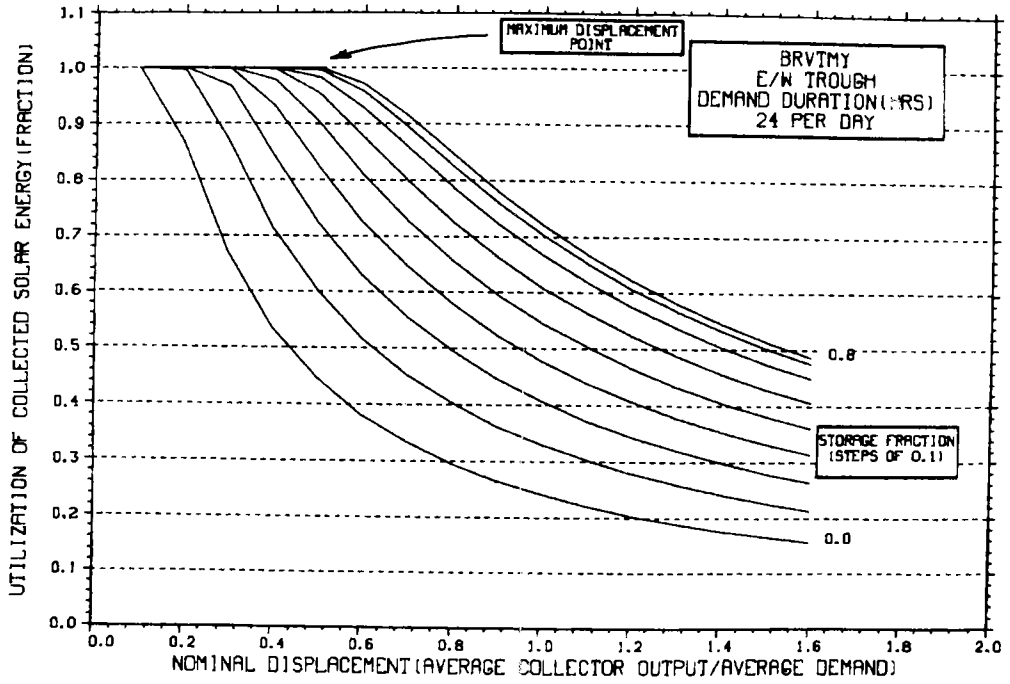

STORAGE SIZING GRAPH FOR CONSTANT ANNUAL DEMAND

NO WEEKEND SHUTDOWN

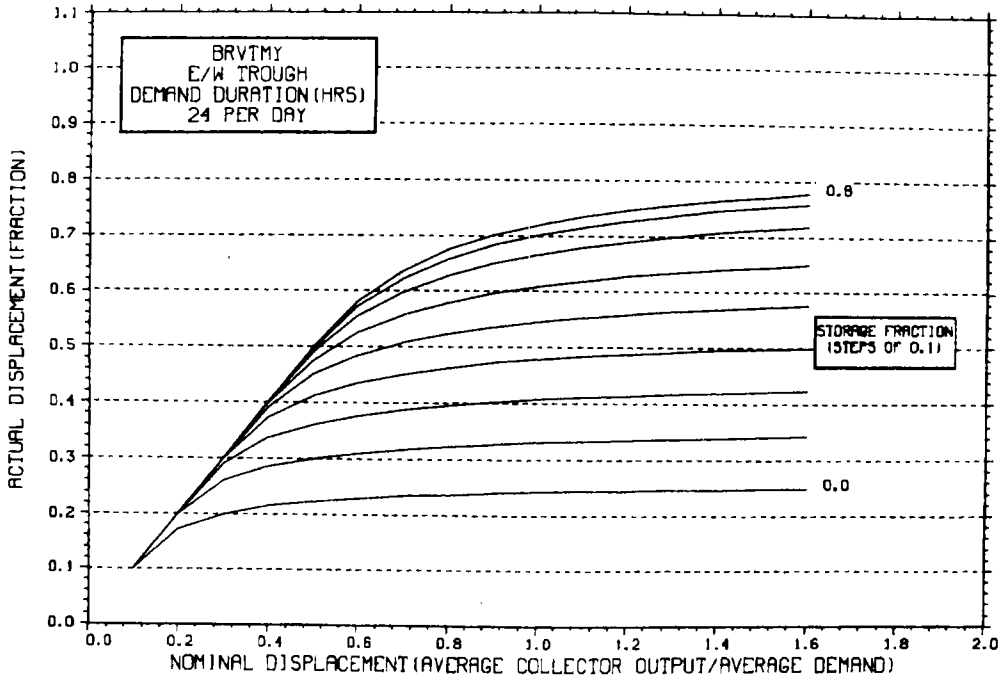

STORAGE SIZING GRAPH FOR CONSTANT ANNUAL DEMAND

NO WEEKEND SHUTDOWN

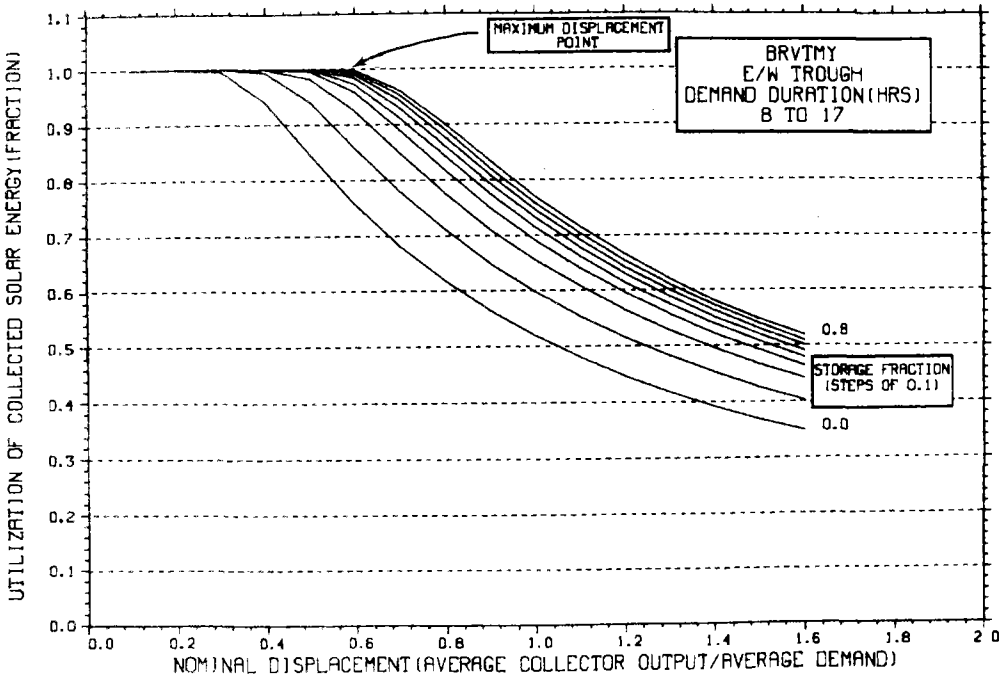

STORAGE SIZING GRAPH FOR CONSTANT ANNUAL DEMAND

NO WEEKEND SHUTDOWN

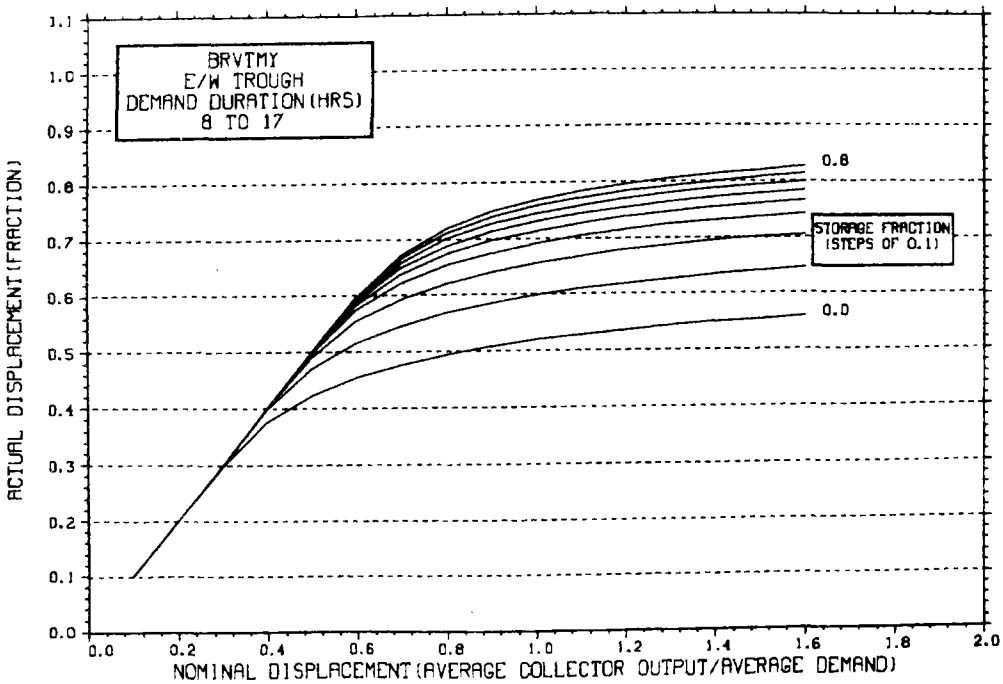

STORAGE SIZING GRAPH FOR CONSTANT ANNUAL DEMAND

NO WEEKEND SHUTDOWN

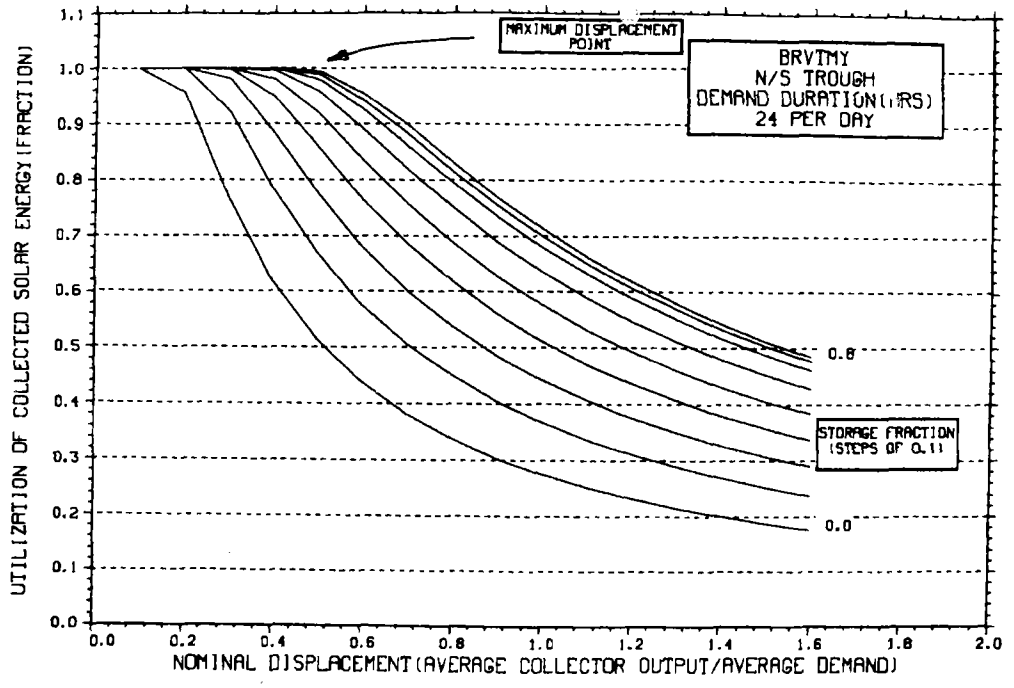

STORAGE SIZING GRAPH FOR CONSTANT ANNUAL DEMAND

NO WEEKEND SHUTDOWN

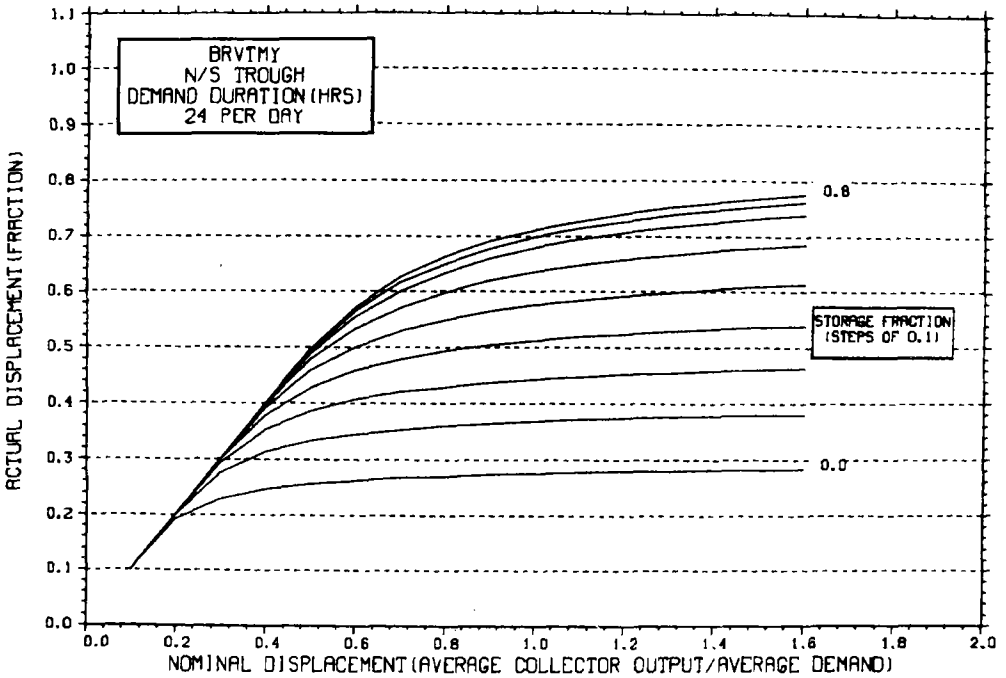

STORAGE SIZING GRAPH FOR CONSTANT ANNUAL DEMAND

NO WEEKEND SHUTDOWN

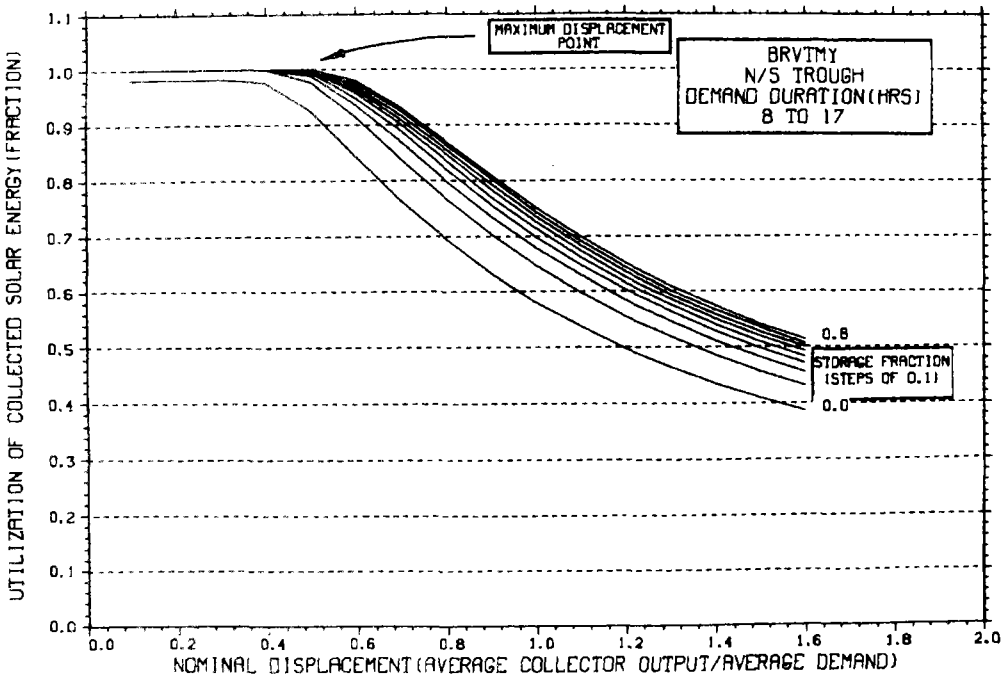

STORAGE SIZING GRAPH FOR CONSTANT ANNUAL DEMAND

NO WEEKEND SHUTDOWN

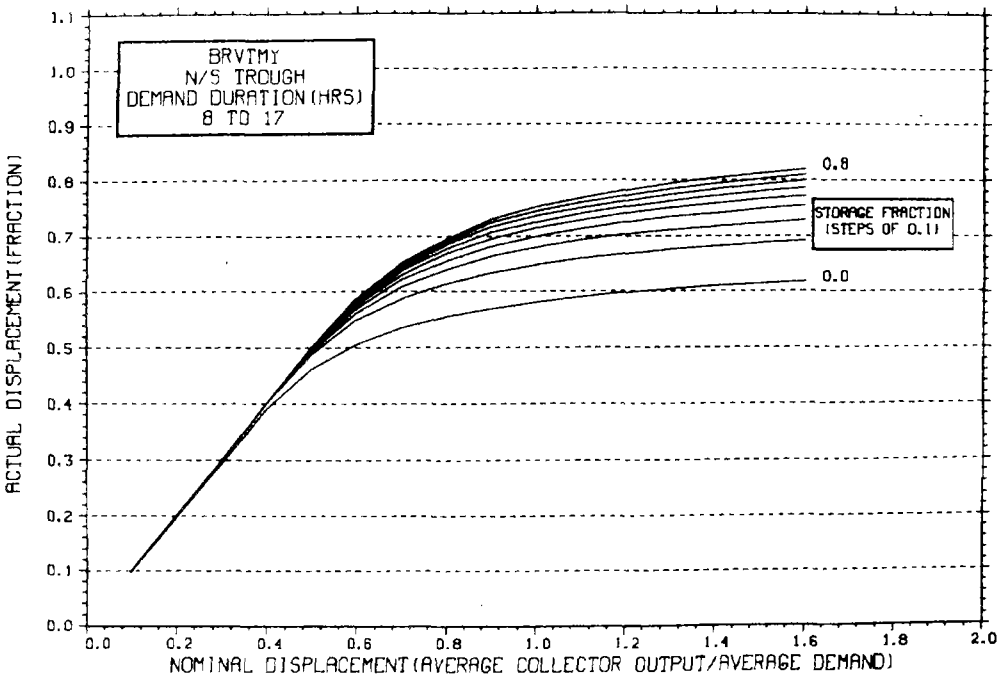

ENERGY INCIDENT ON COLLECTOR APERTURE

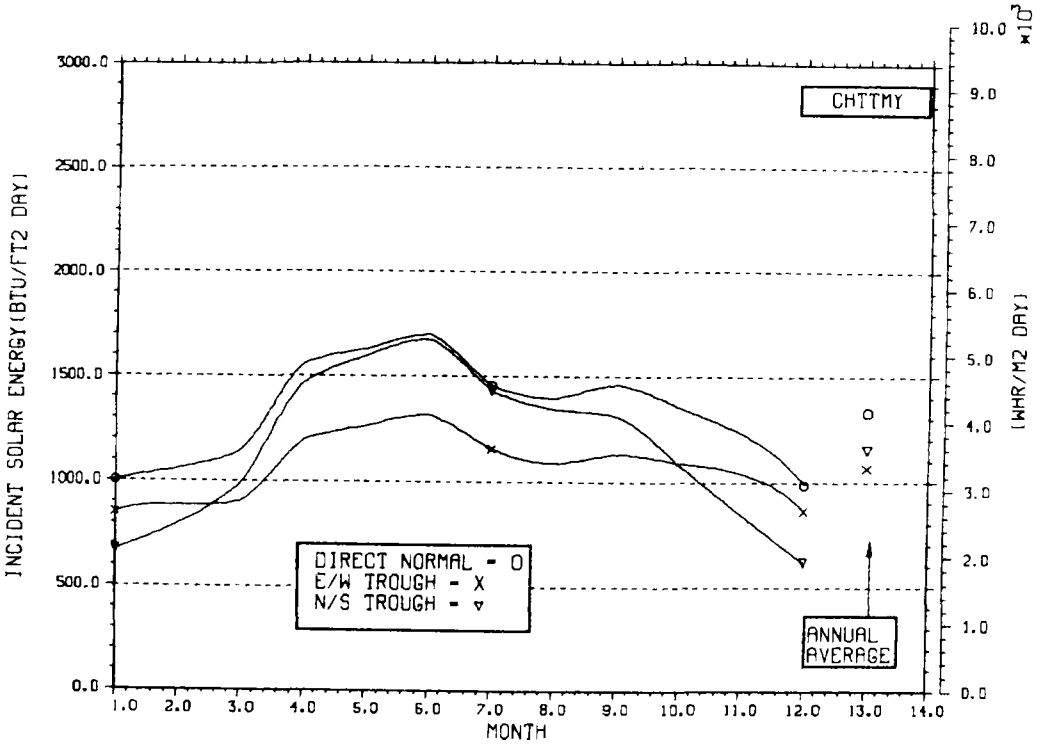

ANNUAL NONFIRST ROW SHADING

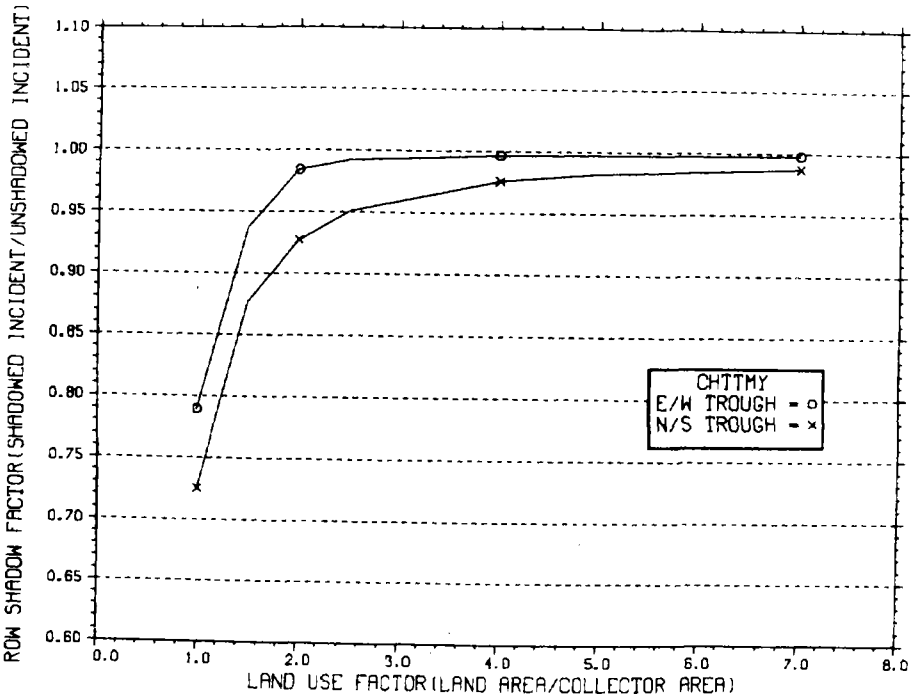

PERFORMANCE VARIATION WITH COLLECTOR AZIMUTH

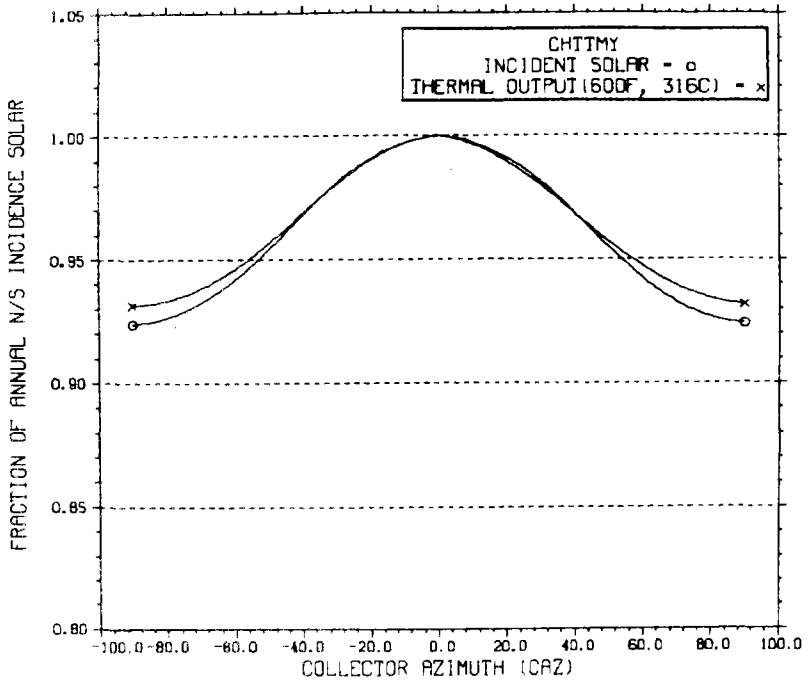

TEMPERATURE DEPENDENCE OF ANNUAL PERFORMANCE

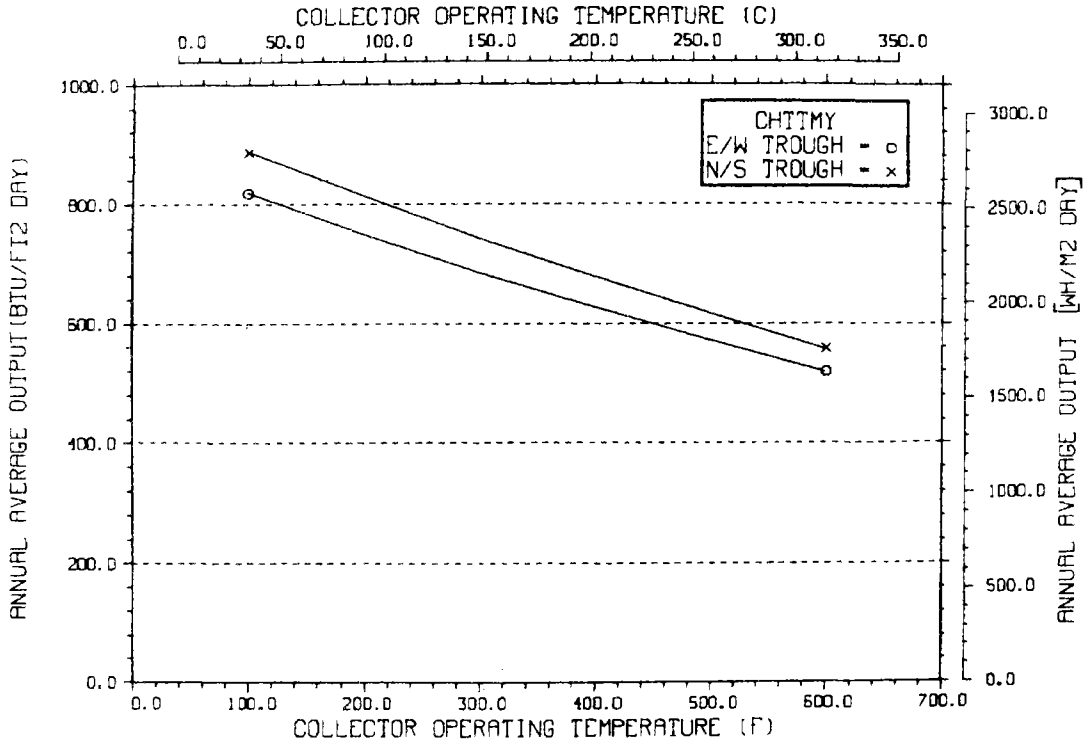

TEMPERATURE DEPENDENCE OF MONTHLY PERFORMANCE

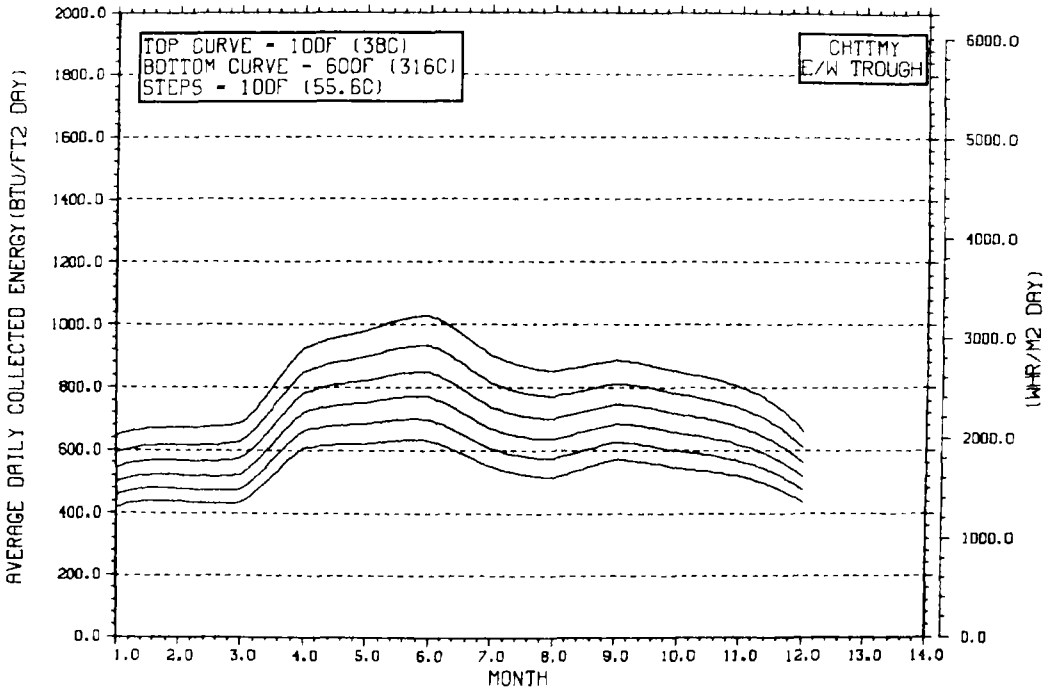

TEMPERATURE DEPENDENCE OF MONTHLY PERFORMANCE

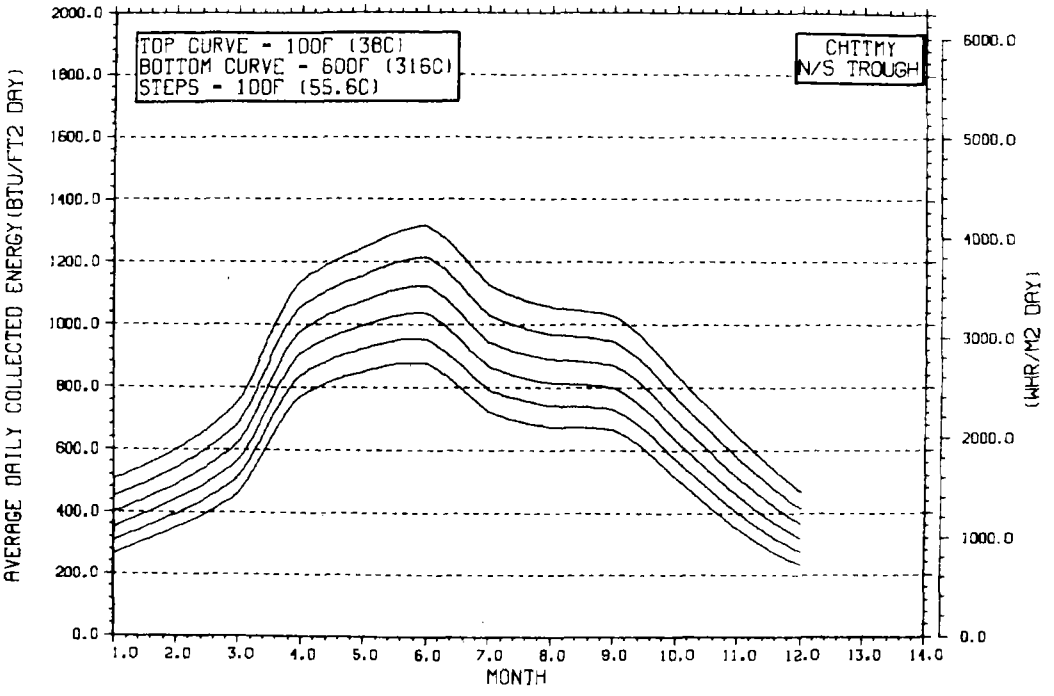

STORAGE SIZING GRAPH FOR CONSTANT ANNUAL DEMAND

NO WEEKEND SHUTDOWN

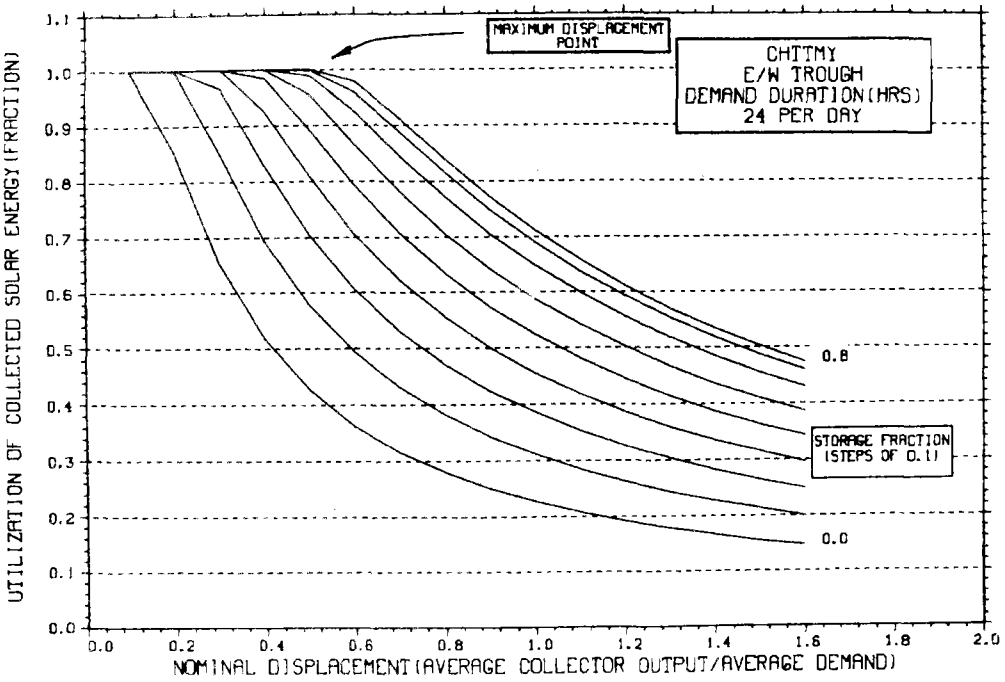

STORAGE SIZING GRAPH FOR CONSTANT ANNUAL DEMAND

NO WEEKEND SHUTDOWN

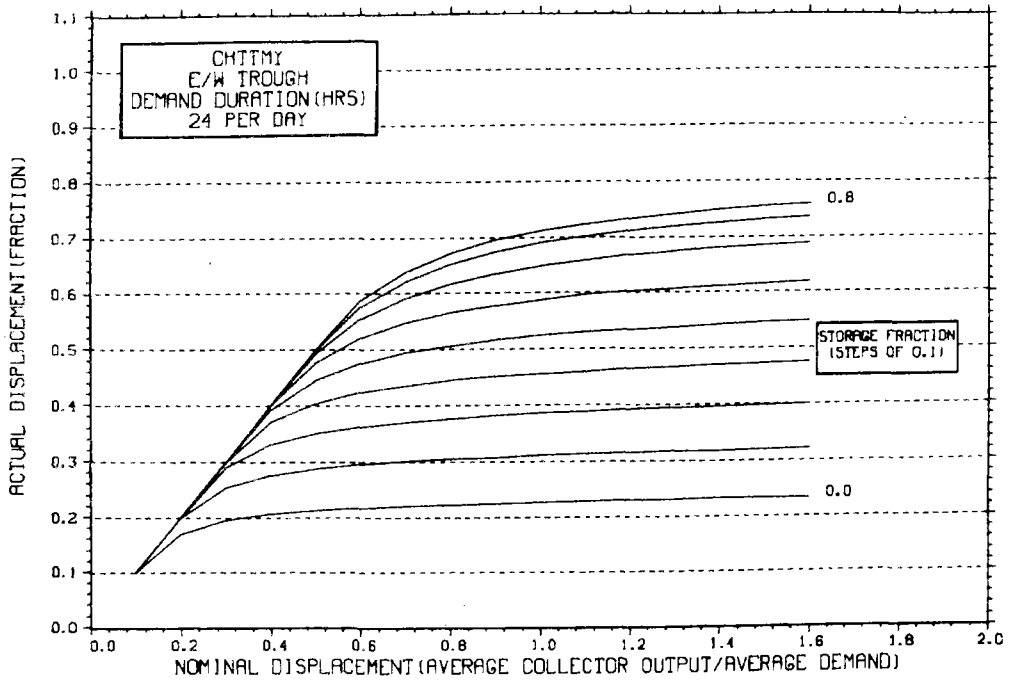

STORAGE SIZING GRAPH FOR CONSTANT ANNUAL DEMAND

NO WEEKEND SHUTDOWN

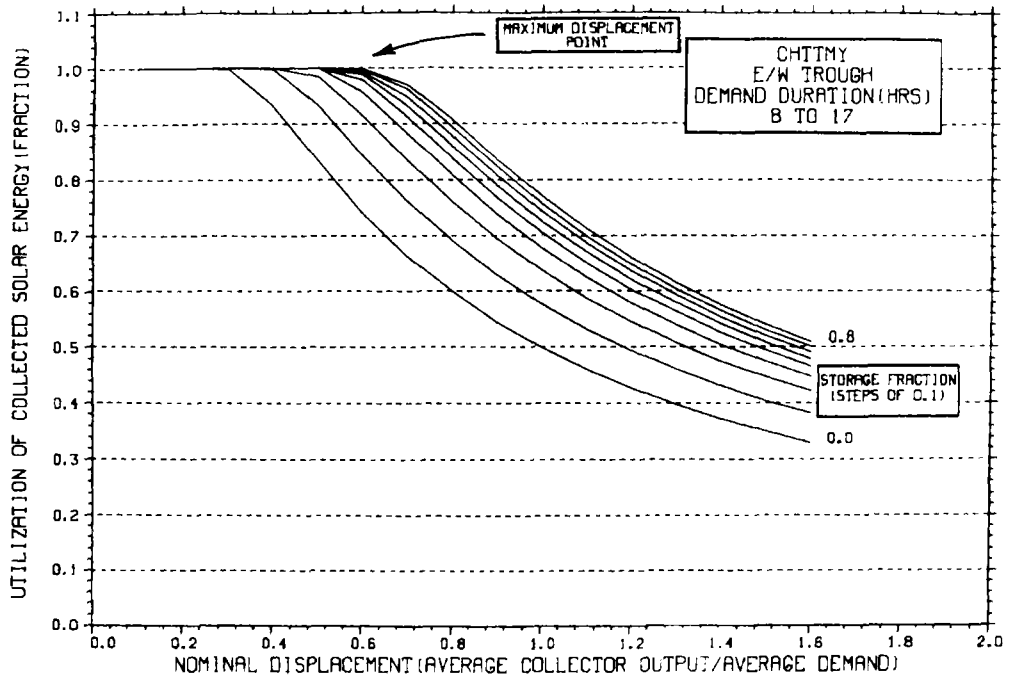

STORAGE SIZING GRAPH FOR CONSTANT ANNUAL DEMAND

NO WEEKEND SHUTDOWN

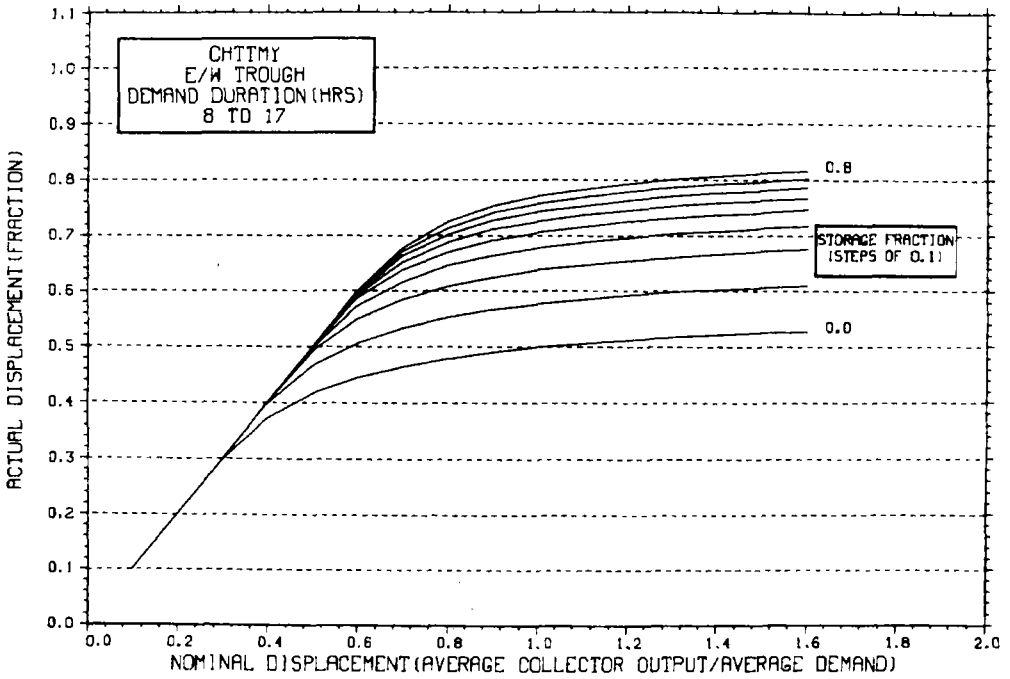

STORAGE SIZING GRAPH FOR CONSTANT ANNUAL DEMAND

NO WEEKEND SHUTDOWN

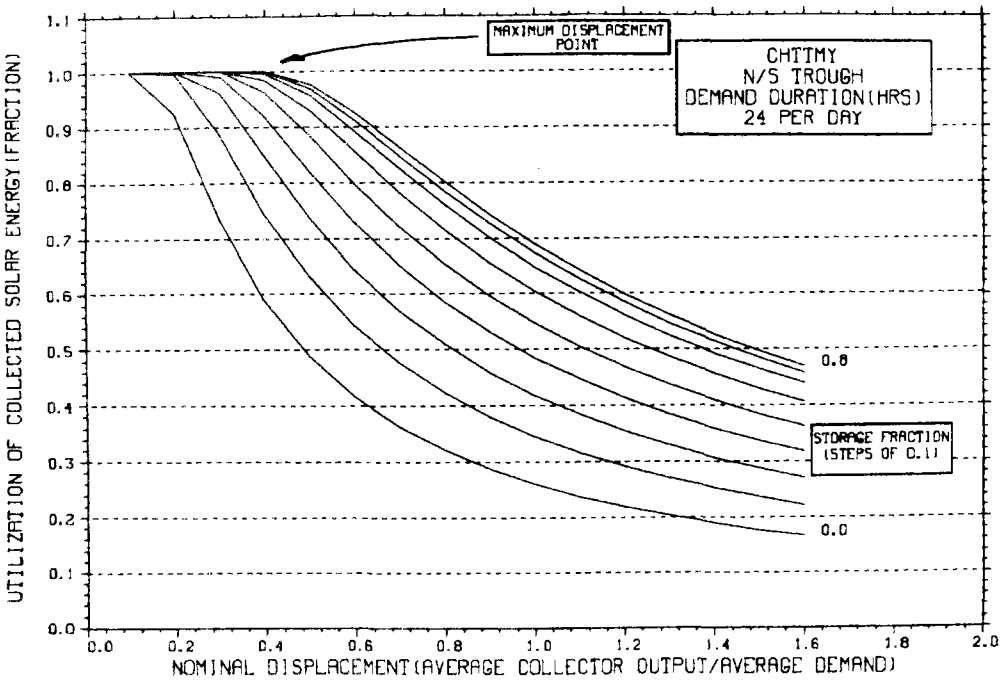

STORAGE SIZING GRAPH FOR CONSTANT ANNUAL DEMAND

NO WEEKEND SHUTDOWN

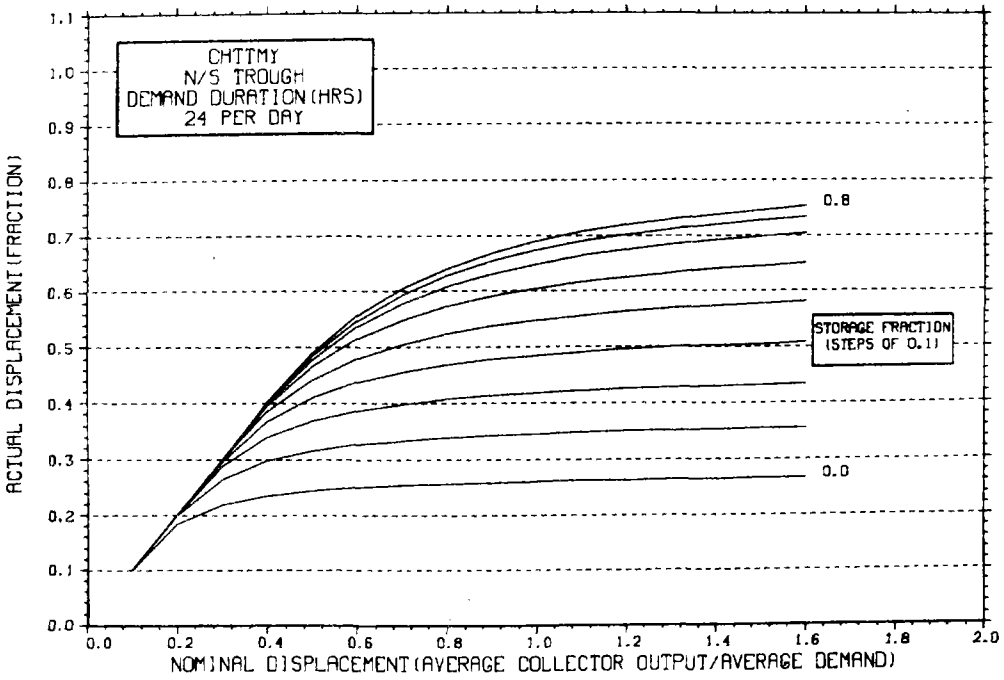

STORAGE SIZING GRAPH FOR CONSTANT ANNUAL DEMAND

NO WEEKEND SHUTDOWN

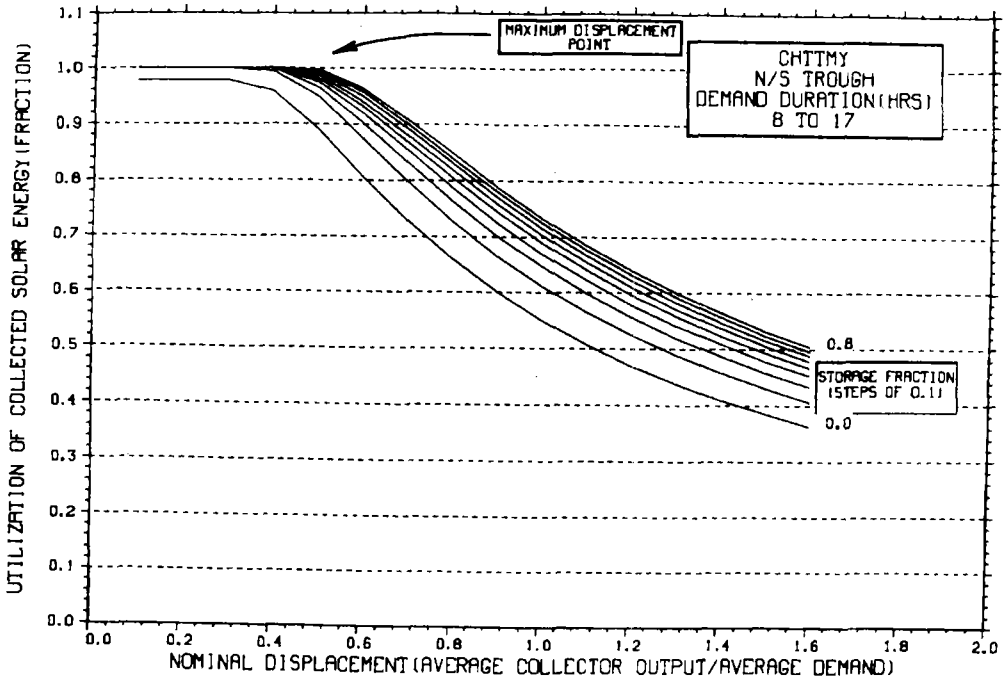

STORAGE SIZING GRAPH FOR CONSTANT ANNUAL DEMAND

NO WEEKEND SHUTDOWN

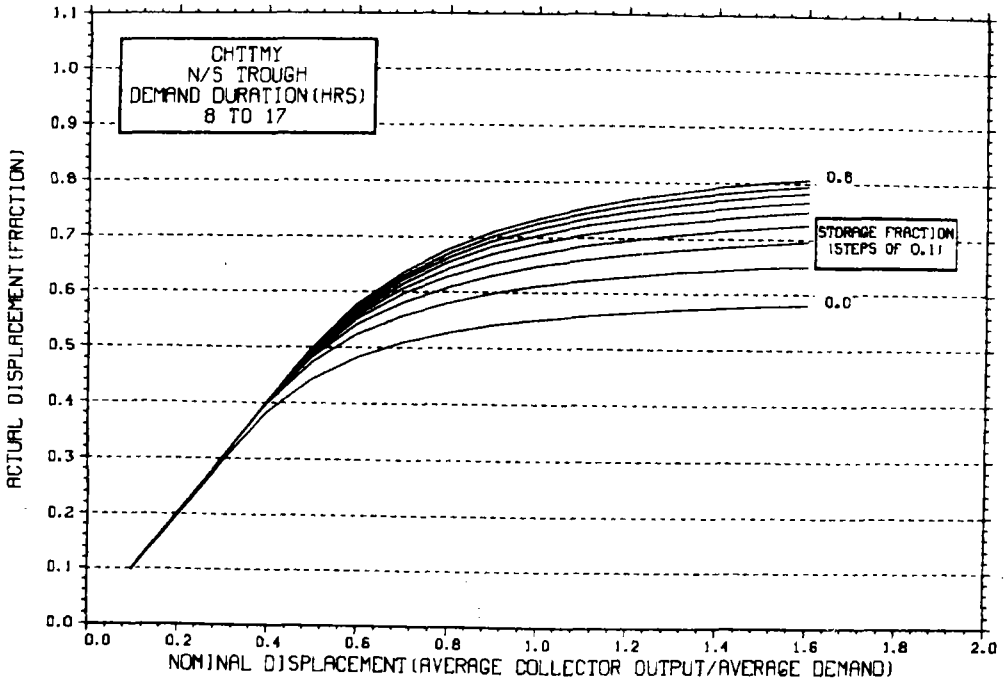

ENERGY INCIDENT ON COLLECTOR APERTURE

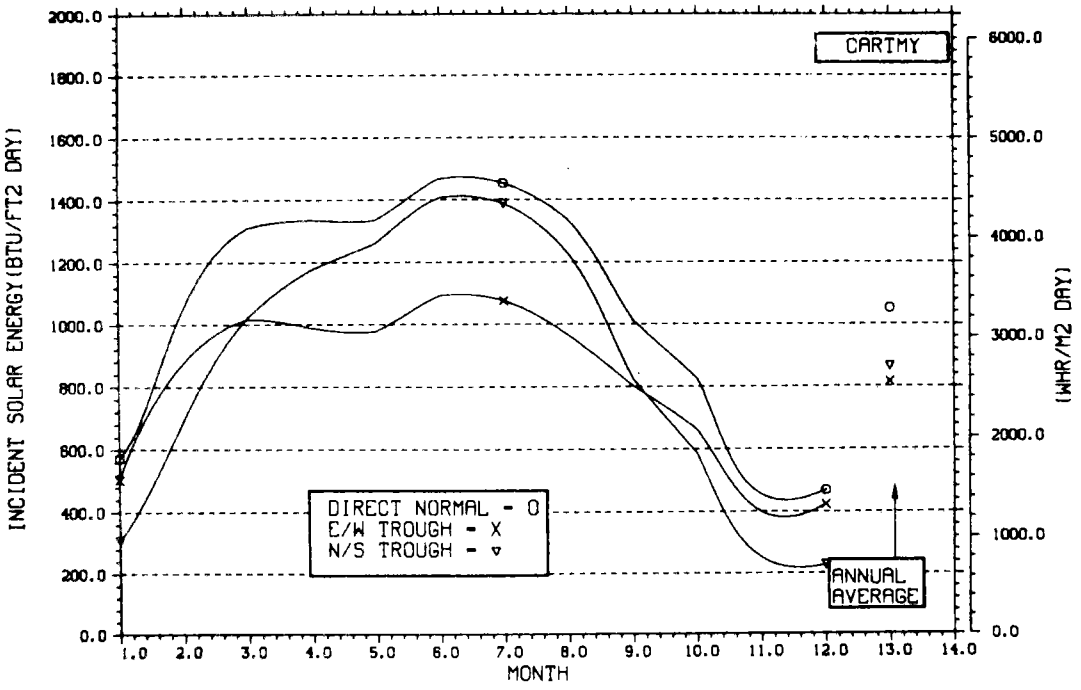

ANNUAL NONFIRST ROW SHADING

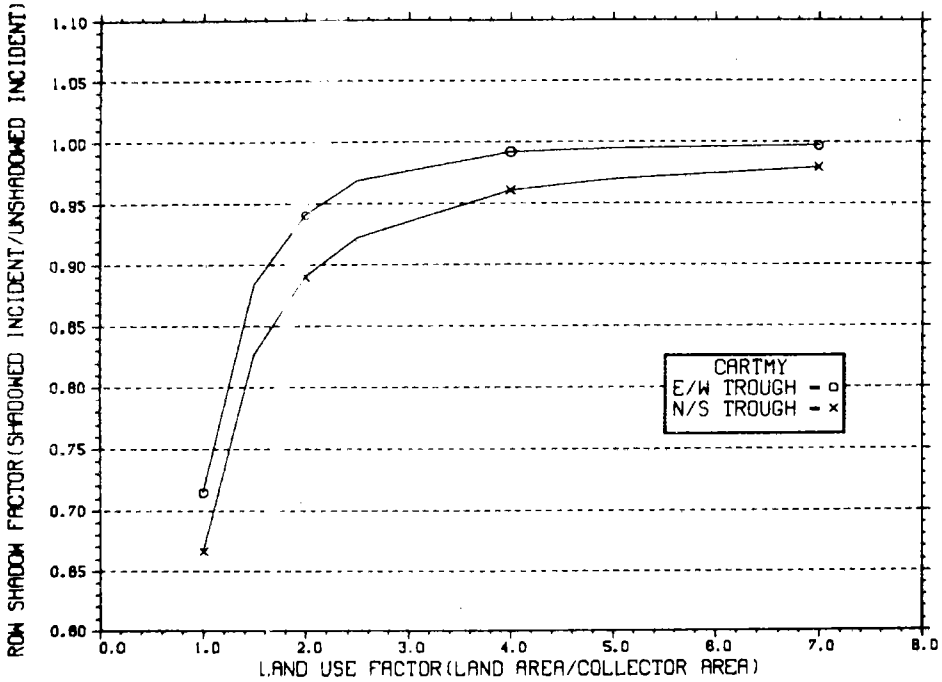

PERFORMANCE VARIATION WITH COLLECTOR AZIMUTH

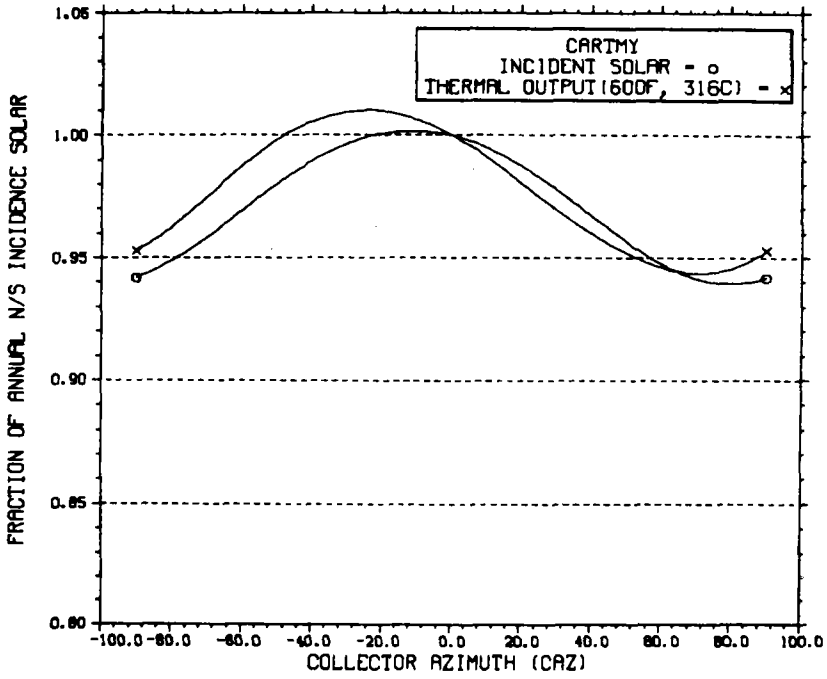

TEMPERATURE DEPENDENCE OF ANNUAL PERFORMANCE

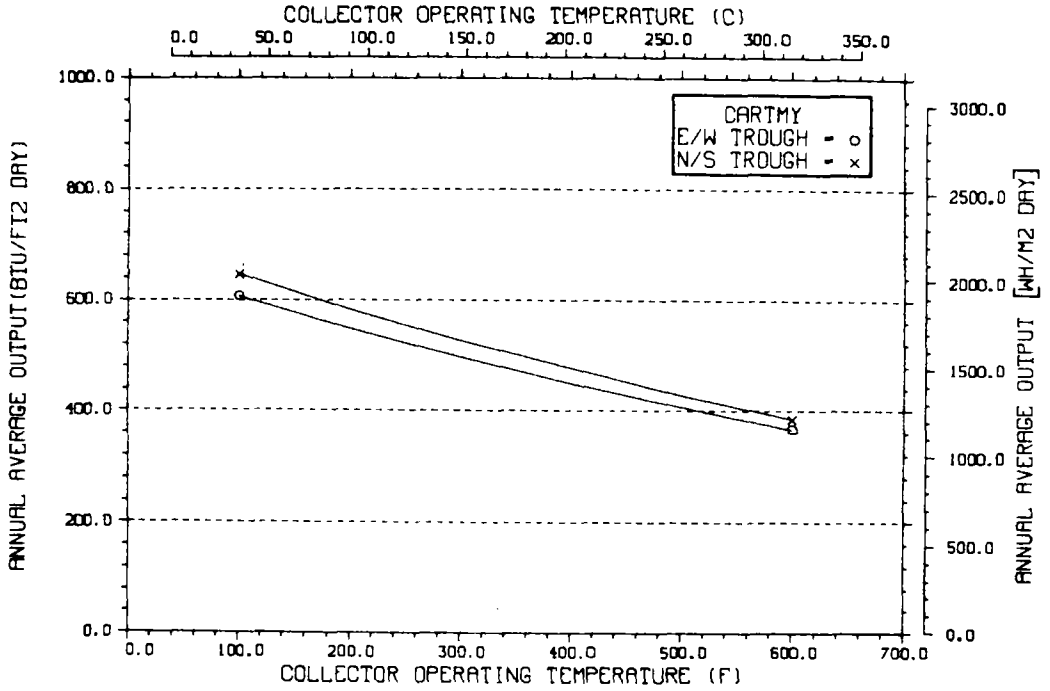

TEMPERATURE DEPENDENCE OF MONTHLY PERFORMANCE

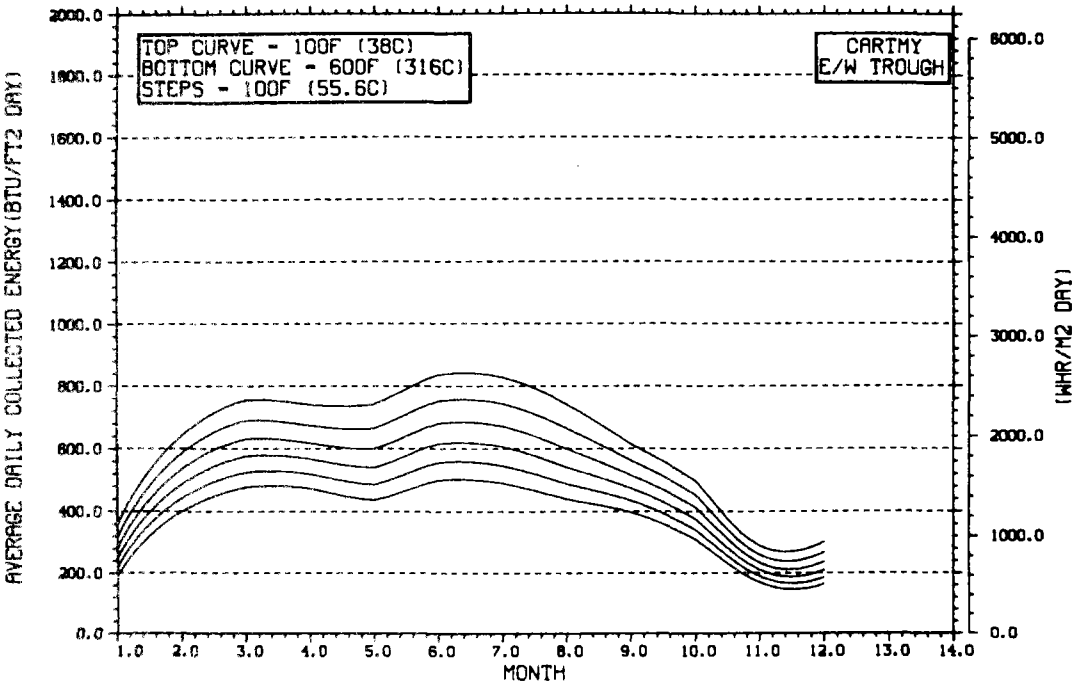

TEMPERATURE DEPENDENCE OF MONTHLY PERFORMANCE

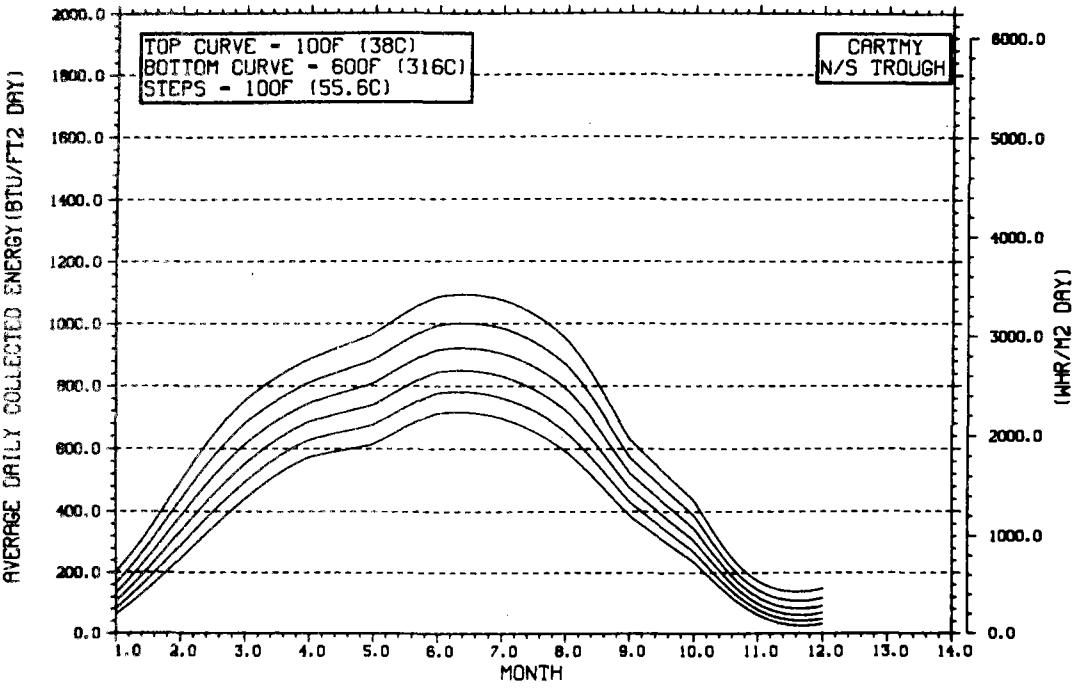

STORAGE SIZING GRAPH FOR CONSTANT ANNUAL DEMAND

NO WEEKEND SHUTDOWN

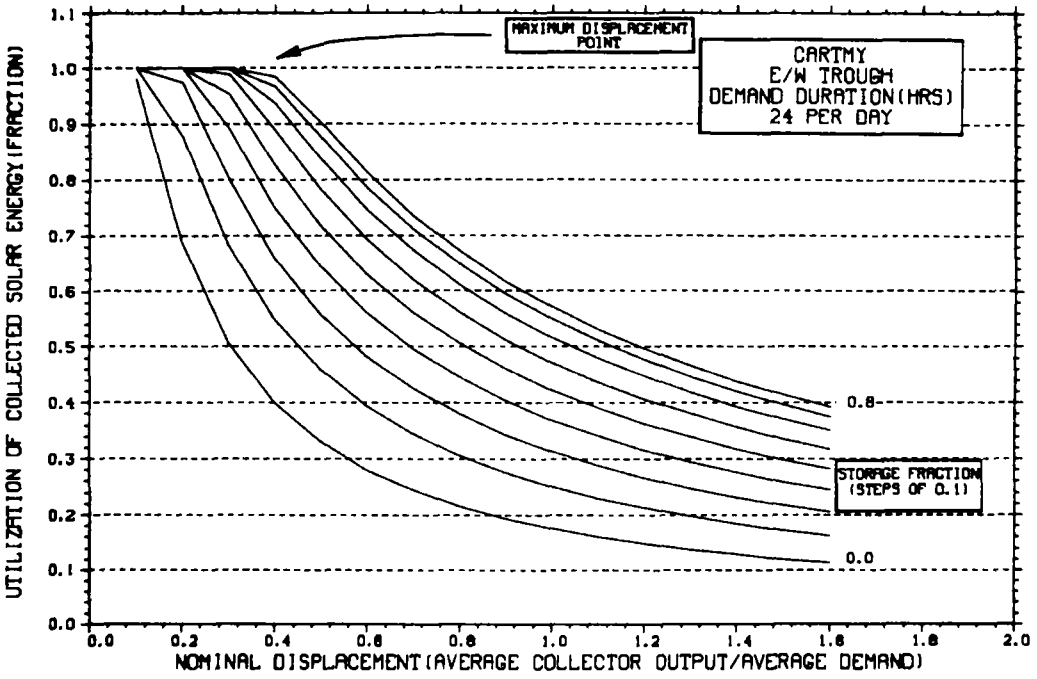

STORAGE SIZING GRAPH FOR CONSTANT ANNUAL DEMAND

NO WEEKEND SHUTDOWN

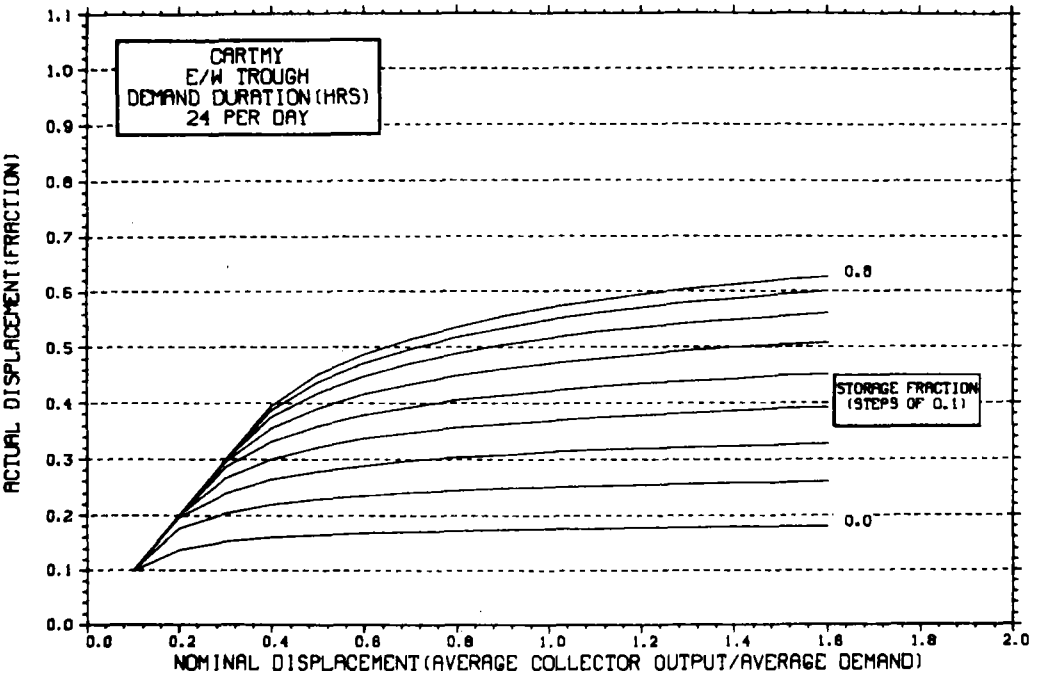

STORAGE SIZING GRAPH FOR CONSTANT ANNUAL DEMAND

NO WEEKEND SHUTDOWN

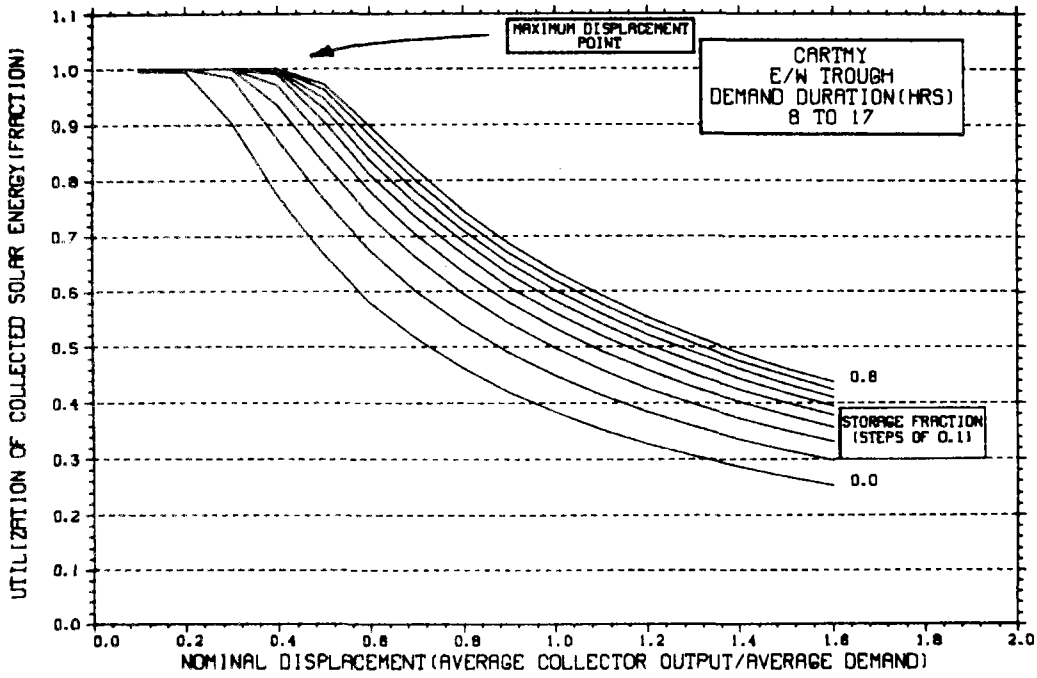

STORAGE SIZING GRAPH FOR CONSTANT ANNUAL DEMAND

NO WEEKEND SHUTDOWN

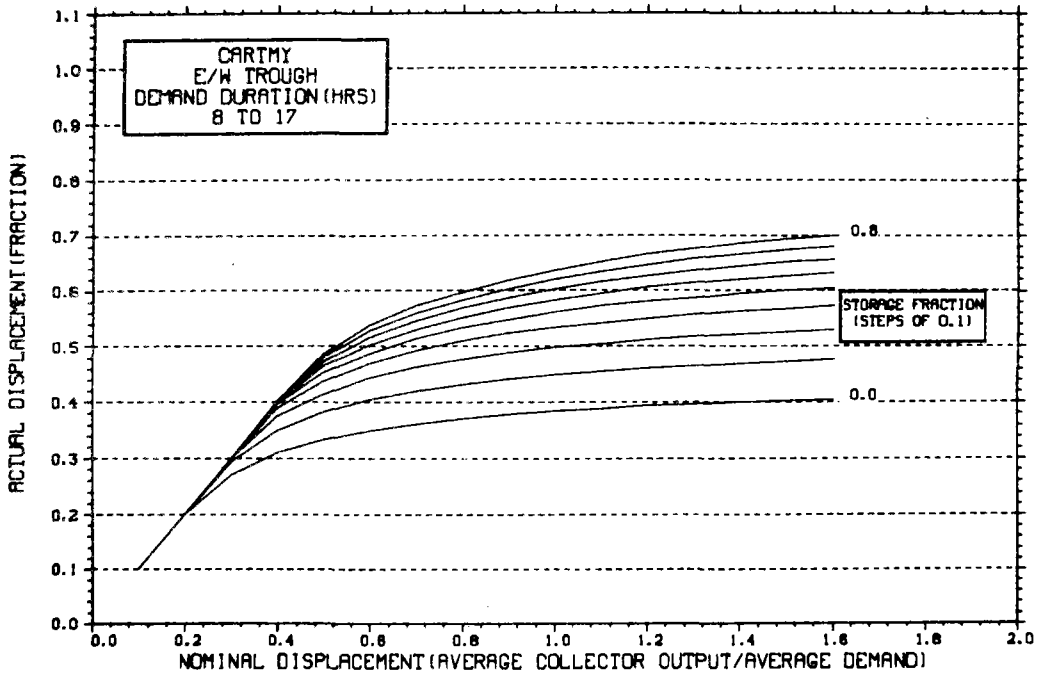

STORAGE SIZING GRAPH FOR CONSTANT ANNUAL DEMAND

NO WEEKEND SHUTDOWN

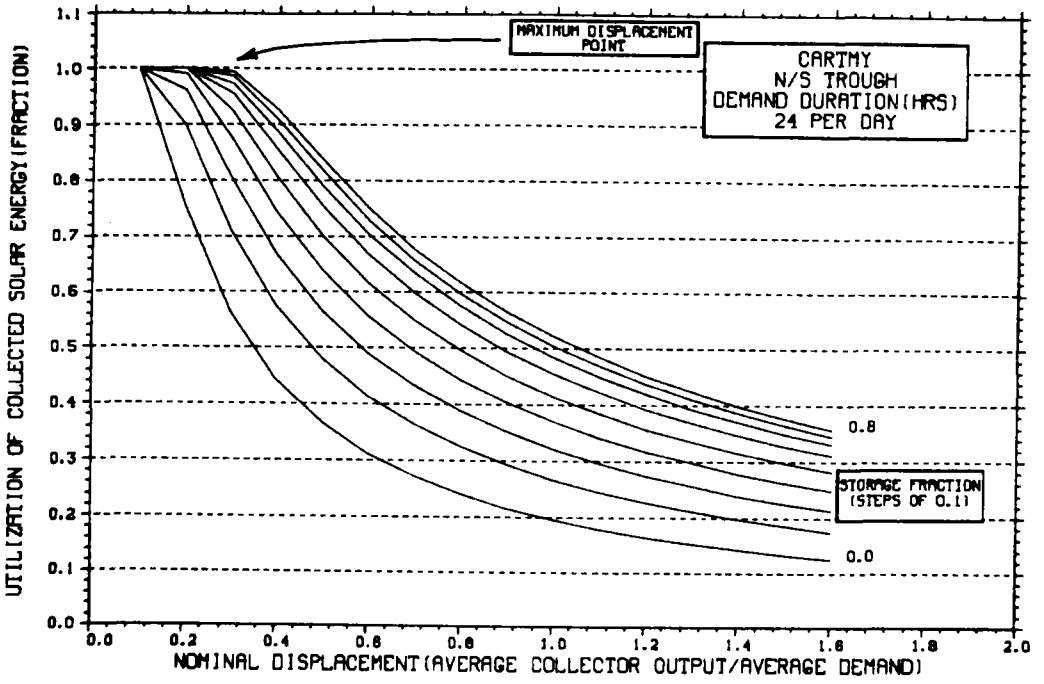

STORAGE SIZING GRAPH FOR CONSTANT ANNUAL DEMAND

NO WEEKEND SHUTDOWN

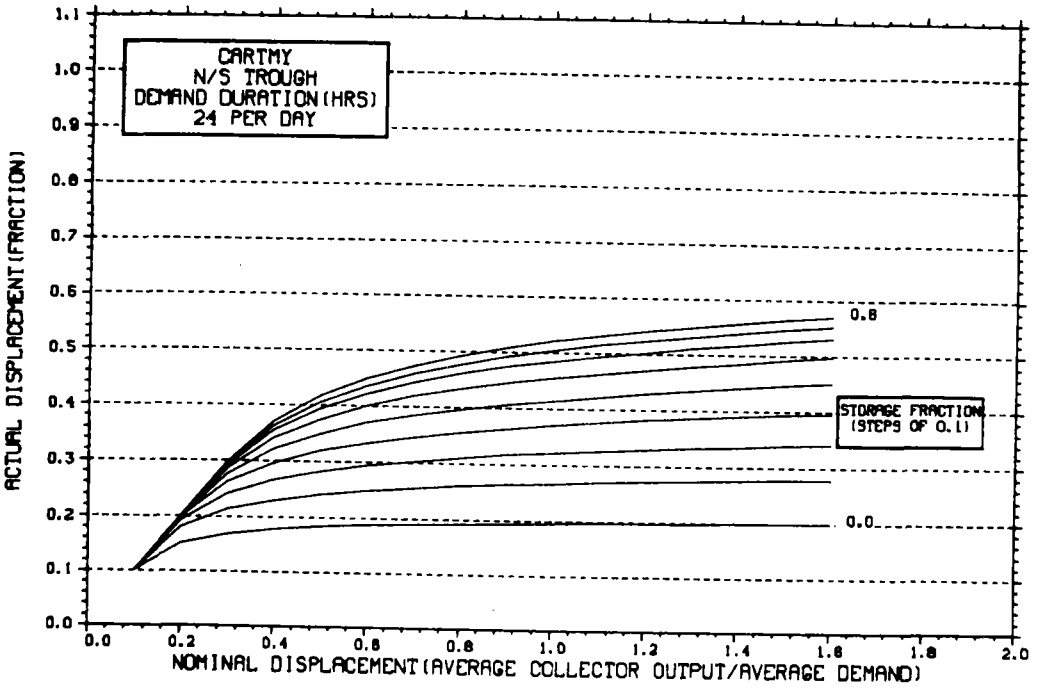

STORAGE SIZING GRAPH FOR CONSTANT ANNUAL DEMAND

NO WEEKEND SHUTDOWN

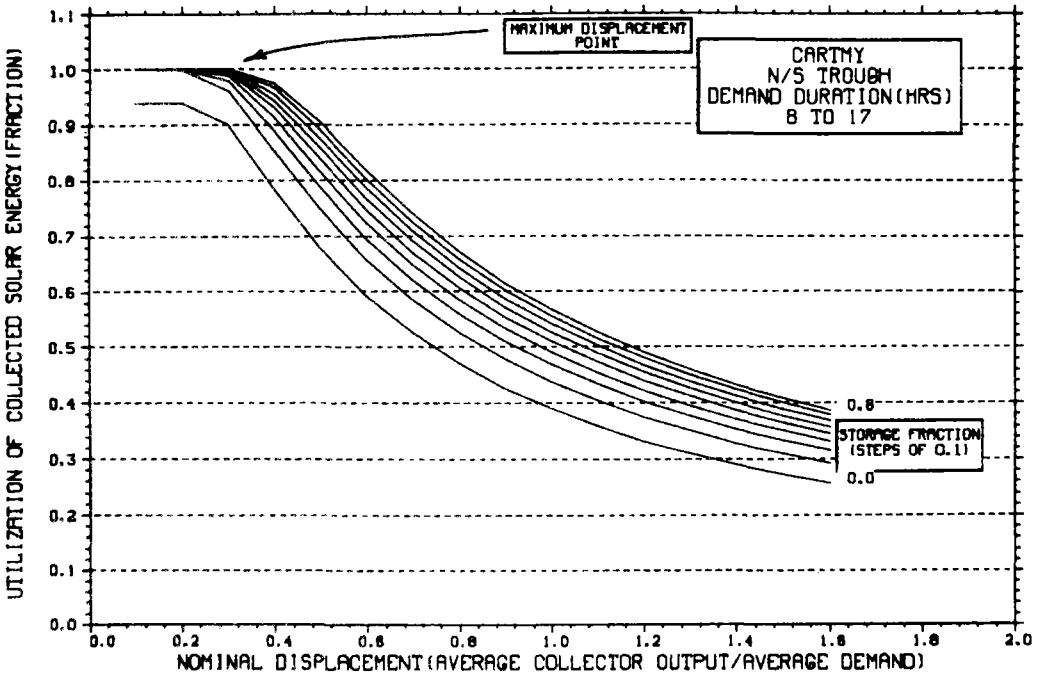

STORAGE SIZING GRAPH FOR CONSTANT ANNUAL DEMAND

NO WEEKEND SHUTDOWN

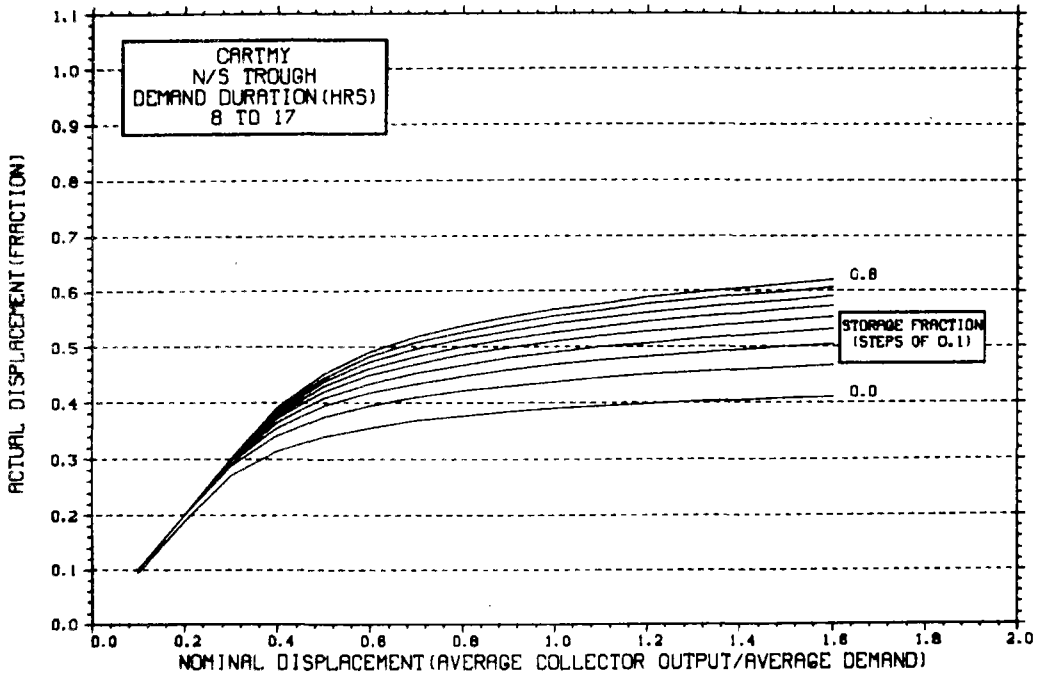

ENERGY INCIDENT ON COLLECTOR APERTURE

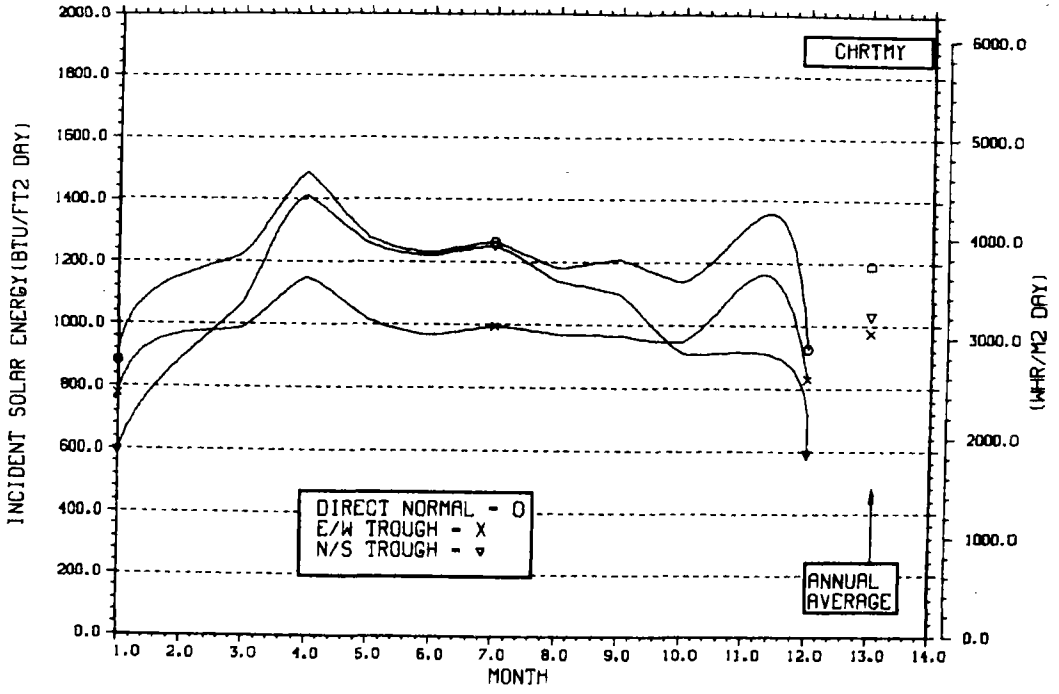

ANNUAL NONFIRST ROW SHADING

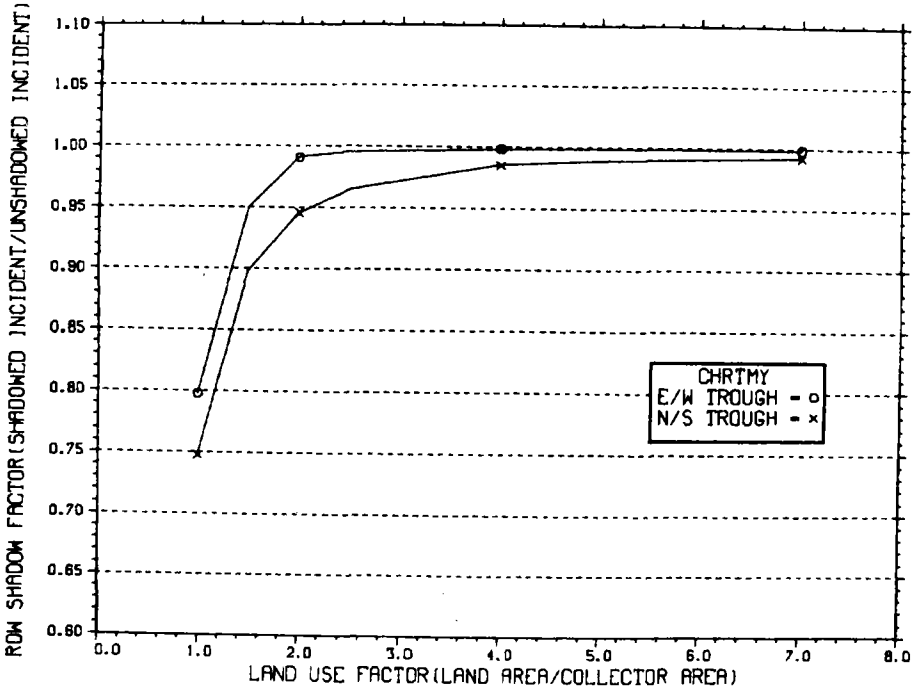

PERFORMANCE VARIATION WITH COLLECTOR AZIMUTH

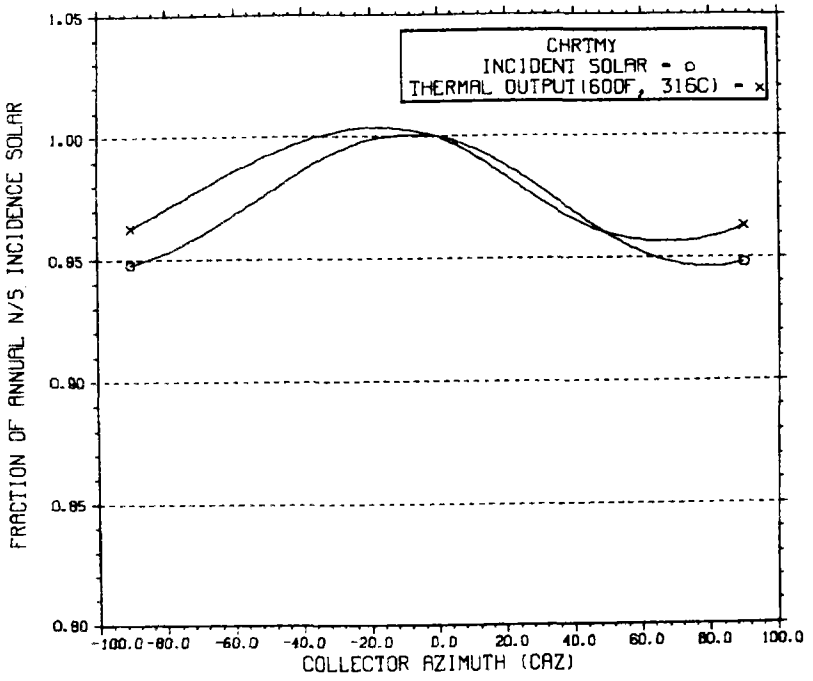

TEMPERATURE DEPENDENCE OF ANNUAL PERFORMANCE

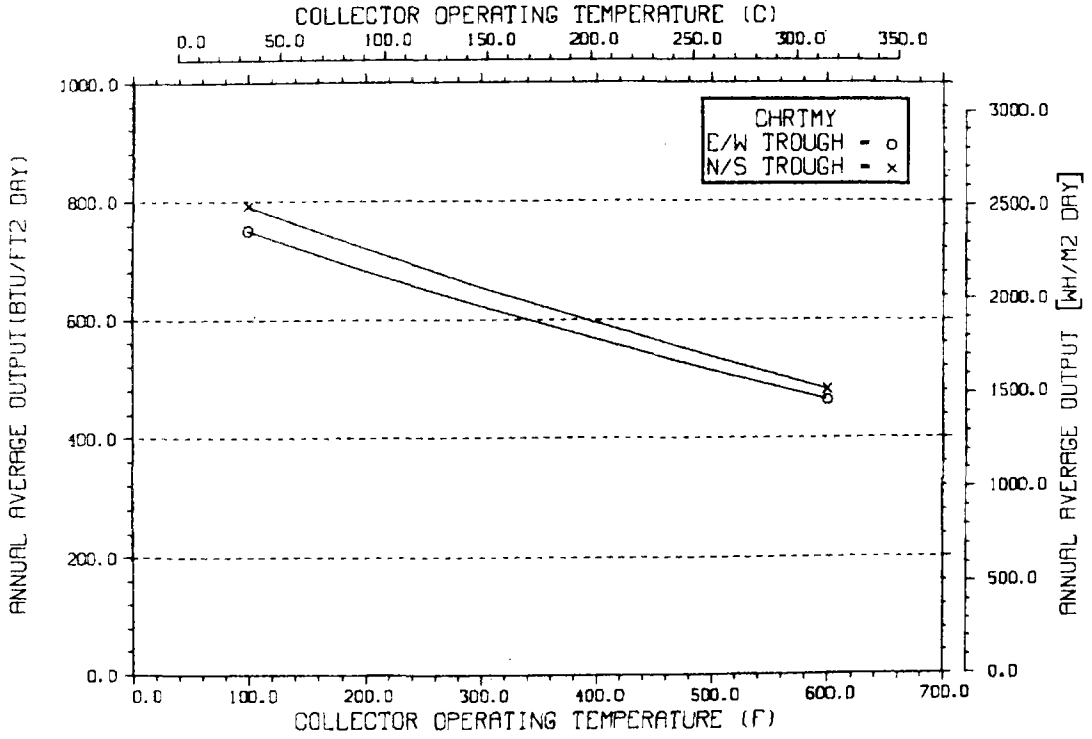

TEMPERATURE DEPENDENCE OF MONTHLY PERFORMANCE

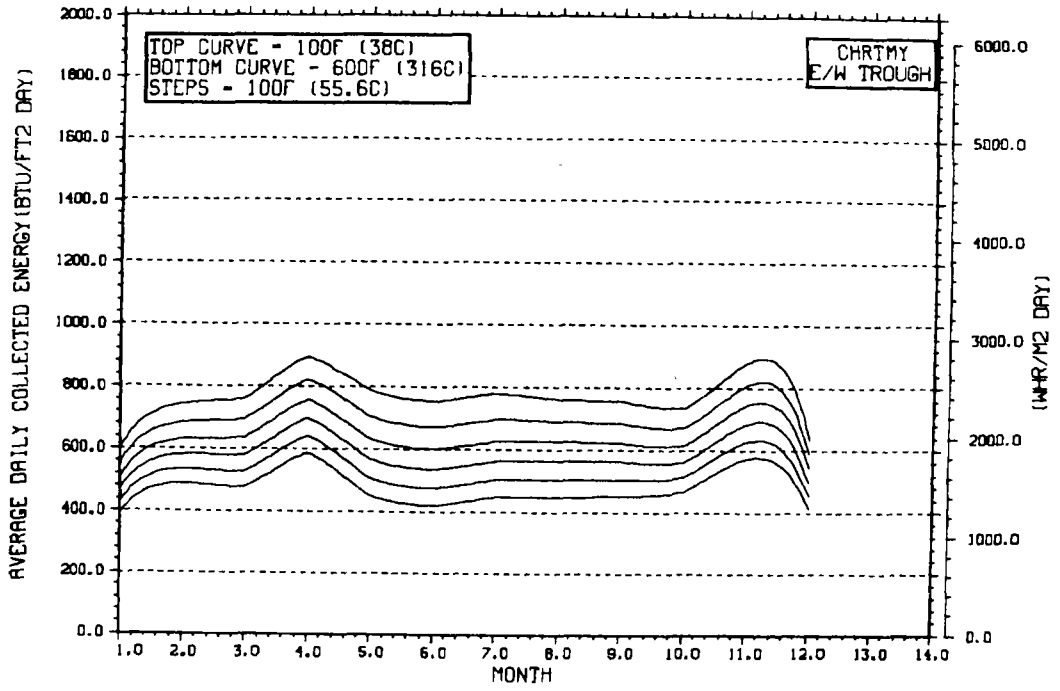

TEMPERATURE DEPENDENCE OF MONTHLY PERFORMANCE

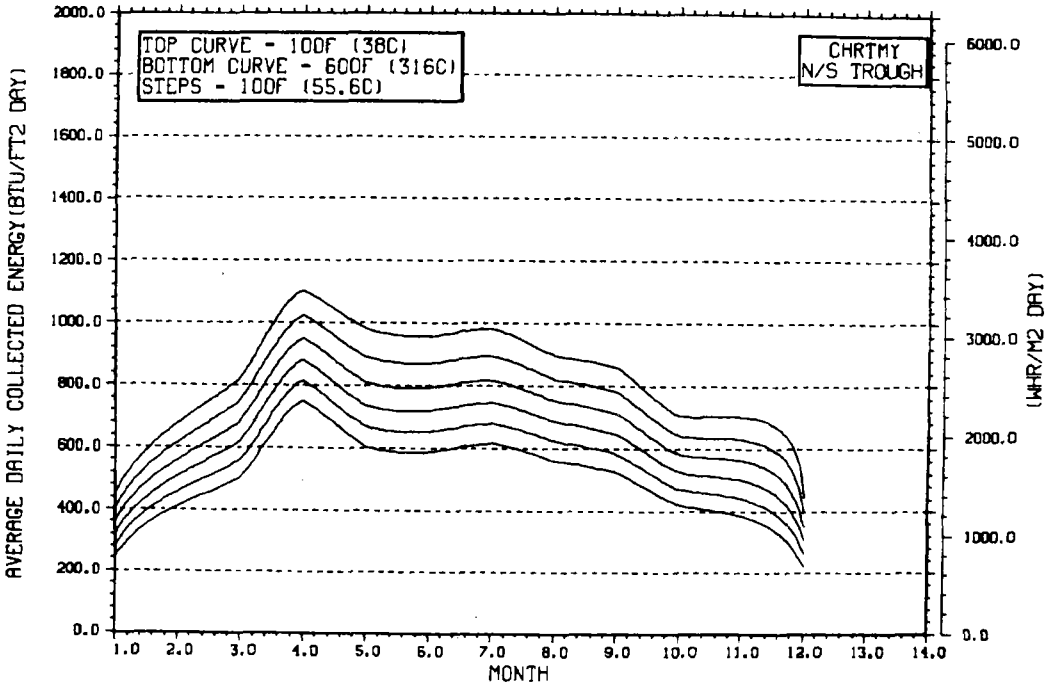

STORAGE SIZING GRAPH FOR CONSTANT ANNUAL DEMAND

NO WEEKEND SHUTDOWN

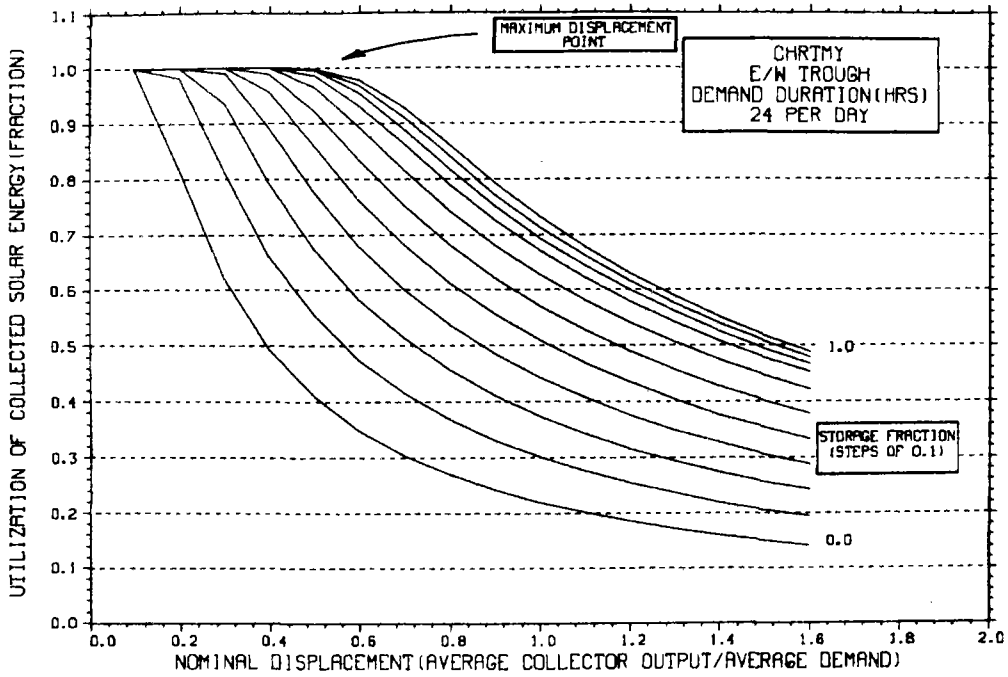

STORAGE SIZING GRAPH FOR CONSTANT ANNUAL DEMAND

NO WEEKEND SHUTDOWN

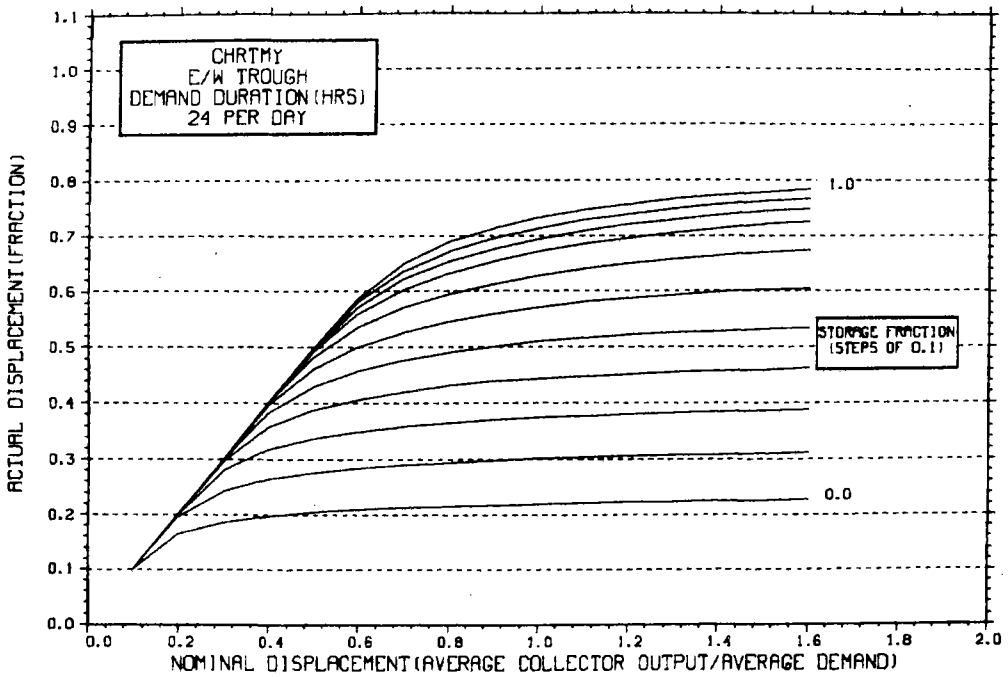

STORAGE SIZING GRAPH FOR CONSTANT ANNUAL DEMAND

NO WEEKEND SHUTDOWN

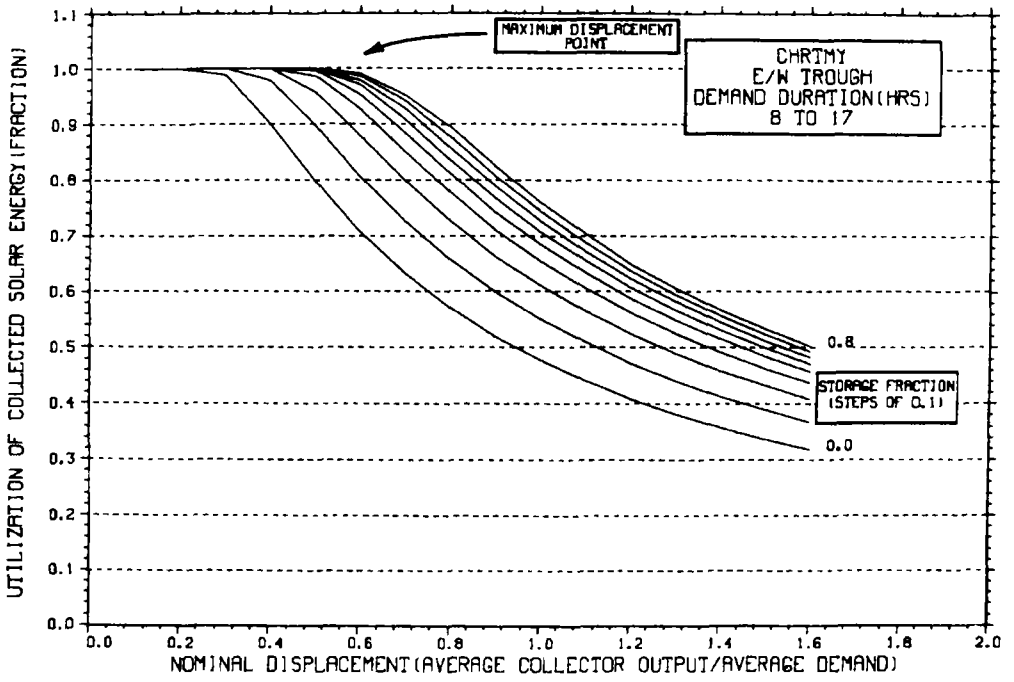

STORAGE SIZING GRAPH FOR CONSTANT ANNUAL DEMAND

NO WEEKEND SHUTDOWN

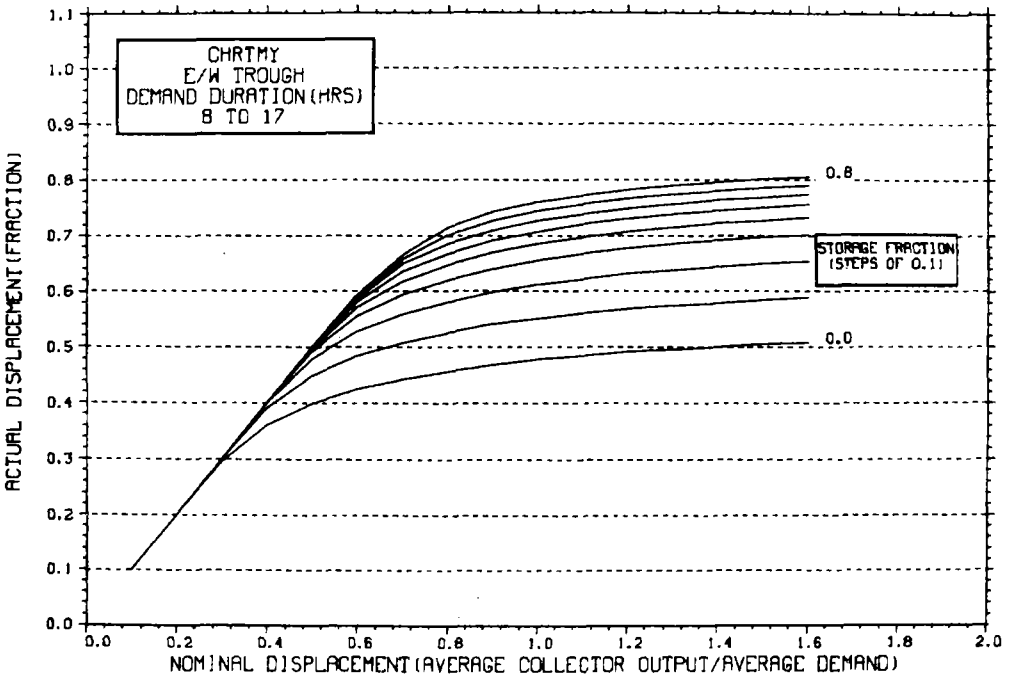

STORAGE SIZING GRAPH FOR CONSTANT ANNUAL DEMAND

NO WEEKEND SHUTDOWN

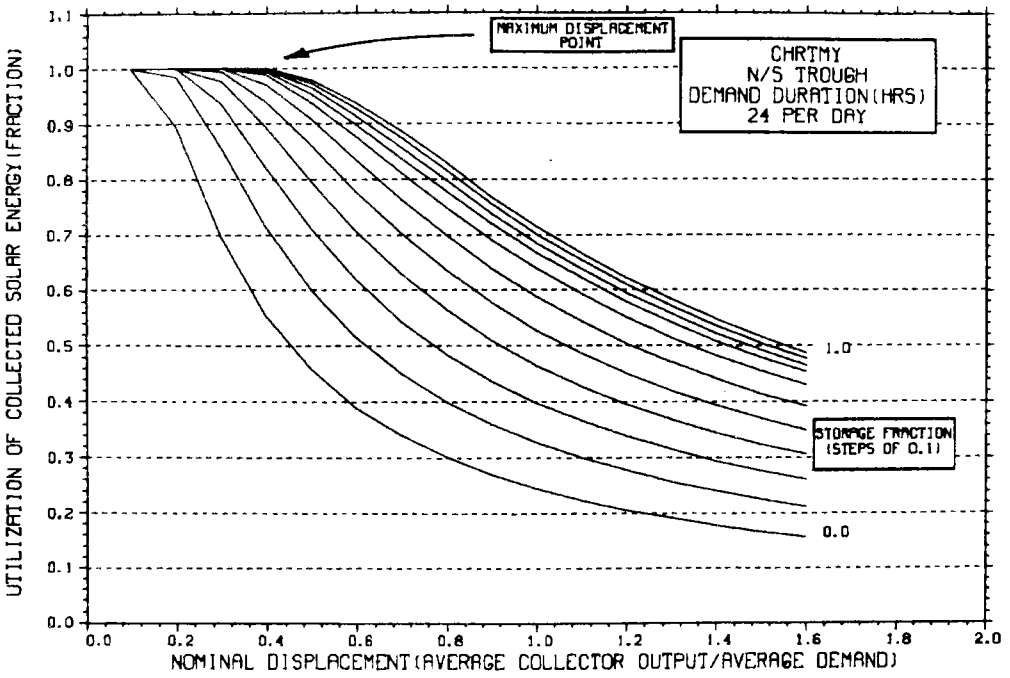

STORAGE SIZING GRAPH FOR CONSTANT ANNUAL DEMAND

NO WEEKEND SHUTDOWN

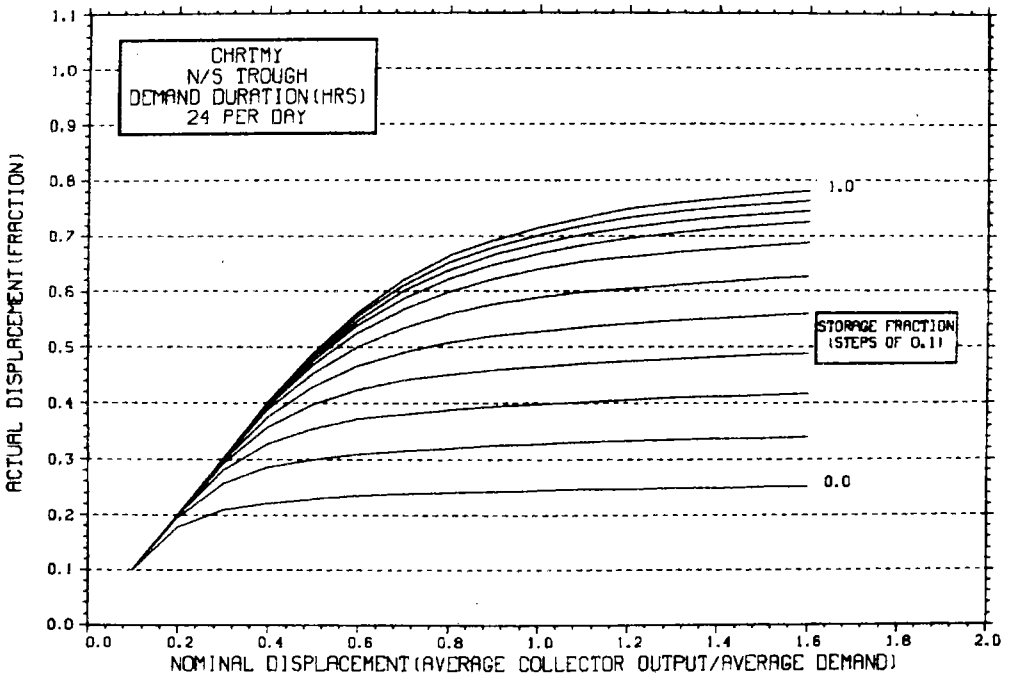

STORAGE SIZING GRAPH FOR CONSTANT ANNUAL DEMAND

NO WEEKEND SHUTDOWN

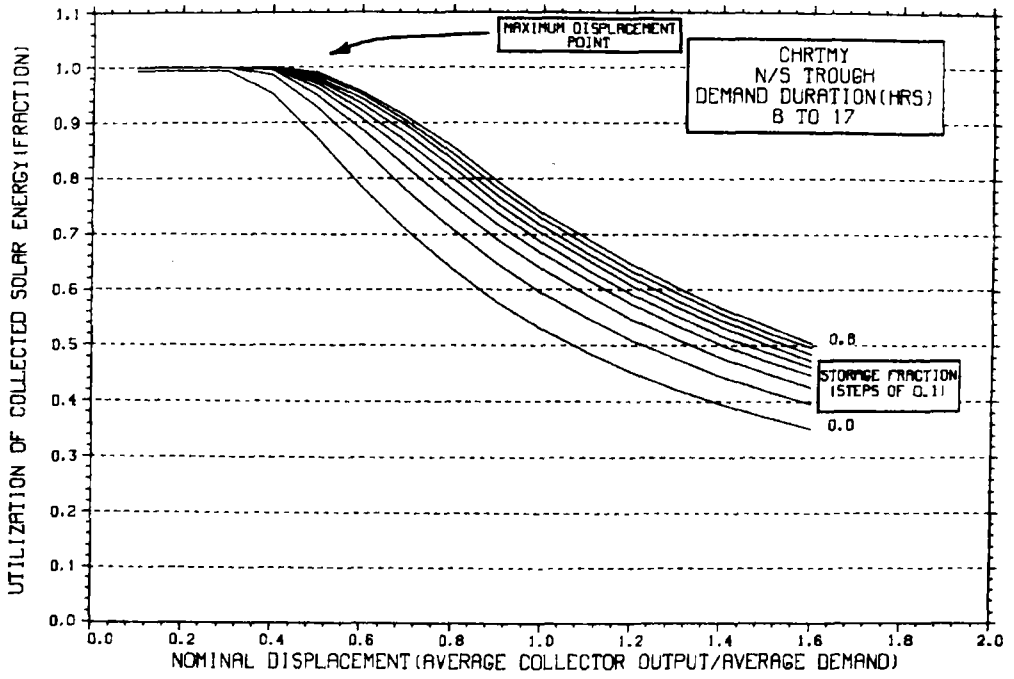

STORAGE SIZING GRAPH FOR CONSTANT ANNUAL DEMAND

NO WEEKEND SHUTDOWN

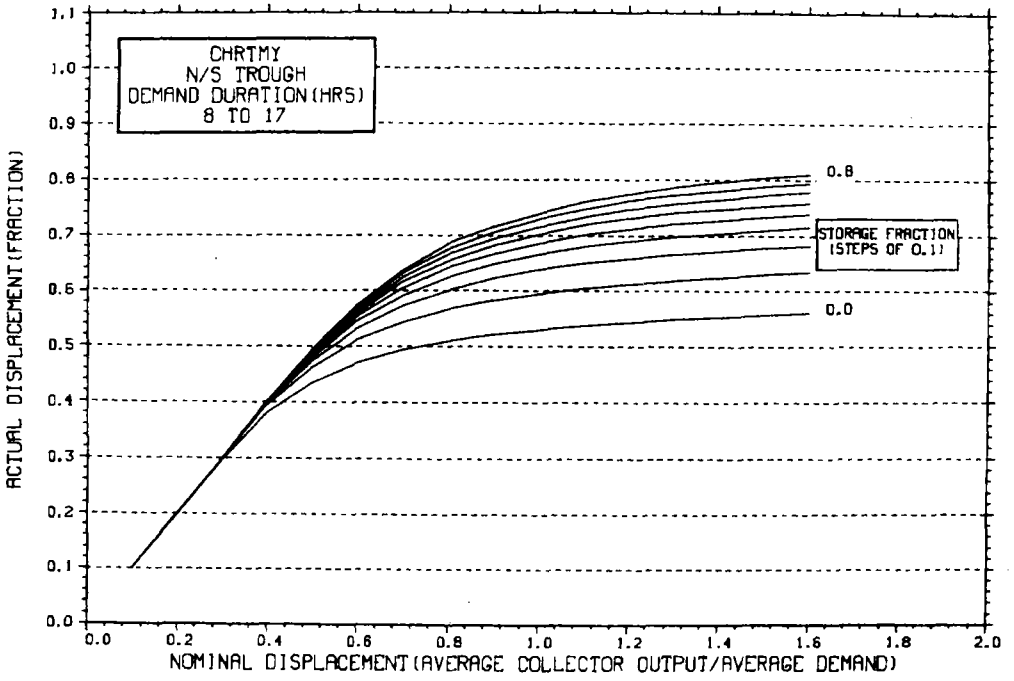

ENERGY INCIDENT ON COLLECTOR APERTURE

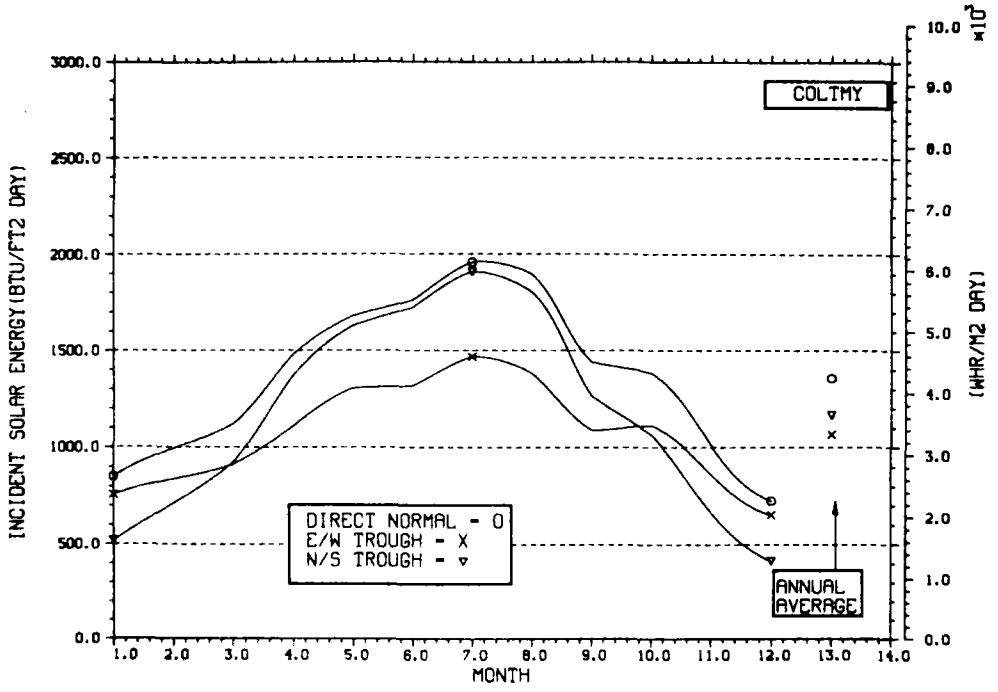

ANNUAL NONFIRST ROW SHADING

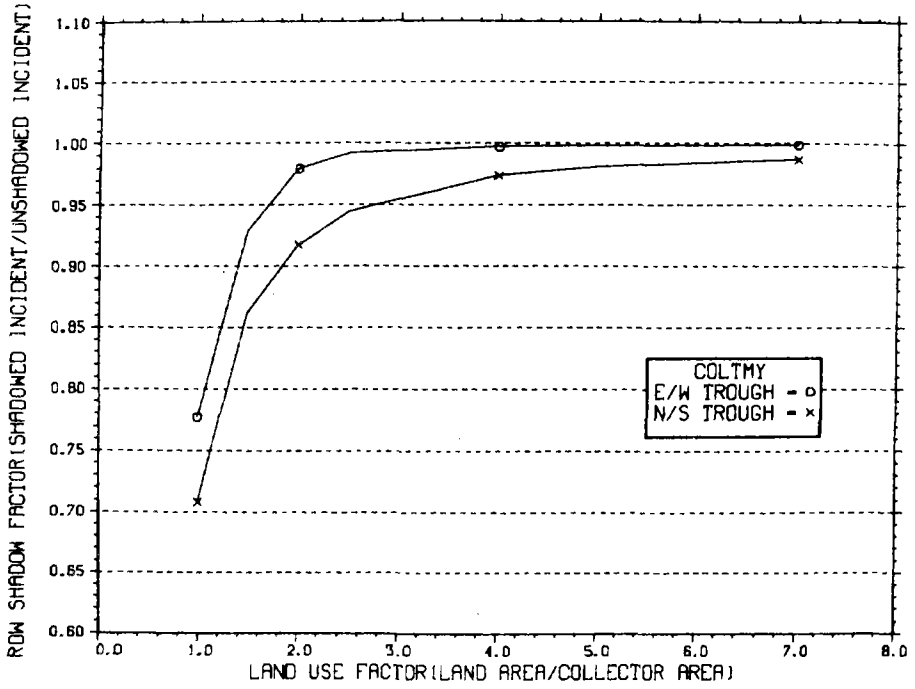

PERFORMANCE VARIATION WITH COLLECTOR AZIMUTH

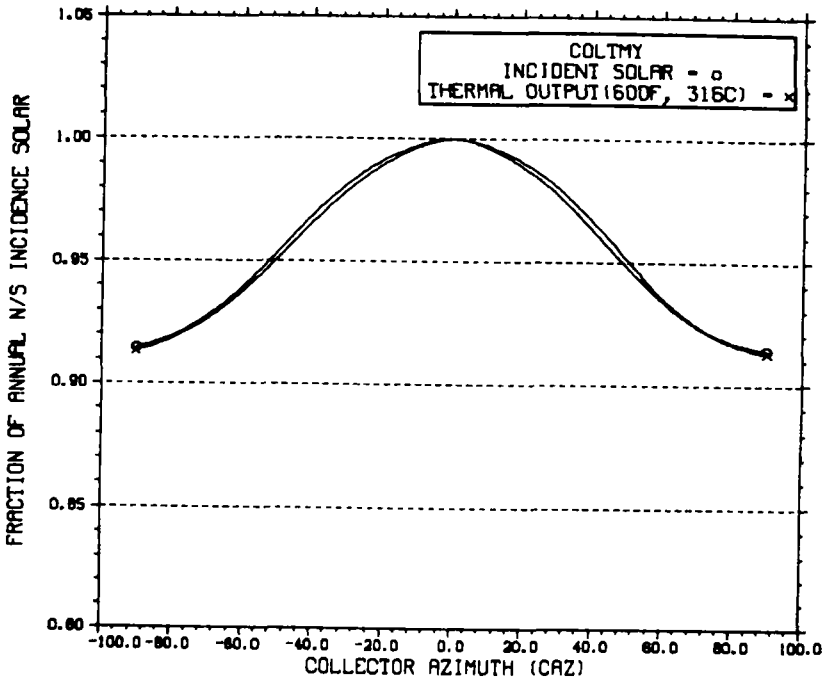

TEMPERATURE DEPENDENCE OF ANNUAL PERFORMANCE

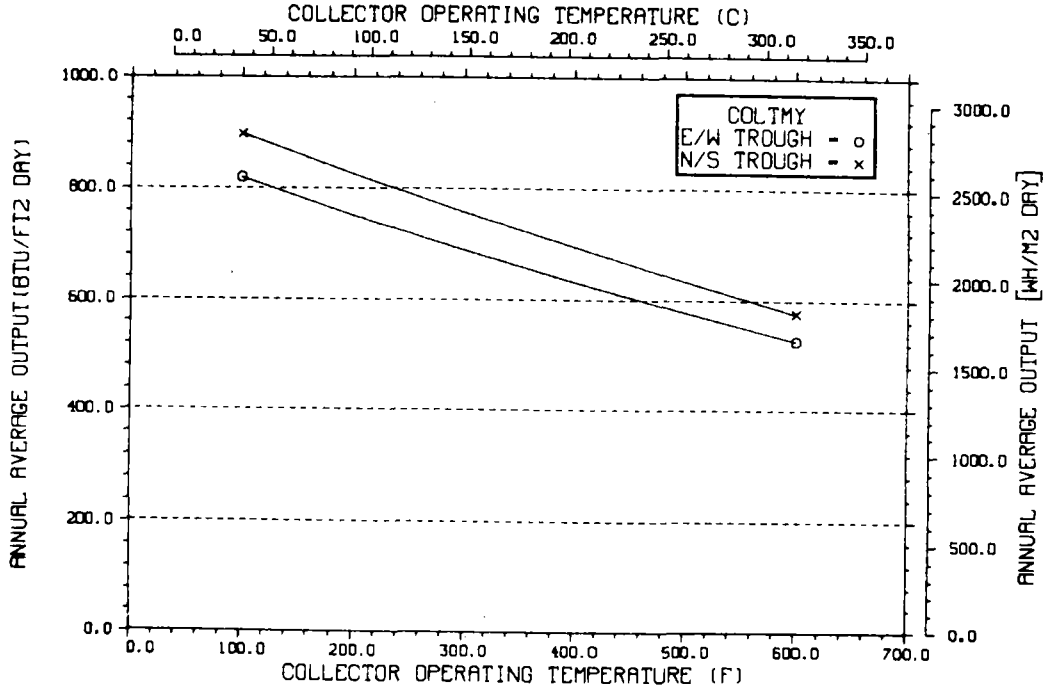

TEMPERATURE DEPENDENCE OF MONTHLY PERFORMANCE

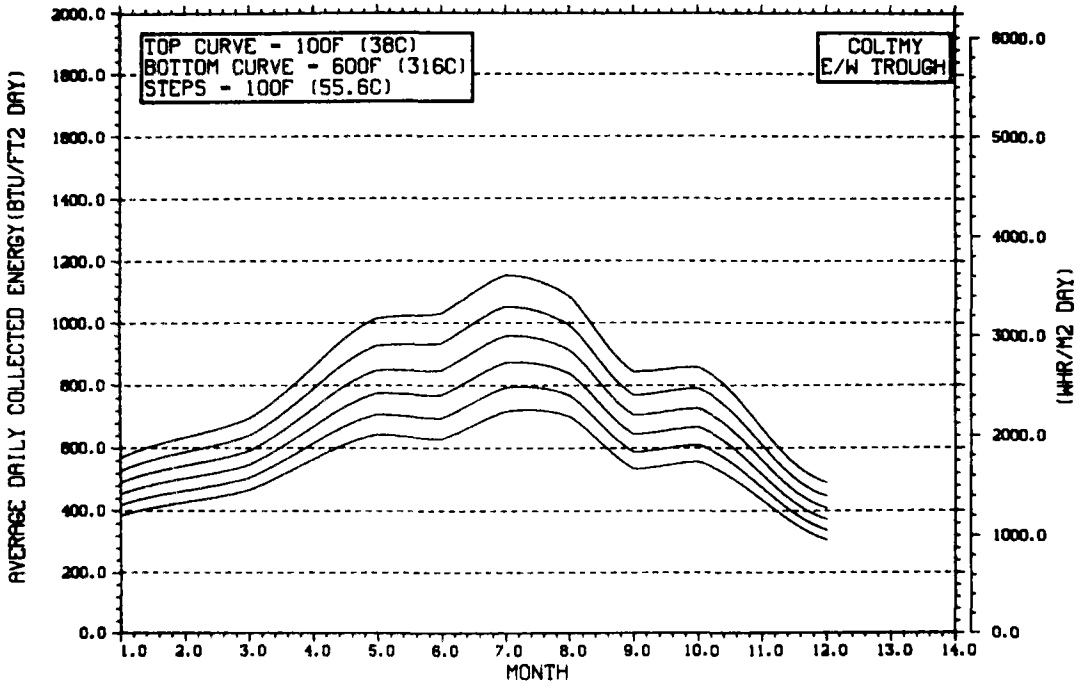

TEMPERATURE DEPENDENCE OF MONTHLY PERFORMANCE

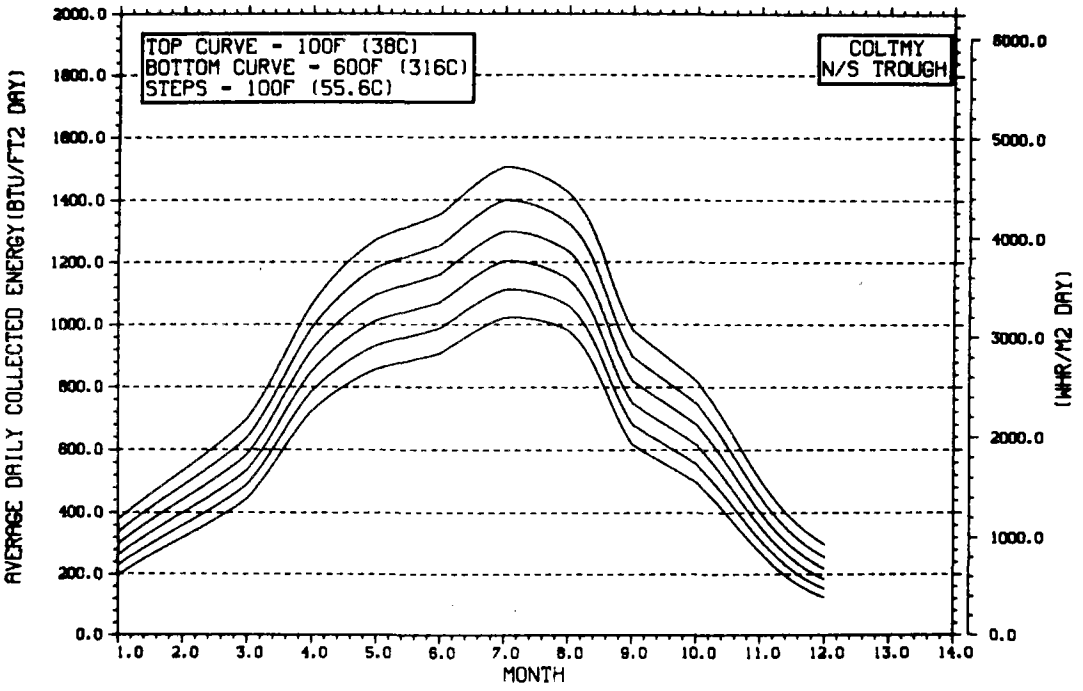

STORAGE SIZING GRAPH FOR CONSTANT ANNUAL DEMAND

NO WEEKEND SHUTDOWN

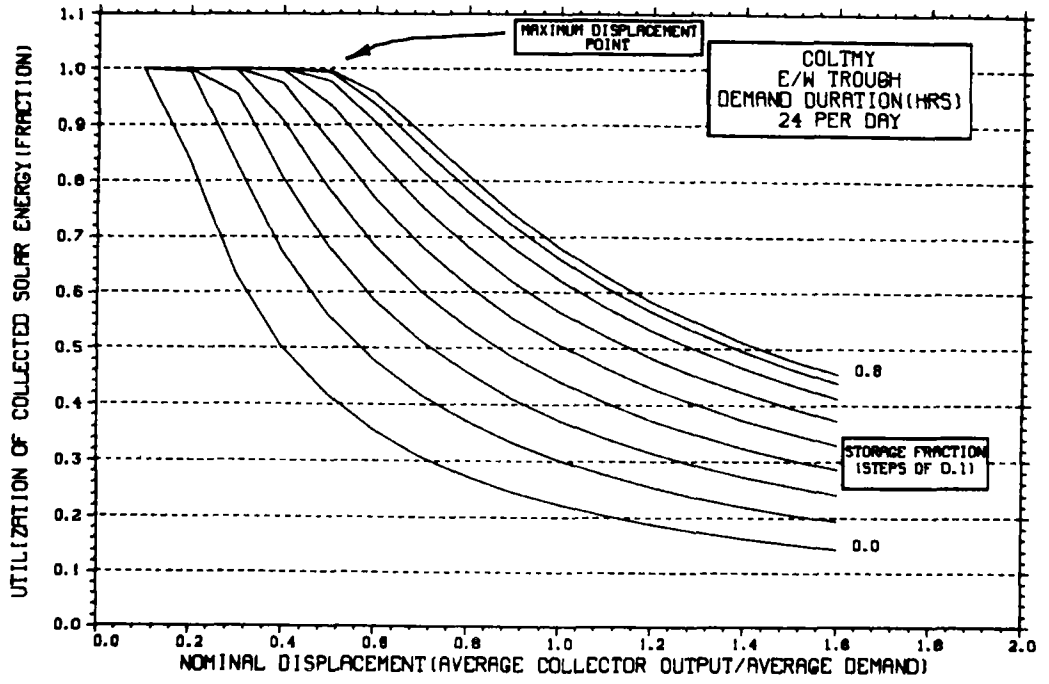

STORAGE SIZING GRAPH FOR CONSTANT ANNUAL DEMAND

NO WEEKEND SHUTDOWN

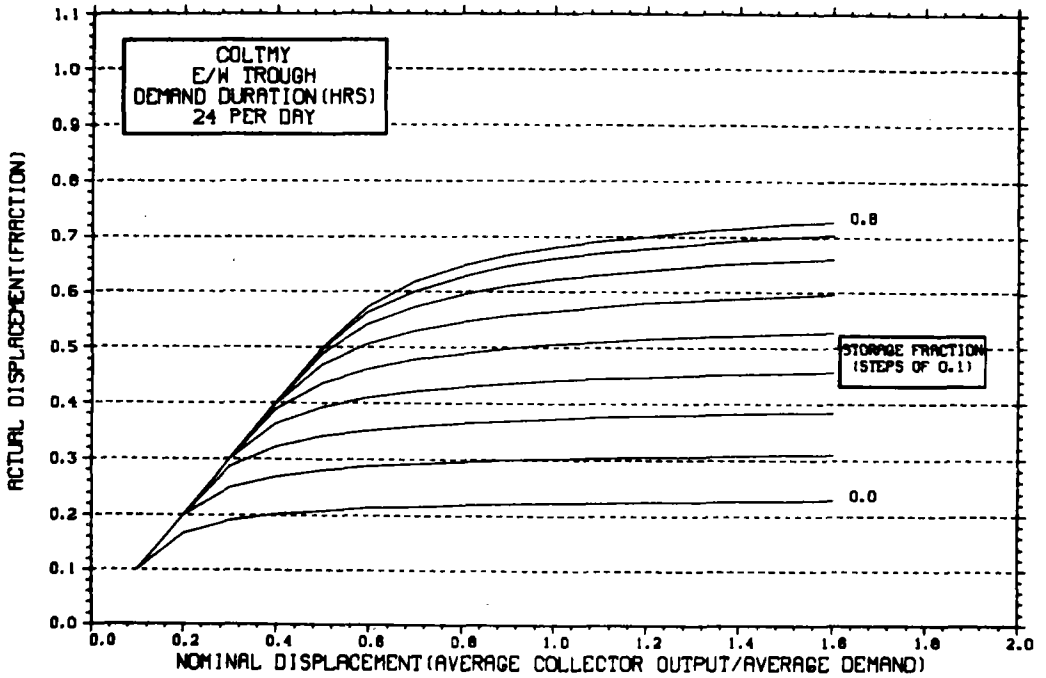

STORAGE SIZING GRAPH FOR CONSTANT ANNUAL DEMAND

NO WEEKEND SHUTDOWN

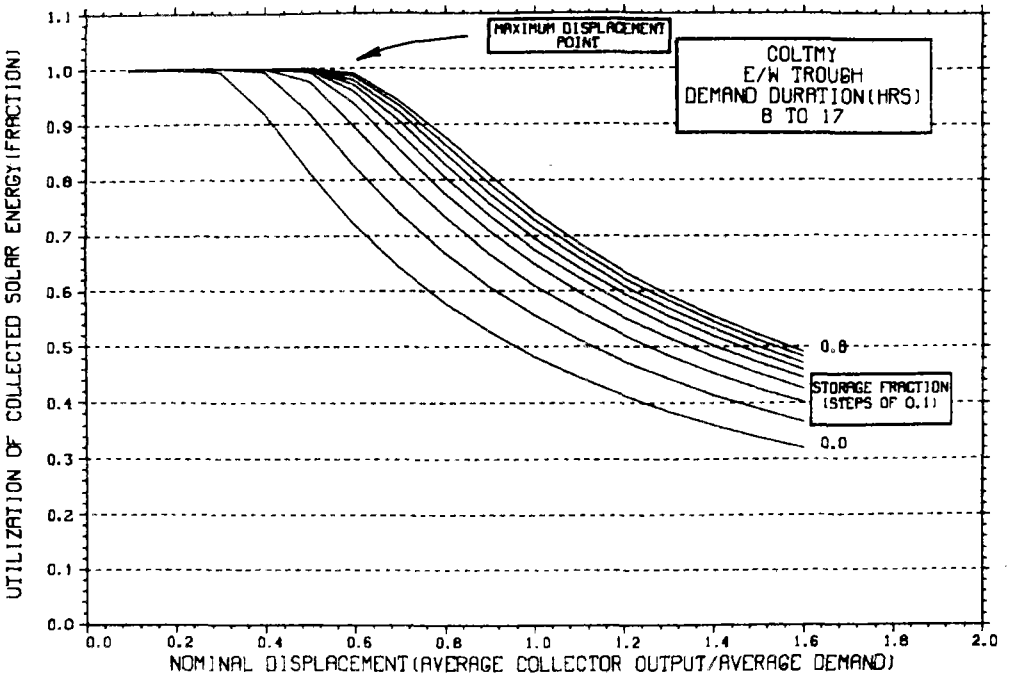

STORAGE SIZING GRAPH FOR CONSTANT ANNUAL DEMAND

NO WEEKEND SHUTDOWN

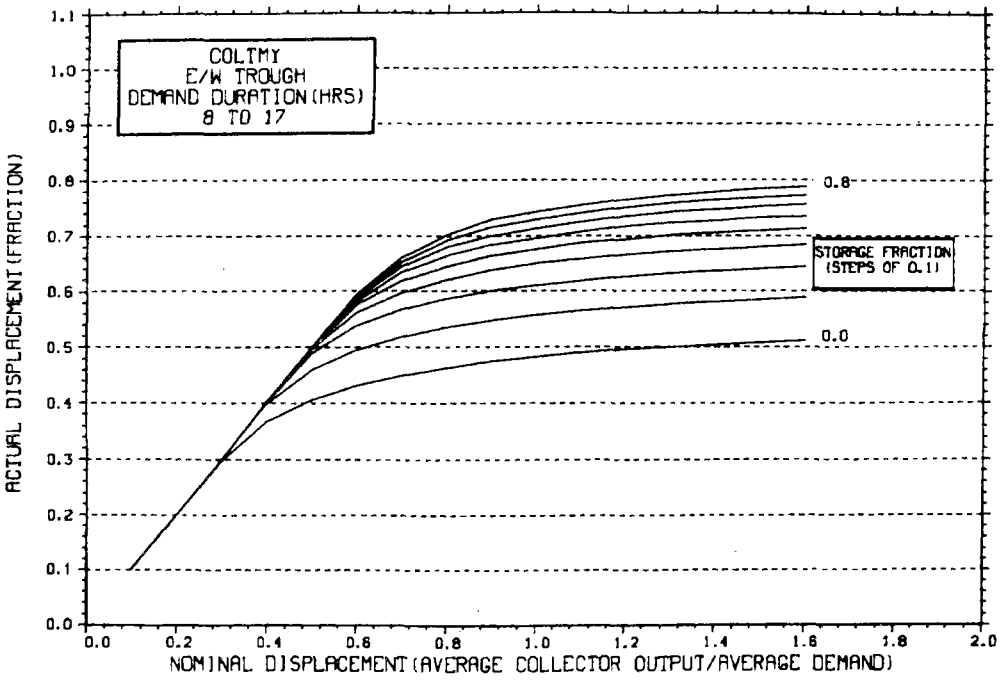

STORAGE SIZING GRAPH FOR CONSTANT ANNUAL DEMAND

NO WEEKEND SHUTDOWN

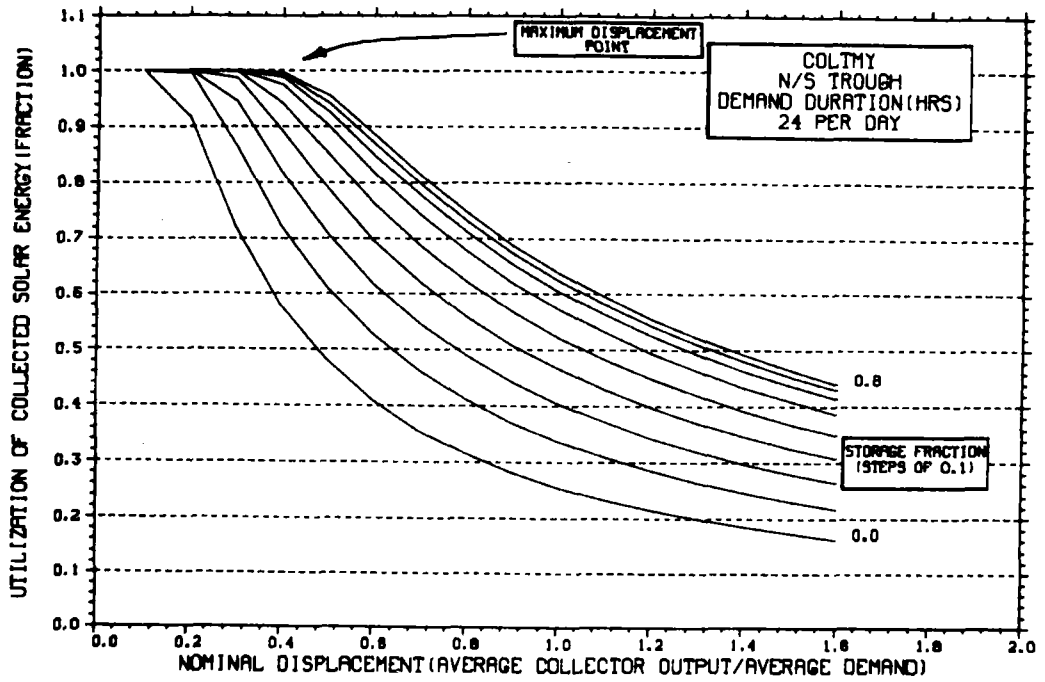

STORAGE SIZING GRAPH FOR CONSTANT ANNUAL DEMAND

NO WEEKEND SHUTDOWN

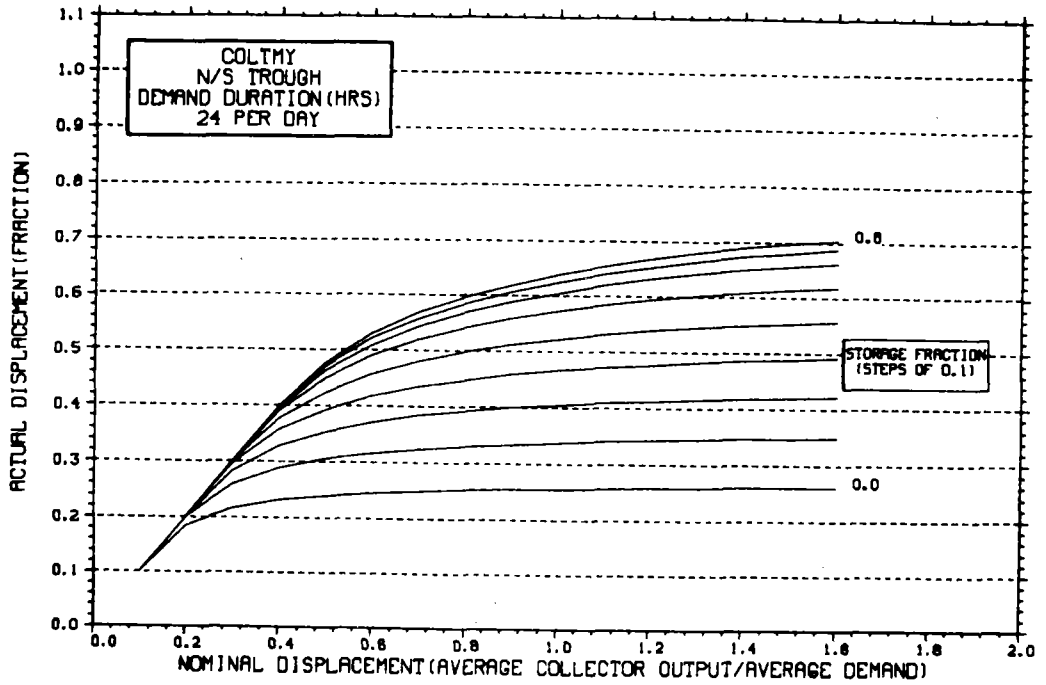

STORAGE SIZING GRAPH FOR CONSTANT ANNUAL DEMAND

NO WEEKEND SHUTDOWN

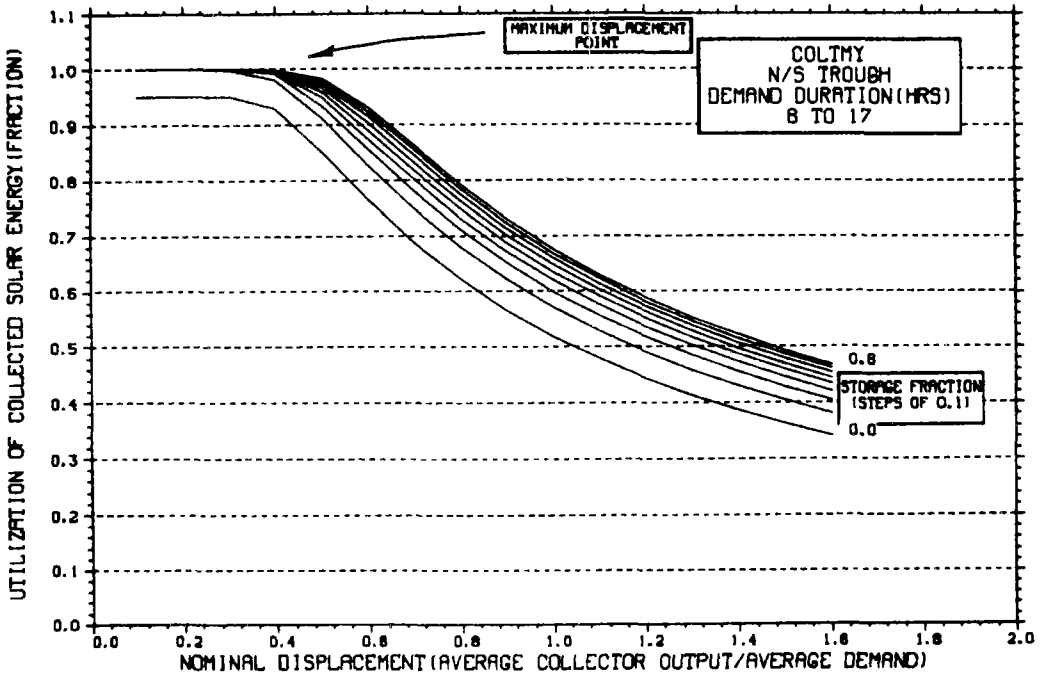

STORAGE SIZING GRAPH FOR CONSTANT ANNUAL DEMAND

NO WEEKEND SHUTDOWN

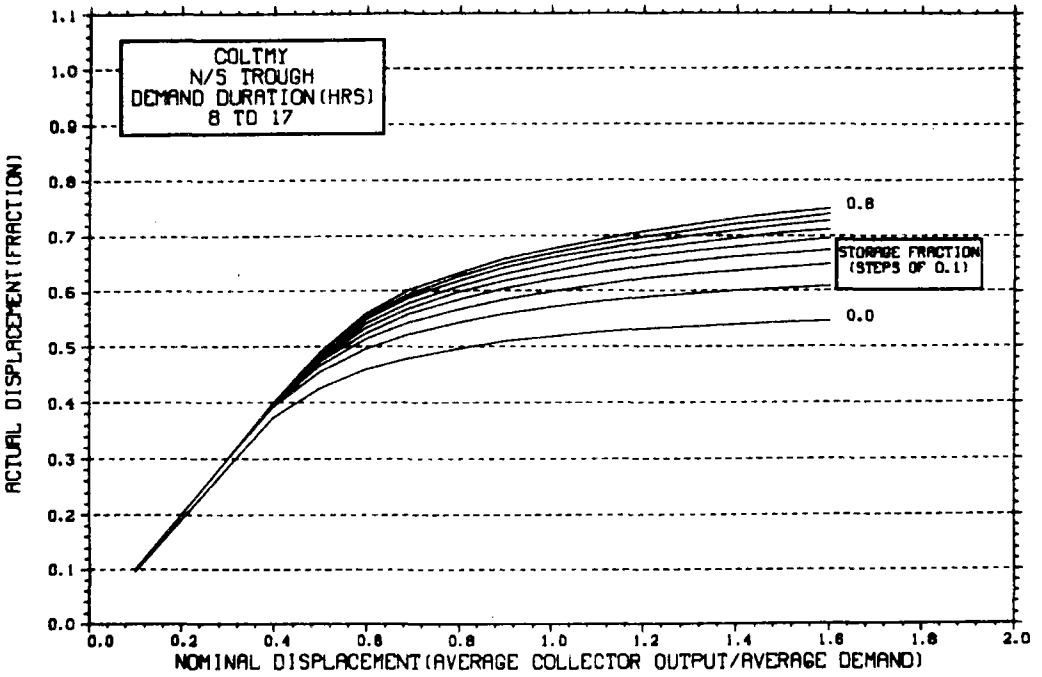

ENERGY INCIDENT ON COLLECTOR APERTURE

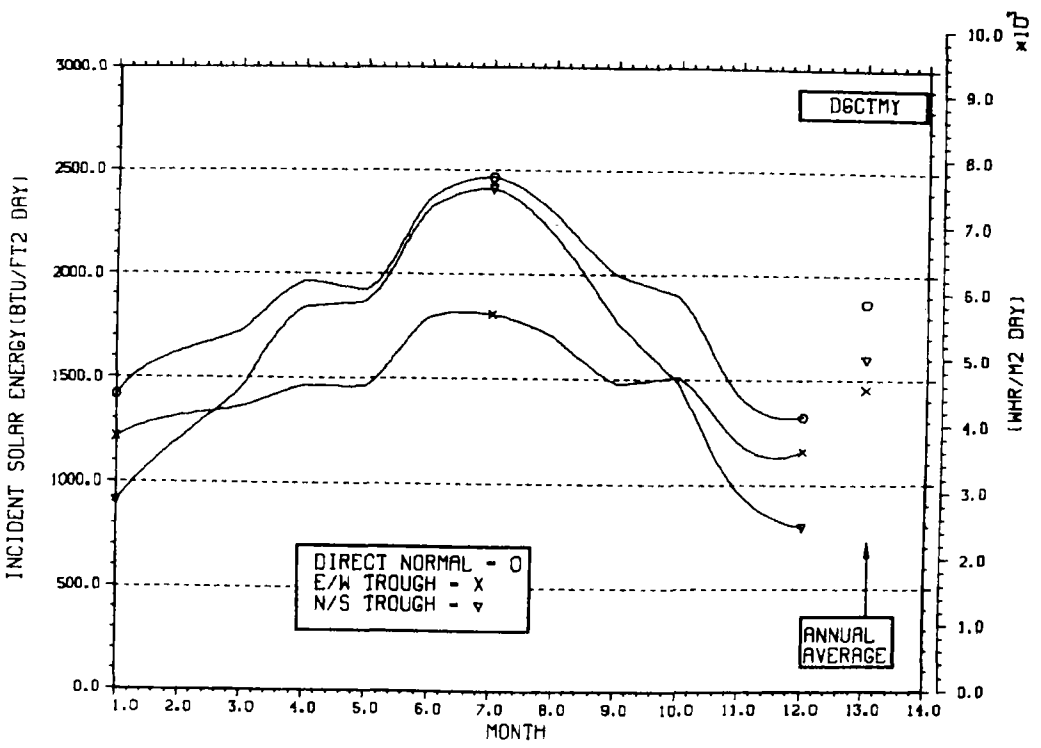

ANNUAL NONFIRST ROW SHADING

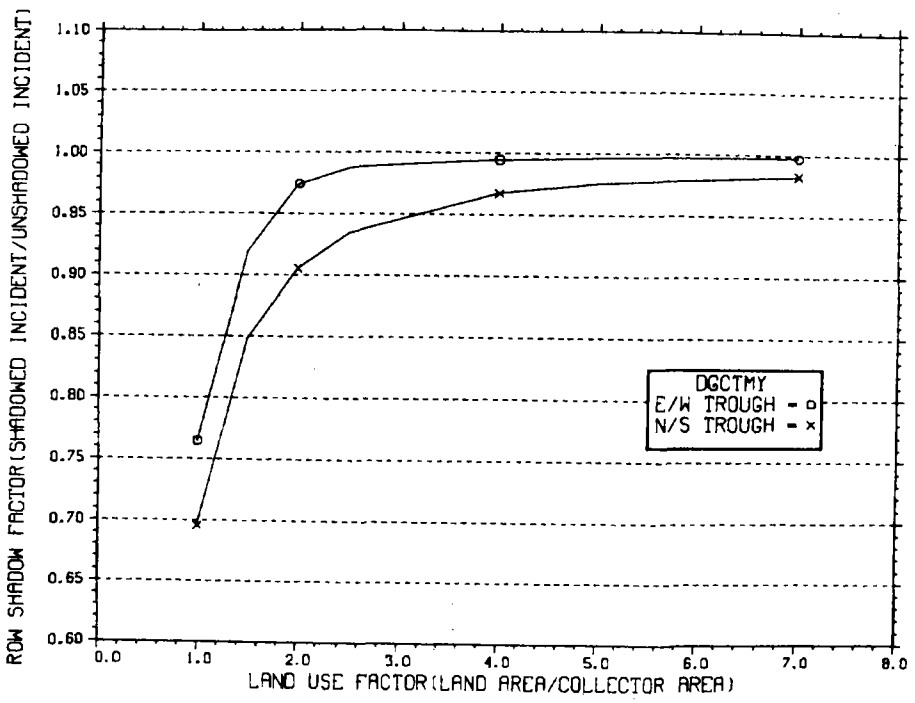

PERFORMANCE VARIATION WITH COLLECTOR AZIMUTH

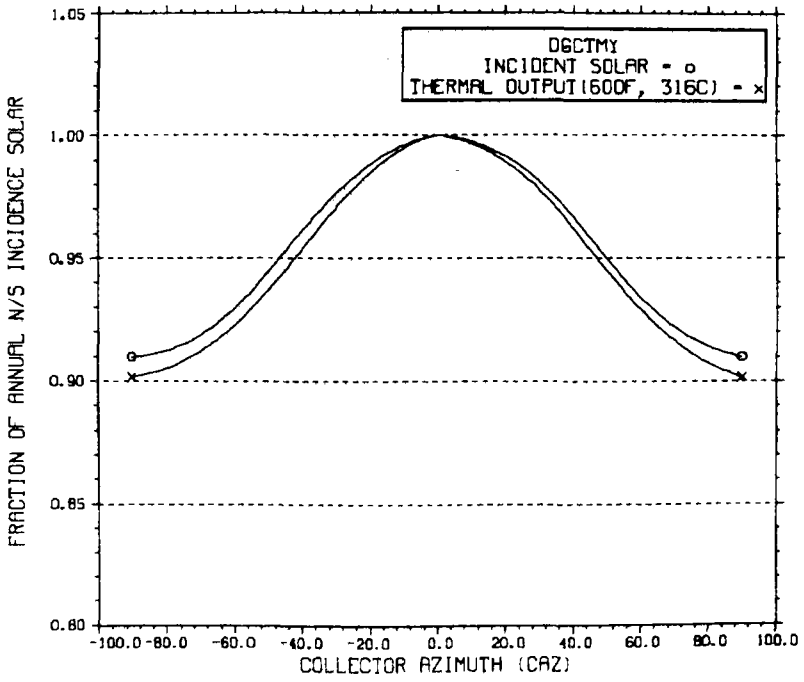

TEMPERATURE DEPENDENCE OF ANNUAL PERFORMANCE

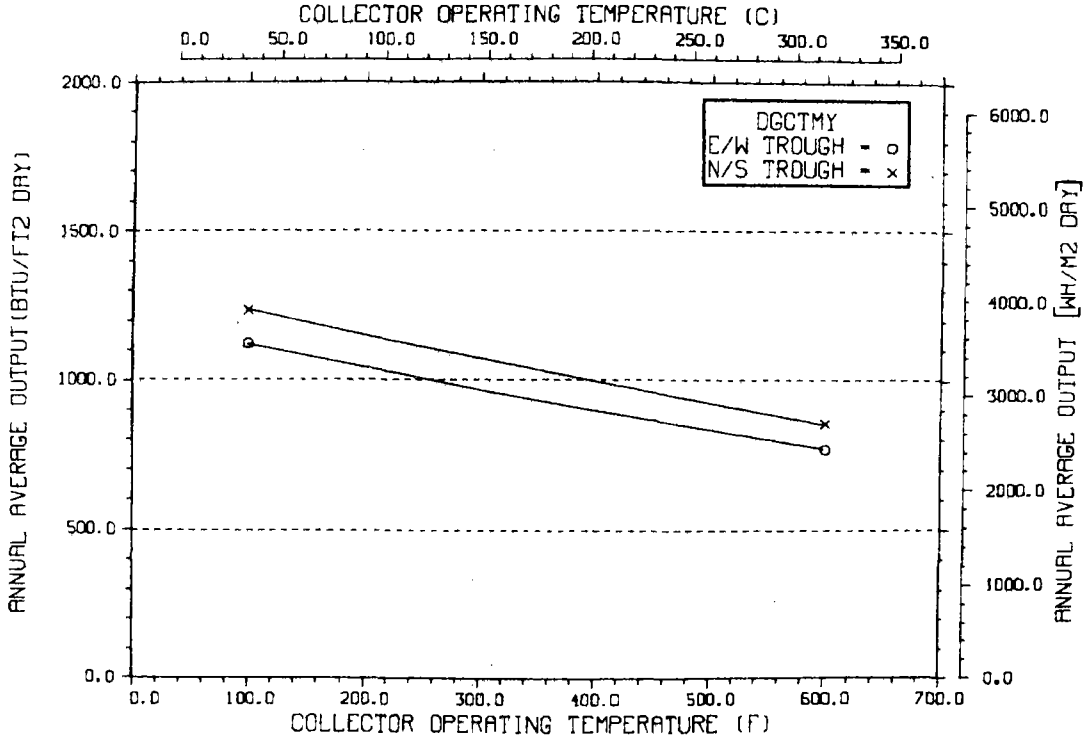

TEMPERATURE DEPENDENCE OF MONTHLY PERFORMANCE

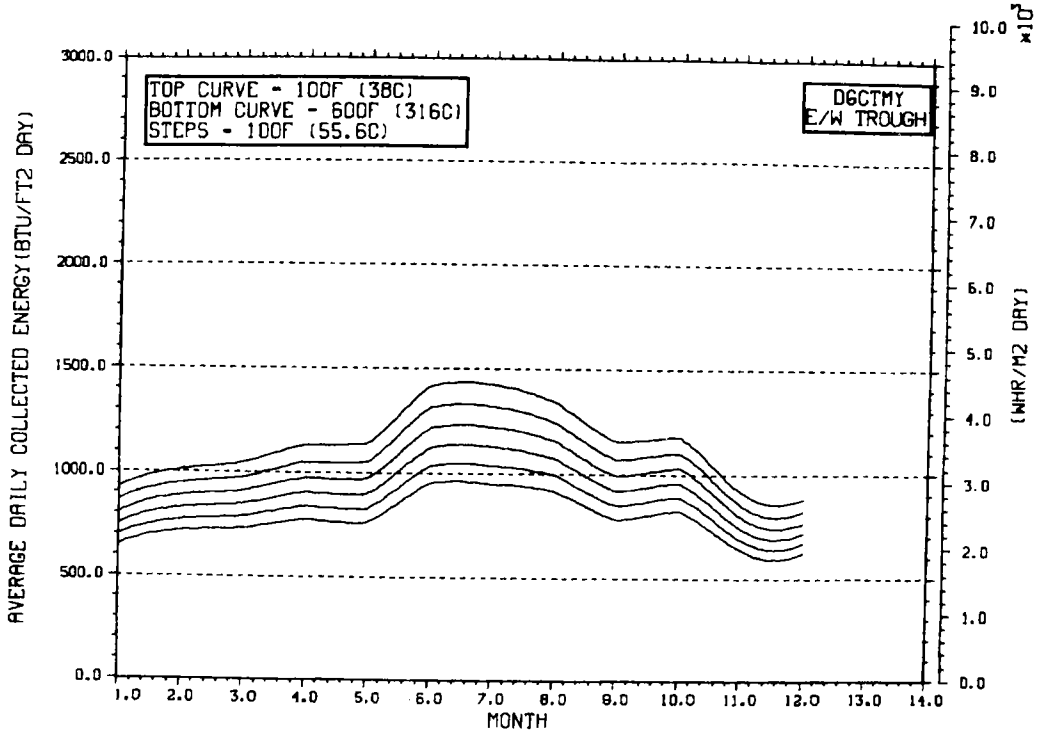

TEMPERATURE DEPENDENCE OF MONTHLY PERFORMANCE

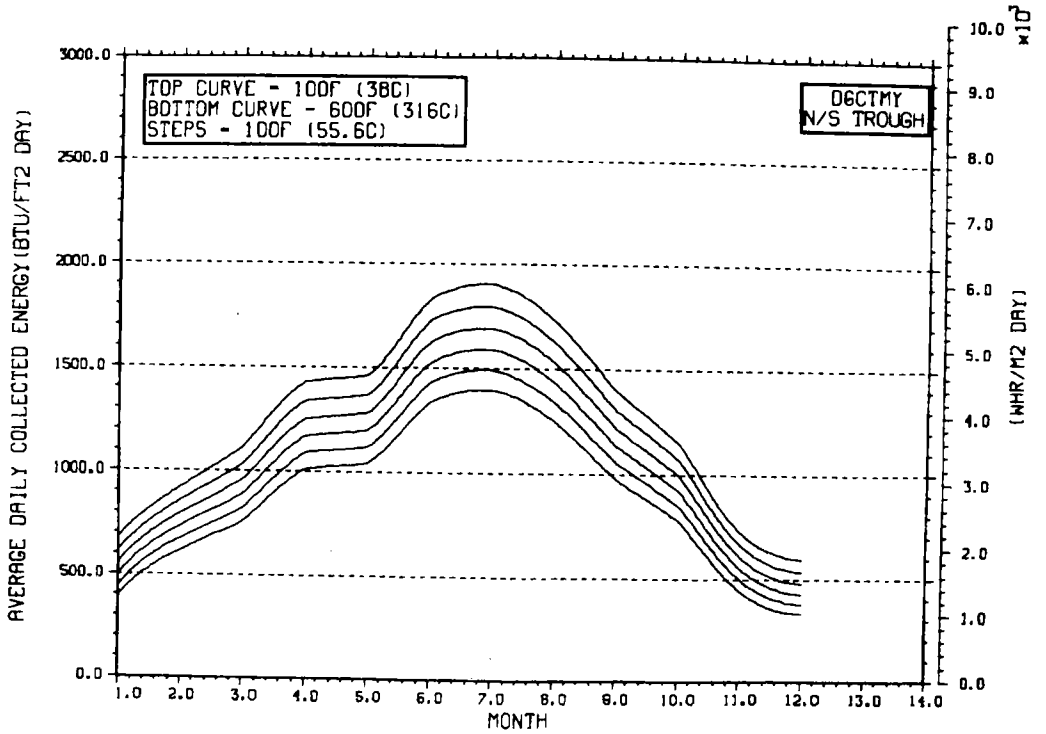

STORAGE SIZING GRAPH FOR CONSTANT ANNUAL DEMAND

NO WEEKEND SHUTDOWN

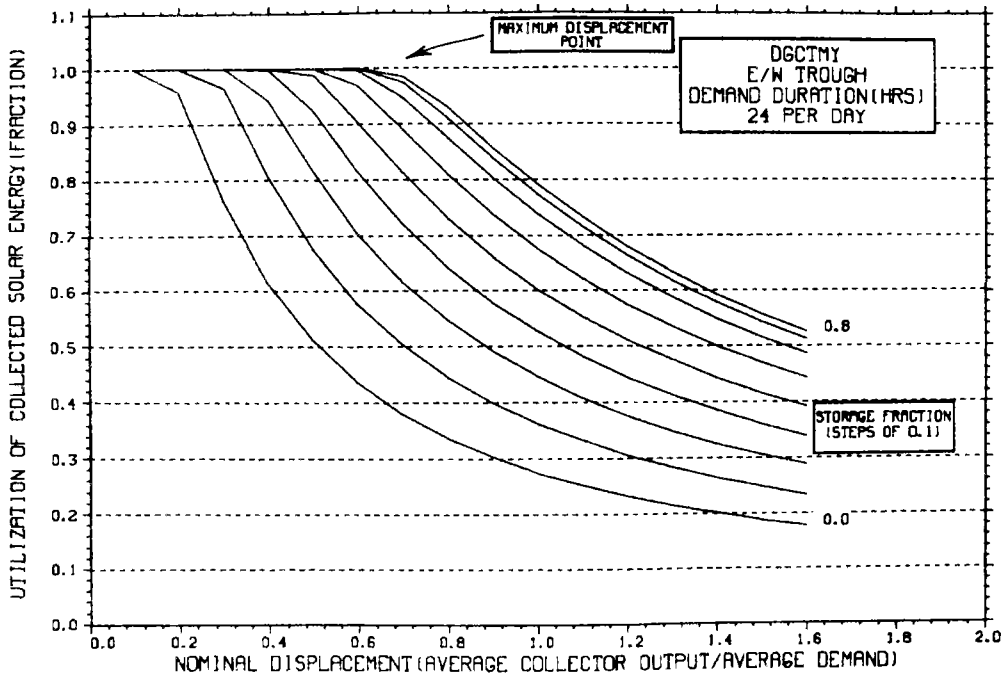

STORAGE SIZING GRAPH FOR CONSTANT ANNUAL DEMAND

NO WEEKEND SHUTDOWN

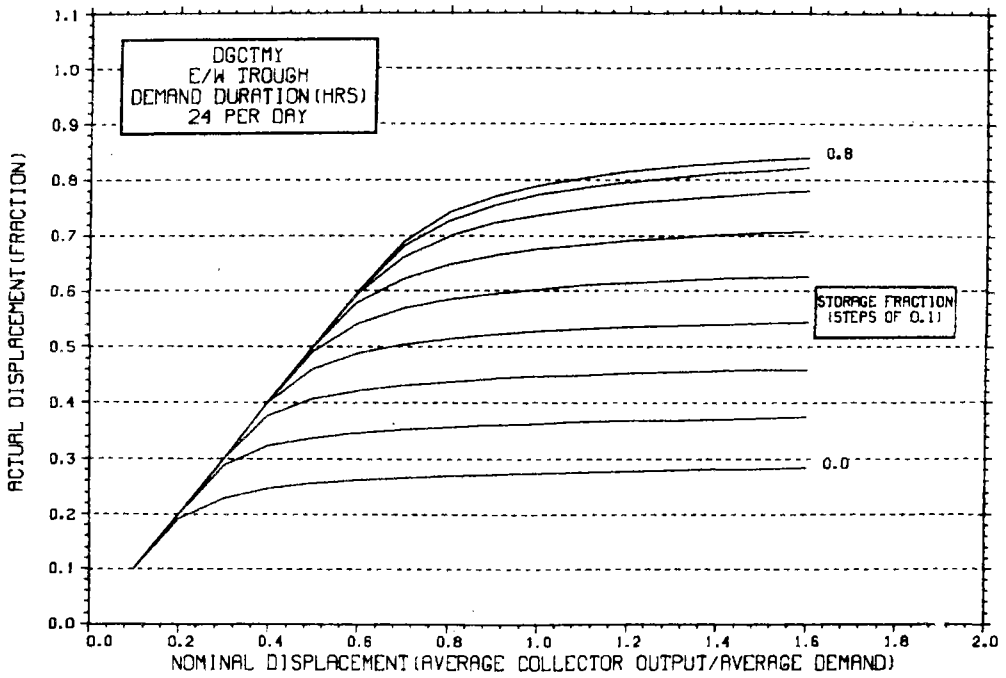

STORAGE SIZING GRAPH FOR CONSTANT ANNUAL DEMAND

NO WEEKEND SHUTDOWN

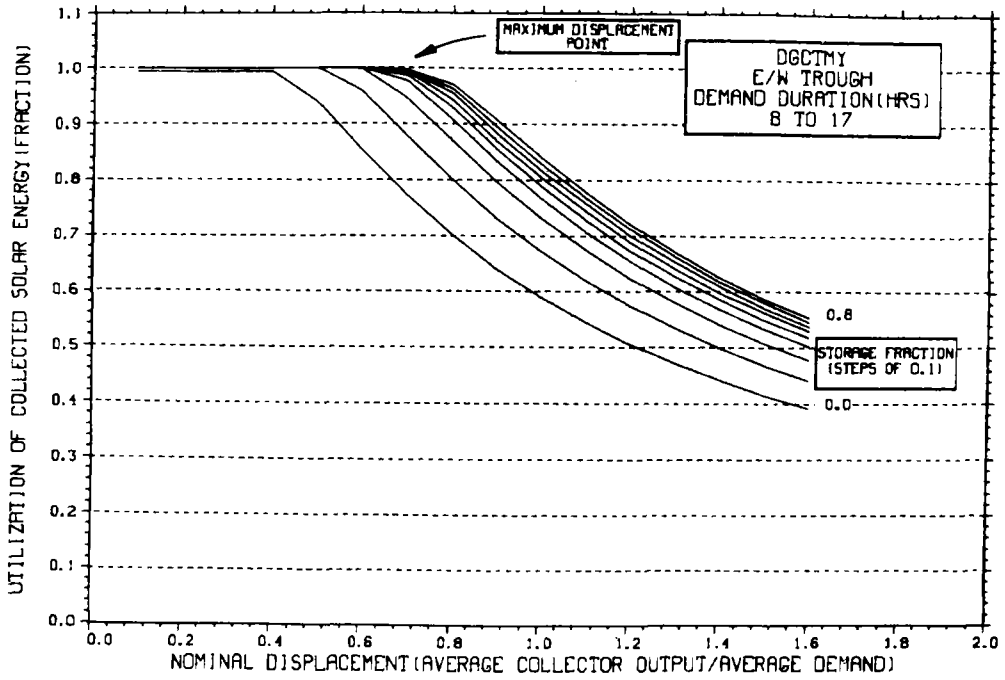

STORAGE SIZING GRAPH FOR CONSTANT ANNUAL DEMAND

NO WEEKEND SHUTDOWN

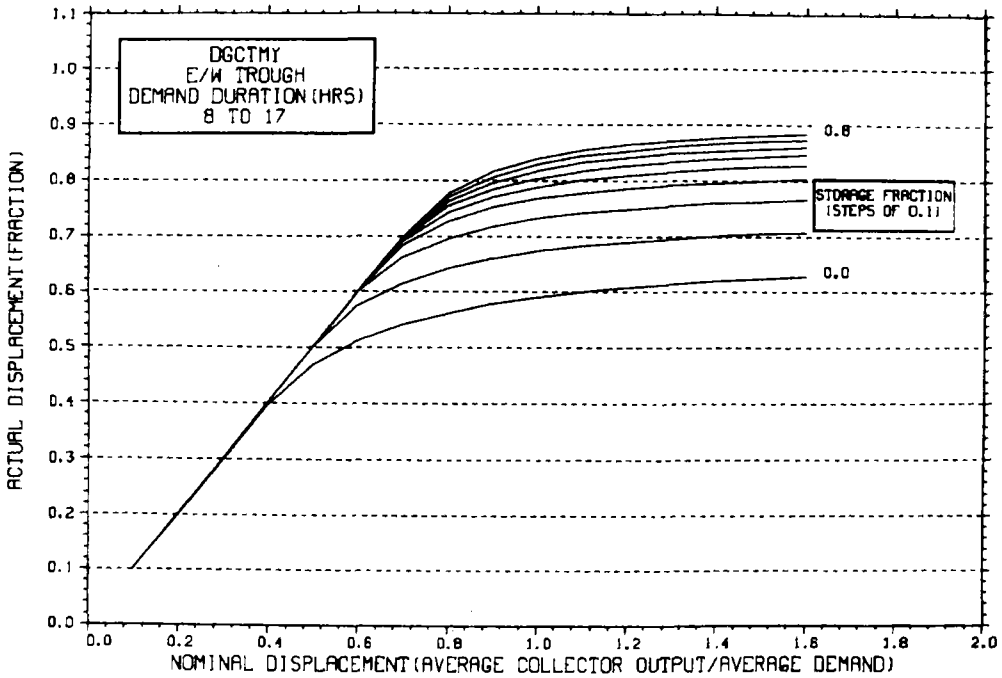

STORAGE SIZING GRAPH FOR CONSTANT ANNUAL DEMAND

NO WEEKEND SHUTDOWN

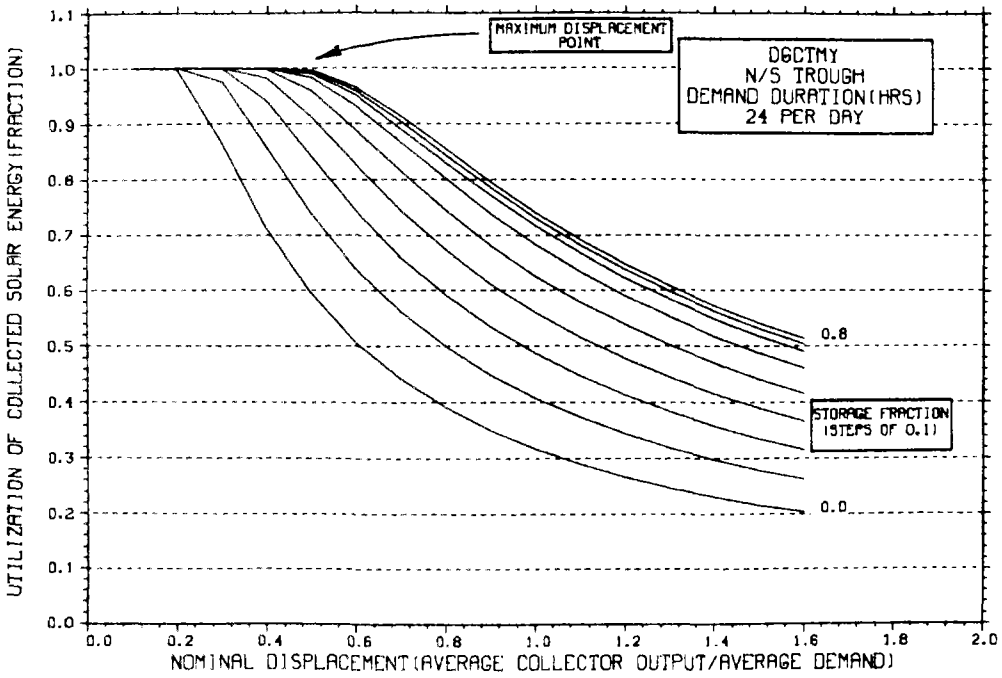

STORAGE SIZING GRAPH FOR CONSTANT ANNUAL DEMAND

NO WEEKEND SHUTDOWN

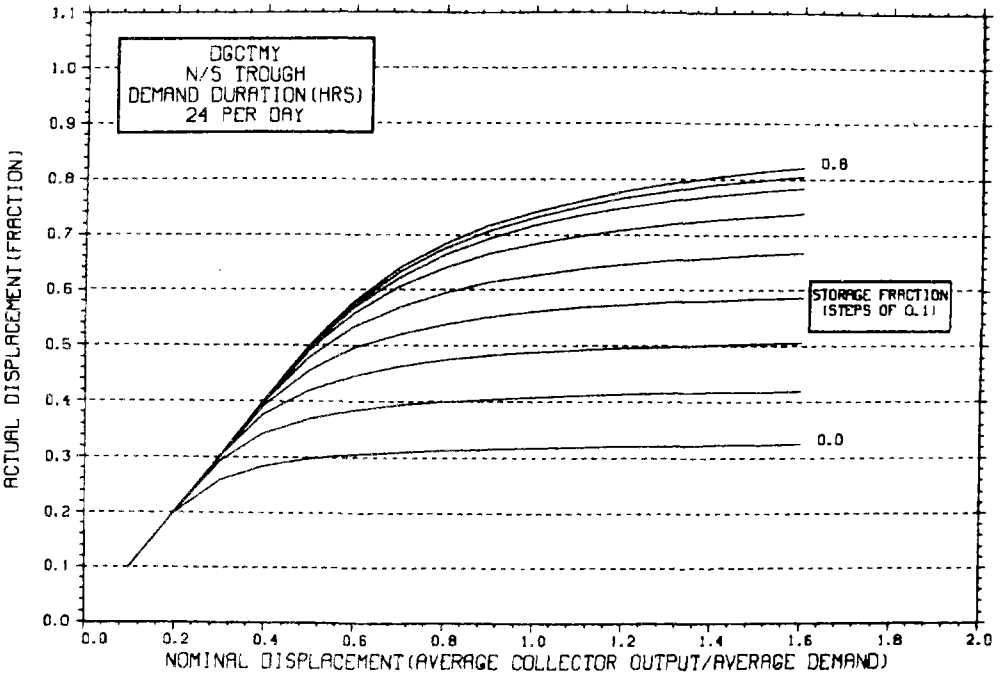

STORAGE SIZING GRAPH FOR CONSTANT ANNUAL DEMAND

NO WEEKEND SHUTDOWN

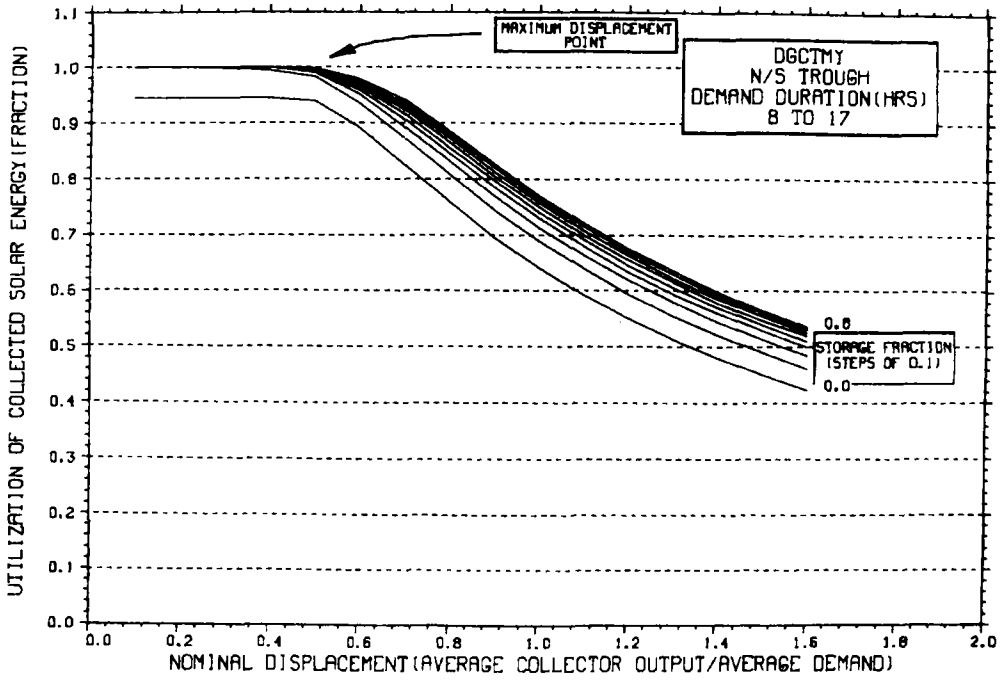

STORAGE SIZING GRAPH FOR CONSTANT ANNUAL DEMAND

NO WEEKEND SHUTDOWN

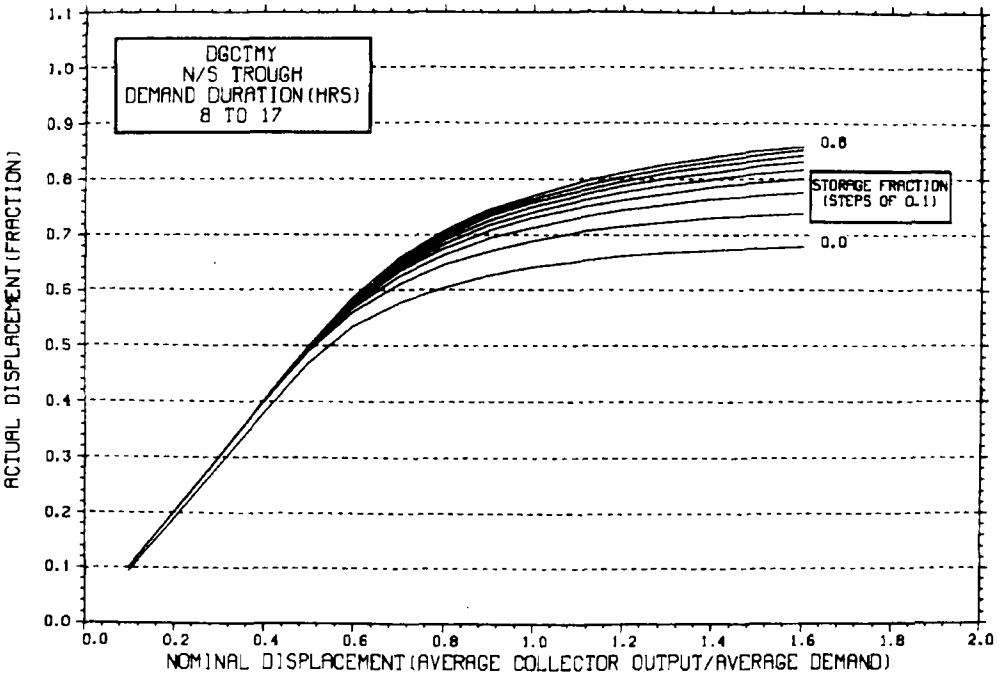

ENERGY INCIDENT ON COLLECTOR APERTURE

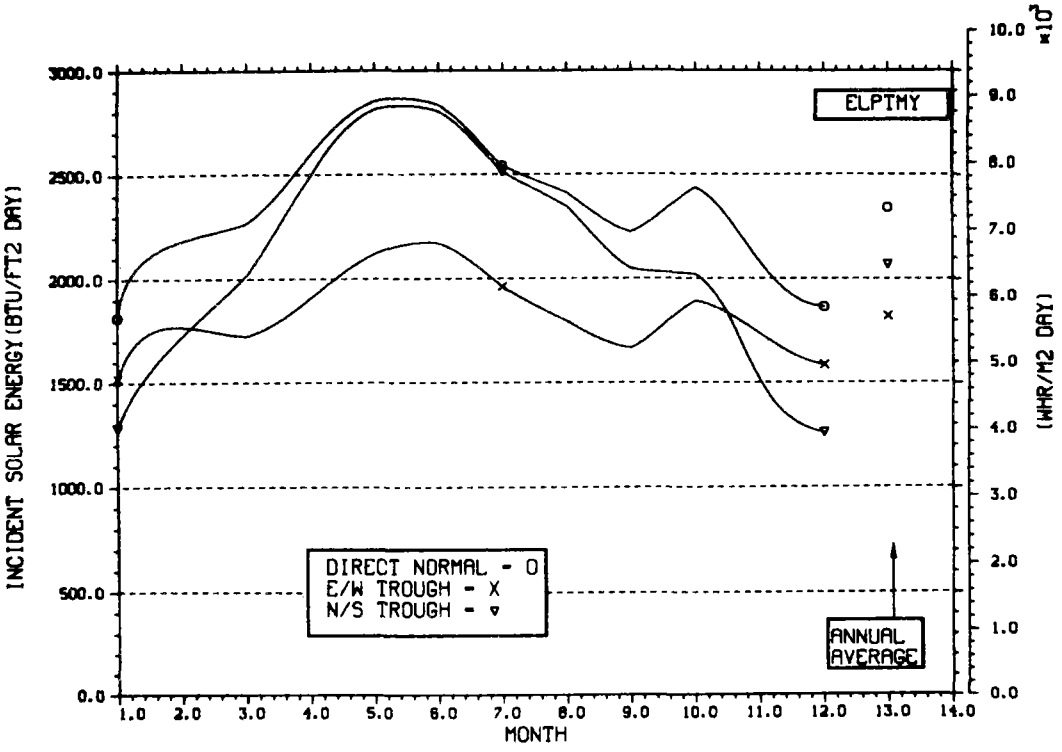

ANNUAL NONFIRST ROW SHADING

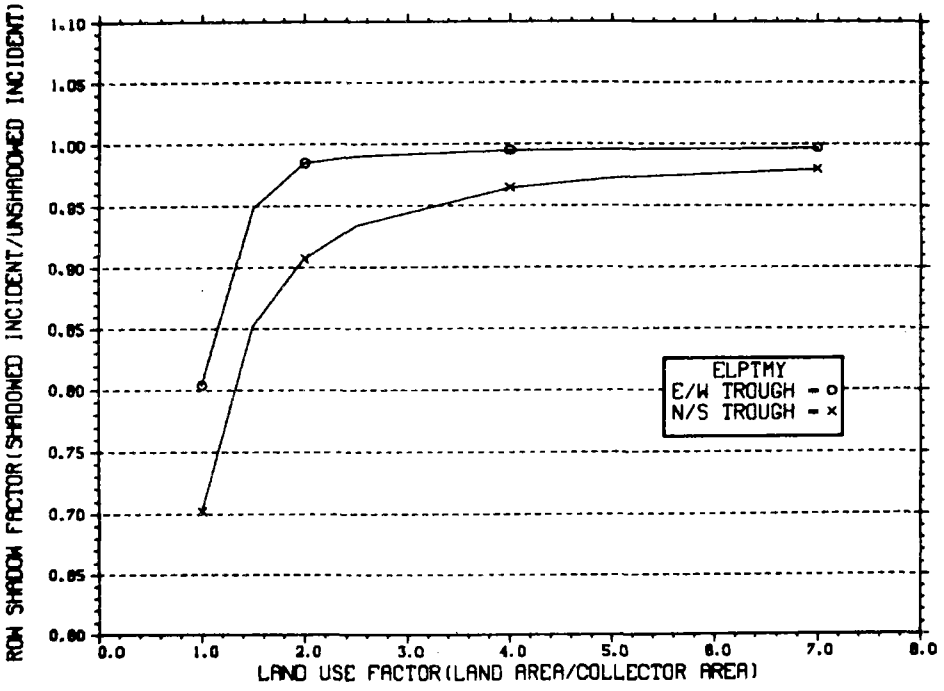

PERFORMANCE VARIATION WITH COLLECTOR AZIMUTH

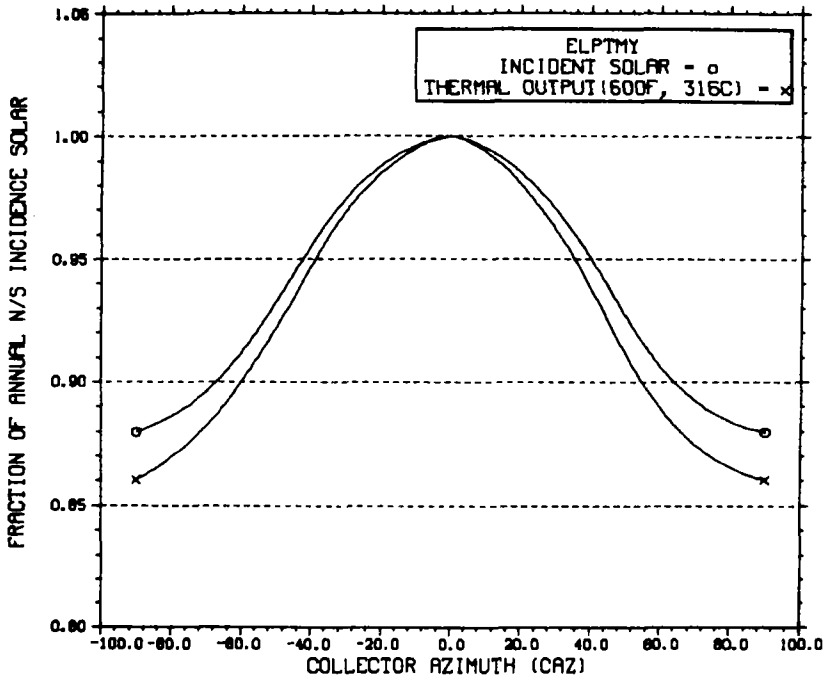

TEMPERATURE DEPENDENCE OF ANNUAL PERFORMANCE

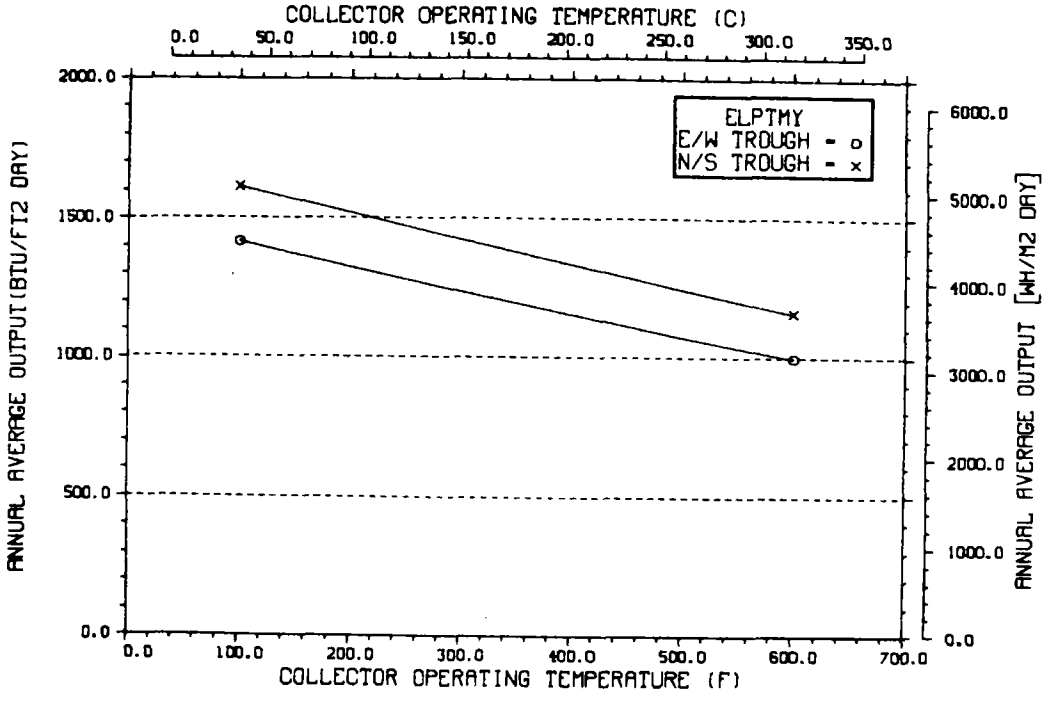

TEMPERATURE DEPENDENCE OF MONTHLY PERFORMANCE

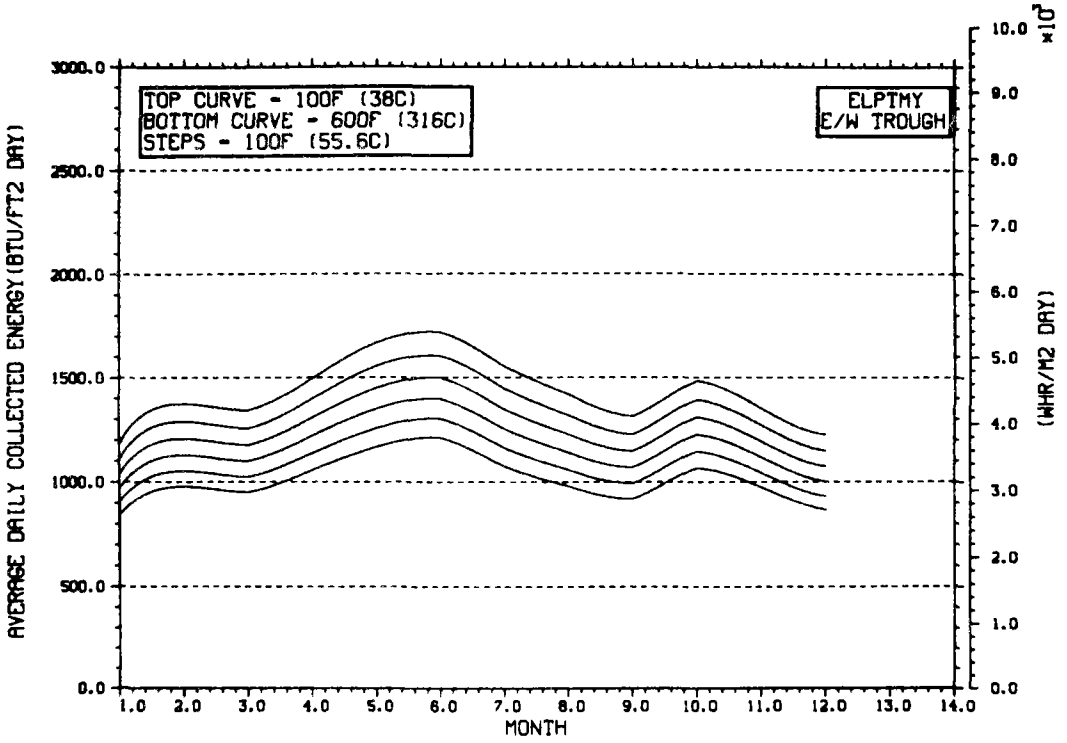

TEMPERATURE DEPENDENCE OF MONTHLY PERFORMANCE

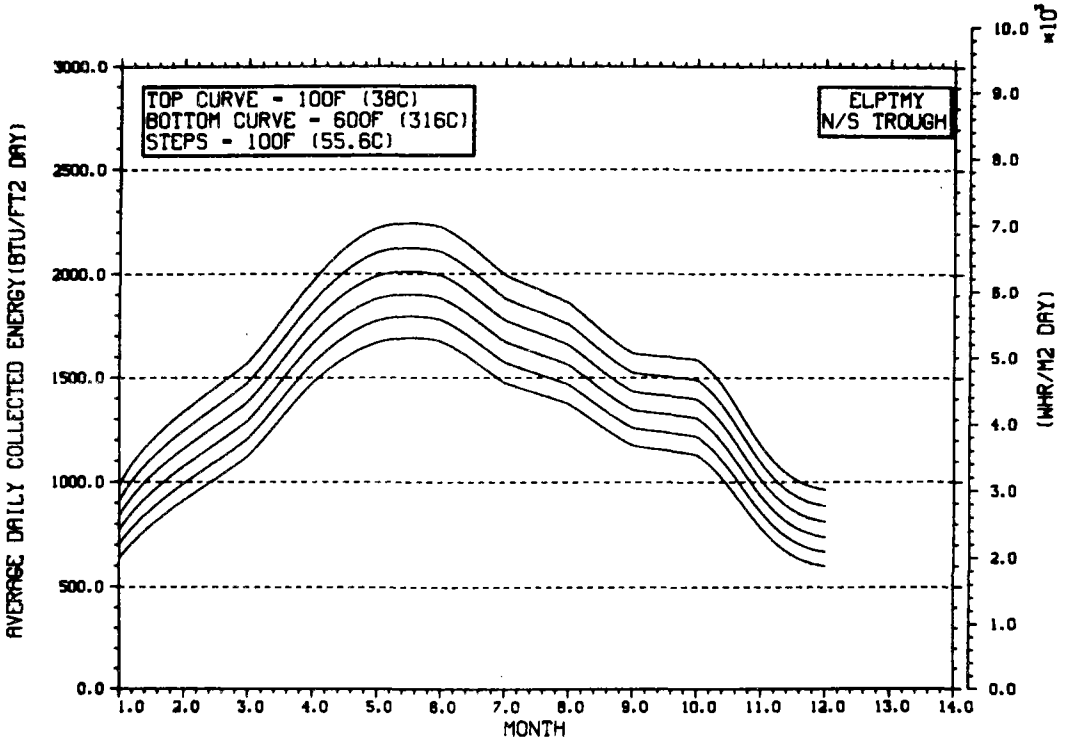

STORAGE SIZING GRAPH FOR CONSTANT ANNUAL DEMAND

NO WEEKEND SHUTDOWN

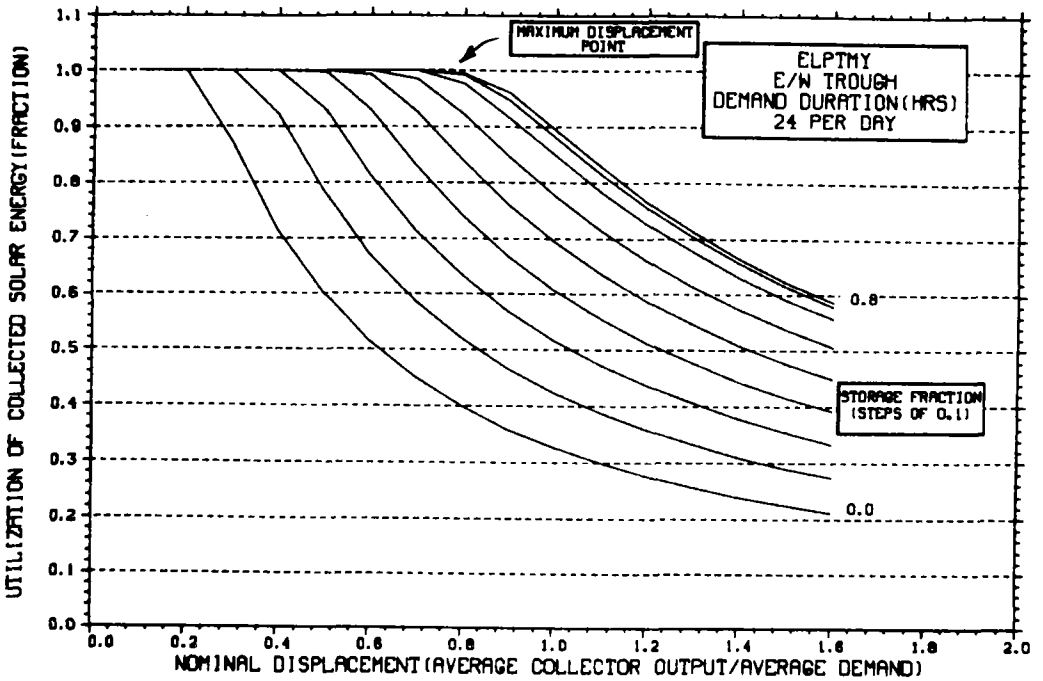

STORAGE SIZING GRAPH FOR CONSTANT ANNUAL DEMAND

NO WEEKEND SHUTDOWN

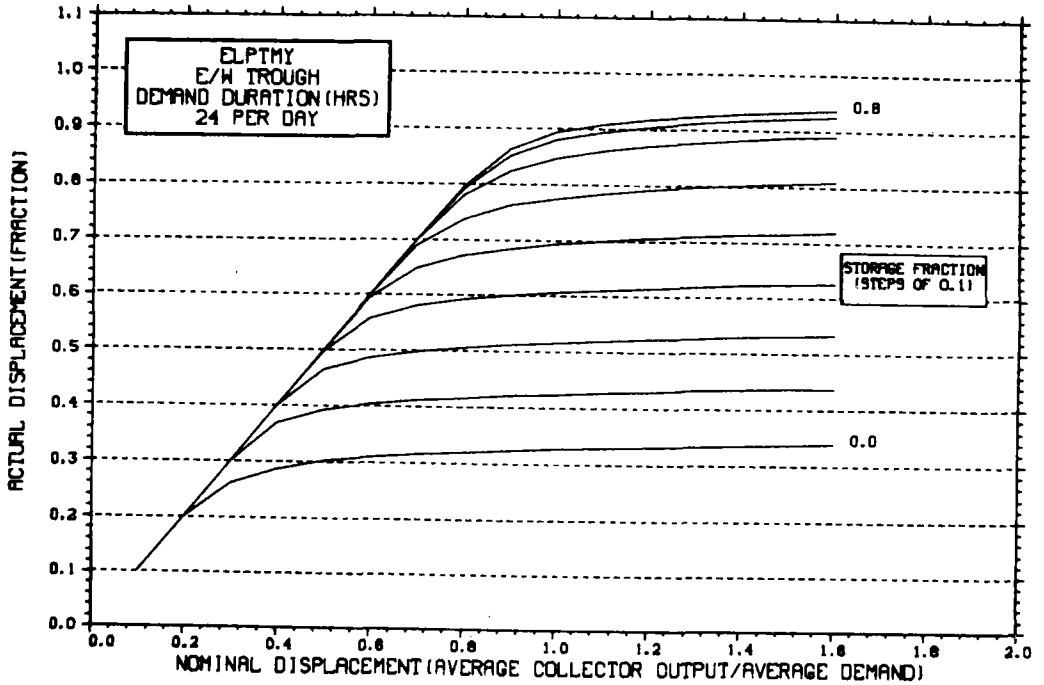

STORAGE SIZING GRAPH FOR CONSTANT ANNUAL DEMAND

NO WEEKEND SHUTDOWN

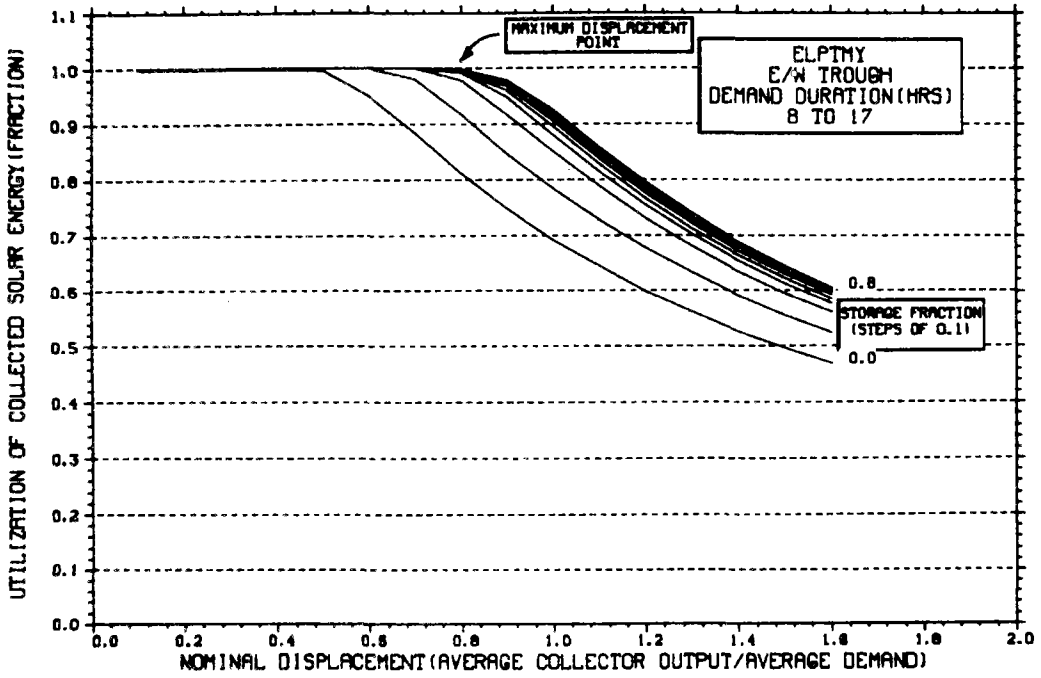

STORAGE SIZING GRAPH FOR CONSTANT ANNUAL DEMAND

NO WEEKEND SHUTDOWN

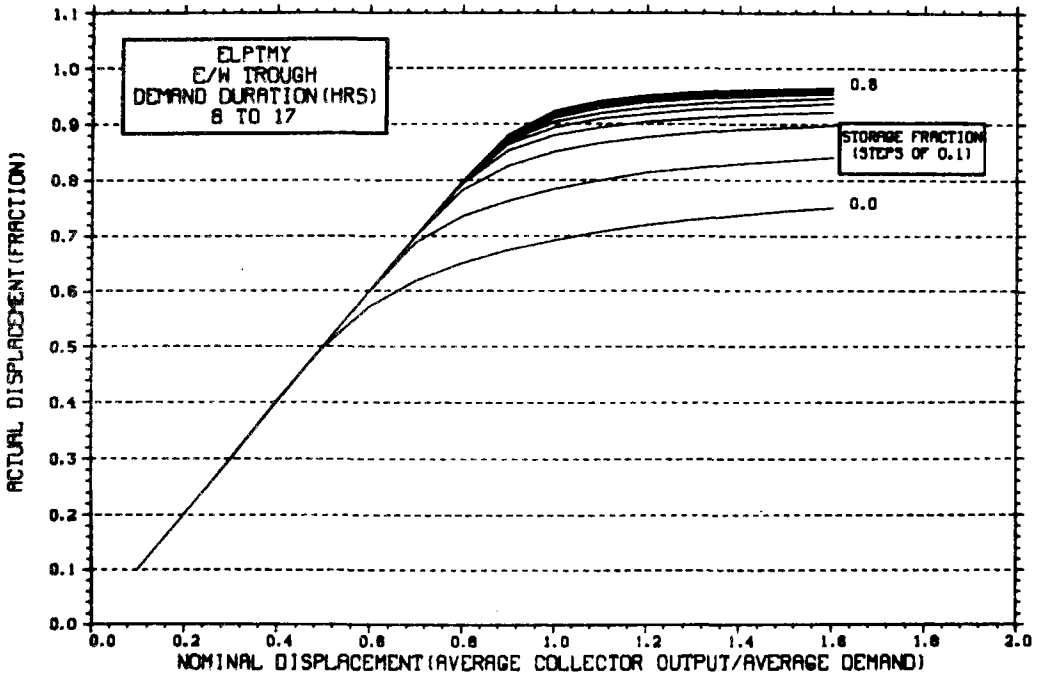

STORAGE SIZING GRAPH FOR CONSTANT ANNUAL DEMAND

NO WEEKEND SHUTDOWN

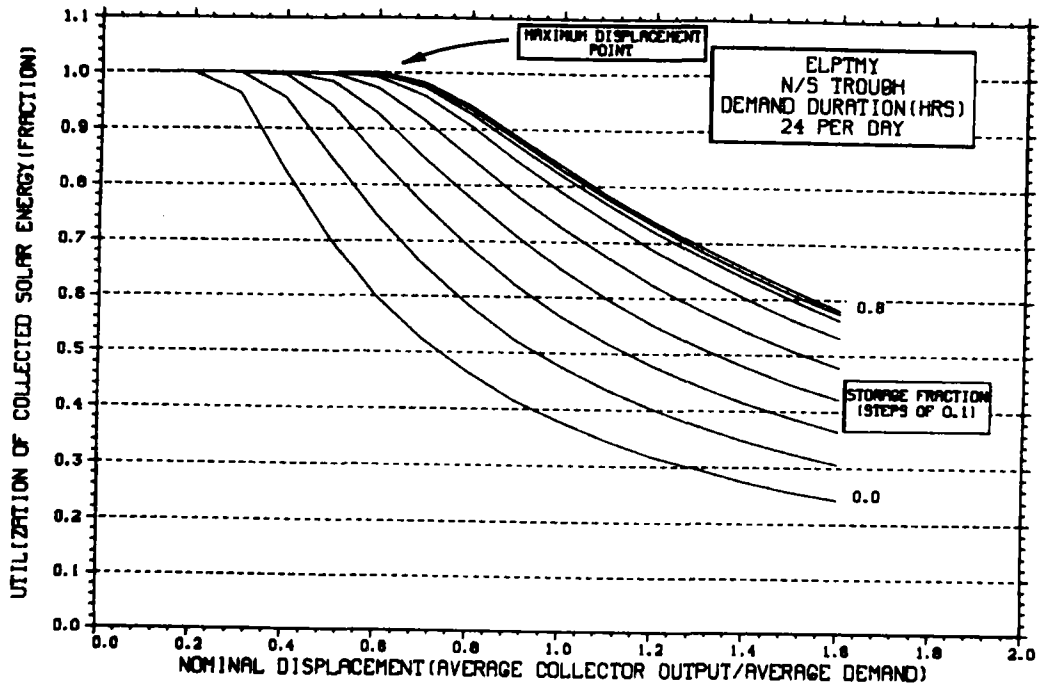

STORAGE SIZING GRAPH FOR CONSTANT ANNUAL DEMAND

NO WEEKEND SHUTDOWN

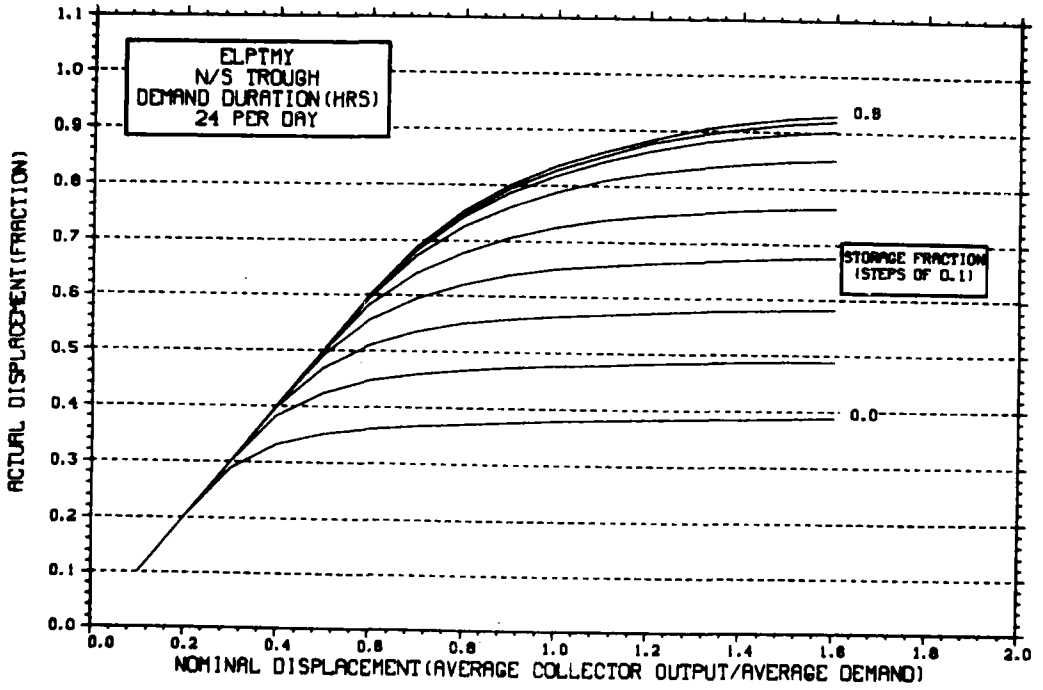

STORAGE SIZING GRAPH FOR CONSTANT ANNUAL DEMAND

NO WEEKEND SHUTDOWN

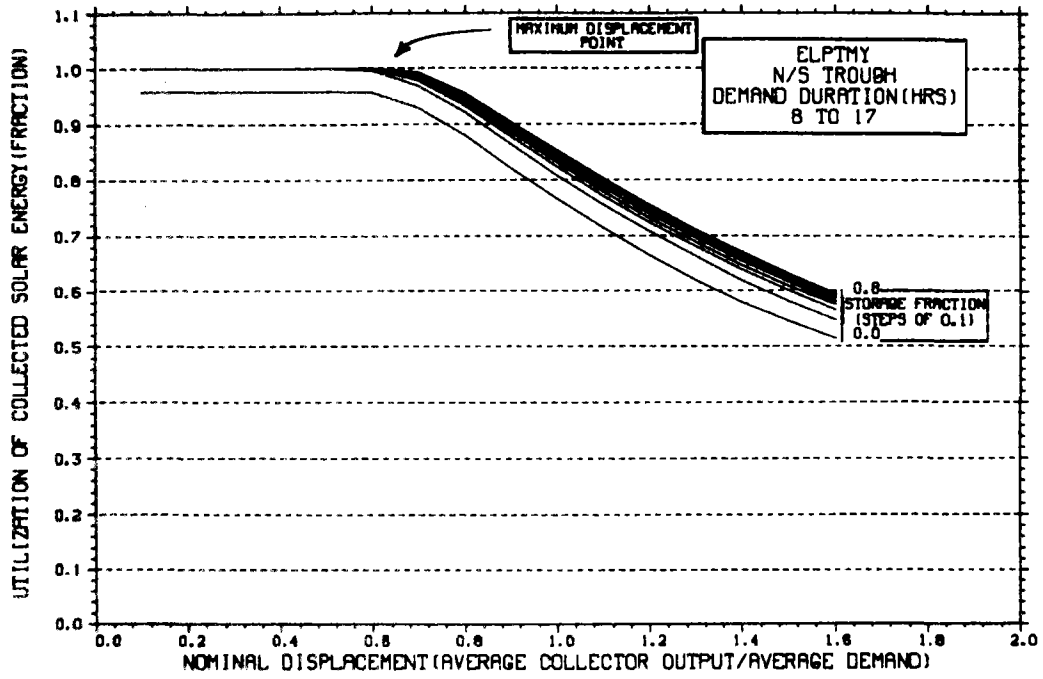

STORAGE SIZING GRAPH FOR CONSTANT ANNUAL DEMAND

NO WEEKEND SHUTDOWN

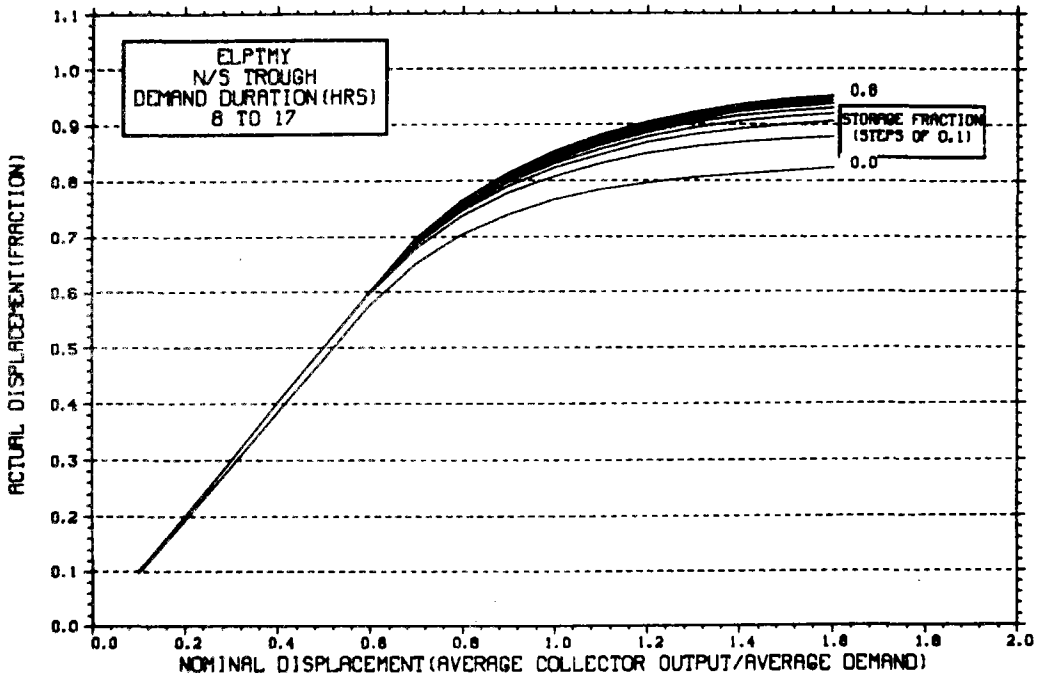

ENERGY INCIDENT ON COLLECTOR APERTURE

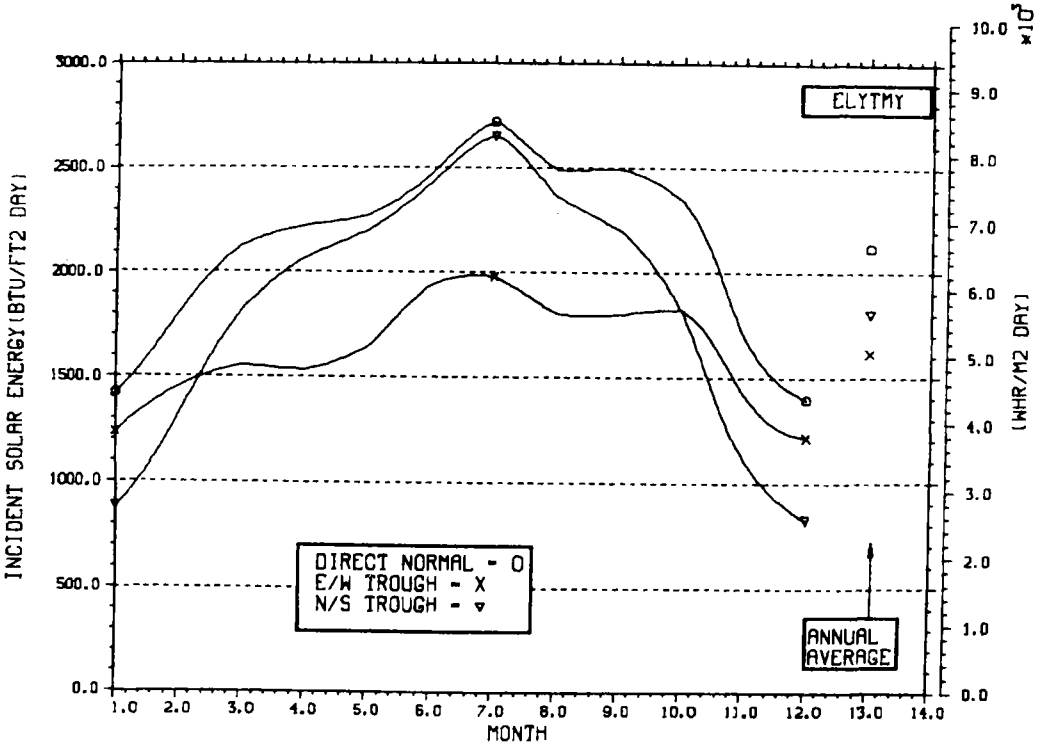

ANNUAL NONFIRST ROW SHADING

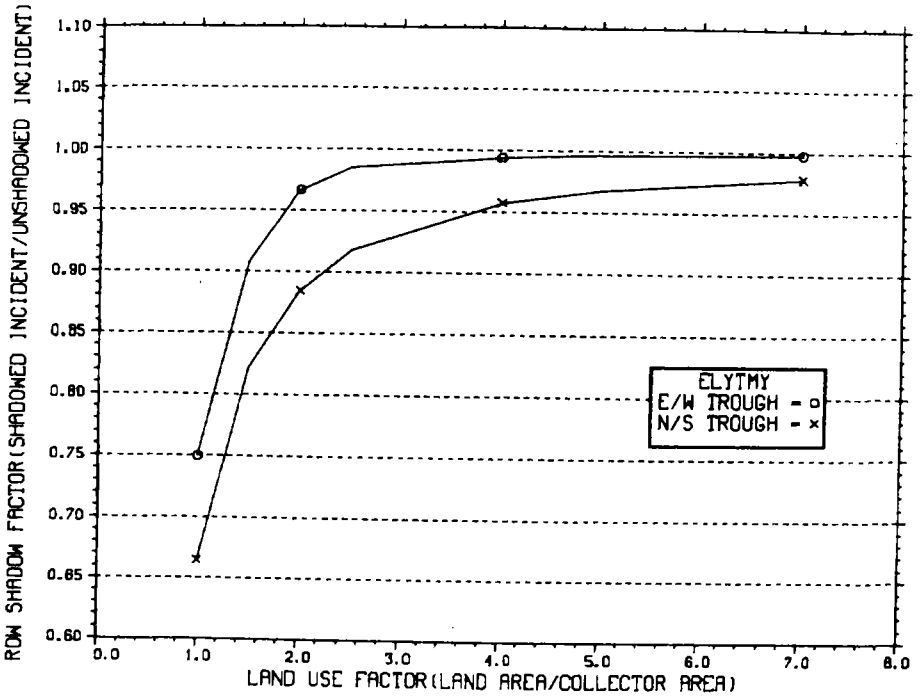

PERFORMANCE VARIATION WITH COLLECTOR AZIMUTH

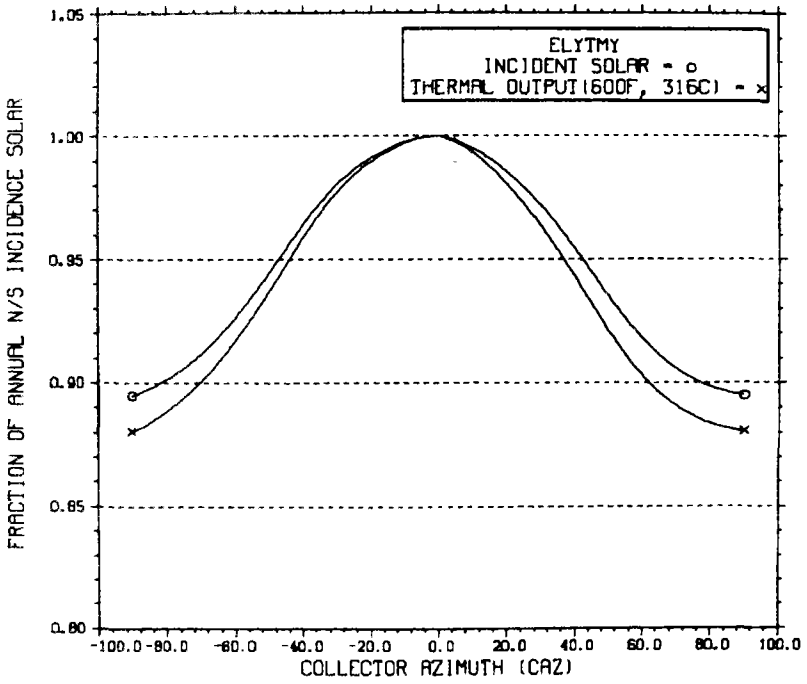

TEMPERATURE DEPENDENCE OF ANNUAL PERFORMANCE

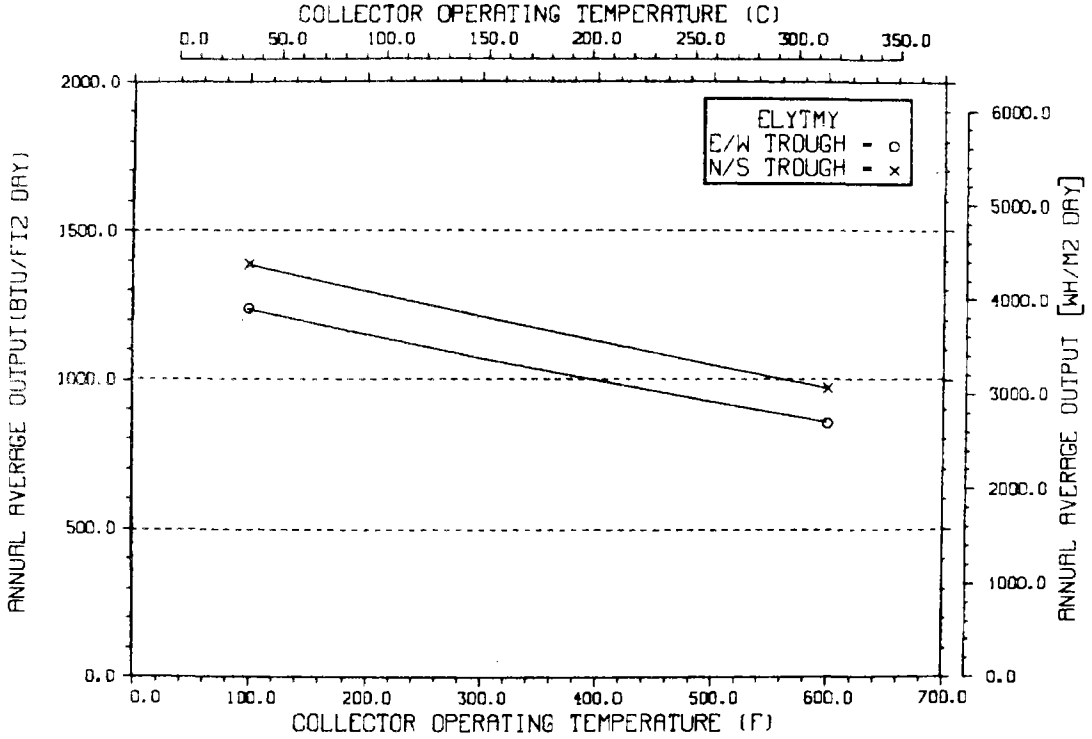

TEMPERATURE DEPENDENCE OF MONTHLY PERFORMANCE

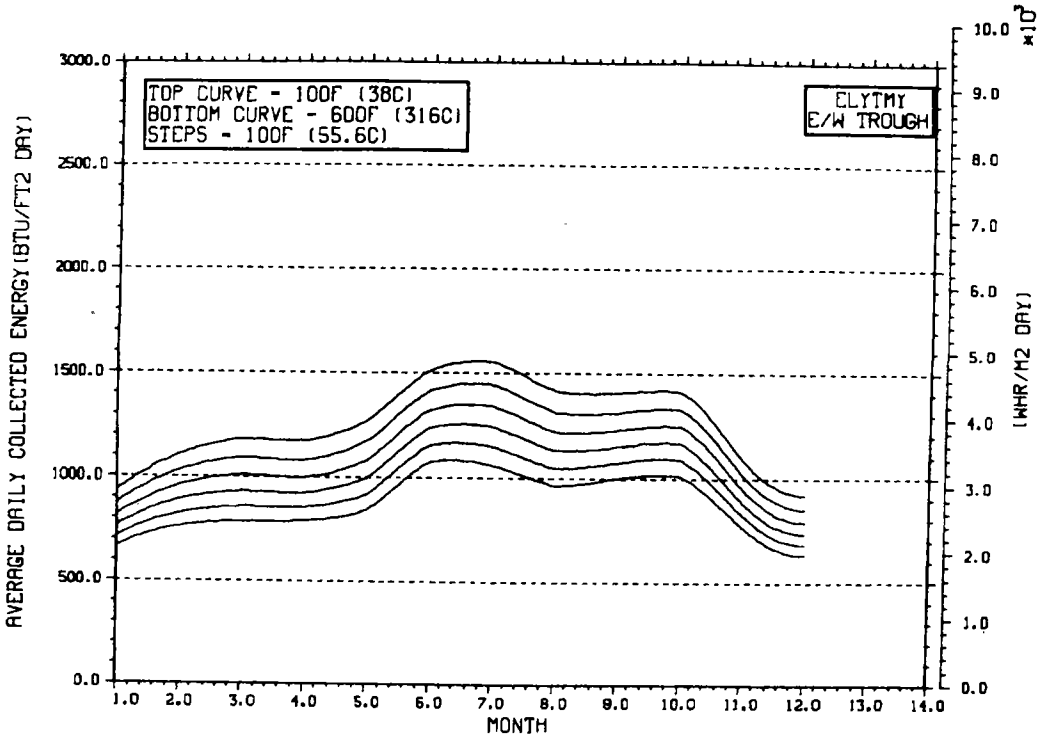

TEMPERATURE DEPENDENCE OF MONTHLY PERFORMANCE

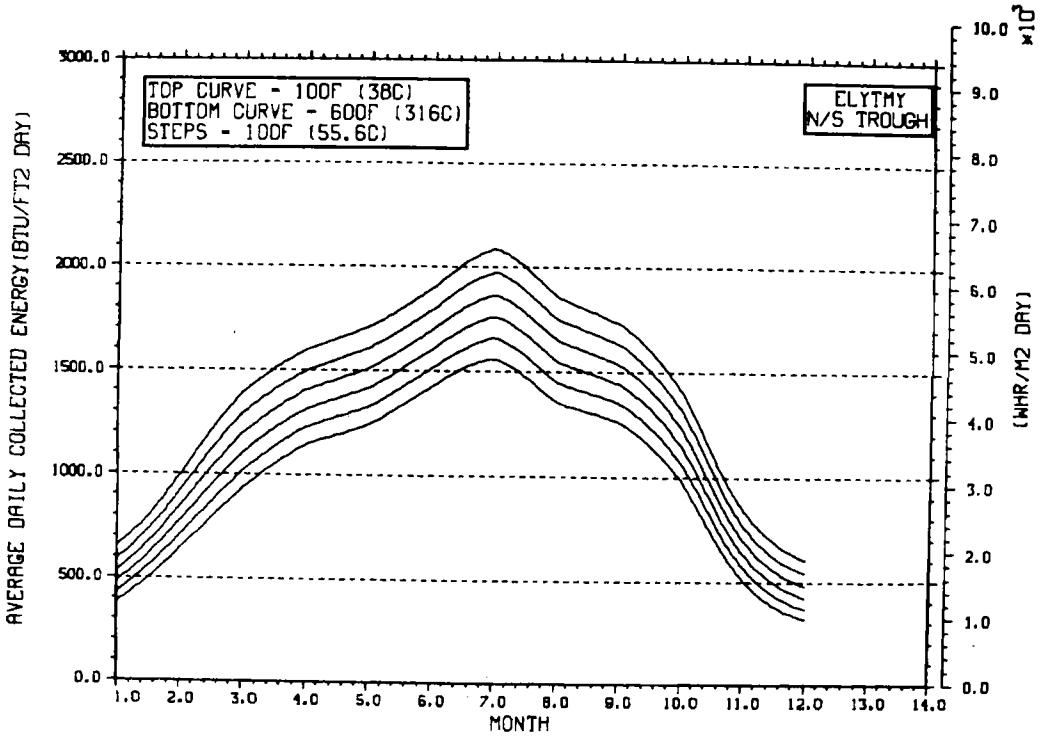

STORAGE SIZING GRAPH FOR CONSTANT ANNUAL DEMAND

NO WEEKEND SHUTDOWN

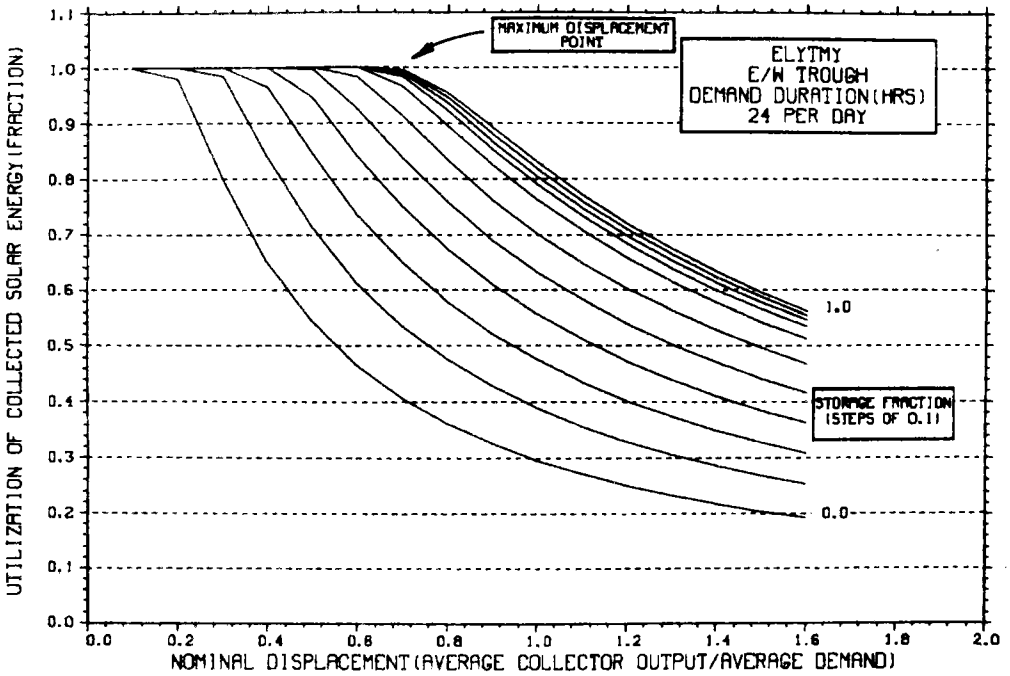

STORAGE SIZING GRAPH FOR CONSTANT ANNUAL DEMAND

NO WEEKEND SHUTDOWN

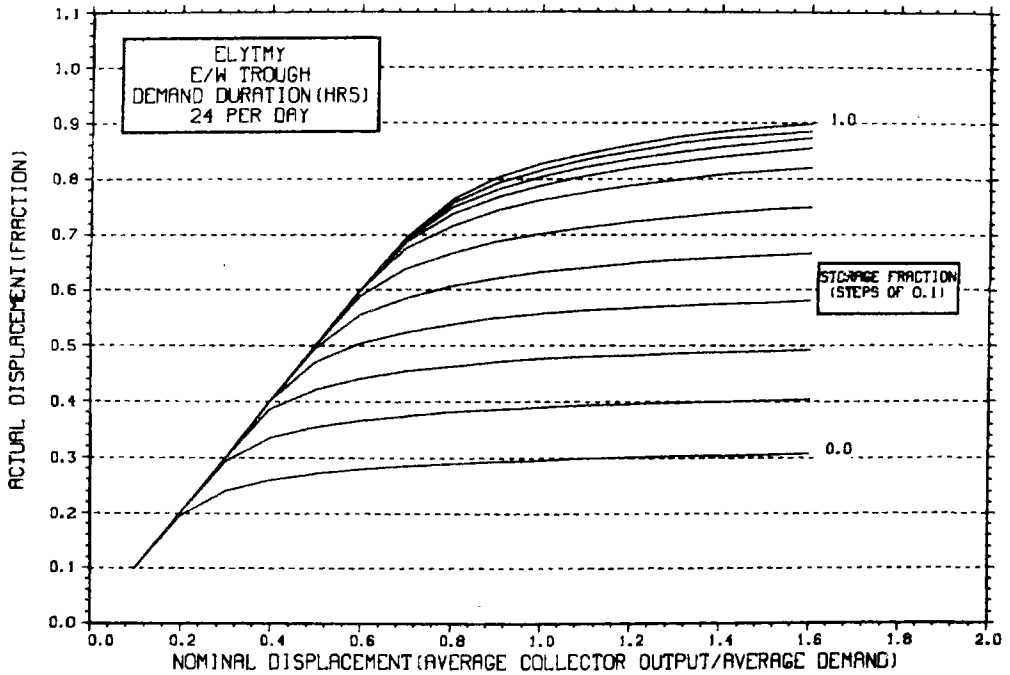

STORAGE SIZING GRAPH FOR CONSTANT ANNUAL DEMAND

NO WEEKEND SHUTDOWN

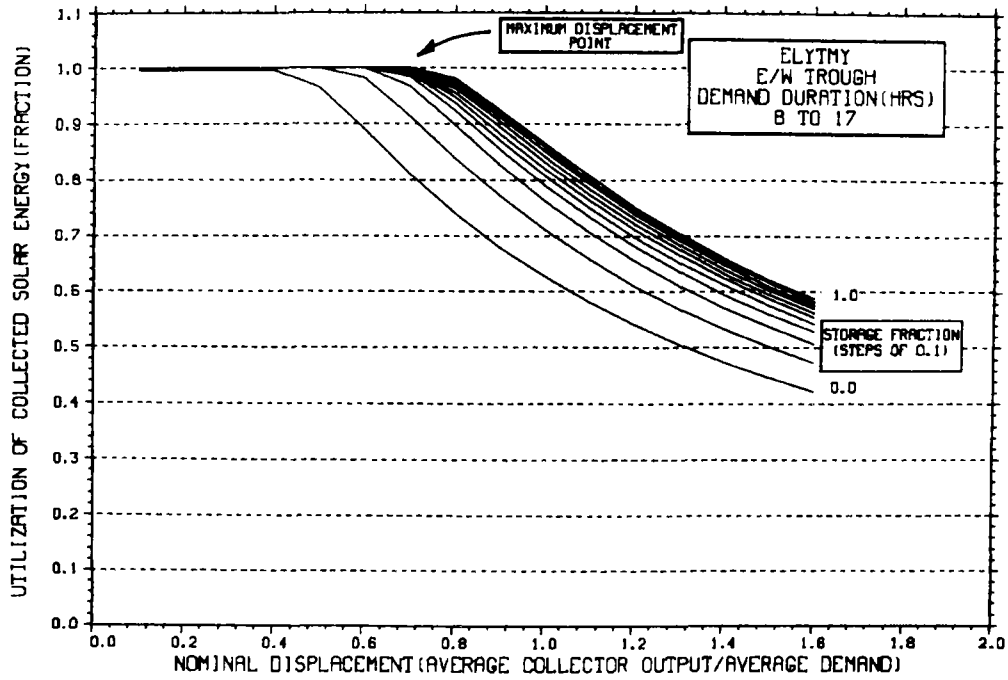

STORAGE SIZING GRAPH FOR CONSTANT ANNUAL DEMAND

NO WEEKEND SHUTDOWN

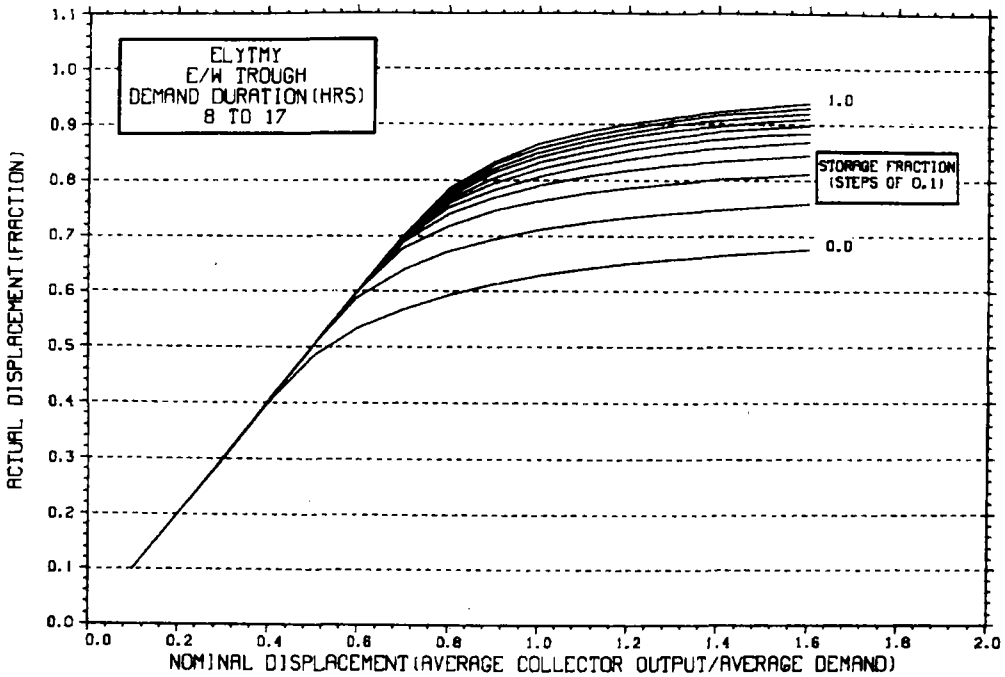

STORAGE SIZING GRAPH FOR CONSTANT ANNUAL DEMAND

NO WEEKEND SHUTDOWN

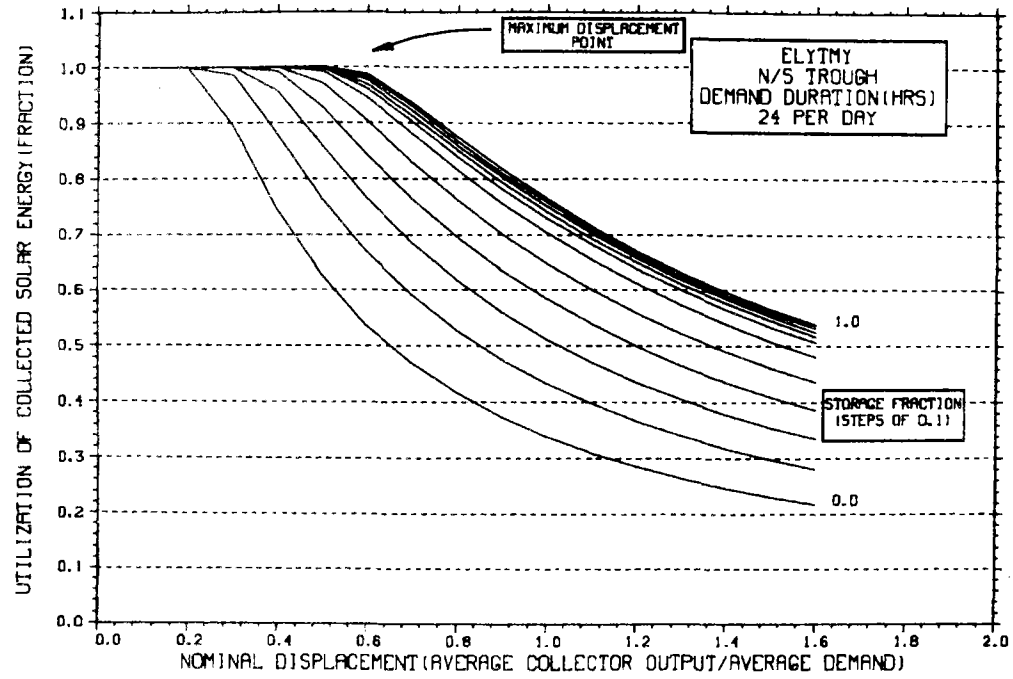

STORAGE SIZING GRAPH FOR CONSTANT ANNUAL DEMAND

NO WEEKEND SHUTDOWN

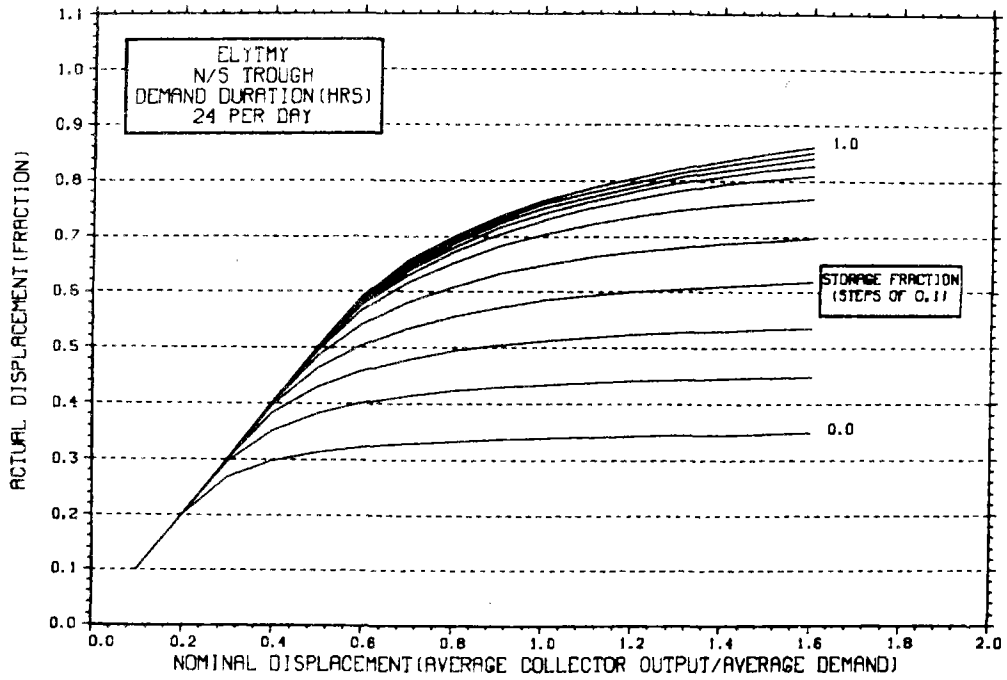

STORAGE SIZING GRAPH FOR CONSTANT ANNUAL DEMAND

NO WEEKEND SHUTDOWN

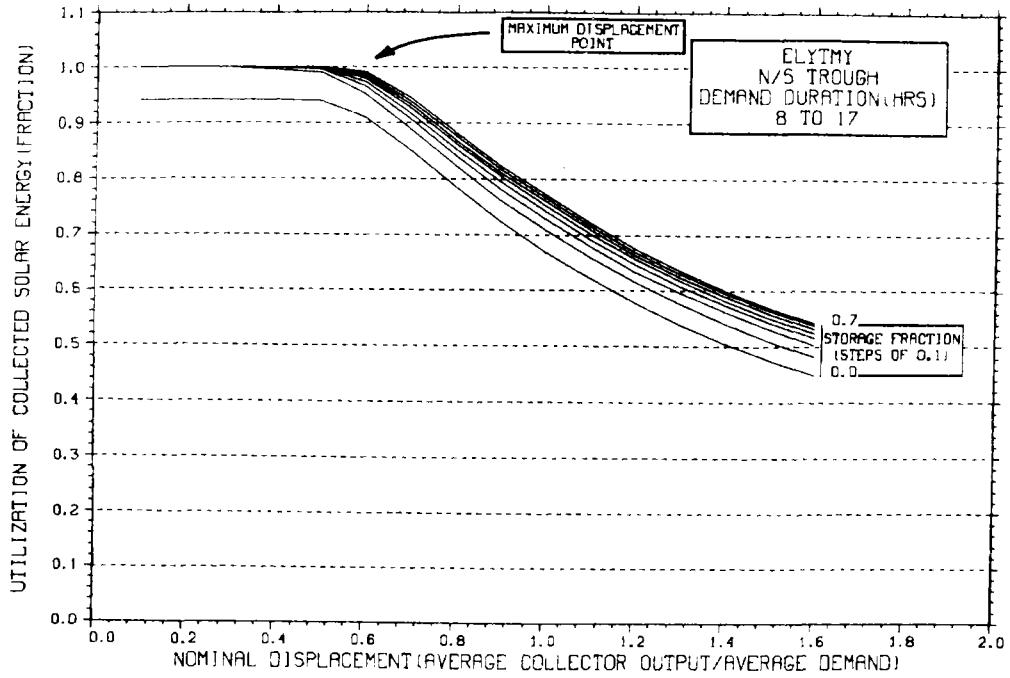

STORAGE SIZING GRAPH FOR CONSTANT ANNUAL DEMAND

NO WEEKEND SHUTDOWN

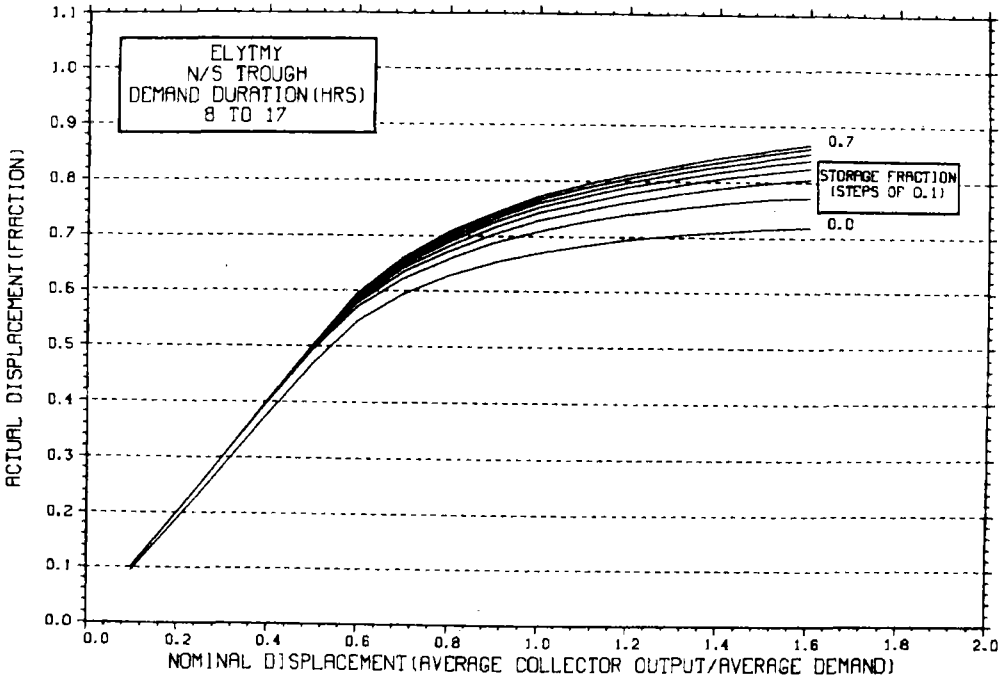

ENERGY INCIDENT ON COLLECTOR APERTURE

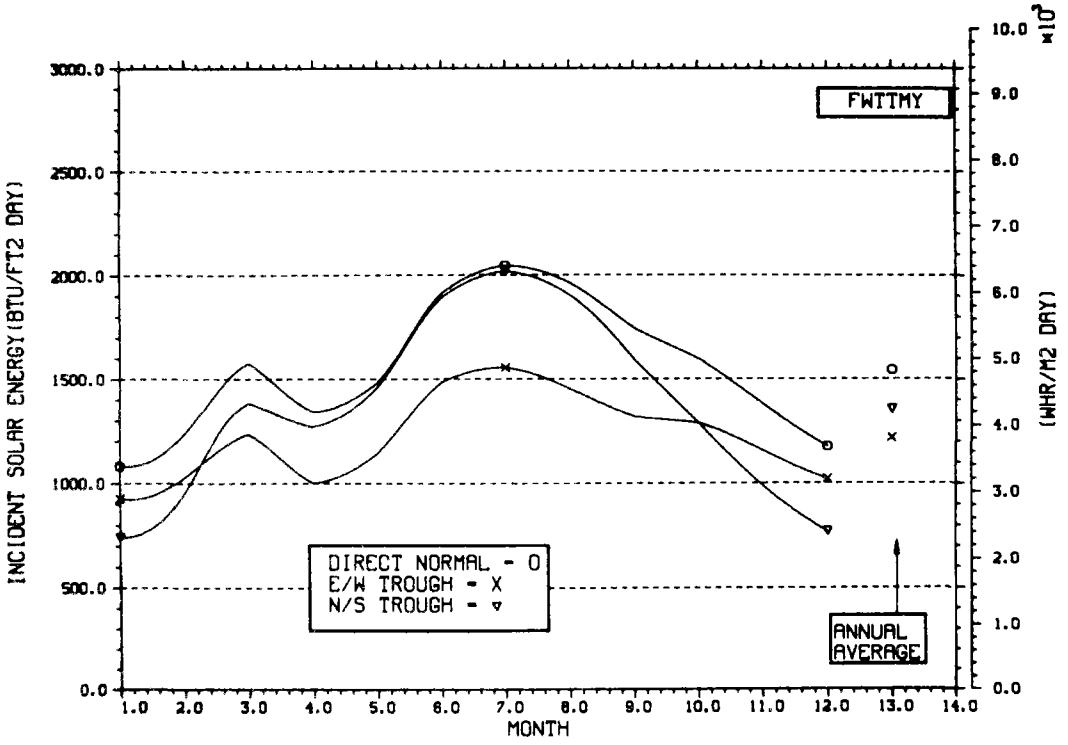

ANNUAL NONFIRST ROW SHADING

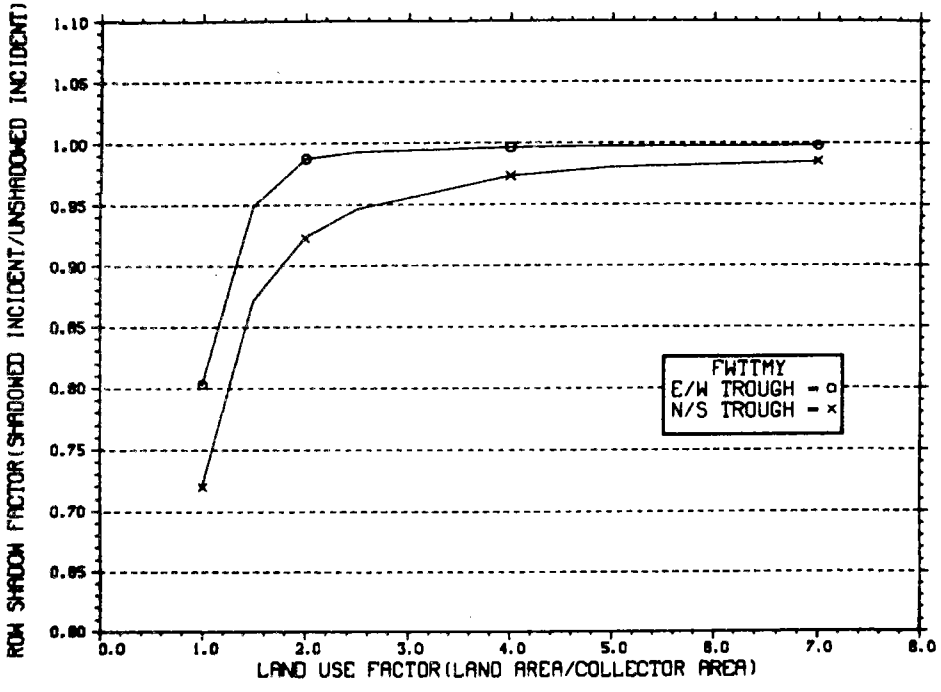

PERFORMANCE VARIATION WITH COLLECTOR AZIMUTH

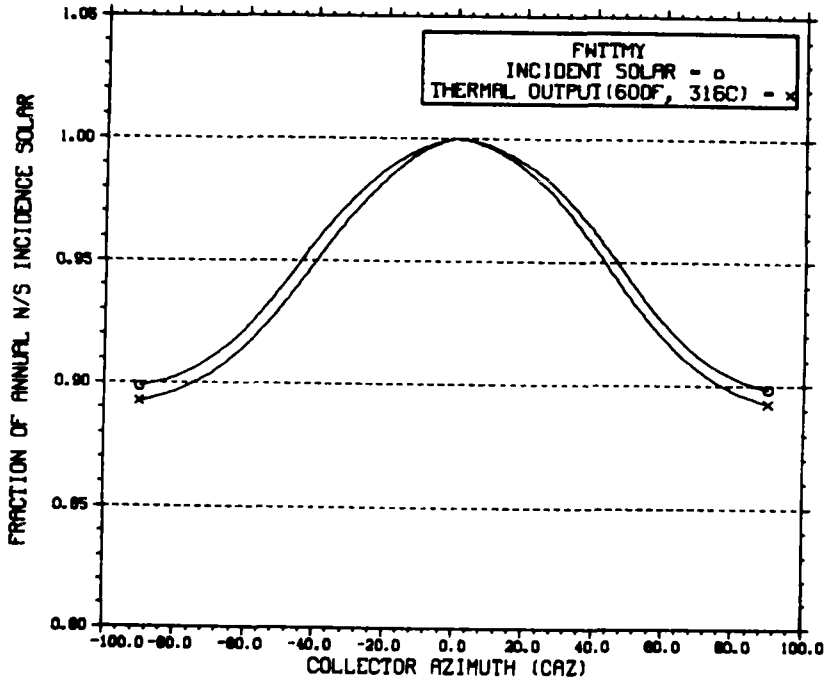

TEMPERATURE DEPENDENCE OF ANNUAL PERFORMANCE

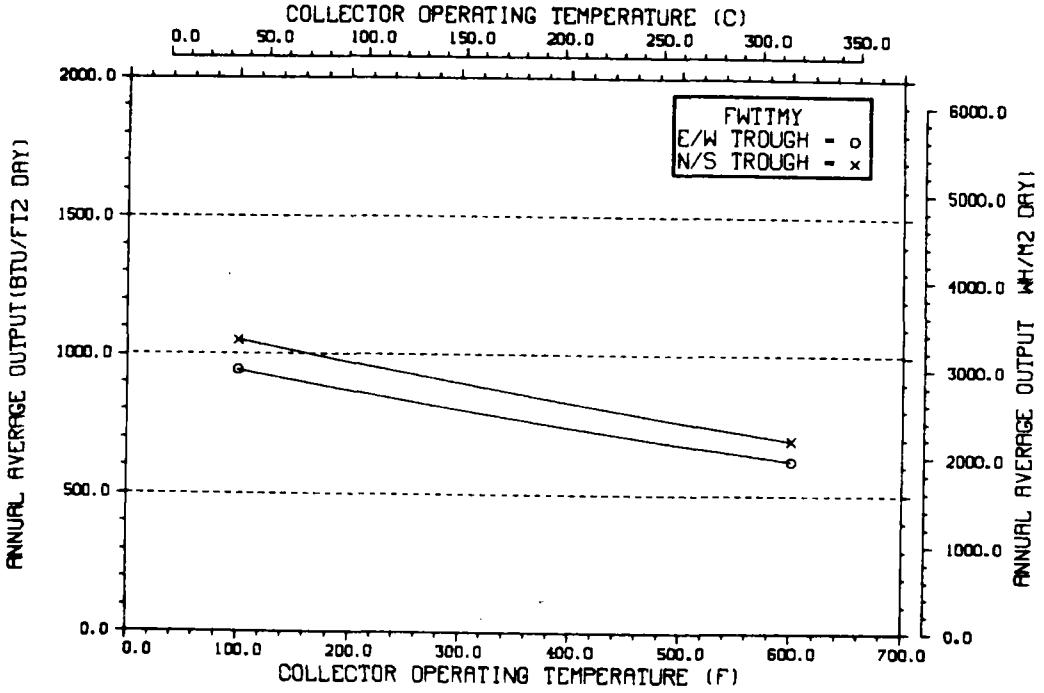

TEMPERATURE DEPENDENCE OF MONTHLY PERFORMANCE

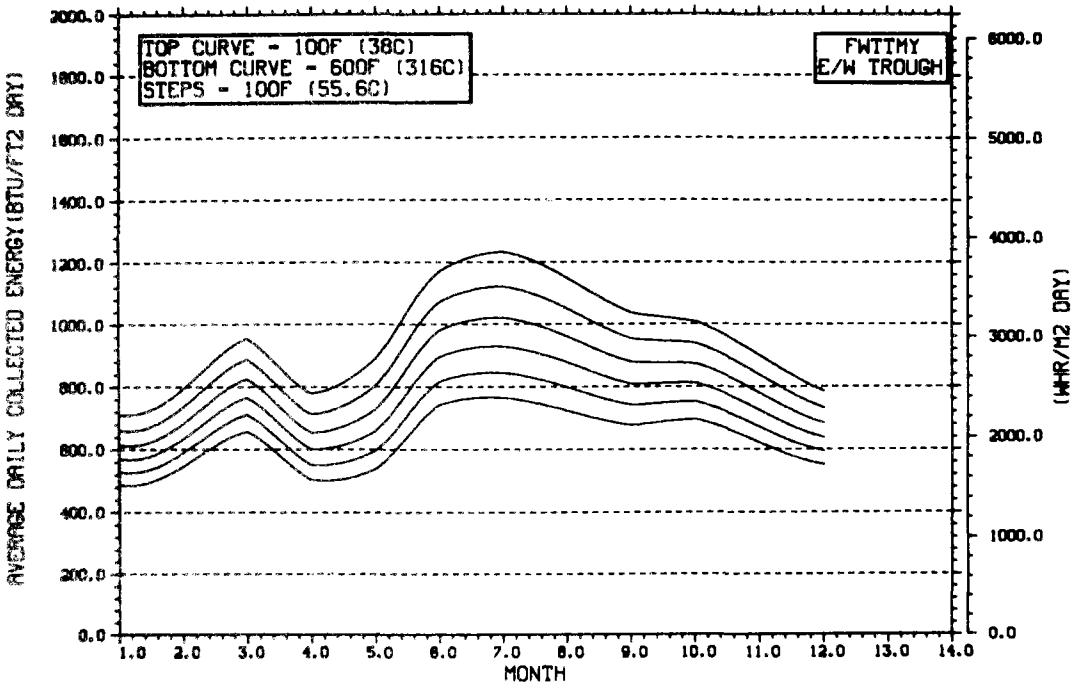

TEMPERATURE DEPENDENCE OF MONTHLY PERFORMANCE

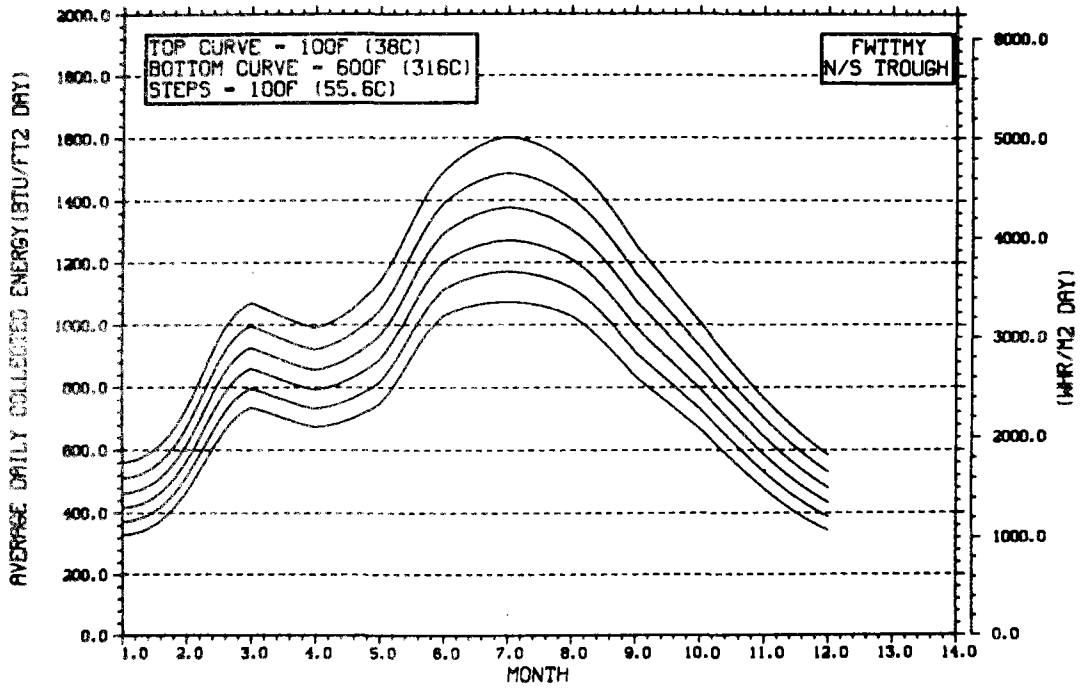

STORAGE SIZING GRAPH FOR CONSTANT ANNUAL DEMAND

NO WEEKEND SHUTDOWN

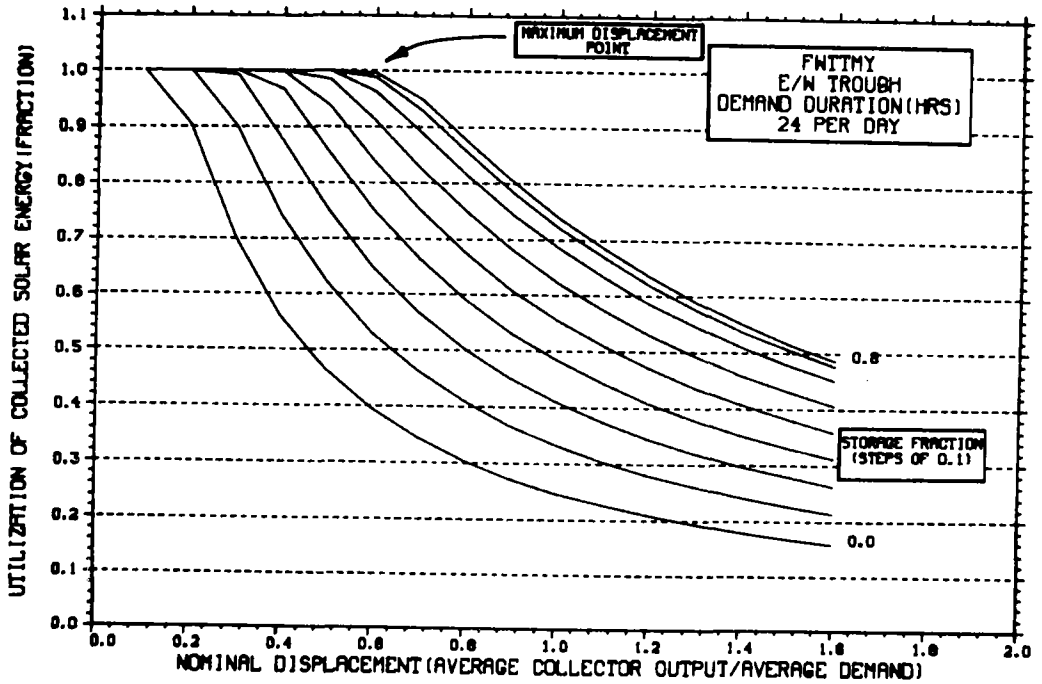

STORAGE SIZING GRAPH FOR CONSTANT ANNUAL DEMAND

NO WEEKEND SHUTDOWN

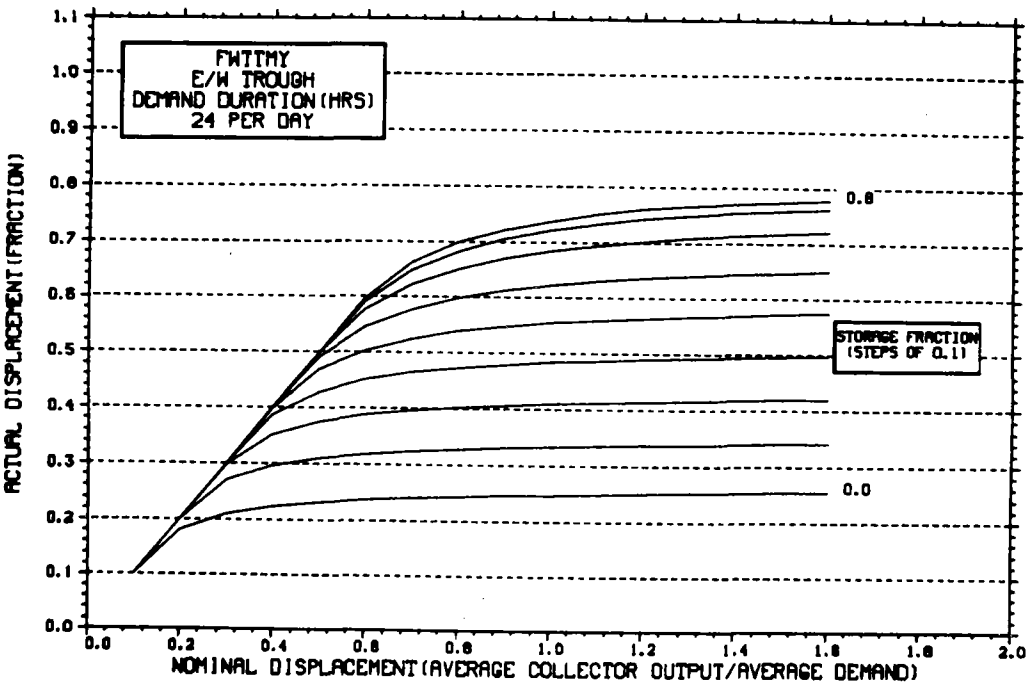

STORAGE SIZING GRAPH FOR CONSTANT ANNUAL DEMAND

NO WEEKEND SHUTDOWN

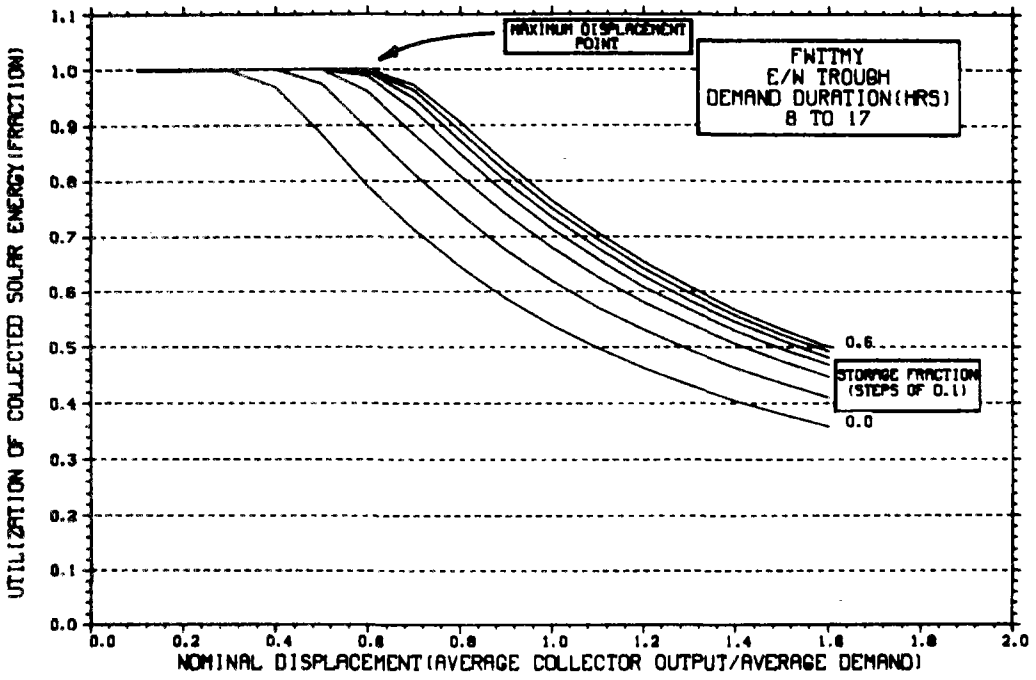

STORAGE SIZING GRAPH FOR CONSTANT ANNUAL DEMAND

NO WEEKEND SHUTDOWN

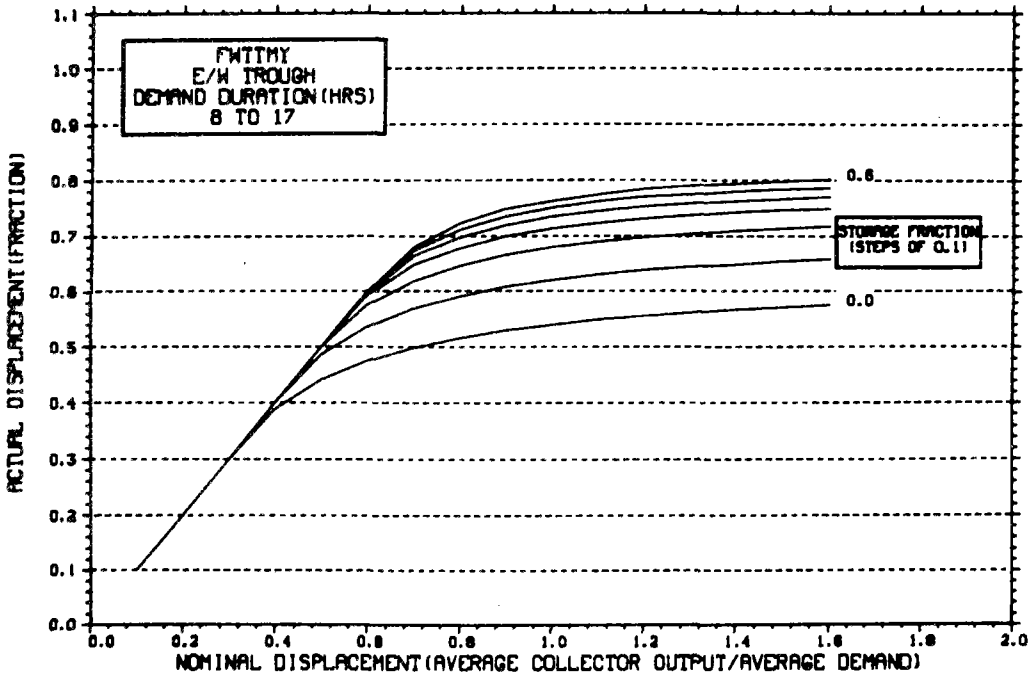

STORAGE SIZING GRAPH FOR CONSTANT ANNUAL DEMAND

NO WEEKEND SHUTDOWN

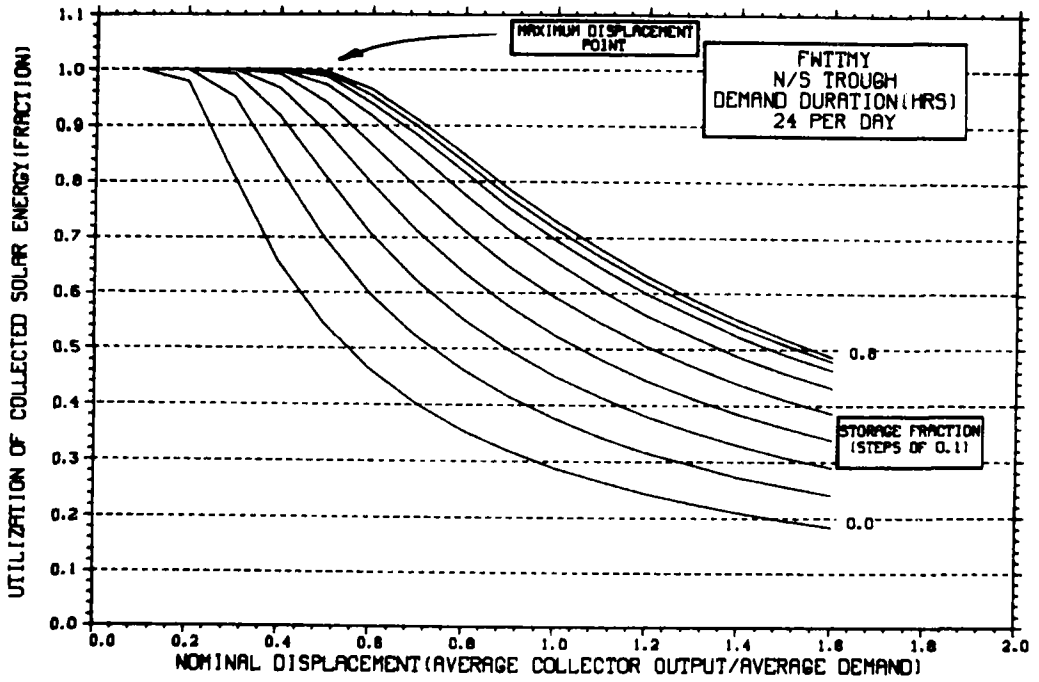

STORAGE SIZING GRAPH FOR CONSTANT ANNUAL DEMAND

NO WEEKEND SHUTDOWN

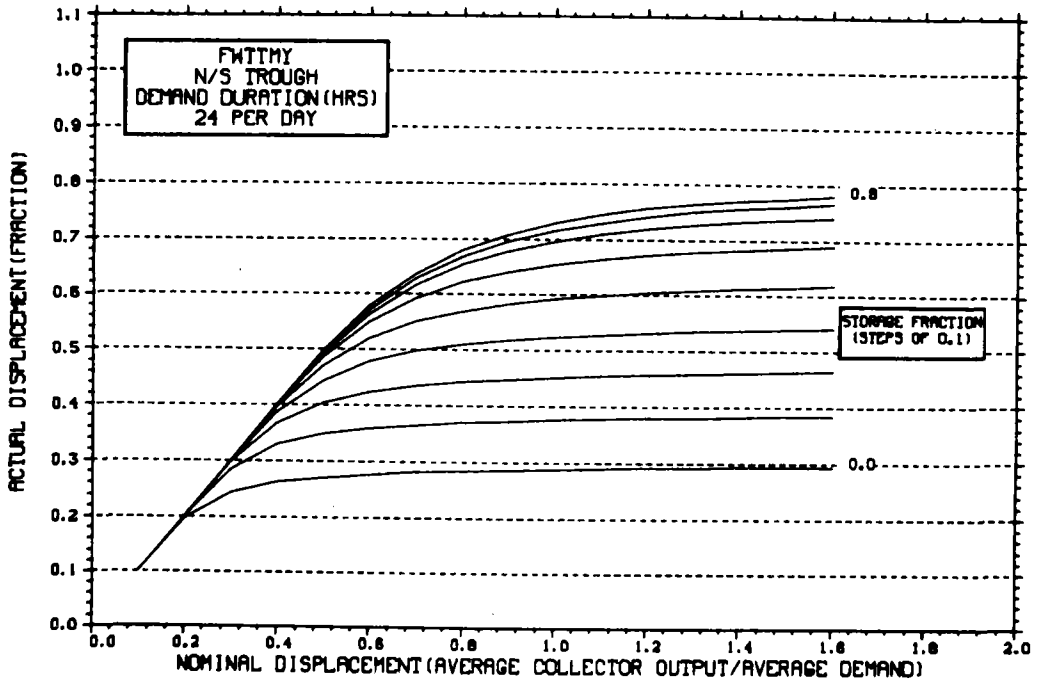

STORAGE SIZING GRAPH FOR CONSTANT ANNUAL DEMAND

NO WEEKEND SHUTDOWN

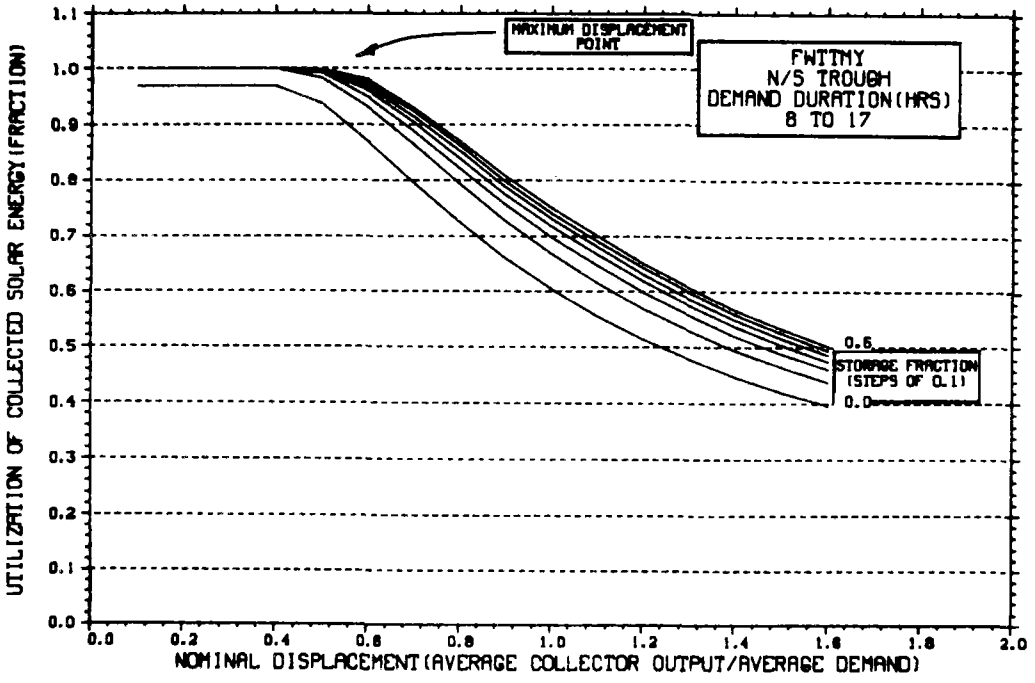

STORAGE SIZING GRAPH FOR CONSTANT ANNUAL DEMAND

NO WEEKEND SHUTDOWN

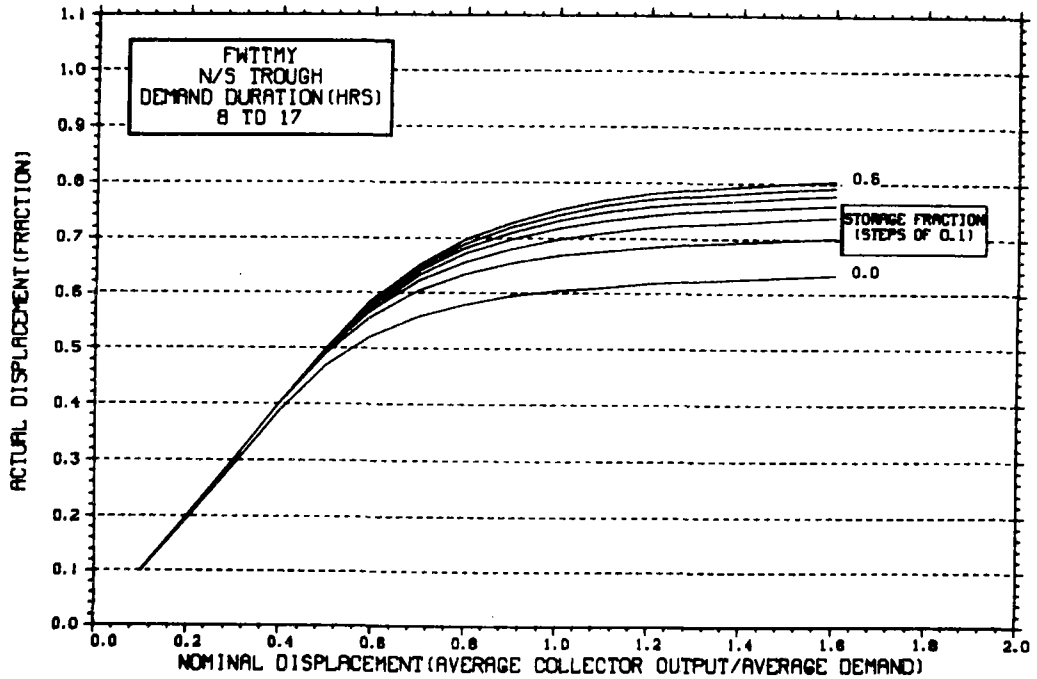

ENERGY INCIDENT ON COLLECTOR APERTURE

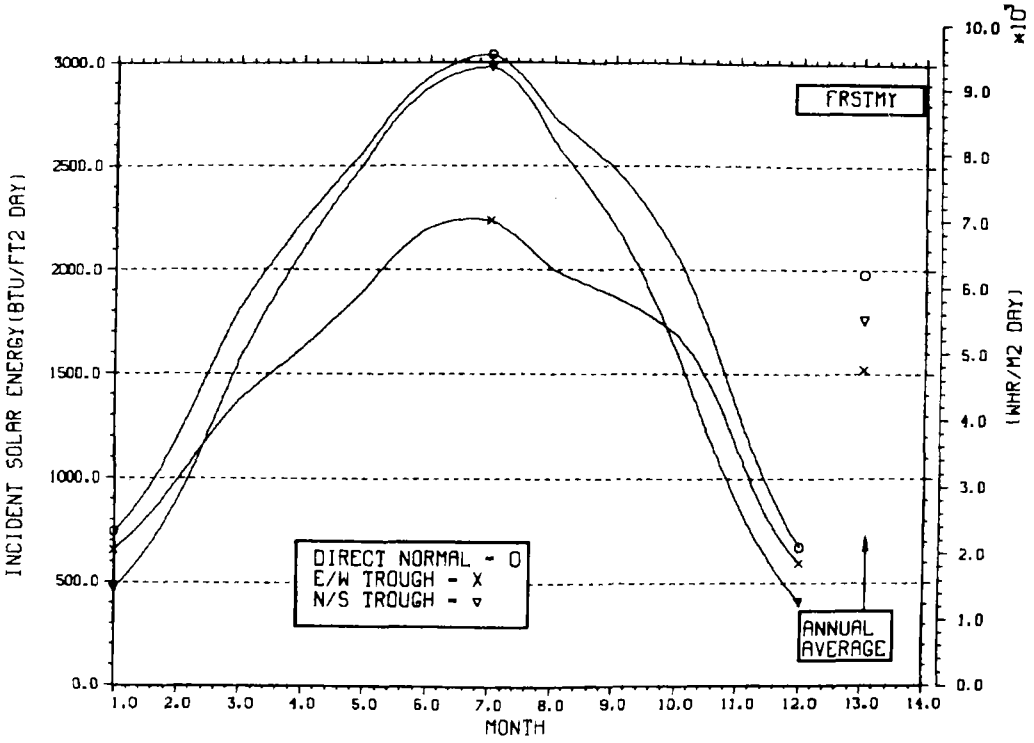

ANNUAL NONFIRST ROW SHADING

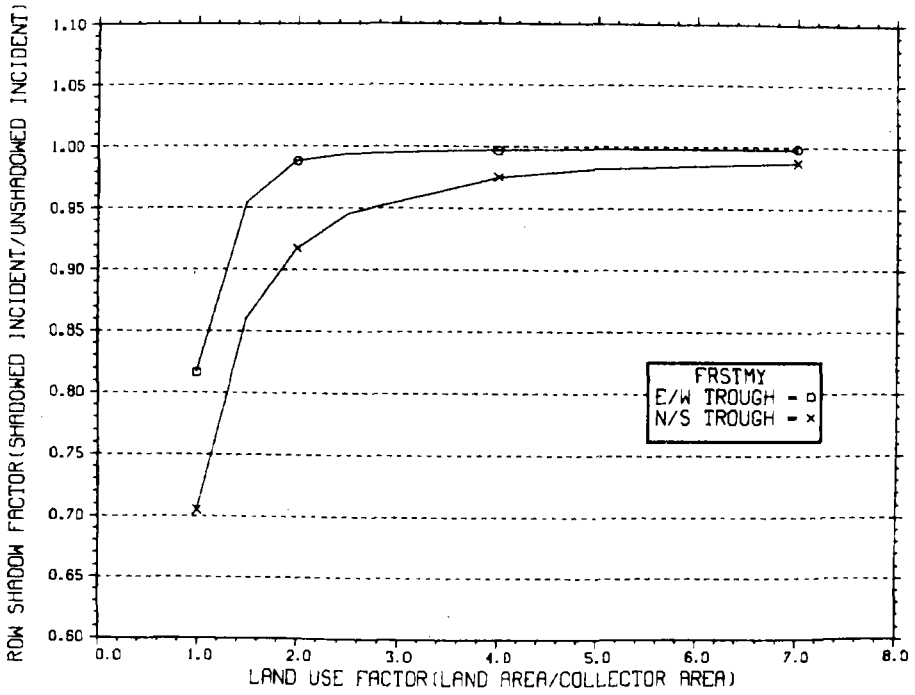

PERFORMANCE VARIATION WITH COLLECTOR AZIMUTH

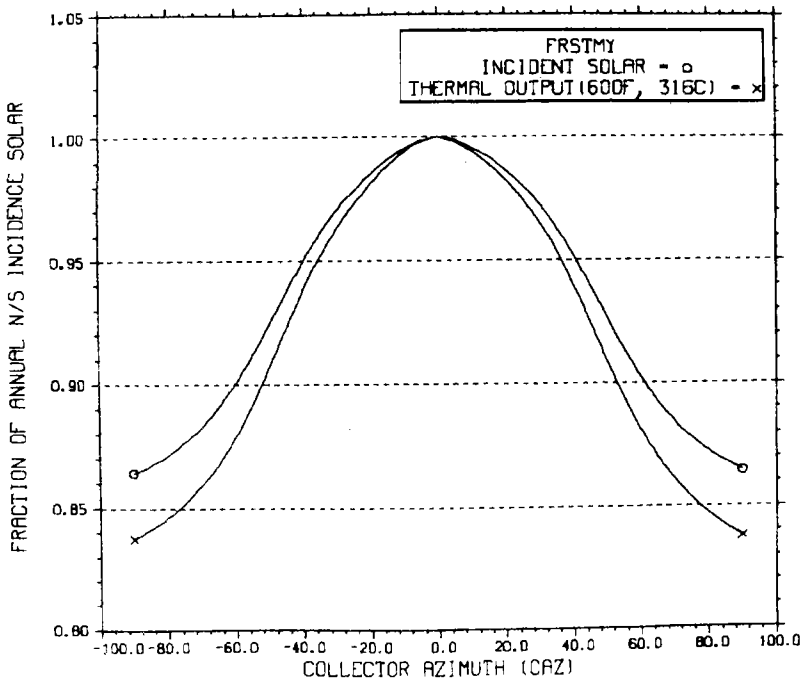

TEMPERATURE DEPENDENCE OF ANNUAL PERFORMANCE

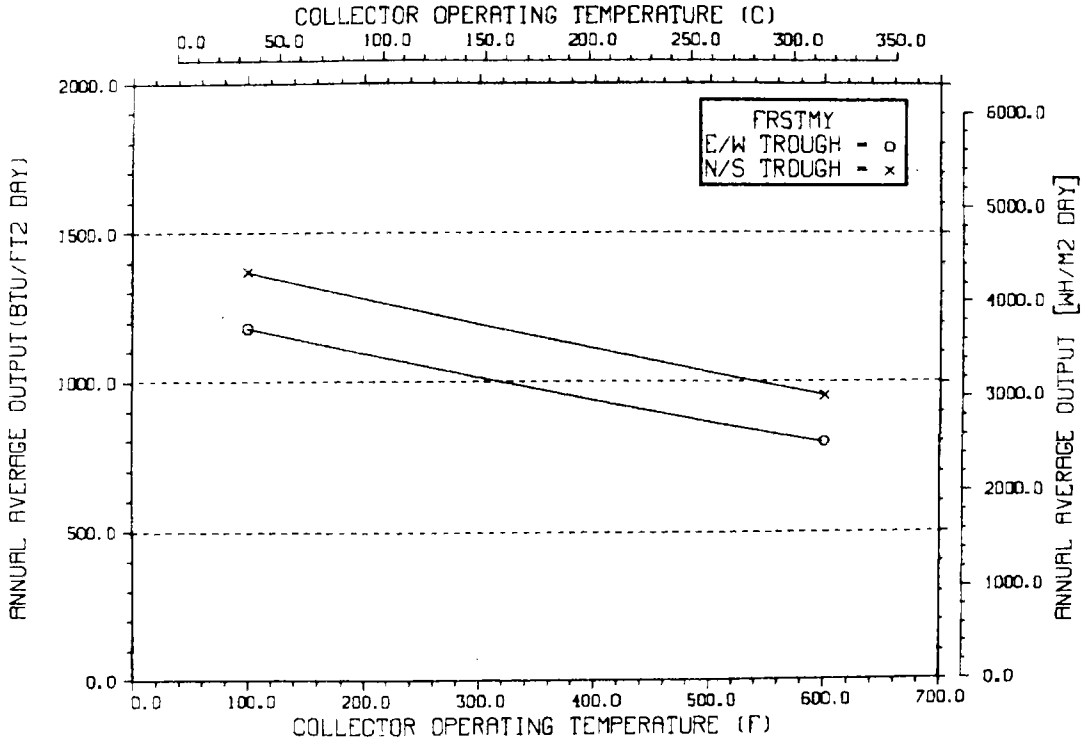

TEMPERATURE DEPENDENCE OF MONTHLY PERFORMANCE

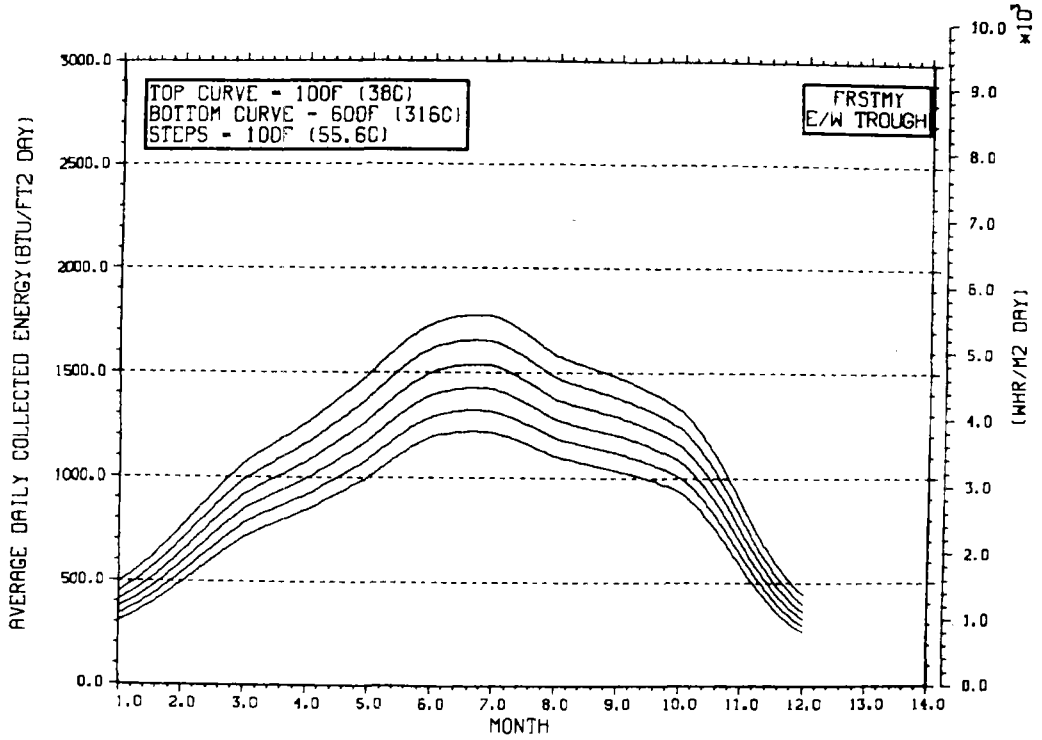

TEMPERATURE DEPENDENCE OF MONTHLY PERFORMANCE

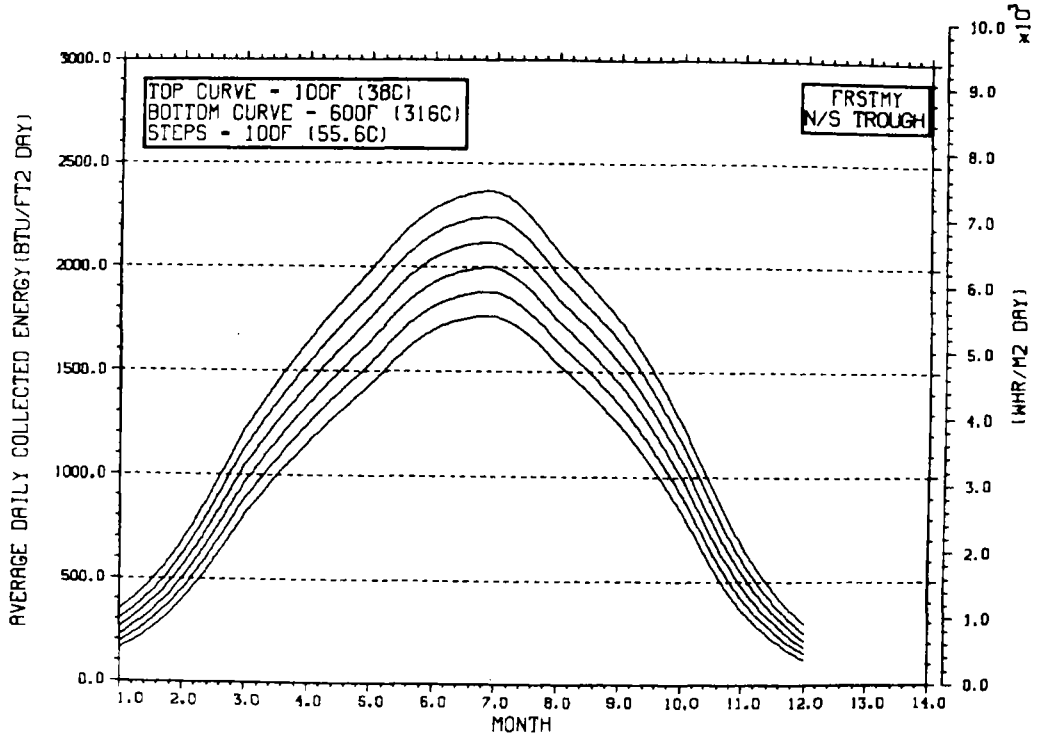

STORAGE SIZING GRAPH FOR CONSTANT ANNUAL DEMAND

NO WEEKEND SHUTDOWN

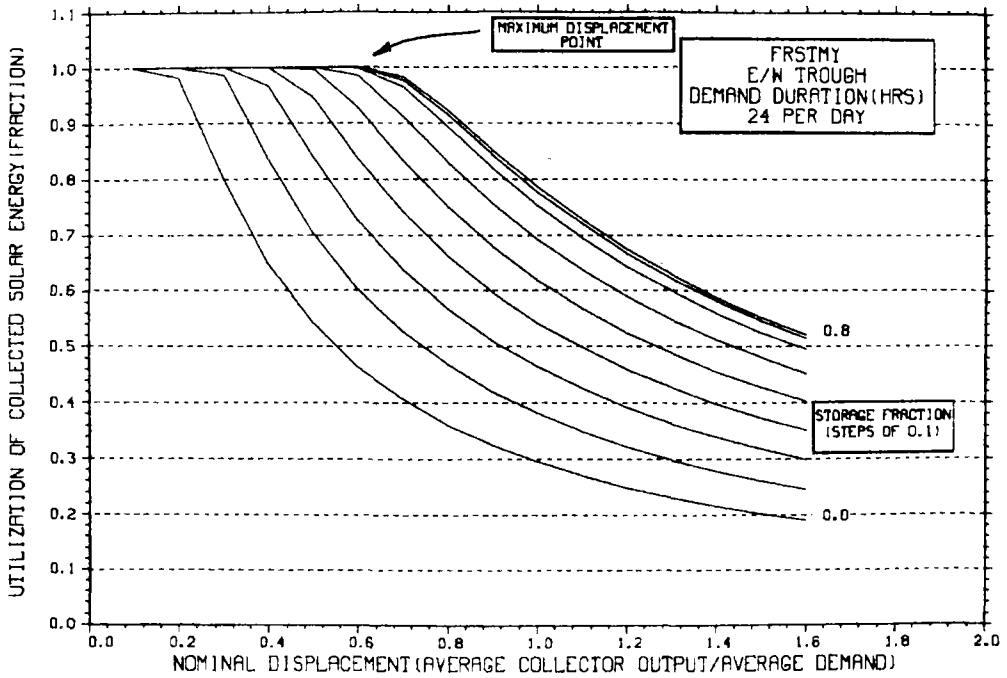

STORAGE SIZING GRAPH FOR CONSTANT ANNUAL DEMAND

NO WEEKEND SHUTDOWN

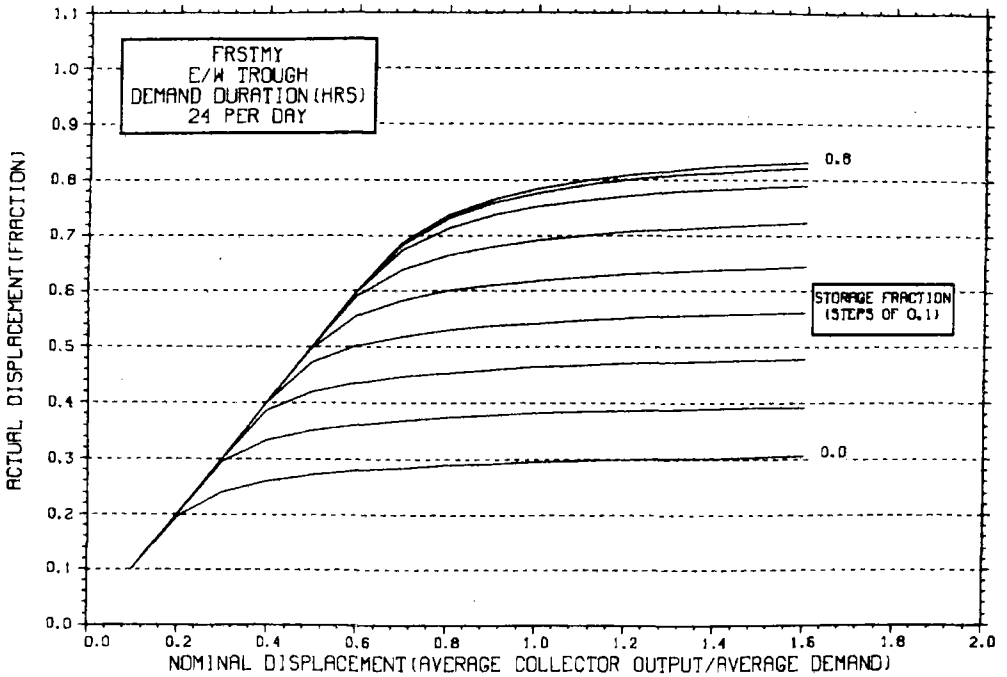

STORAGE SIZING GRAPH FOR CONSTANT ANNUAL DEMAND

NO WEEKEND SHUTDOWN

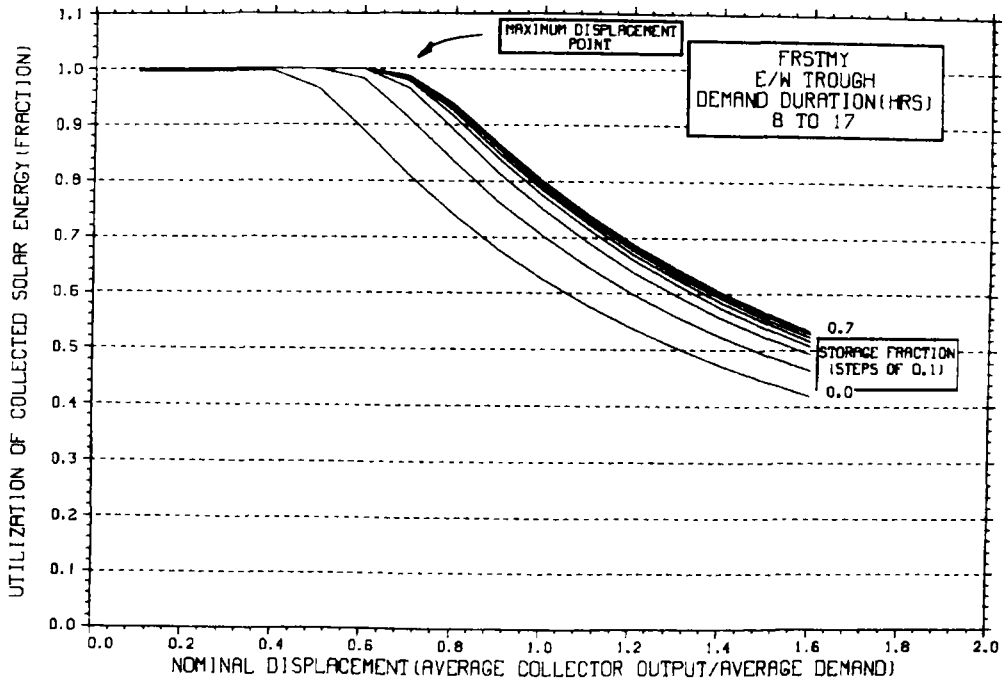

STORAGE SIZING GRAPH FOR CONSTANT ANNUAL DEMAND

NO WEEKEND SHUTDOWN

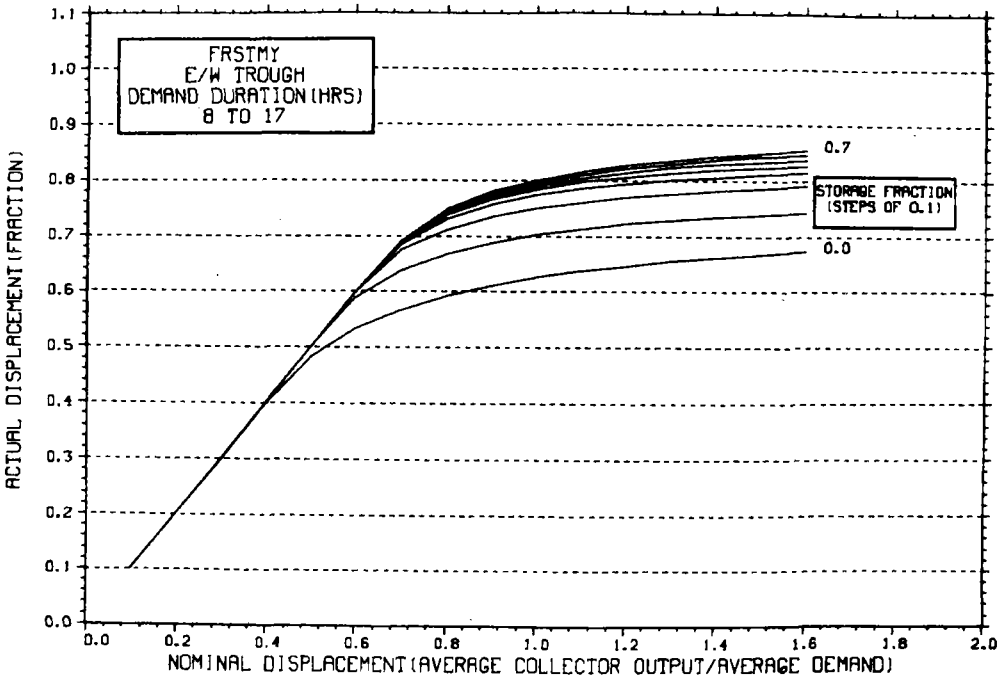

STORAGE SIZING GRAPH FOR CONSTANT ANNUAL DEMAND

NO WEEKEND SHUTDOWN

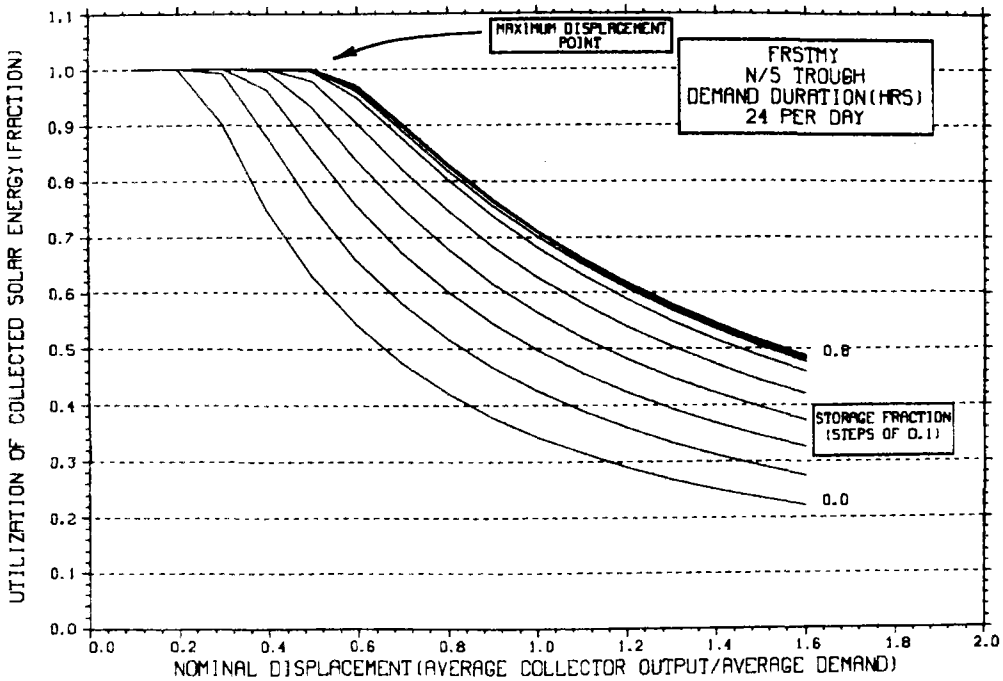

STORAGE SIZING GRAPH FOR CONSTANT ANNUAL DEMAND

NO WEEKEND SHUTDOWN

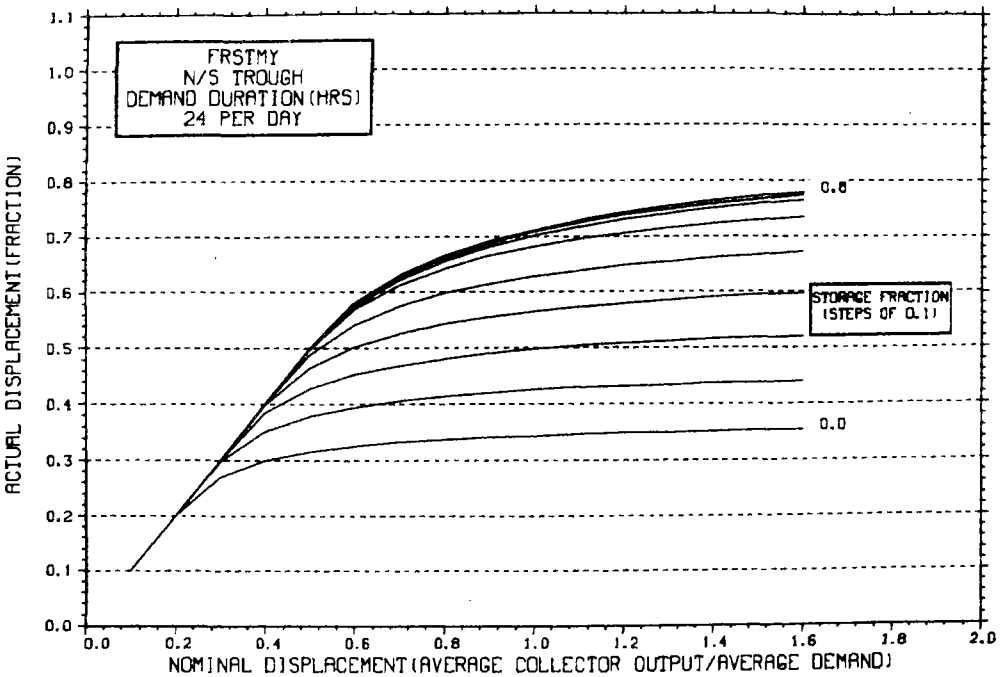

STORAGE SIZING GRAPH FOR CONSTANT ANNUAL DEMAND

NO WEEKEND SHUTDOWN

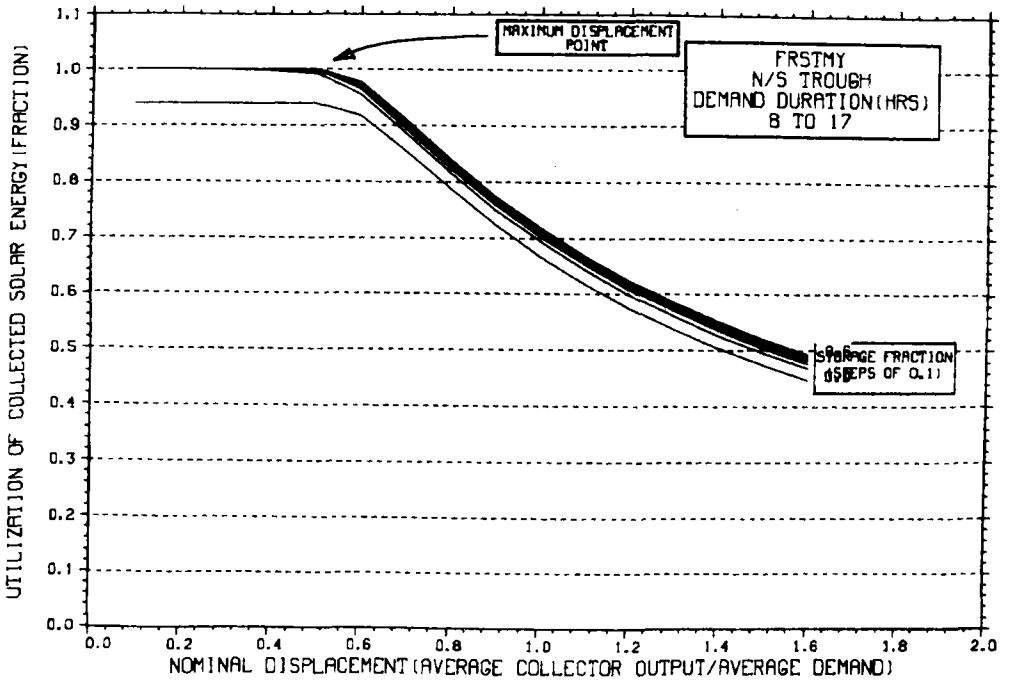

STORAGE SIZING GRAPH FOR CONSTANT ANNUAL DEMAND

NO WEEKEND SHUTDOWN

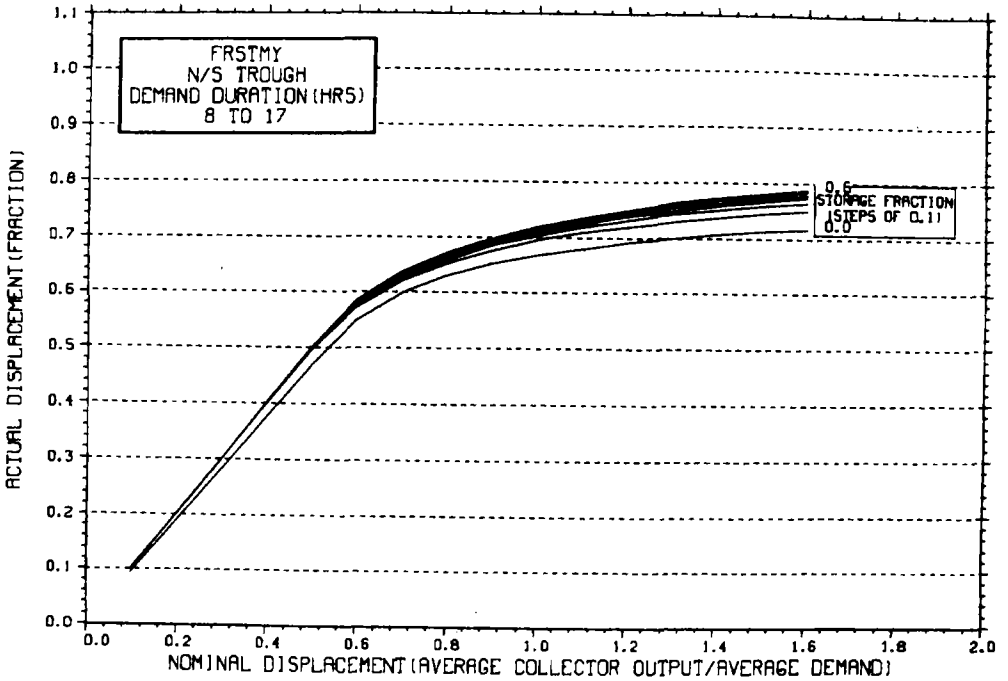

ENERGY INCIDENT ON COLLECTOR APERTURE

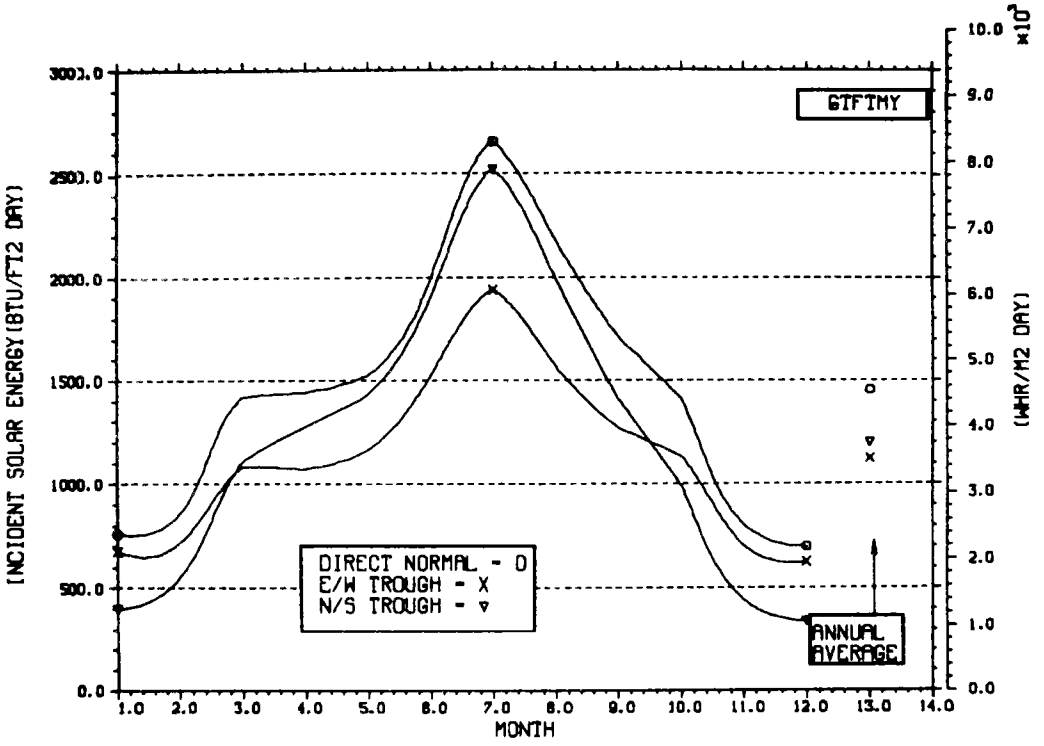

ANNUAL NONFIRST ROW SHADING

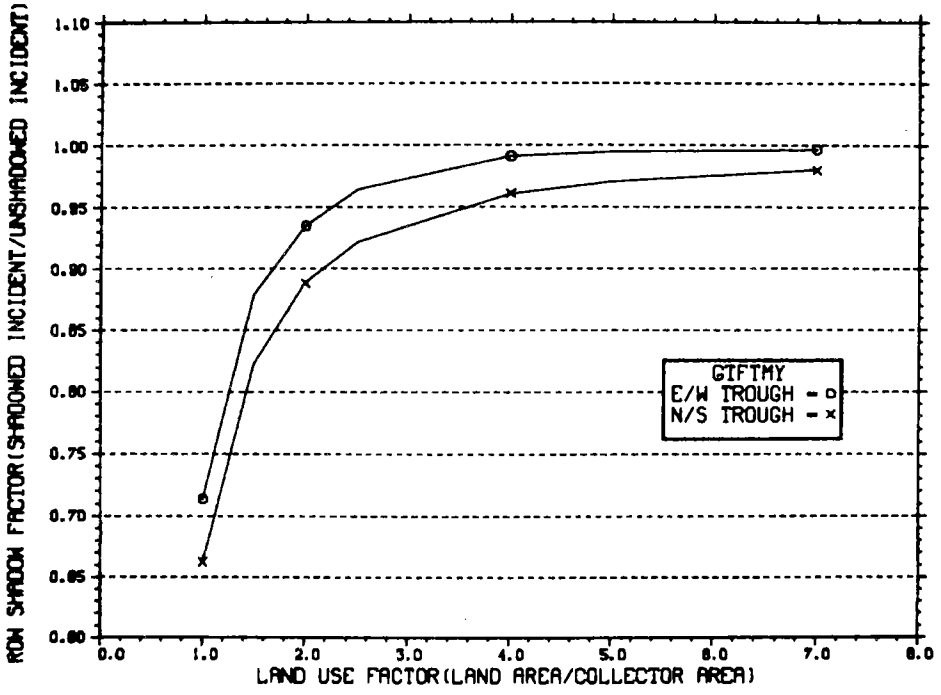

PERFORMANCE VARIATION WITH COLLECTOR AZIMUTH

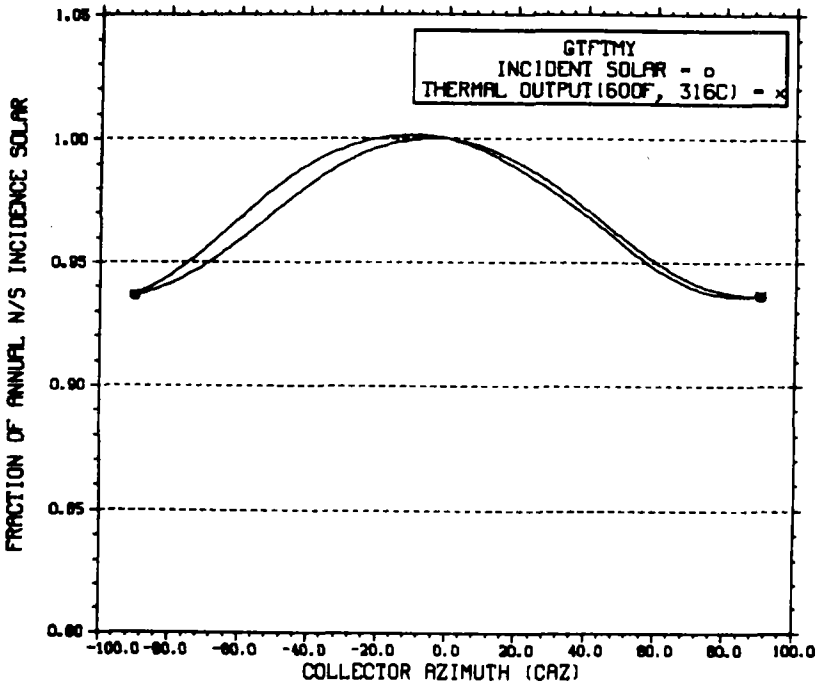

TEMPERATURE DEPENDENCE OF ANNUAL PERFORMANCE

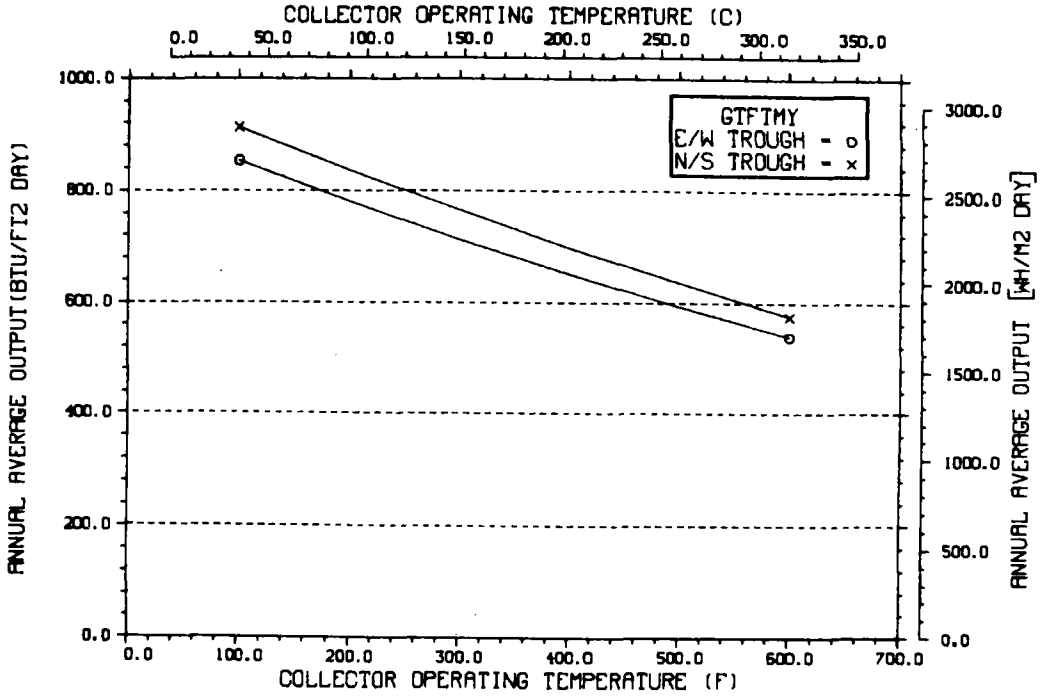

TEMPERATURE DEPENDENCE OF MONTHLY PERFORMANCE

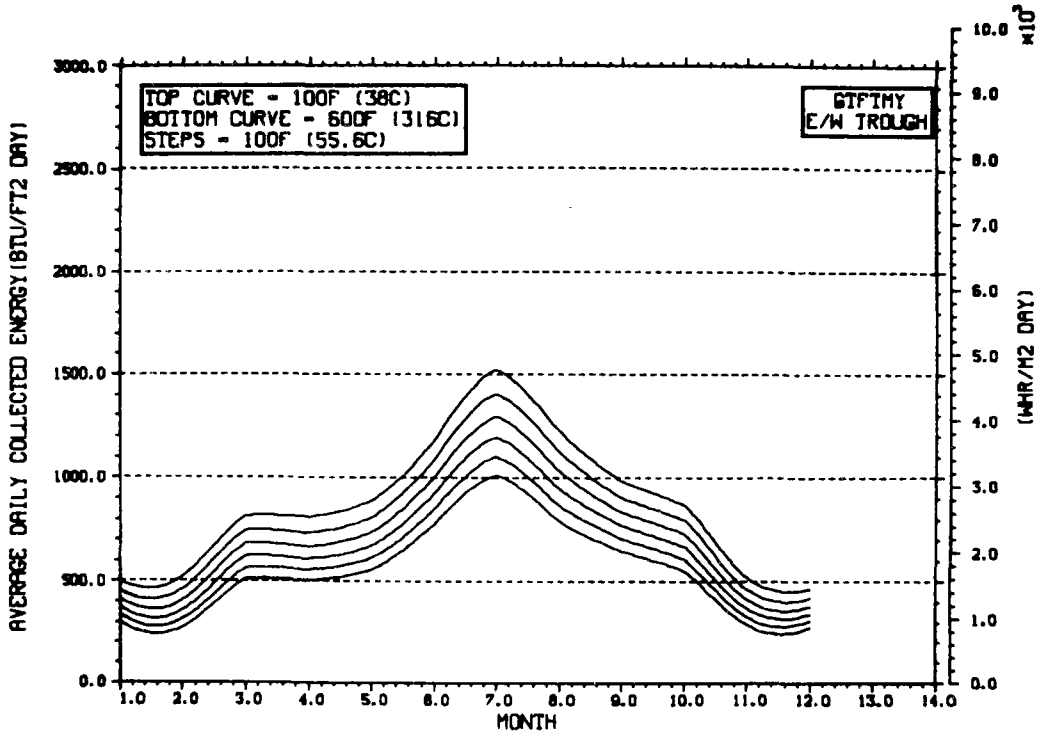

TEMPERATURE DEPENDENCE OF MONTHLY PERFORMANCE

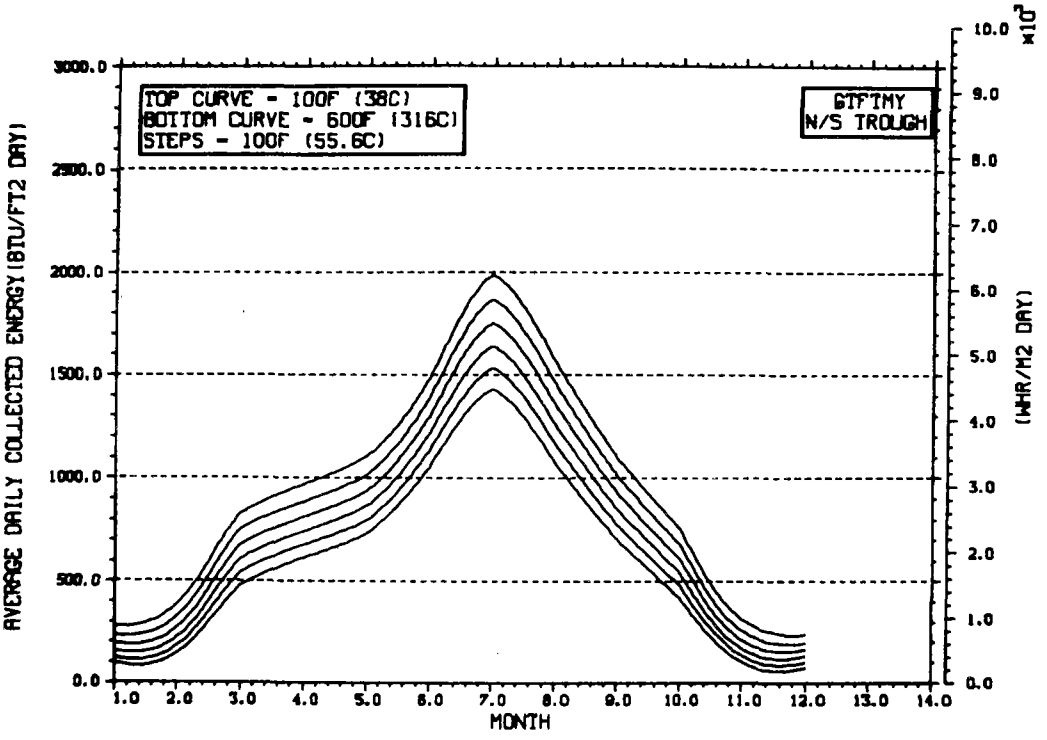

STORAGE SIZING GRAPH FOR CONSTANT ANNUAL DEMAND

NO WEEKEND SHUTDOWN

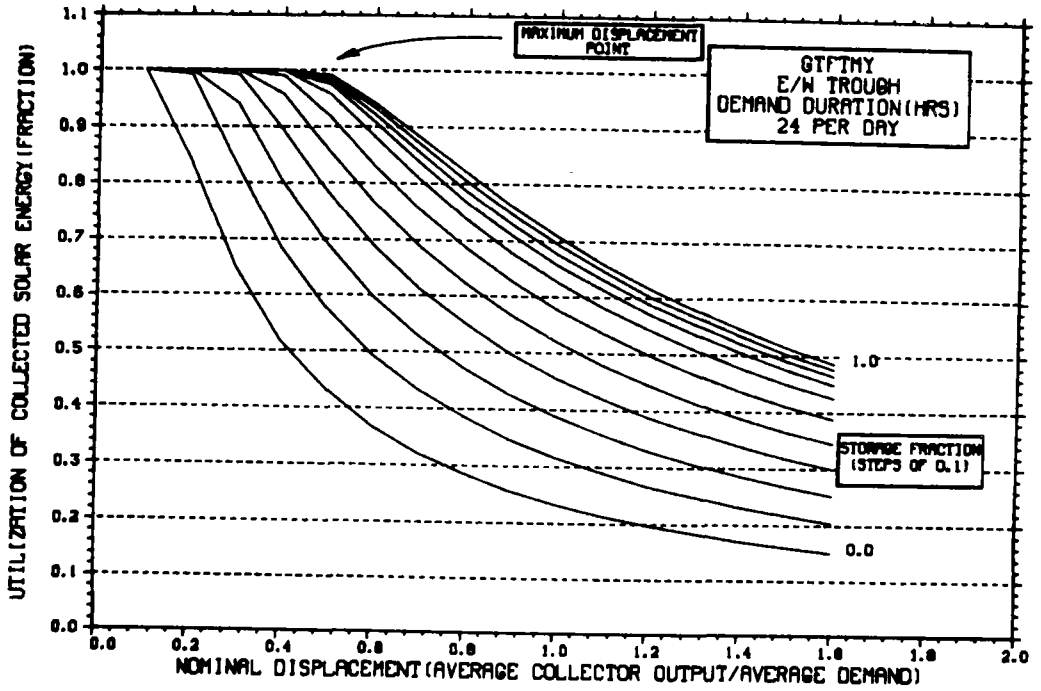

STORAGE SIZING GRAPH FOR CONSTANT ANNUAL DEMAND

NO WEEKEND SHUTDOWN

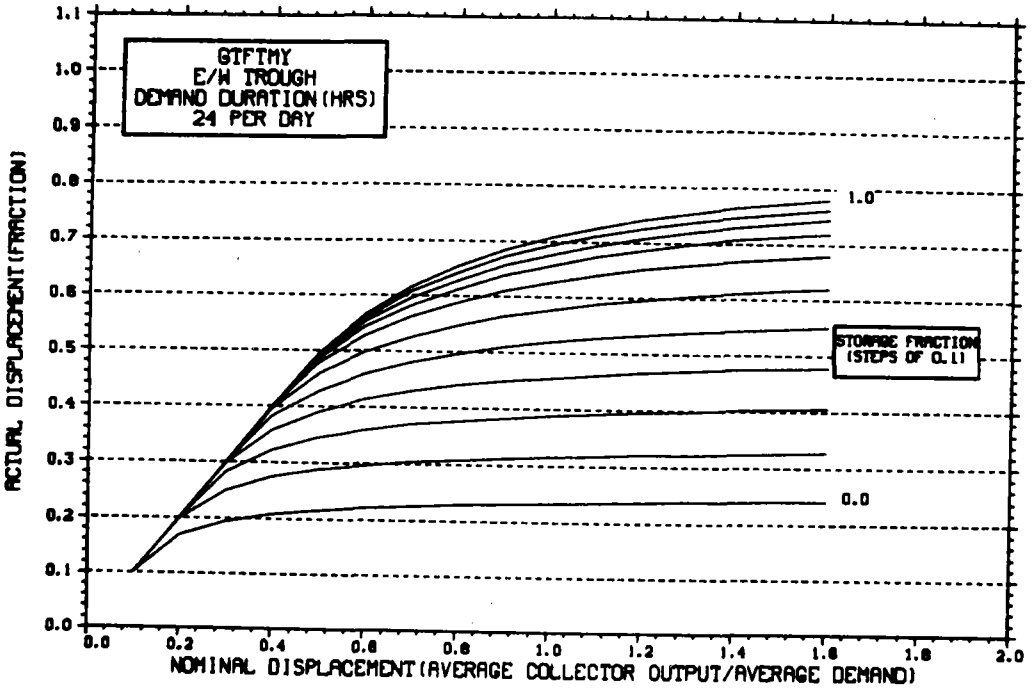

STORAGE SIZING GRAPH FOR CONSTANT ANNUAL DEMAND

NO WEEKEND SHUTDOWN

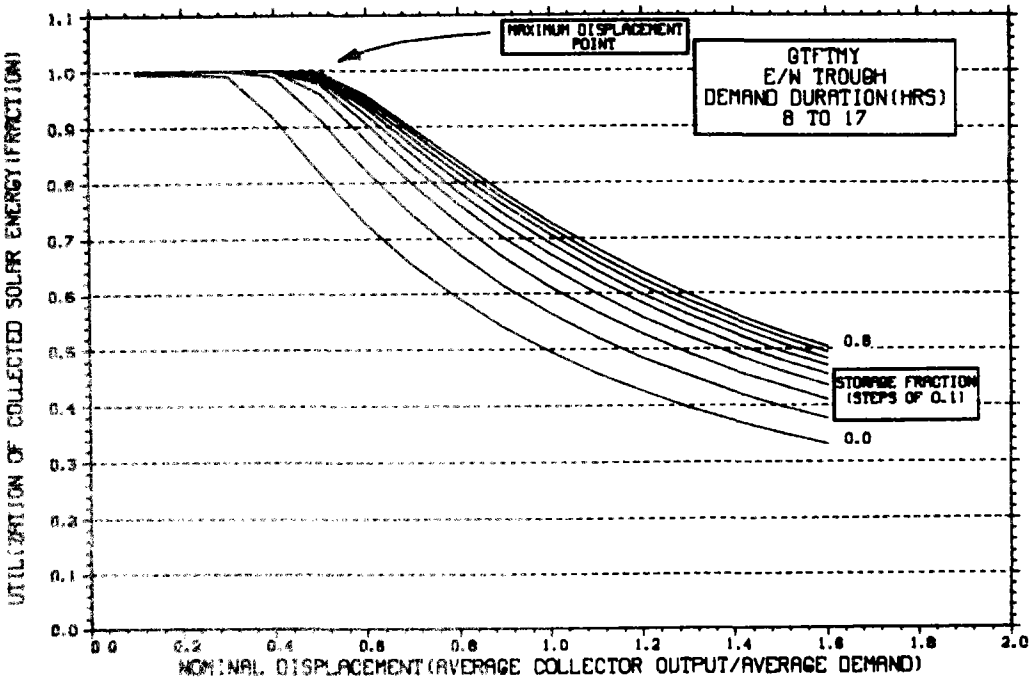

STORAGE SIZING GRAPH FOR CONSTANT ANNUAL DEMAND

NO WEEKEND SHUTDOWN

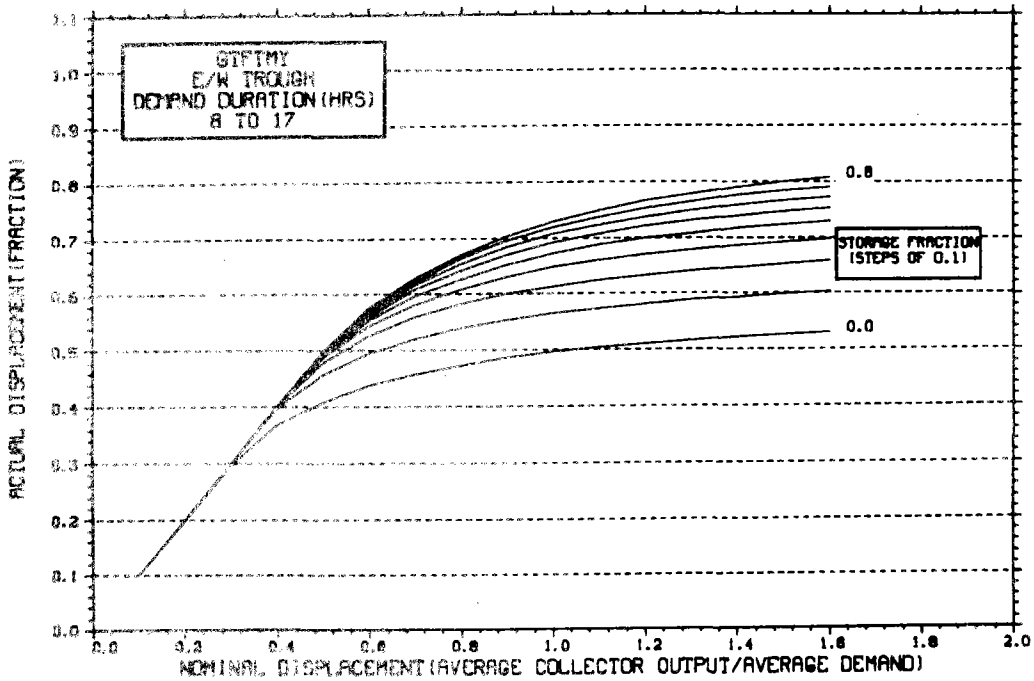

STORAGE SIZING GRAPH FOR CONSTANT ANNUAL DEMAND

NO WEEKEND SHUTDOWN

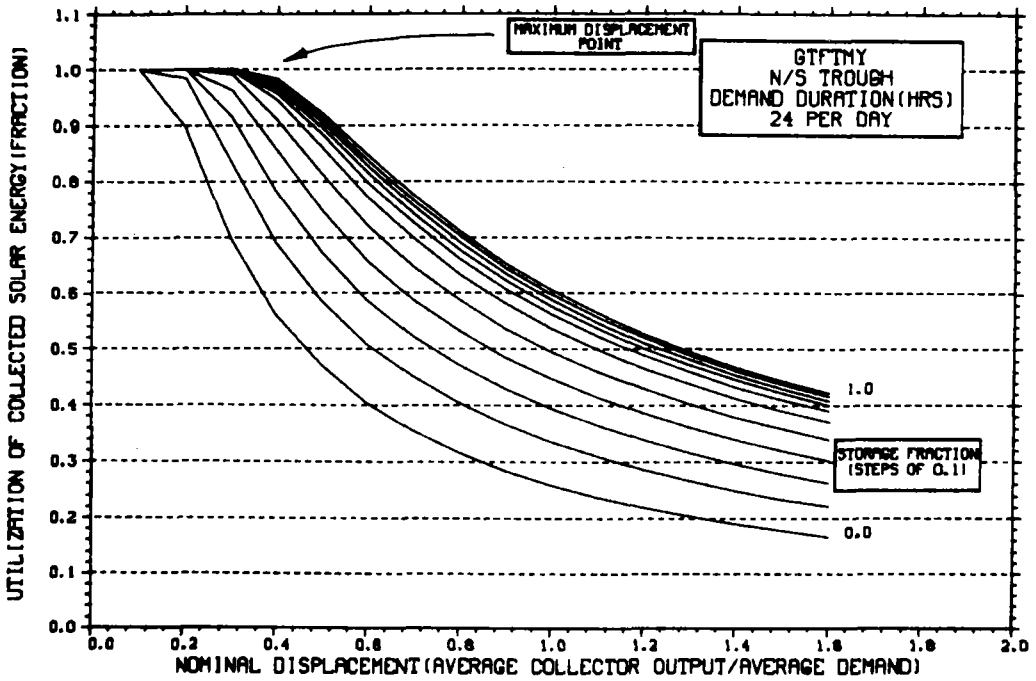

STORAGE SIZING GRAPH FOR CONSTANT ANNUAL DEMAND

NO WEEKEND SHUTDOWN

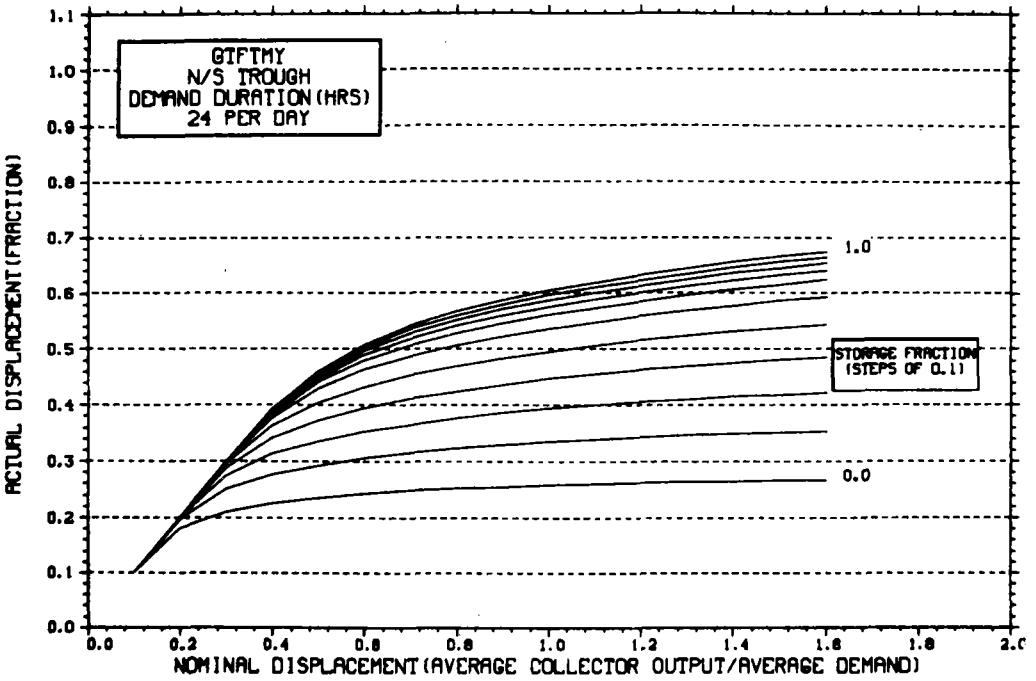

STORAGE SIZING GRAPH FOR CONSTANT ANNUAL DEMAND

NO WEEKEND SHUTDOWN

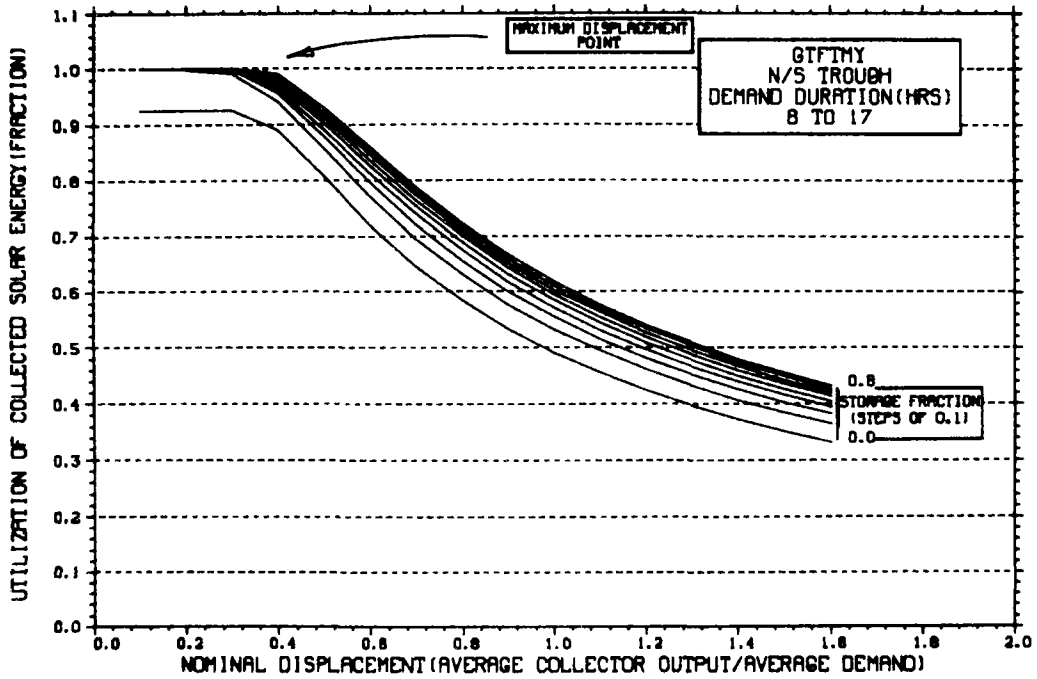

STORAGE SIZING GRAPH FOR CONSTANT ANNUAL DEMAND

NO WEEKEND SHUTDOWN

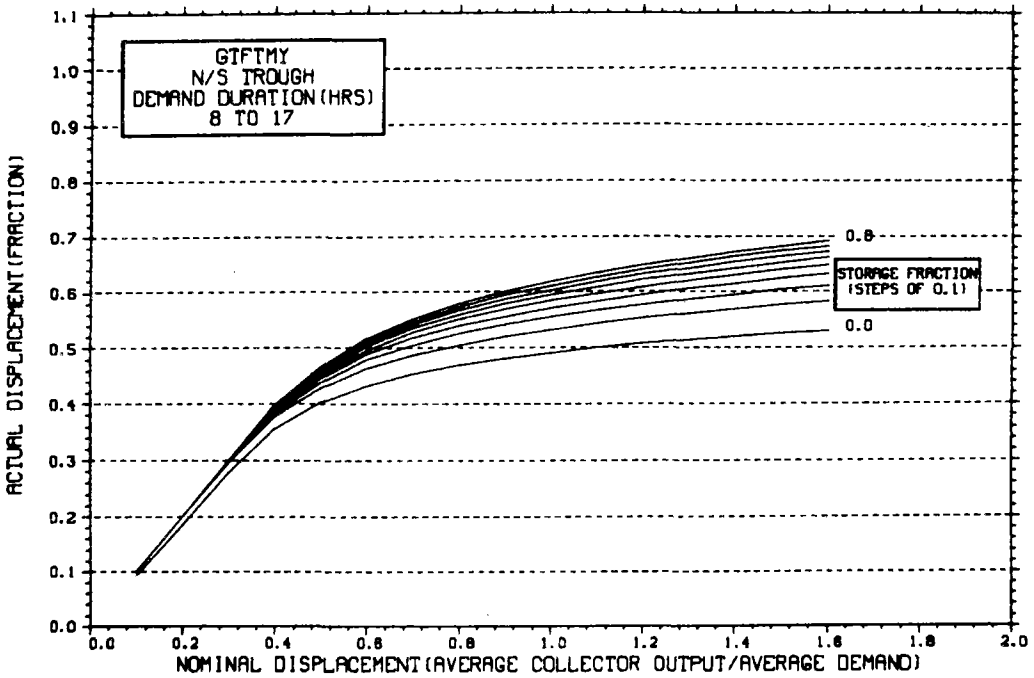

ENERGY INCIDENT ON COLLECTOR APERTURE

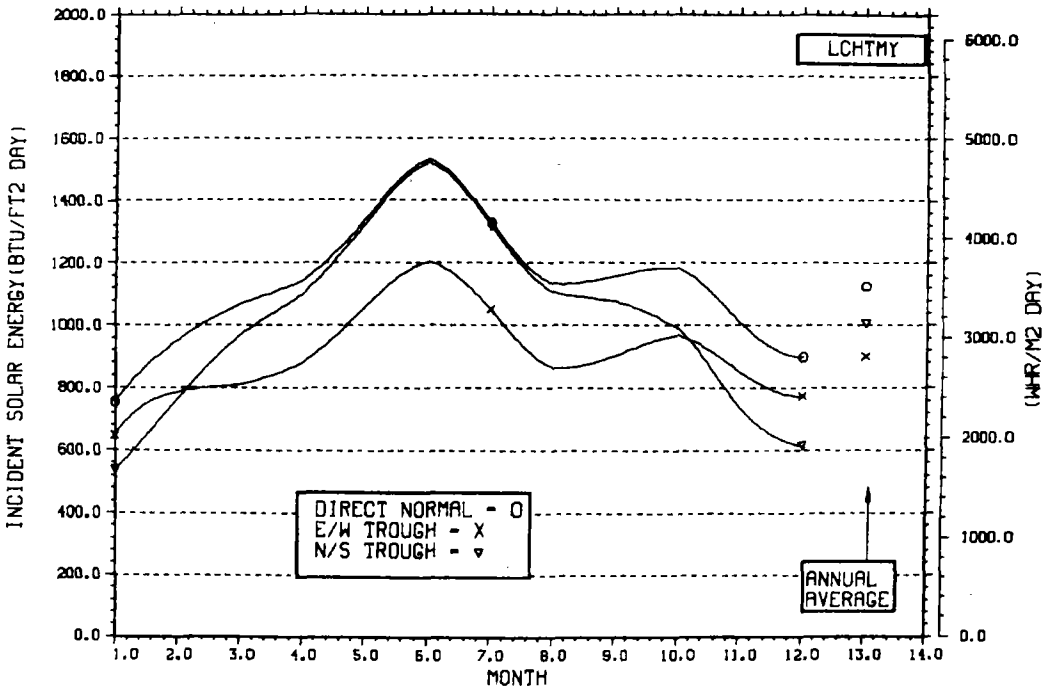

ANNUAL NONFIRST ROW SHADING

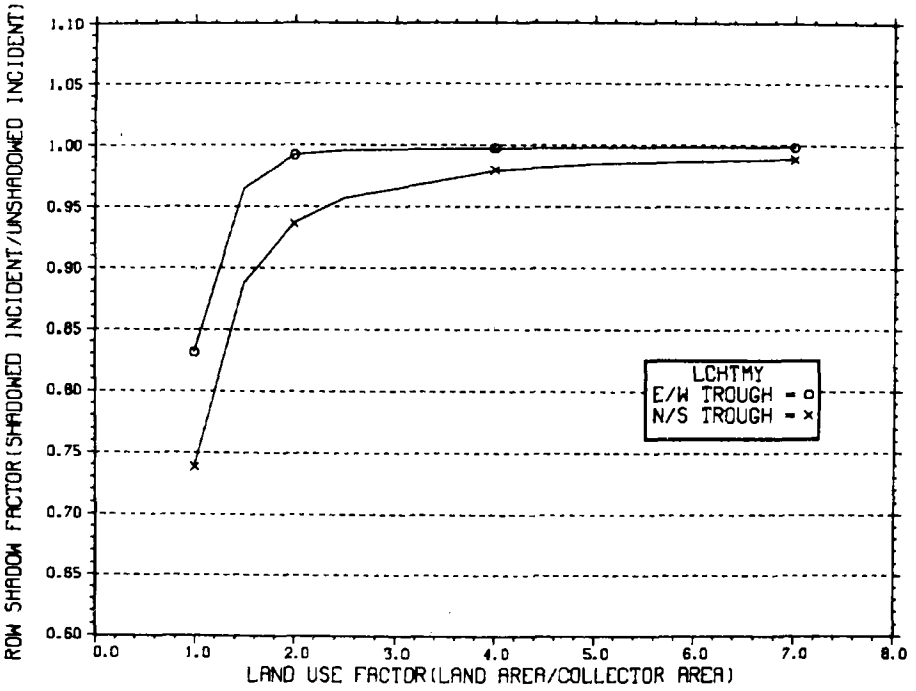

PERFORMANCE VARIATION WITH COLLECTOR AZIMUTH

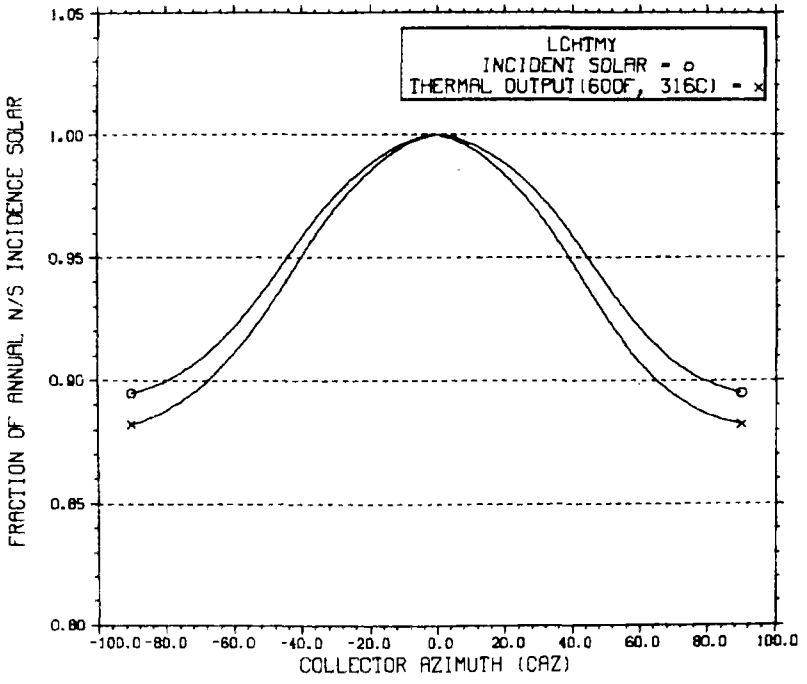

TEMPERATURE DEPENDENCE OF ANNUAL PERFORMANCE

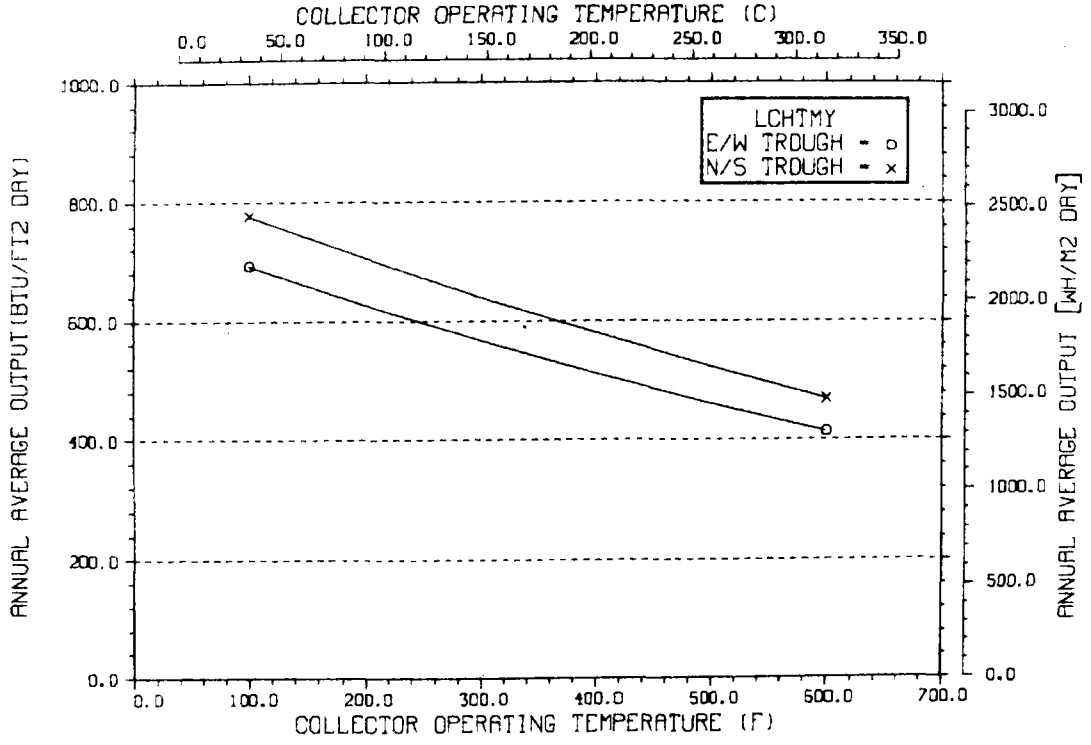

TEMPERATURE DEPENDENCE OF MONTHLY PERFORMANCE

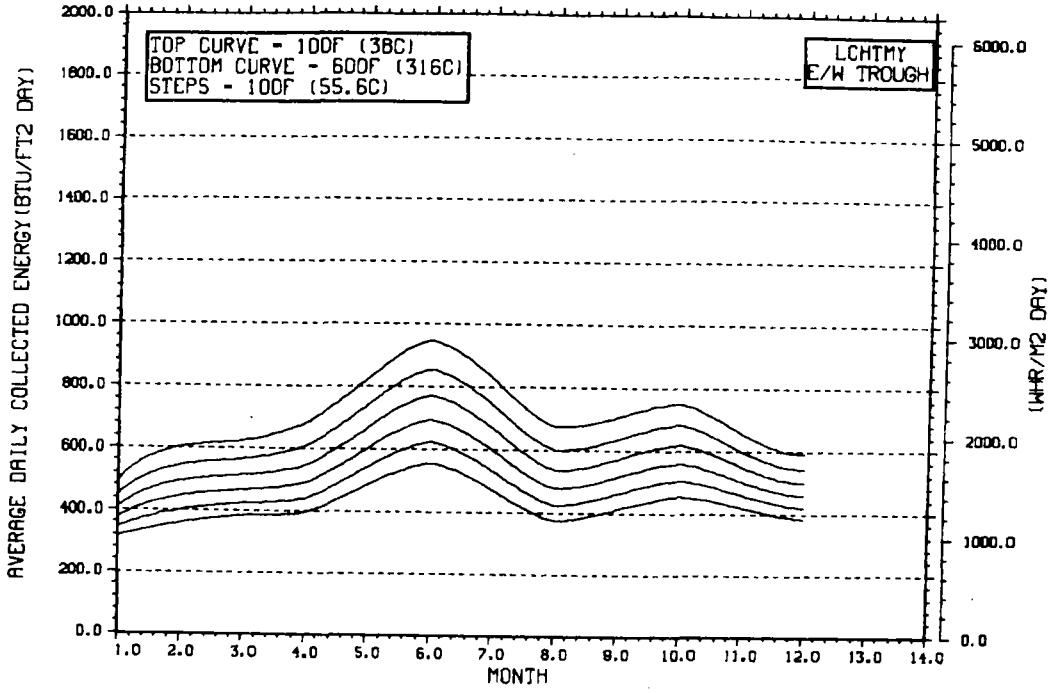

TEMPERATURE DEPENDENCE OF MONTHLY PERFORMANCE

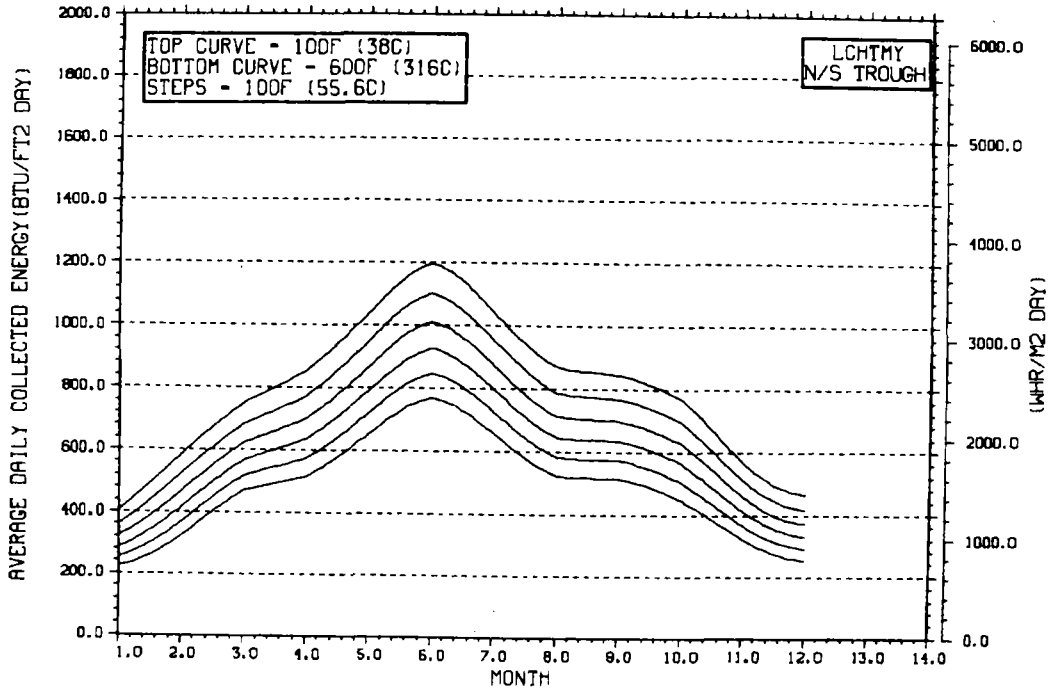

STORAGE SIZING GRAPH FOR CONSTANT ANNUAL DEMAND

NO WEEKEND SHUTDOWN

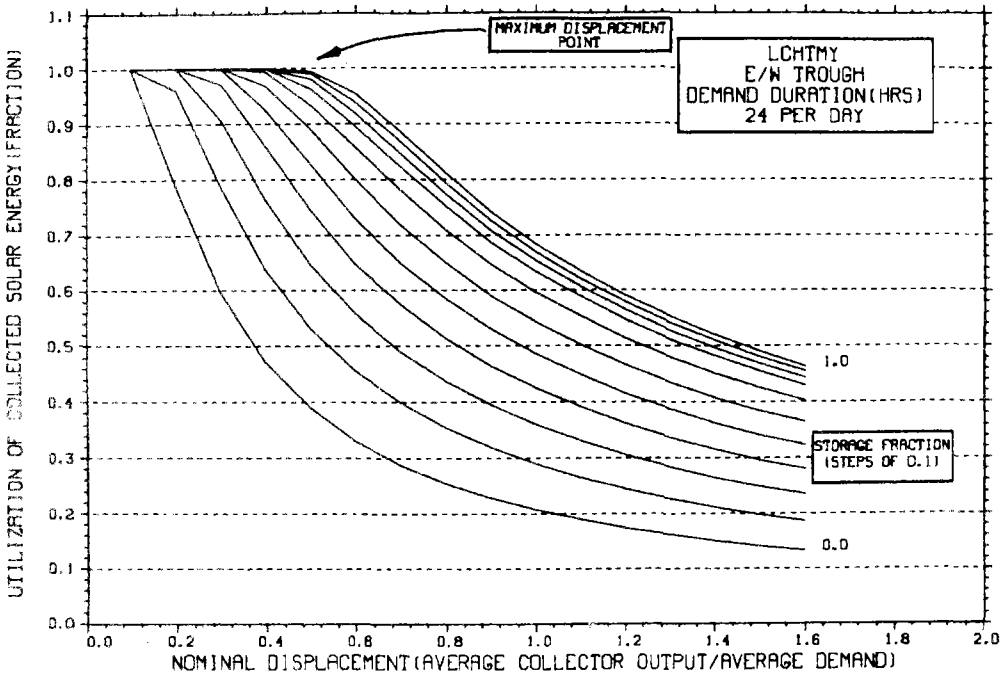

STORAGE SIZING GRAPH FOR CONSTANT ANNUAL DEMAND

NO WEEKEND SHUTDOWN

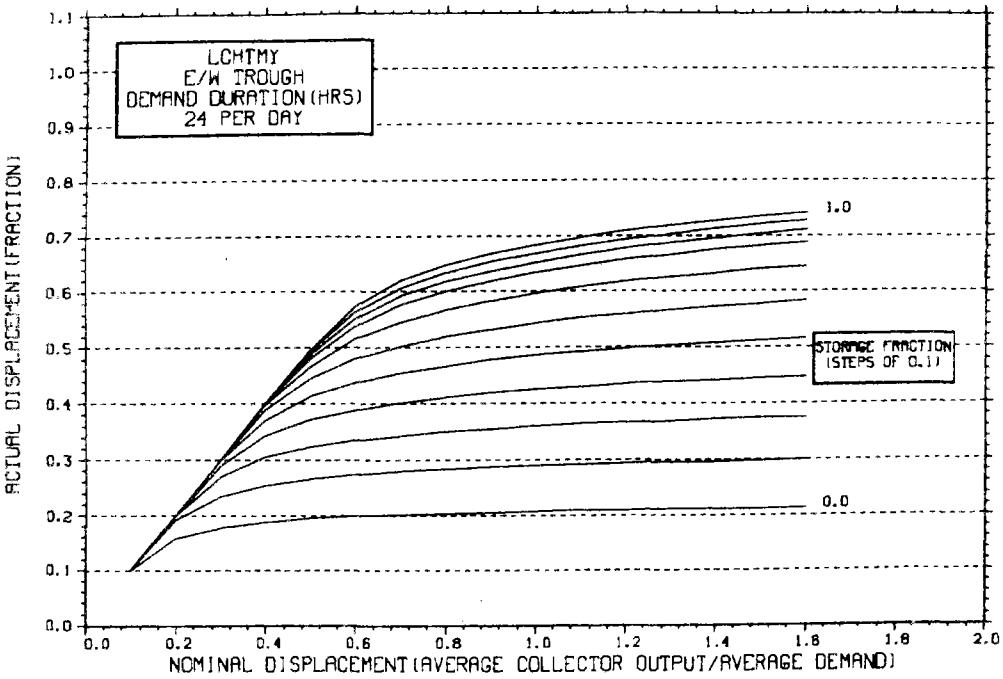

STORAGE SIZING GRAPH FOR CONSTANT ANNUAL DEMAND

NO WEEKEND SHUTDOWN

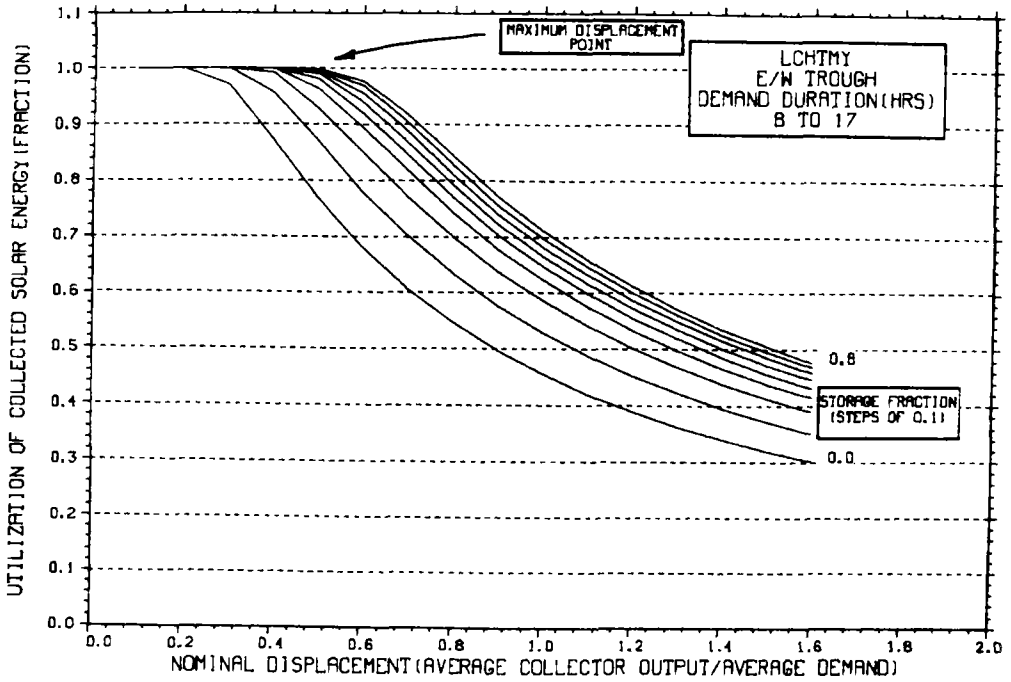

STORAGE SIZING GRAPH FOR CONSTANT ANNUAL DEMAND

NO WEEKEND SHUTDOWN

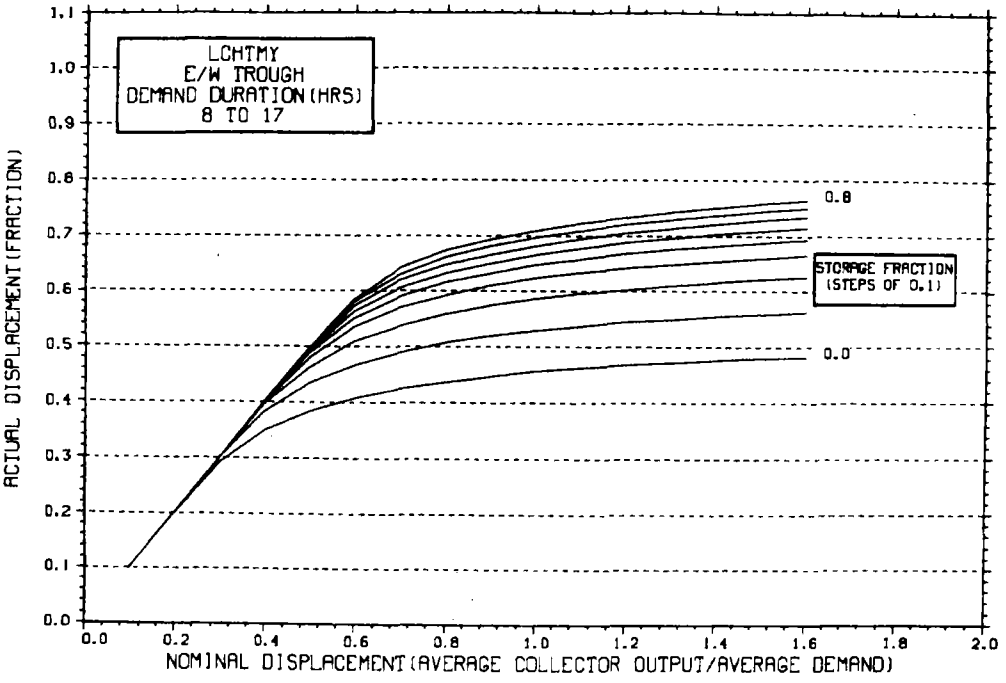

STORAGE SIZING GRAPH FOR CONSTANT ANNUAL DEMAND

NO WEEKEND SHUTDOWN

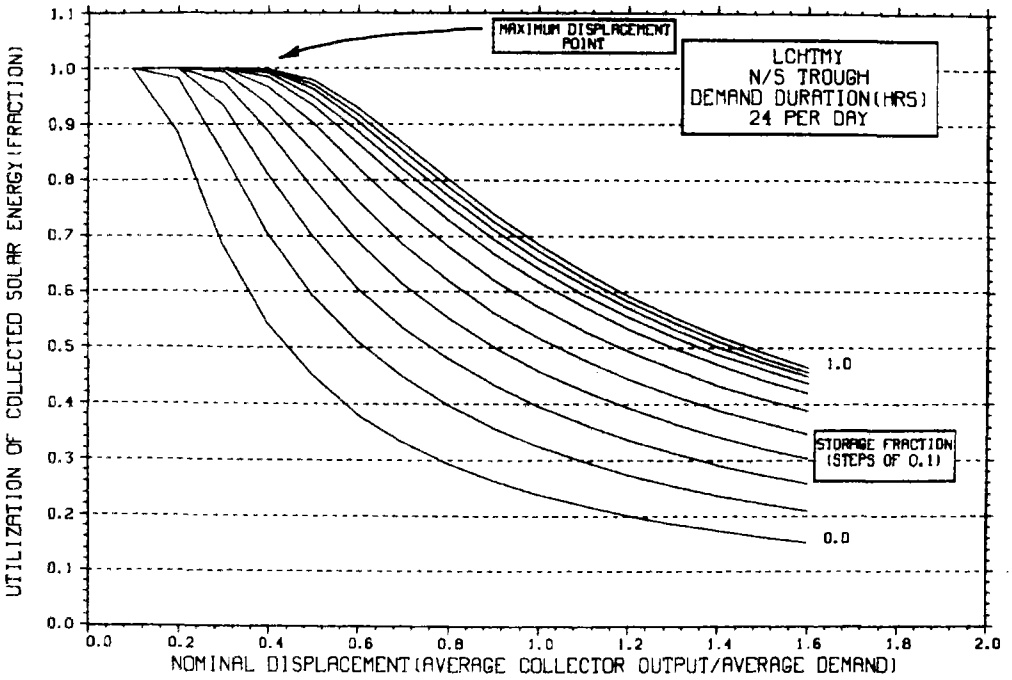

STORAGE SIZING GRAPH FOR CONSTANT ANNUAL DEMAND

NO WEEKEND SHUTDOWN

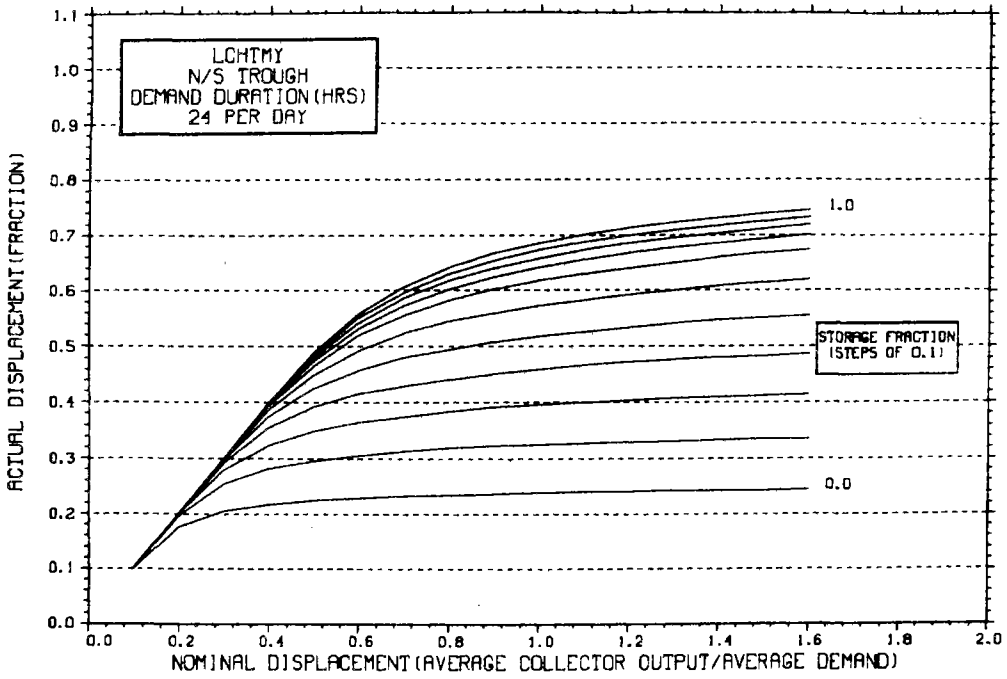

STORAGE SIZING GRAPH FOR CONSTANT ANNUAL DEMAND

NO WEEKEND SHUTDOWN

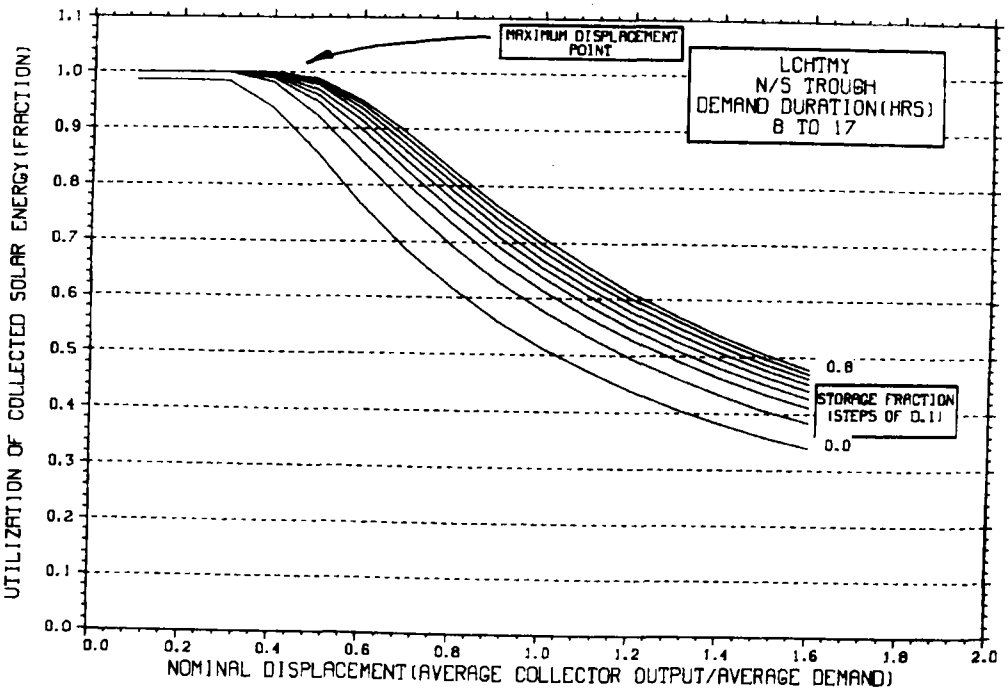

STORAGE SIZING GRAPH FOR CONSTANT ANNUAL DEMAND

NO WEEKEND SHUTDOWN

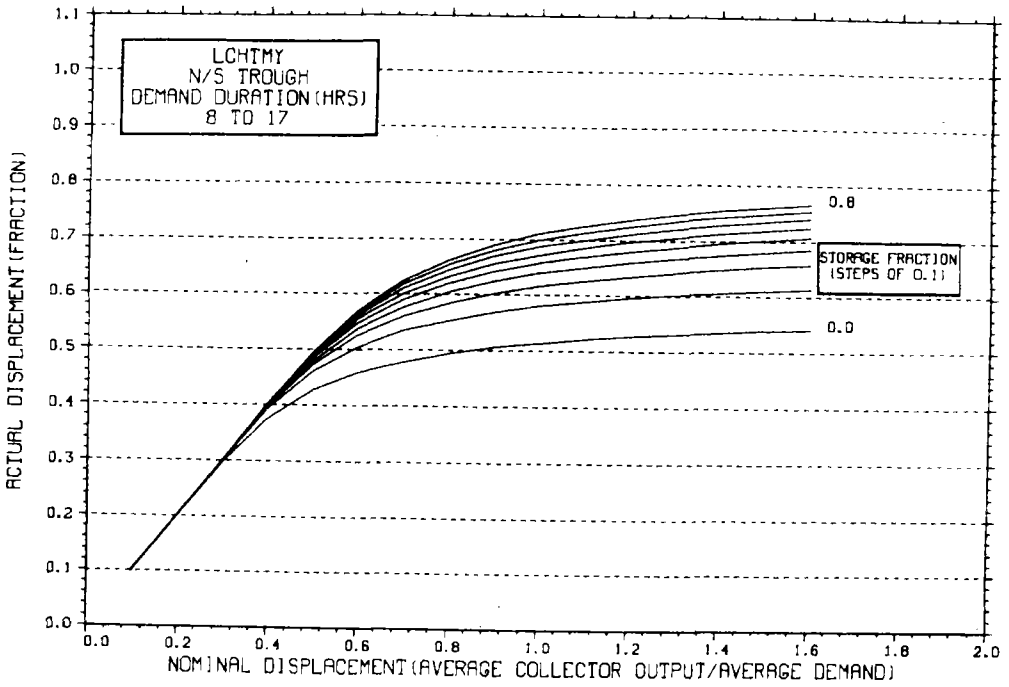

ENERGY INCIDENT ON COLLECTOR APERTURE

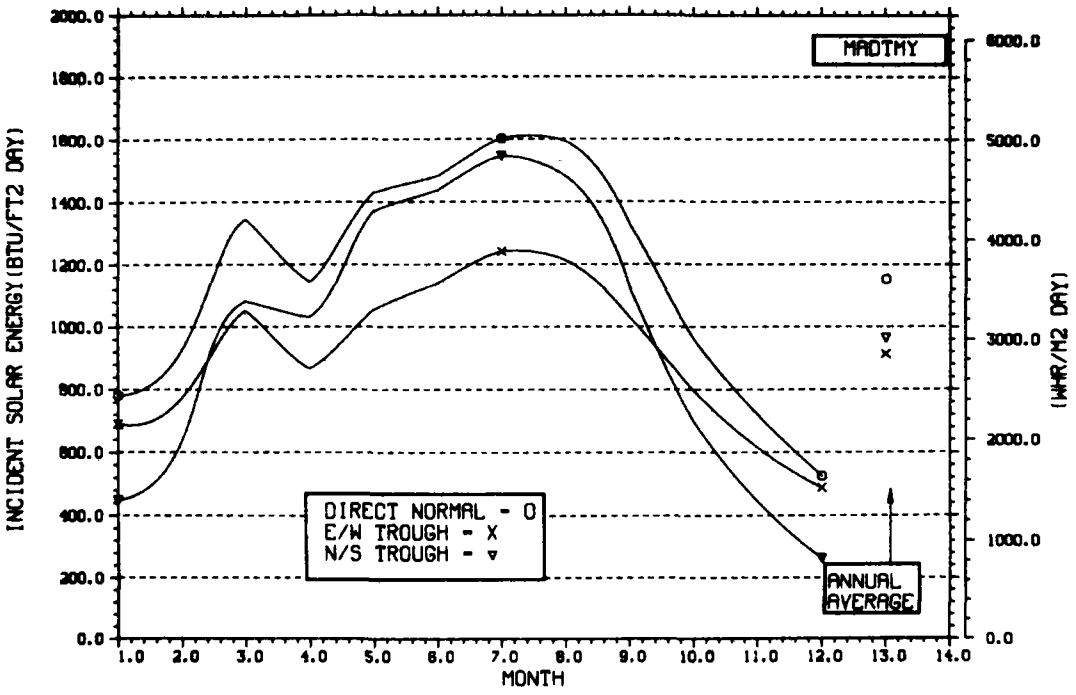

ANNUAL NONFIRST ROW SHADING

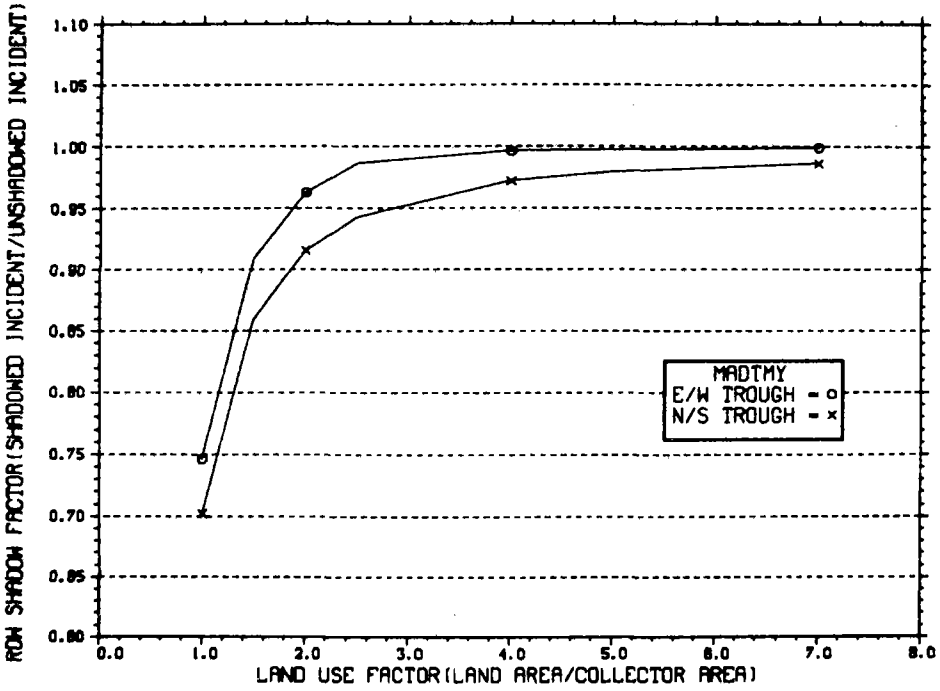

PERFORMANCE VARIATION WITH COLLECTOR AZIMUTH

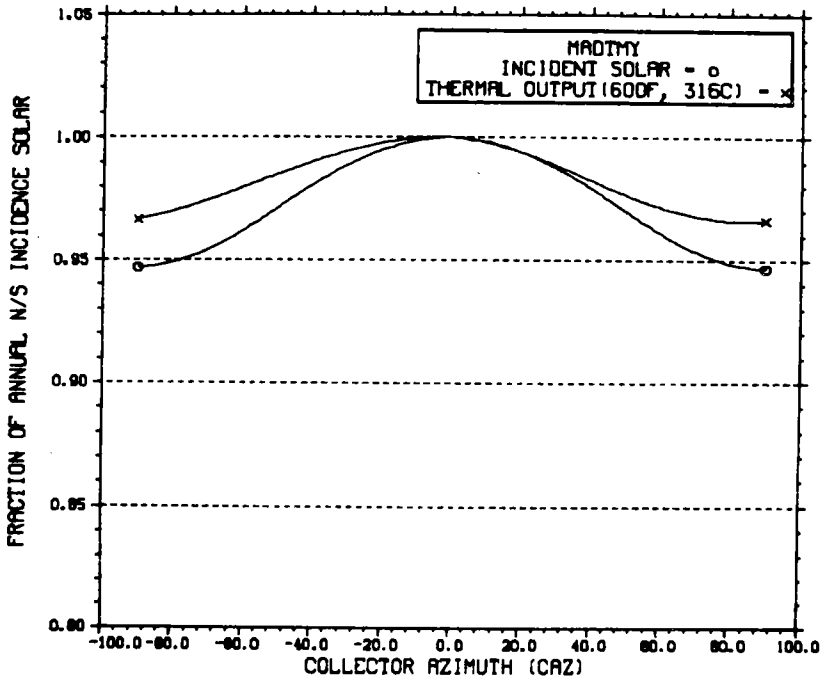

TEMPERATURE DEPENDENCE OF ANNUAL PERFORMANCE

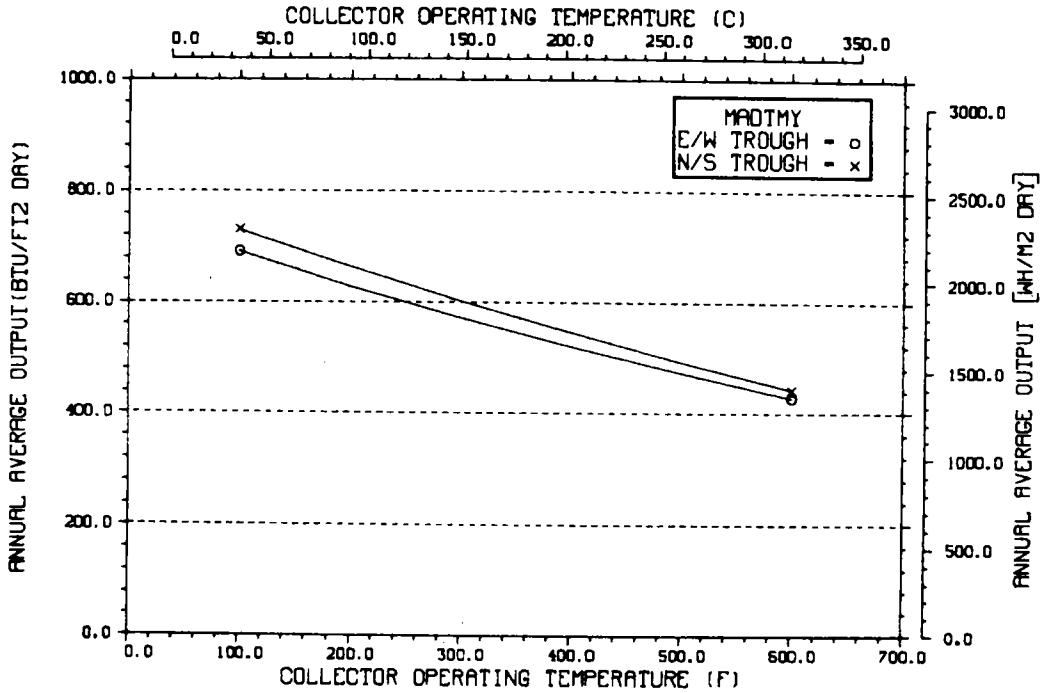

TEMPERATURE DEPENDENCE OF MONTHLY PERFORMANCE

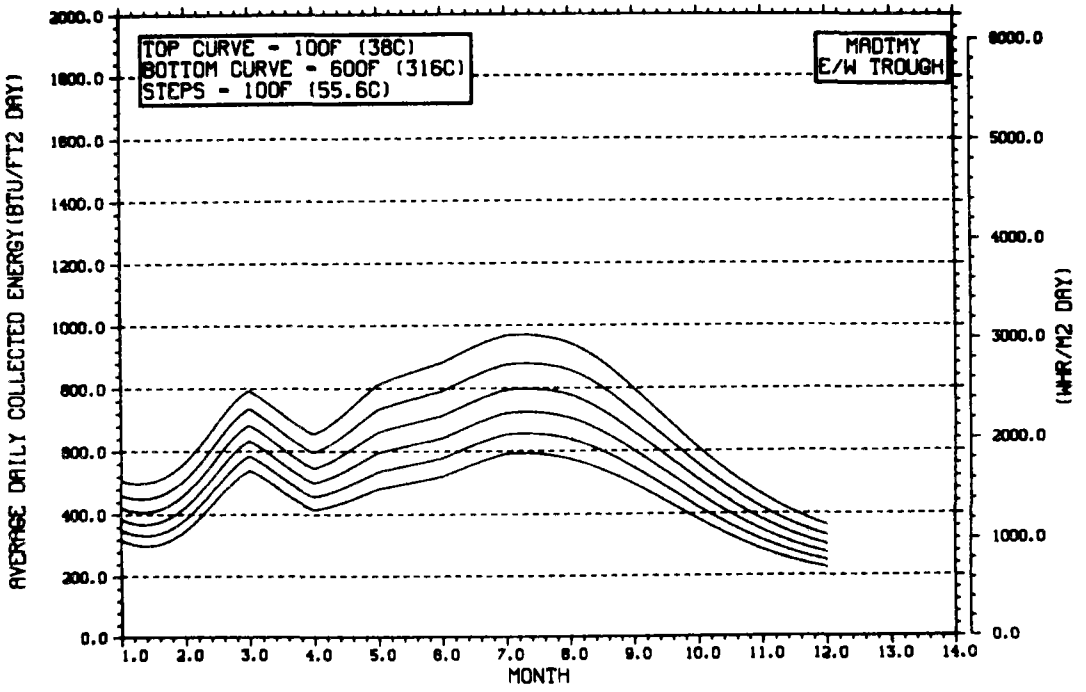

TEMPERATURE DEPENDENCE OF MONTHLY PERFORMANCE

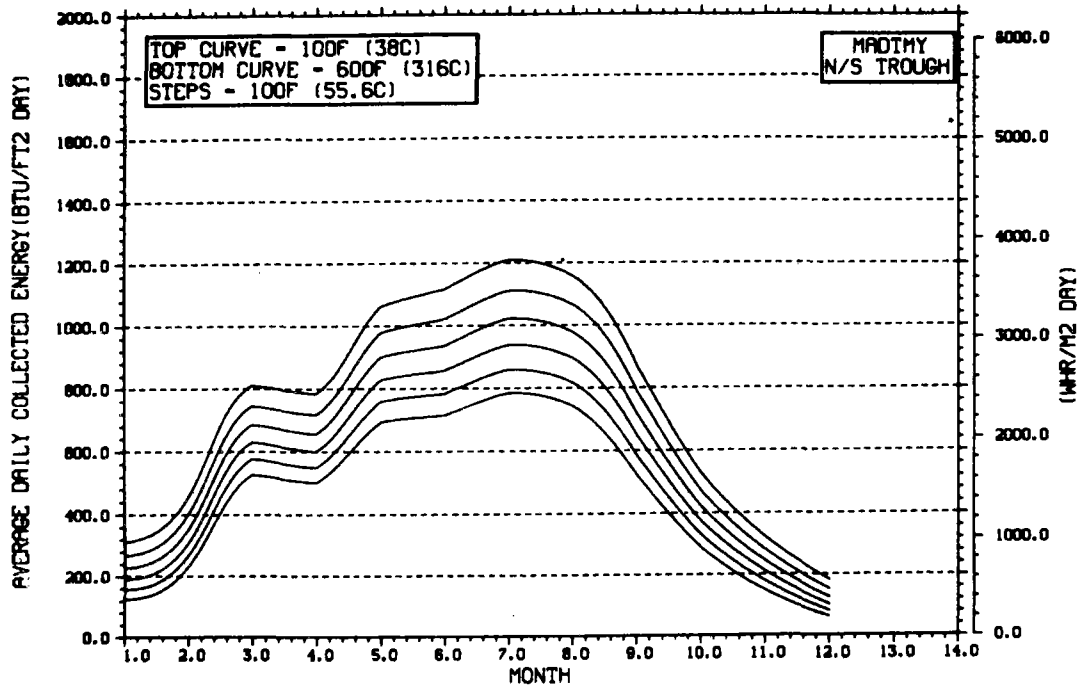

STORAGE SIZING GRAPH FOR CONSTANT ANNUAL DEMAND

NO WEEKEND SHUTDOWN

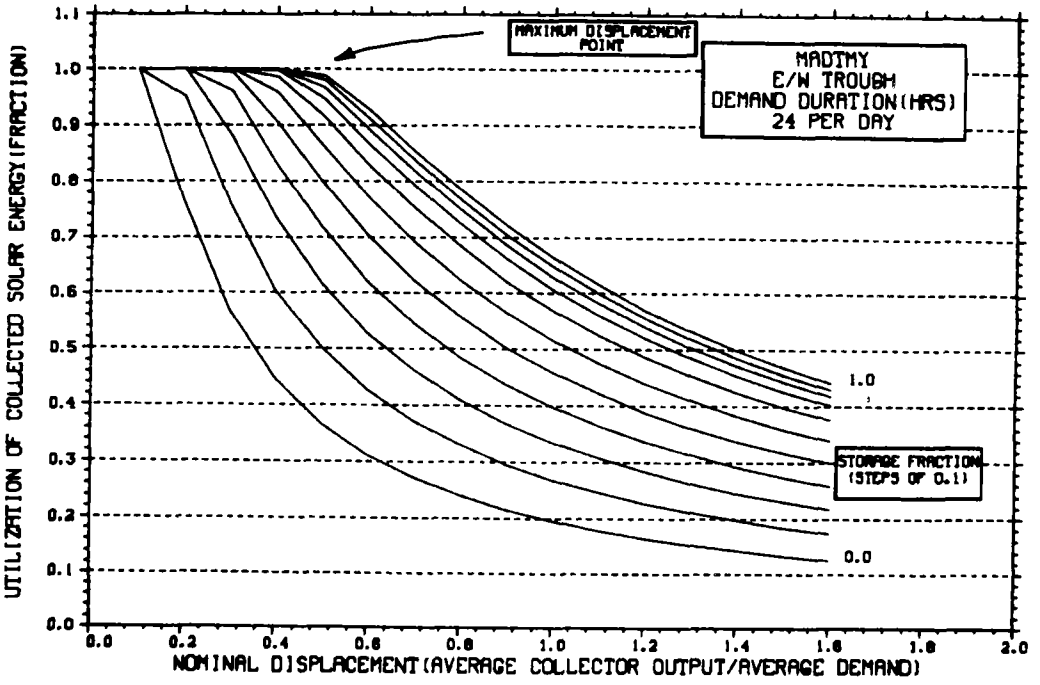

STORAGE SIZING GRAPH FOR CONSTANT ANNUAL DEMAND

NO WEEKEND SHUTDOWN

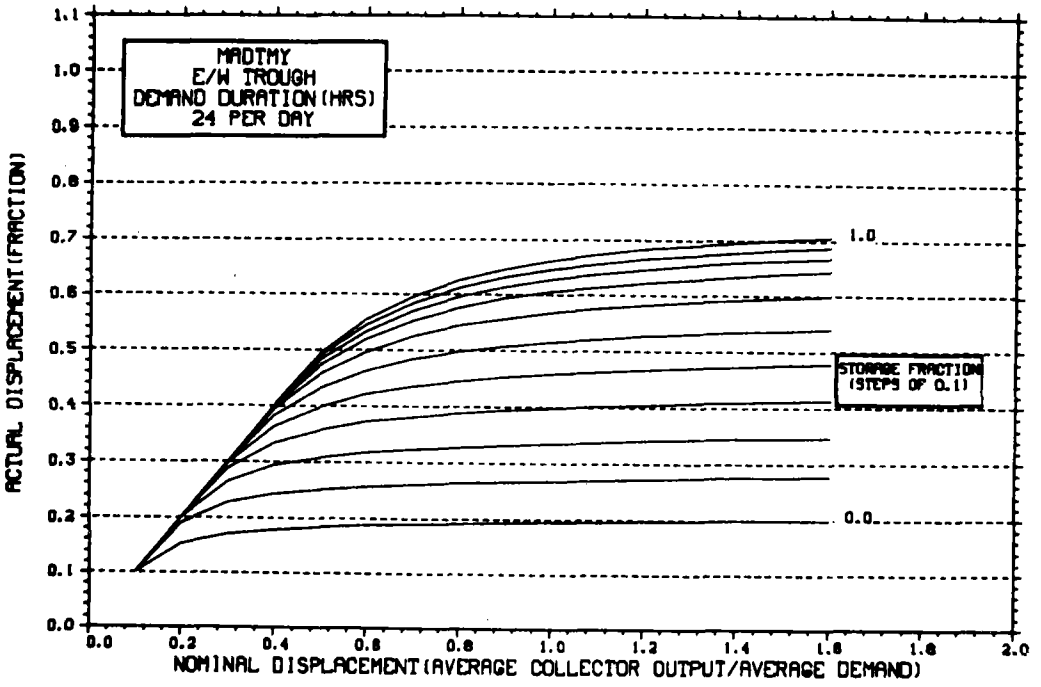

STORAGE SIZING GRAPH FOR CONSTANT ANNUAL DEMAND

NO WEEKEND SHUTDOWN

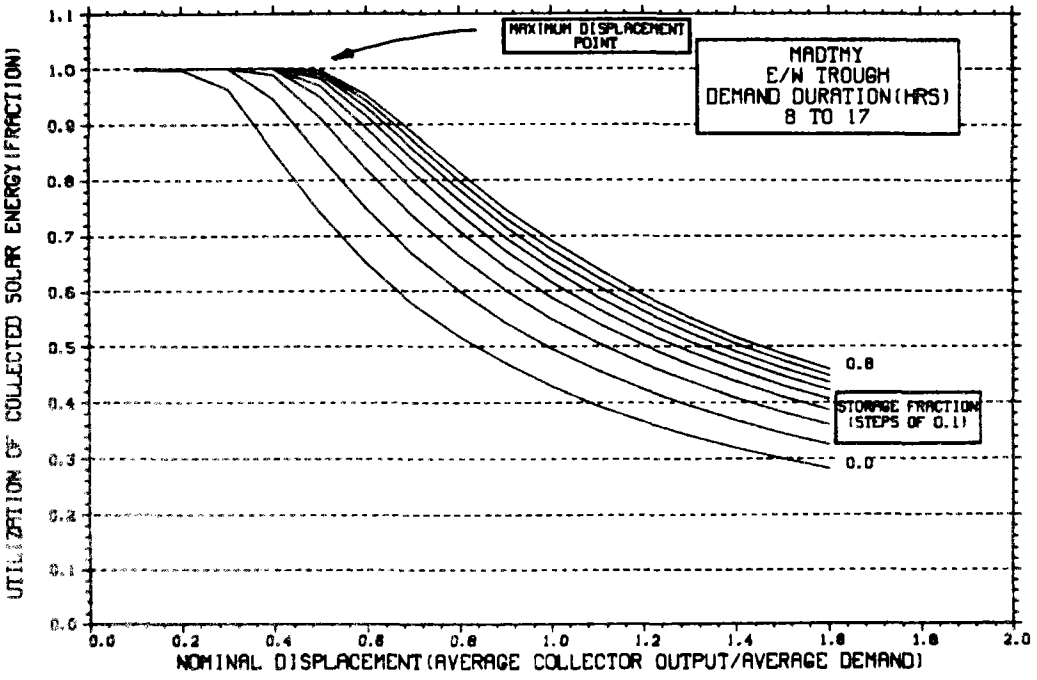

STORAGE SIZING GRAPH FOR CONSTANT ANNUAL DEMAND

NO WEEKEND SHUTDOWN

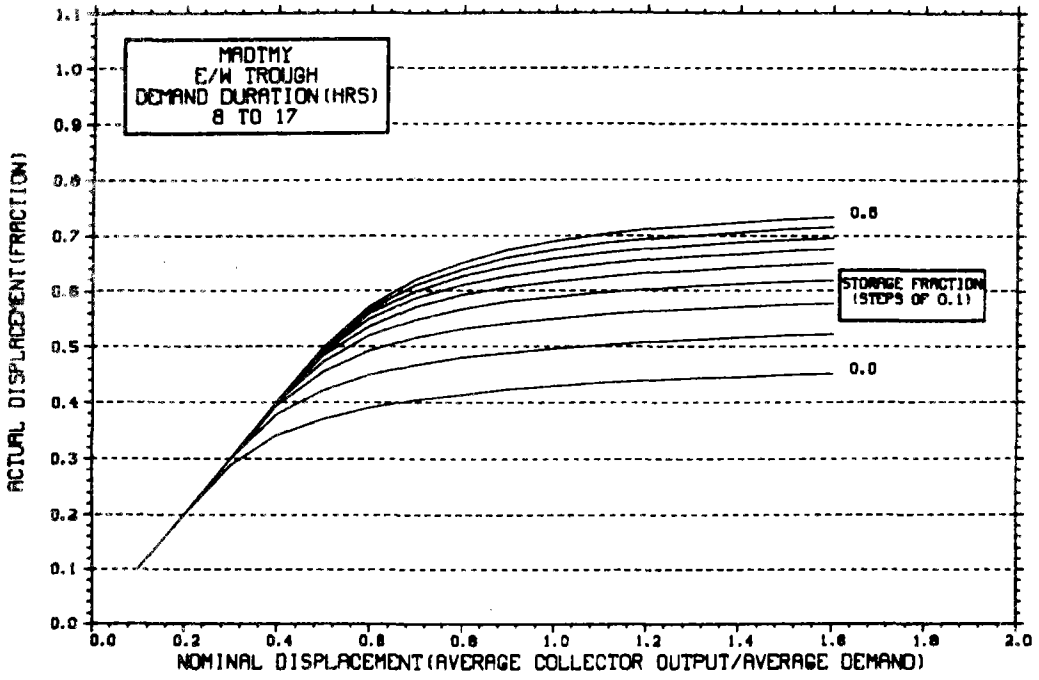

STORAGE SIZING GRAPH FOR CONSTANT ANNUAL DEMAND

NO WEEKEND SHUTDOWN

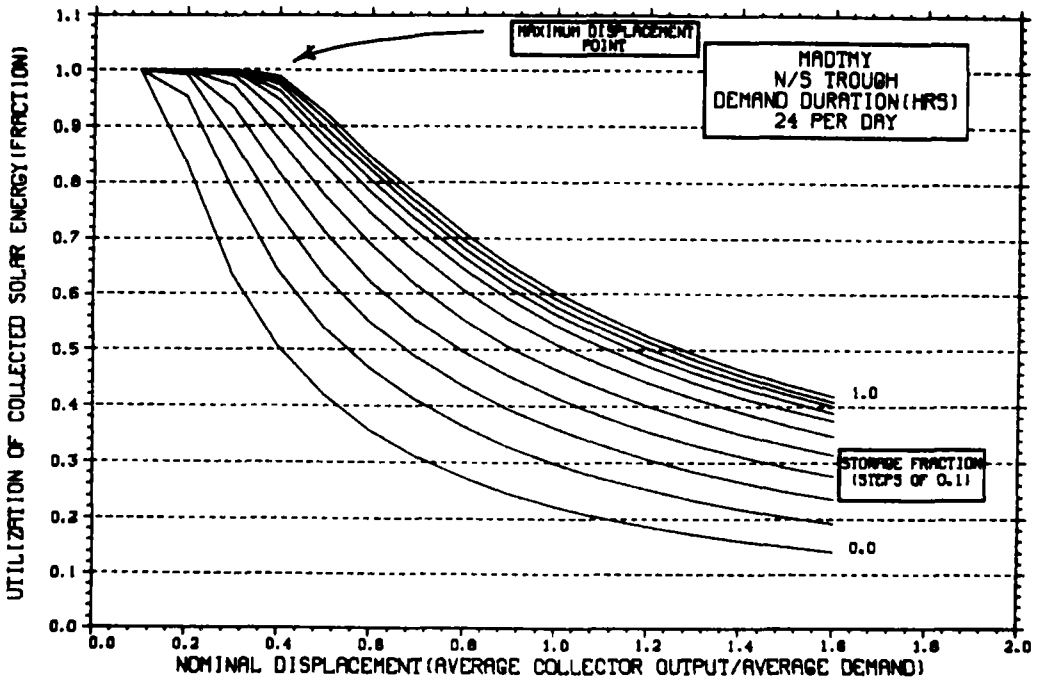

STORAGE SIZING GRAPH FOR CONSTANT ANNUAL DEMAND

NO WEEKEND SHUTDOWN

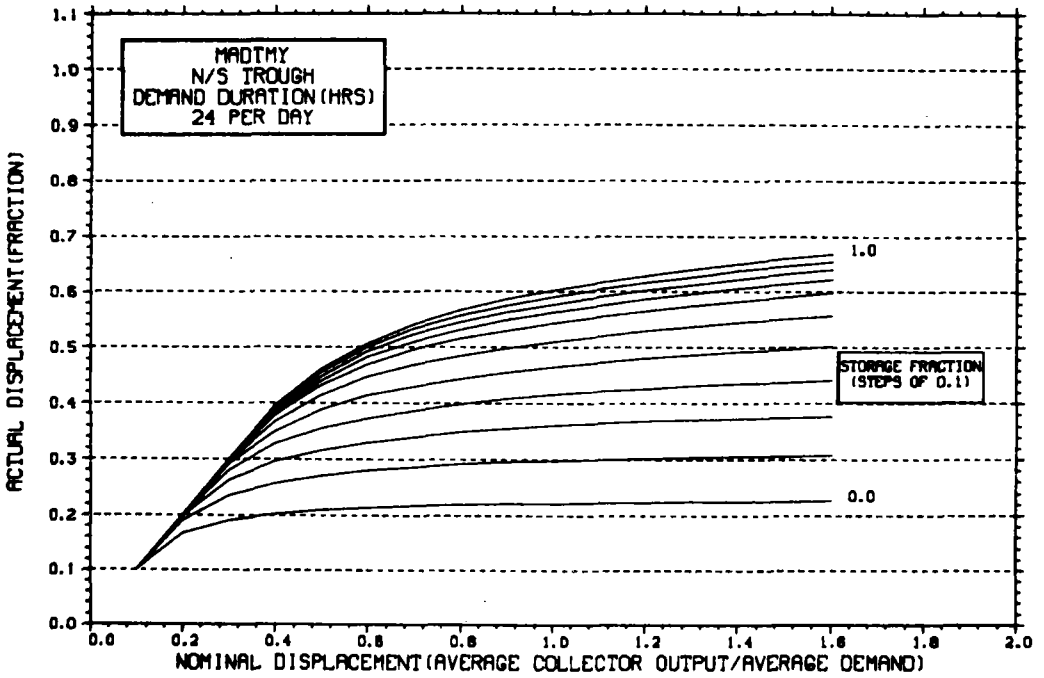

STORAGE SIZING GRAPH FOR CONSTANT ANNUAL DEMAND

NO WEEKEND SHUTDOWN

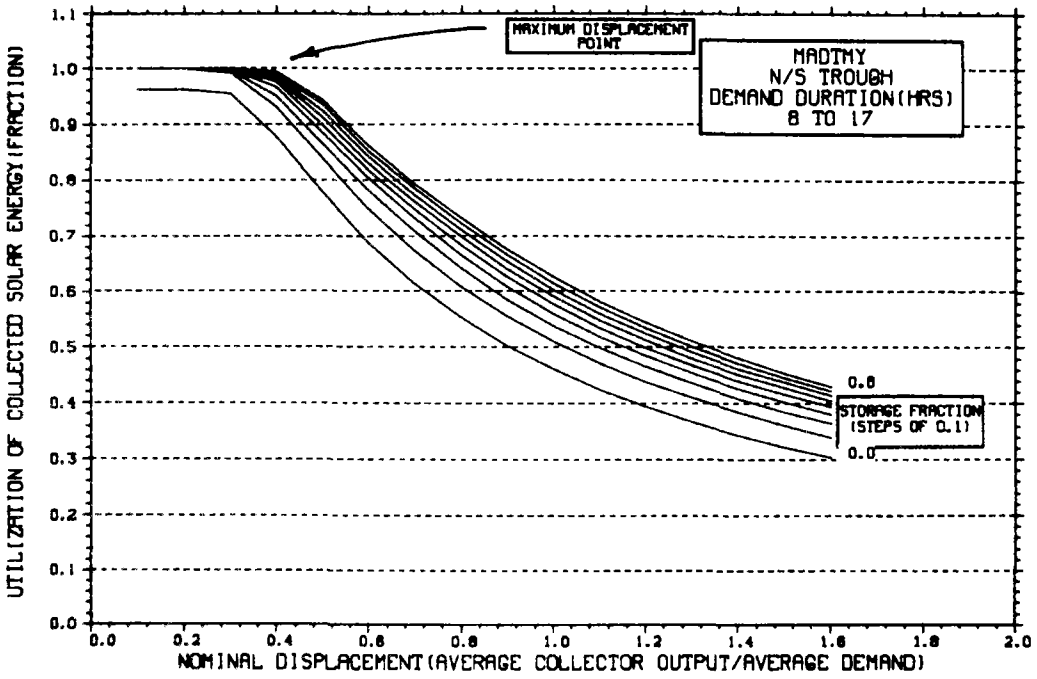

STORAGE SIZING GRAPH FOR CONSTANT ANNUAL DEMAND

NO WEEKEND SHUTDOWN

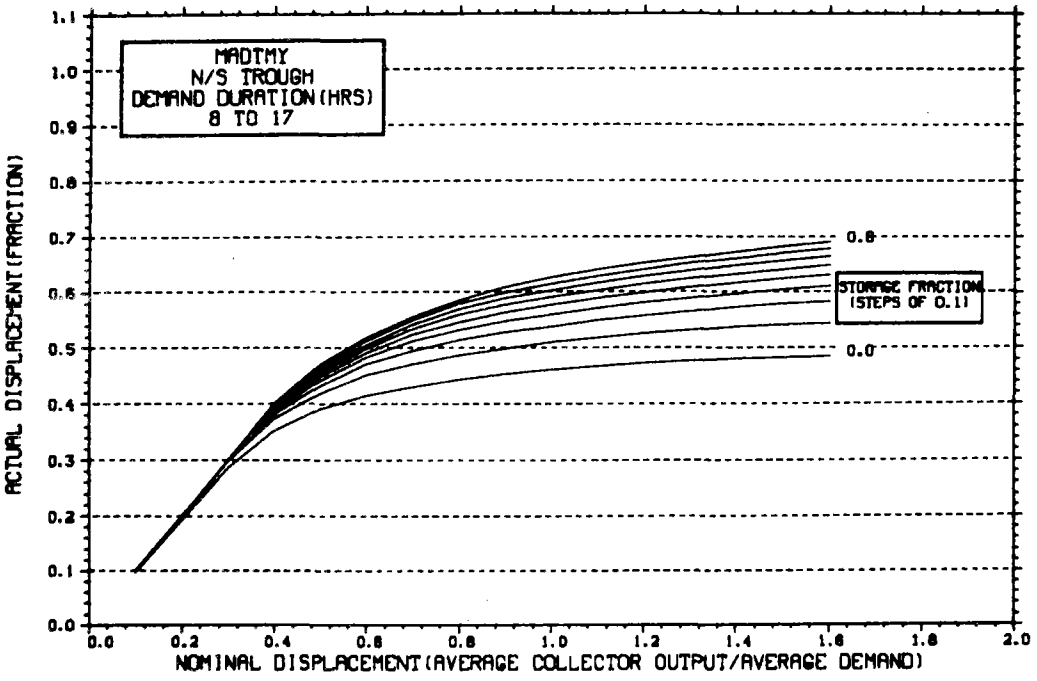

ENERGY INCIDENT ON COLLECTOR APERTURE

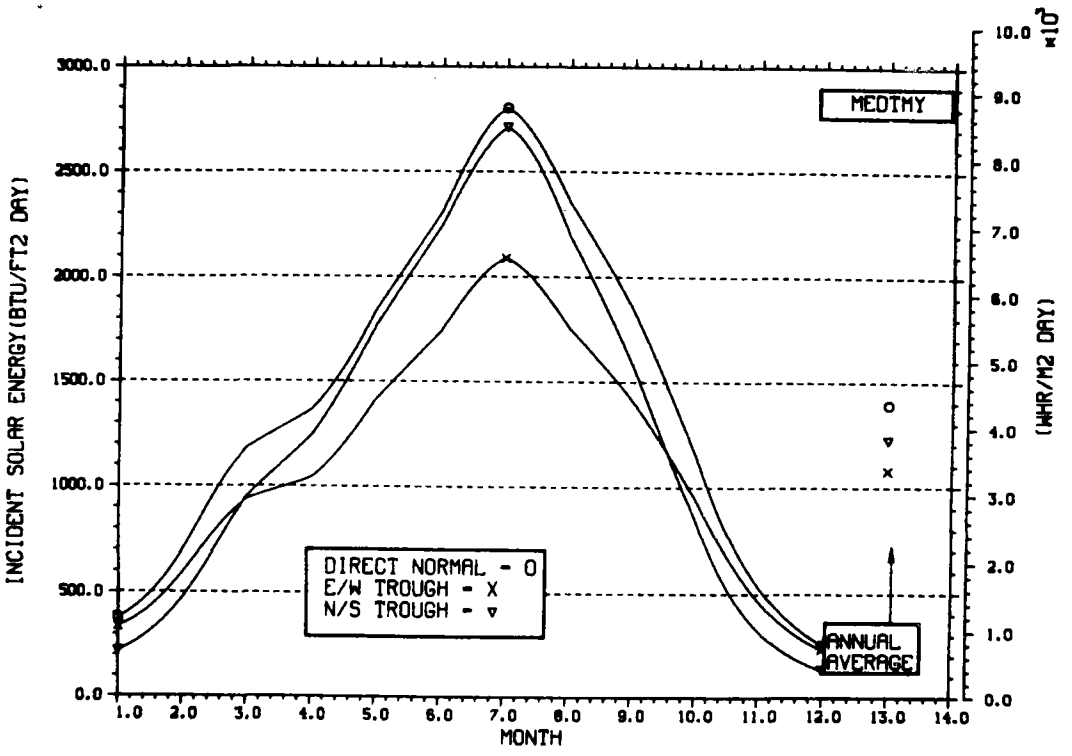

ANNUAL NONFIRST ROW SHADING

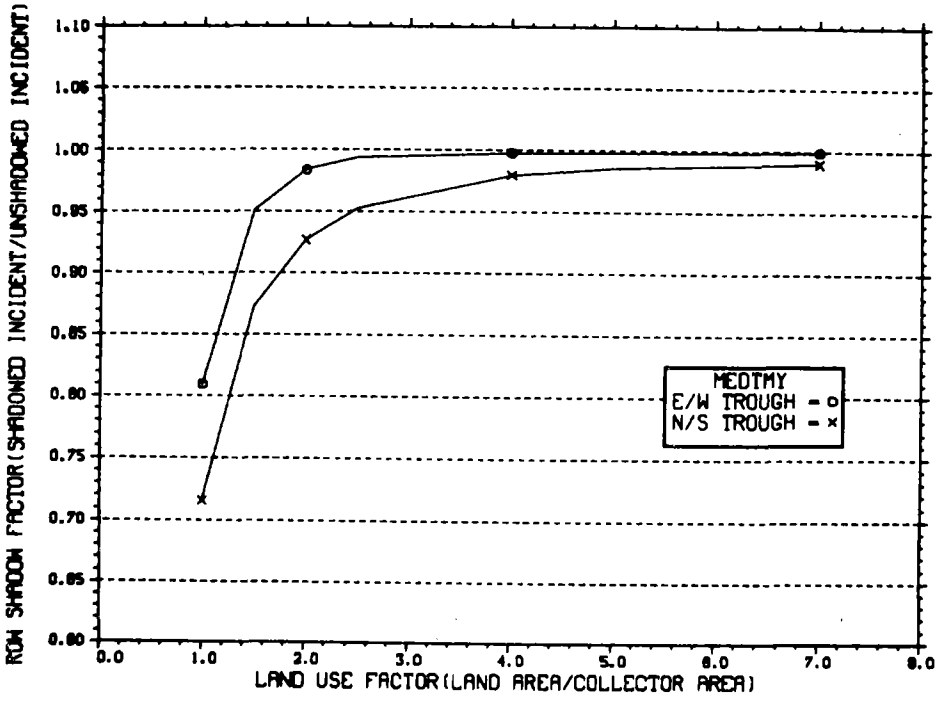

PERFORMANCE VARIATION WITH COLLECTOR AZIMUTH

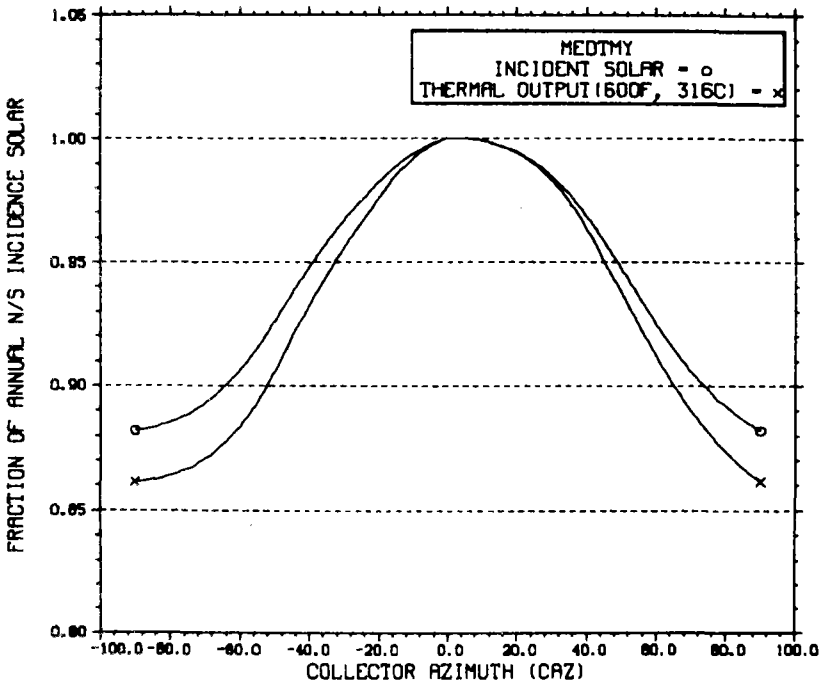

TEMPERATURE DEPENDENCE OF ANNUAL PERFORMANCE

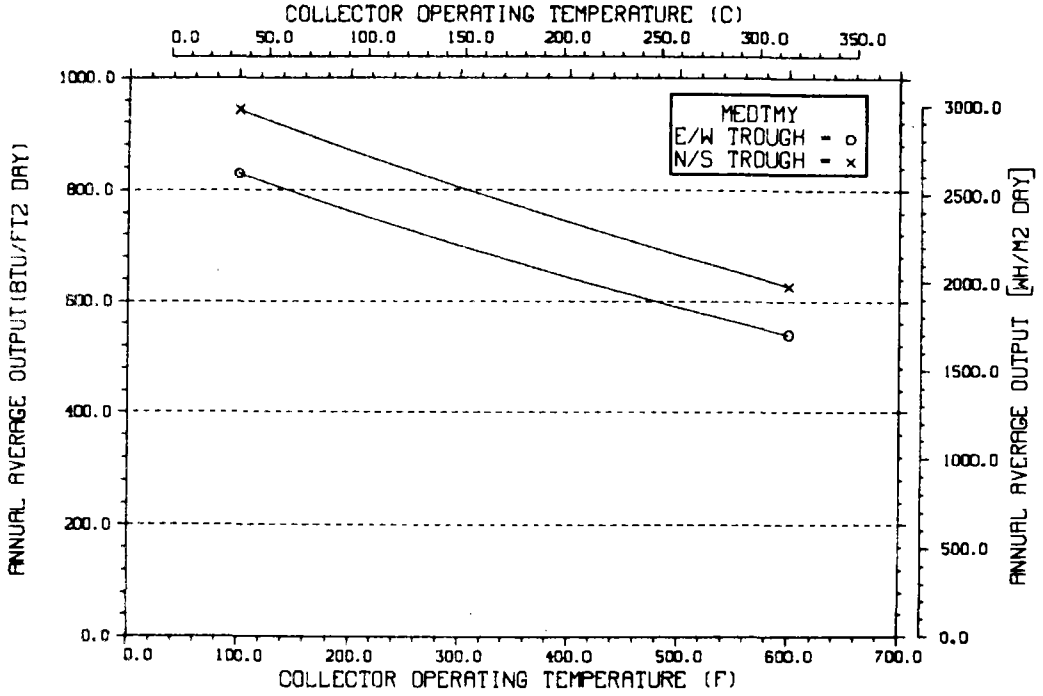

TEMPERATURE DEPENDENCE OF MONTHLY PERFORMANCE

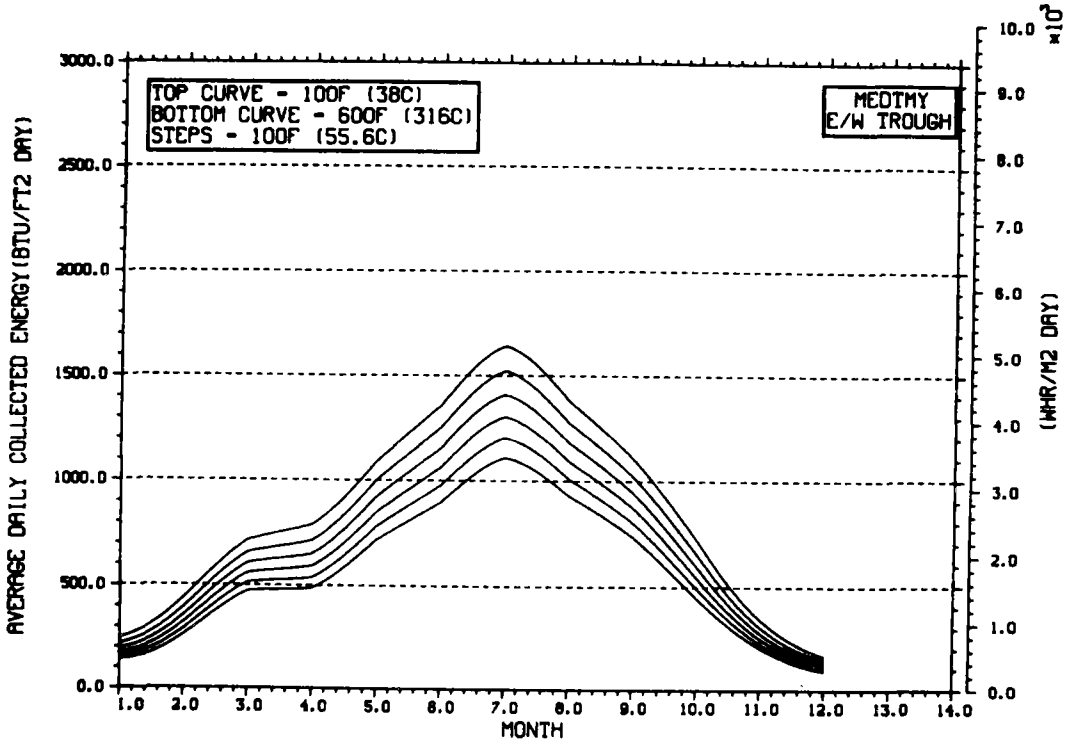

TEMPERATURE DEPENDENCE OF MONTHLY PERFORMANCE

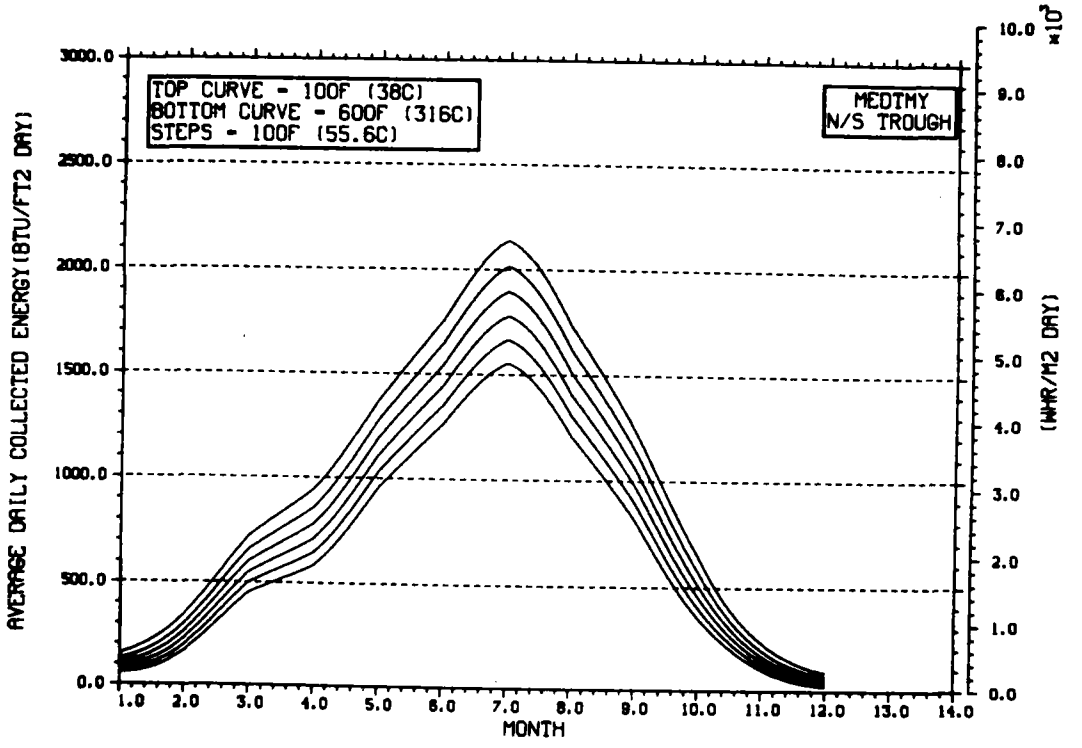

STORAGE SIZING GRAPH FOR CONSTANT ANNUAL DEMAND

NO WEEKEND SHUTDOWN

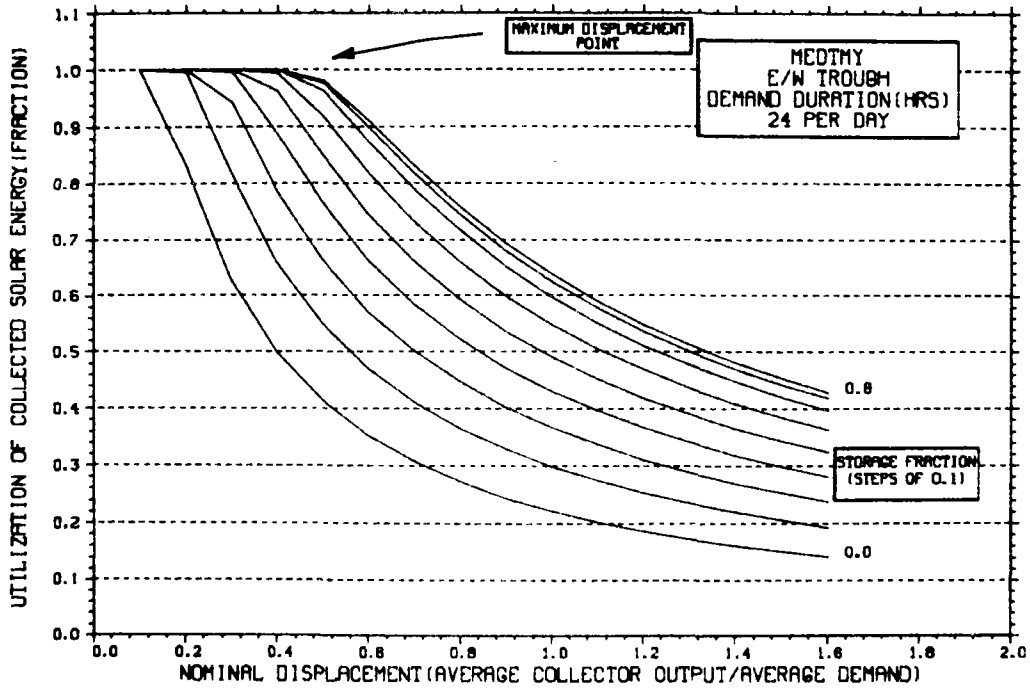

STORAGE SIZING GRAPH FOR CONSTANT ANNUAL DEMAND

NO WEEKEND SHUTDOWN

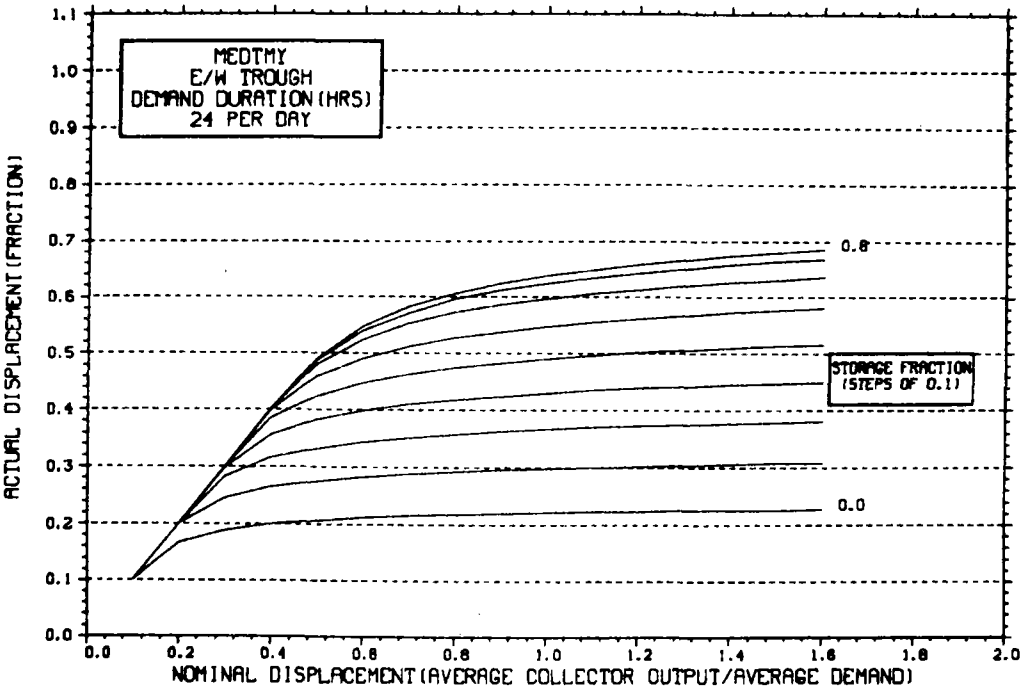

STORAGE SIZING GRAPH FOR CONSTANT ANNUAL DEMAND

NO WEEKEND SHUTDOWN

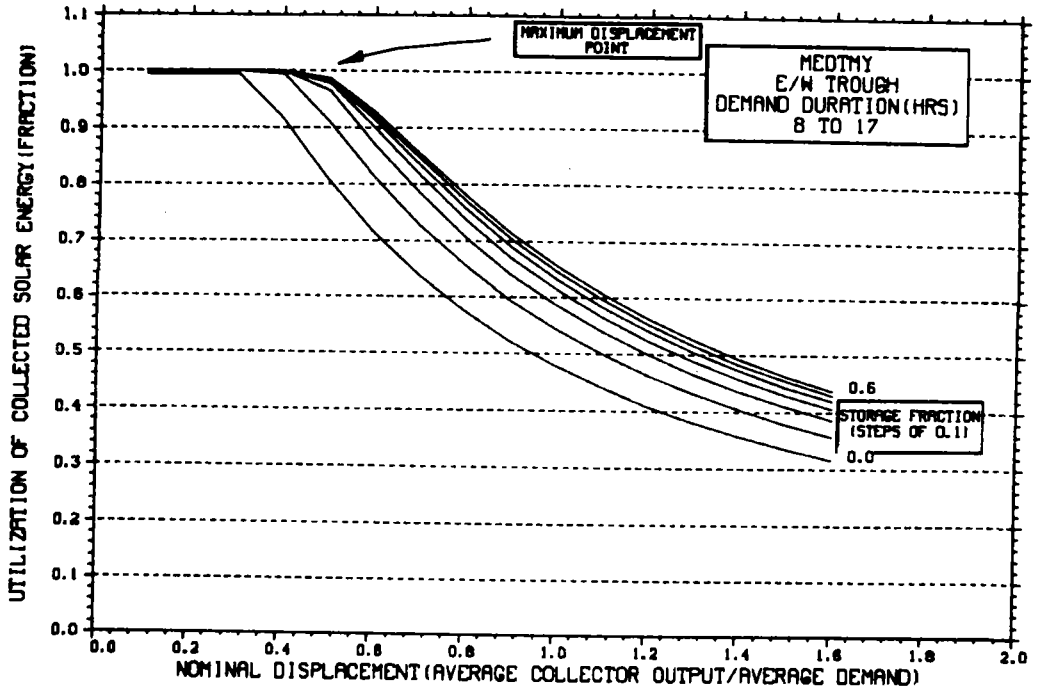

STORAGE SIZING GRAPH FOR CONSTANT ANNUAL DEMAND

NO WEEKEND SHUTDOWN

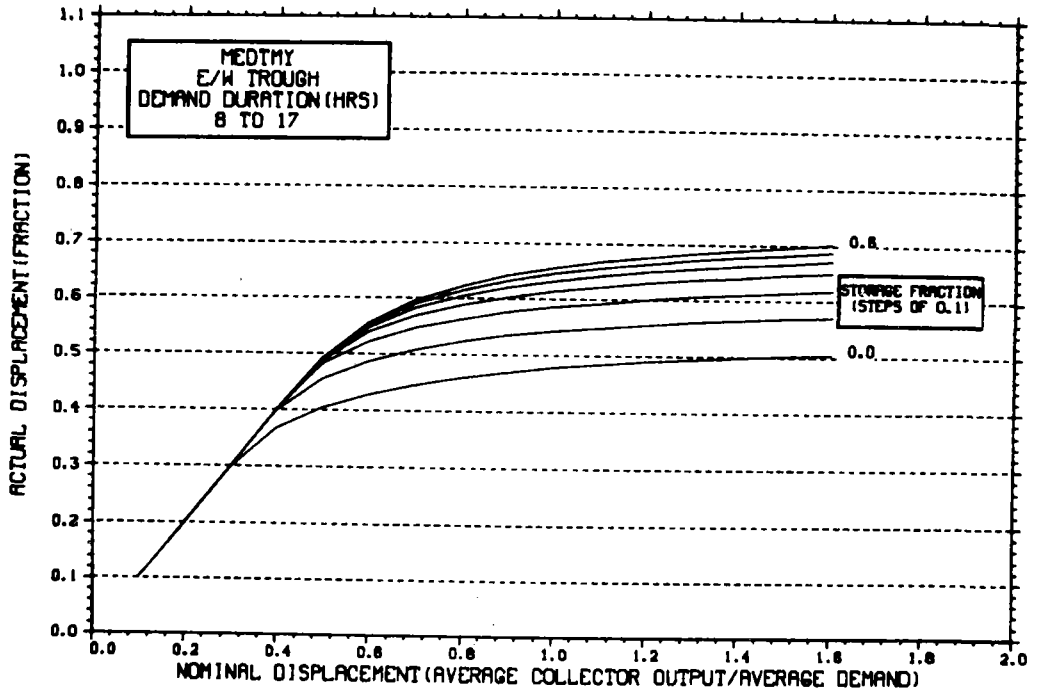

STORAGE SIZING GRAPH FOR CONSTANT ANNUAL DEMAND

NO WEEKEND SHUTDOWN

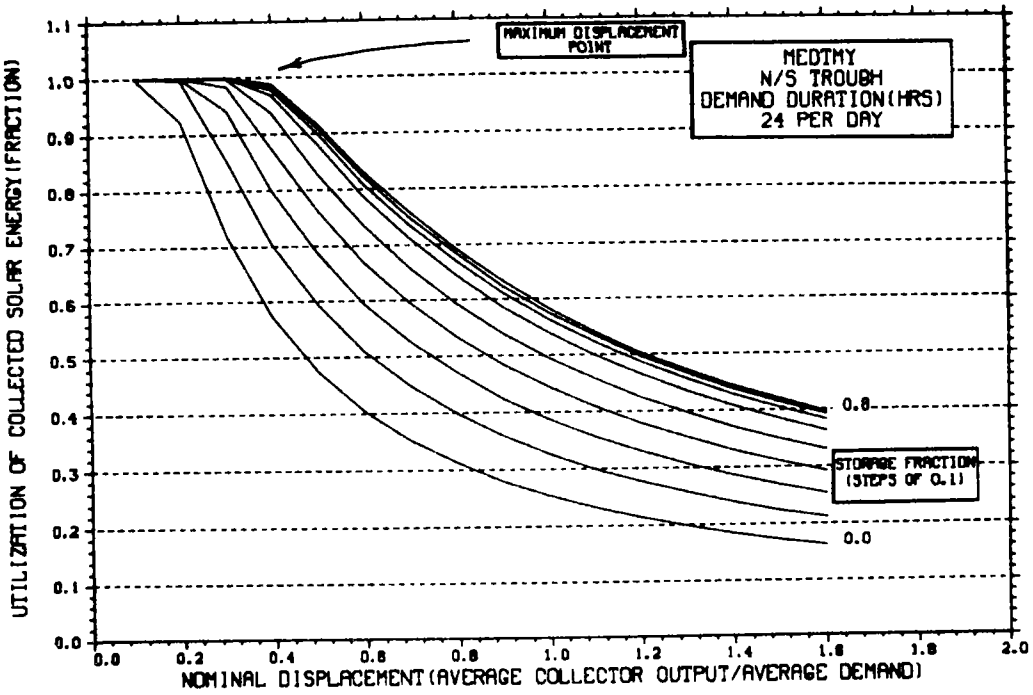

STORAGE SIZING GRAPH FOR CONSTANT ANNUAL DEMAND

NO WEEKEND SHUTDOWN

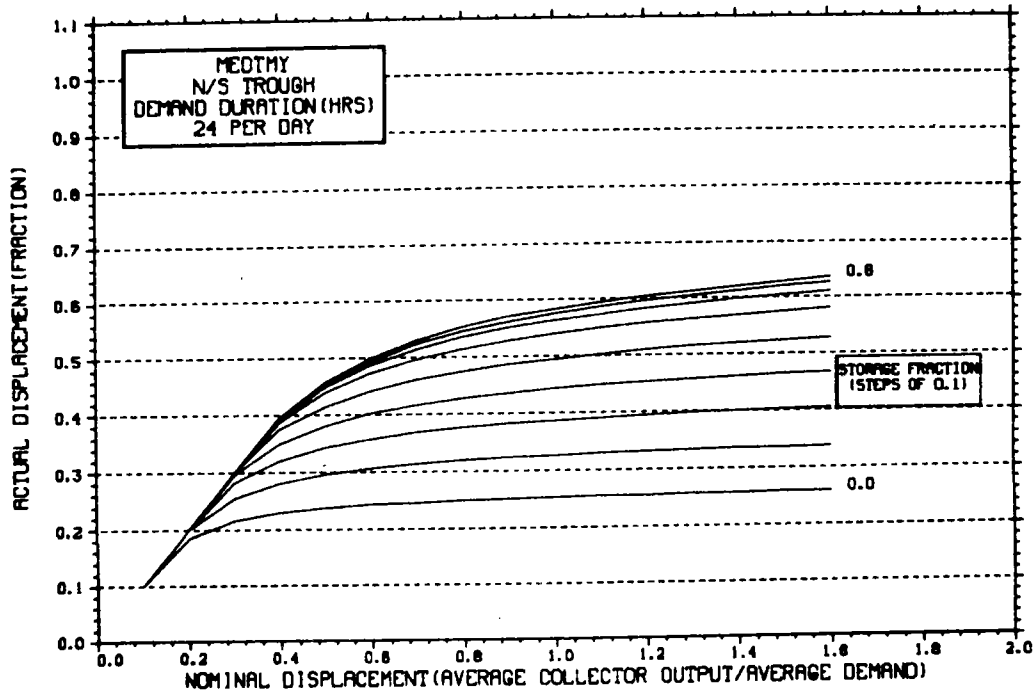

STORAGE SIZING GRAPH FOR CONSTANT ANNUAL DEMAND

NO WEEKEND SHUTDOWN

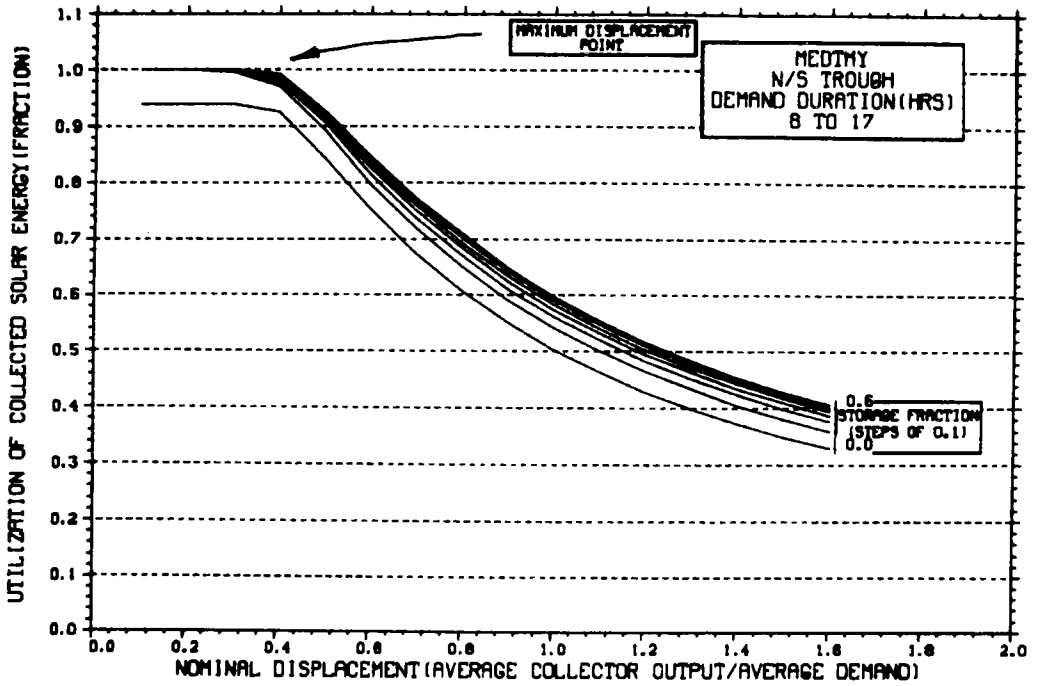

STORAGE SIZING GRAPH FOR CONSTANT ANNUAL DEMAND

NO WEEKEND SHUTDOWN

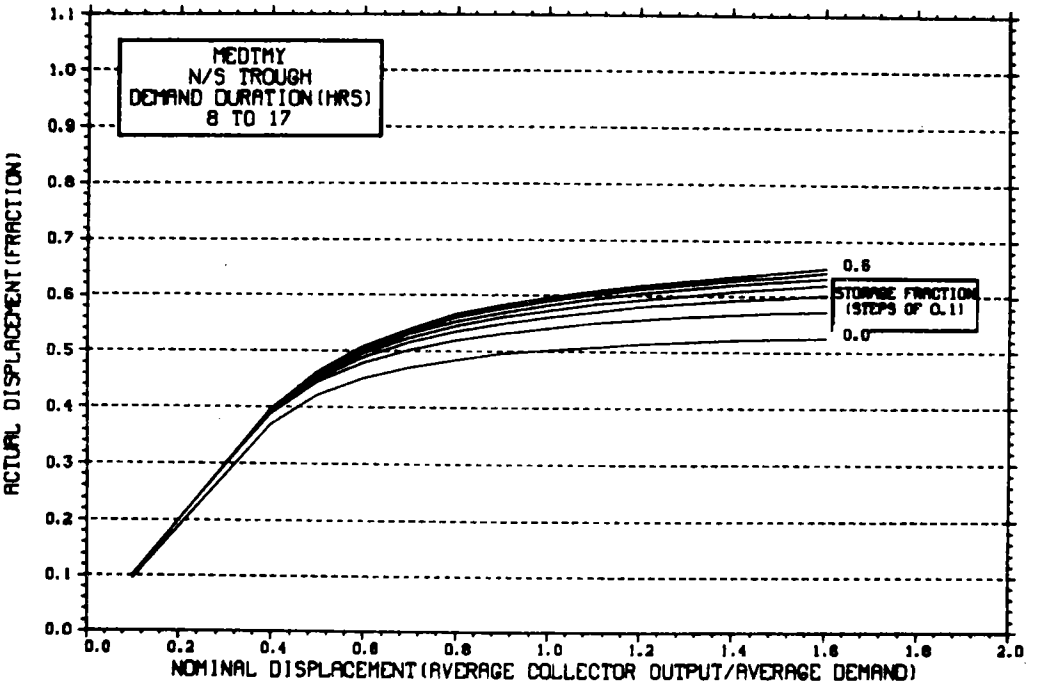

ENERGY INCIDENT ON COLLECTOR APERTURE

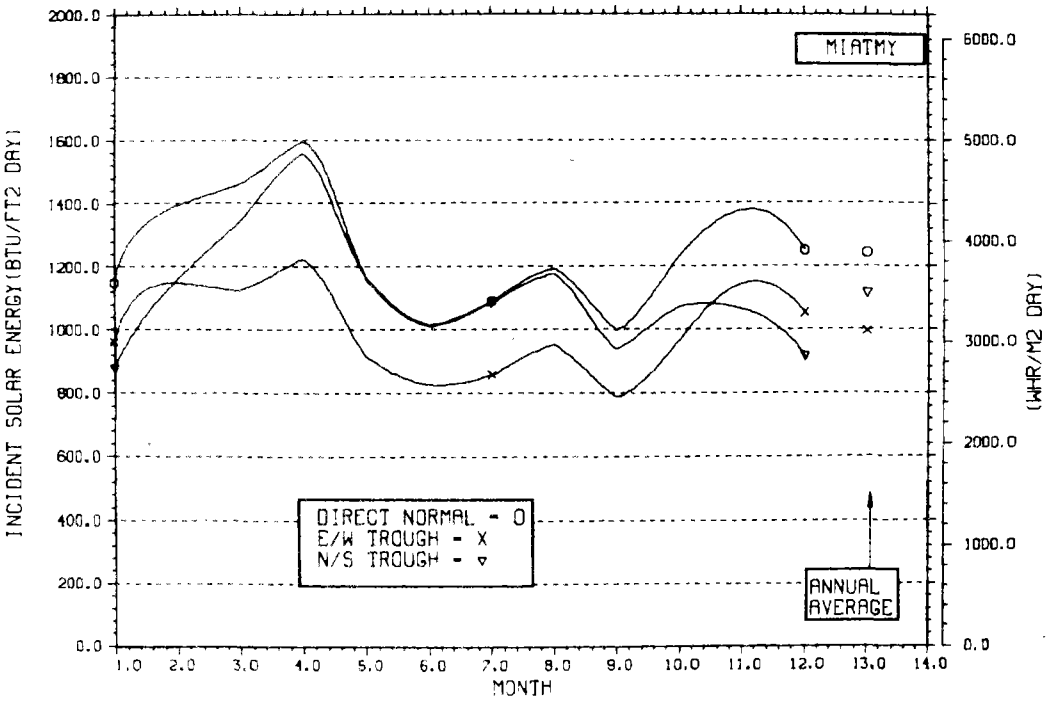

ANNUAL NONFIRST ROW SHADING

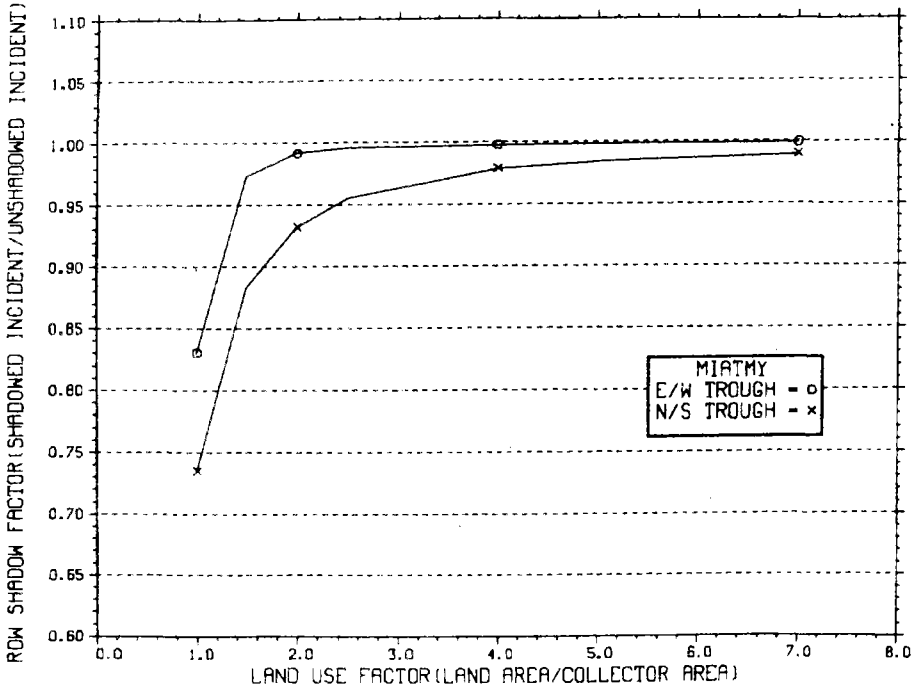

PERFORMANCE VARIATION WITH COLLECTOR AZIMUTH

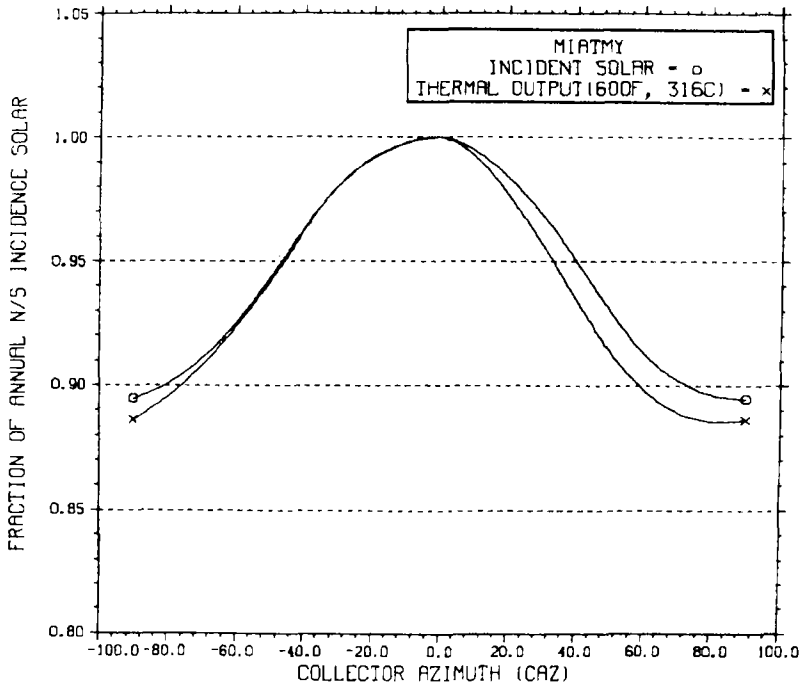

TEMPERATURE DEPENDENCE OF ANNUAL PERFORMANCE

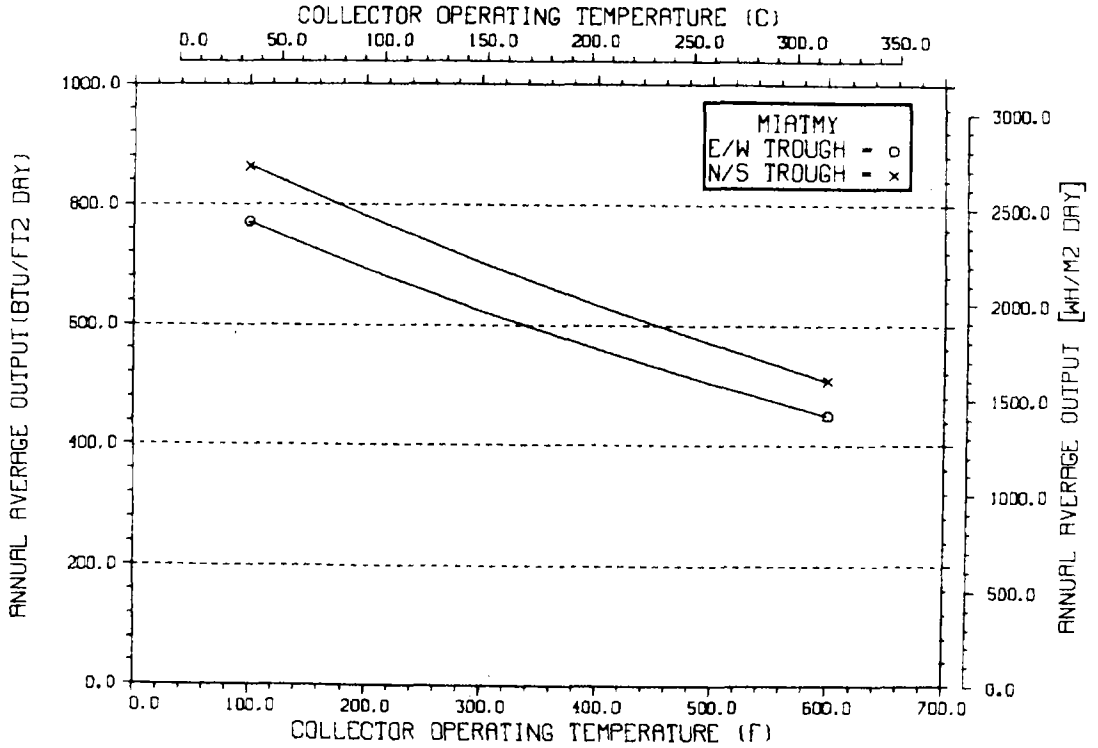

TEMPERATURE DEPENDENCE OF MONTHLY PERFORMANCE

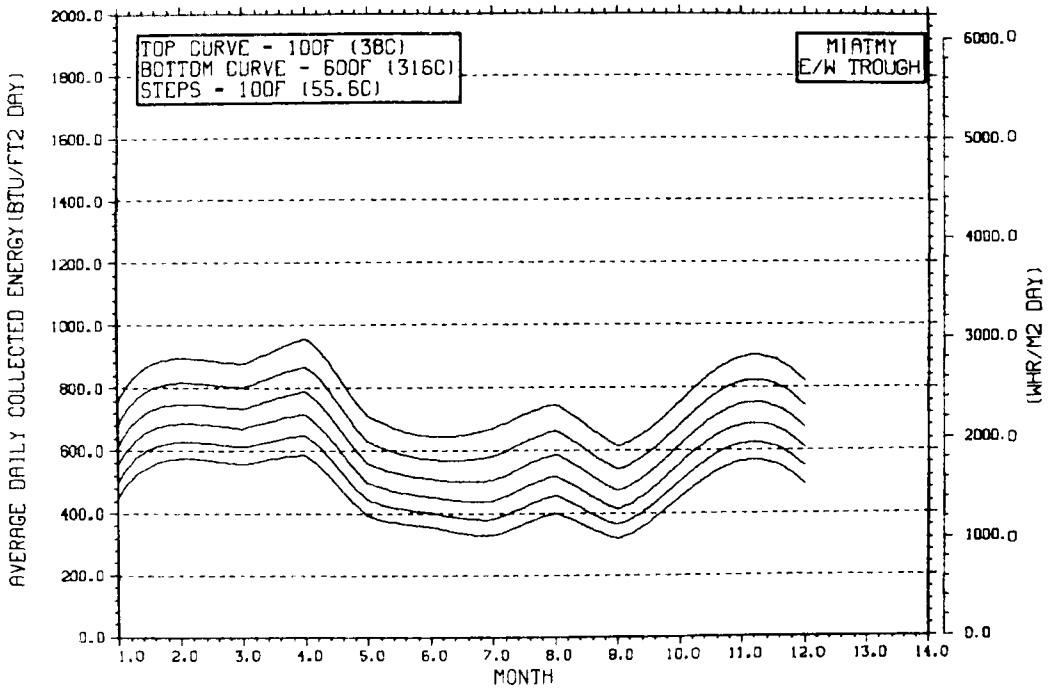

TEMPERATURE DEPENDENCE OF MONTHLY PERFORMANCE

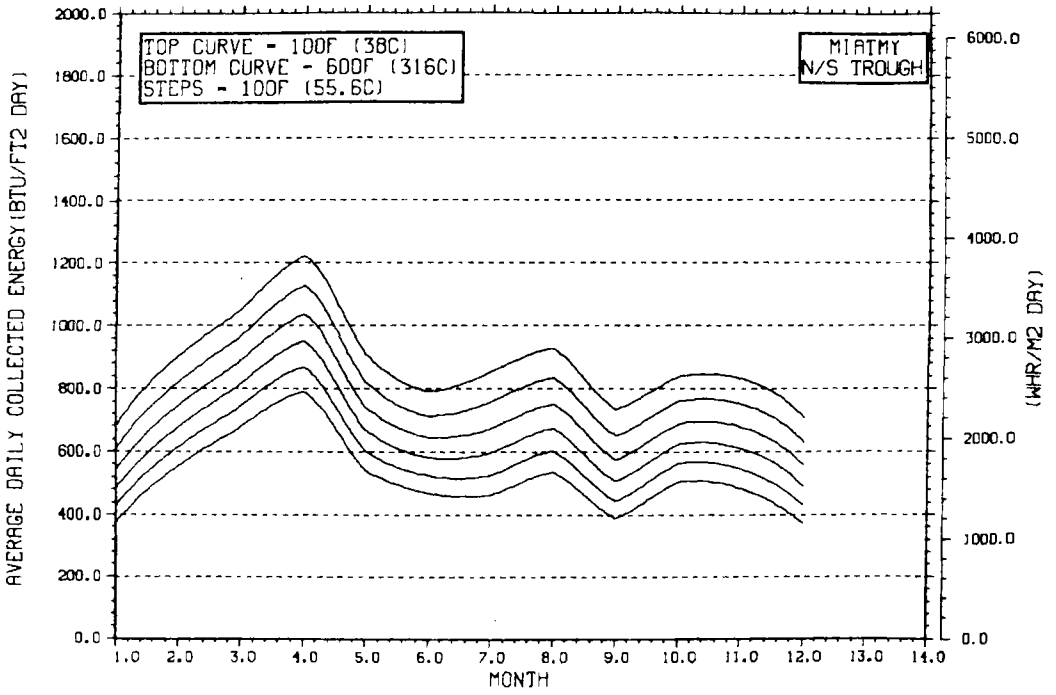

STORAGE SIZING GRAPH FOR CONSTANT ANNUAL DEMAND

NO WEEKEND SHUTDOWN

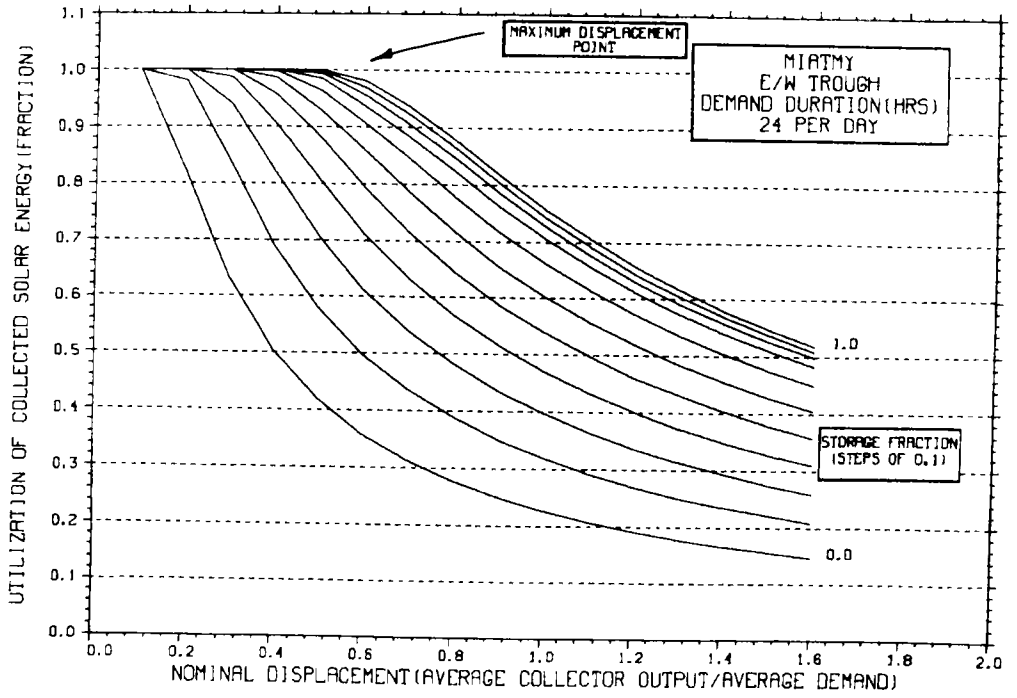

STORAGE SIZING GRAPH FOR CONSTANT ANNUAL DEMAND

NO WEEKEND SHUTDOWN

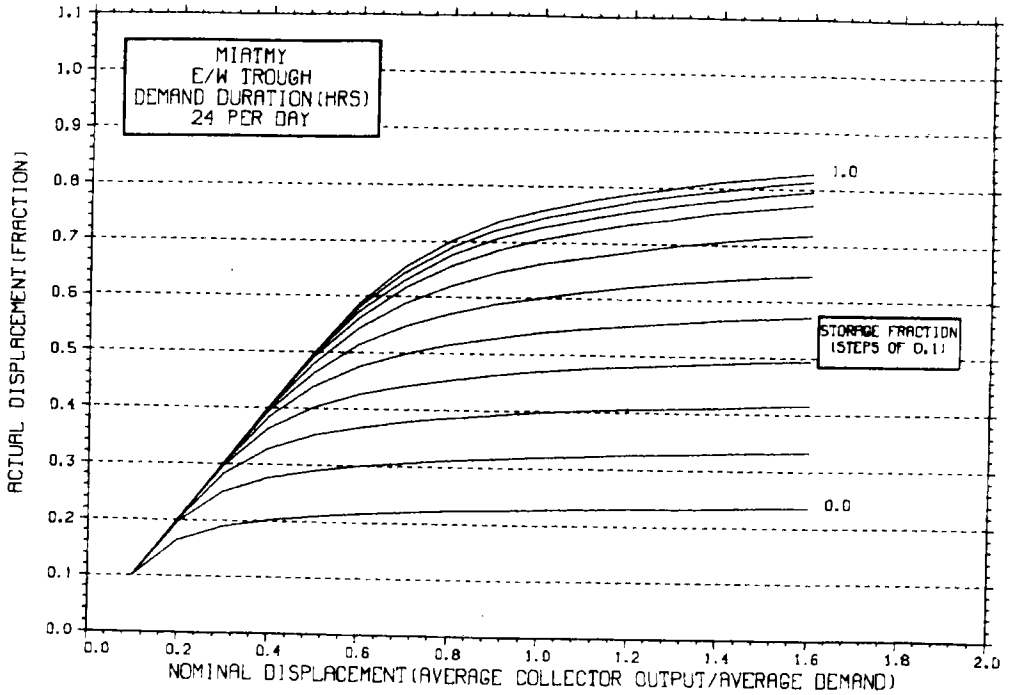

STORAGE SIZING GRAPH FOR CONSTANT ANNUAL DEMAND

NO WEEKEND SHUTDOWN

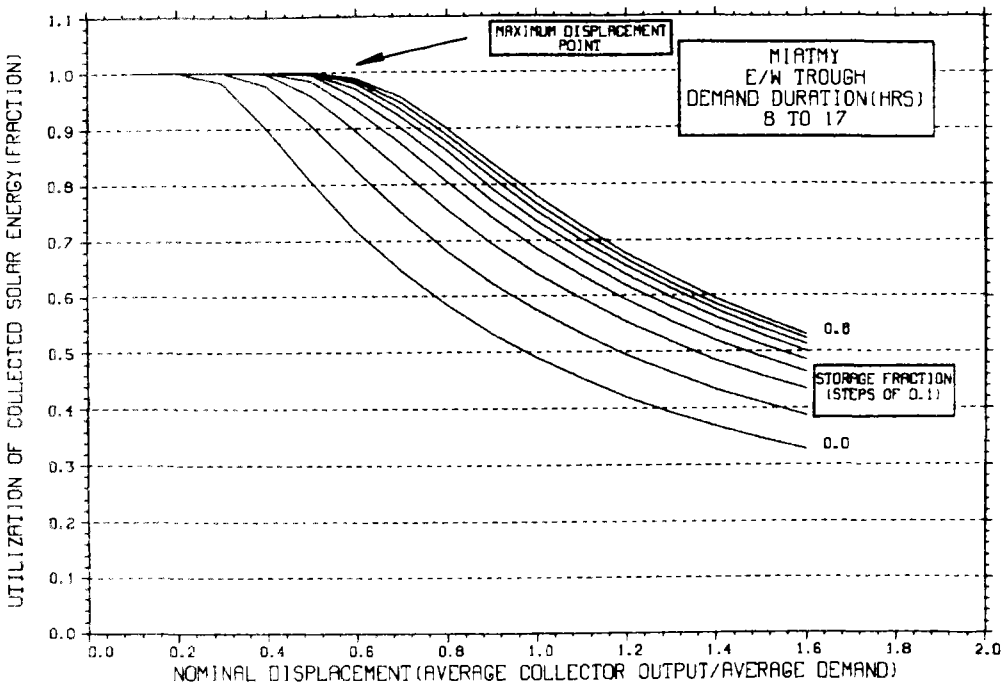

STORAGE SIZING GRAPH FOR CONSTANT ANNUAL DEMAND

NO WEEKEND SHUTDOWN

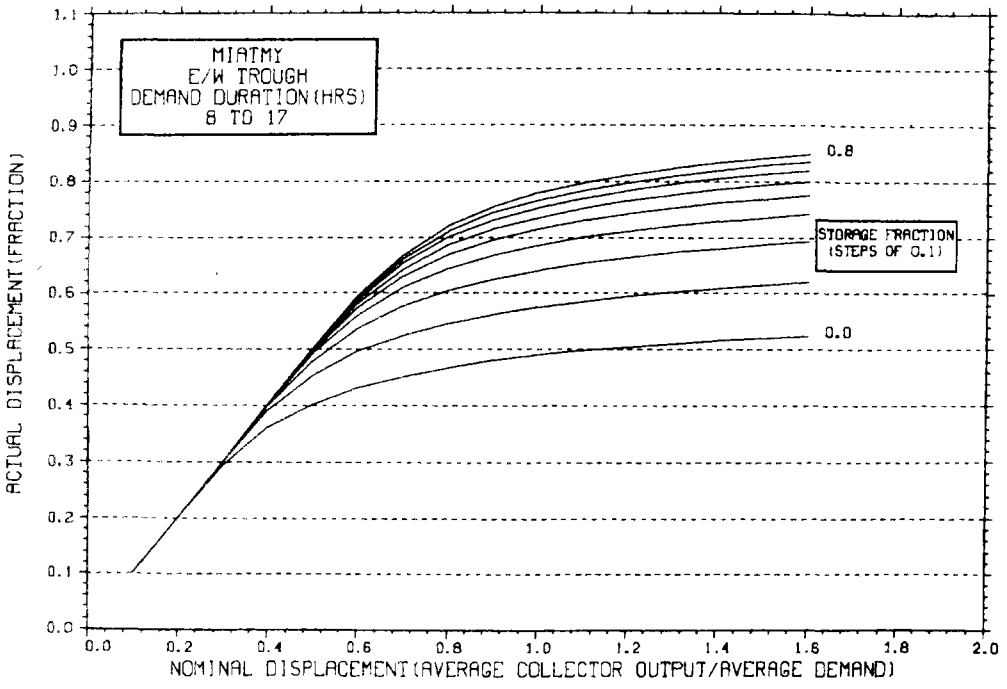

STORAGE SIZING GRAPH FOR CONSTANT ANNUAL DEMAND

NO WEEKEND SHUTDOWN

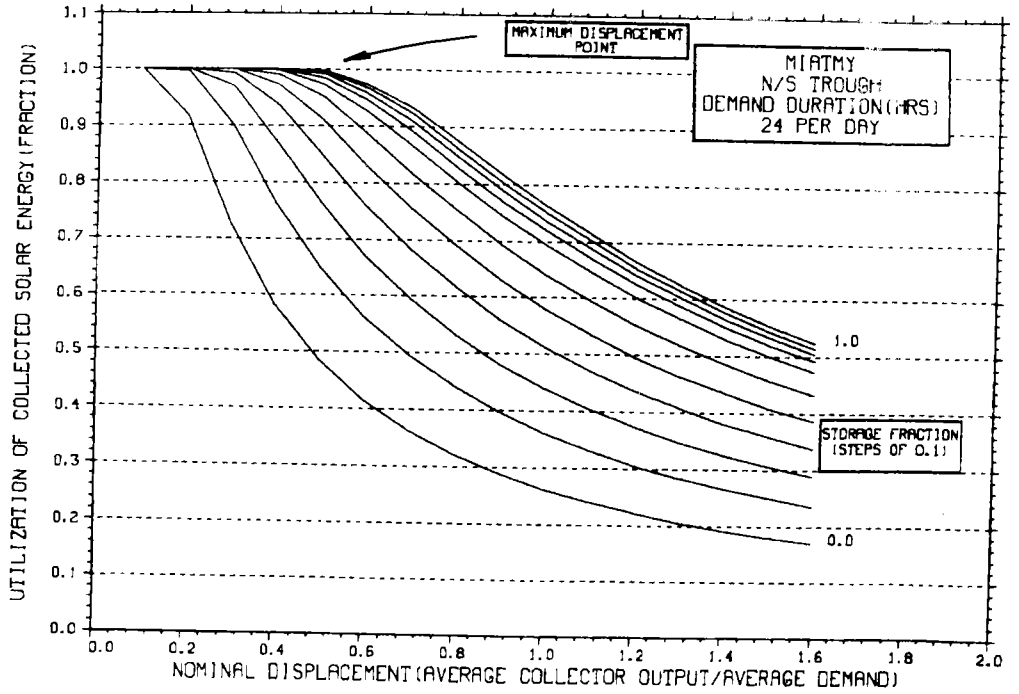

STORAGE SIZING GRAPH FOR CONSTANT ANNUAL DEMAND

NO WEEKEND SHUTDOWN

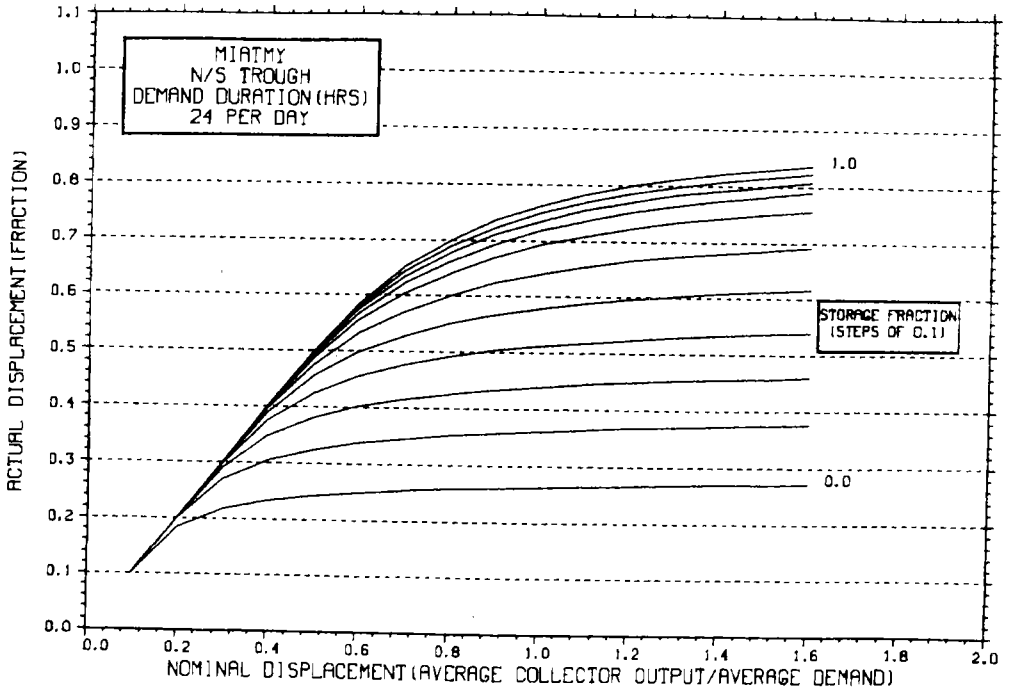

STORAGE SIZING GRAPH FOR CONSTANT ANNUAL DEMAND

NO WEEKEND SHUTDOWN

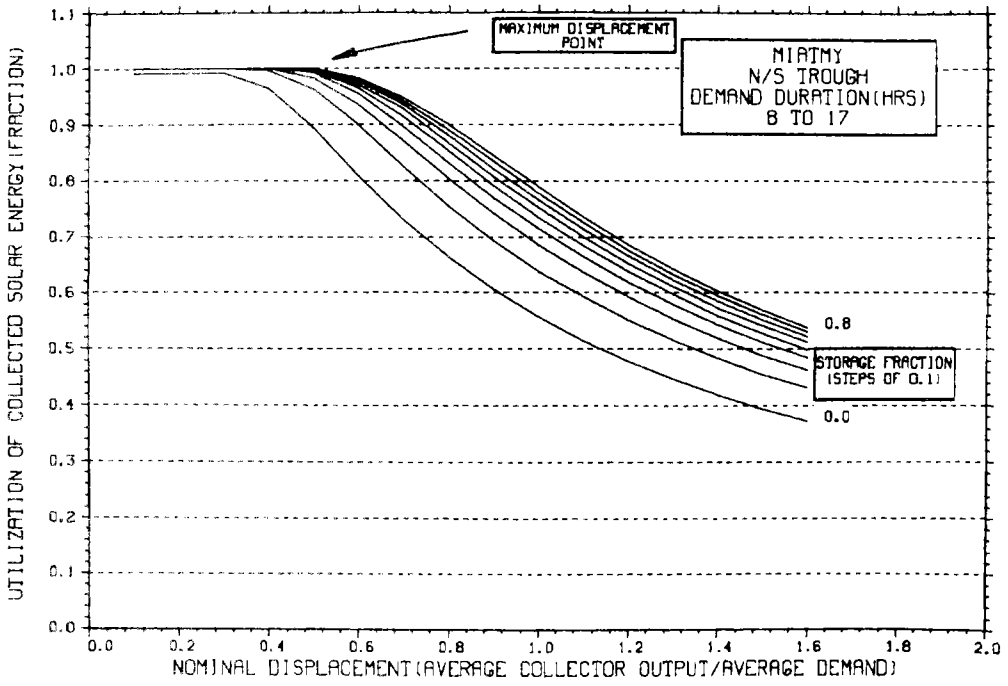

STORAGE SIZING GRAPH FOR CONSTANT ANNUAL DEMAND

NO WEEKEND SHUTDOWN

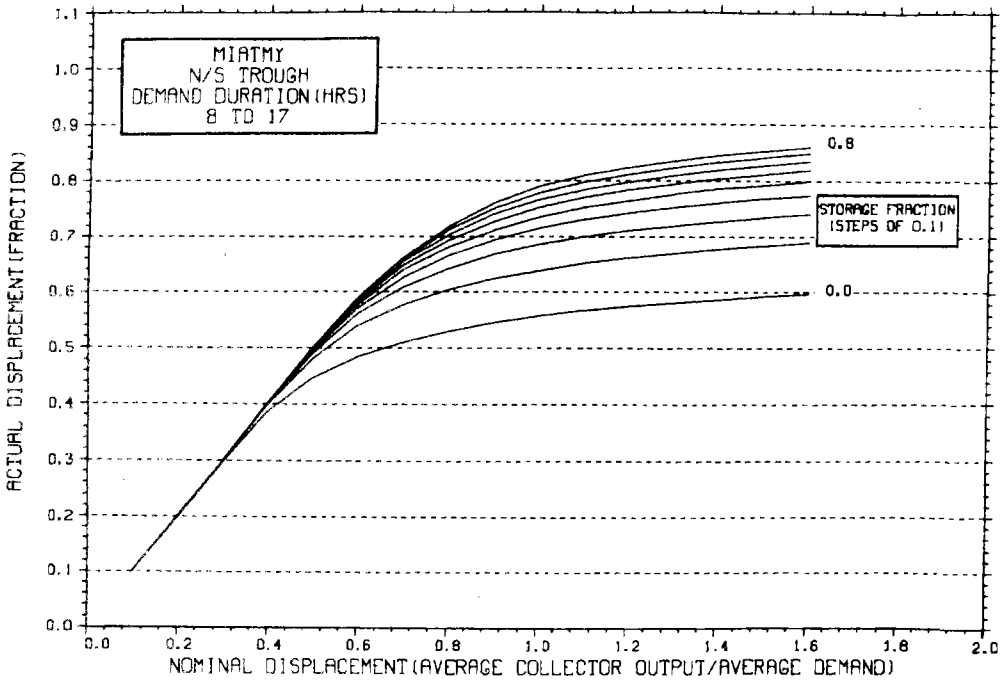

ENERGY INCIDENT ON COLLECTOR APERTURE

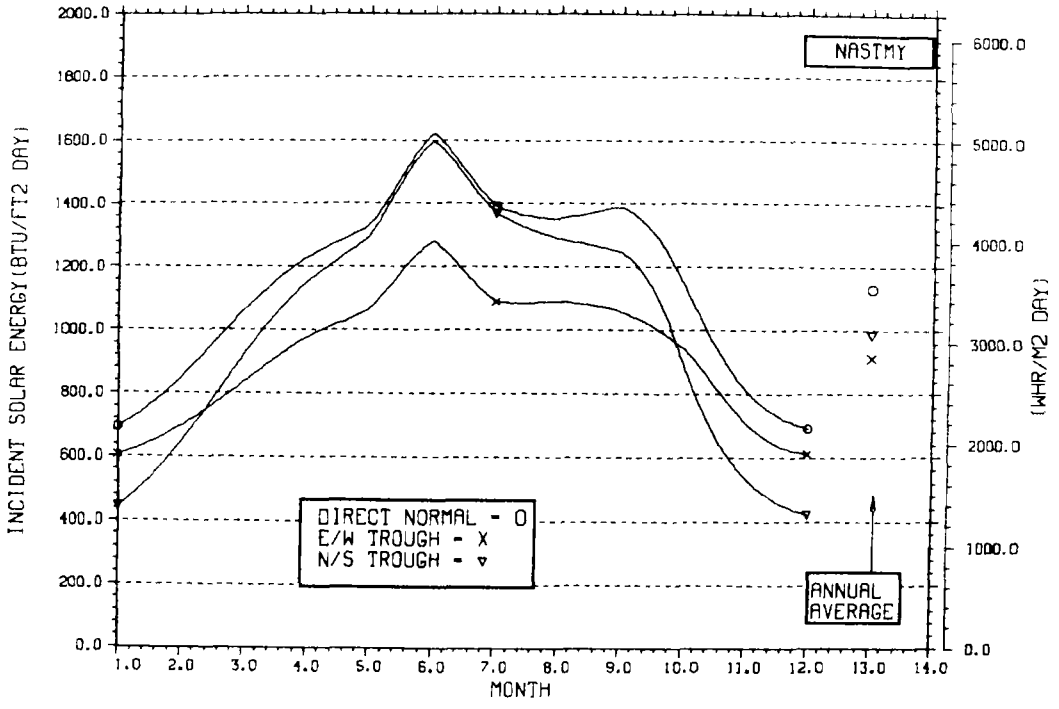

ANNUAL NONFIRST ROW SHADING

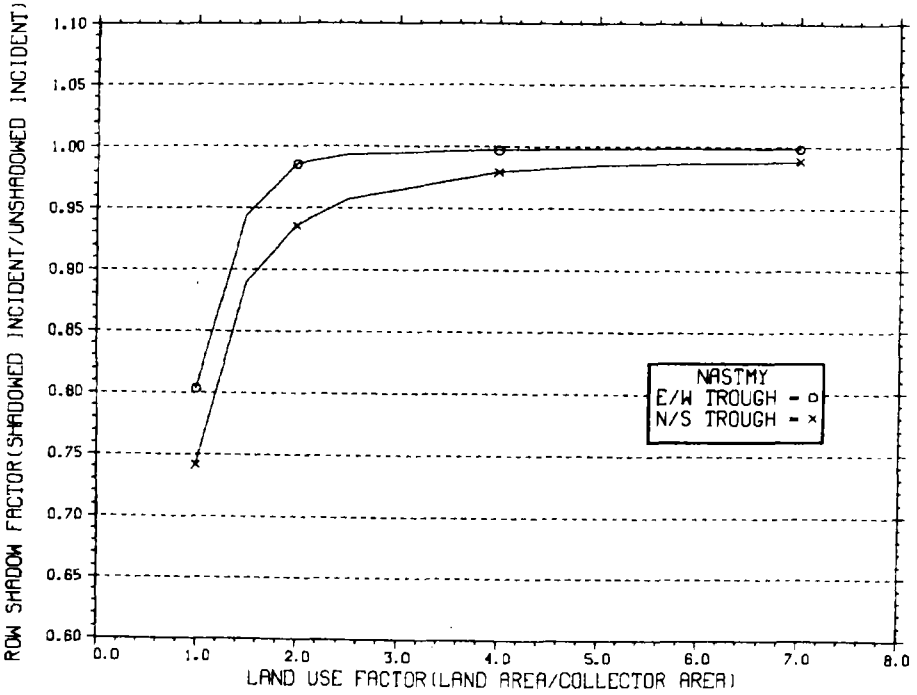

PERFORMANCE VARIATION WITH COLLECTOR AZIMUTH

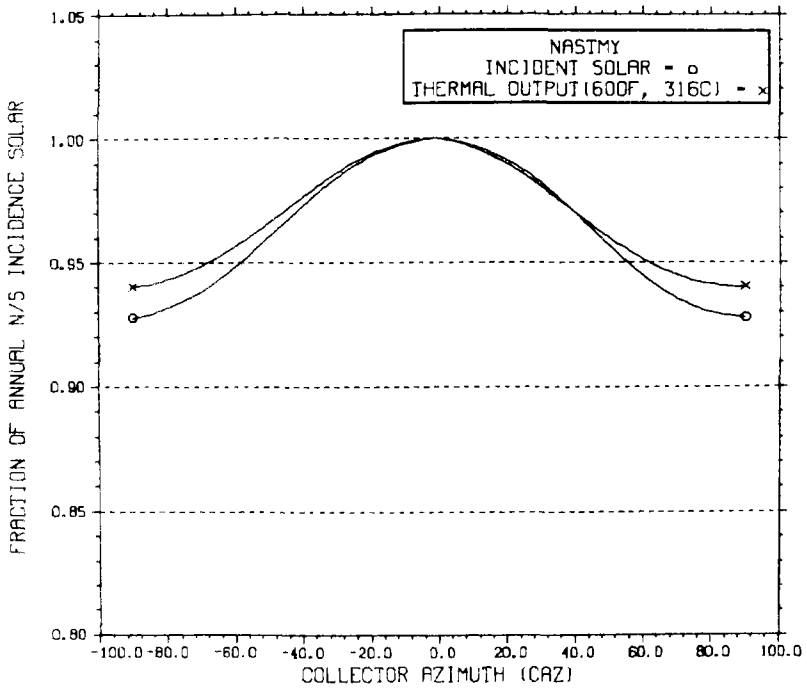

TEMPERATURE DEPENDENCE OF ANNUAL PERFORMANCE

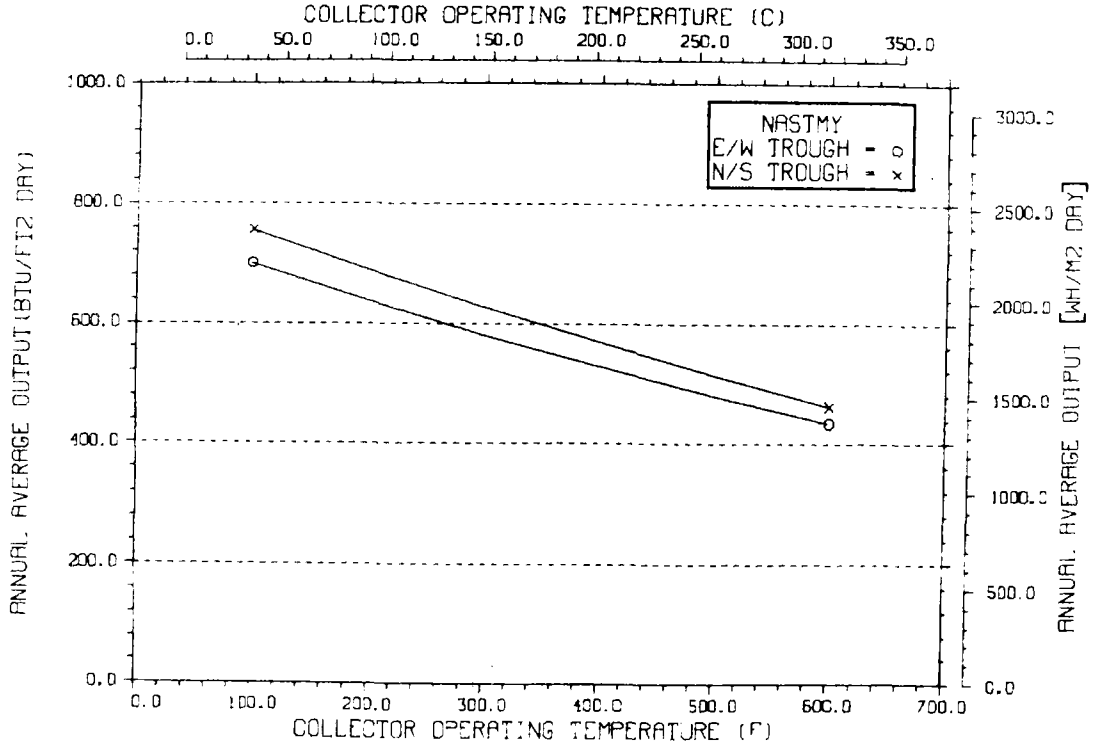

TEMPERATURE DEPENDENCE OF MONTHLY PERFORMANCE

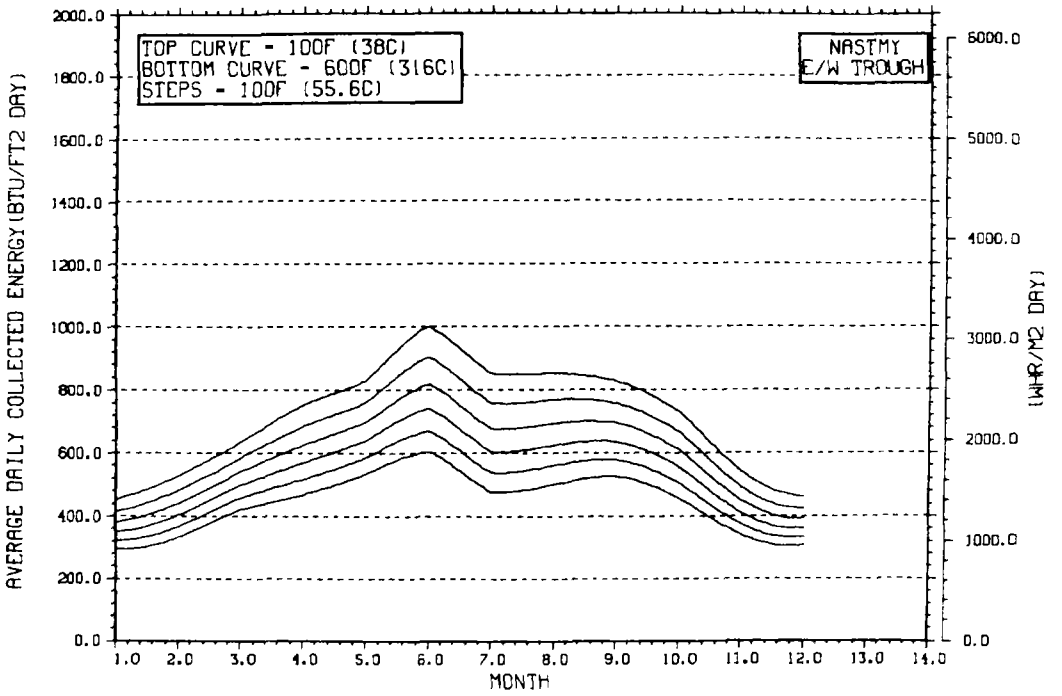

TEMPERATURE DEPENDENCE OF MONTHLY PERFORMANCE

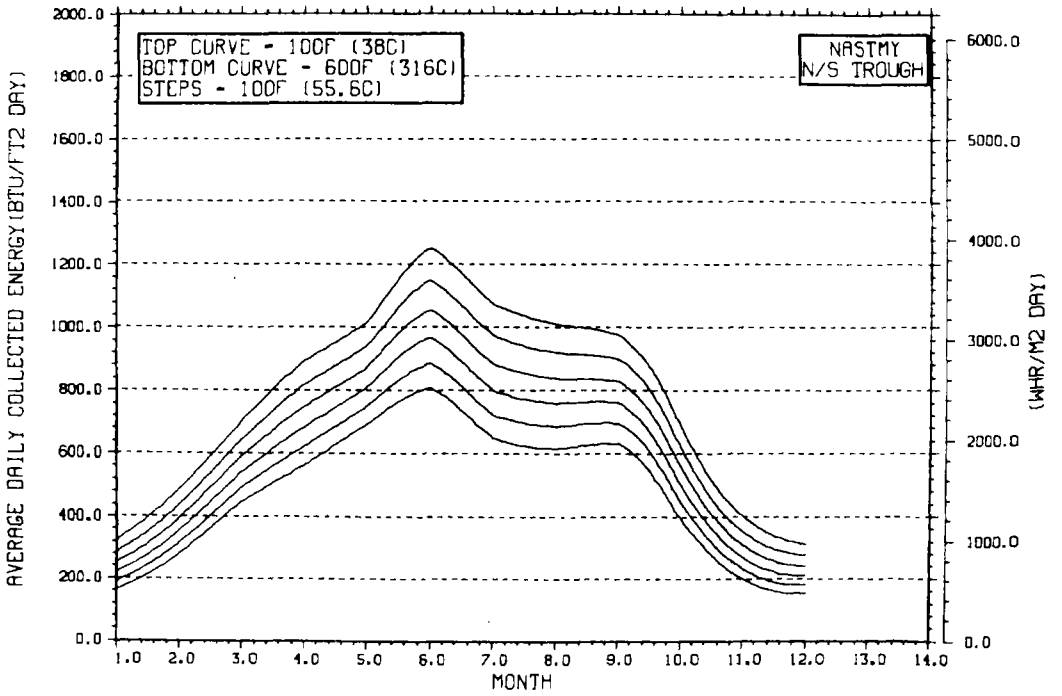

STORAGE SIZING GRAPH FOR CONSTANT ANNUAL DEMAND

NO WEEKEND SHUTDOWN

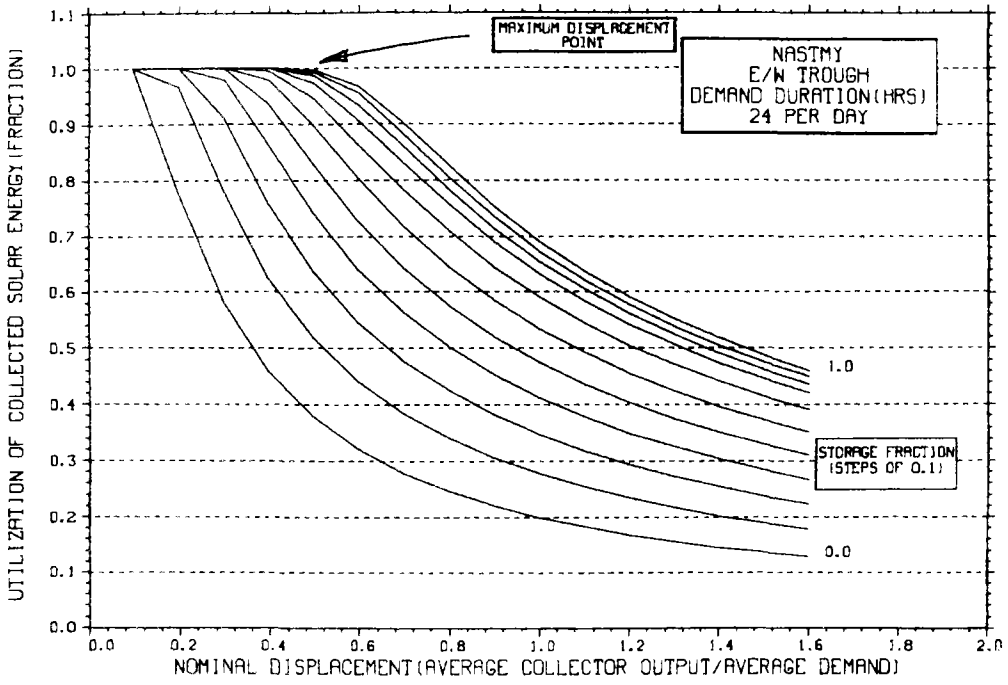

STORAGE SIZING GRAPH FOR CONSTANT ANNUAL DEMAND

NO WEEKEND SHUTDOWN

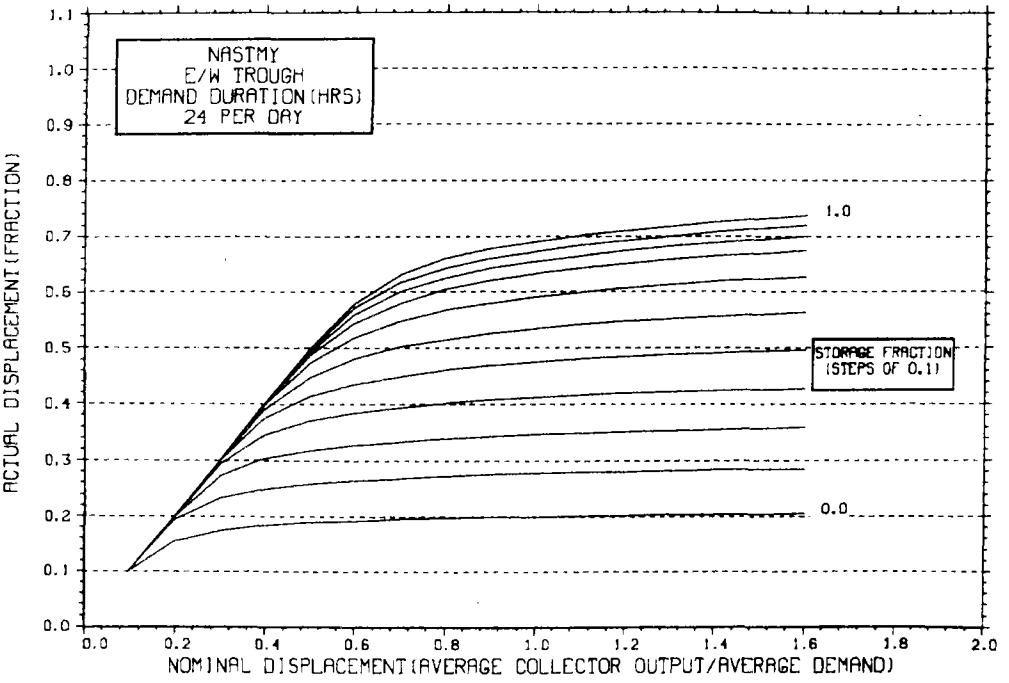

STORAGE SIZING GRAPH FOR CONSTANT ANNUAL DEMAND

NO WEEKEND SHUTDOWN

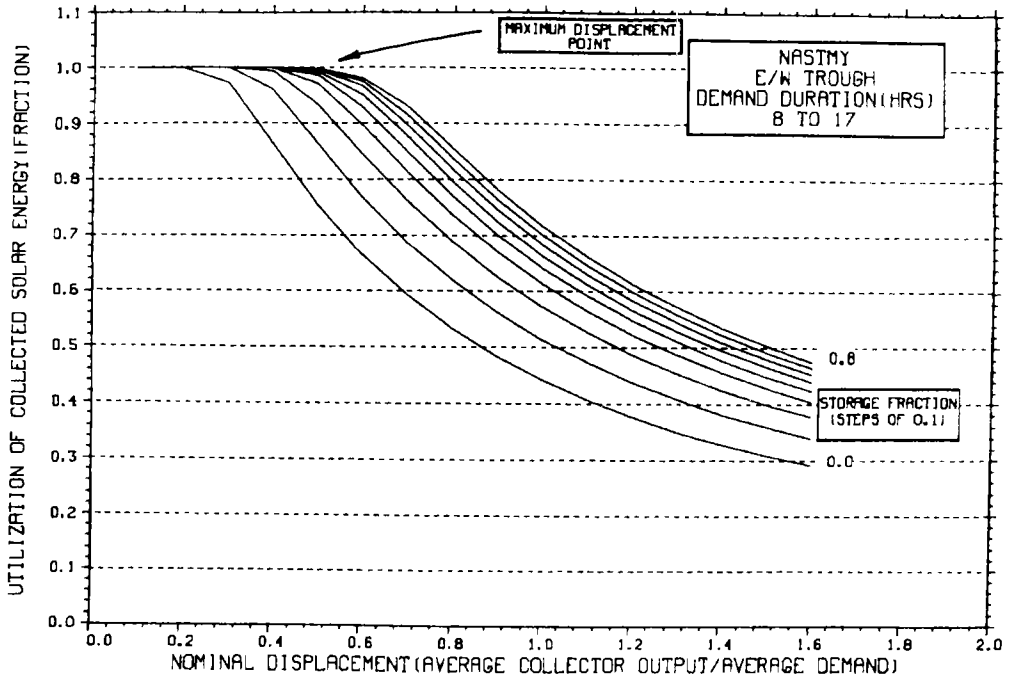

STORAGE SIZING GRAPH FOR CONSTANT ANNUAL DEMAND

NO WEEKEND SHUTDOWN

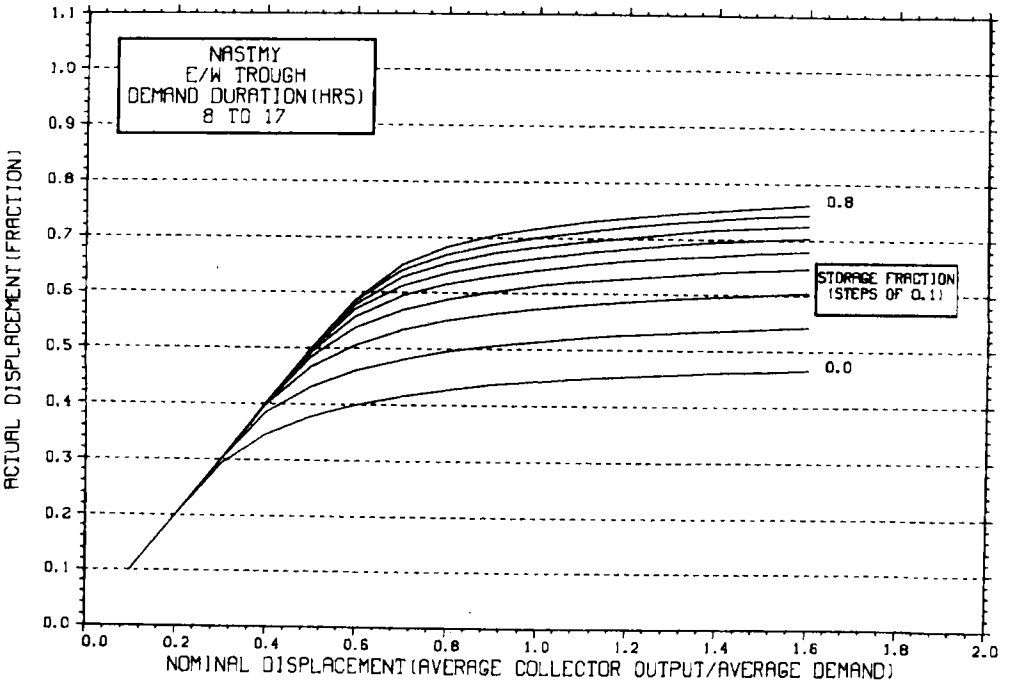

STORAGE SIZING GRAPH FOR CONSTANT ANNUAL DEMAND

NO WEEKEND SHUTDOWN

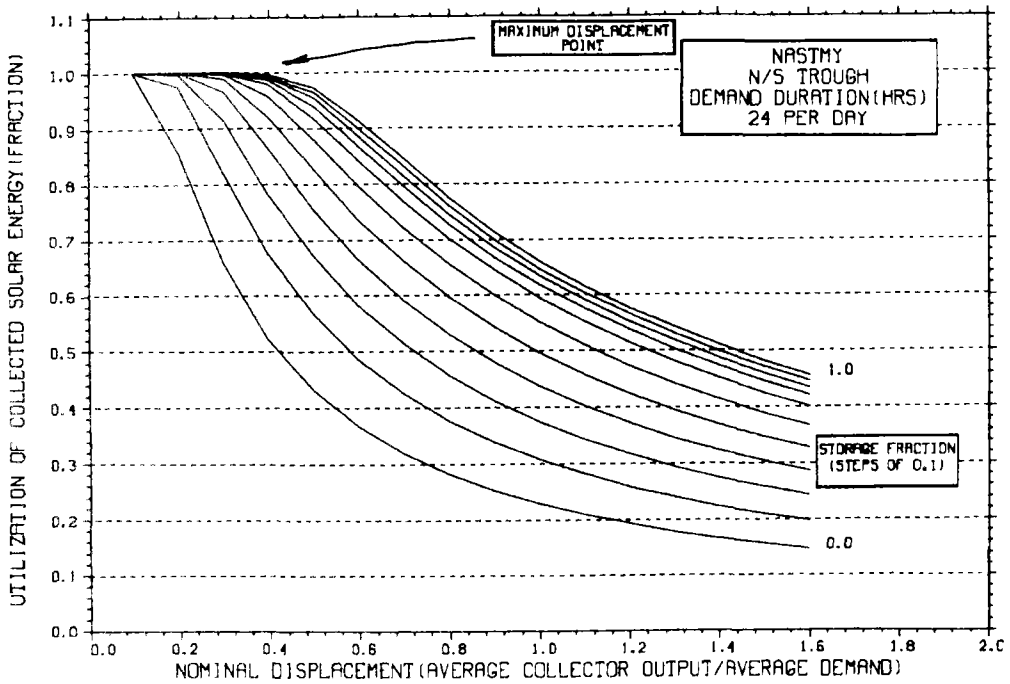

STORAGE SIZING GRAPH FOR CONSTANT ANNUAL DEMAND

NO WEEKEND SHUTDOWN

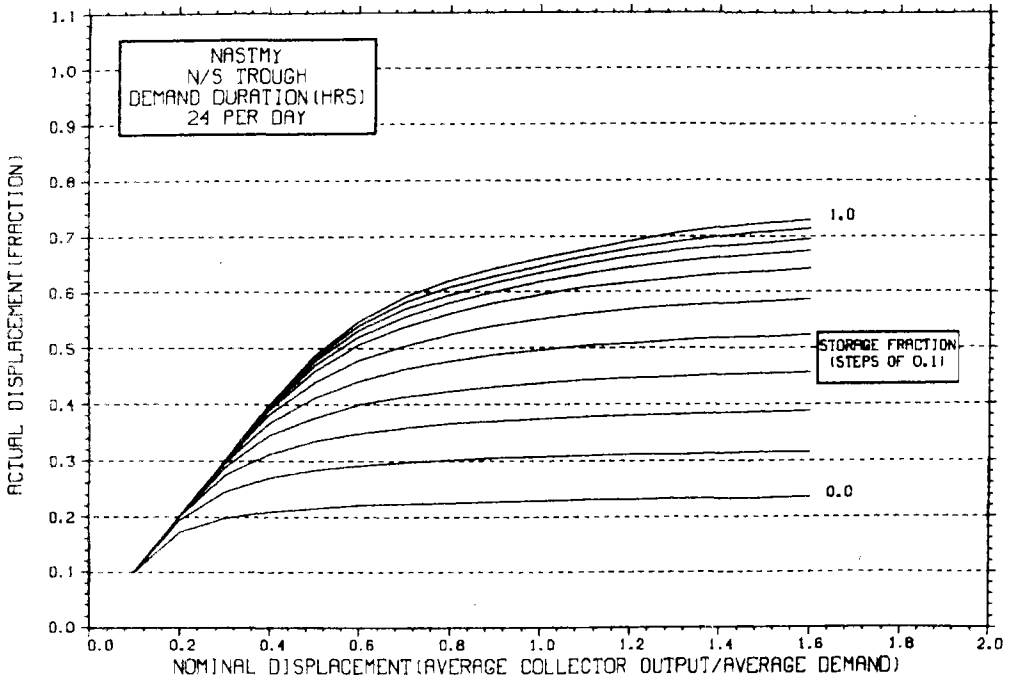

STORAGE SIZING GRAPH FOR CONSTANT ANNUAL DEMAND

NO WEEKEND SHUTDOWN

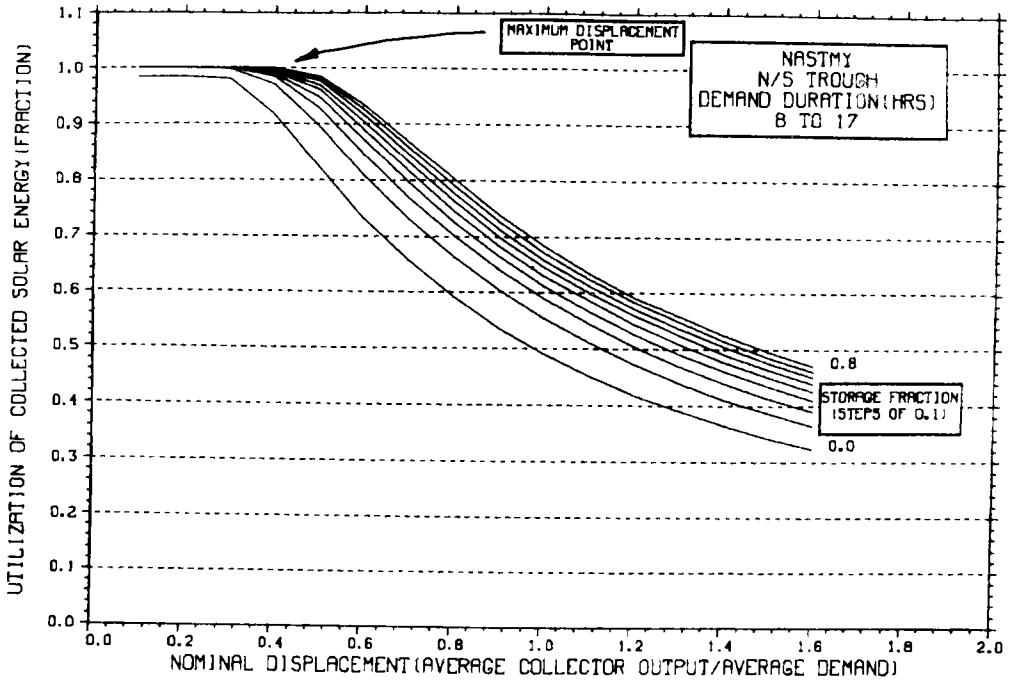

STORAGE SIZING GRAPH FOR CONSTANT ANNUAL DEMAND

NO WEEKEND SHUTDOWN

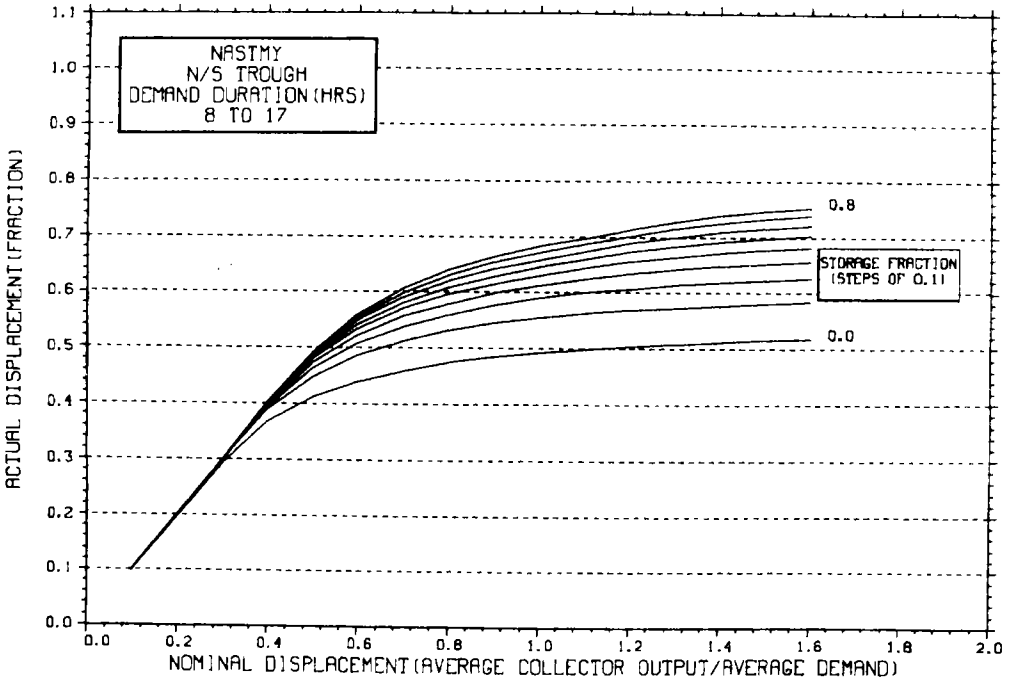

ENERGY INCIDENT ON COLLECTOR APERTURE

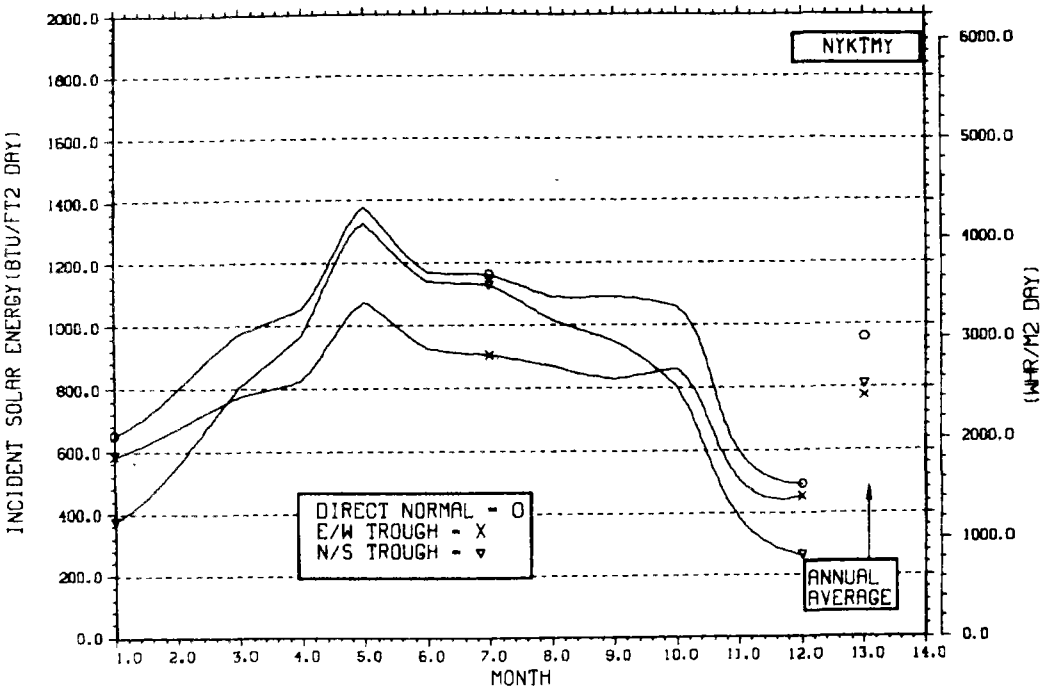

ANNUAL NONFIRST ROW SHADING

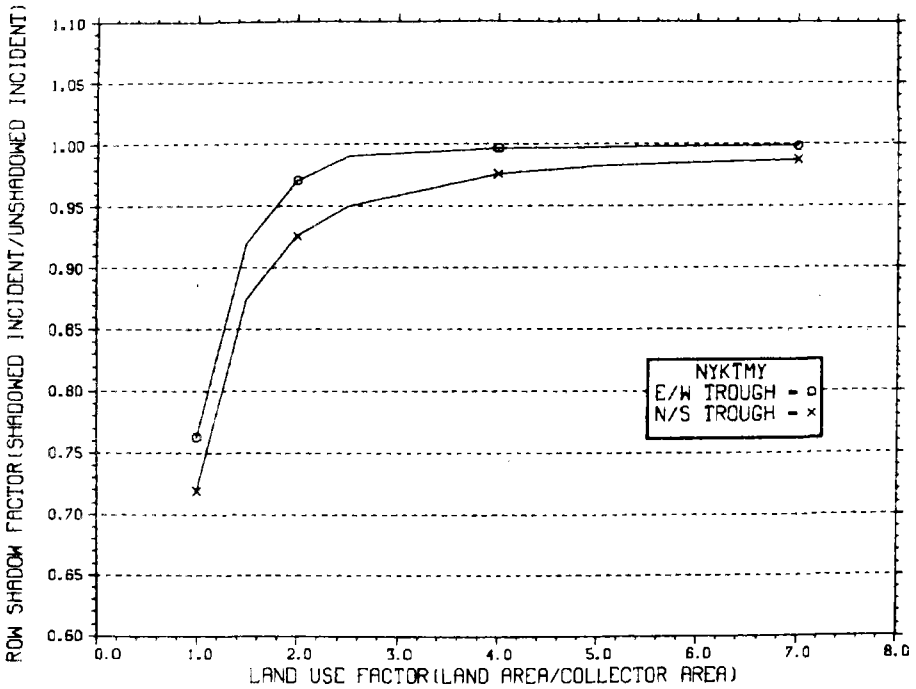

PERFORMANCE VARIATION WITH COLLECTOR AZIMUTH

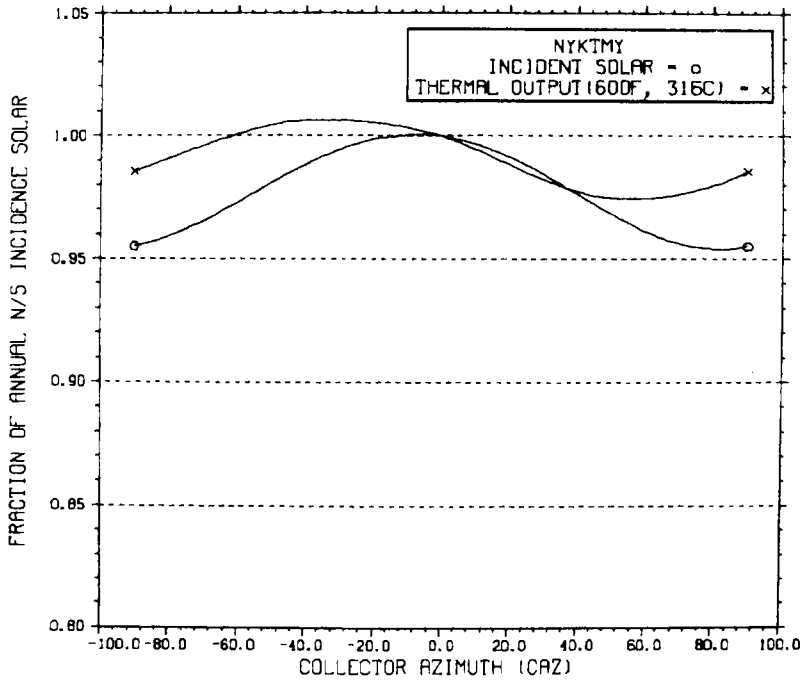

TEMPERATURE DEPENDENCE OF ANNUAL PERFORMANCE

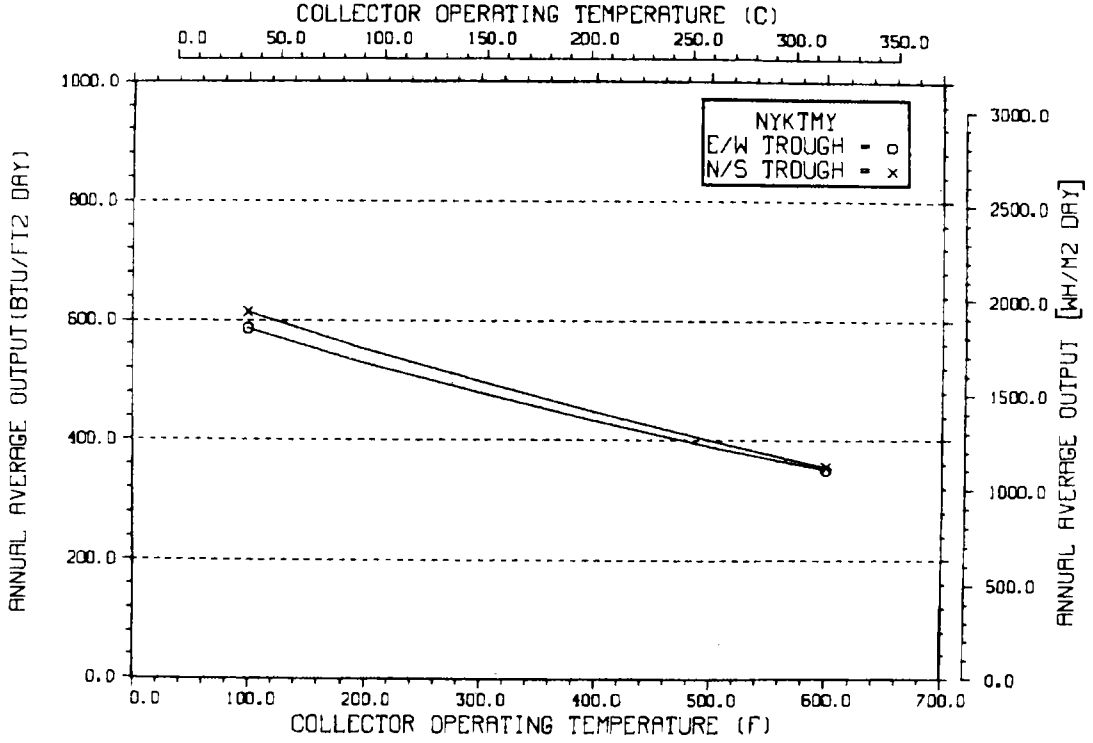

TEMPERATURE DEPENDENCE OF MONTHLY PERFORMANCE

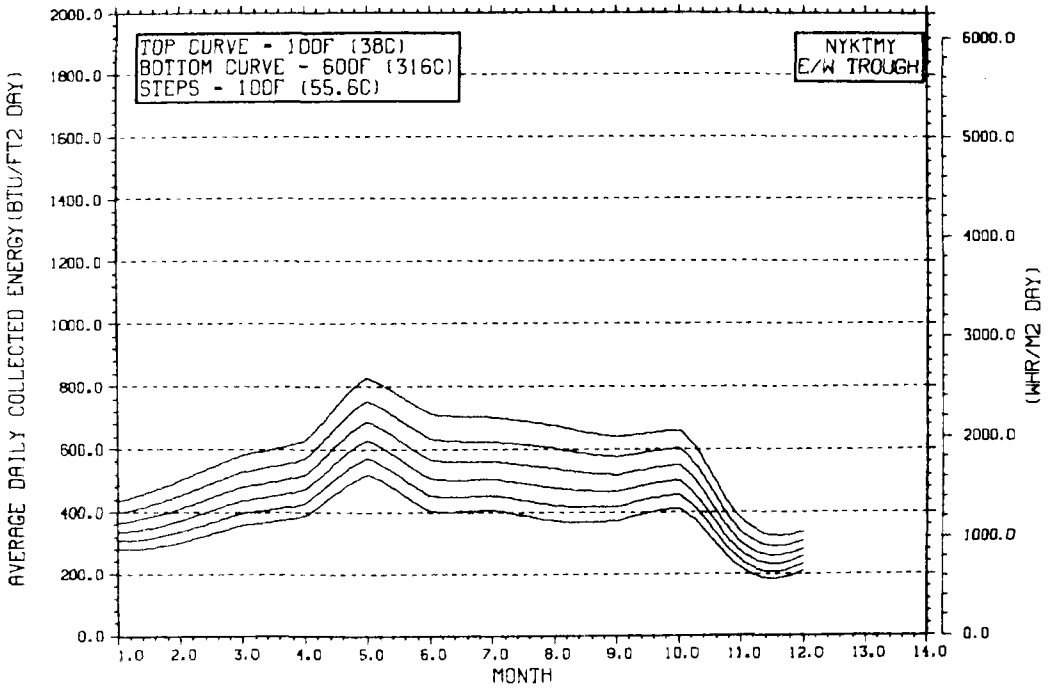

TEMPERATURE DEPENDENCE OF MONTHLY PERFORMANCE

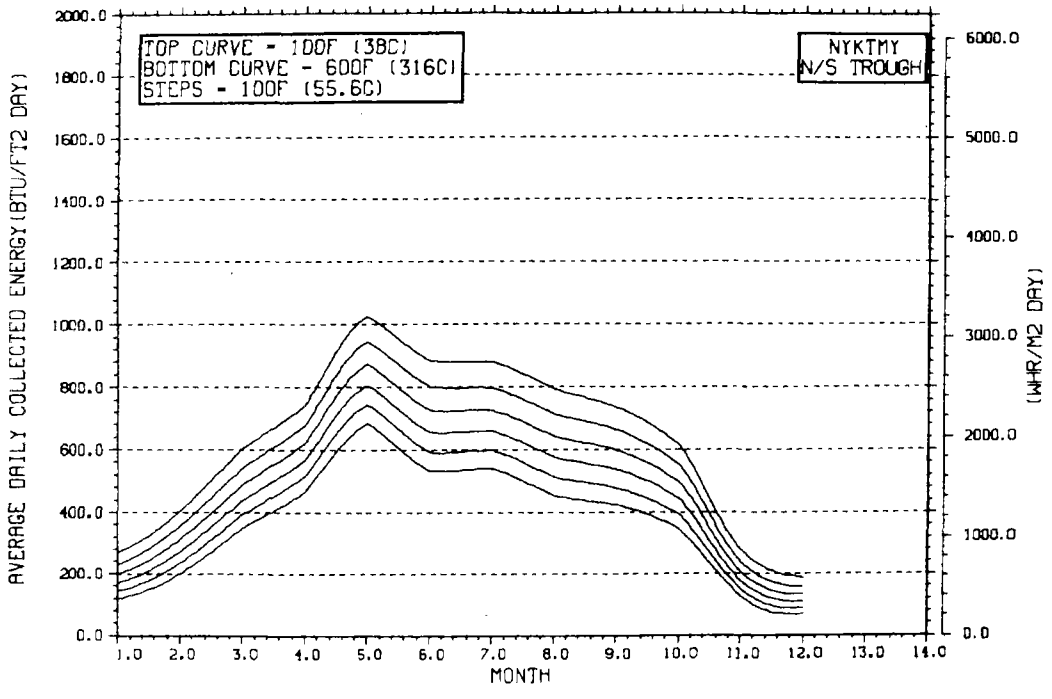

STORAGE SIZING GRAPH FOR CONSTANT ANNUAL DEMAND

NO WEEKEND SHUTDOWN

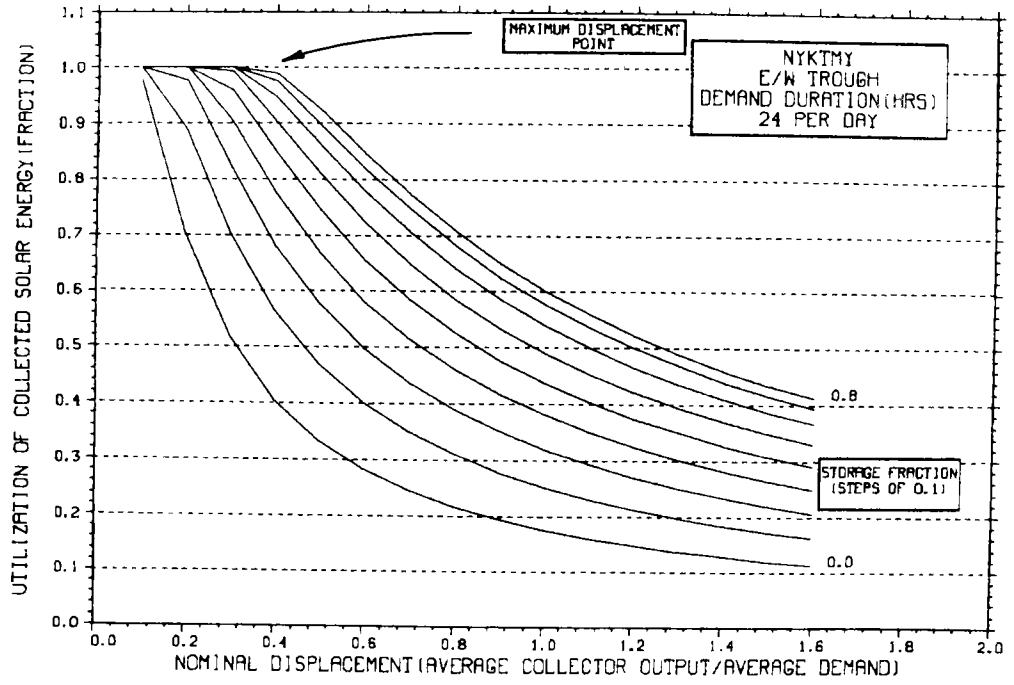

STORAGE SIZING GRAPH FOR CONSTANT ANNUAL DEMAND

NO WEEKEND SHUTDOWN

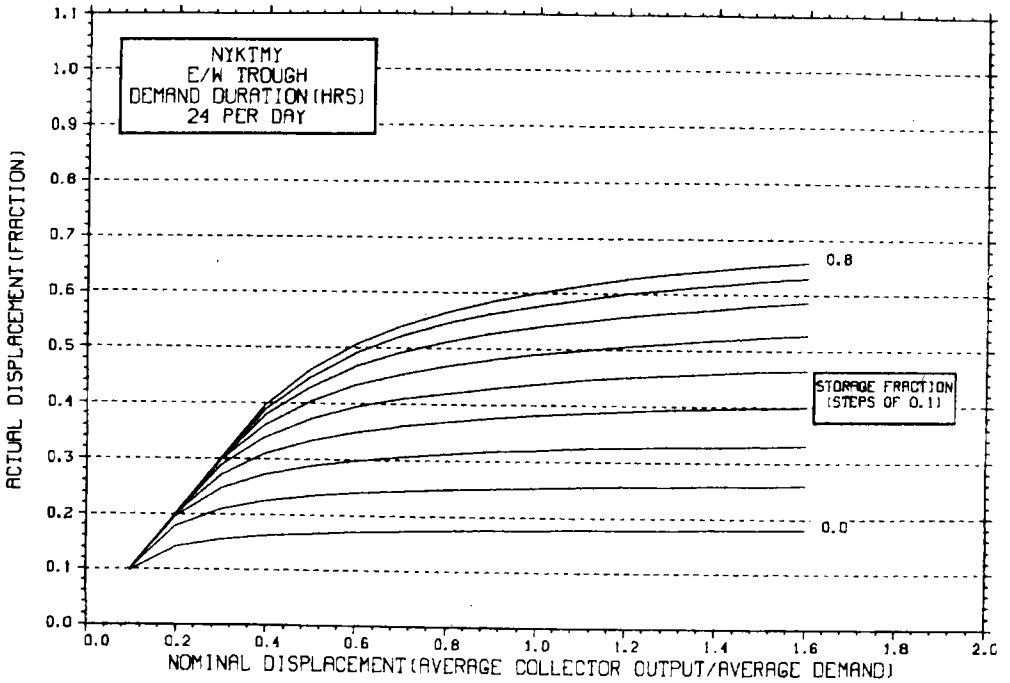

STORAGE SIZING GRAPH FOR CONSTANT ANNUAL DEMAND

NO WEEKEND SHUTDOWN

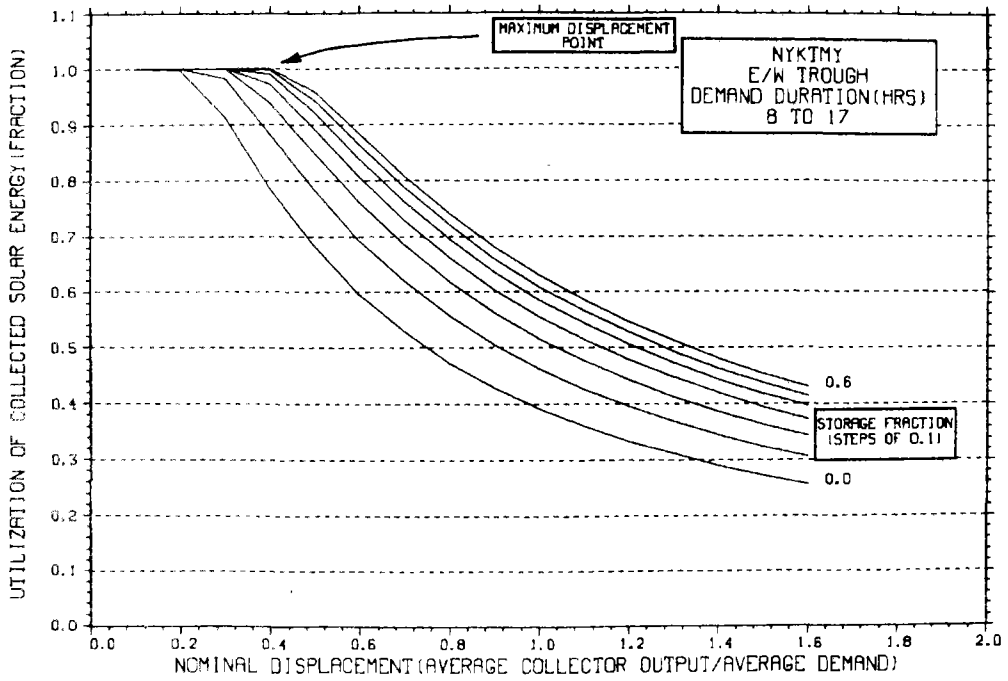

STORAGE SIZING GRAPH FOR CONSTANT ANNUAL DEMAND

NO WEEKEND SHUTDOWN

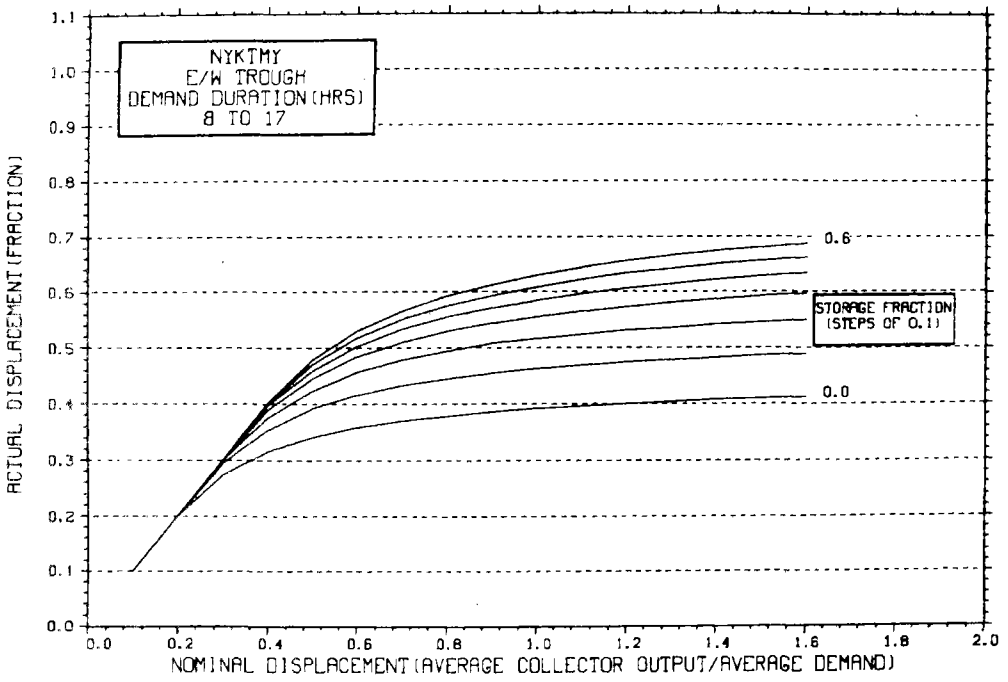

STORAGE SIZING GRAPH FOR CONSTANT ANNUAL DEMAND

NO WEEKEND SHUTDOWN

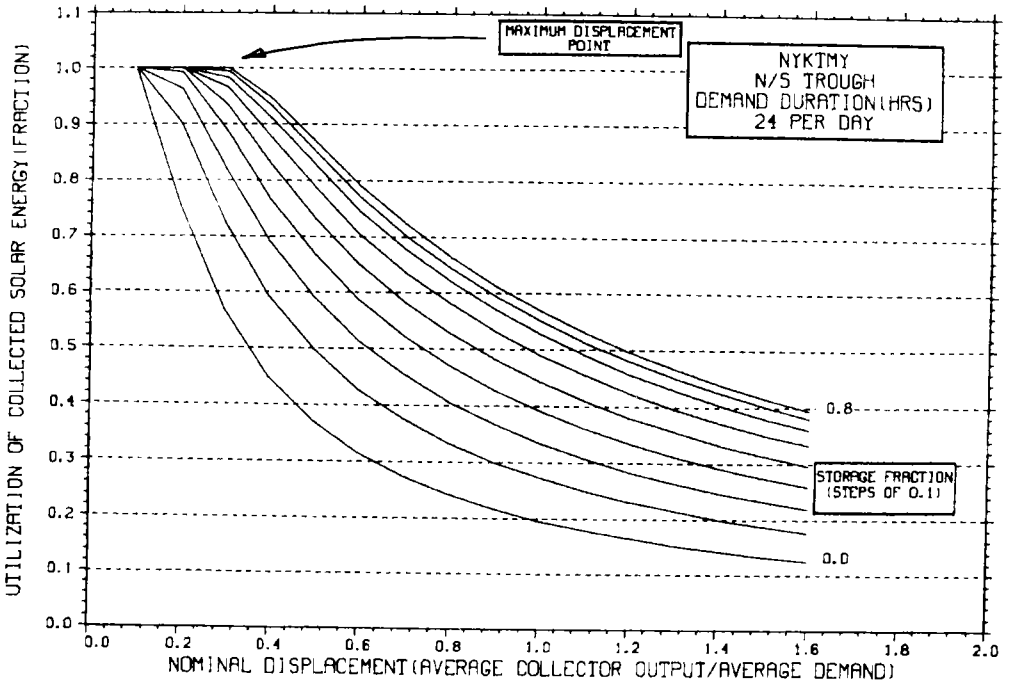

STORAGE SIZING GRAPH FOR CONSTANT ANNUAL DEMAND

NO WEEKEND SHUTDOWN

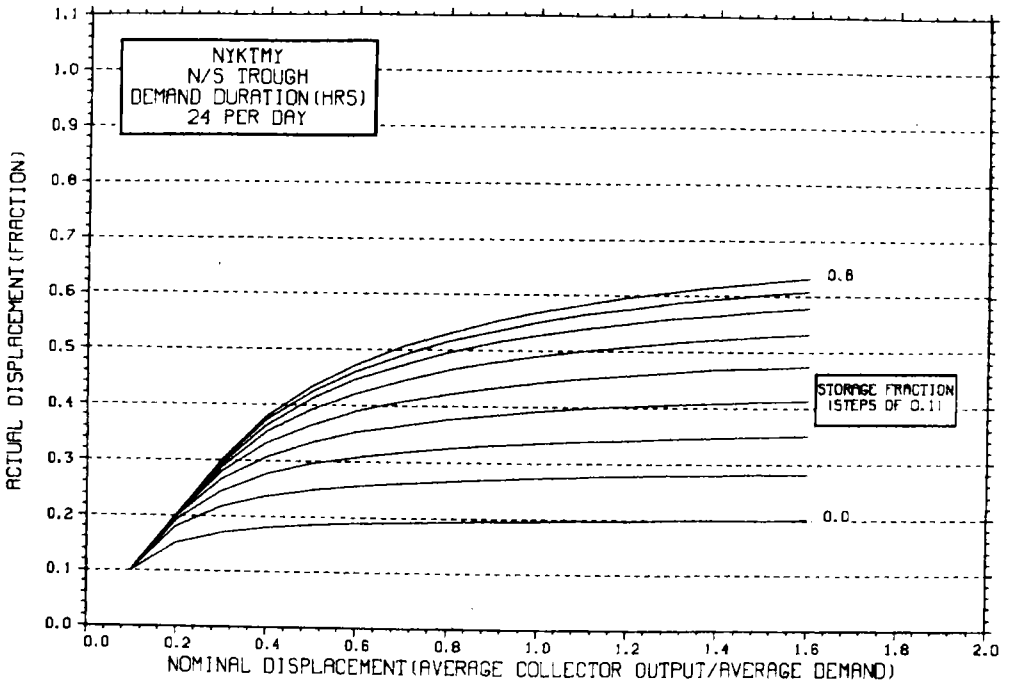

STORAGE SIZING GRAPH FOR CONSTANT ANNUAL DEMAND

NO WEEKEND SHUTDOWN

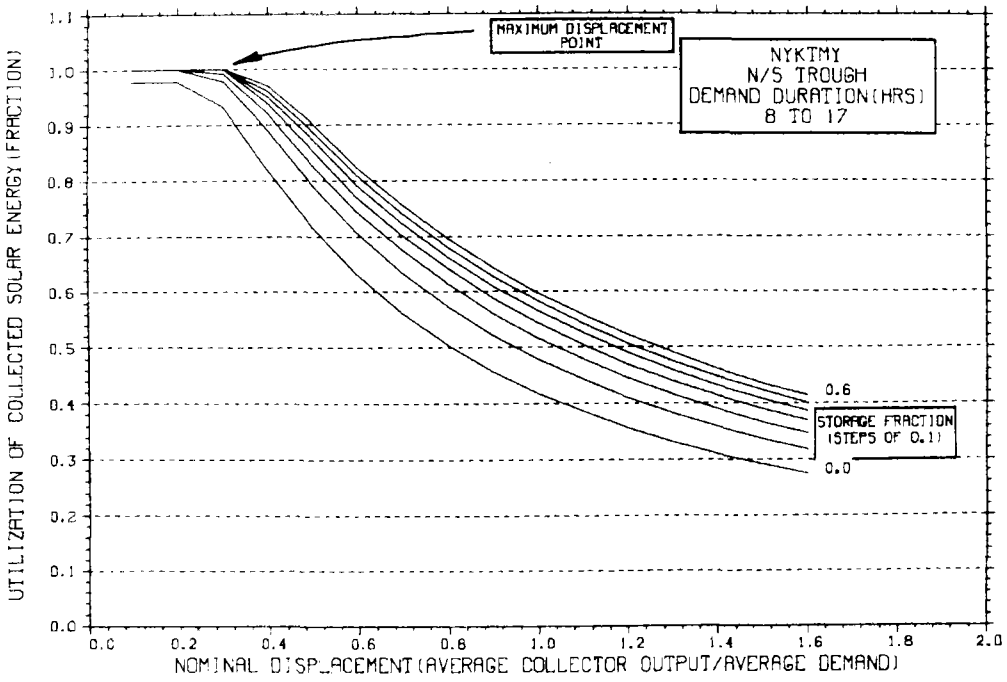

STORAGE SIZING GRAPH FOR CONSTANT ANNUAL DEMAND

NO WEEKEND SHUTDOWN

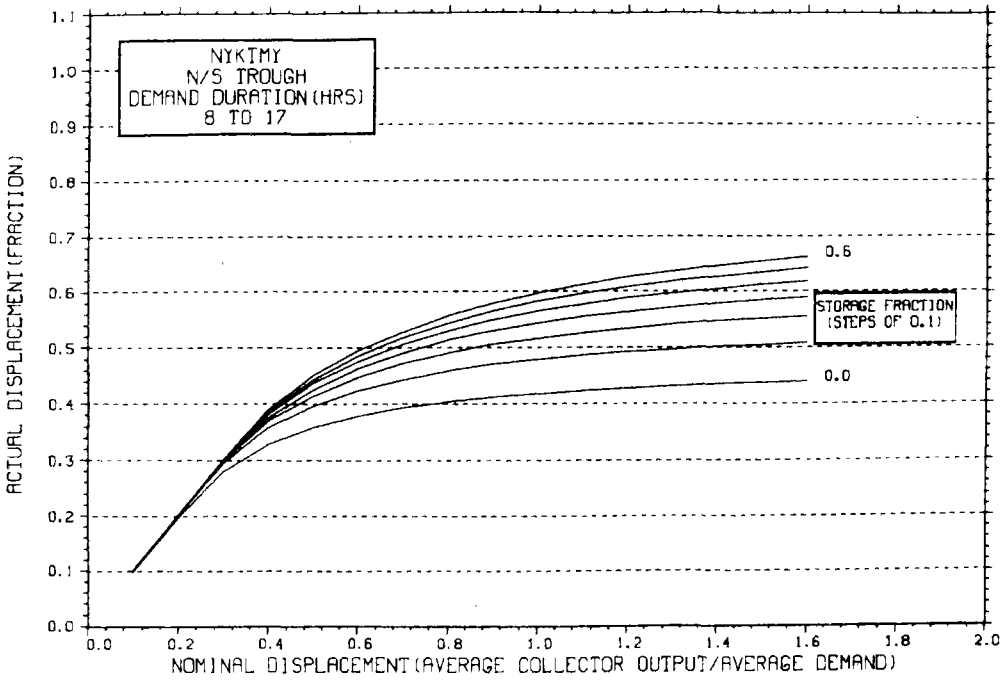

ENERGY INCIDENT ON COLLECTOR APERTURE

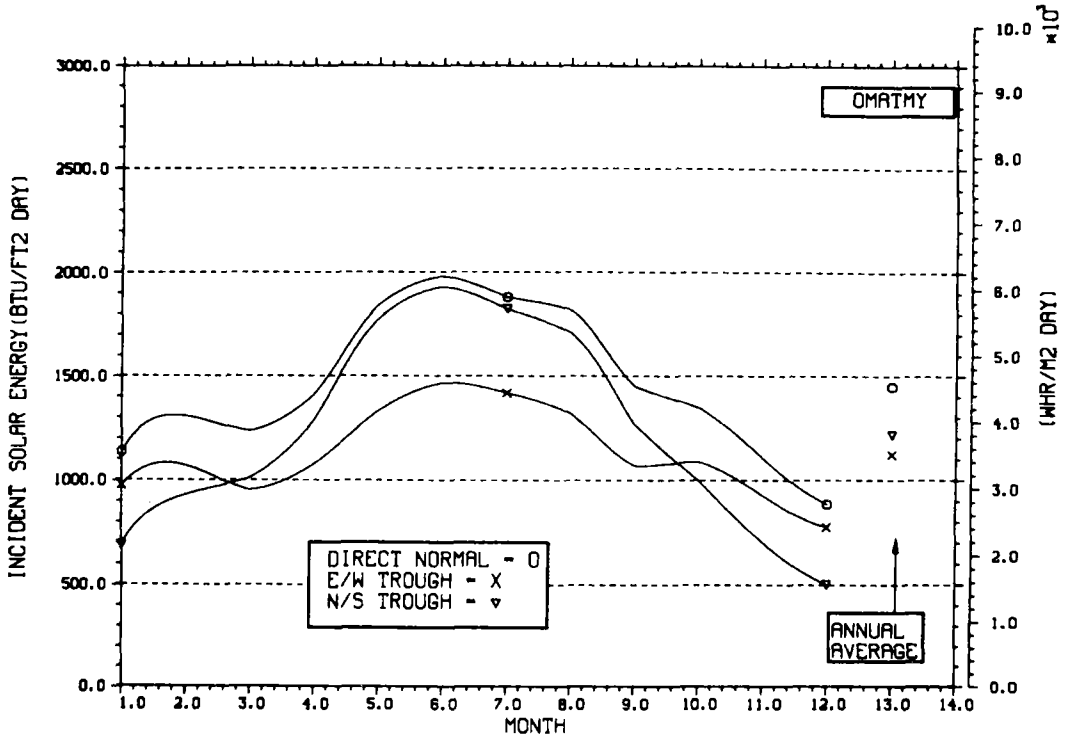

ANNUAL NONFIRST ROW SHADING

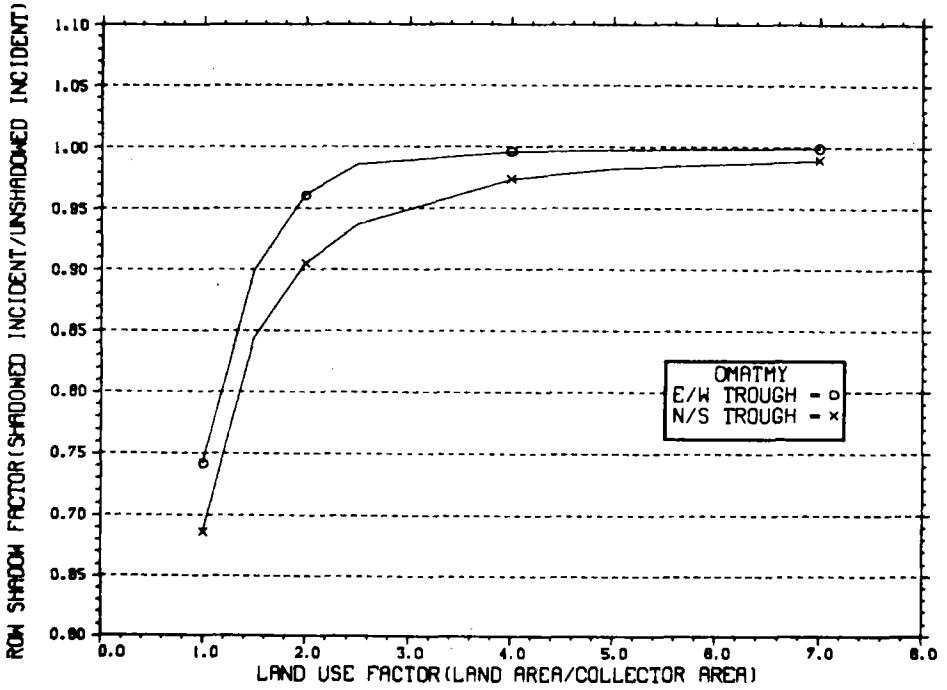

PERFORMANCE VARIATION WITH COLLECTOR AZIMUTH

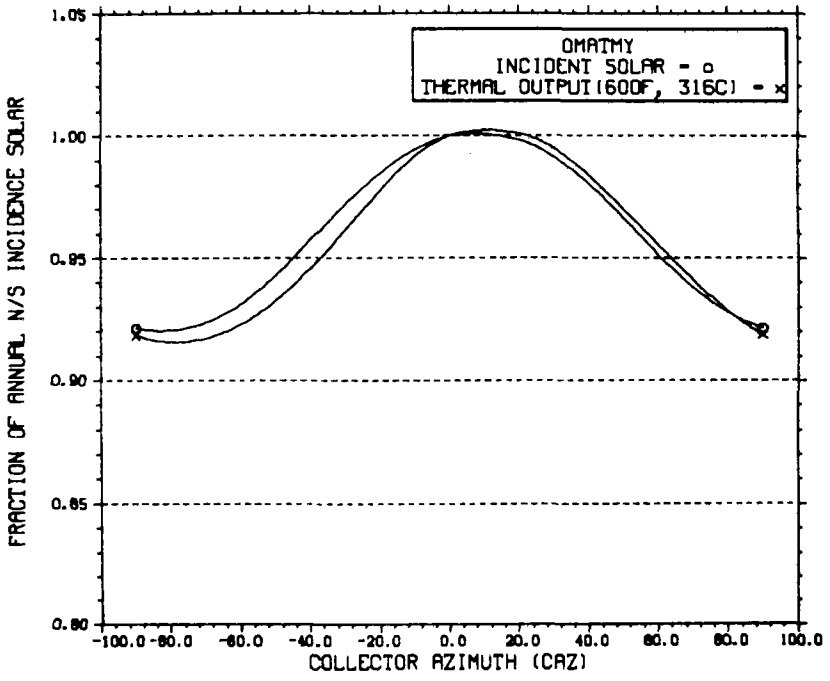

TEMPERATURE DEPENDENCE OF ANNUAL PERFORMANCE

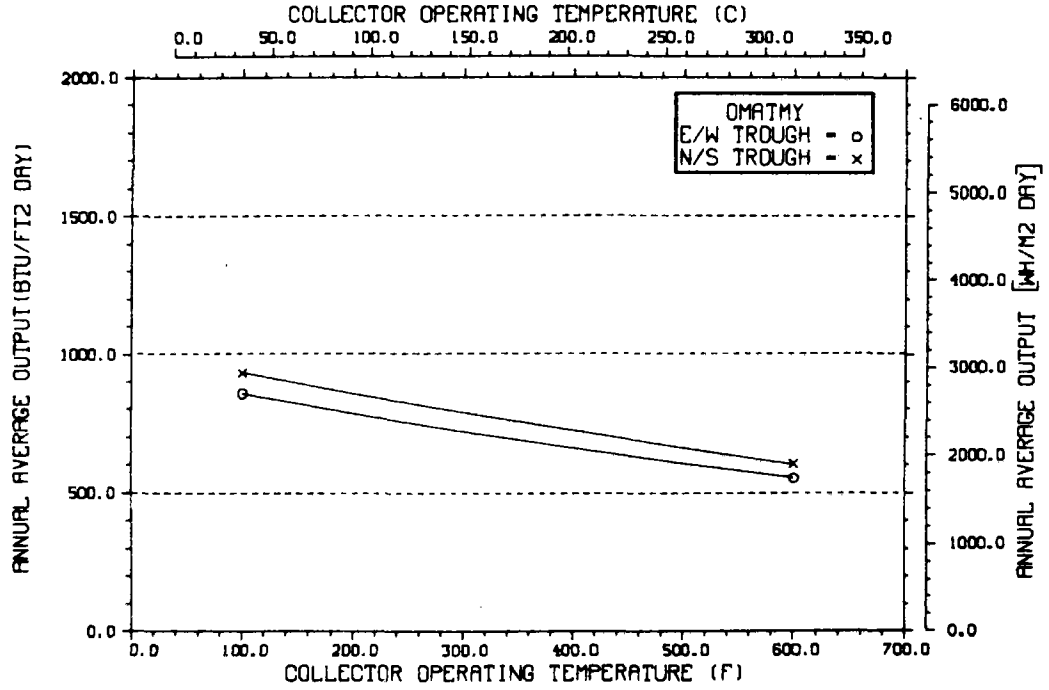

TEMPERATURE DEPENDENCE OF MONTHLY PERFORMANCE

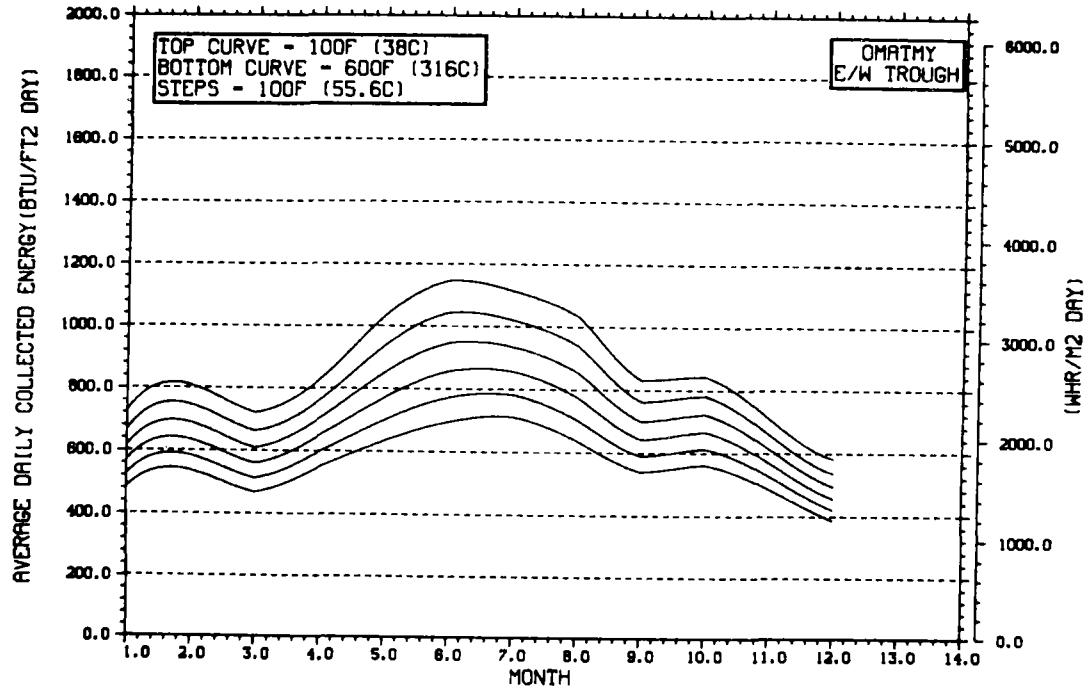

TEMPERATURE DEPENDENCE OF MONTHLY PERFORMANCE

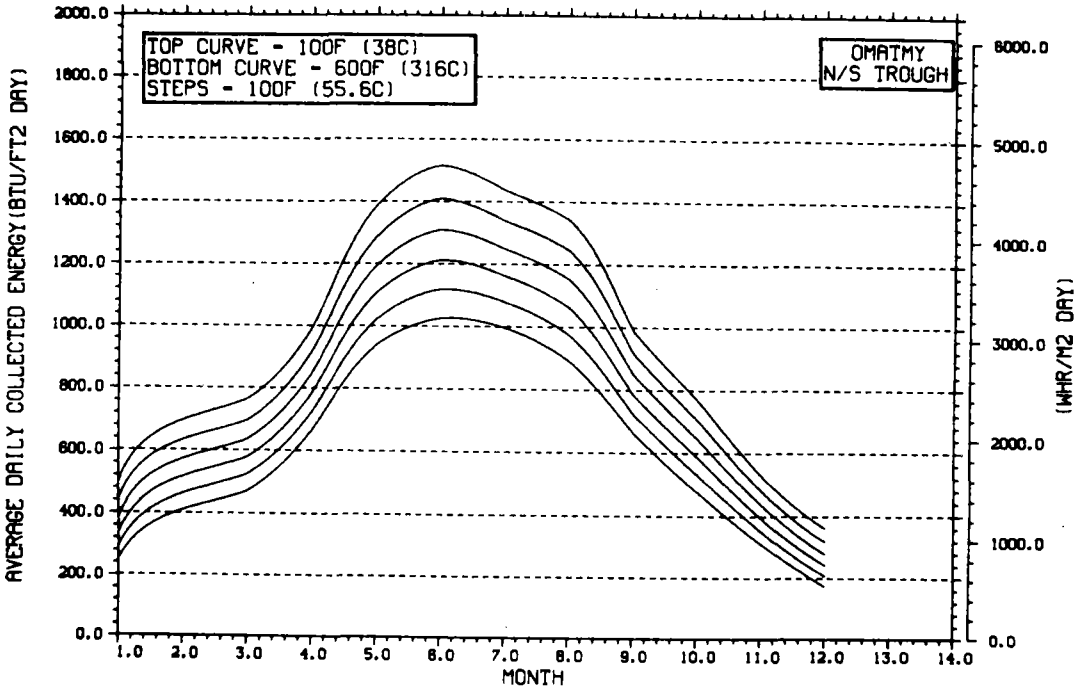

STORAGE SIZING GRAPH FOR CONSTANT ANNUAL DEMAND

NO WEEKEND SHUTDOWN

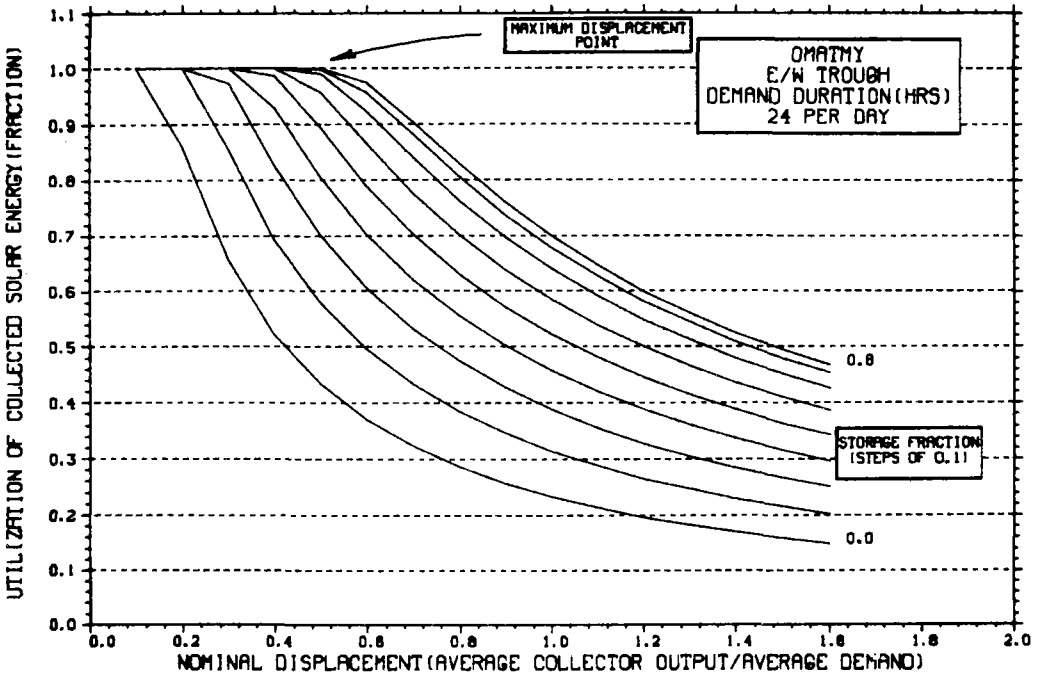

STORAGE SIZING GRAPH FOR CONSTANT ANNUAL DEMAND

NO WEEKEND SHUTDOWN

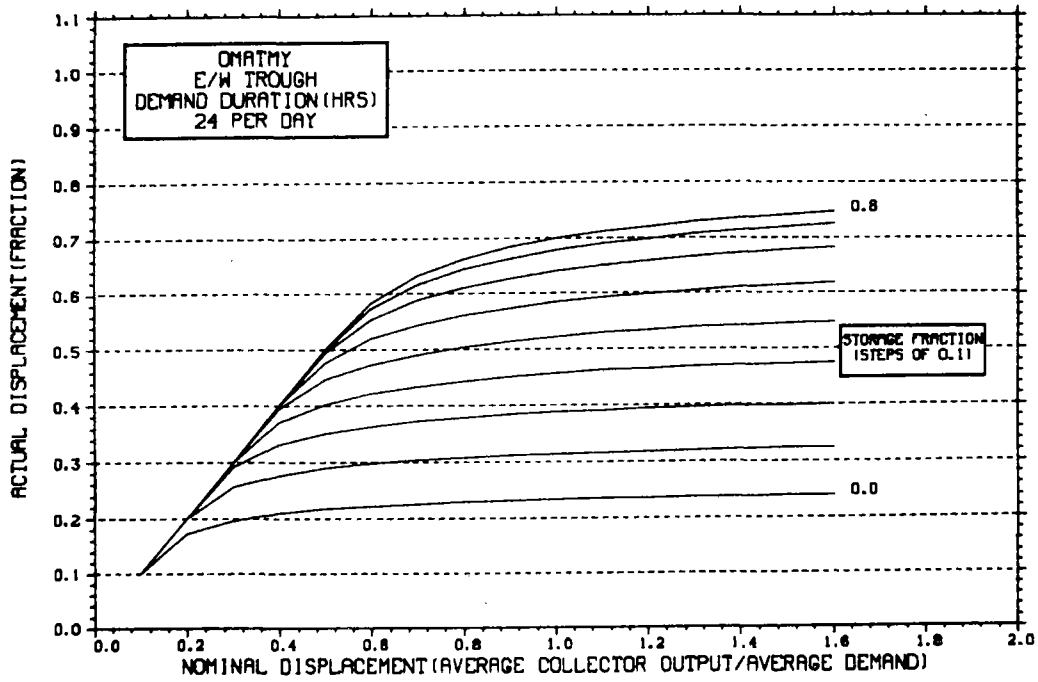

STORAGE SIZING GRAPH FOR CONSTANT ANNUAL DEMAND

NO WEEKEND SHUTDOWN

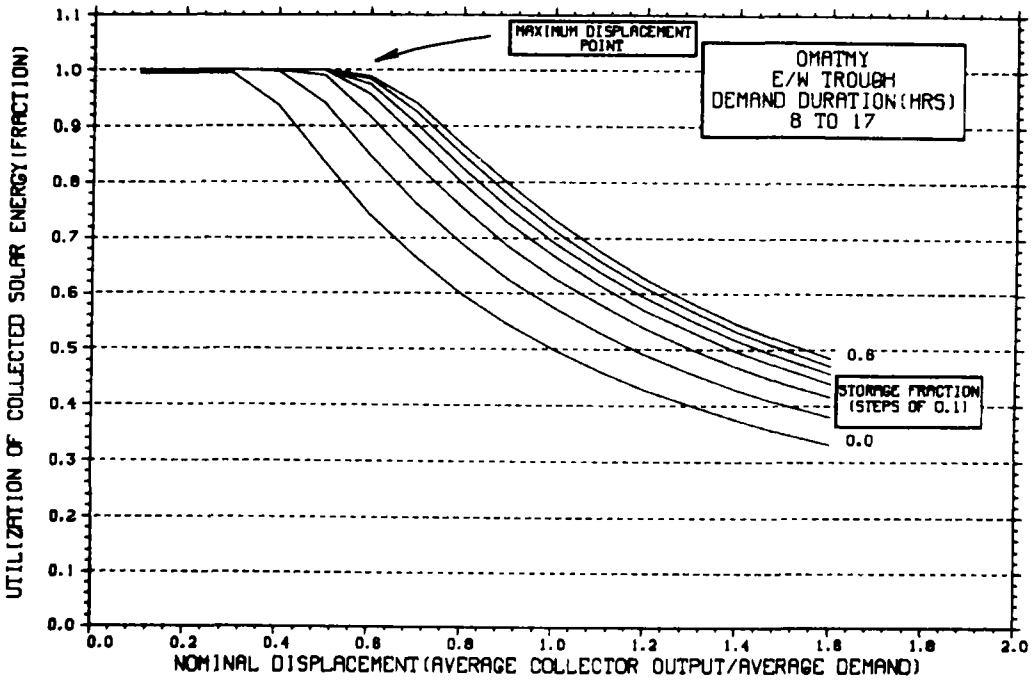

STORAGE SIZING GRAPH FOR CONSTANT ANNUAL DEMAND

NO WEEKEND SHUTDOWN

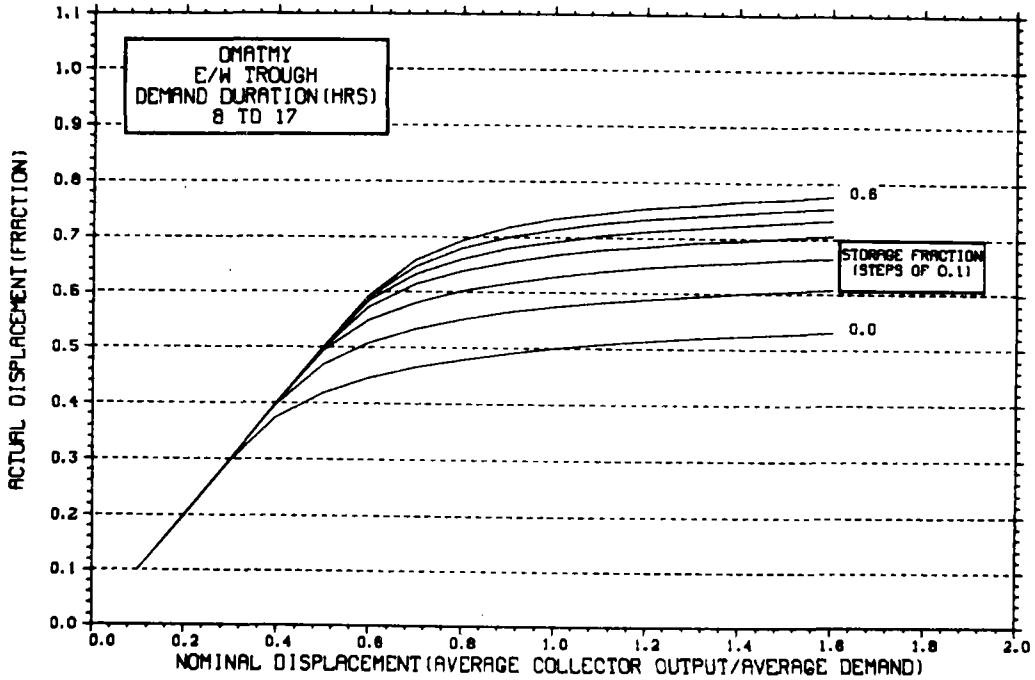

STORAGE SIZING GRAPH FOR CONSTANT ANNUAL DEMAND

NO WEEKEND SHUTDOWN

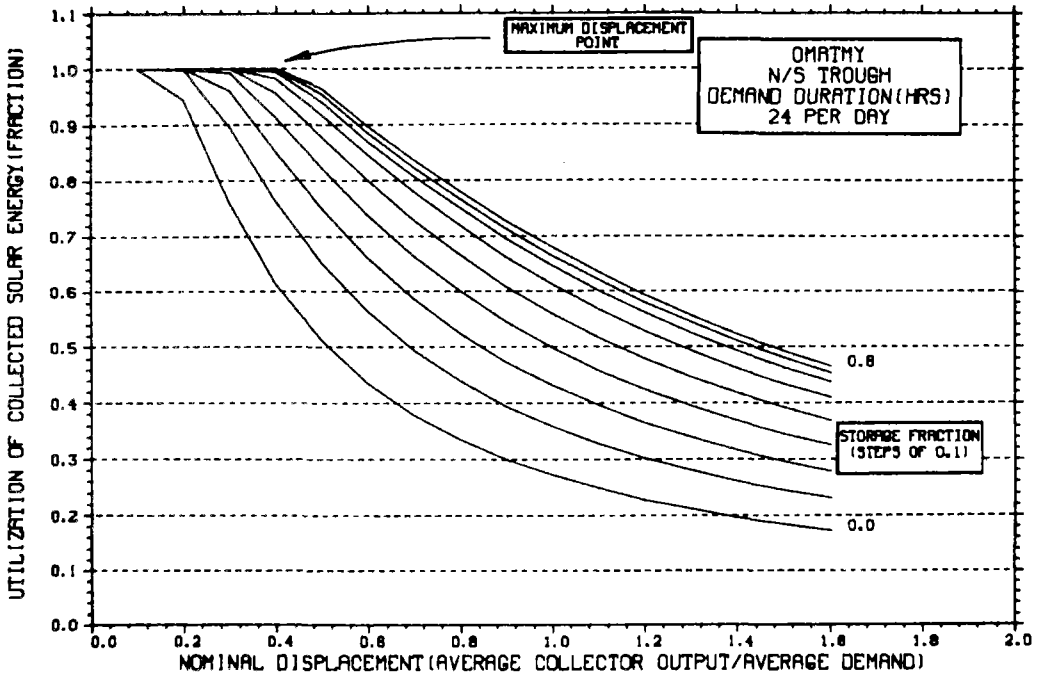

STORAGE SIZING GRAPH FOR CONSTANT ANNUAL DEMAND

NO WEEKEND SHUTDOWN

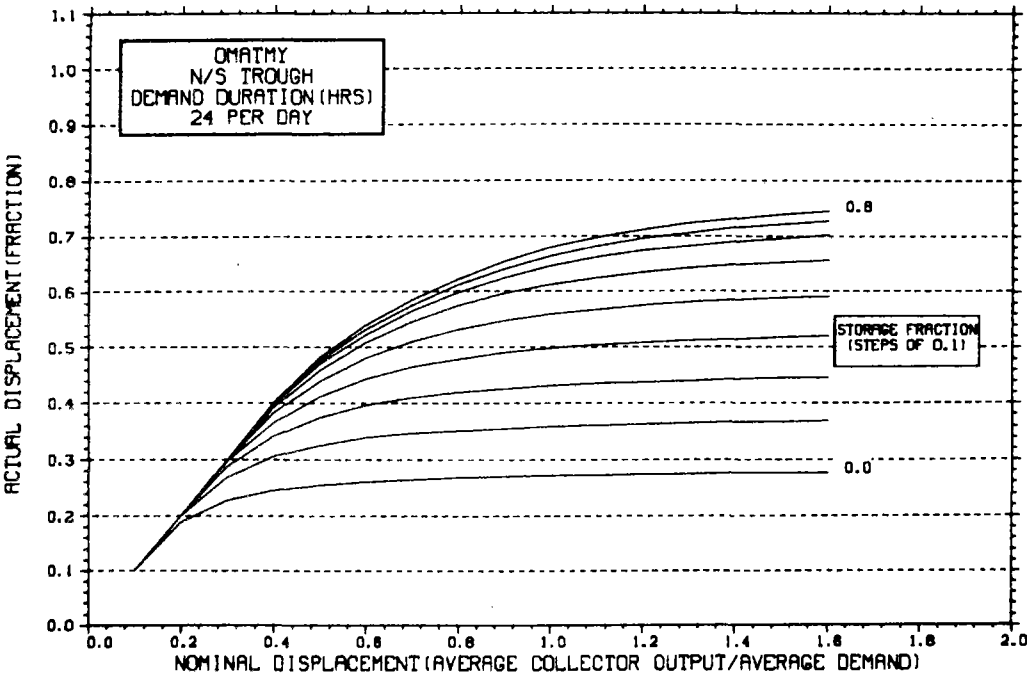

STORAGE SIZING GRAPH FOR CONSTANT ANNUAL DEMAND

NO WEEKEND SHUTDOWN

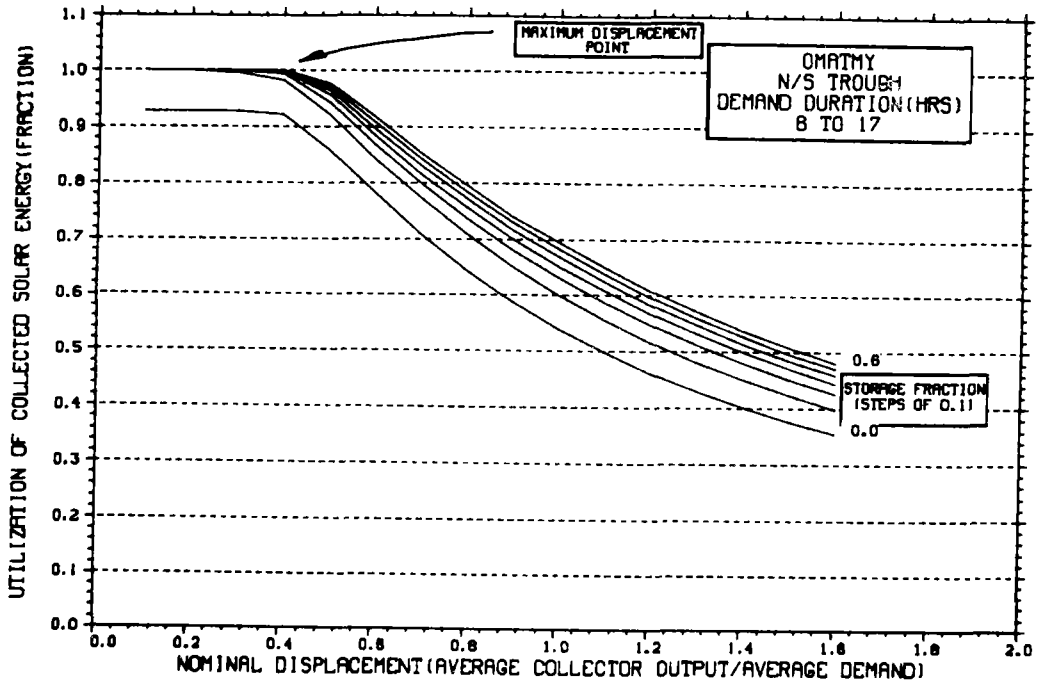

STORAGE SIZING GRAPH FOR CONSTANT ANNUAL DEMAND

NO WEEKEND SHUTDOWN

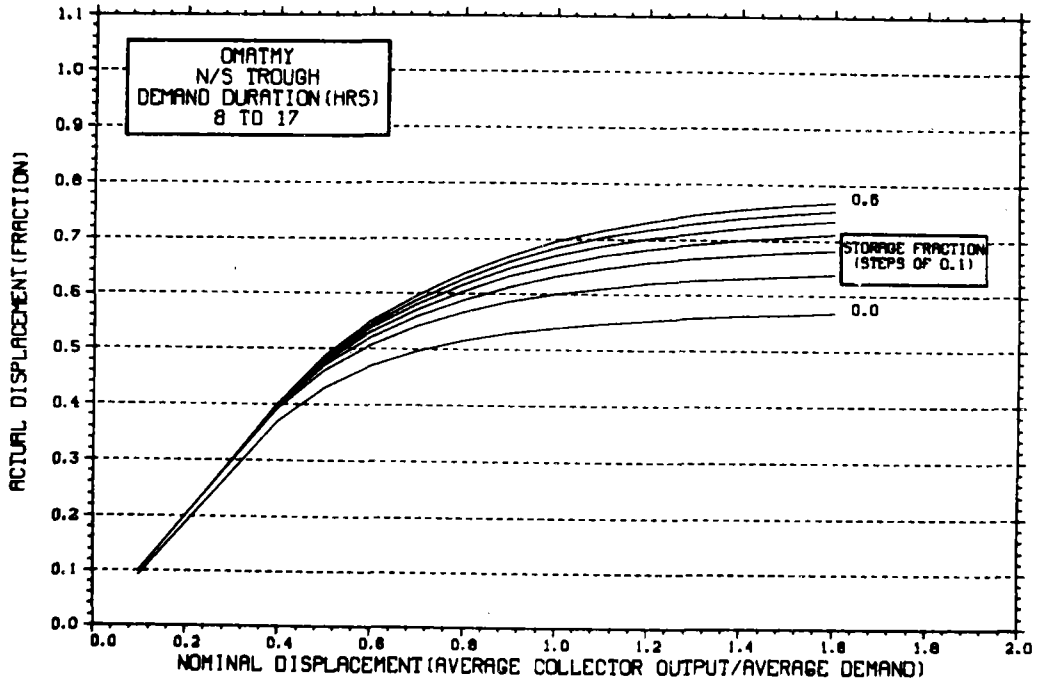

ENERGY INCIDENT ON COLLECTOR APERTURE

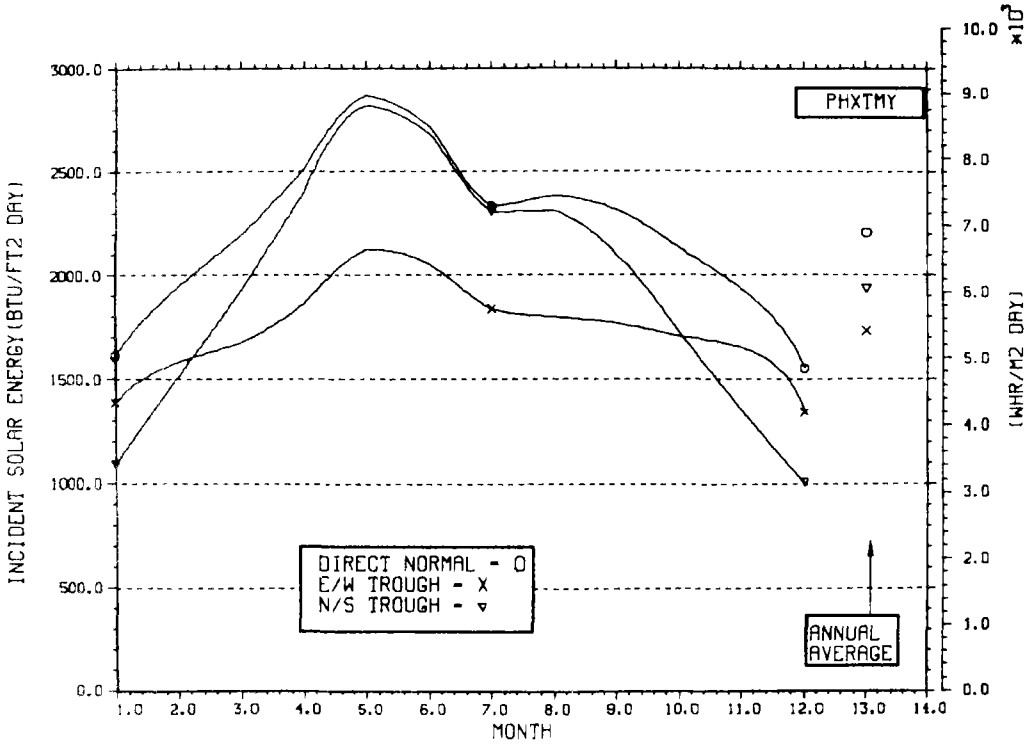

ANNUAL NONFIRST ROW SHADING

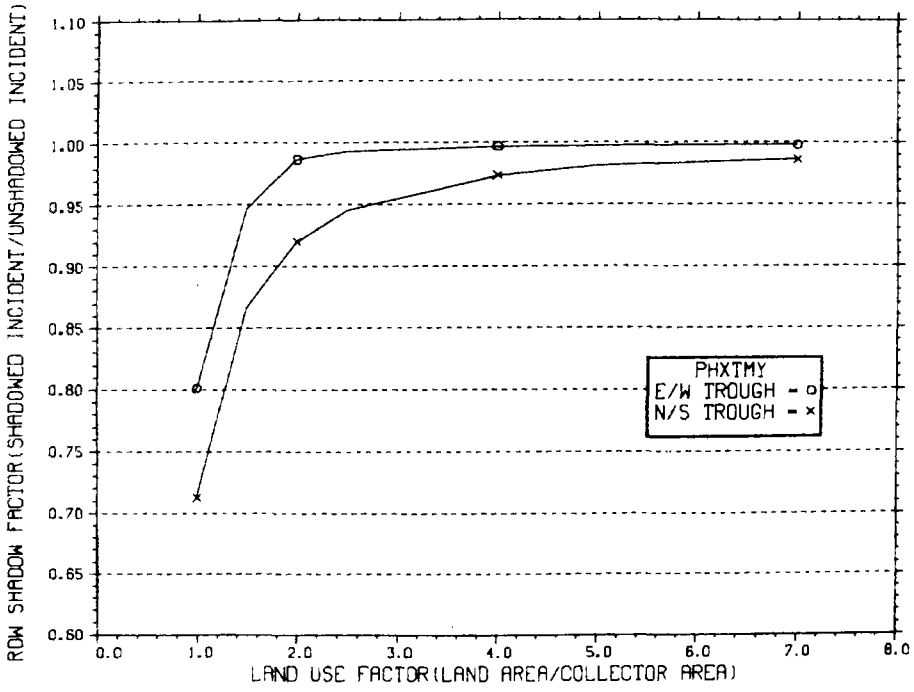

PERFORMANCE VARIATION WITH COLLECTOR AZIMUTH

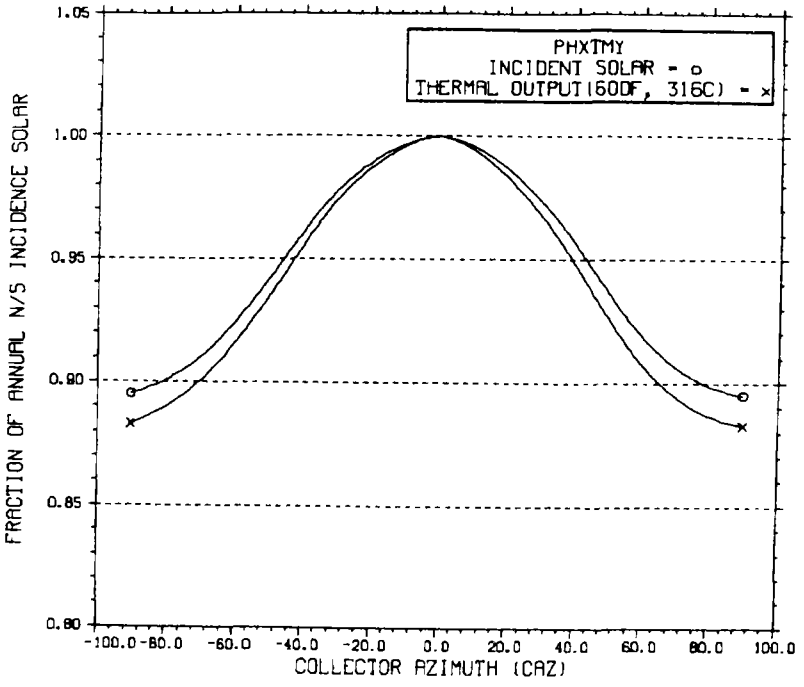

TEMPERATURE DEPENDENCE OF ANNUAL PERFORMANCE

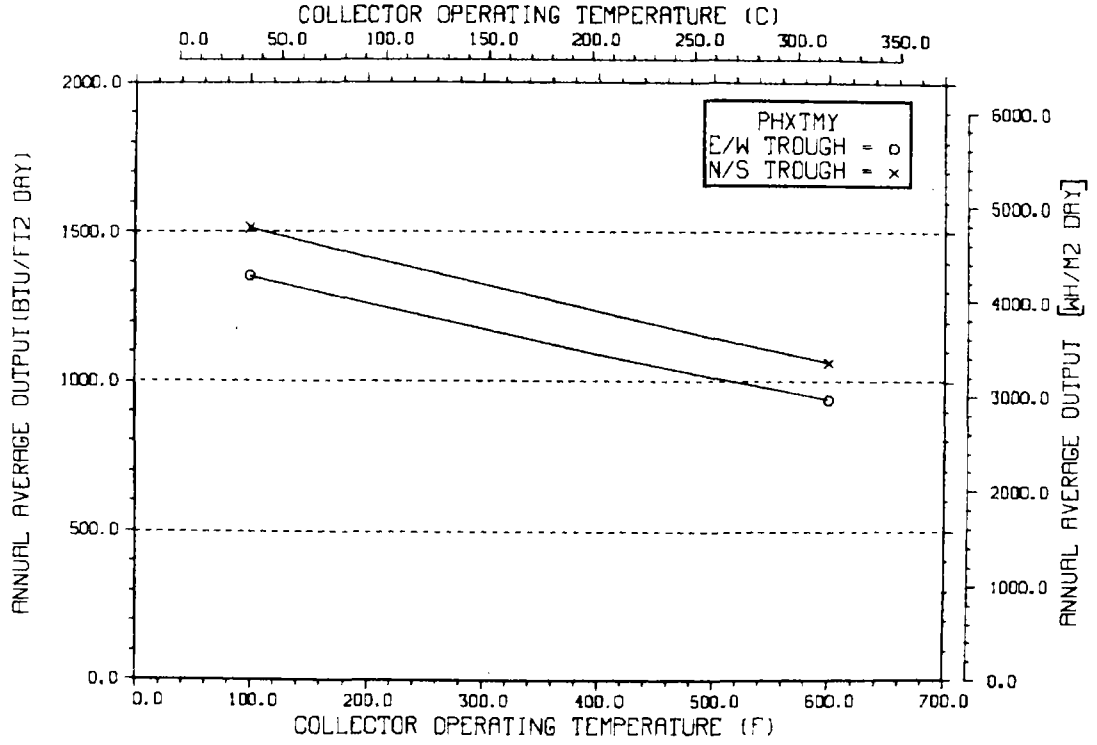

TEMPERATURE DEPENDENCE OF MONTHLY PERFORMANCE

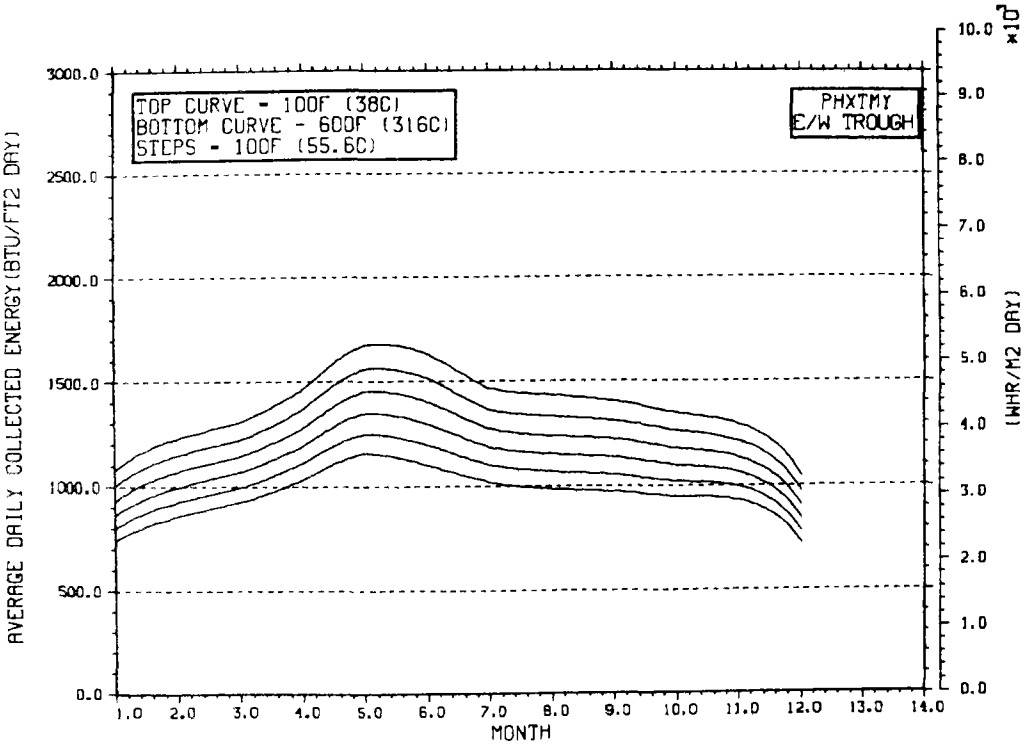

TEMPERATURE DEPENDENCE OF MONTHLY PERFORMANCE

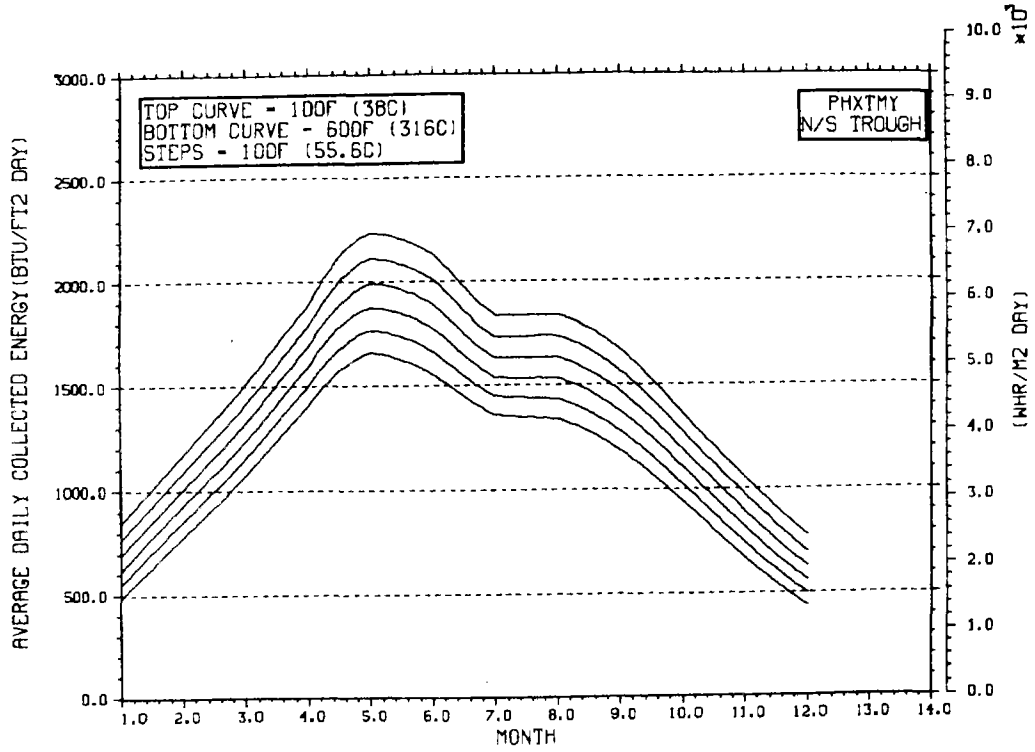

STORAGE SIZING GRAPH FOR CONSTANT ANNUAL DEMAND

NO WEEKEND SHUTDOWN

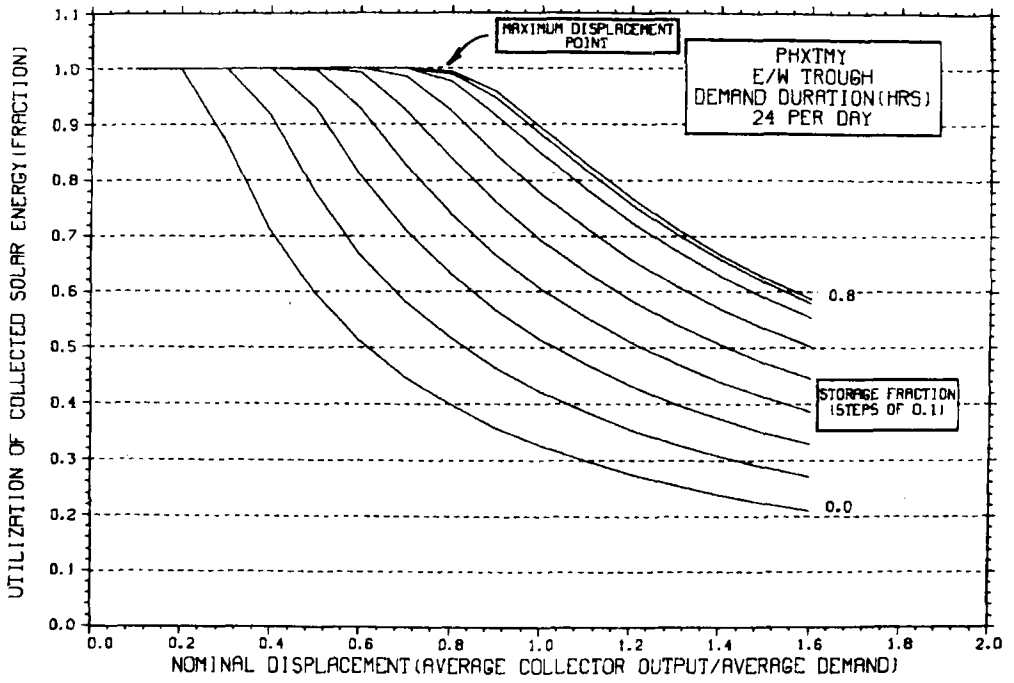

STORAGE SIZING GRAPH FOR CONSTANT ANNUAL DEMAND

NO WEEKEND SHUTDOWN

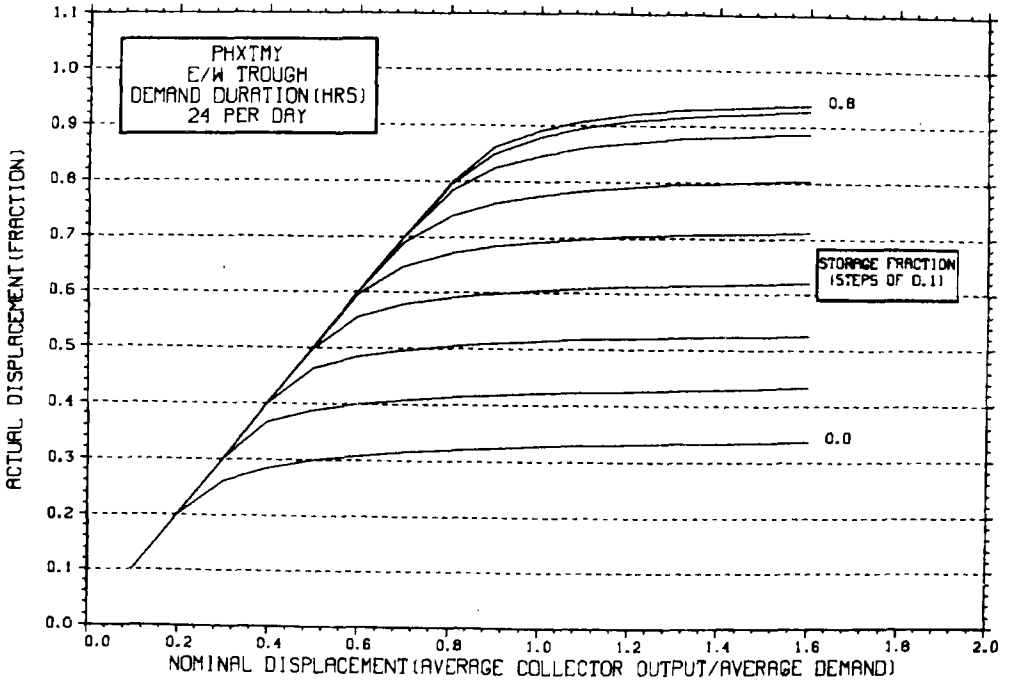

STORAGE SIZING GRAPH FOR CONSTANT ANNUAL DEMAND

NO WEEKEND SHUTDOWN

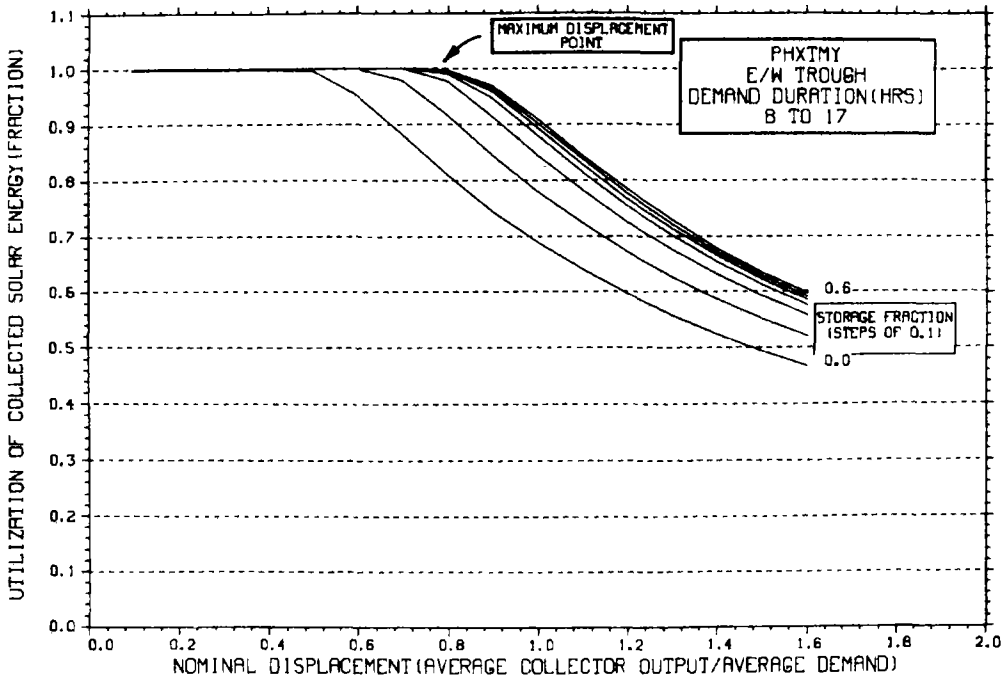

STORAGE SIZING GRAPH FOR CONSTANT ANNUAL DEMAND

NO WEEKEND SHUTDOWN

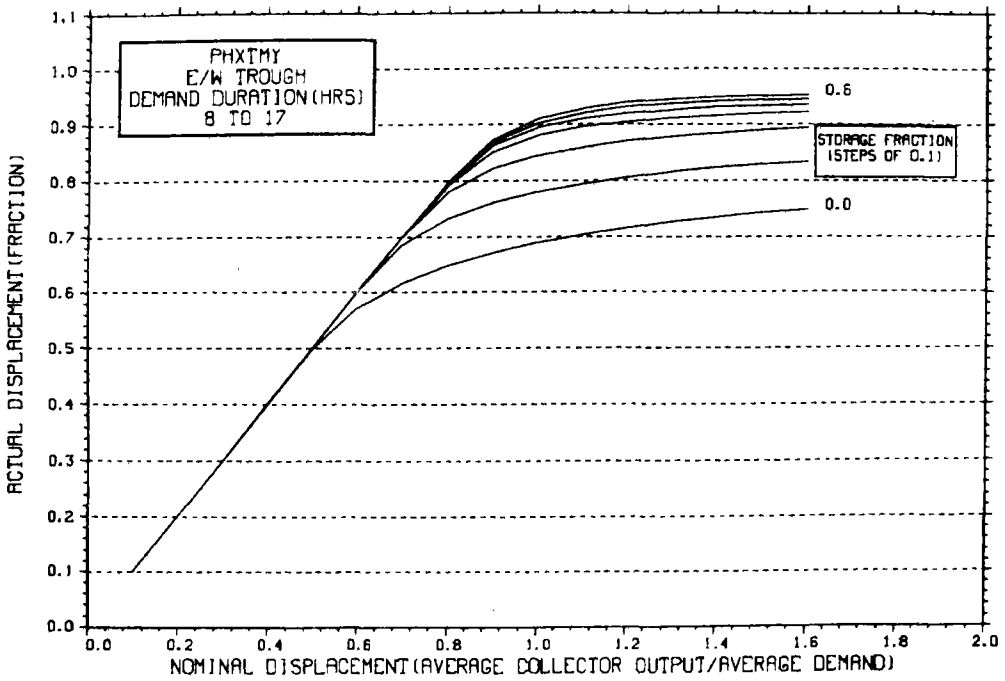

STORAGE SIZING GRAPH FOR CONSTANT ANNUAL DEMAND

NO WEEKEND SHUTDOWN

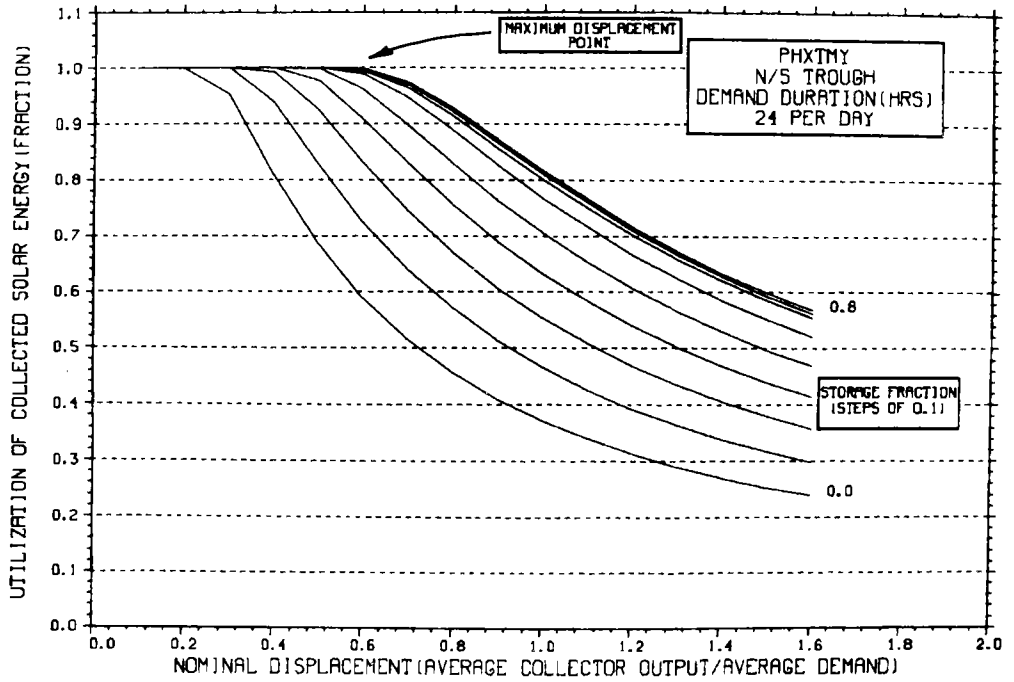

STORAGE SIZING GRAPH FOR CONSTANT ANNUAL DEMAND

NO WEEKEND SHUTDOWN

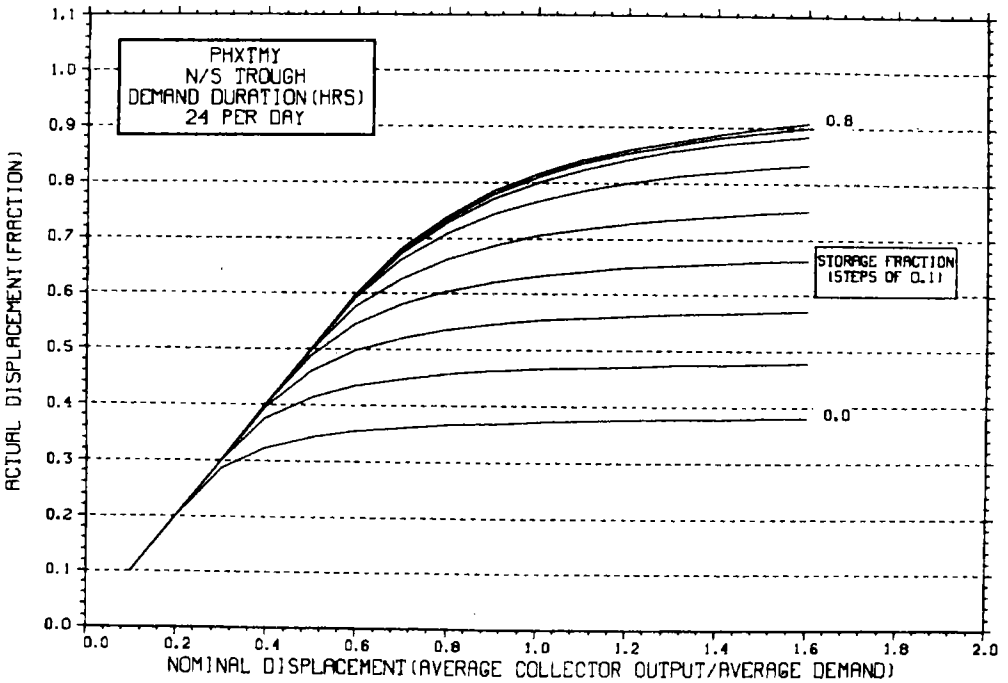

STORAGE SIZING GRAPH FOR CONSTANT ANNUAL DEMAND

NO WEEKEND SHUTDOWN

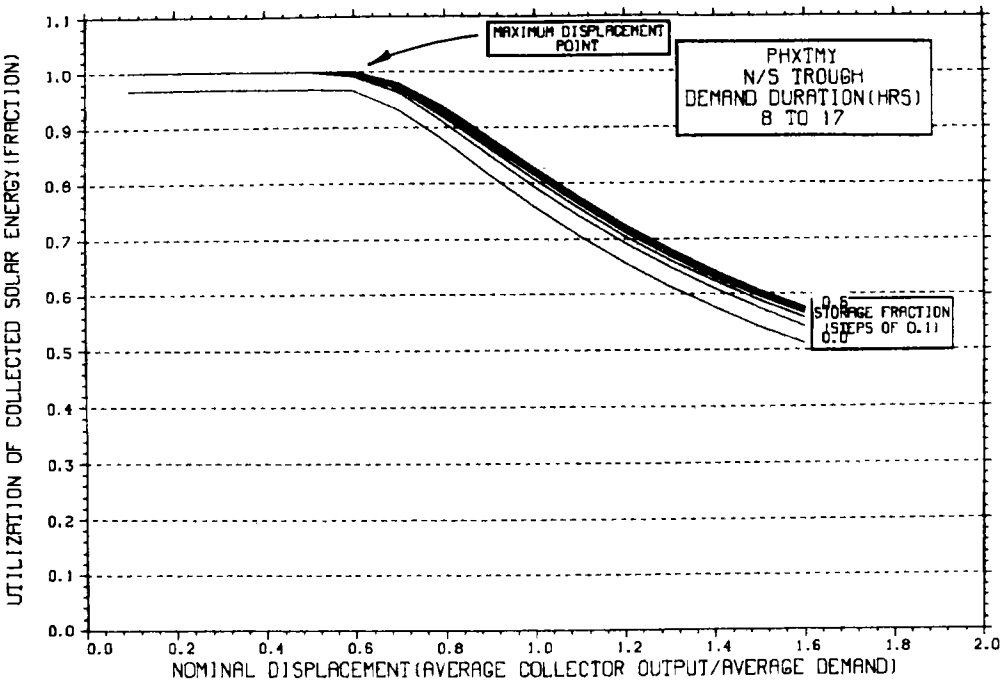

STORAGE SIZING GRAPH FOR CONSTANT ANNUAL DEMAND

NO WEEKEND SHUTDOWN

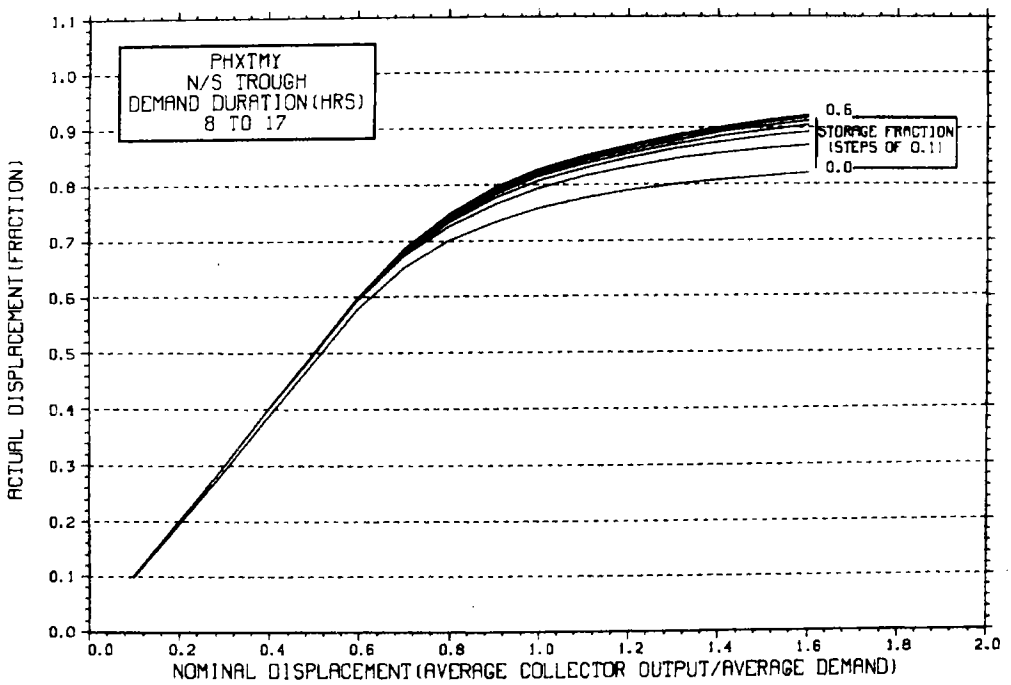

ENERGY INCIDENT ON COLLECTOR APERTURE

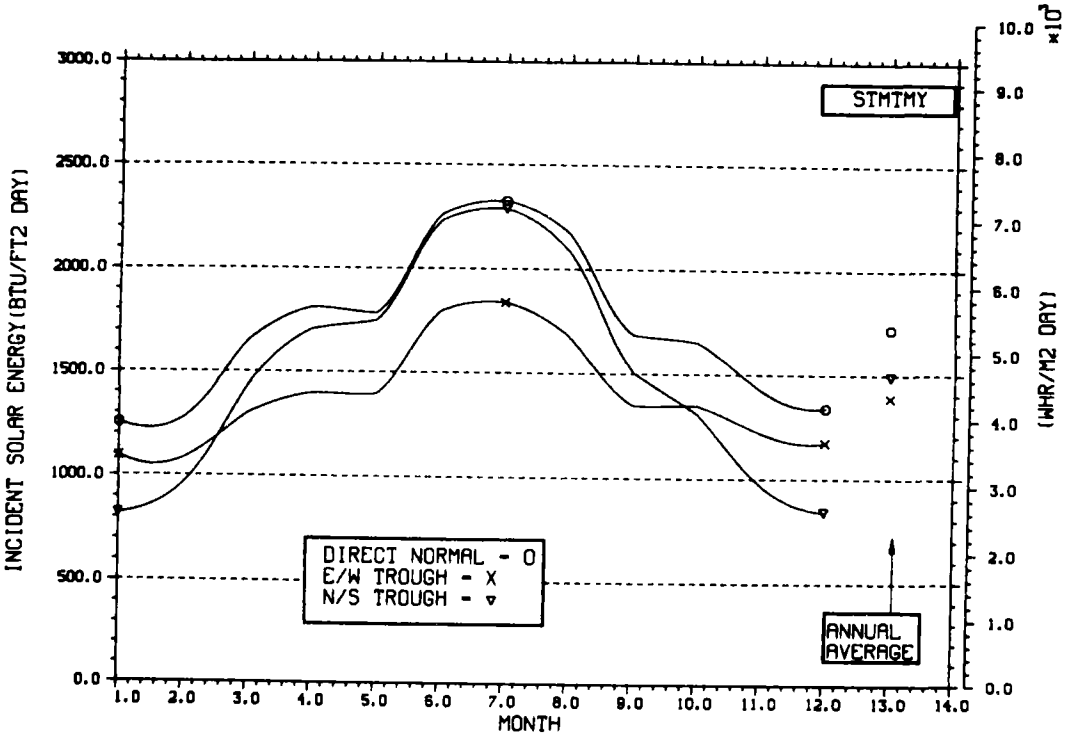

ANNUAL NONFIRST ROW SHADING

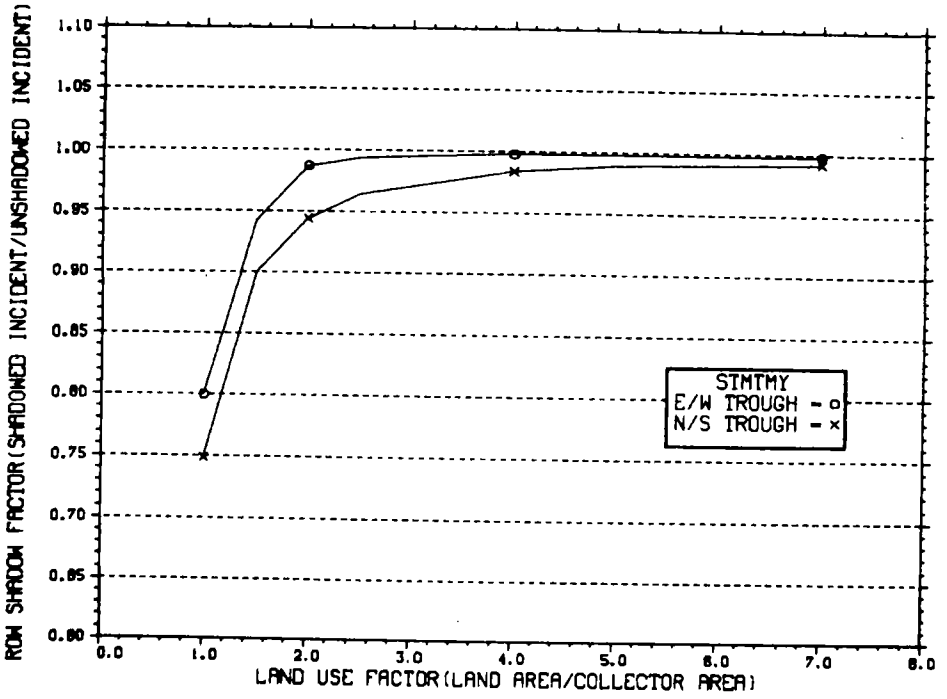

PERFORMANCE VARIATION WITH COLLECTOR AZIMUTH

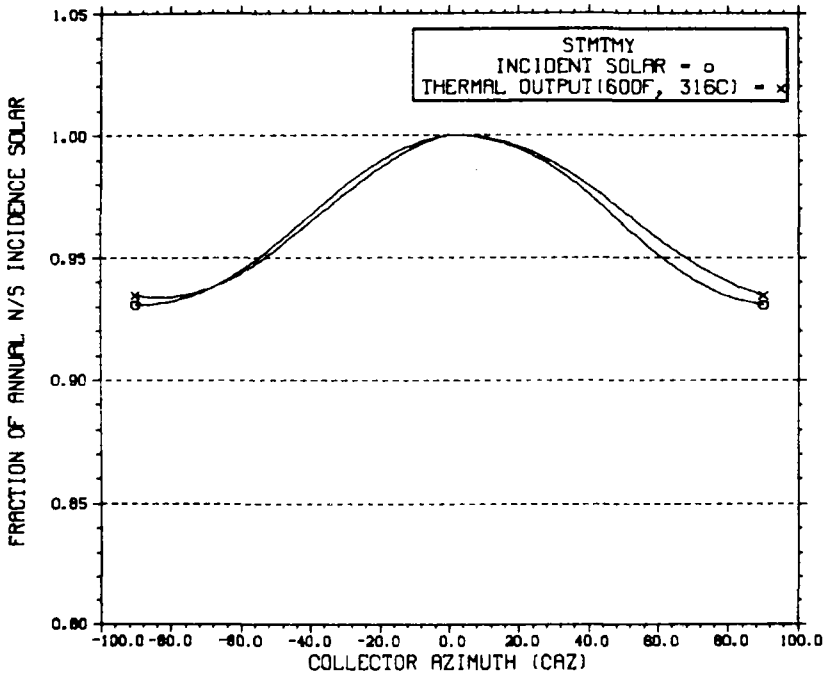

TEMPERATURE DEPENDENCE OF ANNUAL PERFORMANCE

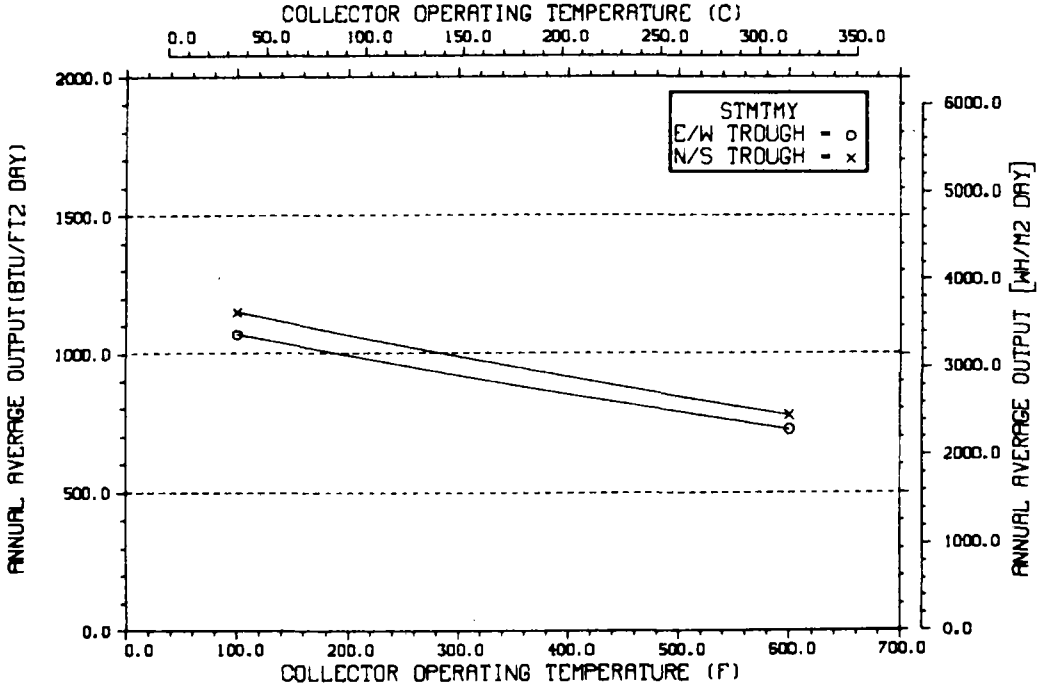

TEMPERATURE DEPENDENCE OF MONTHLY PERFORMANCE

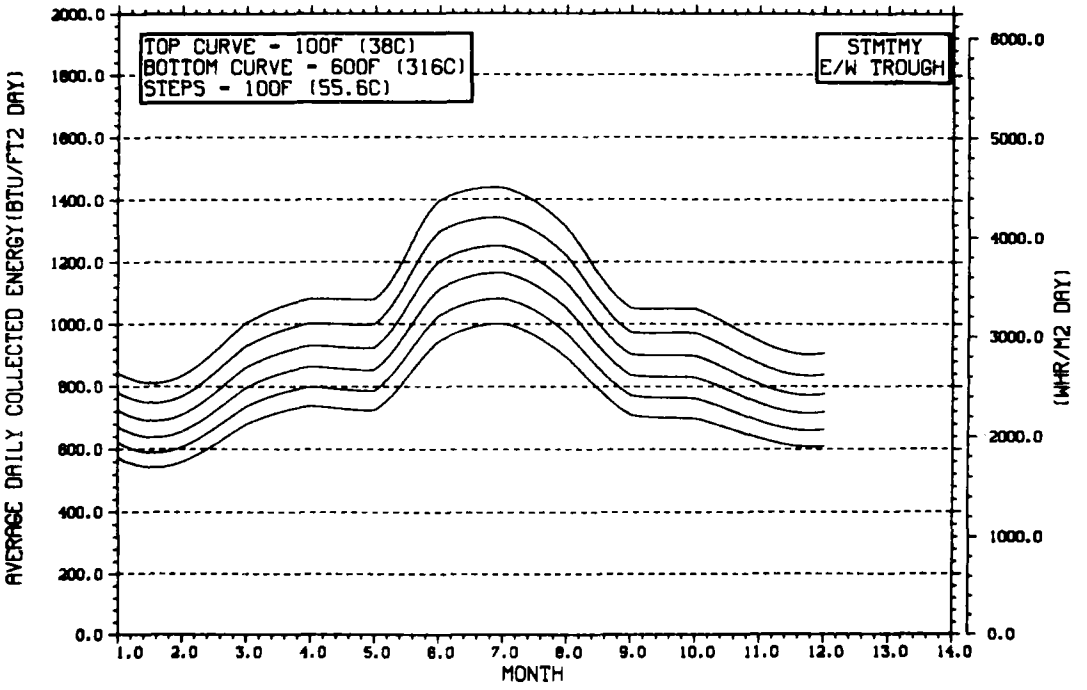

TEMPERATURE DEPENDENCE OF MONTHLY PERFORMANCE

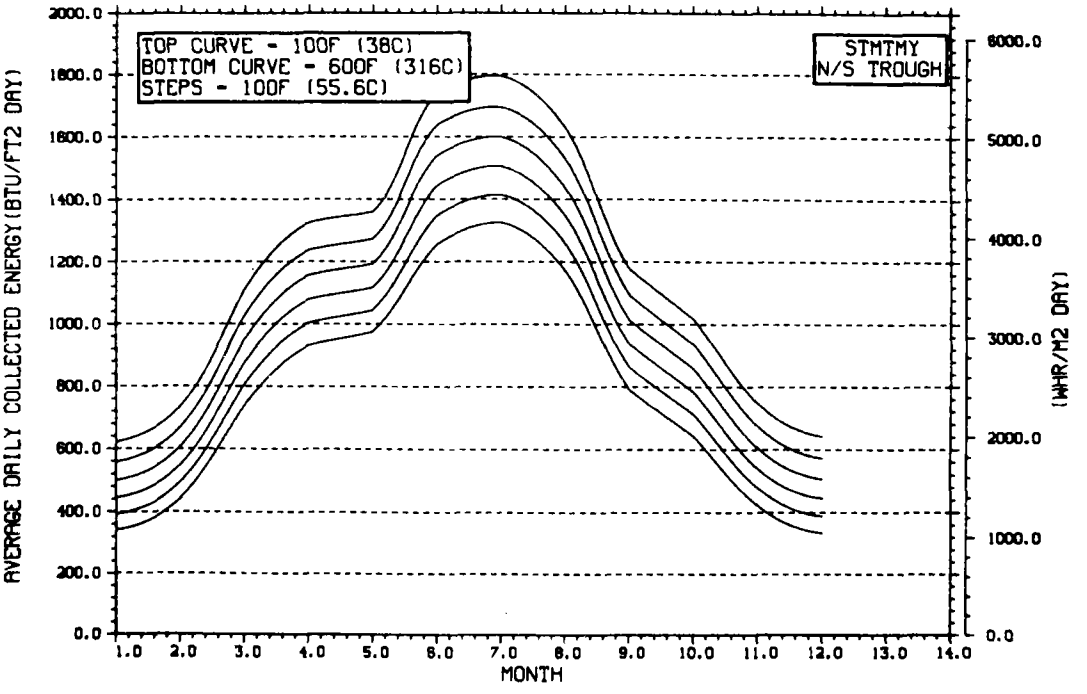

STORAGE SIZING GRAPH FOR CONSTANT ANNUAL DEMAND

NO WEEKEND SHUTDOWN

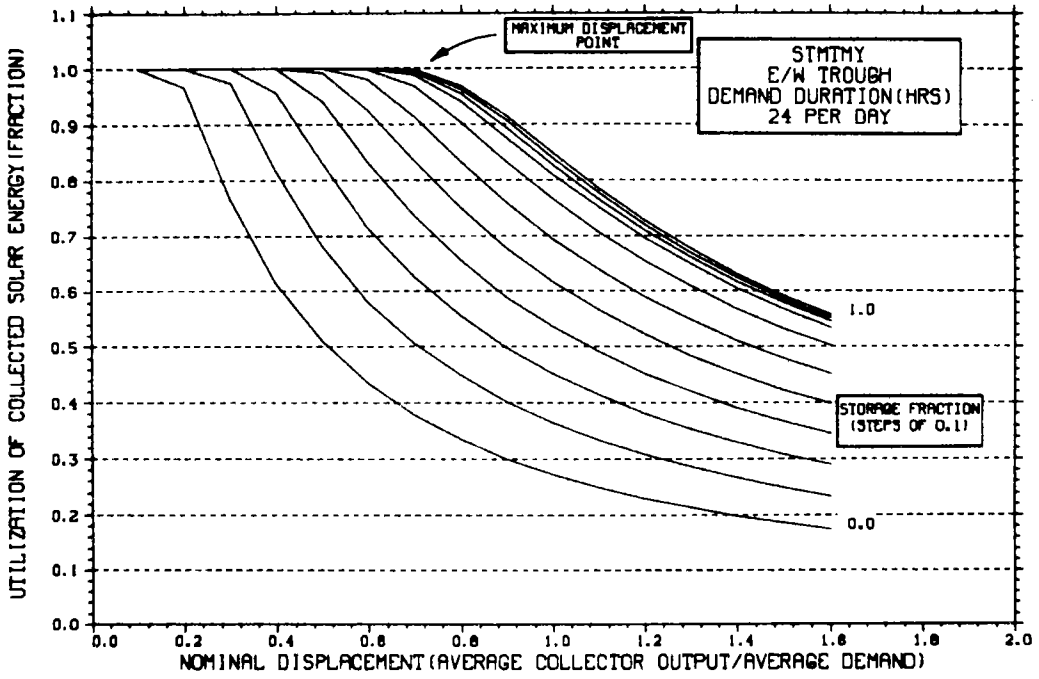

STORAGE SIZING GRAPH FOR CONSTANT ANNUAL DEMAND

NO WEEKEND SHUTDOWN

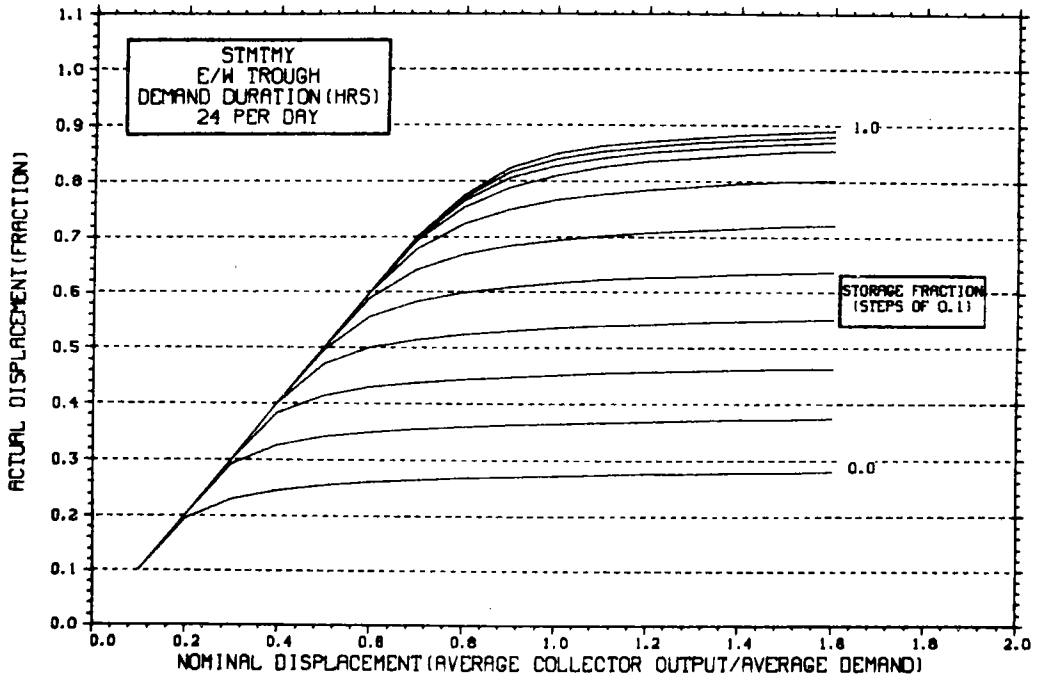

STORAGE SIZING GRAPH FOR CONSTANT ANNUAL DEMAND

NO WEEKEND SHUTDOWN

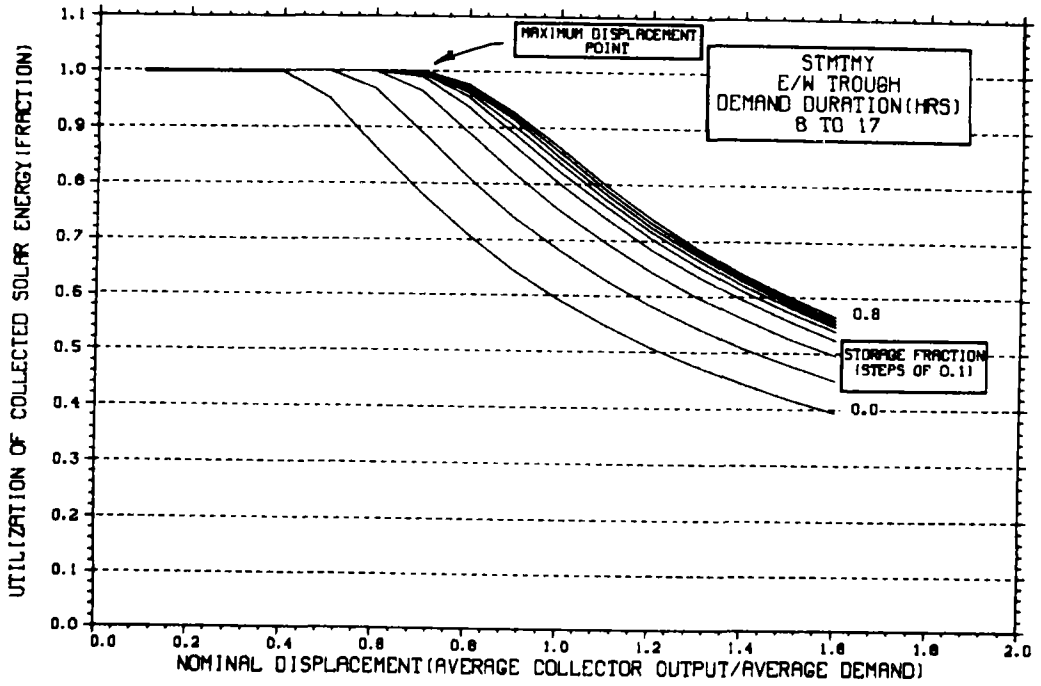

STORAGE SIZING GRAPH FOR CONSTANT ANNUAL DEMAND

NO WEEKEND SHUTDOWN

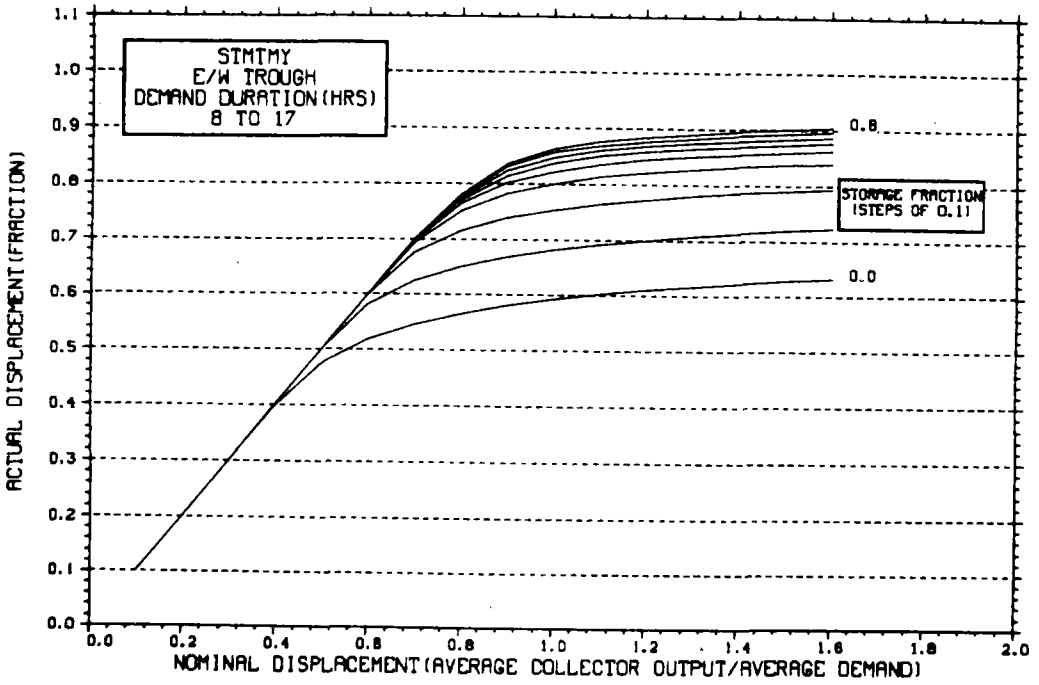

STORAGE SIZING GRAPH FOR CONSTANT ANNUAL DEMAND

NO WEEKEND SHUTDOWN

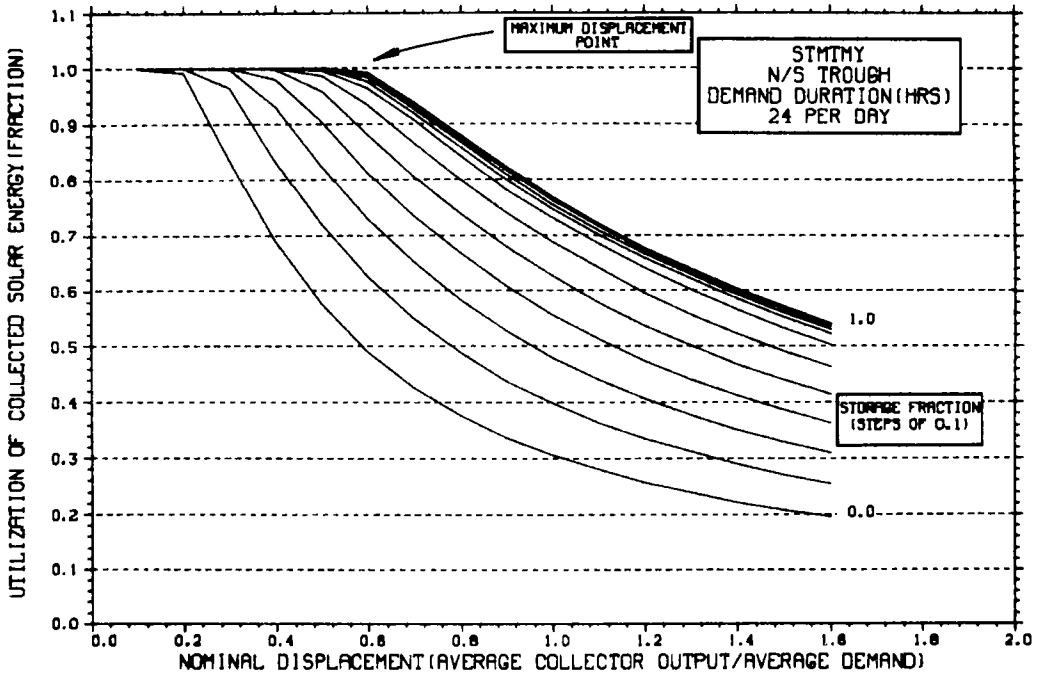

STORAGE SIZING GRAPH FOR CONSTANT ANNUAL DEMAND

NO WEEKEND SHUTDOWN

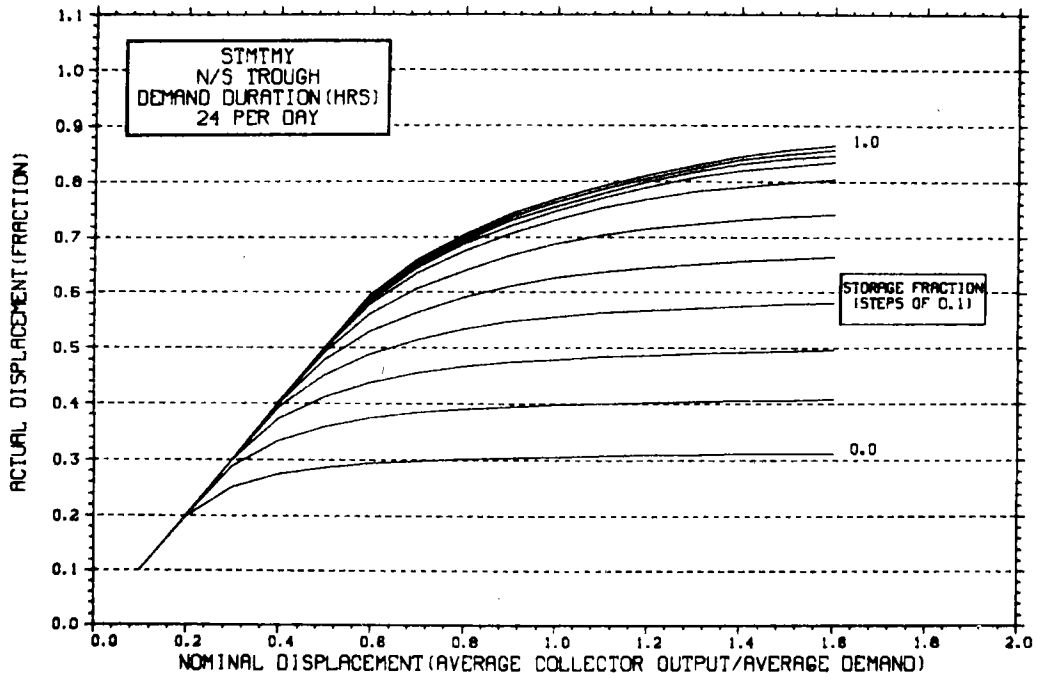

STORAGE SIZING GRAPH FOR CONSTANT ANNUAL DEMAND

NO WEEKEND SHUTDOWN

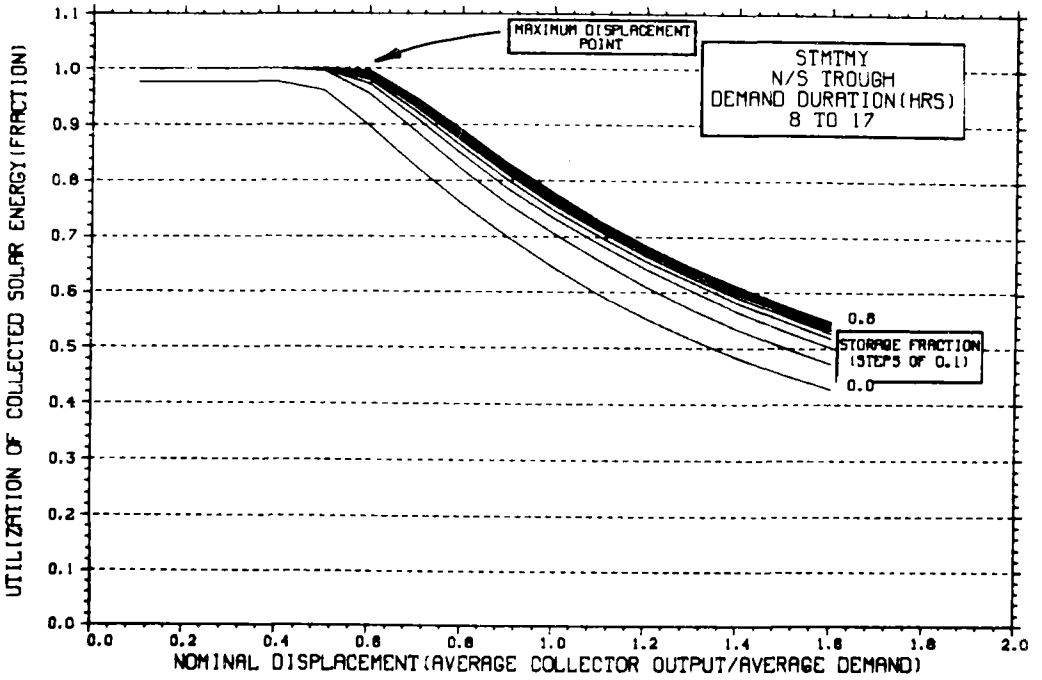

STORAGE SIZING GRAPH FOR CONSTANT ANNUAL DEMAND

NO WEEKEND SHUTDOWN

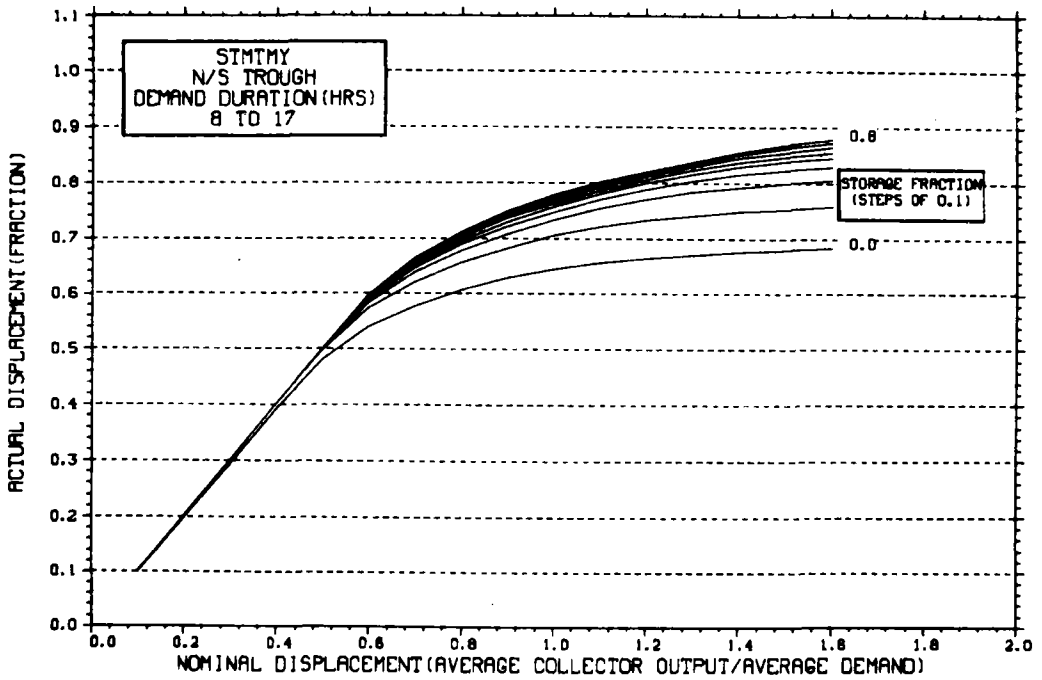

ENERGY INCIDENT ON COLLECTOR APERTURE

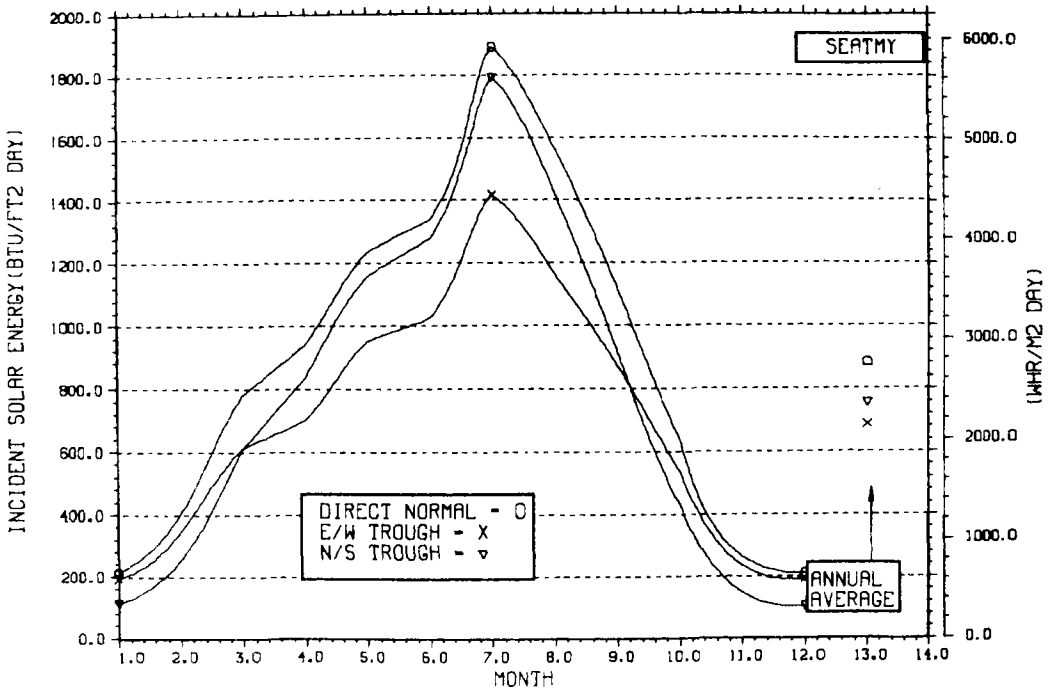

ANNUAL NONFIRST ROW SHADING

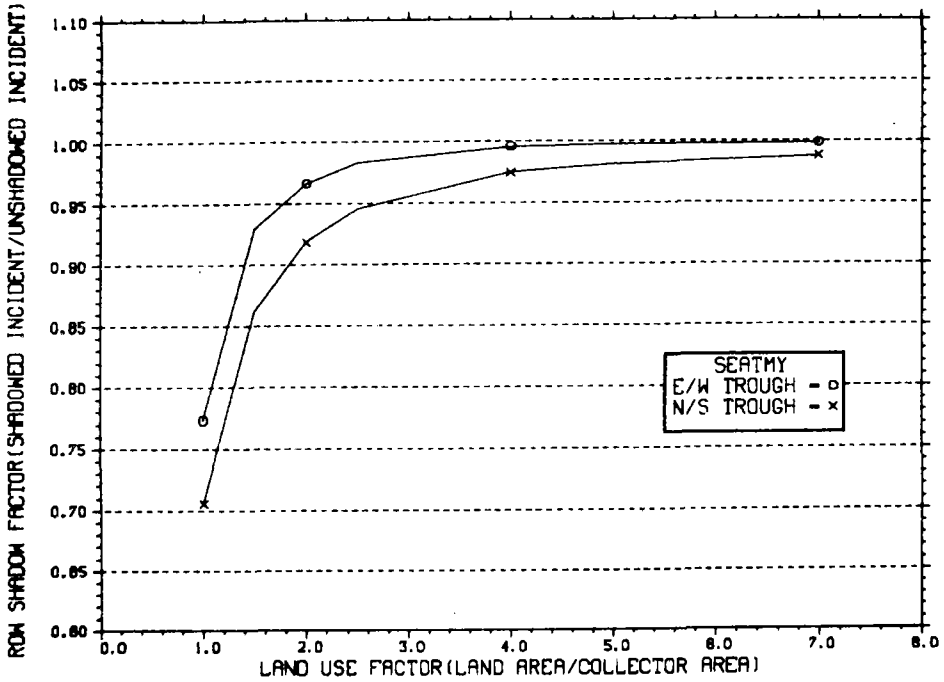

PERFORMANCE VARIATION WITH COLLECTOR AZIMUTH

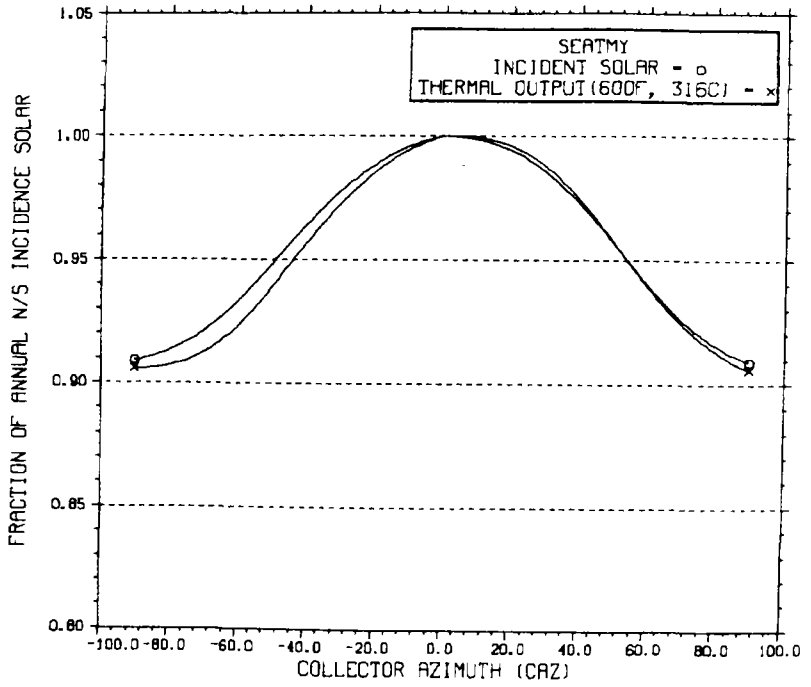

TEMPERATURE DEPENDENCE OF ANNUAL PERFORMANCE

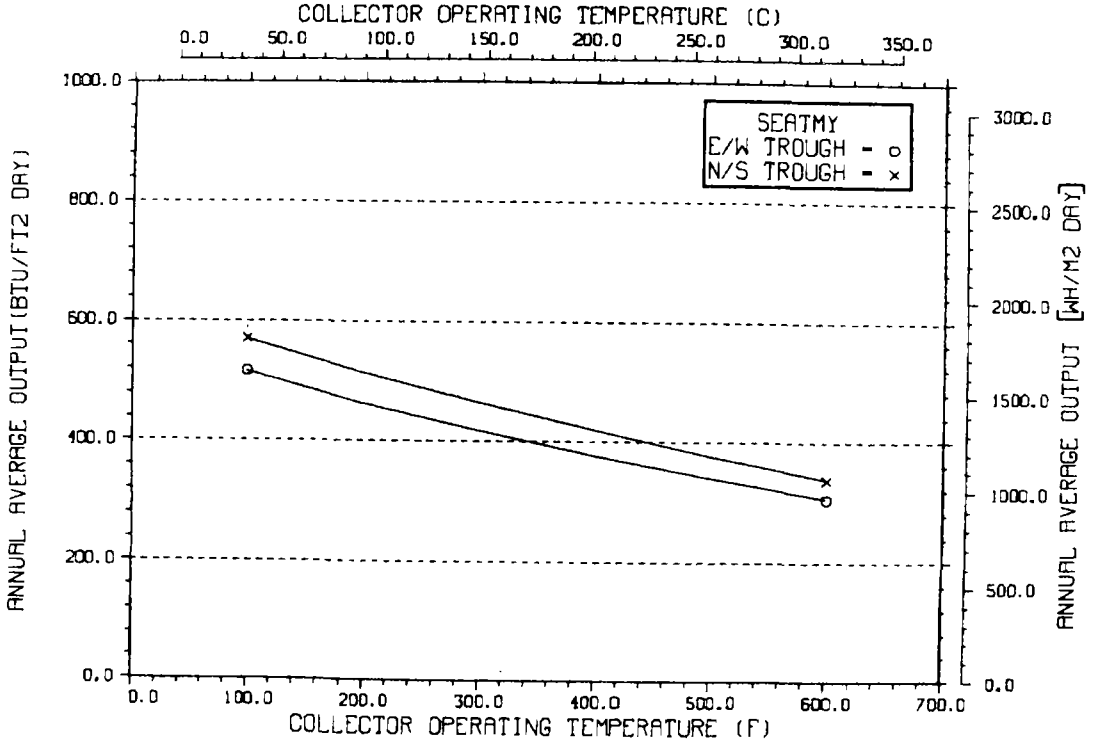

TEMPERATURE DEPENDENCE OF MONTHLY PERFORMANCE

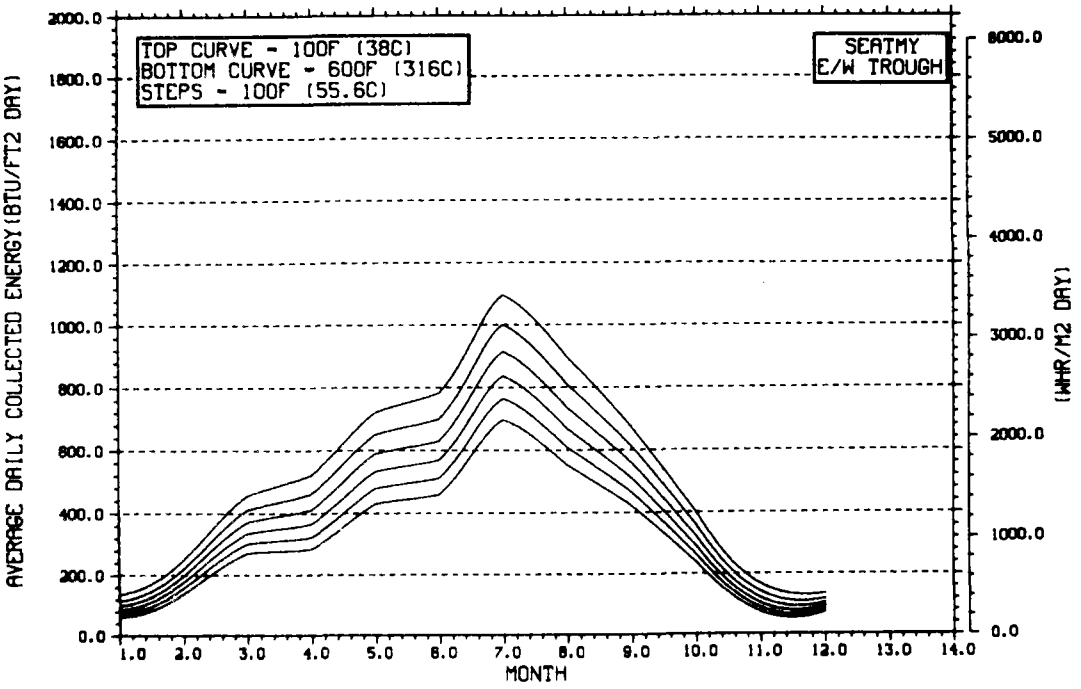

TEMPERATURE DEPENDENCE OF MONTHLY PERFORMANCE

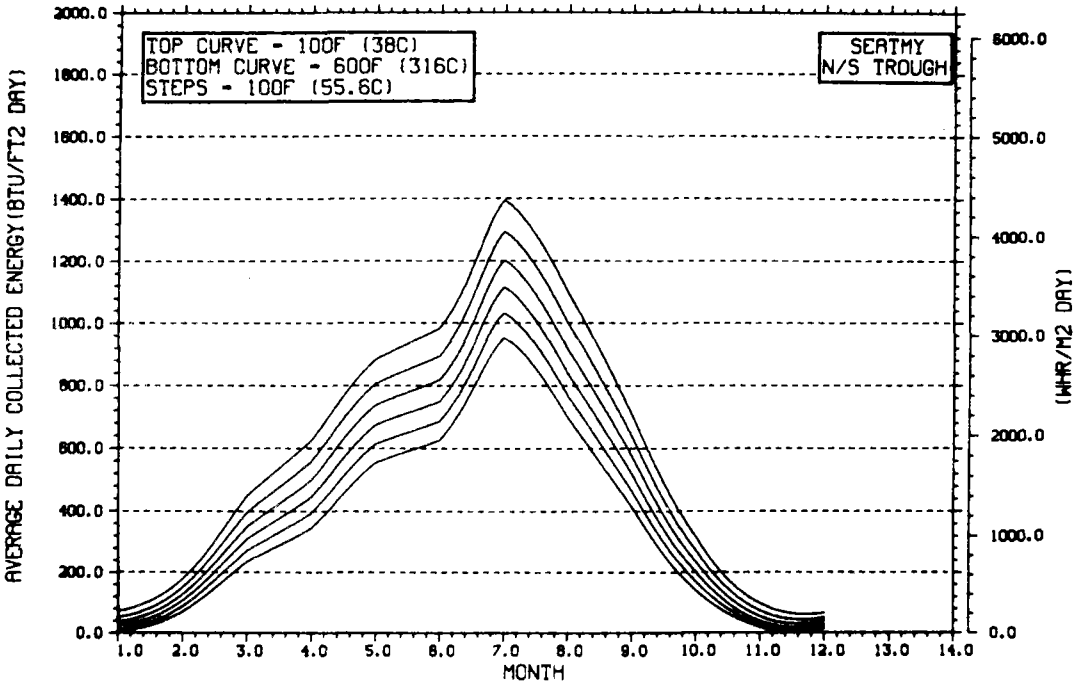

STORAGE SIZING GRAPH FOR CONSTANT ANNUAL DEMAND

NO WEEKEND SHUTDOWN

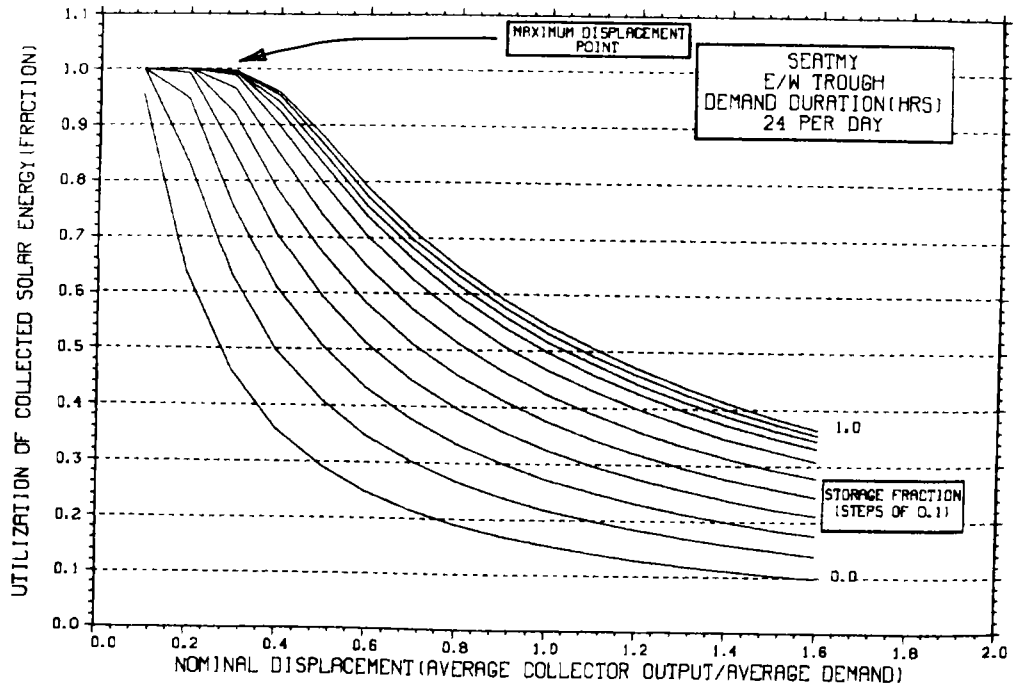

STORAGE SIZING GRAPH FOR CONSTANT ANNUAL DEMAND

NO WEEKEND SHUTDOWN

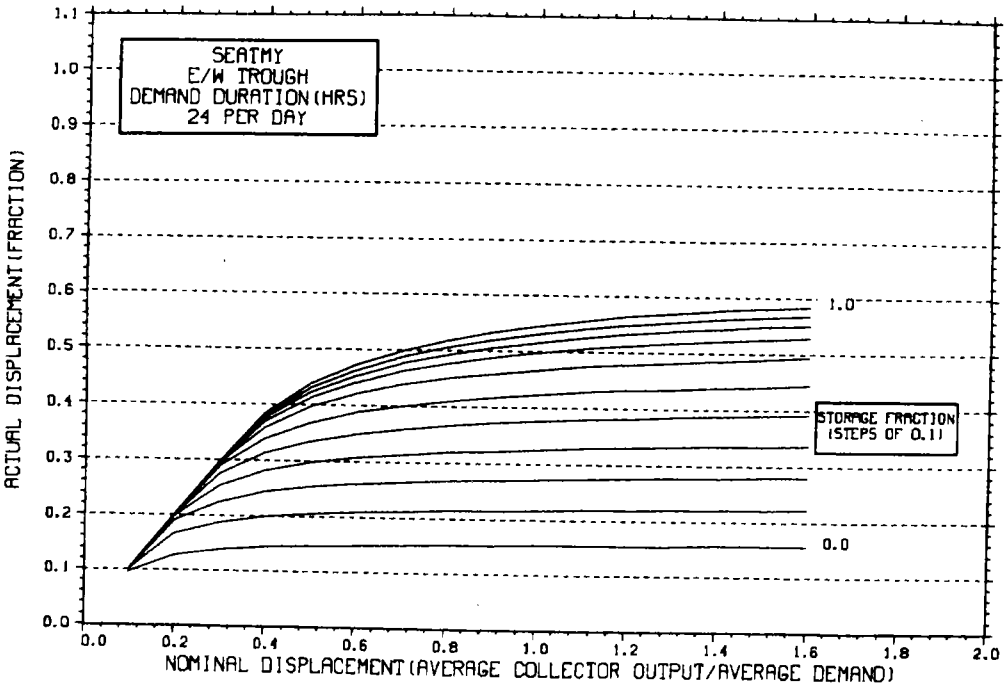

STORAGE SIZING GRAPH FOR CONSTANT ANNUAL DEMAND

NO WEEKEND SHUTDOWN

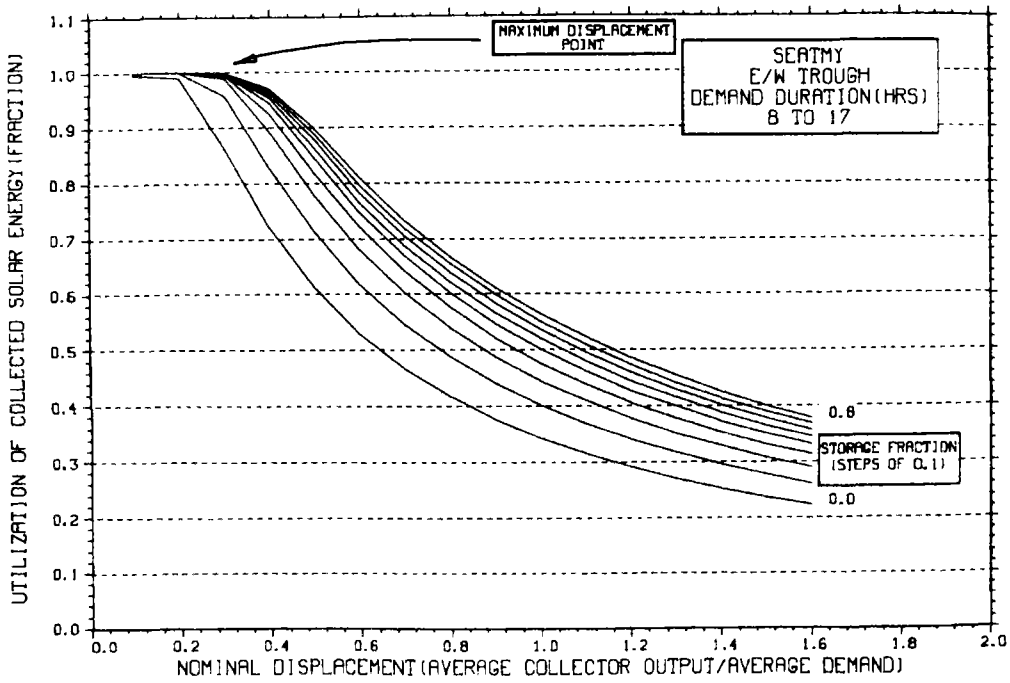

STORAGE SIZING GRAPH FOR CONSTANT ANNUAL DEMAND

NO WEEKEND SHUTDOWN

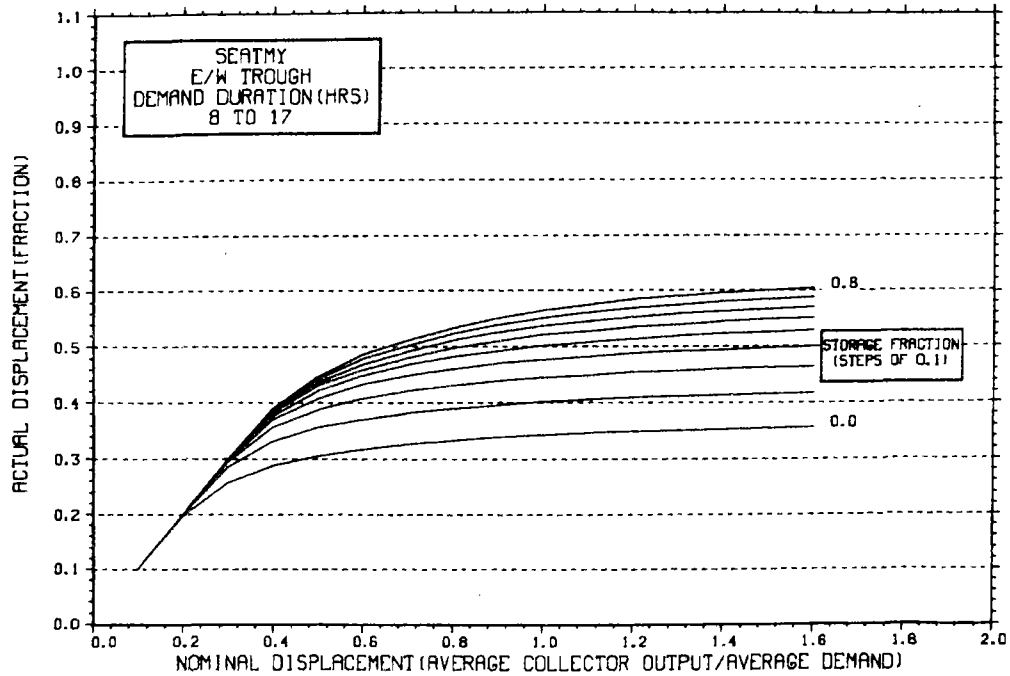

STORAGE SIZING GRAPH FOR CONSTANT ANNUAL DEMAND

NO WEEKEND SHUTDOWN

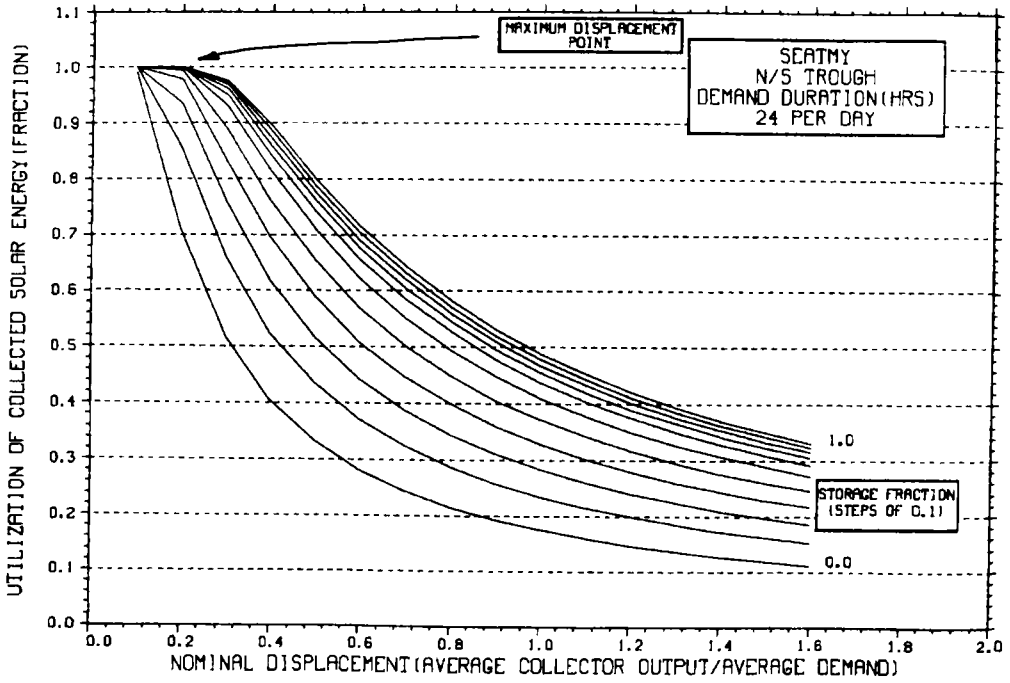

STORAGE SIZING GRAPH FOR CONSTANT ANNUAL DEMAND

NO WEEKEND SHUTDOWN

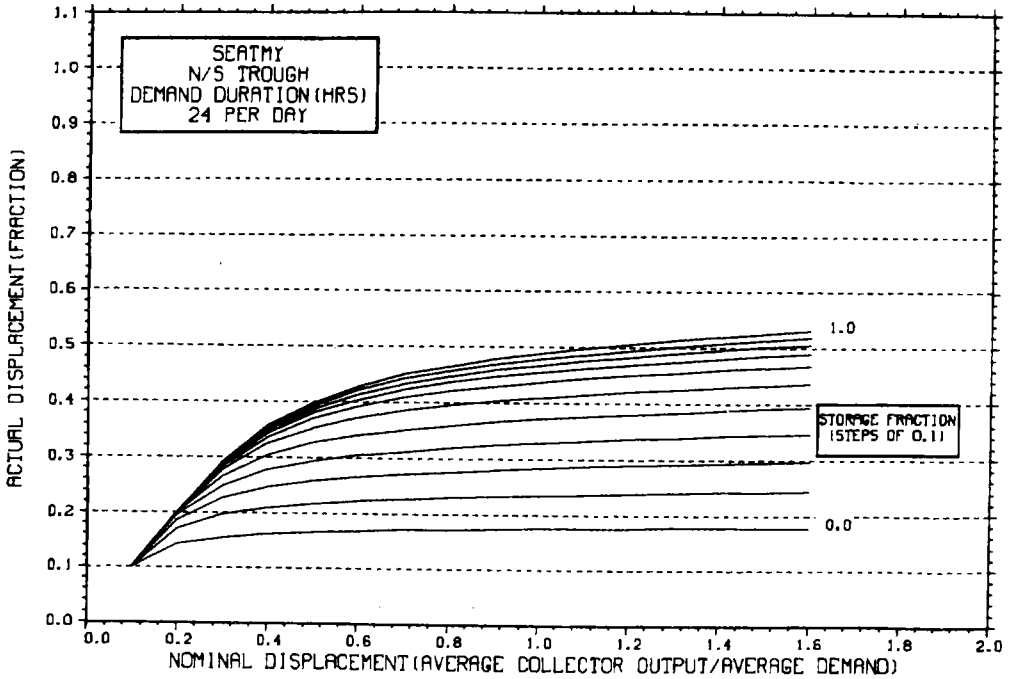

STORAGE SIZING GRAPH FOR CONSTANT ANNUAL DEMAND

NO WEEKEND SHUTDOWN

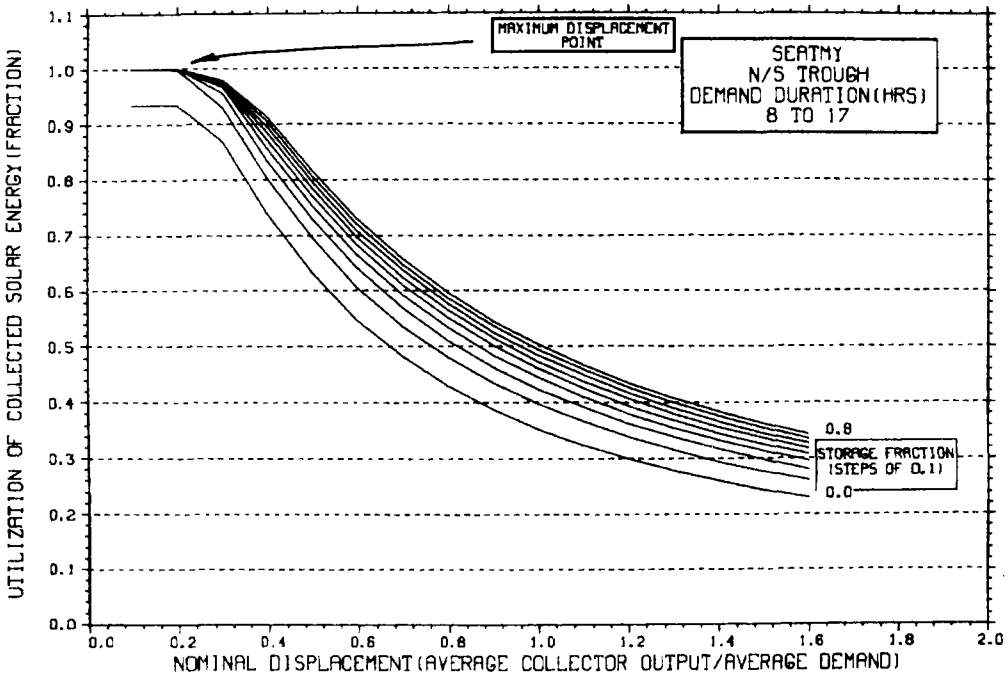

STORAGE SIZING GRAPH FOR CONSTANT ANNUAL DEMAND

NO WEEKEND SHUTDOWN

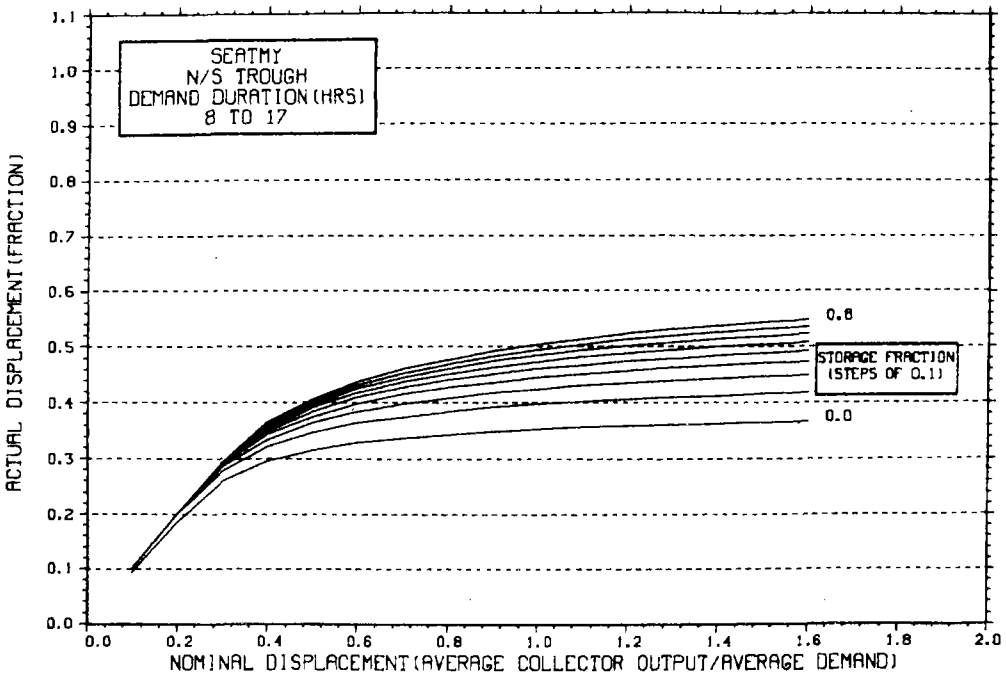

ENERGY INCIDENT ON COLLECTOR APERTURE

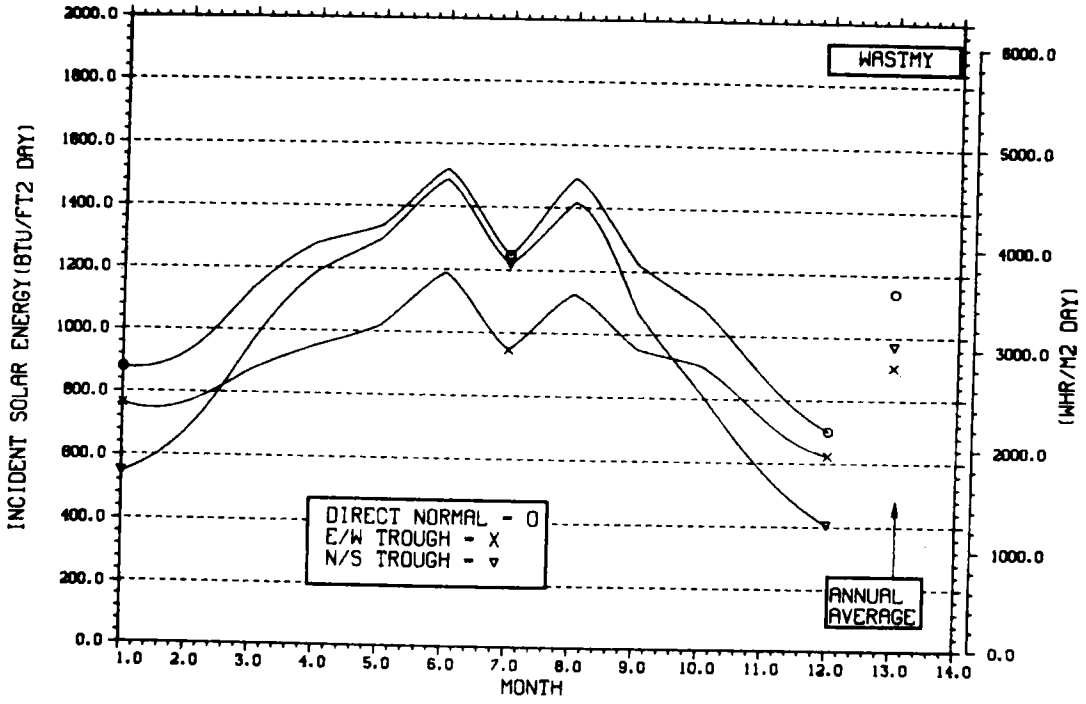

ANNUAL NONFIRST ROW SHADING

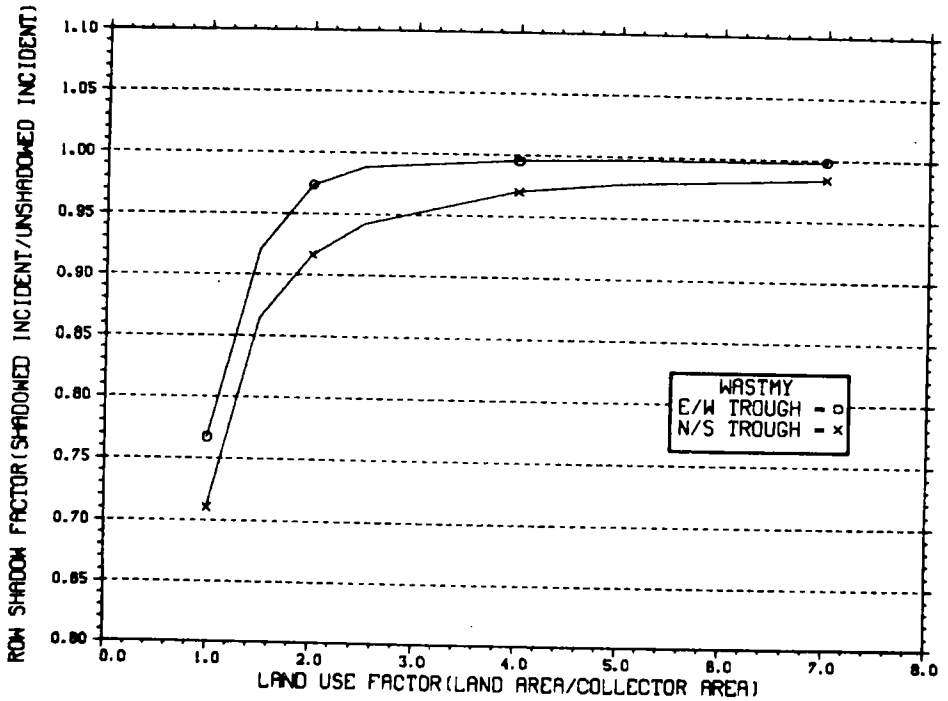

PERFORMANCE VARIATION WITH COLLECTOR AZIMUTH

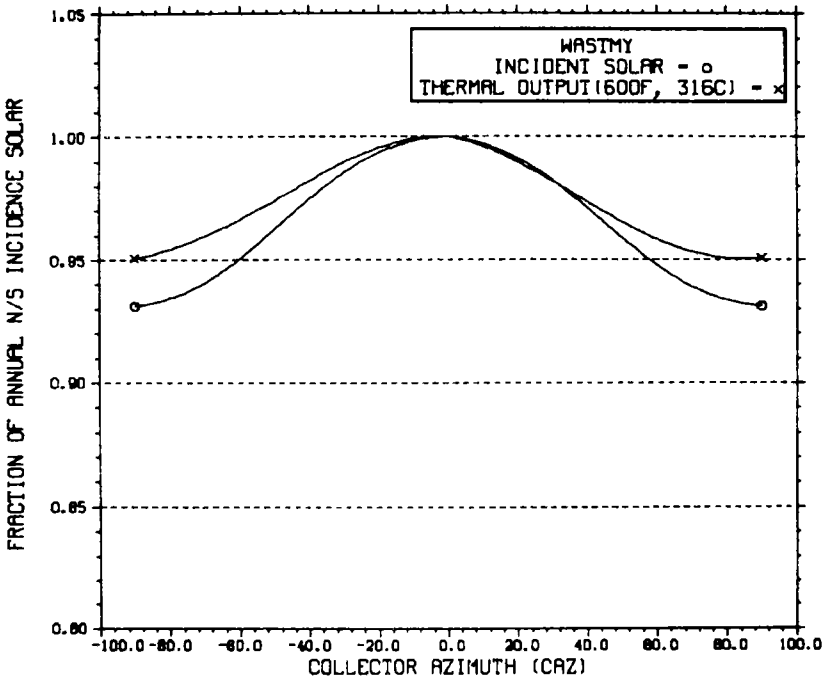

TEMPERATURE DEPENDENCE OF ANNUAL PERFORMANCE

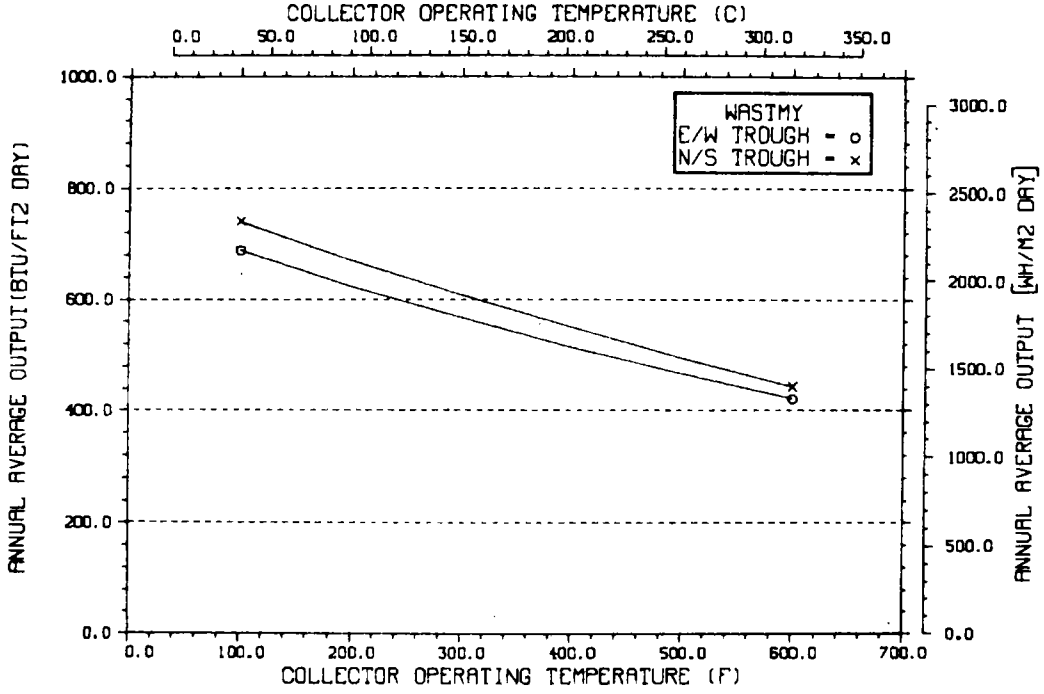

TEMPERATURE DEPENDENCE OF MONTHLY PERFORMANCE

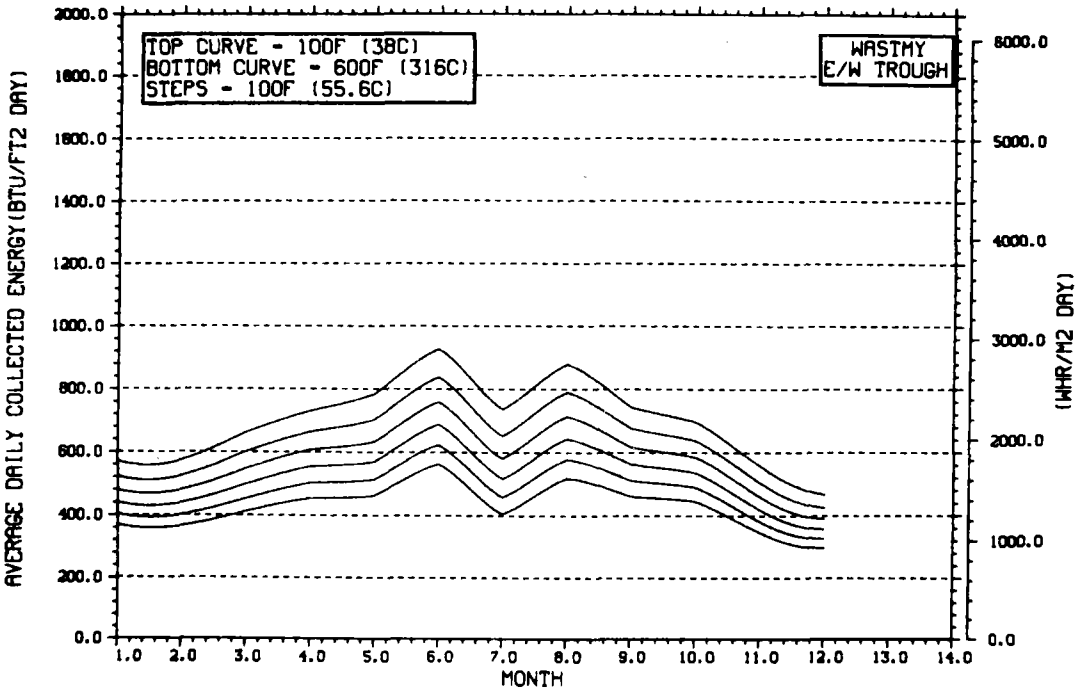

TEMPERATURE DEPENDENCE OF MONTHLY PERFORMANCE

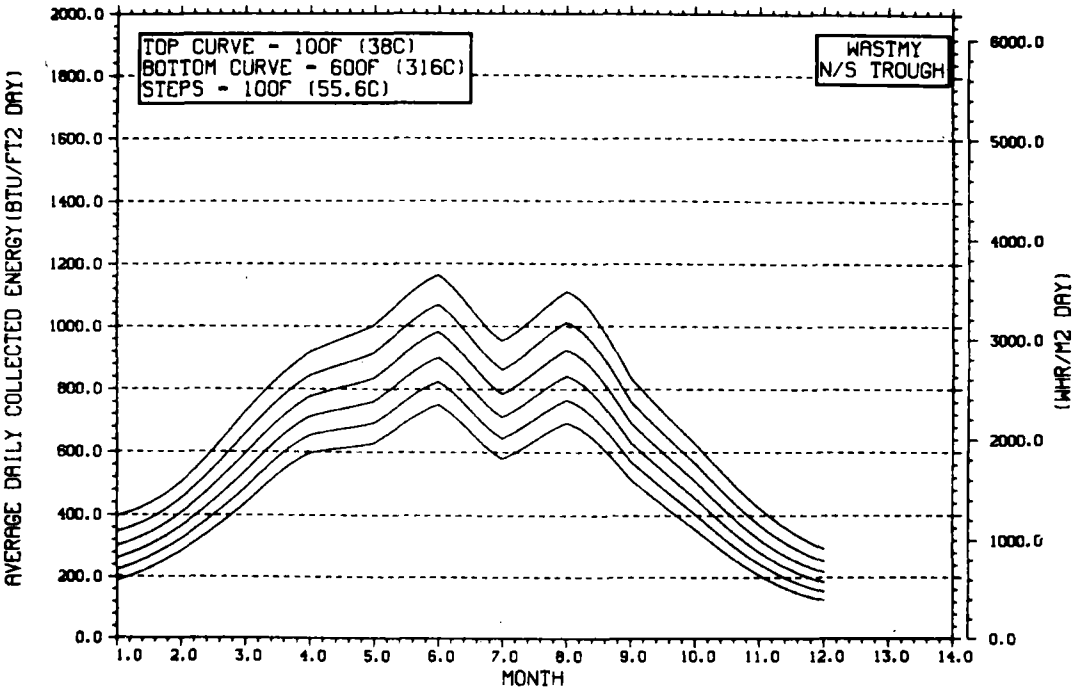

STORAGE SIZING GRAPH FOR CONSTANT ANNUAL DEMAND

NO WEEKEND SHUTDOWN

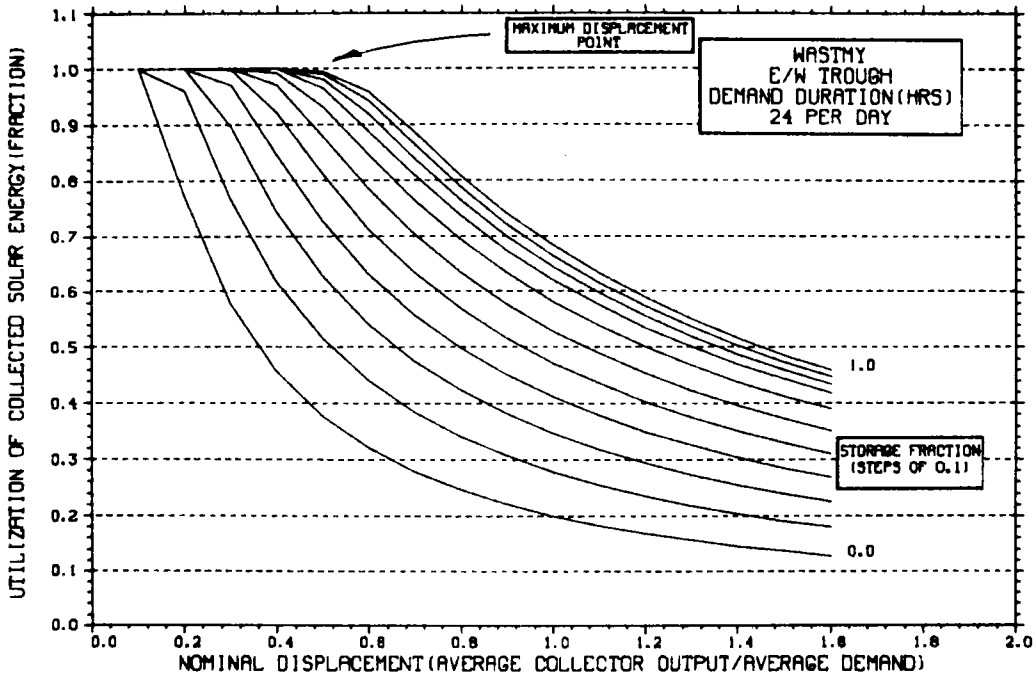

STORAGE SIZING GRAPH FOR CONSTANT ANNUAL DEMAND

NO WEEKEND SHUTDOWN

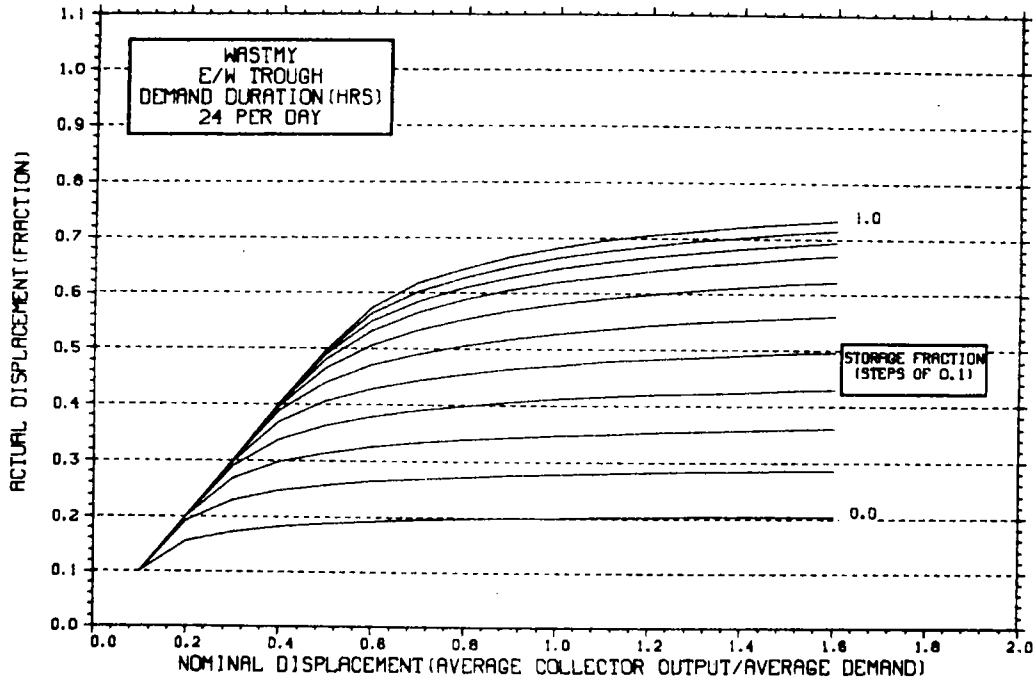

STORAGE SIZING GRAPH FOR CONSTANT ANNUAL DEMAND

NO WEEKEND SHUTDOWN

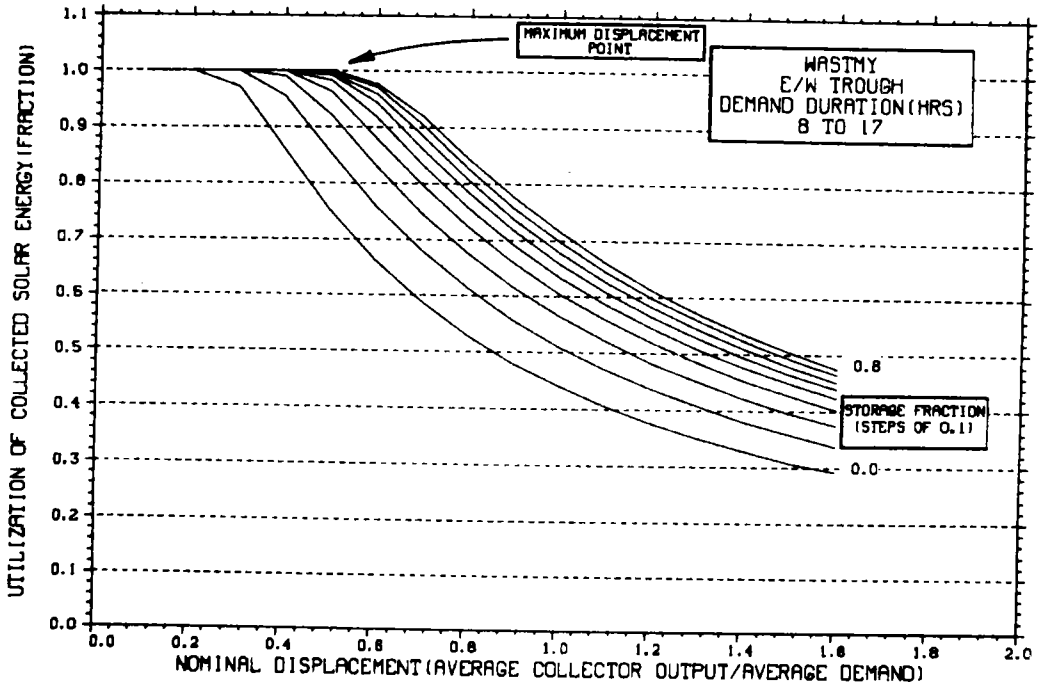

STORAGE SIZING GRAPH FOR CONSTANT ANNUAL DEMAND

NO WEEKEND SHUTDOWN

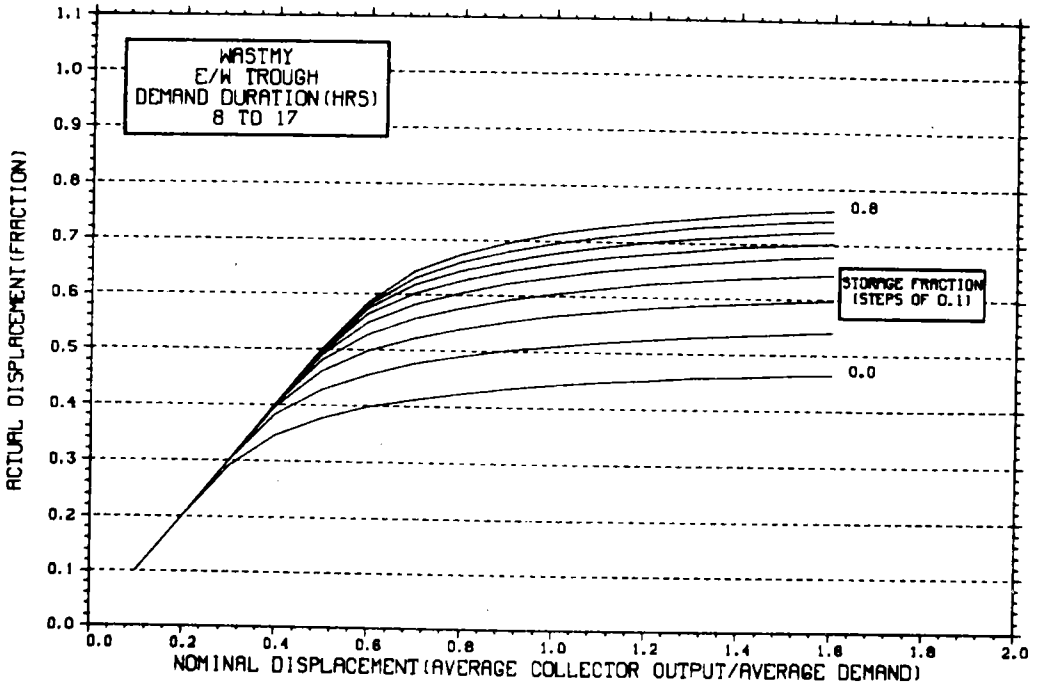

STORAGE SIZING GRAPH FOR CONSTANT ANNUAL DEMAND

NO WEEKEND SHUTDOWN

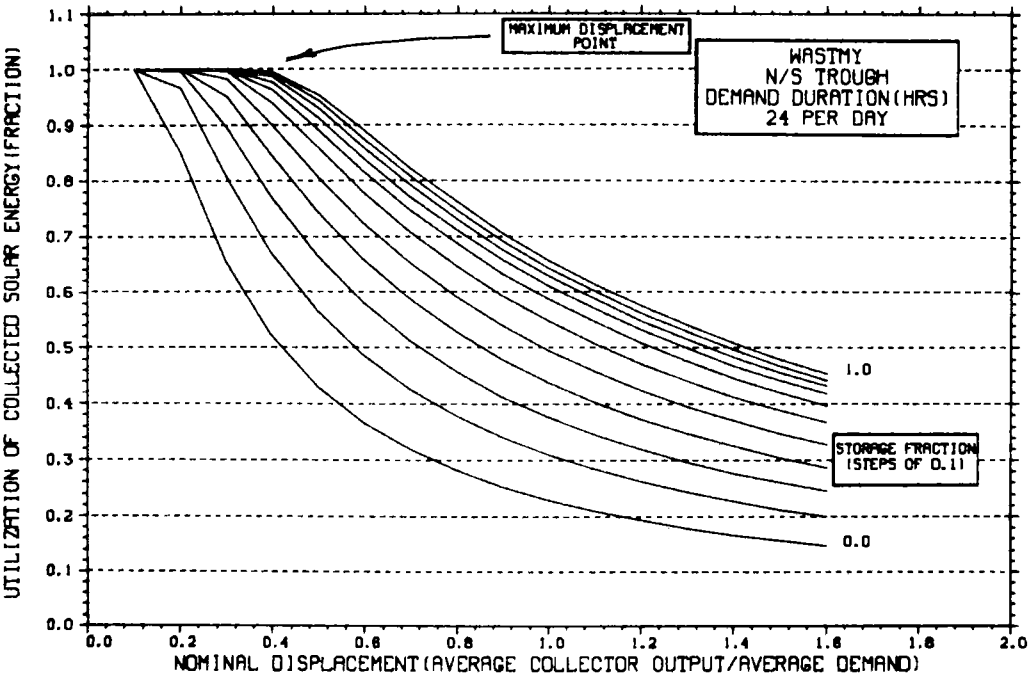

STORAGE SIZING GRAPH FOR CONSTANT ANNUAL DEMAND

NO WEEKEND SHUTDOWN

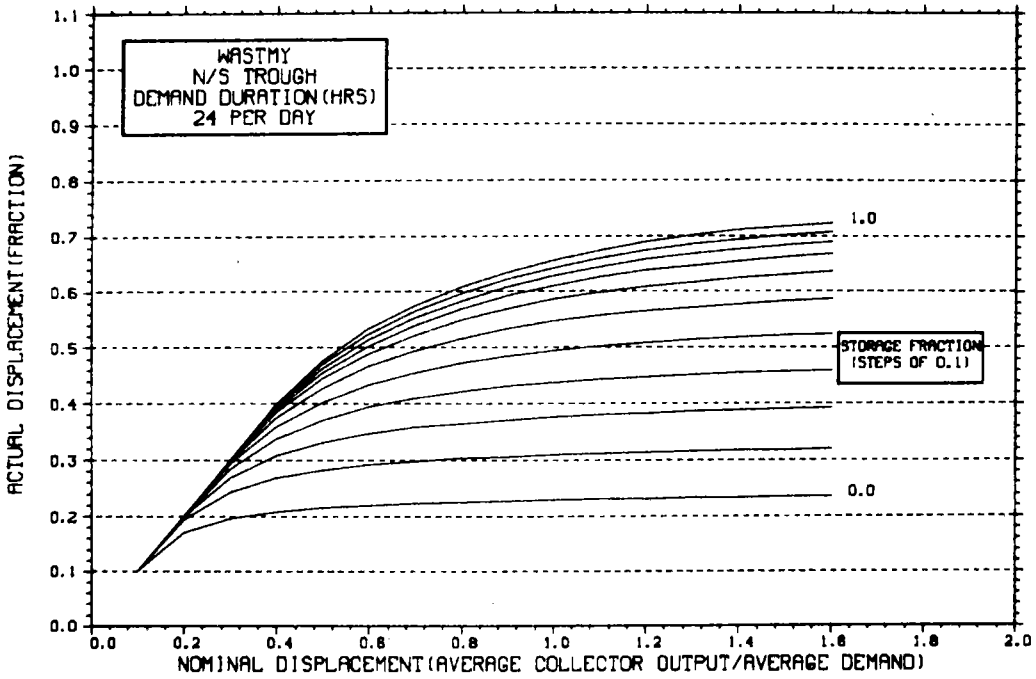

STORAGE SIZING GRAPH FOR CONSTANT ANNUAL DEMAND

NO WEEKEND SHUTDOWN

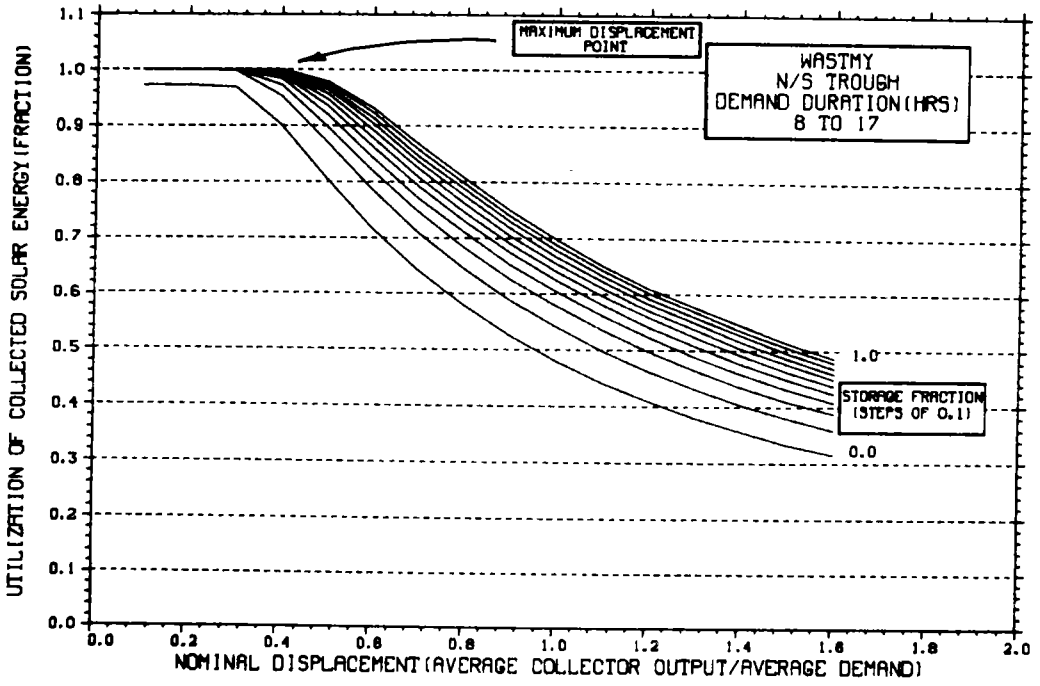

STORAGE SIZING GRAPH FOR CONSTANT ANNUAL DEMAND

NO WEEKEND SHUTDOWN

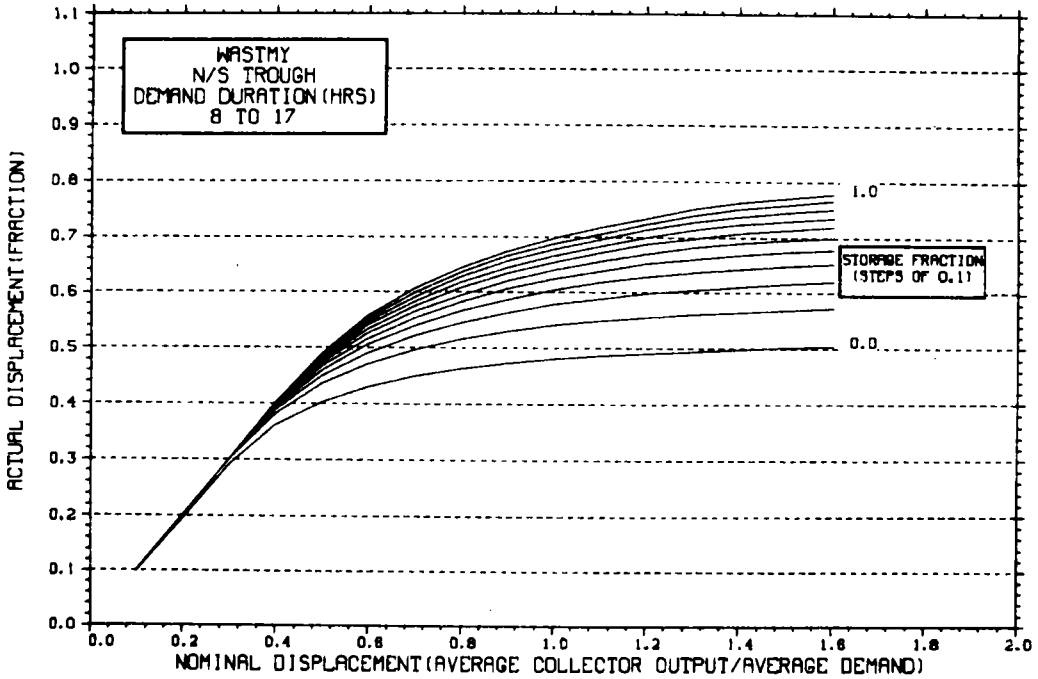

DISTRIBUTION:

AAI Corporation
P.O. Box 6787
Baltimore, MD 21204

Acurex Aerotherm
485 Clyde Avenue
Mountain View, CA 94042
Attn: J. Vindum

Advanco Corporation
999 N. Sepulveda Blvd.
Suite 314
El Segundo, CA 90245
Attn: B. J. Washom

Allison Engr., Inc.
Consulting Mechanical-
Electrical Engrs.
2502 Garfield Ave., SE
Albuquerque, NM

Alpha Solarco
1014 Vine Street
Suite 2230
Cincinnati, OH 45202

American Boa, Inc.
Suite 4907, One World
Trade Center
New York, NY 10048
Attn: R. Brundage

Anaconda Metal Hose Co.
698 South Main Street
Waterbury, CT 06720
Attn: W. Genshino

Applied Concepts Corp.
P.O. Box 2760
Reston, VA 20090
Attn: J. S. Hauger

Applied Solar Resources
490 East Pima
Phoenix, AZ 85004
Attn: W. H. Coady

Arizona Public Service Co.
Box 21666 MS 1795
Phoenix, AZ 85036
Attn: Dr. B. L. Broussard

Argonne National Laboratory (3)
9700 South Cass Avenue
Argonne, IL 60439
Attn: K. Reed
W. W. Schertz
R. Winston

BDM Corporation
1801 Randolph Street
Albuquerque, NM 87106
Attn: T. Reynolds

Battelle Memorial Institute
Pacific Northwest Laboratory
P.O. Box 999
Richland, WA 99352
Attn: K. Drumheller

Bechtel National, Inc.
P.O. Box 3965
50 Beale Street
San Francisco, CA 94119
Attn: E. Y. Lam

Black and Veatch (2)
P.O. Box 8405
Kansas City, MO 64114
Attn: Dr. J. C. Grosskreutz
D. C. Gray

Boeing Space Center (2)
M/S 86-01
Kent, WA 98131
Attn: S. Duzick
A. Lunde

Bovay Engrs., Inc.
3125 Carlisle, NE
Albuquerque, NM 87106

Bridges and Paxton, Inc.
3125 Carlisle Blvd. NE
Albuquerque, NM 87106

Budd Company
Fort Washington, PA 19034
Attn: W. W. Dickhart

Burns & Roe (2)
185 Crossways Park Dr.
Woodbury, NY 11797
Attn: R. J. Vondrasket
J. Wysocki

DISTRIBUTION (Continued):

Carrier Corp.
Energy Systems Div.
Summit Landing
P.O. Box 4895
Syracuse, NY 13221
Attn: R. A. English

Central Solar Energy Research Corp.
328 Executive Plaza
1200 Sixth Street
Detroit, MI 48226
Attn: Ron Nabozny

Congressional Research Service
Library of Congress
Washington, DC 20540
Attn: H. Bullis

Custom Engineering, Inc.
2805 S. Tejon St.
Englewood, CO 80110
Attn: C. A. de Moraes

Del Manufacturing Co.
905 Monterey Pass Road
Monterey Park, CA 91754
Attn: M. M. Delgado

Desert Research Institute
Energy Systems Laboratory
1500 Buchanan Blvd.
Boulder City, NV 89005
Attn: J. O. Bradley

E-Systems, Inc.
Energy Tech. Center
P.O. Box 226118
Dallas, TX 75266
Attn: R. R. Walters

Edison Electric Institute
90 Park Avenue
New York, NY 10016
Attn: L. O. Elsaesser

Electric Power Research Institute (2)
3412 Hillview Avenue
Palo Alto, CA 94303
Attn: Dr. J. Cummings
J. E. Bigger

Energetics
833 E. Arapahoe Street
Suite 202
Richardson, TX 85081
Attn: G. Bond

Energy Institute
1700 Las Lomas NE
Albuquerque, NM 87131

Exxon Enterprises (3)
P.O. Box 592
Florham Park, NJ 07923
Attn: J. Hamilton
P. Joy
Dr. M. C. Noland

Florida Solar Energy Center (2)
300 State Road, Suite 401
Cape Canaveral, FL 32920
Attn: C. Beech
D. Block

General Electric Co. (2)
P.O. Box 8661
Philadelphia, PA 19101
Attn: W. Pijawka
C. Billingsley

General Motors
Harrison Radiator Division
Lockport, NY 14094
Attn: L. Brock

General Motors Corporation
Technical Center
Warren, MI 48090
Attn: J. F. Britt

Georgia Institute of Tech.
Atlanta, GA 30332
Attn: J. D. Walton

Georgia Power Company
270 Peachtree
P.O. Box 4545
Atlanta, GA 30302
Attn: J. Roberts

Honeywell, Inc.
Energy Resources Center
2600 Ridgeway Parkway
Minneapolis, MN 55413
Attn: J. R. Williams

DISTRIBUTION (Continued):

Insights West
900 Wilshire Blvd.
Los Angeles, CA 90017
Attn: J. H. Williams

Jacobs Engineering Co. (2)
251 South Lake Avenue
Pasadena, CA 91101
Attn: B. Eldridge
R. Morton

Jet Propulsion Lab. (3)
4800 Oak Grove Drive
Pasadena, CA 91103
Attn: J. Becker
J. Lucas

Kingston Industries Corporation
205 Lexington Ave.
New York, NY 10016
Attn: M. Sherwood

Lawrence Livermore Lab.
University of Calif.
P.O. Box 808
Livermore, CA 94500
Attn: W. C. Dickinson

Los Alamos National Lab. (3)
Los Alamos, NM 87545
Attn: J. D. Balcomb
C. D. Bankston
D. P. Grimmer

McCarter Corp.
200 E. Washington St.
Norristown, PA 19404
Attn: Roger Powell

McDonnell-Douglas Astronautics Company (3)
5301 Bolsa Avenue
Huntington Beach, CA 92647
Attn: J. B. Blackmon
J. Rogan
D. Steinmeyer

Motorola, Inc.
Government Electronics Division
8201 E. McDowell Road
P.O. Box 1417
Scottsdale, AZ 85252
Attn: R. Kendall

New Mexico State University
Solar Energy Department
Las Cruces, NM 88001

Oak Ridge National Laboratory (3)
P.O. Box Y
Oak Ridge, TN 37830
Attn: S. I. Kaplan
G. Lawson
W. R. Mixon

Office of Tech. Assessment
U.S. Congress
Washington, DC 20510
Attn: R. Rowberg

Progress Industries, Inc.
7290 Murdy Circle
Huntington Beach, CA 92647
Attn: K. Busche

Science Applications, Inc.
P. O. Box 1303
McLean, VA 22102
Attn: Dick Edwards T/9-2

Scientific Applications, Inc.
1200 Mercantile, Commerce Bldg.
Dallas, TX 75201
Attn: Dr. J. W. Doane

Scientific Atlanta, Inc.
3845 Pleasantdale Road
Atlanta, GA 30340
Attn: A. Ferguson

Solar Energy Information Ctr.
1536 Cole Blvd.
Golden, CO 80401
Attn: R. Ortiz

Solar Energy Research Institute (14)
1536 Cole Blvd.
Golden, CO 80401
Attn: B. L. Butler
L. G. Dunham (4)
B. P. Gupta
F. Kreith
J. Thornton
K. Touryan
N. Woodley

DISTRIBUTION (Continued):

D. W. Kearney
C. Bishop
B. Feasby
C. Kutscher

Solar Energy Tech.
Rocketdyne Division
6633 Canoga Avenue
Canoga Park, CA 91304
Attn: J. M. Friefeld

Solar Kinetics Inc.
P.O. Box 47045
8120 Chancellor Row
Dallas, TX 75247
Attn: G. Hutchinson

Southwest Research Institute
P.O. Box 28510
San Antonio, TX 78284
Attn: D. M. Deffenbaugh

Stearns-Rogers
4500 Cherry Creek
Denver, CO 80217
Attn: W. R. Lang

W. B. Stine
1230 Grace Drive
Pasadena, CA 91105

Stone and Webster Engr. Corp.
245 Summer St.
Boston, Mass. 02107
Attn: John M. Lilly
Marketing Engr.

Sun Gas Company
Suite 800, 2 No. Pk. E
Dallas, TX 75231
Attn: R. C. Clark

Sun Heet, Inc.
2624 So. Zuni
Englewood, CO 80110

Sun Heet, Inc.
GED A Division
11965 East 49 Avenue
Denver, CO 80239

Sunpower Systems
510 S. 52nd St.
Tempe, AZ 85281
Attn: W. Matlock

Suntec Systems, Inc.
2101 Woodale Drive
St. Paul, MN 55110
Attn: L. W. Rees

Team, Inc.
120 West Broadway, No. 41
Tucson, AZ 85701
Attn: Roger Harwell

Texas Tech. Univ.
Dept. of Electrical Engr.
P.O. Box 4709
Lubbock, TX 79409
Attn: J. D. Reichert

TRW, Inc.
Energy Systems Group of TRW, Inc.
One Space Park Bldg. R4, Room 2074
Redondo Beach, CA 90278
Attn: J. M. Cherne

Toltec Industries, Inc.
40th and East Main
Clear Lake, IA 50428
Attn: D. Chenault

U.S. Department of Energy (3)
Albuquerque Operations Office
P.O. Box 5400
Albuquerque, NM 87185
Attn: G. N. Pappas
C. B. Quinn
J. Weisiger

U.S. Department of Energy
Division of Energy Storage Systems
Washington, DC 20545
Attn: J. Gahimer

U.S. Department of Energy (8)
Division of Solar Thermal Sys.
Washington, DC 20585
Attn: W. W. Auer
G. W. Braun
J. E. Greyerbiehl
M. U. Gutstein

DISTRIBUTION (Continued):

L. Melamed
J. E. Rannels
F. Wilkins
J. Dollard

U.S. Department of Energy (2)
San Francisco Operations Office
1333 Broadway, Wells Fargo Bldg.
Oakland, CA 94612
Attn: R. W. Hughey

University of Kansas Center for
Research, CRINC
2291 Irving Hall Rd.
Lawrence, KS 66045
Attn: R. F. Riordan

University of New Mexico (2)
Dept. of Mechanical Eng.
Albuquerque, NM 87113
Attn: M. W. Wilden
W. A. Cross

Viking
3467 Ocean View Blvd.
Glendale, CA 91208
Attn: G. Guranson

2320 K. L. Gillespie
2323 C. M. Gabriel
3161 J. E. Mitchell
3600 R. W. Hunnicutt
Attn: H. H. Pastorius, 3640
3700 J. C. Strassell
4000 A. Narath
4700 J. H. Scott
4710 G. E. Brandvold
4713 B. W. Marshall
4717 R. P. Stromberg (20)
4715 R. H. Braasch
4718 E. Burgess
4719 D. G. Schueler (Actg.)
4720 D. G. Schueler
4716 J. F. Banas
4716 R. W. Harrigan (75)
4717 J. A. Leonard
4721 J. V. Otts
4723 W. P. Schimmel
8214 M. A. Pound
8450 R. C. Wayne
8452 A. C. Skinrood
8452 T. Bramlette
8453 W. G. Wilson
3141 L. J. Erickson (5)
3151 W. L. Garner (3)
For DOE/TIC
(Unlimited Release)
3154-3 C. H. Dalin (25)
For DOE/TIC

Org.	Bldg.	Name	Rec'd by *	Org.	Bldg.	Name	Rec'd by *